- Scientia sol mentis est -

KU Leuven
Biomedical Sciences Group
Faculty of Medicine
Department of Microbiology, Immunology, and Transplantation
Laboratory of Immunobiology

KU LEUVEN

DOCTORAL SCHOOL
BIOMEDICAL SCIENCES

THE ROLE OF THE INNATE IMMUNE SYSTEM IN THE PATHOGENESIS OF SYSTEMIC JUVENILE IDIOPATHIC ARTHRITIS: ADVANCES IN UNDERSTANDING

Bert MALENGIER-DEVLIES

Supervisor:	Prof. Dr. Patrick Matthys
Co-supervisors:	Prof. Dr. Carine Wouters
	Prof. Dr. Paul Proost
Chair examining committee:	Prof. Dr. Peter Hoet
Secretary of the jury:	Prof. Dr. Bart Vanaudenaerde
Chair of the public defence:	Prof. Dr. Dominique Bullens
Jury members:	Prof. Dr. Christoph Kessel (University Hospital Muenster)
	Prof. Dr. Nico Wulffraat (UMC Utrecht)
	Prof. Dr. Bart Vanaudenaerde (KU Leuven)
	Prof. Dr. Daan Dierickx (KU Leuven)

Dissertation presented in partial fulfilment of the requirements for the degree of Doctor in Biomedical Sciences

September 2021

ACKNOWLEDGMENT

Wat ik inzag tijdens mijn doctoraat is dat onderzoek niet alleen gaat om nieuwe feiten ontdekken, maar dat het daarentegen gewichtiger is om nieuwe manieren te vinden om over problemen na te denken. Om deze inzichten te vinden is het cruciaal om de verschillende individuele denkvermogens te bundelen en zo SAMEN de eindmeet te halen. Tijdens de afgelopen 5 jaar had ik dan ook het geluk om samen te werken met een groot aantal fantastische mensen, deze hebben mij allemaal helpen groeien tot de onderzoeker die ik nu ben!

In de eerste plaats wil ik mijn promotor prof. Patrick Matthys bedanken. Patrick, bedankt voor het vertrouwen die u mij gaf om te mogen starten in uw labo. Je hebt mij geleerd om goede onderzoeksvragen op te stellen, kritisch na te denken over de resultaten en tot weloverwogen antwoorden te komen. Uw deur stond letterlijk en figuurlijk steeds open. U bleef mij steeds motiveren en onze wetenschappelijke discussies zullen me nog lang bijblijven. Ook mijn copromotoren Prof. Carine Wouters en Prof. Paul Proost wil ik graag bedanken. Prof. Wouters uw klinische inzichten waren van cruciaal belang om de patiënten niet uit het oog te verliezen. Paul, uw expertise in neutrofielen en chemokinen hebben dit onderzoek zeker naar een hoger niveau getild. Jullie passie en enthousiasme voor jullie vak werkten aanstekelijk.

In this paragraph, I want to thank my external jury members prof. Christoph Kessel and prof. Nico Wulffraat for critically evaluating this thesis manuscript as well as their willingness to visit us in Leuven. Ook mijn interne juryleden Prof. Bart Vanaudenaerde en Prof. Daan Dierickx verdienen een bijzondere bedanking voor het opvolgen van dit onderzoek vanaf het prille begin. Prof. Peter Hoet, bedankt om de leescommissie te leiden en Prof. Dominique Bullens om de thesisverdediging voor te zitten.

De kracht van ons “PM-team” ligt naar mijn intentie in onze vele onderlinge samenwerkingen en onze gezamenlijke brainstrom momenten. Laat dit in de toekomst vooral niet verloren gaan! Ellen, Maya en Jessica V als de “oude garde” hebben jullie mij met open armen ontvangen, en herstelde ik zo het mannelijk evenwicht in de groep. Jullie leerden me snel dat een goede voorbereiding en orde van cruciaal belang is. Tegenwoordig is dit nog steeds iets dat ik hoog in het vaandel draag. Kourosh, je versterkte het mannelijke kamp en wordt binnenkort de senior in het labo. Jessica F, bedankt om ons labo de afgelopen 2 jaar te vergezellen met je expertise. Eline, Amber en nu recent ook Margot, net als Kourosh bleven jullie plakken na jullie thesis. Dit toont nog maar eens wat voor een fantastisch team jullie zijn om mee samen te werken. Ik wens jullie alle vier ontzettend veel succes met jullie doctoraat. Alle (oud)-teamleden, wil ik bedanken voor hun grote wetenschappelijke input. Onze lachmomenten, bureau babbels en onderlinge aanmoedigingen zorgden ervoor dat slechte dagen snel vergeten werden. Ons team is natuurlijk niet compleet zonder Tania en Nele. Tania, naast je vele hulp was je er ook steeds voor een hartverwarmende babbel en een luisterend oor. Nele, onze grote muisexperimenten waren zeker nooit zo vlot verlopen zonder jouw goede hulp. Bedankt “team PM” voor de leuke momenten die jullie mij in de afgelopen 5 jaar hebben bezorgd, tijdens, maar zeker ook na de werkuren!

“As scientists, we step on the shoulders of science, building on the work that has come before us - aiming to inspire a new generation of young scientists to continue once we are gone.” Dit is een uitspraak van Stephen Hawking en illustreert wat ik fantastisch vind aan academisch onderzoek: nieuwe onderzoekers inspireren, en hen mijn enthousiasme proberen over te brengen. Lise, Hanne, Eline, Evelyne, Gilles & Jalina, jullie waren stuk voor stuk fantastische studenten. Jullie hebben mijn onderzoek niet enkel sterk vooruitgeholpen maar mij ook op persoonlijk vlak geïnspireerd.

Thanks to all the other (ex)-colleagues from the 7th floor. You created a nice atmosphere every day, which made me feel happy at work. Thanks to Prof. Ghislain Opdenakker, Prof. Philippe Van den Steen, Erik, Lise, Estefi, Jennifer, Vasily, Rafaela, Pierre, Sofie K, Hendrik, Emilie, Leen, Thy, Fran and all colleagues from Bacteriology and Crystallography. Also, at the 6th floor, I felt one of the big family. Thanks to Prof. Sofie Struyf, Prof. Pedro Elias Marques, Noëmie, Helena, Alexandra, Lotte, Mieke DB, Mieke G, Sara AS, Fariba, Pieter, Rik, Vincent, Isabelle, Eva, Karen, Marfa, Mirre, Seppe, Sofie V, Sara S, Luna, Vivian, Ana, Maaike & Matheus. I would like to thank everyone mentioned above for their scientific input and collaborations as

well as their critical assessment of my work. Remember that you don't win a game with the best players, but with the best team! The activities after our experiments, including the daily lunches, (Christmas) parties, (birthday) celebrations, or team building activities, I will continue to cherish. I always was the first in line to organise an afterwork drink, so I hope in the future, the fridge will always be filled for the next Friday evening drink!
Mieke M, samen zijn we aan ons avontuur begonnen en iets na jou heb ik nu ook de eindmeet bereikt. Late avonden hebben we samen in het labo doorgebracht maar de inspanningen hebben zeker geloond! Onze wegen gaan nu uit elkaar, maar ik ben ervan overtuigd dat ze op wetenschappelijk vlak nog zullen kruisen.

Translationeel onderzoek is enkel mogelijk door een nauwe samenwerking met de kliniek. Prof. Lien De Somer, Prof. Ellen De Langhe, Prof. Steven Vanderschueren, Prof. Patrick Verschueren, Prof. Erik Verbeken, Prof. Joost Wauters, Erika, Lore, Cato & Albrecht mijn oprechte dank voor het verzamelen van patiënten materiaal, jullie interesse en klinisch inzicht.

Voor het voltooien van dit doctoraat, maar zeker ook voor een aantal van mijn “zijprojectjes” had ik het geluk te mogen samenwerken met experten in verschillende disciplines. Bedankt Prof. Jeroen Vanoirbeek, Tatjana & Arno voor jullie long expertise, Prof. Greetje Vande Velde, Kaat & Laura voor het uitvoeren van de CT-scans en Prof. Jurgen Vercauteren voor uw statistische inzichten. Bedankt Prof. Georges Leclercq voor uw heldere NK cell doorzichten. To our colleague immunologists from the lab of Adaptive Immunology: Prof. Stephanie Humblet-Baron, Prof. Adrian Liston, Annemarie & Oliver; thanks for our collaborations and thanks to introduce me into the wonderful world of immunology during my master thesis. Prof. Diether Lambrechts en Bram bedank ik graag voor hun single cell sequencing expertise. Eventually, I want to thank all colleagues from the lab of Virology and Chemotherapy, particularly Prof. Johan Neyts, Kai, Ji, Robbert & Mahadesh for our nice collaborations which are still running. Dr. Rebecca Gentek, we recently set up a very nice collaboration and I’m really looking forward to obtaining more insights on immune imprinting in autoimmunity and autoinflammation!

Graag wil ik ook de mensen van het secretariaat bedanken om achter de schermen steeds alles in goede banen te leiden. Bedankt Patrick B, Chantal, Myriam, Dominique, Inge & Cathy. Daarnaast bedankt ik Dieter voor zijn IT-bijstand. Dit doctoraat bevat ook een groot deel muisonderzoek. Het is alom geweten dat “happy animals make good science”, daarom mijn oprechte dank aan alle medewerkers van het animalium; Shana, Greet, Kristof, Nathalie, Annelies, Mirte, Valentijn & Mathias bedankt voor het verzorgen, kweken en opvolgen van mijn muisjes.

Alle vrienden van Team Feest en de KULAK wil ik bedanken voor de leuke en ontspannende momenten de afgelopen jaren. Bij jullie kon ik steeds mezelf zijn en kon ik de stress van me afschudden op de dansvloer, op weekend of één van de vele andere bijeenkomsten. Iedereen is stillaan zijn eigen weg aan het vinden maar ik ben ervan overtuigd dat we er desondanks altijd voor elkaar zullen zijn! De mannen van het koor hebben me geleerd dat doctoreren eigenlijk de studententijd wat verlengen is. Bedankt om 5 jaar lang mijn maandagavond muzikaal in te vullen!

Lieve mama, papa & Heleen, als nuchtere West-Vlamingen zeggen we vaak te weinig wat we echt voelen. Bij deze wil ik nog eens persoonlijk zeggen dat ik zeer veel van jullie hou! Woorden schieten met te kort om te beschrijven wat jullie voor mij betekenen. Ondanks het feit dat jullie niet steeds goed begrijpen waar ik eigenlijk mee bezig ben, zijn jullie altijd geïnteresseerd blijven luisteren en me steeds blijven steunen. Wat de toekomst zal brengen zullen we stap voor stap bekijken maar ik ben ervan overtuigd dat we er altijd zullen blijven staan, dit als een supersterk viertal.

Aan iedereen bedankt!
Thanks to everyone!

Bert

TABLE OF CONTENTS

ACKNOWLEDGMENT ..... **I**

TABLE OF CONTENTS ..... **III**

LIST OF ABBREVIATIONS ..... **IX**

CHAPTER 1: GENERAL INTRODUCTION **2**

1. Autoinflammatory disorders 2

1.1. General features 2

1.2. Innate immune response and inflammasome activation 4

2. Systemic juvenile idiopathic arthritis 6

2.1. Definition, classification, and epidemiology 6

2.2. Aetiology 8

2.3. Clinical and laboratory features 8

2.4. Differential diagnosis 10

2.5. Treatment 10

2.6. Complications 10

2.6.1. Macrophage activation syndrome 11

2.6.2. Lung disease 11

2.7. Mouse models of sJIA 12

3. Pathogenesis of sJIA 13

3.1. Activation of innate immune pathways 14

3.2. Cytokines involved in the pathogenesis of sJIA 15

3.2.1. IL-1β 16

3.2.2. IL-18 16

3.2.3. IFN-γ 17

3.2.4. IL-6 17

3.2.5. IL-10 18

3.2.6. IL-17 18

3.2.7. IL-22 18

3.2.8. TNF-α 19

3.2.9. MIF 19

3.2.10. S100 proteins 19

3.3. Lessons from the CFA-induced sJIA mouse model 20

CHAPTER 2: FACTORS DRIVING EMERGENCY GRANULOPOIESIS IN SYSTEMIC INFLAMMATION **24**

Abstract 24

1. Neutrophils 24

1.1. Introduction 24

1.2. Neutrophil homeostasis 25

1.2.1. Granulopoiesis 26

1.2.2. Circulating pool 30

1.2.3. Marginated pool 32
1.2.4. Tissue pool 32
1.2.5. Apoptosis and neutrophil clearance 34
1.3. Neutrophil function 35
1.3.1. Antimicrobial activities 35
1.3.2. Cellular interactions 37
1.4. Neutrophil heterogeneity 38
1.5. Emergency granulopoiesis in auto-inflammatory disorders 38
1.5.1. Emergency granulopoiesis and extramedullary myelopoiesis 38
1.5.2. Neutrophil-regulating cytokines 42
1.5.2.1. G-CSF 42
1.5.2.2. GM-CSF 44
1.5.2.3. IL-17/IL-23 45
1.5.2.4. IL-1β 46
1.5.2.5. IL-6 46
1.5.2.6. IL-18 47
1.5.2.7. IFN-γ 47
1.5.2.8. FMS-like tyrosine kinase 3 (FLT3) ligand 47
1.6. Physiological regulation of granulopoiesis 48
1.7. Neutrophils in sJIA 48
CHAPTER 3: RESEARCH OBJECTIVES 52
CHAPTER 4: IL-1β DRIVES THE PATHOGENESIS OF SYSTEMIC JUVENILE IDIOPATHIC ARTHRITIS-FEATURES BY STIMULATING PRO-INFLAMMATORY IL-17 AND IL-22 EXPRESSION IN MICE 56
Abstract 56
Introduction 57
Material and Methods 58
Results 60
Increased levels of active IL-1β are found in CFA-challenged IFN-γ KO mice, which are rescued from clinical and haematological abnormalities upon IL-1β neutralisation 60
Reduced extramedullary myelopoiesis and reduced numbers of γδ T cells in anti-IL-1β-treated mice 62
IL-22 levels are increased in CFA-challenged IFN-γ KO mice and IL-22 neutralisation is associated with a partial reduction of sJIA disease symptoms 64
Active-sJIA patients have increased plasma levels of active IL-22, potentiating the release of IL-17 from CD4+ T cells and γδ T cells 66
Discussion 68
Supplementary Tables 71
Supplementary Table 4.1: Patient characteristics 71
CHAPTER 5: ROLE FOR G-CSF IN NEUTROPHILIC EXTRAMEDULLARY MYELOPOIESIS IN SYSTEMIC JUVENILE IDIOPATHIC ARTHRITIS 74
Abstract 74

Introduction 75
Material and Methods 76
Results 78
Active sJIA patients have increased levels of G-CSF that correlates with pro-inflammatory cytokines and number of neutrophils 78
Effects of αG-CSFR antibody on CFA-induced inflammation in IFN-γ KO and WT mice 78
Counteracting effects of G-CSFR-blockage on the development of arthritis 81
Major role for G-CSF-induced extramedullary myelopoiesis 83
Single cell sequencing identifies five neutrophil subsets formed during extramedullary myelopoiesis 85
G-CSFR-blockade alters the relative distribution of neutrophil subsets 87
Discussion 89
Supplementary material 91
Supplementary figures 91
Supplementary Material and Methods 96
Supplementary Tables 97
CHAPTER 6: LUNG FUNCTIONING AND INFLAMMATION IN A MOUSE MODEL OF SYSTEMIC JUVENILE IDIOPATHIC ARTHRITIS 102
Abstract 102
Introduction 103
Material and Methods 104
Results 106
Changes in lung volume and lung density upon immunisation with CFA. 106
Functional lung alterations in CFA-challenged IFN-γ KO mice 108
Histopathology reveals cell infiltration and granulomas in lungs of CFA-challenged mice 110
Lungs of CFA-immunised IFN-γ KO mice present with elevated numbers of neutrophils and activated monocytes/macrophages 112
CFA-immunised IFN-γ KO mice show increased expression of inflammatory mediators in lung tissue 114
Discussion 116
Supplementary Material 119
Supplementary Figures 119
Supplementary Tables 123
CHAPTER 7: GENERAL DISCUSSION AND FUTURE PERSPECTIVES 128
Introduction 128
Current knowledge and gap in the pathogenesis of sJIA 128
Decreasing the knowledge gap by using a sJIA-like mouse model 128
The pathogenesis of sJIA: a summarising model 129
Part I: sJIA is an autoinflammatory disease, initiated by an aberrant inflammasome activation 131
Current insights and new findings 131

Future perspectives 132
PART II: γδ T cells are an important source of IL-17 and IL-22, driving the sJIA-like symptoms 133
Current insights and new findings 133
Future perspectives 134
PART III: Neutrophils are recruited via the IL-17 - G-CSF axis and amplify the innate immune response by releasing pro-inflammatory mediators 134
Current insights and new findings 134
Future perspectives 135
Part IV: Th17 cells and neutrophils are linking the acute autoinflammatory febrile phase to the chronic autoimmune arthritic phase 137
Current insights and new findings 137
Future perspectives 138
Part V: Neutrophil homeostasis: too much, too little? Dual role of neutrophils in sJIA 139
Current insights and new findings 139
Future perspectives 140
Part VI: The lungs are an underestimated target organ in the pathogenesis of sJIA 141
Current insights and new findings 141
Future perspectives 141
ADDENDUM 1: LIMITATIONS OF NEUTROPHIL DEPLETION BY ANTI-LY6G ANTIBODIES IN TWO HETEROGENIC IMMUNOLOGICAL MODELS 144
Abstract 144
Introduction 145
Materials and methods 146
Results 148
Optimising a gating strategy to evaluate the efficiency of neutrophil depletion after injection with anti-Ly6G (clone 1A8) 148
Depletion efficacy in naive BALB/c and C57BL/6 mice 150
Incomplete depletion of neutrophils in both PbNK65-infected C57BL/6 mice and CFA-challenged BALB/c mice 151
Depletion of neutrophils is associated with increased proliferation 152
Discussion 153
Supplementary Material 154
Supplementary Figures 154
ADDENDUM 2: PHENOTYPICAL AND FUNCTIONAL CHARACTERISATION OF NEUTROPHILS IN TWO PYRIN-ASSOCIATED AUTO-INFLAMMATORY DISEASES 158
Abstract 158
Introduction 159
Patients and Methods 160
Results 162
Neutrophils from Patients with PAAND and FMF Show a Primed Gene Expression Profile 162

Neutrophils from Patients with PAAND and FMF Display Phenotypical Differences and Have Altered Maturation States 164
Neutrophils from Patients with PAAND and FMF Display Altered Pro-inflammatory Activities 166
Neutrophils from Patients with PAAND and FMF Show a Primed Phenotype 168
Random Migration and Chemotactic Responses of Neutrophils from PAAND and FMF Patients 170
Discussion 171
Supplementary Material 173
Supplementary Material & Methods 173
Supplementary Figures 174
Supplementary Tables 184
SUMMARY 194
SAMENVATTING 198
REFERENCES 202
ACKNOWLEDGMENTS, PERSONAL CONTRIBUTION, AND CONFLICT OF INTEREST STATEMENT 236
Acknowledgments 236
Author contributions 236
Conflict of interest statement 237
CURRICULUM VITAE 240

LIST OF ABBREVIATIONS

ADA	adenosine deaminase
ADCC	antibody-dependent cellular cytotoxicity
AGS	Aicardi-Goutières syndrome
AHC	hydrocarbon receptor
AIM2	absence in melanoma 2
ALR	AIM2-like receptors
ALT	alanine transaminase
AM	alveolar macrophage
ANA	antinuclear antibodies
AOSD	adult-onset Still's disease
APC	allophycocyanin
APRIL	a proliferation-inducing ligand
APS-1	autoimmune polyglandular syndrome type 1
AS	ankylosing spondylitis
ASC	caspase activation and recruitment domain
AST	aspartate transaminase
ATP	adenosine triphosphate
BAFF	B-cell activating factor
BLTR1, BLT-1	leukotriene B4 receptor
BM	bone marrow
BrDU	5-bromo-2'-deoxyuridine
C/EBP	CCAAT/enhancer-binding protein
C5a(R)	complement component 5a (receptor)
Ca^{2+}	calcium
CAPS	cryopyrin-associated periodic fever syndrome
CCL, CXCL, XCL, or CX_3CL	CC, CXC, XC, or CX_3C chemokine ligand
CCR, CXCR, XCR, or CX_3CR	CC, CXC, XC, or CX_3C chemokine receptor
CD	cluster of differentiation
CD4/8eff cell	CD4/8 effector cell
CD4/8reg cell	regulatory CD4/8 cell
cDNA	complement DNA
CDS	cytosolic DNA sensor
CF	cystic fibrosis
CFA	complete Freund's adjuvant
CI	chemotactic index
CIA	collagen-induced arthritis
CLR	C-type lectin receptors
CR	complement receptors
CRP	C-reactive protein
CSF3R	colony stimulating factor 3 receptor
CyTOF	mass cytometry
DAMP	damage-associated molecular pattern
DC	dendritic cell
DC-SIGN	dendritic cell-specific intercellular adhesion molecule-3-grabbin non-integrin
DEG	differentially expressed gene
DIRA	deficiency of interleukin-1 receptor antagonist
DMARD	disease-modifying anti-rheumatic drug
DNA	deoxyribonucleic acid
EAE	experimental autoimmune encephalomyelitis
EDTA	ethylenediaminetetraacetic acid
ELISA	enzyme-linked immuno sorbent assay
ELP	endogenous lipoid pneumonia

EMH	extramedullary haematopoiesis
ESR	erythrocyte sedimentation rate
F5	factor V
FACS	fluorescence-activated cell sorting
Fc	fragment crystallisable
FCS	foetal calf serum
FDR	false discovery rate
FEV(0.1)	forced expiratory volume (in 0.1s)
fHLH	familial HLH
FITC	fluorescein isothiocyanate
FLC	fibrocyte-like cell
FLT3(L)	FMS-like tyrosine kinase 3 (ligand)
FMF	familial Mediterranean fever
fMLF	N-formyl-Met-Leu-Phe
FSC	forward scatter
FSTL-1	follistatin-like protein 1
FVC	forced vital capacity
G	tissue damping
GCP-2	granulocyte chemotactic protein-2
G-CSF	granulocyte-colony stimulating factor
Gfi-1	growth factor independent-1
GM-CSF(R)	granulocyte-macrophage colony-stimulating factor (receptor)
GMP	granulocyte-macrophage progenitor
GSDMD	gasdermin-D
H&E	haematoxylin and eosin
H_2O_2	hydrogen peroxide
HC	healthy control
HLA	human leukocyte antigen
HLH	hemophagocytic lymphohistiocytosis
HMGB1	high-mobility group box 1
HRP	horseradish peroxidase
HSC	hematopoietic stem cell
HSPC	hematopoietic stem/progenitor cell
HT	Hashimoto's thyroiditis
i.p.	intraperitoneal
IBD	inflammatory bowel disease
ICAM	intercellular adhesion molecule
IDO	indoleamine 2,3-dioxygenase
IFN	interferon
Ig	immunoglobulin
IGF-1	insulin-like growth factor-I
IL	interleukin
IL-18BP	IL-18 binding protein
IL-1R(a)	IL-1 receptor (antagonist)
IL-1RAcP	IL-1 receptor accessory protein
IL-22BP	IL-22 binding protein
ILAR	International League of Associations for Rheumatology
ILC	innate lymphoid cell
ILD	intestinal lung disease
IM	interstitial macrophage
iNKT	invariant NK T cells
iNOS	inducible nitric oxide synthase
IPEX	immunodysregulation polyendocrinopathy enteropathy X-linked syndrome
IQR	interquartile range

IRF	interferon regulatory factors
JAK	Janus kinase
JIA	juvenile idiopathic arthritis
JRA	juvenile rheumatoid arthritis
KC	keratinocyte chemoattractant
KLF5	Krüppel-like factor 5
KO	knockout
LDH	lactate dehydrogenase
LEF1	lymphoid enhancer-binding factor 1
LFA-1	lymphoid function-associated antigen 1
LN	lymph node
LPS	lipopolysaccharide
LRG	leucine-rich α2-glycoprotein
LTB4	leukotriene B4
LXR	liver X receptor
MA	macrophage
(MA-)ARDS	(malaria-associated) acute respiratory distress syndrome
MAS	macrophage activation syndrome
MCP	monocyte chemotactic protein
M-CSF	macrophage colony-stimulating factor
MDSC	myeloid-derived suppressor cell
MFI	mean fluorescent intensity
MG	myasthenia gravis
MIF	macrophage migration inhibitor factor
MIP2	macrophage inflammatory protein 2
MMP	matrix metalloproteinase
MO	monocytes
MPO	myeloperoxidase
MR	mannose receptor
MS	multiple sclerosis
MTX	methotrexate
MyD88	myeloid differentiation primary response gene 88
n.s.	non-significant
NADPH	nicotinamide adenine dinucleotide phosphate
NE	neutrophil elastase
NET	neutrophil extracellular trap
NFDM	non-fat dried milk
NF-κB	nuclear factor kappa B
NH_4Cl	ammonium chloride
NI	non-immunised
NK cell	natural killer cell
NLR	NOD-like receptor
NO	nitric oxide
NOD	nucleotide-binding oligomerisation domain
NPFE	negative pressure forced expiration manoeuvre
NSAID	non-steroidal anti-inflammatory drug
NSE	neurospecific enolase
O_2^-	superoxide anion
(p)Treg cell	(periphery-derived) regulatory T cell
p.i.	post-infection / post-immunisation
PAAND	Pyrin-Associated Autoinflammation with Neutrophilic Dermatosis
PAF	platelet-activating factor
PAH	pulmonary arterial hypertension
PAMP	pathogen-associated molecular pattern

PAP	pulmonary alveolar proteinosis
PBMCs	peripheral blood mononuclear cells
PbNK65	*Plasmodium berghei* NK56-Edinburgh line
PBS	phosphate buffered saline
PCA	principal components analysis
PCR	polymerase chain reaction
PD-L1	programmed death-ligand 1
PE	phycoerythrin
PEF	peak expiratory flow
PerCP	perinidin chlorophyll protein complex
PGE2	prostaglandin E2
PHA	phytohemagglutinin
PLD	parenchymal lung disease
PMA	phorbol 12-myristate 13-acetate
preNeu	neutrophils progenitor
PRR	pathogen recognition receptors
PSGL-1	P-selectin glycoprotein ligand-1
PTT	partial thromboplastin time
RA	rheumatoid arthritis
RAGA	remnant epitopes generate autoimmune disease
RAGE	receptor for advanced glycation end products
RANK(L)	receptor activator of NFκB (ligand)
RBC	red blood cell
RF	rheumatoid factor
RIG-I	retinoic acid-inducible gene-I
RLR	RIG-I-like receptor
Rn	airway resistance
RNA	ribonucleic acid
RNS	reactive nitrogen species
RORγt	retinoic acid receptor-related orphan nuclear receptor γ t
ROS	reactive oxygen species
RT	room temperature
RT qPCR	real-time quantitative PCR
(s)TNFR	(soluble)TNF receptor
s.c.	subcutaneous
(sc)RNAseq	(single cell) RNA sequencing
SCAR	scavenger receptors
SDF	stromal cell-derived factor
SE	standard error
sHLH	secondary HLH
sIL-6R	soluble IL-6R
sJIA	systemic juvenile idiopathic arthritis
SLE	systemic lupus erythematosus
SNP	single nucleotide polymorphism
SOCS	suppressor of cytokine signalling
SPF	specific pathogen-free
SSC	side scatter
STAT	JAK-signal transducer and activator of transcription
T1D	type 1 diabetes
T3SS	type III secretion system
TACE	tumour necrosis factor alpha converting enzyme
TF	transcription factor
TGF	transforming growth factor
Th cell	T helper cell

TLR	toll-like receptor
TNF	tumour necrosis factor
TNFSF	TNF ligand superfamily member
TOF	time of flight
TRAP	tartrate-resistant acid phosphatase
TRAPS	TNFRSF1A-receptor-associated periodic fever syndrome
t-SNE	t-distributed stochastic neighbour embedding
VCAM	vascular cell adhesion protein
VLA	very late antigen
VOI	volume-of-interest
WB	western blot
WBC	white blood cell
WHIM	warts, hypogammaglobinaemia, infection, and myelokathexis
WT	wild type
α-SMA	alpha-smooth muscle actin
ε = G/H	tissue hysteresivity

CHAPTER 1

GENERAL INTRODUCTION

Part of this chapter has been submitted for publication

Bert Malengier-Devlies[1], Paul Proost[2], Carine Wouters[1,3,4], Patrick Matthys[1]

[1]KU Leuven Department of Microbiology, Immunology and Transplantation, Rega Institute for Medical Research, Laboratory of Immunobiology, Leuven, Belgium
[2]KU Leuven Department of Microbiology, Immunology and Transplantation, Rega Institute for Medical Research, Laboratory of Molecular Immunology, Leuven, Belgium
[3]University Hospitals Leuven, Division of Pediatric Rheumatology, Leuven, Belgium
[4]European Reference Network for Rare Immunodeficiency, Autoinflammatory and Autoimmune Diseases (RITA) at University Hospital Leuven, Leuven, Belgium

CHAPTER 1: GENERAL INTRODUCTION

1. Autoinflammatory disorders

1.1. General features

Autoinflammatory and autoimmune diseases are two groups of disorders caused by an abnormal immune response. Although both groups can be placed in the same immunological disease continuum, and conditions with overlapping phenotypes exist, the main distinction is that autoinflammatory diseases are typically defined by a dysfunction of the innate immune system whereas, in autoimmune diseases, aberrant activation of the adaptive immune system dominates (Table 1.1). The main cell types of the innate immune system are neutrophils, eosinophils, basophils, monocytes, macrophages, dendritic cells (DCs), innate lymphoid cells (ILCs) and gamma delta (γδ) T cells. In contrast, in the adaptive immune system, both B and T cells with their highly specific antibodies and T cell receptors against autoantigens evoke the immune response. Autoinflammatory diseases lack high-titer autoantibodies, human leukocyte antigen (HLA) class II associations, or antigen-specific T cells. Clinically, patients often present with recurrent episodes of fever and some signs of abdominal, articular, or cutaneous sterile inflammation (1–3).

Table 1.1: Differences between autoinflammatory and autoimmune diseases (1)

	Autoinflammation	Autoimmunity
Immune dysregulation	Innate immune system	Adaptive immune system
Predominant cell types	neutrophils, eosinophils, basophils, monocytes, macrophages, DCs, ILCs, γδ T cells	T cells, B cells
Features	No autoantibodies No autoreactive T cells No HLA class II associations	Autoantibodies Autoreactive T cells HLA class II associations

The term “autoinflammatory diseases” was proposed for the first time by McDermott *et al*. (4). Since the term was coined in 1999, more than 30 genes affecting different components of the innate immune system have been associated with autoinflammatory diseases (1,5). Autoinflammatory diseases can be divided into at least 8 different categories: interleukin-1β (IL-1β) activation disorders or inflammasomopathies [*e.g.* cryopyrin-associated periodic syndrome (CAPS), familial Mediterranean fever (FMF), or Pyrin-Associated Autoinflammation with Neutrophilic Dermatosis (PAAND)], NK-κB activation syndromes [*e.g.* Tumour necrosis factor receptor-associated periodic syndrome (TRAPS)], protein misfolding disorders [*e.g*. cystic fibrosis (CF)], complement regulatory diseases, cytokine signalling disturbances [*e.g.* Deficiency of interleukin-1 receptor antagonist (DIRA)], macrophages activation syndromes (MAS) (due to *i.e.* mutation in the NLRC4 inflammasome), ubiquitination disorders, and type I interferonopathies [*e.g.* Aicardi-Goutières syndrome (AGS)] (6). Historically, autoinflammatory diseases have been considered as a result of alterations in the innate immune system only. This has been mainly true for monogenic diseases with a clear disease-causing mutation. In contrast, polygenic diseases such as systemic juvenile idiopathic arthritis (sJIA), Adult-onset Still's disease (AOSD), or ankylosing spondylitis (AS) may be considered as polygenic/multifactorial autoinflammatory that have both innate and adaptive immune responses involved. Remark that although sJIA is linked to HLA associations and adaptive immune responses (*vide infra*), no autoantibodies or autoreactive T cells have been found. Therefore, sJIA and AOSD cannot be classified as pure autoimmune diseases. *Vice versa* some monogenic autoimmune diseases [*e.g.* Immunodysregulation polyendocrinopathy enteropathy X-linked syndrome (IPEX) or Autoimmune polyglandular syndrome type 1 (APS-1)] purely depends on monogenic mutations in the adaptive immune system, whereas the main polygenic autoimmune diseases [*e.g.* Rheumatoid arthritis (RA),

Type 1 diabetes (T1D), poly-JIA, or oligo-JIA] also have an important innate component (Figure 1.1) (6,7). Since sJIA forms the thread of this thesis, the disease is described in more detail in section 2.

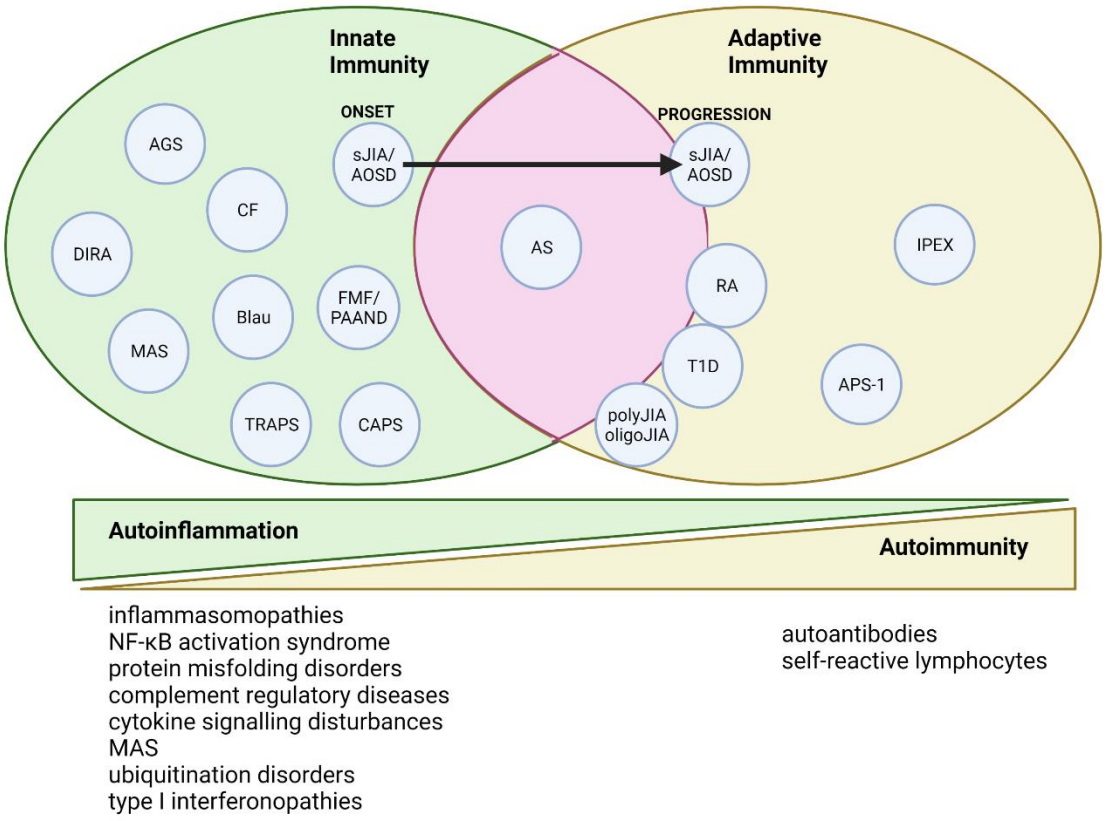

Figure 1.1: Autoimmune and autoinflammatory diseases classified according to the involvement of the innate and adaptive immune systems. The disease spectrum includes rare monogenic diseases at the polar ends of each spectrum. Polygenic diseases involve both the innate and adaptive immune system. CAPS: Cryopyrin-associated periodic syndrome; FMF: familial Mediterranean fever; PAAND: Pyrin-Associated Autoinflammation with Neutrophilic Dermatosis; TRAPS: Tumour necrosis factor receptor-associated periodic syndrome; CF: cystic fibrosis; DIRA: Deficiency of interleukin-1 receptor antagonist; MAS: macrophages activation syndromes; AGS: Aicardi-Goutières syndrome; sJIA: systemic juvenile idiopathic arthritis; AOSD: Adult-onset Still's disease; AS: ankylosing spondylitis; IPEX: Immunodysregulation polyendocrinopathy enteropathy X-linked syndrome; APS-1: Autoimmune polyglandular syndrome type 1; RA: Rheumatoid arthritis; T1D: Type 1 diabetes. Figure adapted from Kessel et al. (6).

1.2. Innate immune response and inflammasome activation

The innate immune system represents the first line of host defence against pathogens and reacts via signalling receptors called pathogen recognition receptors (PRR) detecting different highly conserved structures expressed by pathogens or damaged cells called pathogen-associated molecular patterns (PAMPs) or damage-associated molecular patterns (DAMPs). The first set of extracellular PRRs includes the Toll-like receptors (TLRs), complement receptors (*e.g.* CR1 or CR2), scavenger receptors (*e.g.* SCARA1 or SCARA2), and the C-type lectin receptors (CLRs) (*e.g.* DC-SIGN or dectin 1). There are at least 11 TLR members in humans (TLR1-11) which can be found at the cell membrane or in the endolysosomes. TLR are evolutionarily conserved receptors that are classified in the superfamily of interleukin-1 (IL-1) receptors (IL-1Rs) due to their homology of their cytoplasmic Toll/IL-1R (TIR) domain. Except for TLR3, signalling occurs through the myeloid differentiation primary response gene 88 (MyD88) adaptor protein, activating cytokine-inducing transcription factors such as nuclear factor kappa B (NF-κB) or interferon regulatory factors (IRF). CLRs (including the DC-specific ICAM3-grabbing non-integrin (DC-SIGN) or Dectin-1) recognise aberrant (oligo)saccharides and independently induce an immune response by the activation of NF-κB or can crosstalk with other PRRs. CLRs are mainly expressed by DCs and activation induces T cell polarisation through the expression of specific cytokines. (8–10). The second set of pathogen recognition sensors is present in the cytosol and includes the retinoic acid-inducible gene-I (RIG-I)-like receptors (RLRs), nucleotide-binding oligomerisation domain (NOD)-like receptors (NLRs), absence in melanoma 2 (AIM2)-like receptors (ALR), and pyrin, along with a number of cytosolic DNA sensors (CDS). All these sensors are essential for the detection of intracellular PAMPs, DAMPs, and intracellular homeostasis alterations. Ligation of NLRs, ALRs or pyrin triggers the formation of multiprotein complexes called inflammasomes that generally consist of the sensor molecules, adaptor molecules apoptosis-related speck-like protein containing caspase activation and recruitment domains (ASC), and caspase 1 as an effector molecule. The different components of the inflammasomes are reviewed elsewhere and fall out of the scope of this literature overview (10–16). Eventually, inflammasome activation mediates the proteolytic cleavage and activation of caspase-1, which in turn cleaves pro-IL-1β and pro-IL-18 into their bioactive forms that may be released into the bloodstream. The binding of IL-1β to the IL-1R1, maintains the inflammatory response by the MyD88 promoted transcription of NF-κB-dependent genes, such as NLRP3, pro-IL-1β, pro-IL-18, and IL-6. The inflammatory cascade is shown in Figure 1.2. Activation of caspase 1 also results in pyroptosis by the cleavage of the membrane-pore-forming protein gasdermin-D (GSDMD). Pyroptosis is an inflammatory form of cell death characterised by rapid swelling of the cell and eventually membrane rupture associated with the release of DAMP molecules such as Adenosine triphosphate (ATP) or DNA, perpetuating the inflammatory response. This is in contrast to apoptosis, induced by a different set of caspases (including caspase 9 and caspase 3), in which inflammation is avoided by the release of apoptotic bodies (17,18).

Hereditary monogenic autoinflammatory diseases are characterised by a dysregulation of the innate immune response that can be caused by various mechanisms including increased inflammasome activation and IL-1/IL-18 signalling (inflammasomopathies), constitutive type I IFN signalling and increased NF-kB signalling (6,19). Inflammasomopathies may be caused by mutations in parts of the inflammasome (20,21). Specific mutations in the pyrin-encoding gene *MEFV* for example may lead to two clinically distinct autoinflammatory disorders: FMF and Pyrin-Associated Autoinflammation with Neutrophilic Dermatosis (PAAND) (16,22–24). In the Addendum, we described the phenotypical and functional characteristics of neutrophils in these two distinct auto-inflammatory diseases.

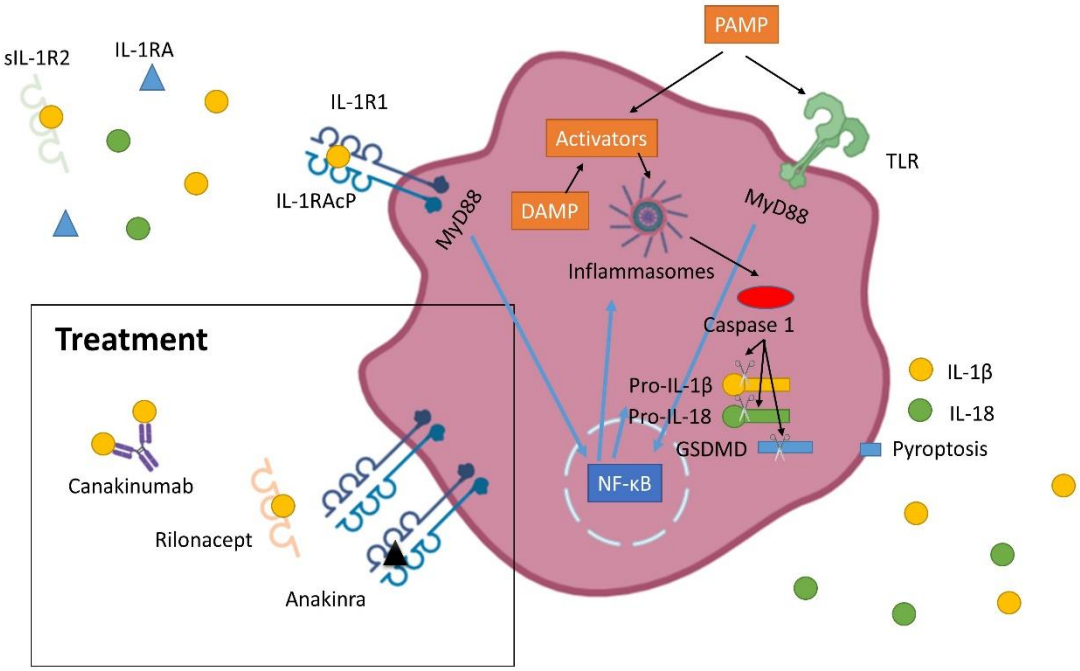

Figure 1.2: Inflammasome activation is tightly regulated and requires at least two signals. First, stimulation of the toll-like receptor (TLR) or the IL-1β receptor (IL-1R) induces MyD88 signalling and NF-κB activation. NF-κB increases the expression of pro-IL-1β, pro-IL-18, gasdermin D (GSDMD), and inflammasome proteins (blue arrows). IL-1R signalling depends on the binding of IL-1β to the heterodimeric IL-1R that consists of an IL-1R type 1 (IL-1R1) and an IL-1R accessory protein (IL-1RAcP). Naturally, the IL-1β receptor antagonist (IL-1RA) and the soluble non-signalling IL-1R type 2 (IL-1R2) regulate the activity of IL-1β. Therapeutically, IL-1β-signalling can be targeted by the use of a monoclonal antibody that binds IL-1β (canakinumab), the use of a dimeric fusion protein of the ligand-binding domains of the IL-1RA and the IL-1RAcP (rilonacept), or a recombinant IL-1RA (anakinra). Next, pathogen-associated molecular patterns (PAMPs) or damage-associated molecular patterns (DAMPs) can activate the inflammasomes resulting in the formation of an inflammasome complex and the subsequent cleavage of inactive pro-caspase-1 into active caspase-1. Caspase-1 in its turn can process pro-IL-1β, pro-IL-18, and GSDMD into active proteins that can be secreted or that can induce pyroptosis (black arrows).

2. Systemic juvenile idiopathic arthritis

sJIA is a unique childhood autoinflammatory immune disorder. In this chapter, we summarise the classification, epidemiology as well as the clinical and laboratory features of the disease. We describe its association with macrophage activation syndrome and more recently reported lung complications that include *i.e.* interstitial lung disease (ILD), and pulmonary alveolar proteinosis (PAP). We will summarise the current knowledge on susceptibility factors and driving pathomechanisms. We describe the potential effects of all different pro- and anti-inflammatory cytokines involved in the pathophysiology and summarise the current treatment strategies. Finally, we will also discuss some novel recent findings made in the sJIA mouse model.

2.1. Definition, classification, and epidemiology

Juvenile idiopathic arthritis (JIA) is an umbrella term for a heterogeneous group of childhood arthritic diseases. The International League of Associations for Rheumatology (ILAR) has defined JIA as arthritis of unknown aetiology that starts before the 16th birthday and persists for 6 weeks and for which known causes are excluded. According to the number of affected joints and the presence of extra-articular symptoms, JIA is defined in six categories including: sJIA, oligoarticular JIA, polyarticular JIA with or without rheumatoid factor (RF), psoriatic arthritis, enthesitis-related arthritis, and undifferentiated arthritis (as summarised in Table 1.2) (25,26).

Table 1.2: JIA subtypes, frequency, main characteristics, age at disease onset, and sex distribution (25,27,28)

	Frequency	Main characteristics	Age at disease onset, sex ratio
Systemic juvenile idiopathic arthritis	5-10%	Arthritis, fever, rash, lymphadenopathy, hepatosplenomegaly, serositis	Throughout childhood, F=M
Oligoarthritis	40-50%	Arthritis in < 5 joints during the first six months	Early childhood, F>M
Polyarthritis (RF negative)	20-25%	Arthritis in ≥ 5 joints, RF negative	Biphasic: peak at 2-4 years and 9-12 years, F>M
Polyarthritis (RF positive)	5%	Arthritis in ≥ 5 joints, RF positive	Late childhood or adolescence, F>M
Psoriatic arthritis	5-10%	Arthritis, Psoriasis	Biphasic peak at 2-4 years and 9-11 years, F>M
Enthesitis-related arthritis	5-10%	Arthritis, Enthesitis	Late childhood or adolescence, M>F
Undifferentiated arthritis	10%	Arthritis, Not fitting in one of the other categories	-
F = Female, M = Male			

sJIA was described for the first time by George Frederic Still in 1896 and is also known as systemic juvenile rheumatoid arthritis (JRA) or Still's disease (29). According to the ILAR, sJIA is diagnosed in the presence of arthritis in one or more joints with or preceded by a quotidian fever of at least 2 weeks and accompanied by an erythematous rash, and enlargement of the lymph nodes (lymphadenopathy), liver and/or spleen (hepatosplenomegaly) or serositis (Table 1.3) (25). The disease can also occur in adults, where it is called Adult-onset Still's disease (AOSD) (30).

Table 1.3: sJIA classification criteria (25)

International League of Associations of Rheumatology (ILAR) classification criteria for systemic juvenile idiopathic arthritis	
Definition	Arthritis in one or more joints with or preceded by fever of at least 2 weeks' duration that is documented to be daily ("quotidian") for at least 3 days, and accompanied by one or more of the following: 1. Evanescent (non-fixed) erythematous rash 2. Generalised lymph node enlargement 3. Hepatomegaly and/or splenomegaly 4. Serositis
Exclusion	a. Psoriasis or a history of psoriasis in the patient or first-degree relative b. Arthritis in a HLA-B27 positive male beginning after the 6th birthday c. Ankylosing spondylitis, enthesitis-related arthritis, sacroiliitis with inflammatory bowel disease, Reiter's syndrome, or acute anterior uveitis, or a history of one of these disorders in a first-degree relative d. The presence of IgM rheumatoid factor on at least 2 occasions at least 3 months apart

JIA is the most common chronic rheumatic syndrome in childhood. It has an incidence of 0.01% and a prevalence of 0.1%. sJIA comprises 5-10% of all JIA cases in Europe and North-America and has a yearly incidence of 0.3-0.9 cases per 100.000 children per year (25,27,28,31). As depicted in Table 1.2, sJIA develops throughout childhood and both sexes are affected with equal frequency (25,32,33).

2.2. Aetiology

The aetiology of sJIA remains largely unknown and requires further research. sJIA is not an infectious disease since, up till now, the condition has not been consistently associated with any pathogen. In view of a seasonal variation in some studies, it has been hypothesised that infectious agents may trigger an excessive immune reaction to a relatively harmless trigger in genetically susceptible children (31,34,35). Indeed, several immunological genetic polymorphisms have been demonstrated to be associated with sJIA, defining sJIA as a multigenic and multifactorial disease. Gene or promoter polymorphisms were found in *i.e.* the interleukin (IL)-1 family (IL1R2, IL1A, IL1F10, and IL1RN), IL-6, IL-10, IL-20, pyrin, tumour necrosis factor (TNF)α, the sulphate transporter SLC26A2, the ATP receptor P2X7 and the macrophage migration inhibitor factor (MIF) (36–46). IL1RN SNPs correlate with higher IL1RN mRNA levels and are also associated with a 6-fold higher risk of non-response (47)**.** Interestingly, a monogenic autosomal-recessive missense mutation was found in the *LACC1* gene, encoding the enzyme laccase domain-containing 1, of five consanguineous Saudi Arabian families presenting with a sJIA phenotype (48). Furthermore, a heterozygous missense variant in the *CASP1* gene (caspase-1), was found in one sJIA patient (49). Finally, mutations in NFIL3 and UNC13D were also linked to the development of juvenile arthritis, sJIA, and MAS (50–52). Although sJIA is considered as an autoinflammatory disease caused by abnormalities of the innate immune system, recent studies have shown that the HLA-DRB1*11 is an important risk factor for sJIA, thereby implicating adaptive immune molecules in the pathogenesis of the disease (53). An increased risk for JIA (including sJIA) was observed among relatives of probands with JIA. Approximately 13% of cases of JIA can be attributed to familial factors (54,55). The “idiopathic” in sJIA mainly refers to the unknown triggers that initiate the onset of the disease (in susceptible individuals).

2.3. Clinical and laboratory features

Clinically, sJIA is characterised by arthritis and fever, accompanied by rash, lymphadenopathy, hepatosplenomegaly, and serositis. Although arthritis is one of the hallmarks of JIA, it can be absent in the early presentation of the disease and only develop at a later stage during the disease course preceded by arthralgia. Arthritis often primarily affects the wrists, ankles, and knees. Rash typically presents as an evanescent erythematous rash on the trunk and proximal extremities. Fever is spiking, with daily peaks over 39°C. Patients also present with fatigue, abdominal pain, and weight loss (31–34). Laboratory findings include (normo- or microcytic) anaemia, thrombocytosis, leukocytosis due to a massive neutrophilia and a high erythrocyte sedimentation rate (ESR). Plasma levels of inflammatory cytokines (IL-6, IL-18) (cytokines are extensively discussed below), acute phase proteins S100A8/A9, and S100A12, and C-reactive protein (CRP) are highly increased. In addition, the level of ferritin and D-dimers and liver enzymes such as aspartate transaminase (AST), alanine transaminase (ALT), and lactate dehydrogenase (LDH) are often elevated as well (31,33,34). An overview of the different clinical and laboratory features is given in Table 1.4. The clinical course of sJIA is highly variable, Singh-Grewal *et al*. showed in a 5-year follow-up study that 40% of the sJIA patients develop a monocyclic course, 7% have a polycyclic course, and half of the patients have a persistent disease course (56).

Table 1.4: Clinical and laboratory features of sJIA and MAS

	sJIA (31–34,57,58)	**MAS** (59–63)
Clinical features		
Fever	Quotidian	Present
Rash	Evanescent	Petechial/macular
Lymphadenopathy	+	+
Splenomegaly	+	+
Hepatomegaly	+	+
Serositis	+	-
Coagulopathy	-	+
CNS dysfunction	±	+
Mucosal bleeding	-	+
Arthritis	+	-
Laboratory features		
Anaemia	+	+
Neutrophil count	↑↑	↓
Leukocyte count	↑↑	↓
Platelet count	↑↑	↓
ESR	↑	~/↓
PT	~	↑
PTT	~	↑
CRP	↑	↑
AST/ALT	~/↑	↑↑
LDH	~/↑	↑↑
Bilirubin	~	~/↑
Albumin	~	↓
Triglycerides	~	↑
Ferritin	~/↑	↑↑
sCD25	~/↑	↑↑
sCD163	~/↑	↑↑
Sodium	~	↓
Fibrinogen	↑	↓
D-dimers	↑	↑↑
Others		
Haemophagocytosis	±	+
NK cell dysfunction	±	+

+ present, ± sometimes present, - not present, ~normal, ↑ increased levels, ↓ decreased levels, ✓ used as a diagnostic marker, CNS = central nervous system, ESR = erythrocyte sedimentation rate, PT = prothrombin time, PTT = partial thromboplastin time, CRP = C-reactive protein, AST = aspartate transaminase, ALT = alanine transaminase, LDH = lactate dehydrogenase, s = soluble

2.4. Differential diagnosis

sJIA has a heterogeneous disease course and the clinical features of sJIA may vary. At the onset of disease, arthritis may be absent, and the first systemic features overlap with many other conditions challenging the diagnosis. The typical spiking fever pattern, especially when accompanied by an evanescent rash, should suggest sJIA, and so is included in the diagnostic criteria (Table 1.4). Often at initial evaluation, only 30% of all patients were found to fulfil the ILAR criteria (33). No diagnostic biomarkers have been identified. More recently a number of proteins including S100A8/A9 (calprotectin), S100A12 (calgranulin C), leucine-rich α2-glycoprotein (LRG), follistatin-like protein 1 (FSTL-1), and IL-18 have been proposed as possible candidates (64–70). The correct diagnosis of sJIA requires exclusion of systemic autoimmune diseases (*e.g.* systemic lupus erythematosus), monogenic autoinflammatory diseases (*e.g.* FMF), infections (*e.g.* sepsis), malignancies, or systemic disorders associated with vasculitis (*e.g.* Kawasaki disease). Furthermore, genetic testing can exclude some of the monogenic autoinflammatory syndromes presenting with fever, rash and joint/muscle pain.

2.5. Treatment

Early diagnosis is crucial for the appropriate treatment of sJIA patients. Typically, patients are initially treated with non-steroidal anti-inflammatory drugs (NSAIDs). Often, corticosteroid therapy is needed to control the systemic inflammation, however, chronic steroid therapy should be avoided due to the adverse reaction of long-term corticosteroid treatment certainly in children (*e.g.* growth retardation or osteoporosis) (31,32,35). Disease-modifying anti-rheumatic drugs (DMARDs) (*e.g.* methotrexate or hydroxychloroquine) are commonly used in RA but are less effective in sJIA. Only methotrexate had arthritis-controlling properties in sJIA (31,32,71). About 10 years ago, the therapeutic benefit use of biologicals was demonstrated. Patients can be treated successfully with IL-1 blocking-agents such as the recombinant IL-1 receptor antagonist (IL-1Ra) anakinra (72–77), the monoclonal antibody canakinumab (75–78), or the IL-1 neutralising fusion protein rilonacept (76,79). Also the use of IL-6 blocking agents such as the IL-6 receptor monoclonal antibody tocilizumab has shown beneficial effects in sJIA (75,76,80–83). IL-1 blocking therapies are reportedly beneficial equally as first-line therapy, underlining the importance of IL-1β at the disease onset (74,84). This is in line with the "window of opportunity" that has been proposed by Nigrovic (85). In his review, it has been described that sJIA follows a biphasic clinical course, in which innate immune system hyperactivation is mainly involved at disease initiation, followed by the involvement of the adaptive immune system which ultimately contributes to the arthritic phenotype (85). The use of TNF inhibitors has been shown to be very effective in other subtypes of JIA but not to control systemic inflammation in sJIA (31,32,75,86). Unfortunately, not all patients are responsive to the current therapies, and an initial response may disappear with time. This shows the current need for further research. A final resort might be the use of autologous stem cell transplantation but this should be limited since an increased mortality risk (87–89).

2.6. Complications

Amongst the different JIA subtypes, sJIA has the highest mortality rate since the disease is associated with life-threatening complications including macrophage activation syndrome (MAS) and amyloidosis (31). MAS can be considered as an excessive inflammatory reaction associated with inappropriate activation and proliferation of macrophages and cytotoxic T cells causing an overwhelming cytokine storm and hemophagocytosis (59). MAS is diagnosed in around 10-15% of all sJIA patients although subclinical MAS was reported in up to 50% of the patients (90,91). The pathogenesis is further described in 2.6.1. Amyloidosis is characterised by deposition of amyloid A, an important acute-phase protein, eventually leading to organ dysfunction. In the past, amyloidosis was observed in up to 16% of the sJIA patients but currently manifests less frequently presumably due to a better disease control (32,92). Next to MAS and amyloidosis, chronic inflammation of sJIA may also result in osteoporosis,

and growth retardation. In a number of patients, refractory destructive joint disease (*e.g.* hip involvement) causes long-term functional limitations (93,94). More recently, it has become clear that patients may also develop lung complications (discussed in paragraph 2.6.2).

2.6.1. Macrophage activation syndrome

Clinically, patients with MAS present with persistent high fever, hepatosplenomegaly, and lymphadenopathy. In addition, patients typically also manifest liver and central nervous system involvement, which are associated with increased liver enzymes, coagulation problems and mental status changes. Severe coagulopathy may eventually result in multi-organ failure and death. Laboratory abnormalities include a cytopenia, with decreased number of red blood cells (RBCs), platelets, and leukocytes. MAS is also characterised by increased levels of CRP, lactate dehydrogenase, D-dimers and liver enzymes AST and ALT. Next, increased bilirubin levels, hypoalbuminemia, hyponatremia, and hypertriglyceridemia are found in patients. Furthermore, decreased levels of fibrinogen may result in a sudden fall in ESR in MAS patients. Highly increased ferritin levels derived from activated macrophages are an important marker of MAS. Finally, the presence of (CD163+) hemophagocytic macrophages in the bone marrow (BM) or tissue biopsies are a good diagnostic marker, however frequently absent at initial stages of MAS (59,60,63,95,96). The different clinical, laboratory, and diagnostic features are indicated in Table 1.4. Since the symptoms of MAS and sJIA are partially overlapping, diagnosis of MAS is challenging but ultimately important since its life-threatening features. Thanks to a collaborative effort of expert physicians, classification criteria for MAS complicating sJIA have been described (97). No specific biomarker has been described, however, elevated levels of soluble (s)CD25 and sCD163, ferritin, neopterin, TNF-α, soluble TNF receptors (sTNFR), interferon (IFN)-γ, IFN-γ-induced chemokines (including CXCL9, CXCL10, and CXCL11), IL-18 levels, and adenosine deaminase 2 (ADA2) activity are used to predict the development of MAS (59,98–103). Clinically and at the level of laboratory markers, MAS resembles hemophagocytic lymphohistiocytosis (HLH). HLH comprises both familial HLH (fHLH) and secondary HLH (sHLH). MAS is considered as a form of sHLH that occurs as a complication of autoimmune or autoinflammatory diseases. Next to sJIA, MAS has been described in SLE, Kawasaki disease, AOSD, RA, CAPS, and FMF (60,104). A detailed description of fHLH and sHLH falls out of the scope of this literature overview and has been provided elsewhere (105,106).

2.6.2. Lung disease

In recent years, an increased number of children with severe and life-threatening lung disease have been reported. The first report was made in 2013, when 25 patients with sJIA were described as having pulmonary arterial hypertension (PAH), intestinal lung disease (ILD), and pulmonary alveolar proteinosis (PAP) (107). PAP is a diverse group of lung diseases characterised by alveolar surfactant accumulation filling the alveolar space. PAP can be induced by a hereditary or autoimmune disruption of granulocyte-macrophage colony-stimulating factor (GM-CSF) signalling, an impaired macrophage number or function, or a congenital surfactant production disorder. In two recent papers, the lung pathology was extensively described. Radiographically, patients demonstrated ground-glass opacities, subpleural reticulation, interlobular septal thickening, and lymphadenopathy. Histopathological analysis confirmed the existence of PAP-like features with an important infiltration of lymphocytes. At the gene transcription level, high levels of IFN-γ and T cell activation-genes were measured. The authors propose that the altered external inflammatory milieu may promote an altered macrophage activation resulting in defective surfactant recycling (108,109). Interestingly, the pathological features differed from the early-described lung pathology in sJIA, characterised by a nonspecific interstitial pneumonitis with interstitial and nodular infiltrates, assuming that the new lung pathology can be considered as a new disease entity (110,111). Remarkably, the increased incidence coincides with the increased use of biologicals and so requires further attention (112).

2.7. Mouse models of sJIA

Three mouse models have been described to study sJIA pathogenesis. The first model was described by De Benedetti *et al*. and is based on a NSE/hIL-6 construct that carries the rat neurospecific enolase (NSE) promoter driving the expression of human IL-6 cDNA (113). Some of these transgenic lines presented with growth retardation and high serum levels of IL-6 due to a leaky expression of IL-6 in other organs than the central nervous system, where the NSE promoter is normally activated. Food intake was normal and IL-6 blockade could rescue the growth retardation. The model provides us with an understanding of the role of IL-6 in the growth retardation observed in sJIA. Decreased levels of insulin-like growth factor-I (IGF-I) were measured in the leaky transgenic mouse lines and may directly affect the growth hormone, in line with the low IGF-I levels measured in patients (113,114). Interestingly, when the IL-6 transgenic mice were injected with lipopolysaccharide (LPS), a TLR4 ligand, mice develop an excessive immune response resembling MAS. Mice presented with a decreased number of platelets and neutrophils, reduced haemoglobin levels, high sCD25 levels, hyperferritinemia, and a cytokine storm (115). Furthermore, it was shown that IFN-γ plays an important role in driving the pathogenesis (116). Also, in patents, it has been reported that MAS may occur in sJIA patients after an infectious trigger (117).

The second model introduced by Kawane *et al*. relies on the use of DNase II-deficient mice. These mice develop polyarthritis and an inflammatory cytokine storm in the joints. DNase II-deficient mice are characterised by an accumulation of undigested DNA, which subsequently activates the production of IFN-β, ultimately causing lethal embryonic anaemia. However, double DNase II and type I IFN receptor KO mice or DNase II inducible KO mice developed polyarthritis in adulthood, as seen in RA or sJIA. Joint inflammation was dependent on IL-1β, IL-6, and TNF-α since inhibition of one of these cytokines could inhibit the development of the arthritic symptoms (118–120). Concluding, the model shows that chronic activation of macrophages may induce a cytokine storm of the joints that subsequently results in arthritic symptoms.

The third model of sJIA was developed in our laboratory by Avau *et al*. The model is based on the subcutaneous injection of complete Freund's adjuvant (CFA) in BALB/C mice. When wild-type (WT) mice are injected, the animals develop a transient inflammation with splenomegaly, lymphadenopathy, thrombocytosis, neutrophilia, and increased expression of cytokines. When IFN-γ knockout (KO) mice are used, they develop full-blown sJIA-like features including weight loss, arthritis, anaemia, hemophagocytosis, and increased plasma levels of IL-6. The model was the first animal model of sJIA that included both the development of systemic inflammation and arthritis and can be used to further elucidate the pathogenesis of sJIA (extensively described in paragraph 3.3) (121). In this thesis, this model was used to understand the role of the innate immune system, focusing on the involvement of IL-1β, IL-22, G-CSF, neutrophils, and γδ T cells. Furthermore, we show that this model can also be used to study lung pathology as an important complication of sJIA.

3. Pathogenesis of sJIA

Although the aetiology of sJIA is still unknown (0), more insights into the disease mechanisms have been obtained during the last years. Patients with sJIA are characterised by an excessive activation of the innate immune system leading to an increased production of particular cytokines and S100 proteins (122). The involved immune cells and cytokines are described in paragraph 3.1 and paragraph 3.2 and summarised in Figure 1.3. The use of our mouse model allowed us to further unravel the disease mechanisms of sJIA, and the main findings are summarised in paragraph 3.3.

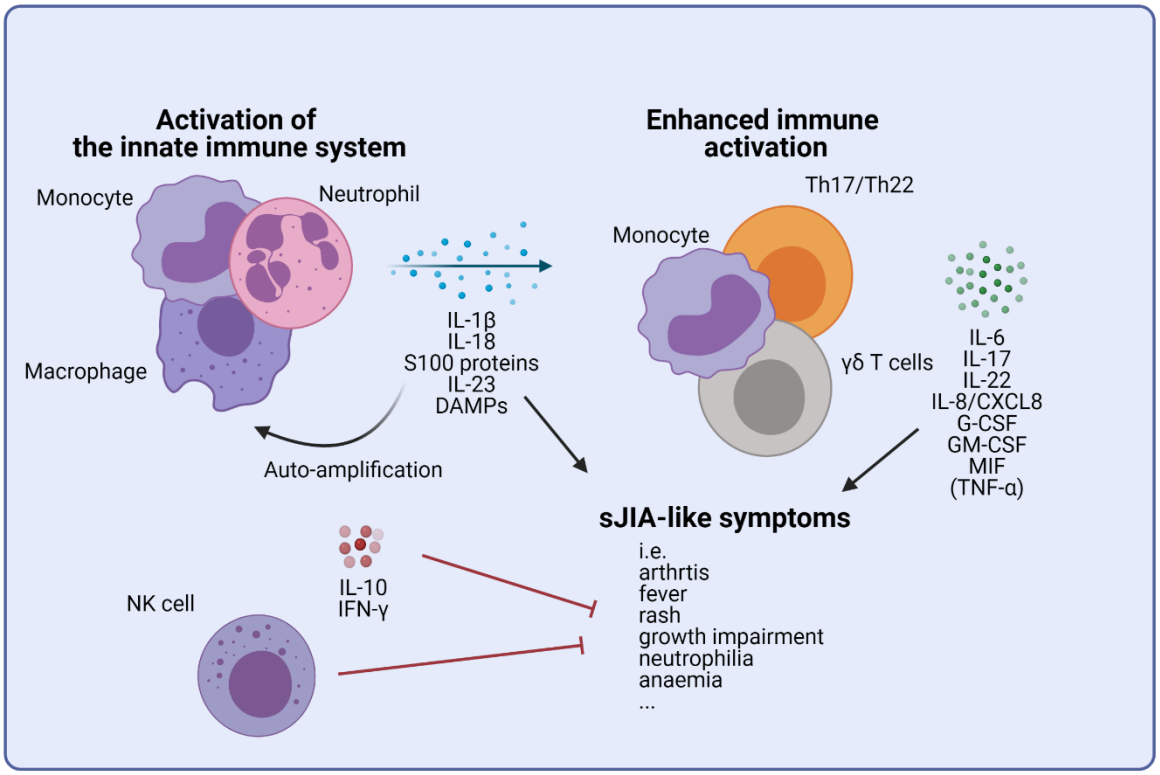

Figure 1.3: The pathogenesis of systemic juvenile idiopathic arthritis (sJIA)
A biphasic clinical model has been proposed in the pathophysiology of sJIA. Initially, a relatively unharmful agent triggers excessive activation of the innate immune system in genetically susceptible children. Innate immune activation is associated with the release of pro-inflammatory molecules and DAMPs, which further enhance both innate and adaptive immune responses. Triggering of the adaptive immune system ultimately contributes to the arthritic phenotype at a later stage of the disease. Different mediators explain the observed clinical sJIA-like symptoms and are extensively described in paragraph 3.2. Remark that both IL-10 and IFN-γ rather have a counterbalancing role in the sJIA-like features, as well as NK cells.

3.1. Activation of innate immune pathways

The constitutive activation of the innate immune system is one of the hallmarks of autoinflammatory disorders (see paragraph 1). In sJIA, innate immune activation was demonstrated at both gene expression and cellular levels. Gene expression profiling of the peripheral blood mononuclear cells (PBMCs) of sJIA patients showed increased expression of genes involved in the IL-1, IL-6, or TLR signalling or genes related to macrophage and neutrophil activation or differentiation (73,123–127). Interestingly, a relation between PRR activation and disease activity was uncovered since patients showed an increased expression of the TLR8 (recognising ssRNA), which was directly correlated with the IL-1β levels and the disease activity (128). Increased circulating numbers of monocytes and (immature) neutrophils are found in patients. Neutrophils are thought to play an important role in the activation of the inflammatory pathways via the release of inflammatory mediators (*i.e.* IL-1β or S100 proteins), especially at the early stages of disease (85,129–131). The function and formation of new neutrophils (granulopoiesis) seen in autoinflammatory disorders are further described in paragraph 1 and were investigated thoroughly in this dissertation. Transcriptional, cellular and molecular analyses showed that circulating monocytes of sJIA patients had an activated state, under-expressed the IL-1 inhibitor aryl hydrocarbon receptor (AHR), and had a mixed M1/M2-like phenotype that was directly correlated with the disease activity in patients (61,126,127,132,133). Furthermore, monocytes from sJIA patients showed an impaired response to IFN-γ. This might result in a dysregulated immune response to an infectious agent that subsequently contributes to the pathogenesis of sJIA (134,135). Natural killer (NK) cells are another important group of innate immune cells involved in the pathogenesis of sJIA. A normal number or decreased number of NK cells was reported in sJIA patients (132,136–139). Several studies showed a defective NK cell function with abnormalities in the IL-18-induced IFN-γ production, granzyme K expression, or perforin expression (137,139–144). This could, however, not always be confirmed (137,145). The role of NK cells in sJIA and MAS has recently been reviewed by Vandenhaute *et al* (146). Finally, a pathological role has been attributed to the γδ T cells. Although normal levels of γδ T cells have been reported in patients with sJIA, cells were characterised by an increased protein expression of IL-17, further driving the innate immune response (132,138,147).

3.2. Cytokines involved in the pathogenesis of sJIA

Table 1.5: cytokine profile in sJIA (168)

	Production by leukocytes				Plasma or serum levels	
	Ex vivo (a)		*In vitro (b)*			
IL-1β	=	(123–126)	↑, ↓, =	(45,61,136,148)	↑, ↓, =	(45,68,137,147–153)
IL-1RA	ND		=	(45,136)	↑↑	(45,68,136,151,153)
IL-6	↑	(124,125)	↑, =	(61,136,148,154)	↑↑	(45,68,133,147,149,150,152,153,155–160)
IL-8	ND		ND	(61,136,154,158,161)	↑, =	(149,150)
IL-10	↑	(124,125)	↑, ↓, =	(61,136,154,158,161)	↑, =	(45,149,152,157,158)
IL-17	ND		↑	(147,162)	↑, =	(45,147,152)
IL-22	ND		ND		=	(163)
IL-18	↑	(164)	=	(45)	↑↑	(45,68,133,139,147,152,155–158,164)
TNFα	ND		=	(61,136,148)	↑, =	(45,149,150,152,153,157,160)
IFN-γ	=	(126)	↑, ↓, =	(147,157,161,162)	↑, =	(45,147,152,157,160)
S100 proteins	ND		ND		↑↑	(67,165,166)
G-CSF	ND		ND		↑↑	(45)
GM-CSF	ND		ND		↑↑	(45)
MIF	ND		ND		↑	(152,167)

(a) mRNA level in PBMCs or whole blood cells; (b) protein level after stimulation of leukocytes with LPS, PMA-ionomycin, PHA or ant-CD3/CD28 *in vitro*; ↑, elevated; ↑↑strongly elevated; = undetectable or not elevated; ↓, lower than healthy controls; more than one symbol, conflicting results in literature. Abbreviations: G-CSF, granulocyte-colony stimulating factor; GM-CSF, granulocyte macrophage-colony stimulating factor; IFN, interferon; IL, interleukin; ND, not described; Ra, receptor antagonist; TNF, tumour necrosis factor; MIF, macrophage migration inhibitory factor

3.2.1. IL-1β

IL-1β is an important cytokine with many pro-inflammatory activities. Several inflammatory cell-types including activated monocytes, neutrophils or macrophages secrete the cytokine via a two-step mechanism. As described in paragraph 1, PAMPS or DAMPS induce the transcription of pro-IL-1β. Subsequent processing into active IL-1β by inflammasomes-requires the presence of a second stimulus (169). IL-1β can bind its IL-1R type I (IL-1RI) that, together with the IL-1 receptor accessory protein (IL-1RAcP), induces MyD88-dependent signalling. IL-1β promotes secretion of cytokines (*e.g.* IL-6) and chemokines (*e.g.* CXCL8/IL-8) and induces the expression of enzymes involved in the production of inflammatory mediators (*e.g.* prostaglandin E2 and nitric oxide (NO)). Furthermore, IL-1β contributes to the maturation of osteoclasts, bone erosion, and eventually arthritis (20). IL-1β together with IL-23 induces IL-17 and IL-22 production in γδ T cells and induces the differentiation of T helper (Th) 17 cells mediating autoimmune inflammation (170). Many of the symptoms observed in sJIA patients including fever, rash, thrombocytosis, neutrophilia, and arthritis, can be explained by the increased production of IL-1β (20). However, plasma IL-1β levels are hard to measure and multiple studies failed to show increased plasma or serum IL-1β levels (137,147,149–152). Neither was an increased IL-1β gene expression profile observed in patients (123–125). Increased IL-1β production was demonstrated upon stimulation of PBMCs with serum of sJIA. However, a reduced IL-1β secretion by monocytes of sJIA patients was reported, suggesting that other cellular sources, such as neutrophils might play an important role in the production of IL-1β (45,61,148). The successful treatment with IL-1-blocking agents such as anakinra, canakinumab, and rilonacept was the first proof of importance of IL-1 in sJIA (75,148,150,171,172). A localised action of IL-1β might explain the absence of elevated plasma IL-1β signature (173). Further experimental studies and single nucleotide polymorphisms (SNPs) in IL-1-related genes have clearly strengthened the concept of a pathological role for IL-1β in sJIA (45,73,124,174).

The pro-inflammatory activity of IL-1β is tightly regulated by its two-step activation mechanism, by the naturally occurring IL-1 receptor antagonist (IL-1Ra) and by the IL-1 receptor type 2 (IL-1R2) (175). IL-1Ra blocks the binding of IL-1 to its signalling receptor. IL-1R2, which is mainly expressed on neutrophils and their precursors, lacks the signalling Toll/IL-1R domain and regulates the pro-inflammatory activity of IL-1β by acting as a decoy receptor (176,177). The IL-1R2 has a higher affinity for IL-1 than for the IL-1Ra and thus further enhances the anti-inflammatory function of IL-1Ra (178). The surface expression of IL-1R2 is tightly regulated. Anti-inflammatory molecules such as glucocorticoids may augment the surface expression of IL-1R2 and may in part explain the beneficial effects of glucocorticoid treatment in sJIA (179,180). Pro-inflammatory molecules such as reactive oxygen species (ROS), LPS, TNF-α, leukotriene B4, and N-formyl-Met-Leu-Phe (fMLF) can initiate a rapid proteolytic cleavage of the membrane-bound IL-1R2 by different proteases (179,181). Increased levels of IL-1Ra are measured in the plasma of sJIA although to a lower degree than in polyarticular JIA, suggesting that the inhibition of IL-1β is insufficient to suppress the inflammation in sJIA (45,68,136,151,153,173)

3.2.2. IL-18

IL-18 is a pro-inflammatory cytokine constitutively expressed by monocytes, keratinocytes, and epithelial cells. Like IL-1β, the cytokine is produced in a premature form (pro-IL-18) that needs to be cleaved by caspase-1 upon activation of the inflammasome (182,183). High plasma levels of IL-18 were measured in active sJIA patients and have been proposed as a candidate biomarker. Also in patients with inactive disease, moderately increased levels of IL-18 were measured (101,137,152,156,184). IL-18 is considered as an important cytokine involved in the pathogenesis of sJIA and high levels of IL-18 are preludes to the development of MAS (101). IL-18 can bind the IL-18 receptor expressed on lymphocytes, DCs, and mesenchymal cells. The cytokine signals like IL-1β in a MyD88-dependent way

and exerts its pro-inflammatory action by increasing cell adhesion molecules, induction of chemokines, and increasing joint inflammation (183).
IL-18 is a potent inducer of IFN-γ and is often referred to as "IFN-γ-inducing factor". IFN-γ, in turn, regulates the activity of IL-18 via the induction of an IL-18 endogenous inhibitor, the IL-18 binding protein (IL-18BP), causing in this way an important negative feedback loop (182). In sJIA, the levels of IL-18BP were found only moderately increased, insufficient to counteract the high levels of IL-18 (139,164).

3.2.3. IFN-γ

IFN-γ is a cytokine with both pro- and anti-inflammatory properties. IFN-γ production by activated T cells and NK cells can be induced by IL-12 and IL-18 (185–187). The cytokine binds to its specific IFN-γ receptor that signals in a Janus kinase (JAK) signal transducer and activator of transcription (STAT)-dependent way. IFN-γ stimulates the immune response by activating macrophages and increasing its antigen presentation capacity via major histocompatibility class I and II (MHC-I and II) molecules. Furthermore, IFN-γ is an important cytokine in B cell maturation and Th1 polarisation. Next, it induces the expression of chemokines [*e.g.* CXCL9 (MIG) and CXCL10 (IP-10)], and cell adhesion molecules [*e.g.* intercellular adhesion molecule 1 (ICAM-1) and vascular cell adhesion protein 1 (VCAM-1)]. IFN-γ also has important anti-inflammatory properties including the inhibition of Th17 polarisation and the promotion of regulatory T (Treg) cell development. Indoleamine 2,3-dioxygenase (IDO) can be induced by IFN-γ and inhibits T cell proliferation by limiting the access of cells to free tryptophan. Next, the cytokine inhibits the expression of neutrophil-specific chemokines (*i.e.* CXCL8/IL-8) and the release of important neutrophilic factors (*i.e.* matrix metalloproteinases (MMPs) and serine proteases), by which IFN-γ can inhibit inflammation-induced tissue damage (187–190). In sJIA patients, the role of IFN-γ is still unclear. The levels of IFN-γ are moderately increased and are low in comparison to its upstream inducer IL-18 (45,137,152). An increased number of IFN-γ producing T cells were found in patients. However, a lower IFN-γ expression was measured in these cells. *In vitro* stimulation of PBMCs resulted in a decreased IFN-γ production in patients when compared to healthy individuals (147,162). Likewise, sJIA patients display an absent IFN-γ gene signature in their PBMCs (124–126), NK cells (157), and synovial tissues (135). NK cells of sJIA patients produced less IFN-γ due to a defective phosphorylation of the IL-18 receptor upon signalling (137,139). Since monocytes of sJIA patients were able to respond to IFN-γ, a limited *in vivo* exposure was hypothesised in patients (135).

3.2.4. IL-6

IL-6 can be produced by almost all stromal and immune cells in response to *e.g.* IL-1β, TNF-α, or TLR ligands. IL-6 binds the IL-6 receptor (IL-6R) which is expressed on a wide variety of cell types and subsequently signals in a JAK-dependent way (191,192). In sJIA, the gene expression of IL-6 (124,125) and IL-6 serum levels were strongly elevated in patients as compared to healthy controls (HCs) (45,68,133,147,149,150,152,153,155–160). Furthermore, increased levels were measured in the synovial fluid of sJIA patients (152). Interestingly, high IL-6 levels were associated with more active joint inflammation (101). Several sJIA symptoms can be explained by the elevated levels of IL-6 including fever, thrombocytosis, and growth impairment. IL-6 may be responsible for the microcytic anaemia, by blocking the iron supply to the developing erythroid cells and induces furthermore the production of acute-phase proteins (*e.g.* CRP) in hepatocytes (114,168,173,193). Together with transforming growth factor (TGF)-β, IL-6 preferentially promotes the differentiation of Th17 cells that play a crucial role in the induction of several autoimmune diseases (194). The crucial role of IL-6 in sJIA was confirmed by the successful use of the humanised anti-IL-6 receptor antibody tocilizumab (75,76,80).

3.2.5. IL-10

IL-10 is an important anti-inflammatory cytokine, limiting excessive inflammation and autoimmunity. Multiple cell types including T cells, monocytes, macrophages, eosinophils, neutrophils, DCs, NK cells, and B cells secrete IL-10. The cytokine has multiple functions including the inhibition of the secretion of pro-inflammatory cytokines (*e.g.* TNF-α, IL-1β, IL-6, IL-23, and G-CSF) or prostaglandins, stimulating the release of anti-inflammatory molecules (*e.g.* IL-1Ra), and inhibiting the production of chemokines (*e.g.* CXCL8/IL-8). Furthermore, IL-10 may inhibit antigen presentation or adhesion molecule expression and stimulates the differentiation of Tregs. IL-10 signals after binding the IL-10 receptor that signals in a JAK-STAT-dependent way (195–202). In sJIA, polymorphisms in the IL-10 gene or promoter were described (38,41,42). Although two haplotypes in the IL-10 promoter point towards a decreased IL-10 expression, increased expression of IL-10 has been reported in monocytes and PBMCs of patients (42,124,125,161). In addition, elevated plasma levels are described in patients with sJIA (133,149,152,157). In contrast, whole blood cell stimulation resulted in a decreased IL-10 production in patients when compared to HCs (136). Insufficient IL-10 production or signalling might be involved in the pathogenesis of sJIA. Indeed, a decreased IL-10-induced suppression of IL-6 production was reported in patients (124,154). Furthermore, we recently showed that patients with sJIA had a reduced ratio of IL-10 to the inflammatory mediators CRP, IL-6, and IL-18 (158).

3.2.6. IL-17

IL-17 is a pro-inflammatory cytokine that is mainly secreted by Th17 cells and γδ T cells. The secretion of IL-17 is often accompanied by the co-release of IL-22 (further discussed in 3.2.7). IL-17 expression can be induced by high levels of IL-1β, IL-23, TGF-β, and IL-6. Upon secretion, IL-17 can bind the IL-17 receptor expressed on multiple tissues that signal in an Act1-dependent way. The cytokine induces the production of many other cytokines [*e.g.* IL-6, G-CSF, GMCSF, IL-1β, and TNF-α], and chemokines [*e.g.* CXCL8/IL-8 and CCL2/monocyte chemotactic protein (MCP)-1]. Furthermore, IL-17 may induce the release of prostaglandins such as PGE2 and may drive chronic arthritis (203–205). The cytokine has been linked to many autoimmune and autoinflammatory diseases including RA, asthma, and multiple sclerosis (MS). In sJIA, plasma or serum levels were either normal or increased in patients when compared to HCs (45,147,152). With the use of intracellular staining it was shown that IL-17 is expressed in γδ T cells. Furthermore, an increased number of IL-17-producing T cells in patients was reported (147,206). The development of anaemia was linked to IL-17 since a positive correlation was seen between IL-17 and the erythropoiesis signature in sJIA patients (131). In addition to the development of anaemia, high IL-17 levels explain multiple disease symptoms including arthritis, fever, and neutrophilia (34,85). Nevertheless, no reports exist on the beneficial use of IL-17 blocking agents (such as secukinumab, ixekizumab or bimekizumab) in the treatment of sJIA.

3.2.7. IL-22

IL-22 is a cytokine with both pro- and anti-inflammatory properties (207,208). Activated T cells, γδ T cells, subsets of NK cells, NKT cells, and group 3 innate lymphoid cells (ILC3) are the predominant IL-22 producing cells (209–212). The cytokine is often co-released with IL-17 and was quickly associated with Th17 cells (213). However, in contrast to Th17-associated cytokines, its expression does not depend on the transcription factor (TF) retinoic acid receptor-related orphan nuclear receptor γ t (RORγt) but is rather regulated by the aryl hydrocarbon receptor or STAT3. The cytokine can be induced by IL-23, IL-1β or IL-6 (214,215). IL-22 signals via the heterodimeric IL-22R - that is mainly expressed on keratinocytes, hepatocytes and epithelial cells - in a JAK-STAT-dependent way (216–218). The soluble IL-22R homolog IL-22 binding protein (IL-22BP) tightly regulates the activity of IL-22 (219,220). Interestingly, a close regulation exists between IL-18 and IL-22. IL-18 can downregulate IL-22BP expression, thus enhancing IL-22 activity. *Vice versa*, IL-22 can upregulate the levels of IL-18 by

enhancing the expression of pro-IL-18 in human keratinocytes and murine intestinal epithelial cells (221–224).
IL-22 plays an important role in the epithelial barrier homeostasis and has important anti-apoptotic and proliferative properties. The cytokine can induce the production of *e.g.* β-defensin, lipocalin-2, RegIIIg, and mucins (225–228) and acts synergistically with IL-17 or TNFα in the expression of *e.g.* IL-6 or G-CSF by epithelial cells (213,225,226). Excessive production of the cytokine can have pathological consequences and has been linked to autoinflammatory and autoimmune disorders. In RA for example, IL-22 induces the proliferation of synovial fibroblasts and expression of receptor activator of NFκB ligand (RANKL). Furthermore, IL-22 may induce IL-1β production and promotes osteoclastogenesis that may result in bone erosion (229–232). In psoriasis, the cytokine is responsible for skin inflammation (233) but in the liver of the gastro-intestinal tract, IL-22 was found to be mainly protective (234–236). In sJIA, the role of IL-22 is currently unknown but some of the symptoms including arthritis or neutrophilia can be explained by the action of IL-22. One study showed no increased serum levels of IL-22, however only three sJIA patients were included in this study (163).

3.2.8. TNF-α

TNF-α is a pro-inflammatory cytokine secreted by *e.g.* monocytes, macrophages, and activated T cells. The cytokine can bind two receptors: the TNF receptor-1 (TNFR1) and the TNFR2. Downstream signalling plays an important role in various physiological and pathological processes including the activation of neutrophils (described below) and the development of arthritic symptoms (237,238). Gene polymorphisms correlating with high expression of TNF-α were described in patients. Nevertheless, plasma levels of TNF-α in patients with sJIA are usually low (149,152,157). Furthermore, no alterations in TNF-α were detected upon stimulation of whole blood or PBMCs from patients when compared to HCs (61,73,136). Anti-TNF-α treatment (etanercept) was very effective in RA and other non-systemic forms of JIA but is less effective in sJIA. This underlines the fact that TNF-α only plays a minor role in the pathogenesis of sJIA (75,86).

3.2.9. MIF

Migration inhibitory factor (MIF) is a proinflammatory molecule that can be secreted by many immune cells. The molecule can signal via the MIF receptor (CD74) and may induce pro-inflammatory cytokines (*e.g.* IL-1β, TNF-α, IL-8, and IL-18) or MMPs and contributes to the development of arthritis (167,239,240). In sJIA patients, increased plasma and serum levels of MIF are reported, of which the levels were correlated with the systemic features and the number of inflamed joints (152,167).

3.2.10. S100 proteins

The S100 proteins S100A8 (calgranulin or myeloid-related protein), S100A9 (calgranulin B), and S100A12 (calgranulin C) are alarmins with important pro-inflammatory and cellular homeostatic properties. Upon cellular stress, they are released from activated monocytes (S100A8/A9) or granulocytes (S100A8/A9 and S100A12), acting in this way as DAMPs (241). S100 proteins can bind TLR4 or the receptor for advanced glycation end products (RAGE), which signals via various pathways (147,242–246). The proteins can induce the secretion of cytokines by monocytes (*e.g.* IL-1β, IL-18, IL-6, and TNF-α) and up-regulate adhesion molecules on endothelial cells. Next, S100 proteins can enhance degranulation or phagocytosis in neutrophils or monocytes and may be involved in the development of arthritis (241,247–251). High concentrations of heterodimeric S100A8/A9 (also known as calprotectin) and S100A12 were measured in patients with sJIA. Comparing the different subtypes of JIA, the highest serum levels of S100A12 were measured in serum from patients with sJIA, confirming the systemic nature of the disease. S100 proteins were proposed as good candidate biomarkers since the high levels were closely associated with the disease activity and were absent in other forms of inflammatory arthritis as well as in other autoimmune, autoinflammatory or infectious

diseases except for FMF. In sJIA, a positive feedback loop with IL-1β was demonstrated (67,166,241,244,250,252,253). Interestingly, Kessel *et al.* showed that S100A12 together with IL-1β or IL-18 could induce IL-17 expression in γδ T cells to levels similar to those observed in sJIA patients (147).

3.3. Lessons from the CFA-induced sJIA mouse model

The sJIA mouse model, based on the subcutaneous injection of CFA at the tail base of BALB/C mice, is a well-recognised clinically relevant animal model to study sJIA pathology (Figure 1.4) (100,121,147,254) CFA is a relatively general trigger that contains killed mycobacteria with multiple PAMPs such as peptidoglycans and CpG. Upon binding to TLRs, CFA activates the innate immune system including monocytes/macrophages, DCs, γδ T cells, and NK cells (255). The local inflammation further results in the infiltration of neutrophils and eventually leads to the stimulation of an adaptive immune response with the activation of T helper cells, B cells, and cytotoxic cells in the secondary lymphoid organs. In the absence of IFN-γ, mice develop an important systemic inflammation with full-blown sJIA-like features whereas WT mice only show minor inflammation (121). Mounting a potent Th1 response is essential to remove the mycobacteria that, by nature, is difficult in BALB/C mice and deficient in the absence of IFN-γ. This results in ineffective CFA clearance in IFN-γ KO mice and a long-lasting immune activation (255). IFN-γ KO mice are furthermore also characterised by inborn defects in NK cells (256). NK cells may contribute to the termination of the immune response by the elimination of autologous activated cells. Interestingly, an important regulatory role of NK cells in the prevention of sJIA has recently been described in our mouse model (257). The NK cells of CFA-challenged IFN-γ KO mice display an aberrant balance of activating and inhibitory NK cell receptors, show a lower expression of cytotoxic proteins, and have a defective NK cell cytotoxicity. Depletion of NK cells or blockade of the NK cell activating receptor NKG2D in WT mice result in an aggravation of the symptoms as seen in the IFN-γ KO mice and are associated with increased numbers of activated inflammatory monocytes (257). We additionally demonstrated that susceptibility of IFN-γ KO mice to develop sJIA could also, at least partially, be explained by acquired defects in IL-10 production as IL-10 defects were found in B cells, Treg cells, and NK cells (158). Neutralisation of IL-10 in WT mice resulted clinically in a chronic immune-inflammatory disorder, haematologically reminiscent of sJIA (158). The persistent stimulation of CFA and the unterminated immune response eventually results in an important imbalance between the pro- and anti-inflammatory pathways. Indeed CFA-immunised IFN-γ KO mice were characterised by increased expression of pro-inflammatory cytokines (*e.g.* IL-1β, IL-6, and IL-18), increased plasma IL-6 levels, and inappropriate expansion of IL-17 producing γδ T cells and CD4+ T cells. Using the mouse model, we showed that IL-17 is an essential cytokine in the induction of the sJIA-like symptoms since neutralisation of IL-17 resulted in almost complete inhibition of the symptoms. In addition, neutralisation of the IL-12/IL-23p40 also results in an important amelioration of the sJIA-like symptoms. Although p40 is a subunit of both IL-12 and IL-23, the effect of the p40 antibody is most likely due to its neutralising capacity on IL-23 and, since no differences in IL-12 expression were seen after the CFA challenge (121). IL-23 can directly strengthen the Th17 cell expansion and pathogenicity (187,258) and furthermore stimulates γδ T cells to produce IL-17, amplifying the *in vivo* Th17 response (170).

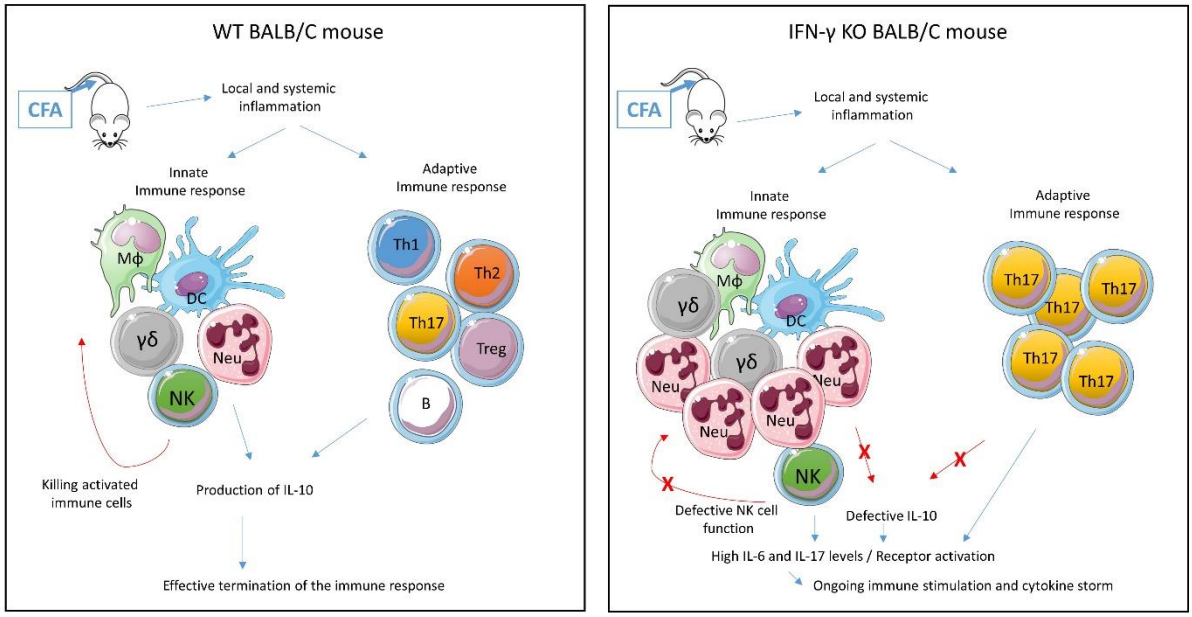

Figure 1.4: Current insights in the pathogenesis of the murine model of sJIA. Complete Freund's adjuvant (CFA) injection results in a local and systemic inflammatory reaction and activation of innate as well as adaptive immune cells. In WT mice, the immune response results in effective clearance of the CFA components. The inflammatory response is dampened via the production of IL-10 and the elimination of activated autologous immune cells by NK cells. In the IFN-γ KO mice, CFA-immunisation also leads to the activation of innate and adaptive immune cells. However, a defective NK cell activity and a defective production of IL-10 and IFN-γ results in an ongoing immune response. Immunised mice show increased cytokine levels of IL-6 and IL-17, which leads to the observed sJIA-like symptoms. Mϕ, macrophage; Th, T cell helper cell; Treg, regulatory T cell; NK, natural killer cell; Neu, neutrophil; γδ, γδ T cell; DC, dendritic cell; B, B cell.

CHAPTER 2

FACTORS DRIVING EMERGENCY GRANULOPOIESIS IN SYSTEMIC INFLAMMATION

Part of this chapter has been submitted for publication

Bert Malengier-Devlies[1], Mieke Metzemaekers[2], Paul Proost[2], Patrick Matthys[1]

[1]KU Leuven Department of Microbiology, Immunology and Transplantation, Rega Institute for Medical Research, Laboratory of Immunobiology, Leuven, Belgium
[2]KU Leuven Department of Microbiology, Immunology and Transplantation, Rega Institute for Medical Research, Laboratory of Molecular Immunology, Leuven, Belgium

CHAPTER 2: FACTORS DRIVING EMERGENCY GRANULOPOIESIS IN SYSTEMIC INFLAMMATION

Abstract

Neutrophils are key cell types of the innate immune system endowed with both oxidative and non-oxidative defense mechanisms. More recently, a more complex role for neutrophils was described with sophisticated functions including neutrophil extracellular trap formation, interactions with innate and adaptive immune cells and cytokine production. Neutrophils are short-lived in homeostatic conditions and are continuously released from the bone marrow. Fully mature neutrophils develop from undifferentiated hematopoietic stem cells via different immature subtypes and are fully equipped to ensure a fast and an appropriate immune response. During excessive inflammation, there is a high need for additional neutrophils. The hematopoietic system rapidly adapts to this increased demand by switching from a steady state to an emergency granulopoiesis. During this emergency granulopoiesis, the *de novo* production of neutrophils is augmented, additionally, neutrophils are formed at extramedullary sites, and mature neutrophils are rapidly released from the marginated pools. Although neutrophils can protect hosts against microorganisms, excessive activation causes tissue damage in neutrophil-rich diseases. Therefore, tight regulation of neutrophil homeostasis is warranted. In this review, we discuss the kinetics of neutrophil ontogenesis in homeostatic and emergency situations and describe different molecular mediators involved in this regulation. Furthermore, we substantiate this chapter with the example of an autoinflammatory disease, *i.e.* systemic juvenile idiopathic arthritis.

1. Neutrophils

1.1. Introduction

Neutrophils are the most abundant leukocytes in the human blood and protect our body from harmful agonists (3,259). The importance of these cells is demonstrated in patients with neutropenia, leukocyte adhesion deficiency or chronic granulomatous disease which are prone to (fatal) microbial infections (260). For a long time, neutrophils were considered as simple, short-lived polymorphonuclear innate phagocytes with rapid antibacterial and antifungal actions. However, discoveries in recent years revealed the complexity of neutrophil functions. The different neutrophilic properties are described in paragraph 1.3. Neutrophils are an important source of pro-inflammatory mediators such as proteases, cytokines, chemokines, and alarmins including S100A8/A9 and S100A12, amplifying the innate immune response. Neutrophils may interact with other leukocytes and have both disease-promoting and disease-limiting properties, indicative of the existence of different neutrophil subsets with unique immunomodulatory functions (261–264). For many years, neutrophils were seen as a relatively homogenous cell population. However, the existence of neutrophil subsets with transcriptional, functional and phenotypic heterogeneity has recently emerged in both humans and mice (265). The neutrophil heterogeneity is further described in paragraph 1.4. The production and storage of new neutrophils are tightly regulated (described in paragraph 1.2). In normal conditions, neutrophils are short-lived cells with variable lifetimes across multiple tissues and are produced at a rate of 1-2 x 10^{11} cells/day in humans and 1 x 10^{7} cells/day in mice (266,267). However, during an excessive inflammatory immune response, when there is a high demand for new neutrophils, the life span of neutrophils may increase up to 7 days and the production of new neutrophils may increase tenfold during infection (268,269). During such excessive neutrophil production - often described as ‘emergency granulopoiesis’ - the production may additionally take place outside the bone marrow (BM) in a process called extramedullary myelopoiesis (270,271). Both autoimmune and autoinflammatory diseases are characterised by important emergency granulopoiesis and an important role of neutrophils has been described in these diseases. Emergency granulopoiesis and its main drivers in autoinflammatory diseases are extensively described in paragraph 1.5. In the final paragraph (paragraph 1.7), we describe the pathophysiological role of neutrophils in sJIA.

1.2. Neutrophil homeostasis

Neutrophil homeostasis is tightly regulated since an excessive neutrophil accumulation or activation may be detrimental (259,272–277) while defects in development, migration, or function can result in severe immunological problems (275,278–282). Regulation of neutrophil homeostasis involves the formation of new neutrophils in the BM (granulopoiesis), the release of new neutrophils into the circulation, the storage of neutrophils outside the BM (marginated pool), the infiltration of neutrophils into the site of inflammation (tissue pool) and eventually the clearance of (aged) neutrophils (262,268). The different components of regulation are further discussed in the following paragraphs and summarised in Figure 2.1.

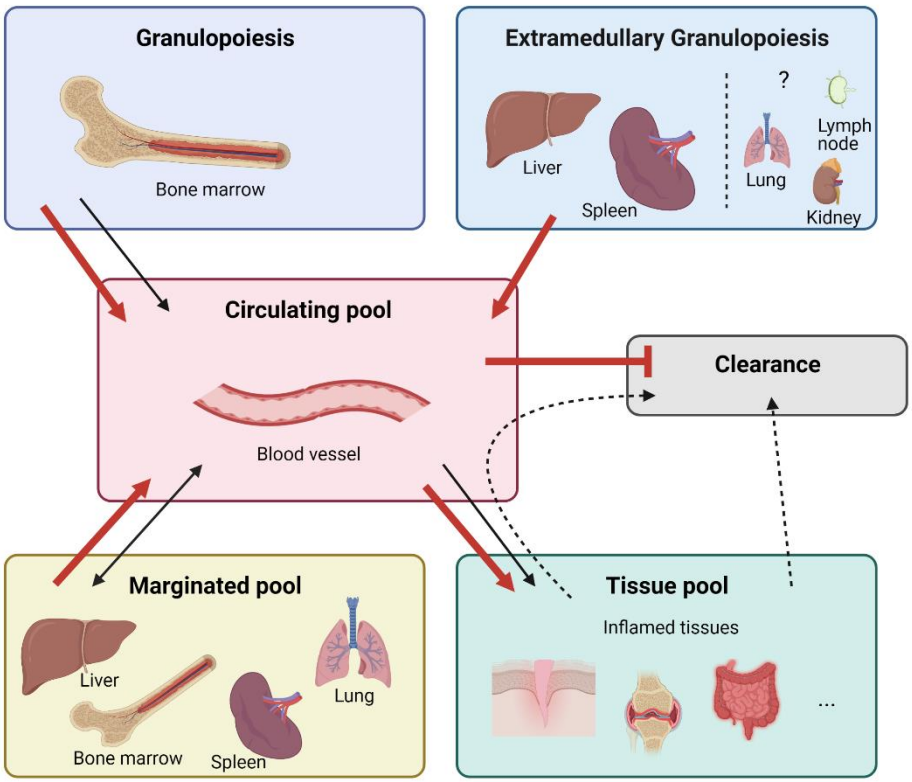

Figure 2.1: Neutrophil homeostasis is tightly regulated
In homeostatic conditions (black arrows) neutrophils mature in the bone marrow from undifferentiated hematopoietic stem cells (HSCs), replenishing the mitotic stem cell pool that gives rise to mature neutrophils via different immature stages of myeloblast, promyelocyte, myelocyte, metamyelocyte, immature band cells, and mature neutrophils. These neutrophils are stored in the bone marrow upon release before entering the blood circulation. Different organs store a pool of neutrophils, referred to as marginated pool, and are forming a reservoir of mature neutrophils. In response to inflammation, neutrophils can exit the bloodstream and enter the tissue pool. Senescent neutrophils are cleared in the bone marrow by stromal macrophages or by tissue-resident macrophages in the periphery. During excessive inflammation (red arrows), neutrophils are massively attracted to the site of inflammation and their clearance is decreased by increasing their lifespan. Demanding the high need of neutrophils, increased numbers of neutrophils are released from the bone marrow. Furthermore, neutrophils are formed and released from extramedullary sites. Cytokine stimulation, including epinephrine, can additionally quickly release neutrophils from the marginated pool.

1.2.1. Granulopoiesis

The BM is the main source of new neutrophils. Neutrophils that mature in the BM can be subdivided into three pools *i.e.* the stem cell pool, the mitotic pool and the post-mitotic pool. The hematopoietic stem cells (HSC) of the stem cell pool give rise to the granulocyte-macrophage progenitor (GMP) cells that gradually mature under influence of different cytokines or growth factors (discussed in paragraph 1.5.2), into mature neutrophils. Complete neutrophil maturation takes more than 10 days (283,284).

HSC locate in BM niches provided mainly by perivascular cells that express a membrane-bound form of stem cell factor and the chemokine CXCL12 (also known as stromal cell-derived factor 1 or SDF-1), which are the ligands for the stem cell antigen CD117 (C-kit) and CXC chemokine receptor (CXCR) 4, respectively (285,286). Two models are proposed that describe the differentiation of these HSC. In the first classical or hierarchical model, HSC give rise to myeloid-committed common myeloid progenitors (CMP) that eventually gives rise to GMPs. During the differentiation, the capacity to differentiate into any other cell type is lost (287–289). In the alternative model, cells rather have a mixed-lineage potential with transcriptional and functional heterogeneity (287). The absence of oligopotent intermediates with mixed cell markers, having a limited differentiation potential, is favouring this second model described (290–292). Here, the CMP compartment contains predestined subpopulations which are transcriptionally primed towards either erythrocytes, megakaryocytes, DCs, monocytes, neutrophils, eosinophils, or basophils (292–294).

The mitotic pool includes promyelocytes and myelocytes. Finally, the most differentiated non-dividing cells include both the immature neutrophils and the mature neutrophils. Microscopically, the different neutrophil precursors can be distinguished. Promyelocytes are defined as large cells with an oval nucleus and a dark cytoplasm. Myelocytes have a less dense cytoplasm, and a rounder nucleus. Metamyelocytes, band cells and mature neutrophils are smaller cells and have a clear cytoplasm. In humans, metamyelocytes and band cells have a kidney-like nucleus whereas in mice these cells have doughnut-like band-shaped nucleus. Finally, mature neutrophils are characterised by their typical segmented nucleus (295–300). The different neutrophil precursors are shown in Figure 2.2.

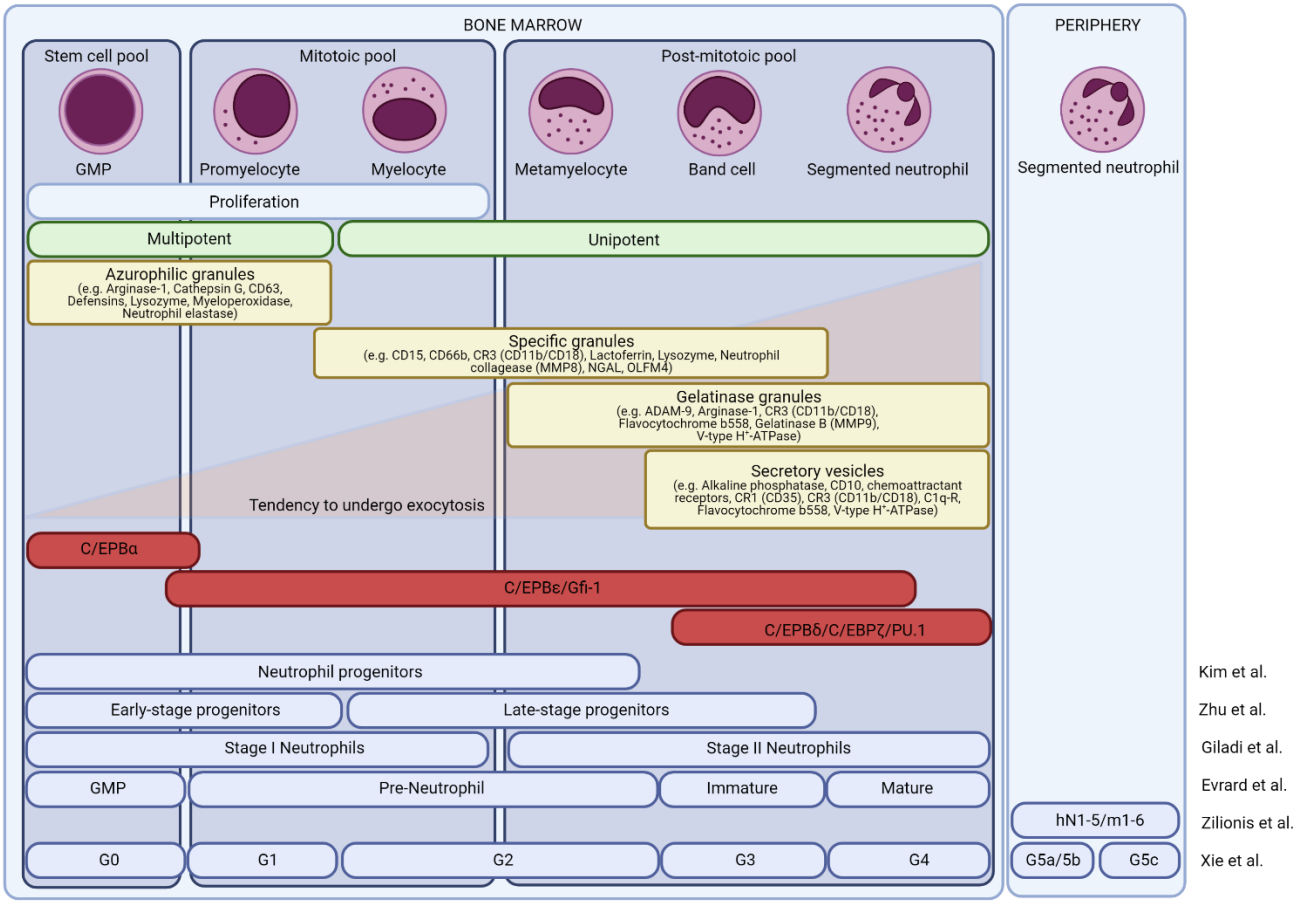

Figure 2.2: Neutrophil development in the bone marrow (BM)
Overview of the different neutrophil subsets in the BM. Morphologically, neutrophils are divided into granulocyte-monocyte progenitor cells (GMPs), promyelocytes, myelocytes, metamyelocytes, band neutrophils, and mature neutrophils. Based on their proliferative and differentiation capacity, the cells are divided into a stem cell pool, a mitotic pool, and a post-mitotic pool. Neutrophil maturation is associated with changes in transcription factors and granule protein expression. At least four types of granules are formed in the neutrophils, each obtaining a unique set of effector molecules. The different granules are released hierarchically, opposite to their formation. Recently, single-cell sequencing or CyTOF reassessed the different neutrophil subsets and different groups have proposed a new neutrophil nomenclature. Figure adapted from Xie et al. (301).

The differentiation of neutrophils is associated with changes in TFs and granule production. The main TF driving granulopoiesis includes CCAAT/enhancer-binding protein (C/EBP) α and PU.1 (Figure 2.3). High expression of C/EBPα or PU.1 is associated with granulocyte or monocyte commitment, respectively. Runx1 and lymphoid enhancer-binding factor 1 (Lef1) are regulating the C/EBPα expression and defects result in a neutrophil maturational block (299,302,303). C/EBPα itself, negatively regulates the expression of cMyc. Consistently, C/EBPα mutant mice have an early block in granulocyte differentiation (304–306). Another major TF in involved in neutrophil development includes Krüppel-like factor 5 (KLF5), which is mainly active at early stages and controls neutrophil production at the expanse of eosinophils (307). In addition, growth factor independent-1 (Gfi-1) also drives the initial neutrophil development and represses the monocyte-promoting TFs PU.1 and Irf8 (292,308–314). Mutations in Gfi-1 block neutrophil maturation at the promyelocyte stage (299,303,313). The expression of Gfi-1 and C/EBPα decreases from the myeloblast stage and is associated with an increased expression of C/EBPε that peaks at the myelocyte stage. C/EBPε regulates the transition from promyelocytes to myelocytes and represses genes involved in cell cycling. The deletion of C/EBPε leads to neutrophil progenitor arrest and neutropenia (292,315–318). Further myelocyte maturation is driven by an upregulation of C/EBPβ, C/EBPγ, C/EBPδ, and C/EBPξ.

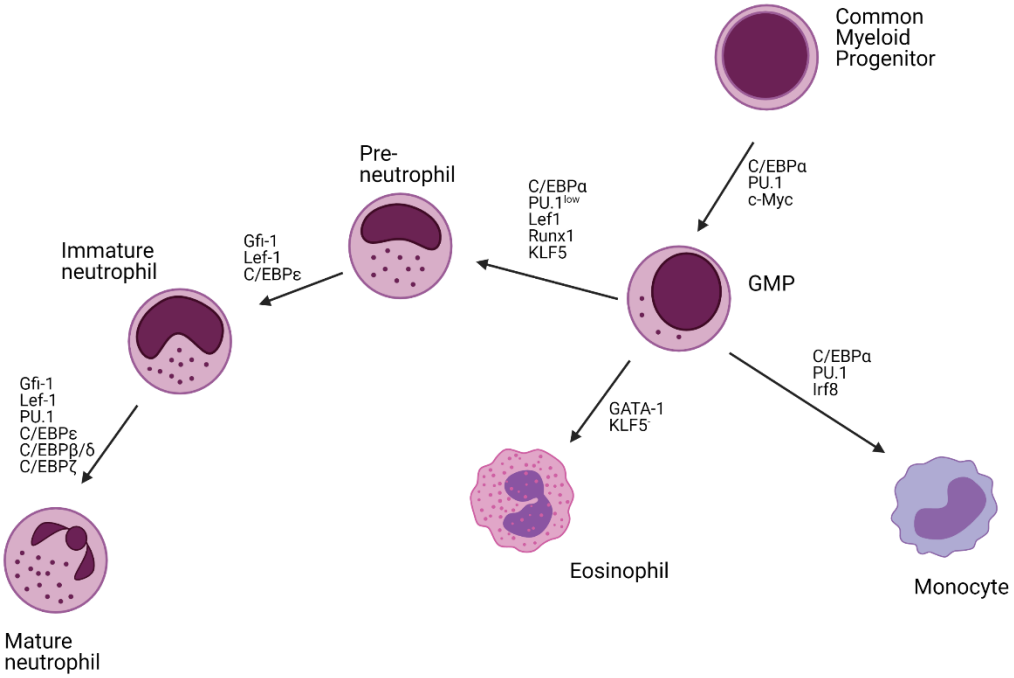

Figure 2.3: Transcription factors regulating neutrophil differentiation.
Neutrophils mature from hematopoietic stem cells (HSCs) in the bone marrow (BM). These HSCs are self-reviewal and can differentiate into all immune cells. The common myeloid progenitor (CMP) cells give rise to the myeloid lineage including neutrophils, monocytes, and eosinophils. C/EBPα is the main transcription factor driving myeloid differentiation. Together with PU.1, and c-Myc, C/EBPα drives granulocyte-monocyte progenitor cell (GMP) differentiation. High levels of C/EBPα, PU.1 and Irf8 further drive monocyte development, high levels of GATA-1 eosinophil development, whereas C/EBPα, Lef1, Runx1, KLF5 together with low expression of PU.1 enhance neutrophils development. Neutrophil maturation is further driven by Gfi-1, Lef-1, C/EBP transcription factors (C/EBPε, C/EBPβ, C/EBPδ, C/EBPζ), and PU.1. C/EBP, CCAAT/enhancer-binding protein; Irf8, Interferon regulatory factor 8; Lef1, Lymphoid enhancer-binding factor 1; Runx1, Runt-related transcription factor 1; KLF5, Krüppel Like Factor 5; GFI1, Growth Factor Independent 1 Transcriptional Repressor.

The different maturational stages are associated with a sequential formation of primary (azurophilic), secondary (specific), tertiary (gelatinase), and secretory granules (300). Primary granules are mainly formed during the myeloblast stage (GMP, promyelocyte) and the main granule proteins include myeloperoxidase (MPO), α-defensins, bactericidal/permeability-increasing protein (BPI), and distinct serine proteinases such as elastase or cathepsin G. The main secondary granule proteins are lactoferrin (LTF) and are mainly formed during the myelocytes stage (myelocyte, metamyelocyte). Tertiary granules are rich in gelatinases and are formed during the band cell stage (banded immature neutrophils). Secretory vesicles are mainly formed at the final stages of neutrophil maturation and mainly include early activation surface proteins that facilitate neutrophil migration. All granules are stored in the mature neutrophils until activation. Upon neutrophil activation these granules are sequentially released according to the "formed-first-released-last model" (319).

Using new techniques including single-cell RNA sequencing (scRNAseq) and mass cytometry (CyTOF), the granulopoiesis in the BM can be re-assessed and the old nomenclature can be replaced by new neutrophil subsets that better represent the true heterogeneity. Evrard *et al*. performed CyTOF analysis on murine BM cells and revealed the existence of three neutrophils subsets. The neutrophils subsets include a proliferative neutrophils progenitor group (preNeu) and a non-proliferating immature and mature group (316). PreNeu express CD117 (c-kit) but did not express markers for other leukocyte lineages. Phenotypically, preNeu were defined as $Lin^{-}c\text{-}kit^{int}CD11b^{+}CXCR4^{+}$ and expressed primary and secondary granules. The human counterparts of the preNeu were defined as $Lin^{-}CD34^{-}CD101^{-}CD15^{+}CD66b^{+}$ cells. Immature and mature neutrophils can be discriminated based on the differential expression of CXCR2 and CD101. Immature neutrophils are $Lin^{-}c\text{-}kit^{-}CD11b^{+}CXCR4^{-}CXCR2^{-}CD101^{-}$ (or $Lin^{-}CD11b^{+}CD115^{-}Ly6G^{low}Ly6B^{int}$) and are mainly expressing secondary granule proteins. Mature neutrophils are $CD11b^{+}CD115^{-}Ly6G^{+}$ $CXCR2^{+}CD101^{+}$ and are expressing gelatinase granule proteins (316). In humans, immature and mature neutrophils are defined as $Lin^{-}CD34^{-}CD101^{+}CD15^{+}CD66b^{+}CD10^{-}CD16^{-}$ and $CD101^{+}CD15^{+}CD66b^{+}CD10^{+}CD16^{+}$, respectively (320,321). Kim *et al*. confirmed the existence of a murine neutrophil precursor and defined these cells as $lin^{-}c\text{-}kit^{+}CD11b^{+}Ly6G^{low}Ly6B^{int}CD115^{-}GFI1^{+}$ cells (322). Later Zhu *et al*. showed that two populations of neutrophil precursor cells can be distinguished based on the expression of CD34 in. Early-stage and late-stage precursor cells were defined as $c\text{-}kit^{+}Gfi1^{low}CEBPA^{hi}Ly6G^{low}$ and c-kit+$Gfi1^{high}CEBPA^{low}$Ly6G+ cells respectively (323). The overlay between the different neutrophil subsets are visualised in Figure 2.4 (320).

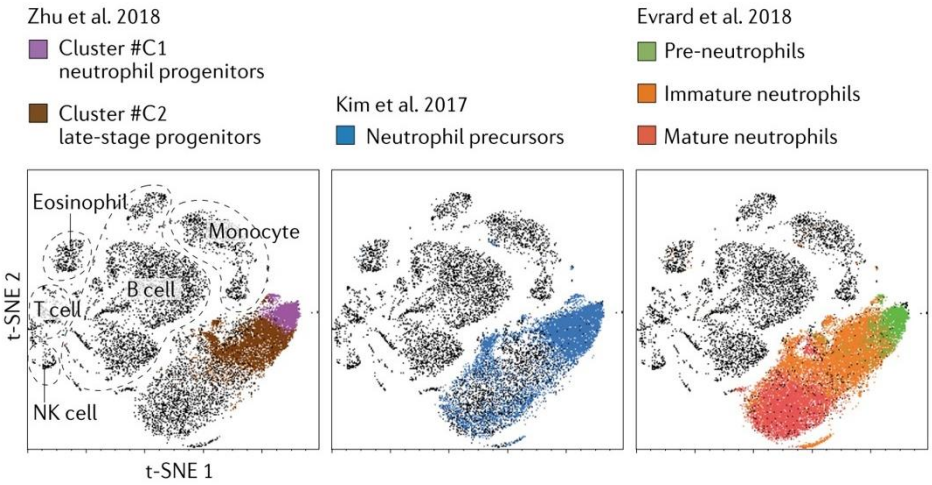

Figure 2.4: T-distributed stochastic neighbour embedding (t-SNE) plot representing the overlap between the different proposed neutrophils subsets in the murine bone marrow (BM). Evrard et al. demonstrated the presence of pre-neutrophils (green), immature neutrophils (orange), and mature neutrophils (red) (316). Blue cells represent the neutrophils precursors proposed by Kim et al (322). These neutrophil precursor cells were further subdivided by Zhu et al in #C1 (pink) and #C2 (brown) neutrophil progenitor cells (323). Figure from Ng et al. and reproduced with permission (320).

Just recently, Xie *et al*. performed single-cell sequencing on differentiating and mature mouse neutrophils and revealed eight neutrophil populations with a distinct molecular signature of which three were peripheral mature neutrophils and five were BM neutrophils. In the BM, three dividing subsets (including the GMP population) and two post-mitotic maturing subsets were described (324). Also, in healthy and tumorous lungs, different neutrophil subsets were investigated by single-cell sequencing. Five and six different neutrophil subsets were found in mice and humans respectively, including three conserved subsets. One of these subsets expressed canonical markers such as MMPs, or S100 proteins, one was tumour-specific, and one showed high expression of type I interferon-genes (325).

1.2.2. Circulating pool

Mature neutrophils can be stored in the BM and are released into the circulation upon stimulation (Figure 2.5) (259,262). The balance of the chemokine receptors CXCR4 and CXCR2 tightly regulates the release of neutrophils. Upregulation or downregulation of CXCR2 and CXCR4, respectively, is associated with release (326). CXCR4 is the main receptor for CXCL12, expressed by the stromal cells of the BM that retains the neutrophils in the bone marrow (268). Enhanced activity of CXCR4 delays the release of mature neutrophils from the bone marrow and is described in WHIM syndrome patients (327). Also the adhesion molecule VCAM-1, expressed by the BM epithelial cells is retaining the neutrophils in the BM by its interaction with the integrin very late antigen (VLA) 4 expressed on neutrophils (268). In contrast, human CXCR2 can bind the seven ligands CXCL1, CXCL2, CXCL3, CXCL5, CXCL6, CXCL7 and CXCL8 stimulating the release of neutrophils from the BM. G-CSF (further described in paragraph 1.5.2.1) lowers the threshold of release by decreasing CXCL12 production (328) and CXCR4 expression (329) and by increasing the amounts of mobilising signals (*e.g.* CXCL1) (330). AMD3100 is a CXCR4 antagonist that is used in the clinic for mobilising myeloid stem cells into the blood stream (331). The release of neutrophils outside the BM is assisted by the release of granule proteins including MMP-9, paving the transendothelial/transcellular way through the sinusoidal endothelium (332,333). Interestingly, the transit from the BM to the peripheral blood is associated with large transcriptomic and epigenetic differences (334).

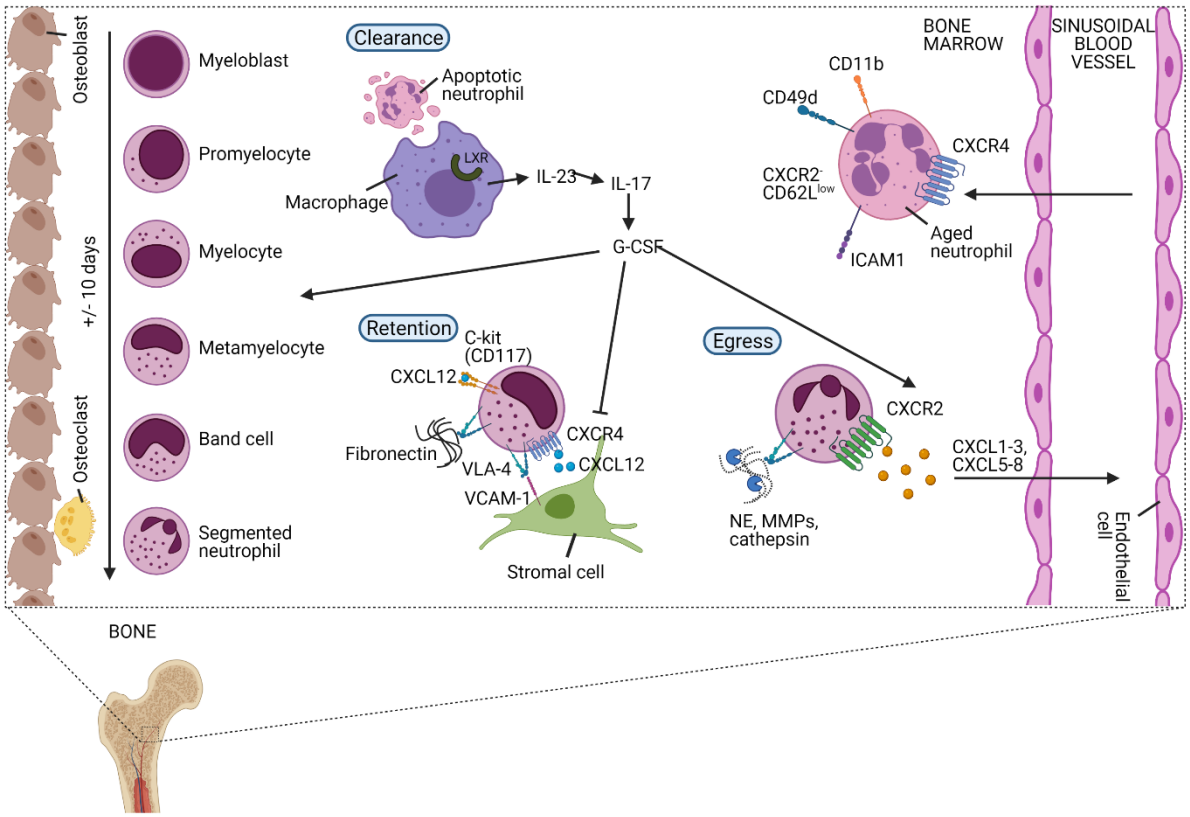

Figure 2.5: The release of neutrophils from the bone marrow (BM) is tightly regulated in homeostatic conditions

In the BM, neutrophils differentiate from undifferentiated hematopoietic stem cells (HSCs) into mature neutrophils via different immature stages of myeloblast, promyelocyte, myelocyte, metamyelocyte, immature band cells, and mature segmented neutrophils. Neutrophils are retained in the BM via the homing CXCR4 receptor or the stem cell antigen CD117 (C-kit) which both bind CXCL12, released by stromal cells. Additionally, the integrin very late antigen 4 (VLA-4) expressed on neutrophils are retaining neutrophils in the BM by binding the adhesion molecule vascular cell adhesion protein 1 (VCAM-1) or fibronectin. Granulocyte colony-stimulating factor (G-CSF) is an important growth factor that regulates the proliferation, differentiation, and egress of neutrophils in the BM. It aborts the CXCR4/CXCL12 interactions and releases neutrophilic chemoattractants including CXCL1-3 and CXCL5-8 that bind CXCR2. During the release of neutrophils from the BM, granule proteins are released degrading the fibronectin and mediating trans-endothelial transport. Aged neutrophils are characterised by the expression of diverse receptors including upregulated CXCR4, ICAM1, CD11b, CD49d, and low expression of CXCR2 and CD62L. Aged neutrophils migrate back to the BM where they are engulfed by macrophages. Upregulation of the liver X receptor (LXR) family induces the expression of interleukin-23 (IL-23) that may enhance the release of new neutrophils, balancing the homeostasis of neutrophils, via the IL-23/IL-17/G-CSF-axis.

Generally, it was believed that neutrophils exit the BM into the peripheral blood upon maturation. Unexpectedly, recent single-cell RNA sequencing exposed an additional complexity and showed that neutrophils can enter the peripheral blood without going through the most mature stage (324). This is in line with the observations made during emergency granulopoiesis (further described in paragraph 1.5.1).

1.2.3. Marginated pool

Margination refers to the prolonged transit of neutrophils through organs, resulting in discrete intravascular (marginated) pools. Marginated pools can be found within the spleen, liver and BM. Lung margination may be specific only for certain species such as primate, mice, and dogs (326,335–338). During infection or inflammation, cytokine stimulation, including epinephrine (adrenaline), can quickly release the marginated neutrophils into the circulation (339–341).

1.2.4. Tissue pool

Neutrophils are the first immune cells that enter the site of inflammation and can clear pathogens by a wide range of antimicrobial actions (described in paragraph 1.3.1). Neutrophils need to enter the inflamed tissue via extravasation, a process that is coordinated by selectins and integrin ligand binding Figure 2.6. Furthermore, multiple steps of the neutrophil migration cascade depend on chemoattractants and their receptors. The different chemoattractants belong to either the host chemotactic lipids [*e.g.* leukotriene B4 (LTB4)], the chemokines [CXCL1 to CXCL3 and CXCL5 to CXCL8 in humans or KC, macrophage inflammatory protein (MIP)2 and granulocyte chemotactic protein-2 (GCP-2) in mice], complement anaphylatoxins (C3a and C5a), or bacterial formyl peptides (*e.g.* fMLF), and were all recently described by Metzemaekers *et al*. (342–344).

In brief, neutrophil extravasation encompasses four different steps. First, pro-inflammatory cytokines (including TNF-α, IL-1β, and IL-17) or bacterial stimulants (including LPS or fMLF) induce the expression of adhesion molecules (*i.e.* P-selectins and E-selectins) on the endothelial cells. These adhesion molecules can bind glycoproteins *e.g.* P-selectin glycoprotein ligand-1 (PSGL-1) expressed on the neutrophil surface, mediating rolling of the neutrophils along the endothelium. Next, the glycosaminoglycan-captured chemokines signalling, and the L-selectin (CD62L) binding to *e.g.* GlyCAM-1 on endothelial cells can activate lymphoid function-associated antigen 1 (LFA-1) on neutrophils. This integrin binds ICAM1 and ICAM-2 on endothelial cells and mediates a firm adhesion and arrest. Afterward, neutrophils crawl along the endothelium mainly via the paracellular route. Assisted by the release of granule proteins, neutrophils reach the site of inflammation via the interaction of ICAM-1 and ICAM-2 with Mac-1 and LFA-1. Neutrophils may also follow a transcellular path directly through the endothelial cell body without the loss of the integrity of the plasma membrane of either cell. Finally, neutrophils further migrate towards increasing concentrations of chemokines (338,345–351).

At the site of inflammation, neutrophils can be primed by cytokines (IL-1β, IL-6 or TNF-α), PAMPs (*e.g.* LPS), DAMPs (*e.g.* ATP), or complement-opsonised particles via their vast repertoire of PRRs (352). Morphologically, primed neutrophils are characterised by a hyper-mature phenotype with up to five nuclear lobes and are phenotypically defined by increased CD16 or CD11b/CD18 expression levels and CD62L shedding. In comparison with quiescent cells, primed neutrophils display a more aggressive action upon subsequent activation with a second inflammatory stimulus, illustrated by enhanced ROS production, degranulation, phagocytosis, and an increased tendency to release neutrophil extracellular traps (NETs) (353).

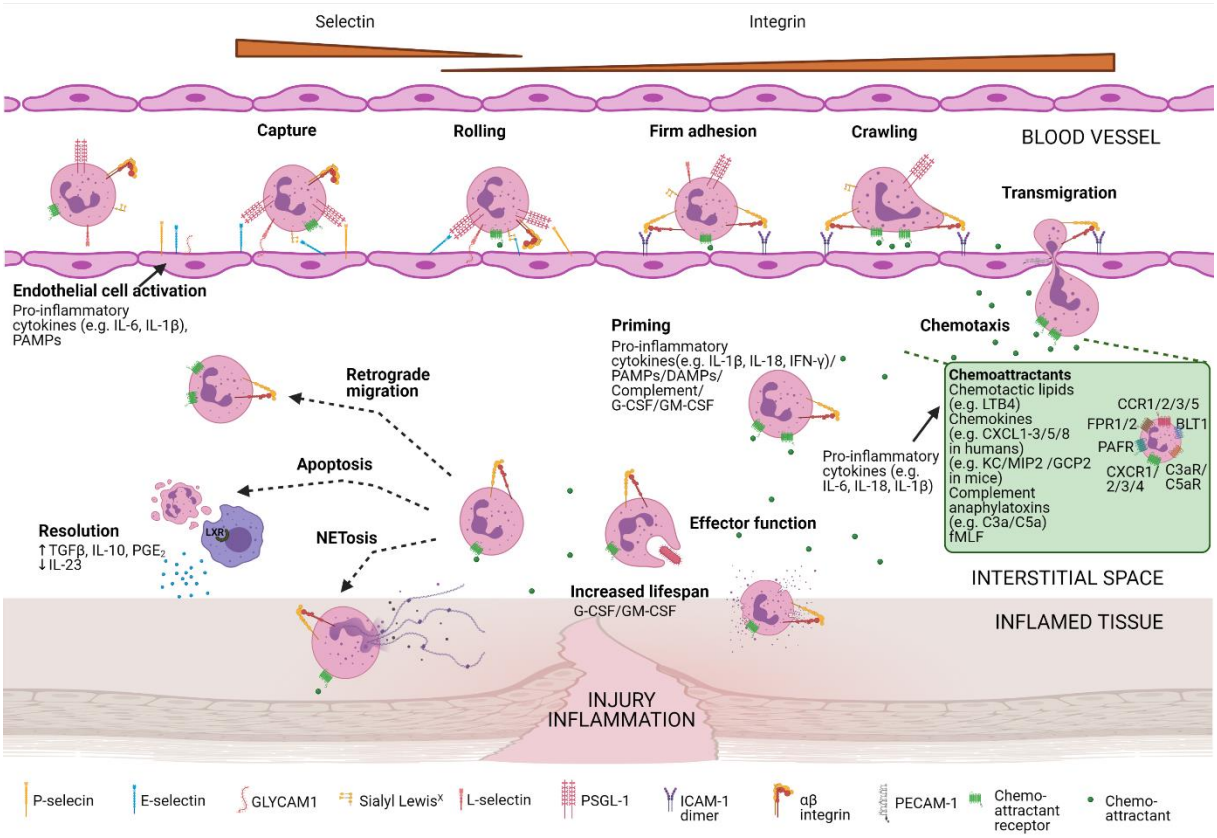

Figure 2.6: Neutrophil recruitment towards the site of inflammation
Neutrophil mobilisation and internalisation involve different steps including the capture of the cells, rolling, firm adhesion, crawling, and transmigration. Diverse neutrophil surface receptors are involved in this process. Pro-inflammatory cytokines or pathogen-associated molecular patterns (PAMPS) activate endothelial cells, allowing them to express adhesion molecules (e.g. P-selectins and E-selectins). These adhesion molecules bind mucins expressed on the neutrophil surface capturing and slowing the neutrophil. Slow rolling of the cells allows chemoattractants to bind their respective chemoattractant receptors. Subsequent signalling results in integrin activation and eventually firm adhesion. Next, neutrophils are crawling along with the endothelial cells and transmigrate at cell-cell junctions (paracellular migration) or by endothelial cell bodies (transcellular migration). Once migrated, neutrophils are further attracted towards the centre of inflammation by a gradient of chemoattractants. An overview of the main chemoattractants is shown in the green box. Chemoattractants are mainly released by pro-inflammatory cytokines. At the focus of inflammation, neutrophils are primed by proinflammatory cytokines, PAMPs, DAMPs, complement molecules, and/or growth factors enhancing their effector function and additionally increases their lifespan. In vivo studies in animals suggest that extravasated neutrophils can back-migrate (retrograde migration). Otherwise, neutrophils undergo NETosis or apoptosis. Apoptotic neutrophils are engulfed by tissue-resident macrophages that upregulate TFs of the liver X receptor (LXR) family, potentiating resolution at the site of inflammation. Figure adapted from Metzemaekers et al. (344).

1.2.5. Apoptosis and neutrophil clearance

Under homeostatic conditions, senescent 'aged' neutrophils upregulate CXCR4 and CD11b and downregulate CD62L (354,355). Interestingly, aged neutrophils were shown to lose their granule content and have a blunted capacity to produce NETs, limiting their tissue-damaging potential (356). Aged neutrophils transmigrate into the BM where they are cleared by the resident stromal macrophages. This results in the induction of TFs of the liver X receptor (LXR) family. Macrophages and LXRs are essential components for the modulation of the hematopoietic niche and may cause downregulation of CXCL12, which subsequently results in an increased neutrophil mobilisation (357). In addition, the microbiome may affect the neutrophil numbers by increasing the number of aged neutrophils through a TLR and MyD88-dependent mechanism (86).

After fulfilling their effector functions, neutrophils can undergo terminal NET formation (*vide supra*), necrosis or apoptosis. Apoptotic neutrophils can be phagocytosed by resident macrophages and subsequently upregulate LXR (358,359). This induces a reduced IL-23 production and subsequent reduced IL-17 and G-CSF that terminates the inflammatory recruitment of new neutrophils. Furthermore, it stimulates the secretion of the anti-inflammatory cytokines TGF-β and IL-10, which further decreases the neutrophil chemo-attraction (7).

1.3. Neutrophil function

1.3.1. Antimicrobial activities

Upon priming, neutrophils have diverse functions which are illustrated Figure 2.7. Their antimicrobial properties are the best known and include phagocytosis, degranulation, ROS production, and NET formation (338,360,361).

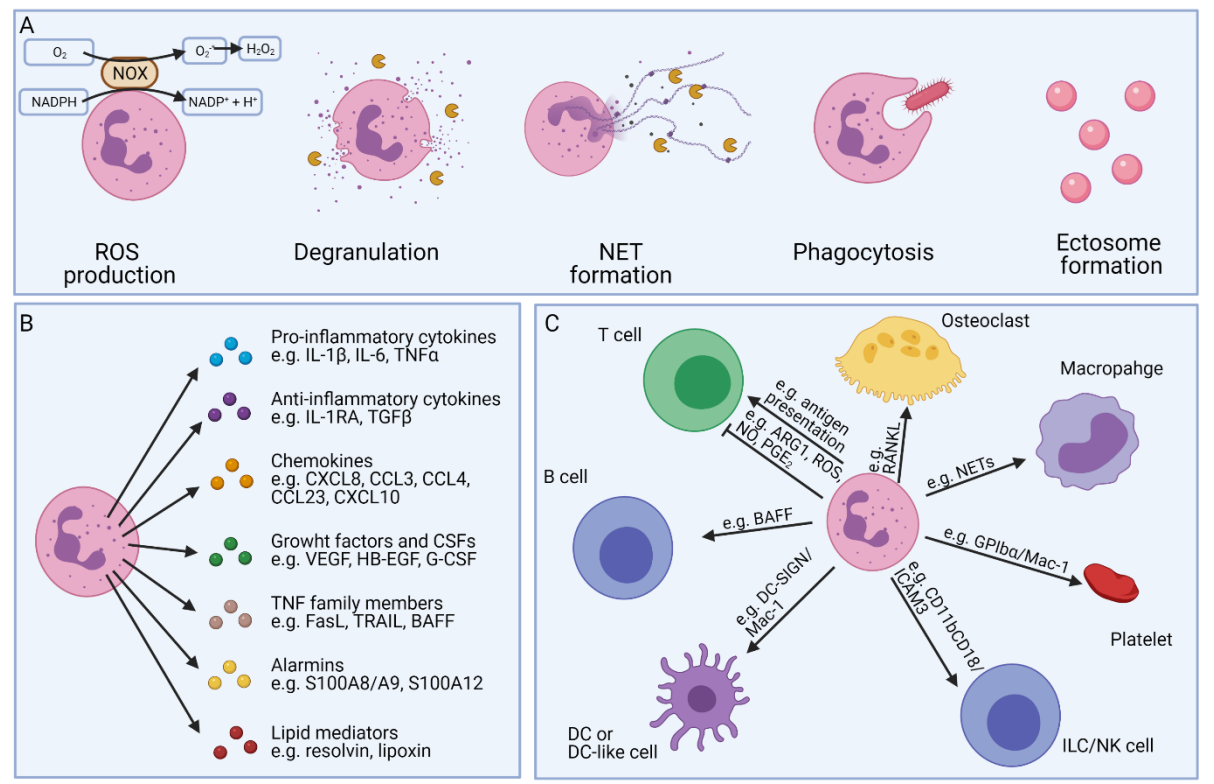

Figure 2.7: Overview of the different neutrophil effector functions
Neutrophils possess different defence mechanisms including both oxidative and non-oxidative mechanisms (panel A). Neutrophils can produce reactive oxygen species (ROS) and release soluble mediators stored pre-made granules (degranulation). Neutrophils show a unique form of cell death, called NETosis, where neutrophils expel neutrophil extracellular traps (NETs), consisting of decondensed DNA together with histones, cytokines, and granule proteins. Furthermore, neutrophils are professional phagocytes able to engulf foreign particles for internal digestion. Neutrophils can also transform into anuclear cytoplasts (ectosomes), regulating the inflammatory microenvironment, intercellular communication, and exert antimicrobial functions. Next to the release of granule proteins, neutrophils also release a bunch of soluble mediators (panel B). Although the release per individual cell is limited, neutrophils are an important source, due to their high abundance in the blood. Neutrophils interact with different cells of both the innate and adaptive immune system (panel C). Neutrophils can carry antigens and act as antigen-presenting cells, activating T cells. In contrast, myeloid-derived-suppressor neutrophils can inhibit the proliferation of T cells. Neutrophils can stimulate the maturation of antibody-producing B cells and play an essential role in the generation of NK cells in the BM. Furthermore, neutrophils may also interact with platelets, macrophages, dendritic cells (DCs), or osteoclasts.

Among the different leukocytes, the population of neutrophils have the highest phagocytic capacity. During phagocytosis, neutrophils can engulf pathogens or cellular debris (346,362,363). The main phagocytic receptors include the C-type lectin receptors (*e.g.* the mannose receptor (MR) and scavenger receptors), fragment crystallisable (Fc) receptors, and complement receptors (CR) (360,362,364,365). Upon phagocytosis, a phagolysosome is formed which can fuse with granule proteins, releasing its antibacterial proteins or activate a membrane-bound nicotinamide adenine dinucleotide phosphate (NADPH)-oxidase that induces the production of superoxide anions (O_2^-) that in turn is metabolised into hydrogen peroxide (H_2O_2) or other ROS (366). These granule proteins can also be released upon stimulation in a process called degranulation. The granule proteins can eliminate extracellular pathogens [*i.e.* by neutrophil elastase (NE), MPO, or lactoferrin] or degrade extracellular matrix proteins [*i.e.* by neutrophil collagenase (MMP8) or neutrophil metalloproteinase 9 (MMP-9)], facilitating the neutrophil migration. During the release of granule proteins, granules are released in the reverse order of their formation, starting from the secretory vesicles (314,338,346,367,368). The secreted granule proteins also influence the inflammatory activities of the surrounding cells and promote cytokine, chemokine, and ROS production, cell activation, extravasation, and pathogen uptake by opsonisation (*e.g.* by the binding of cationic antimicrobial peptides such as defensins or cathelicidins). The importance of proper degranulation is underlined in Papillon-Levèfre syndrome patients who have neither elastase nor other serine proteases (*e.g.* cathepsin C). Patients are characterised by a reduced monocyte accumulation at the site of inflammation and show an important susceptibility to systemic infections (367,369–372). Degranulation is often linked to the production of ROS in a process called the respiratory burst. The ROS can interact with hydrogen and potassium ions or can be converted by the granule superoxide dismutase MPO into hydroxyl radical, hypochlorite and hypobromite, all having strong antimicrobial properties (338,373–377). The importance of ROS production is demonstrated in patients with chronic granulomatous disease, who have a defect in their NADPH oxidase (378). Human neutrophils can also generate membrane vesicles, called ectosomes, upon stimulation with specific agonists. These ectosomes express phosphatidylserine, as well as various membrane proteins, and contain diverse granule proteins, which play a role in modulating the inflammatory microenvironment, intercellular communication and exert antimicrobial functions (379–382). A more recently discovered antimicrobial mechanism, unique to neutrophils, is the expulsion of NETs via a process called NETosis (383). NETs consist of decondensed double-stranded DNA, antibacterial cytosolic and granule proteins such as NE or MPO, and histones. NETs can capture and immobilise pathogens, facilitating their clearance (338,384). Furthermore, NETs were described to catch pro-inflammatory cytokines and can proteolytically degrade them to resolve the inflammation in gout (385). NETs are also highly immunogenic since they were linked to the development of several autoimmune diseases including RA and SLE (386–394). The formation of NETs is a multi-step process that is not yet completely understood. Until now, three different types of NETosis have been described (suicidal NETosis, vital NETosis, and vital NETosis with the release of mitochondrial DNA). A complete description of these different processes falls out of the scope of this literature overview and has been provided elsewhere (384,395,396).

1.3.2. Cellular interactions

Next to the important antimicrobial properties, neutrophils can interact with other immune cells and are critical in establishing a good immune response. As described previously, neutrophils are one of the first cell types to enter the sites of inflammation and can secrete both pro-inflammatory cytokines (*e.g.* TNF-α, IL-18, and IL-1β), anti-inflammatory cytokines (*i.e.* IL-10, and IL-1RA), and chemokines (*e.g.* CCL2, CXCL8, CXCL9, CXCL10, and CCL20), further recruiting new immune cells to the site of inflammation (397–402). Although low secretion levels and limited capacity for *de novo* protein synthesis were proposed, neutrophils and their activation products can play an important contribution since they are so abundant (403). The neutrophil-derived proteases may additionally modulate the signalling network via their cytokine and chemokine processing capacity (404–406). Neutrophils also produce growth factors and angiogenic factors (G-CSF and VEGF) via which they may influence different biological processes including tumorigenesis (397,407,408) or may induce immunoglobulin class switching and somatic hypermutations in B cells by the secretion of B-cell activating factor (BAFF), a proliferation-inducing ligand (APRIL), also known as TNF ligand superfamily member 13 (TNFSF13), and IL-21 (409–412). Neutrophils can also regulate the inflammatory outcome by changing the composition of the secreted lipids. At early stages, neutrophils synthesise pro-inflammatory lipids such as prostaglandins, and leukotrienes, whereas later lipoxins, resolvins and protectins are secreted tempering the inflammatory response (360).

Neutrophils can directly interact with innate and adaptive immune cells such as DCs, T cells, and NK cells (Figure 2.7). Neutrophils interact with DCs through glycosylation-dependent interactions between Mac-1 and dendritic cell-specific intercellular adhesion molecule-3-grabbin non-integrin (DC-SIGN), elucidating DC maturation and activation, DC-mediated Th1 polarisation, and furthermore can give DCs access to antigens (413–420). Upon stimulation with GM-CSF neutrophils can also directly serve as antigen-presenting cells and can upregulate antigen-presenting molecules (*e.g.* MHCII) and co-stimulatory molecules (*e.g.* CD80 and CD86). These cells are called neutrophil-DC hybrid cells and may stimulate T cell activation and proliferation (421–424). In contrast, myeloid-derived suppressor cells (MDSCs) can suppress the activation and proliferation of T cells and are described in various infections or inflammatory conditions and cancer (425,426). Suppression can be induced by the induction of NO via the inducible nitric oxide synthase (iNOS) (427), the release of hydrogen peroxide (428), the depletion of L-arginine in an arginase-dependent way (429) or by direct cell contact via programmed death-ligand 1 (PD-L1) or Mac-1 (430,431). Neutrophils can also interact with NK cells and play an important role in their BM maturation (432). Additionally, neutrophils express a functionally active membrane-bound RANKL, the ligand for receptor activator of NF-kB (RANK) and so can activate osteoclastogenesis (433).

1.4. Neutrophil heterogeneity

The existence of different neutrophil subsets with functional and phenotypical heterogeneity has recently emerged in humans and mice [reviewed in (264,434–436)]. Both in steady-state and malignant conditions, several subsets were described, having specific activities or characteristics. Among the different tissues, phenotypic diversity was shown (266,437) and even in the blood of healthy controls, two neutrophil subsets were described (438). The two most well-known subsets include those that can be found in malignancies and transplantation including the anti-tumoural N1 versus the tumour-promoting N2 neutrophils (439–445). Depending on the microenvironment, an important plasticity between the two subtypes was described, shifting along with the tumour progression. This indicates high plasticity of neutrophils as they adapt their activity depending on the need of the microenvironment (438,446,447). Other reported subsets include the MDSC (431,448,449), the so-called neutrophil-dendritic (DC) hybrids (expressing both neutrophil and DC markers) (421), reversed migration neutrophils (defined as $ICAM^{hi}/CXCR1^{lo}$ neutrophils) (450,451), angiogenic neutrophils (defined as $CD49d^{+}VEGFR1^{hi}CXCR4^{hi}$ neutrophils) (452,453) and low-density granulocytes (LDG) (454–456). Remark that currently it is not clear whether the different neutrophil subsets present a distinct subgroup of neutrophils formed in the BM or rather reflect a different activation state defined by different environmental conditions. The different neutrophil subsets can be divided according to their causing stimuli or conditions (*i.e.* inflammation or tumour), according to their maturity-status (mature and immature neutrophils), according to their age or cell density (low-density neutrophils and high-density neutrophils) (320,357,435,436,438,446,447,457–461). Although the existence of heterogeneity among neutrophils is now recognised, the mechanism and biological relevance of this diversity remains under debate. Most research focused on blood neutrophils and little is known about the tissue-infiltrated neutrophil subsets. Furthermore, it remains to be clarified if there exists overlap between neutrophil subsets in specific pathophysiological contexts (320). The current neutrophils' nomenclature is confusing and contributes to controversies regarding the neutrophil function and ontogeny. A better understanding of neutrophil heterogeneity in auto-inflammatory diseases was part of this dissertation.

1.5. Emergency granulopoiesis in auto-inflammatory disorders

1.5.1. Emergency granulopoiesis and extramedullary myelopoiesis

In homeostatic conditions, the formation of neutrophils is tightly regulated (*vide supra*). However, in specific conditions such as infection, bleeding, cancer, auto-inflammation or autoimmunity, large numbers of functional neutrophils are required. To meet the high demand for these cells, the production of neutrophils is increased in a process called 'emergency granulopoiesis' (462–467). Emergency granulopoiesis involves a series of shared cascading events and is well documented during infection (468,469). First, pathogens are sensed via the PRR that recognises different PAMPs. In the BM, the hematopoietic stem/progenitor cell (HSPC) expresses PRR (470,471) and can directly be activated. Activation stimulates their survival, proliferation, differentiation, and migration (259,271,471–478) or can induce the release of growth factors such as IL-6 or G-CSF (470,479). Pathogens can also indirectly be recognised by specialised cell types in the peripheral tissues or BM. Recognition is translated by the release of different growth factors and cytokines, including G-CSF, GM-CSF, IL-6, IL-1β, IL-3, or FMS-like tyrosine kinase (FLT3) ligand (Figure 2.8) (480–487).

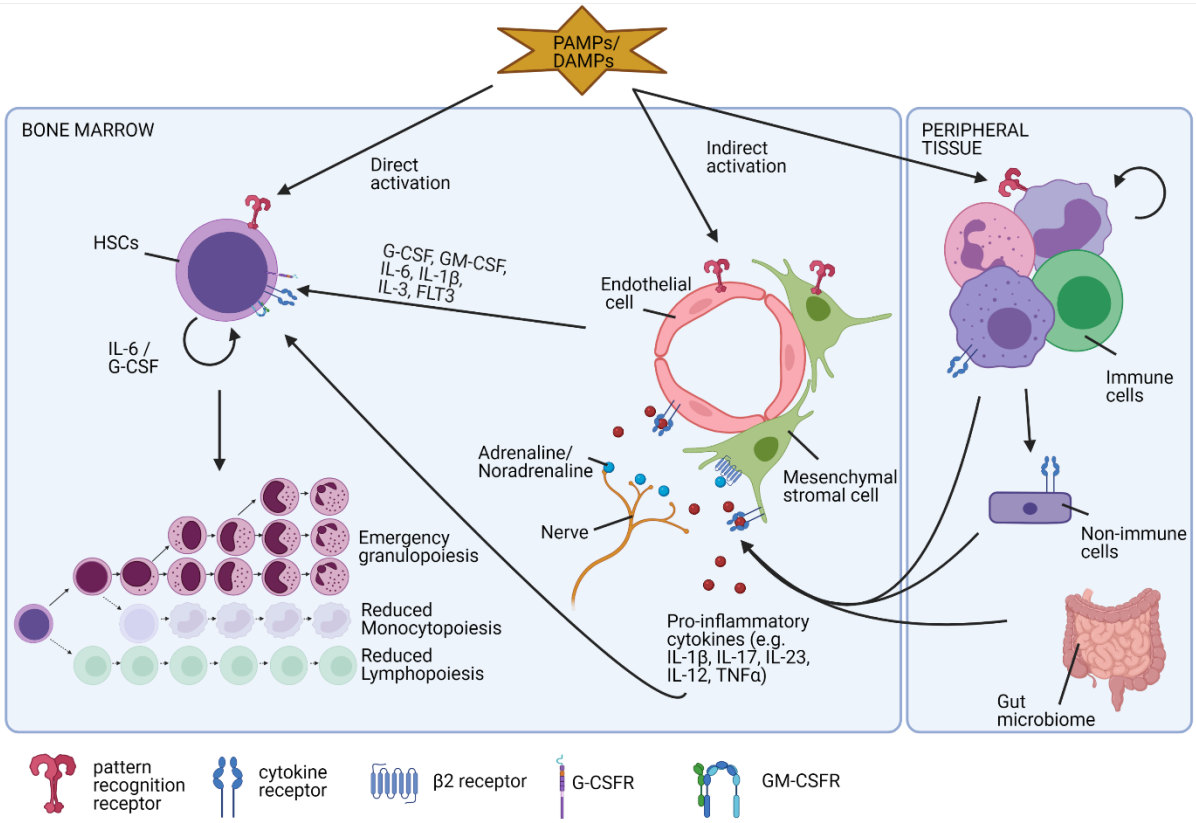

Figure 2.8: Factors involved in the induction of emergency granulopoiesis.
During excessive inflammation, there is a high need for new neutrophils (emergency granulopoiesis). Different direct and indirect mechanisms are involved in the differentiation and release of new neutrophils. Damage-associated molecular patterns (DAMPs) or pathogen-associated molecular patterns (PAMPs) bind diverse pattern recognition receptors, expressed on diverse cell types. In hematopoietic stem cells (HSCs), binding directly stimulates the release of interleukin-6 (IL-6) and granulocyte colony-stimulating factor (G-CSF), inducing their proliferation and differentiation into neutrophils. Indirectly, the molecular pattern molecules bind endothelial cells or stromal cells, providing an important source of pro-inflammatory molecules and growth factors. Additionally, these endothelial cells or mesenchymal cells are stimulated by pro-inflammatory cytokines released by immune cells or non-immune cells of the periphery that encountered invading pathogens or cell damage. The neuronal release of adrenalin or noradrenalin additionally stimulates the release of new neutrophils. Finally, also food intake and the gut microbiome tightly regulate neutrophil homeostasis.

The main hematopoietic growth factors are discussed in paragraph 1.5.2. Next, granulopoiesis is stimulated by different growth factors, and neutrophils are released into the circulation. Finally, after the inflammation has resolved, the neutrophil homeostasis is restored.

Emergency granulopoiesis is characterised by an increased release of immature neutrophils, such as myelocytes, metamyelocytes, and band cells into the circulation, known as 'the left shift' (488). Clinically, the left shift is described as a blood leukocytosis with an increased appearance of immature neutrophil precursor cells in the peripheral blood, which are normally only present in the BM during physiological steady-state conditions. In sepsis, the presence of immature neutrophils in the circulating blood is often used as a clinical indicator (489,490). In humans, mature and immature neutrophils can be distinguished based on the CD10 expression that is observed on mature neutrophils only (321). Furthermore, based on expression levels of CD16 and CD62L (L-selectin) neutrophils can be subdivided into mature, immature, and hyper-mature neutrophils. In non-inflammatory conditions, nearly all circulating neutrophils have a mature phenotype and are $CD16^{high}CD62L^{high}$ cells. In inflammatory settings, an increased number of immature neutrophils ($CD16^{dim}CD62L^{high}$) and hypersegmented neutrophils ($CD16^{high}CD62L^{dim}$) are found (431,491,492). Recently, a single-cell sequencing experiment was performed in a bacterial infection-induced mouse-model. In this study, researchers showed that the emergency granulopoiesis is associated with an augmented proliferation of the early stage neutrophil progenitor cells in the BM and accelerated post-mitotic maturation of the neutrophils. Interestingly, the overall neutrophil differentiation in the BM remains intact but a substantial difference in the transition between the subpopulations was reported (324).

Today, it remains challenging to determine clear boundaries between steady-state and emergency haematopoiesis. During searches for mechanisms involved in the emergency granulopoiesis, researchers showed that granulopoiesis can be induced by cytokines in the absence of C/EBPα and suggested alternative pathways under emergency conditions (Figure 2.9) (493). It was found that especially C/EBPβ plays a crucial role in the stress-induced haematopoiesis, which was hampered in C/EBPβ KO mice (462,493–499). Whereas both C/EBPα and C/EBPβ share downstream genes involved in the granulocyte differentiation (500), a less pronounced cell cycle inhibition was linked to C/EBPβ as compared to C/EBPα (304,493,501–503). The importance of C/EBPβ in stress-induced granulopoiesis has been confirmed in diverse mouse models and a zebrafish model (504–506). Interestingly, in chronic myeloid leukaemia, the breakpoint cluster region-Abelson murine leukaemia virus (BCR-ABL) fusion protein may drive a myeloid expansion by activating the emergency granulopoiesis in a C/EBPβ-dependent way (495,496).

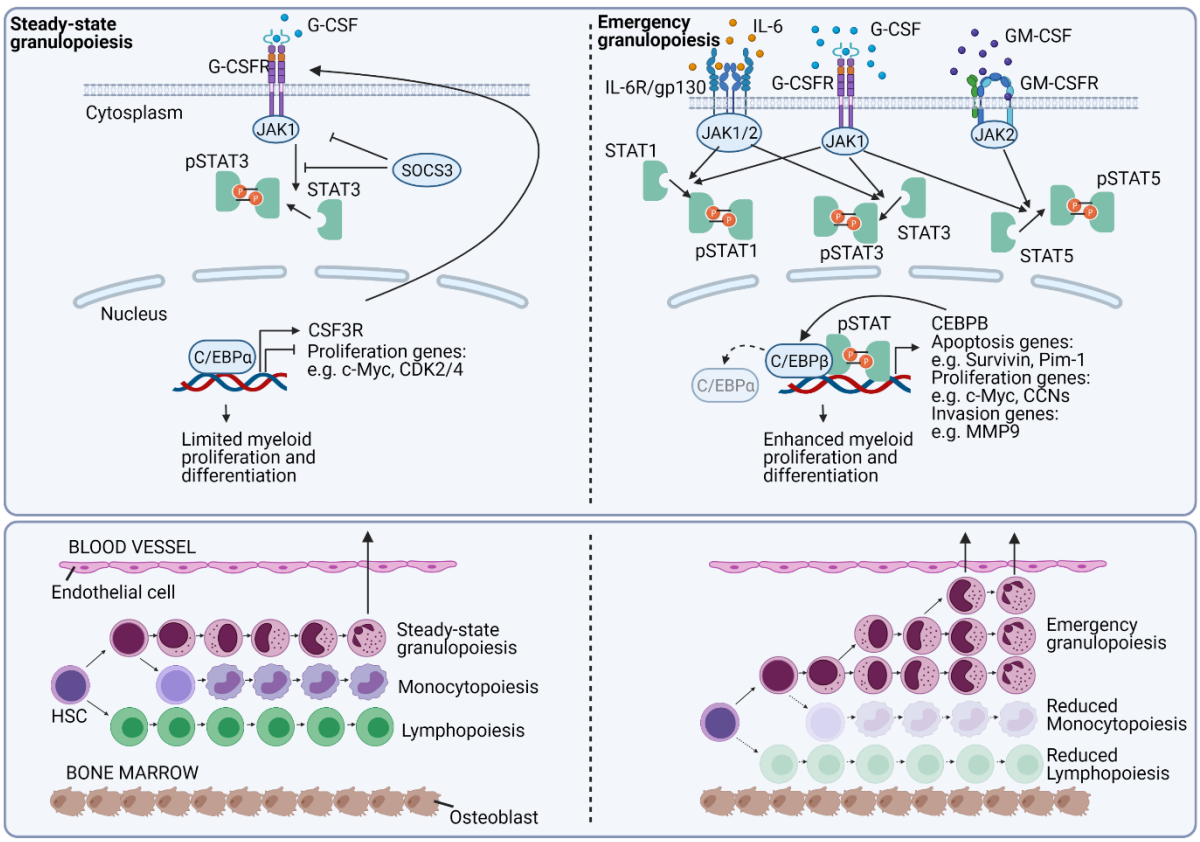

Figure 2.9: Growth factor signalling regulates emergency granulopoiesis
In homeostatic conditions, granulocyte colony-stimulating factor (G-CSF) is the main growth factor that regulates neutrophil development. G-CSF signals via the G-CSF receptor (G-CSFR) (encoded by the CSF3R gene), and signals via the Janus kinase (JAK)-signal transducer and activator of transcription (STAT) pathway. Via unknown mechanisms, G-CFSR signalling induces the CCAAT-enhancer-binding protein-α (C/EBPα). C/EBPα is the major transcription factor involved in myelopoiesis. The transcription factor enhances the expression CSF3R, whereas it inhibits genes required for the cell cycle, eventually causing a limited myeloid proliferation and differentiation. During excessive inflammation, neutrophils massively migrate to the site of inflammation. To counterbalance neutrophil depletion and to provide newly needed neutrophils, emergency granulopoiesis is initiated. Emergency granulopoiesis is characterised by a large-scale de novo generation of new neutrophils from neutrophil progenitor cells. Interleukin-6 (IL-6), G-CSF, and granulocyte-macrophage colony-stimulating factor (GM-CSF) are mainly stimulating the proliferation and differentiation of new neutrophils. IL-6 binds the IL-6 receptor (IL-6R)/gp130 and signals in a JAK-STAT1 or STAT3-dependent way. Excessive G-CSFR signalling induces both STAT1, STAT3, and STAT5 phosphorylation and signalling, whereas GM-CSF receptor (GM-CSFR) signalling mainly tempts STAT5 activation. Upon activation, the pSTAT molecules are translocated to the nucleus where they directly stimulate genes involved in the regulation of apoptosis, proliferation, and cellular translocation. Additionally, pSTAT signalling stimulates the expression of the transcription factor C/EBPβ. C/EBPβ replaces C/EBPα, and releases the brake on proliferative genes, cranking myelopoiesis. During emergency granulopoiesis, not only mature neutrophils are leaving the BM, but also more immature neutrophils are being released. This process is called "left shift". Figure adapted from Manz et al. (462).

In homeostatic conditions, neutrophils are exclusively formed in the BM, but during emergency granulopoiesis, neutrophils can also be formed outside the BM in a process called 'extramedullary myelopoiesis'. The extramedullary myelopoiesis mainly takes place in spleen and liver and, more controversially, also in LNs, lungs, and kidney as shown in patients and mice (462,507–511). Extramedullary myelopoiesis was supported by circulating HSPC found in the blood-stream (512). Under acute or chronic stress conditions such as infection, these HSPC can seed in the extramedullary tissues (510). In the murine spleen, the HSPCs were localised close to transcription factor 21 (Tcf21) positive stromal cells that can secrete niche factors such as CXCL12 and stem cell factor to support the splenic extramedullary haematopoiesis (EMH) (513). Although the BM niche and splenic stroma are quite different, neutrophil development in the spleen during EMH follows the same hierarchical developmental order as described in the mouse BM and in this way the spleen provides a unique reservoir able to supply additional myeloid cell during the immune challenge (316,514,515).

Remarkably, upon stress, neutrophils are released at different stages of maturation, which all have diverse chromatin and transcriptional landscapes. It is important to understand how the neutrophil epigenome is established during differentiation. Pre-existing differences in the chromatin landscape between the different neutrophil subsets in the bone marrow or blood may contribute to observed heterogeneity since the same environmental trigger may induce a different biological output (112).

Emerging evidence from cancer studies suggests that neutrophils generated from the BM are functionally different from those derived from extramedullary sites such as the spleen. Driven by the cancer microenvironment, HSPCs can generate MDSC in the spleen (514,516,517). Interestingly, C/EBPβ can regulate the expression of enzymes such as arginase and inducible nitric oxide synthase both of which are required for the lymphocyte inhibitory activities of the MDSC (57) and the absence of C/EBPβ could reduce the tumour metastasis (518,519). Note that no validated markers have been identified that can discriminate between suppressive and pro-inflammatory neutrophil subpopulations and that currently distinction is based only on functional assays performed on isolated cells (460). Recently however, CD84 was proposed as surface marker for MDSCs in breast cancers (517).

The term 'reactive granulopoiesis' has been proposed in settings where an emergency granulopoiesis is induced by a non-infectious trigger such as during autoimmunity or auto-inflammation. It will be necessary to understand the different cytokines that fine-tune the granulopoiesis and understand the molecular differences between emergency and reactive granulopoiesis.

1.5.2. Neutrophil-regulating cytokines

While several (chemotactic) cytokines can activate neutrophils, in this paragraph only cytokines that are involved in granulopoiesis and neutrophil homeostasis will be discussed.

1.5.2.1. G-CSF

Granulocyte colony-stimulating factor (G-CSF) is the main haematopoietic growth factor required for the proliferation and differentiation of haematopoietic precursor cells into neutrophils (520–525). G-CSF regulates the commitment of progenitor cells to the myeloid lineage (526), induces the proliferation of granulocytic precursor cells (527), reduces the transit time through the granulocytic compartment (527), and controls the viability of the BM neutrophil pool (524,525,528). Furthermore, it induces the release of mature neutrophils from the BM into the blood by the internalisation and consequent downregulation of CXCR4 (529,530) or by downregulation of CXCL12 in the BM (531). In contrast, G-CSF can also impede the CXCR2-induced neutrophil mobilisation by negatively regulating CXCR2-mediated intracellular signalling which under specific bacterial infections, acts as a negative regulator of neutrophil mobilisation (532). Both *in vitro* and *in vivo,* G-CSF acts on mature neutrophils and may enhance ROS production, adherence, phagocytosis, killing, antibody-dependent cellular

cytotoxicity (ADCC), and may induce phenotypic alterations such as increased expression of CD11b (533). G-CSF also affects the expression of the pro-survival protein survivin which increases the lifespan of mature neutrophils (534,535).

In addition, G-CSF induces the release of prostaglandin E2 and induces fever (536). Furthermore, G-CSF can stimulate the peripheral sympathetic nervous system to release catecholamines (85) which may reduce the number of osteoblast and the CXCL12 production (537,538). Interestingly, G-CSF is a strong inhibitor of the NK cell function, altering its receptor expression and reducing its cytotoxic capacity and cytokine production (539,540).

Many tissues including endothelial cells, macrophages, epithelial cells, fibroblasts, and BM stromal cells produces G-CSF when stimulated with inflammatory stimuli such as LPS, IL-1β, or TNF-α (541–544). IL-17 and IL-23 have been implicated as major upstream regulators of G-CSF (discussed below) (521,542,545). The G-CSF levels are rapidly increased in response to infection or during emergency granulopoiesis and stimulate the expansion of neutrophils in the peripheral blood (481,482,546). Interestingly, during emergency granulopoiesis, the endothelial cells were shown as the main cellular source of G-CSF (547).

G-CSF signals via its G-CSFR homodimeric receptor (548) and signals in a JAK/STAT-dependent way. G-CSF can stimulate three members of the STAT family (STAT 1, 3, and 5) (549–553). The role of STAT1 and STAT5 in the granulopoiesis is however limited (554–559) and myeloid differentiation is mainly induced by STAT3 (560). In steady-state conditions, the G-CSFR signalling is controlled in a suppressor of cytokine signalling 3 (SOCS3)-dependent way (561) and STAT3 KO mice are marked by peripheral neutrophilia (562–565). In steady-state granulopoiesis, the expression of the G-CSFR is regulated by C/EBPα. C/EBPα drives the expression of many genes that encode proteins that are required for myeloid progenitor proliferation and granulocyte differentiation. Next, it restricts excessive proliferation by inhibiting the expression of genes required for cell cycle progressions *e.g.* the genes encoding MYC, cyclin-dependent kinase 2 (CDK2) or CDK4 (271,566). During emergency granulopoiesis, when G-CSF levels are markedly increased, STAT3 is directly stimulating the expression of MYC and C/EBPβ, which in turn further stimulates MYC transcription by replacing C/EBPα at the promoter region (Figure 2.9) (271,505).

G-CSFR KO mice have lower amounts of immature granulocytic precursors and neutrophils in the BM, have a 70-80% reduction of circulating neutrophils (due to a defective release), and are defective in certain mature neutrophil cell functions (524,525,567,568). Similarly, humans expressing dominant negative receptor mutations in G-CSFR are neutropenic (569,570). Additionally, mutations in the haematopoietic cell-specific Lyn substrate 1-associated protein X1 (HAX1), which contributes to the G-CSFR signalling pathway cause severe neutropenia in humans (571,572). Interestingly, emergency granulopoiesis, however, can occur in a G-CSF-independent way and G-CSFR KO can still mount a granulopoietic response in a sterile model of peritonitis or during a *Candida albicans* infection. In contrast, G-CSFR KO mice showed a more severe disease during infection with *Listeria monocytogenes* (525,573–576).

The exogenous administration of G-CSF mimics the physiological responses that are observed during emergency granulopoiesis and increase the neutrophil count in peripheral blood (469,470). Upon G-CSF treatment, also HSC can be mobilised from the BM into the blood (577,578). Currently, G-CSF is used in clinics to treat neutropenia patients (579–581) or to mobilise hematopoietic progenitors for transplantation (582,583).

In RA, G-CSF plays a pro-inflammatory role in the development of arthritis by promoting neutrophil trafficking into the inflamed joints. G-CSF KO or G-CSFR KO mice are protected from the development of arthritis (545,584), and injection of G-CSF in the collagen-induced arthritis (CIA) model can

exacerbate disease symptoms (585). Targeting the G-CSFR could also reduce neutrophil trafficking and joint inflammation in an antibody-mediated inflammatory arthritis model and ameliorates arthritic pain (586–588). In JIA patients, G-CSF was demonstrated as a major regulator of the neutrophil gene expression signature (589,590). In sJIA patients, increased G-CSF plasma levels are measured when compared to healthy controls. Furthermore, the highest levels were found in patients with an incomplete response or nonresponse to anakinra (45). The observed neutrophilia and NK cells defects seen in sJIA, may also in part be explained by the increased G-CSF levels but the exact role of G-CSF in sJIA remains incompletely understood. In this dissertation, we investigated the exact role of G-CSF in the sJIA mouse model.

1.5.2.2. GM-CSF

Granulocyte-macrophage colony-stimulating factor (GM-CSF) is a cytokine secreted by a variety of cells. The major sources include activated T and B cells, monocytes/macrophages, endothelial cells, fibroblasts but also neutrophils, eosinophils, epithelial cells, mesothelial cells, chondrocytes, Paneth cells, and tumour cells may secrete GM-CSF (591–593). In T cells, the release of GM-CSF is triggered by IL-1β and IL-23 or IL-1β and IL-12 in mice and humans respectively (594–596). In fibroblasts, endothelial cells, chondrocytes, and smooth muscle cells, TNF-α and IL-1 are the main inducers whereas in macrophages/monocytes GM-CSF is released upon TLR-stimulation (591). GM-CSF can form a positive feedback loop by activating macrophages and DCs to produce IL-23, IL-1β, and IL-6 activating Th17 and Th1 cells that in turn express GM-CSF (597). The production can be inhibited by IFN-γ (598), IL-4 (599), IL-10 (600), and glucocorticoids (601).

GM-CSF is required for the *in vivo* development of neutrophils, monocytes and macrophages from the BM precursor cells and plays a crucial role in the maintenance of the innate immune homeostasis (602–605). Depending on the dose, GM-CSF can have different effects on myeloid cell survival, proliferation, or differentiation (534,606–608). GM-CSF also upregulates the antimicrobial function of mature neutrophils and enhances ROS production, adherence, killing, phagocytosis, and ADCC both *in vitro* and *in vivo* (533,609). Furthermore, GM-CSF phenotypically alters neutrophils and can upregulate the expression of the integrin CD11b, which facilitates adhesion and tissue entry (533,610). Following chemo- or radiotherapy, exogenous GM-CSF can be used to restore the myeloid populations (611). In addition to its effect on neutrophils, GM-CSF also stimulates activities of macrophages, DCs, and B cells [reviewed elsewhere (612)].

GM-CSF signals via the GM-CSF receptor (GM-CSFR) that is composed of one α chain and one β chain with low and high-affinity binding to GM-CSF, respectively. The β chain is shared with IL-3 and IL-5 receptors (607). The GM-CSFR is expressed on myeloid cells and some non-hematopoietic cells, but not on T cells (613). Four main signalling pathways can be triggered by the G-CSFR (614–616). The main pathway involves the JAK2/STAT5 pathway that activates genes such as pim-1, CIS, and cyclin to induce cell myeloid differentiation and proliferation (617–619). Next, both the phosphatidylinositol-3-kinase (PI3K) and JAK/STAT-Bcl-2 signalling pathway are involved in cell survival (620). Eventually, the ERK1/2 and NK-κB pathways mediate cell differentiation and inflammation (621,622).

Whereas GM-CSF-deficient mice have an impaired reproductive capacity and develop pulmonary alveolar proteinosis (PAP), GM-CSF KO mice have a normal basal granulopoiesis and show no alterations in peripheral blood counts (575,623,624). This indicates that other growth factors aside from GM-CSF have a redundant role in myeloid cell development and differentiation under steady-state conditions. In emergency granulopoiesis, GM-CSF plays an important role and GM-CSF KO mice fail to control infections with *Listeria monocytogenes* or *Mycobacterium avium* (574,625). In contrast, mice lacking the three myeloid colony-stimulating factors [G-CSF, GM-CSF, and macrophage colony-stimulating factor (M-CSF)] still mount an inflammatory response in a sterile model of peritonitis (576). Interestingly, GM-CSF (but also IL-3 and IL-6, discussed below) can restore the lack of G-CSFR

expression in C/EBPα-deficient mice and can initiate a C/EBPα-independent granulopoiesis (626–628). *In vitro* studies suggested C/EBPβ as the driving transcription factor in this process, since C/EBPβ-deficient hematopoietic cells had impaired responsiveness to GM-CSF (504).

GM-CSF has a pathological role in Th17-driven auto-immune diseases such as multiple sclerosis (MS) and RA (594,597,629). Consequently, the ablation of GM-CSF signalling could suppress the disease in models of arthritis, MS, and lung disease (608,630–632). In contrast, in autoimmune diseases driven by humoral responses such as myasthenia gravis (MG), Hashimoto's thyroiditis (HT) and systemic lupus erythematosus (SLE), GM-CSF rather has a protective role (629). Interestingly, in invasive breast cancer, prolonged G-CSF may induce the development of immunosuppressive neutrophils in the spleen (517,633). In patients with JIA, the frequency of GM-CSF producing T helper cells was significantly increased in the synovial fluid when compared to the PBMCs and was furthermore correlated with an increased ESR (634,635). sJIA patients show increased plasma levels of GM-CSF as compared to healthy controls and a significantly decreased level was observed in the anakinra responder group (81).

1.5.2.3. IL-17/IL-23

Already since the first reports of IL-17, an indirect role of the cytokine on neutrophil proliferation and differentiation was demonstrated (542). IL-17 mainly functions on epithelial, endothelial, and stromal cells, inducing the expression of pro-inflammatory cytokines, growth factors, and chemokines that regulate granulopoiesis, recruitment, and life span of new neutrophils (636). IL-6 was the first identified gene target of IL-17, regulating granulopoiesis (637). Furthermore, IL-17 induces the production and release of the two main granulocytic growth factors G-CSF and GM-CSF (542,638,639). IL-17 also induces the production of other pro-inflammatory cytokines including TNFα, IL-1β as well as cyclooxygenase 2 (COX2) and inducible nitric oxide synthase (iNOS), which all directly or indirectly regulate the formation of new neutrophils (640). Next, IL-17 also regulates the attraction of neutrophils via the induction of various chemokines *i.e.* CXCL1 (KC), CXCL2 (MIP2), CXCL6 (GCP-2), or CXCL8 (IL-8) (641). Furthermore, IL-17 can stimulate endothelial expression of P-selectins, E-selectins, and integrin ligands including ICAM-1 and VCAM, enhancing the neutrophil mobilisation (642). Remark that neutrophils themselves can form a positive feedback loop during neutrophil recruitment by releasing pro-inflammatory cytokines and chemokines (263).

Th17 cells, which are the main source of IL-17, are induced from naïve T cells in the presence of both TGFβ and IL-6 (in mice) or IL-1β (in humans). The pro-inflammatory cytokines TNF-α and IL-1β can synergistically increase IL-6 production, further contributing to Th17 cell differentiation. Following activation, RORγt is induced, which promotes the expression of IL-17 and the IL-23 receptor (IL-23R). Subsequent IL-23-signalling further increases the RORγt and IL-17 expression in a STAT3-dependent way (643). Although IL-17 was described as a T cell-secreted cytokine, much of the IL-17 released during an inflammatory response is produced by innate immune cells such as the γδ T cells (644). Since these cells do not require induction of the IL-23R, these cells may induce a fast IL-17 response to IL-1β or IL-23 without any T cell receptor engagement (170).

IL-23 is released by macrophages and DCs upon TLR-triggering. Subsequently, IL-23 can enhance the development of new neutrophils via the well-established "IL-23-IL-17-G-CSF axis" (645). Remark that this axis also plays a pivotal role during neutrophil homeostasis (see 0). Here, phagocytosis of dying neutrophils by specialised macrophages in the tissue *i.e.* lung, BM, or spleen, may block the secretion of IL-23 and subsequent IL-17-regulated neutrophil release (359,646).

1.5.2.4. IL-1β

Myelopoiesis is stimulated both directly and indirectly upon binding of IL-1β to its receptor. IL-1β itself or IL-1β in synergy with other growth factors (*e.g.* G-CSF), can induce the proliferation and differentiation of HSPCs and GMPs. This induction is based on the activation of PU.1 and can be blocked in IL-1R1 KO mice (647,648). In naïve conditions, IL-1R1 KO mice have no defects in myeloid cell numbers (649). Alternatively, IL-1β can indirectly regulate granulopoiesis by the production of neutrophilic growth factors and inflammatory mediators including IL-3, IL-6, G-CSF, and GM-CSF (493,650–652). More importantly, IL-1β is a potent inducer of IL-17 expression in CD4+ T cells or γδ T cells (427). IL-1β additionally regulates the recruitment of neutrophils by the production of neutrophil attracting chemokines such as CXCL1, CXCL2, or CXCL8 (IL-8) and by the induction of adhesion molecules on endothelial cells (650,653,654). Interestingly, IL-1β can also directly prime neutrophils for ROS production or NET formation and may prolong the lifespan of our neutrophils (130,535,655–657).

1.5.2.5. IL-6

Although IL-6 is not necessary for maintaining neutrophil homeostasis (658), the cytokine plays a critical role during emergencies (659–661) and may stimulate granulopoiesis in the absence of both G-CSF and GM-CSF (651). Administration of IL-6 induces a biphasic neutrophilia in animals via a rapid mobilisation of neutrophils from the marginated pool into the circulation (662–664), followed by an accelerated release of neutrophils from the bone marrow, which is induced by a stimulated myeloid cell differentiation (662,665–667). IL-6 deficient mice show an impaired neutrophil response after *C. albicans* infection (668) and patients treated with the humanised monoclonal anti-IL-6R antibody tocilizumab, show transient neutropenia, all demonstrating the neutrophil mobilising properties of IL-6 (669–674). Interestingly, in C/EBPα KO mice, IL-6 can induce neutrophil differentiation by restoring the colony stimulating factor 3 receptor (Csf3R) expression (271,675).

Classically, IL-6 signals upon binding to its membrane-bound IL-6-receptor alpha subunit (IL-6Rα), resulting in gp130 homodimerisation, phosphorylation of STAT3 and STAT1 proteins, and downstream signalling (676). IL-6 can also promote IL-6 trans signalling in cells that express gp130 but lack the IL-6Rα which requires the binding of IL-6 to the soluble IL-6Rα (sIL-6Rα) into an IL-6/IL-6Rα complex. Neutrophils are an important source of sIL-6Rα. IL-6Rα can proteolytically be cleaved via the TNFα converting enzyme-like enzyme (677) upon stimulation with CRP, CXCL8, C5a, LTB4, or platelet-activating factor (PAF) (677). In this way, neutrophils promote IL-6 trans signalling in other cell types and favour resolution by the transition from neutrophil to monocyte-mediated inflammation (678–680). Together with IL-6, the IL-6/IL-R complex activates endothelial cells to secrete monocyte chemoattractant protein (MCP-1)/CCL2 and induce expression of adhesion molecules (such as ICAM1 or VCAM), decreasing neutrophil and favouring monocyte recruitment (681,682). This could explain why in animal models of inflammation, the neutrophilic infiltrate is more dominant in IL-6 KO than in WT animals (679,683). The recruitment of monocytes is protective in acute models, whereas, during chronic inflammation such as CIA, colitis or experimental autoimmune encephalomyelitis (EAE), IL-6 is rather pro-inflammatory by favouring mononuclear-cell accumulation, angioproliferation, B cell maturation, and by promoting the anti-apoptotic properties of T cells (683–687).

Conflicting results regarding the direct role of IL-6 on neutrophil function were reported (688–693). Recently it was demonstrated that granulocytes are unable to induce STAT-signalling upon stimulation with IL-6 since the expression of gp130 is lost during the maturation of granulocytes (694). So the conflicting functional effects described upon IL-6R inhibition are presumably induced by contaminating cell populations (695).

1.5.2.6. IL-18

IL-18 has pleiotropic effects on neutrophil activation, including pro-inflammatory cytokine expression, degranulation, and priming of the oxidative burst (338,696,697). Since activation of neutrophils induces inflammasome-mediated IL-18 release, the cytokine can trigger a positive activation loop (698). IL-18 has no direct effect on granulopoiesis, but can stimulate the secretion of CXCL1 and CXCL2, two chemokines involved in the recruitment of neutrophils (699). Indirectly, IL-18 may alter neutrophil homeostasis by inducing IFN-γ in T cells and NK cells (182).

1.5.2.7. IFN-γ

Contradictory results were obtained when HSPCs were stimulated with IFN-γ (469). Whereas some studies reported that IFN-γ may induce quiescent HSPCs to enter the cell cycle, other studies showed that IFN-γ rather has anti-proliferative effects (469,700,701). In the myeloid lineage, IFN-γ favours the production of monocytes at the expense of neutrophils. On the one hand, IFN-γ can induce the expression of SOCS3 in GMPs, blocking the G-CSF-induced activation of STAT3 (505,701–703). On the other hand, IFN-γ regulates the expression of PU.1 and IRF-8 in these GMPs, further boosting monocyte development (701,703). Consequently, when human progenitor cells were stimulated with IFN-γ, monocyte development was induced, whereas G-CSF-induced granulopoiesis was blocked (704). Indirectly, IFN-γ also inhibits the $CD4^+$ T cell-mediated IL-17 production and neutrophil recruitment (705,706). All these findings support the fact that IFN-γ KO mice are marked by massive granulopoiesis during infection with *Mycobacterium tuberculosis* or *Toxoplasma gondii* (707,708).

IFN-γ can also directly stimulate neutrophils and can alter the expression of genes involved in *i.e.* migration, chemotaxis, phagocytosis, or apoptosis (709). IFN-γ-stimulated neutrophils have a prolonged life span, and increased phagocytic capacity, oxidative burst, or NET formation, and show an enhanced pro-inflammatory cytokine expression (710,711). IFN-γ also induces the expression of PD-L1 on neutrophils, involved in the suppression of lymphocyte proliferation (430). Besides, IFN-γ tempts the expression of genes involved in antigen-presentation, resulting in the neutrophil-DC hybrid cells (421,709,710).

1.5.2.8. FMS-like tyrosine kinase 3 (FLT3) ligand

FMS-like tyrosine kinase 3 (Flt3) ligand (Flt3L) is a transmembrane protein expressed on various cells including T cells and fibroblasts. The protein can be shed from the membrane by the enzyme tumour necrosis factor alpha converting enzyme (TACE) or a disintegrin and metalloproteinase domain 17 (ADAM17) (712,713). Flt3L signals via Flt3 (CD135), a transmembrane receptor tyrosine kinase expressed on HSCs and early precursor cells (714,715). Flt3 induces several pathways including the MAPK, PI3K/AKT, and JAK2/STAT5 signalling pathways (716,717), and promotes the growth, proliferation, and differentiation of progenitor cells (718). Flt3L mainly regulates the development of DCs, and a large expansion of DCs can be observed in healthy human volunteers receiving Flt3L (719). Flt3L or Flt3 KO mice have a reduced number of DCs, but the mice also show reduced numbers of hematopoietic precursors, neutrophils, NK cells, or monocytes and show a defective early B cell development (718,720). On its own, Flt3L is a modest mobiliser of neutrophils but synergistic action between Flt3L and other cytokines, including G-CSF, GM-CSF, SCF, IL-3, and IL-6, can promote the expansion of neutrophils (721–724). Interestingly, Flt3L also can expand and activate murine MDSCs. The activation of the suppressive function was demonstrated to be dependent on STAT3-signalling (725). In RA patients, elevated serum and synovial fluid levels of Flt3L are found (726,727). Flt3 can induce osteoclastogenesis (728) and Flt3L KO mice were protected from developing arthritis (729). In the context of sJIA, no data about Flt3L is available.

1.6. Physiological regulation of granulopoiesis

Neutrophil homeostasis is regulated through a density-dependent feedback system in the BM (3,730). In this feedback system, BM macrophages engulf senescent or apoptotic neutrophils and subsequently produce G-CSF to replace these cells (730,731). Apoptosis and other types of cell elimination (*e.g.* ferroptosis) of neutrophils in the peripheral organs leads to a direct or indirect (IL-23/IL-17 axis-mediated) suppression of G-CSF production, tempering excessive inflammation (359,730,732). Hypocellularity (*e.g.* during antibody depletion), can also be sensed in the BM. This results in an enhanced HSPC proliferation and might be mediated by a reduced competition for available G-CSF (or other growth factors) (463,730).

Finally, circadian rhythm and food intake via microbiota-derived signals also regulate the number, maturation, and gene expression of neutrophils. A full description of the intrinsic clockworks or diurnal rhythm variations in systemic and local factors falls out of the scope of this literature overview [reviewed in (733–736)].

1.7. Neutrophils in sJIA

Patients with active sJIA show an increased number of circulating neutrophils which is in line with the peripheral expansion of immature $CD34^{+}CD33^{+}$ myelomonocytic precursors (126,173). In addition, increased levels of neutrophil-derived mediators such as S100 proteins, MMP8, MMP9, elastase, and proteins involved in adhesion and chemotaxis of neutrophils (*e.g.* soluble E-selectin and soluble ICAM-1) were measured in the plasma of patients with sJIA. Furthermore, a positive correlation was found between increased numbers of neutrophils and levels of inflammatory mediators CRP, ferritin, S100A8/A8, S100A12, MMP-8, and soluble E-selectin. An increased number of immature $CD16^{dim}$ neutrophils was reported in patients with sJIA. The increased percentage of immature neutrophils in the peripheral blood cell count (banded neutrophils and granulocyte precursors) was confirmed by cytospin (130). Also patients with sJIA had a higher proportion of $CD62L^{low}$ neutrophils compared to healthy controls (129,130). The shedding of CD62L, mediated by membrane-proximal cleavage, reflects a primed phenotype and is often associated with nuclear hypersegmentation (353,737–739). Whereas one study failed to show an increased number of hypersegmented neutrophils, another study showed, by imaging cytometry, that patients with systemically active disease and features of early/subclinical MAS had substantially more hypersegmented neutrophils (129,130). The primed phenotype of the neutrophils was reflected by an increased intracellular *ex vivo* ROS production upon fMLP stimulation and by an enhanced secretory vesicle degranulation. The increased degranulation was demonstrated by the increased surface expression of CD35 and CD64, and by the enhanced release of S100A8/A9 upon PMA stimulation (130). Also in patients with AOSD, an upregulation of CD64 has been reported (740). Neutrophil transcriptome analysis showed an inflammatory gene expression profile. Upregulated genes included neutrophil granule proteins, IL-1 family members, components of inflammasomes, high-affinity IgG receptor CD64, IL-8, and genes involved in the NF-κB pathway. Interestingly, the gene expression profile was overlapping with the transcriptome of sepsis (129,130,589). Remarkably, neutrophil protease genes (including MMP-8, and MMP-9) could also be found in PBMC microarray datasets of sJIA patients and might reflect the presence of LDG in the PBMC fraction, which was confirmed by flow cytometry analysis (589). Remark that also in AOSD, increased levels of LDGs were reported, correlating with disease activity (741). In sJIA, the number of neutrophils was rapidly normalized in inactive patients and after treatment with anakinra (130). A high (immature) neutrophil count was correlated with a good response to anakinra and a short disease duration assuming that the effect of anakinra is mainly due to its effects on neutrophils (45,130). Indeed, IL-1β has been demonstrated as an important cytokine in the priming of neutrophils, and priming of neutrophils could be reverted upon anakinra treatment (130). Also in patients with AOSD, a strongly elevated neutrophil number was associated with an upregulated IL-1 gene expression profile and a pronounced upregulation of canakinumab-responsive genes (742). In addition, S100 proteins have

been proposed as important activators of neutrophils in sJIA. Like LPS, S100 proteins are strong TLR4 activators which may explain the overlapping gene expression profile of sJIA and sepsis (130). Finally, the treatment of patients with sJIA with tocilizumab was also associated with a significantly different neutrophilic gene expression profile (743). The role of neutrophils in the development of sJIA-associated arthritis remains unknown but in RA, it was demonstrated that phagocytes are extensively involved in the synovial inflammation by its release of various pro-inflammatory mediators (386,744,745). Remark that in JIA patients, we recently showed that neutrophils in inflamed joints have an activated phenotype (746). Concluding, neutrophils in sJIA are increased in the circulation and display an activated pro-inflammatory phenotype. However, their extract role in the development of systemic inflammation and arthritis further needs to be elucidated. In this dissertation, we further investigated the role of neutrophils in sJIA using the CFA-based sJIA mouse model. In this model, an increased number of (immature) neutrophils was reported. In contrast to sJIA patients, the model allows us deplete neutrophils, block their development, or study the role of extramedullary myelopoiesis in systemic inflammation.

CHAPTER 3

RESEARCH OBJECTIVES

CHAPTER 3: RESEARCH OBJECTIVES

Autoinflammatory diseases are caused by an abnormal innate immune response, resulting in systemic inflammation (1–3). sJIA is a rare childhood autoinflammatory disease and is characterised by arthritis, fever, rash, lymphadenopathy, hepatosplenomegaly, and weight loss. Patients additionally present with anaemia, thrombocytosis, neutrophilia, and a cytokine storm with high levels of IL-6 and IL-18 (31–33,173). The aetiology of sJIA remains largely unknown but patients follow a biphasic clinical course, in which the innate immune system is mainly involved at disease initiation, followed by activation of the adaptive immune system which is considered to ultimately contribute to the arthritic phenotype (85). sJIA is also associated with potential severe joint damage and severe life-threatening complications including MAS, amyloidosis, and lung disease (31,108,109). About 10 years ago, the treatment of sJIA improved dramatically by the introduction of biologicals targeting either IL-1 or IL-6 (72–83). The efficiency of IL-1 and IL-6 antagonism as a treatment for sJIA patients is beyond question, but a sufficient explanation for its successful effect has not yet been reported. Additionally, some patients do not respond to these therapies or escape after an initial good response. The general aim of this doctoral thesis was **to provide further insights into the pathogenesis of sJIA, focusing on the innate immune system, by using a mouse model of sJIA** that was developed at our laboratory. As described by Avau *et al*. (121), sJIA-like disease can be induced in IFN-γ KO BALB/C mice upon CFA challenge. By using this translational approach, we **focused on neutrophils**, because these cells are considered - but not proven - to play a pathological role in the disease. At the molecular level, we **investigated the innate immune cytokines IL-1β, IL-17, IL-22, and G-CSF**, four cytokines that are strongly associated with innate immune cell activation and highly expressed in the CFA-immunised IFN-γ KO sJIA-like mouse model. Furthermore, we studied **the development of lung complications in our sJIA mouse model**. Three main objectives were addressed in this project (see below). Additionally, **neutrophils were phenotypically and functionally characterised in two pyrin-associated autoinflammatory diseases**: Familial Mediterranean Fever and Pyrin-Associated Autoinflammation with Neutrophilic Dermatosis (**Addendum 2**).

Objective 1: Elucidate the role of IL-1β and IL-22 in the pathogenesis of our sJIA mouse model

IL-1β has been involved in the pathogenesis of sJIA, but its exact role remains unknown. In sJIA patients, therapeutic IL-1 blockade was associated with a reduced IL-17 expression in γδ T cells (147). γδ T cells are an unconventional innate subset of T lymphocytes and are excellent inflammatory cytokine-producing cells (747). Normal levels of γδ T cells have been reported in patients with sJIA, but cells were characterised by an increased protein expression of IL-17. Using our sJIA mouse model, we previously identified IL-17 as a disease-promoting cytokine (121). Since IL-17 can be induced in γδ T cells by IL-1β, we aimed to study the effect of IL-1β neutralisation on γδ T cell (numbers, phenotype and cytokine production) and the development of sJIA (**Chapter 4**). We explored the hypothesis that enhanced production of IL-1β in IFN-γ KO mice, as compared to WT mice, might explain the aggravated phenotype. Next, IL-17 production is often accompanied by the production of IL-22, a cytokine that belongs to the IL-10 superfamily (121,215). IL-22 has both pro- and anti-inflammatory activities and may upregulate the expression of pro-inflammatory molecules or synergise with IL-17 in the production of both IL-6 and G-CSF (211). Increased expression levels of IL-22 are measured in our sJIA mouse model, but its exact role remains unknown. Considering the pathological role of IL-22 in rheumatic disease (*e.g.* by stimulating IL-1β production or by promoting osteoclastogenesis), we wanted to test the relevance of IL-22 in sJIA as a potential new target (**Chapter 4**).

Objective 2: Elucidate the role of neutrophils in the pathogenesis of a sJIA mouse model, and identify factors that drive neutrophilia, and neutrophil subsets formed during extramedullary myelopoiesis

Neutrophils are the most abundant innate immune cells in human circulation (259). These short-lived cells can rapidly infiltrate the site of inflammation (338). Inappropriate activation of neutrophils in sterile settings is described in autoinflammatory disorders and may result in tissue damage. In sJIA, the role of neutrophils in systemic inflammation or arthritis remains largely unknown. Increased numbers of immature and mature neutrophils are reported, and neutrophils show an activated phenotype and inflammatory gene expression (129,130). Here, we hypothesised that neutrophils are involved in the induction of sJIA via the release of inflammatory mediators including IL-1β or S100 proteins, or by their immunosuppressive properties. Using our mouse model, we investigated the exact role of neutrophils in the pathophysiology of sJIA (**Chapter 5**). One way to study the *in vivo* function of neutrophils is by using neutrophil-depleting antibodies, these were tested in our model (**Addendum 1**). Next, we aimed to understand the pro-inflammatory factors that drive the enhanced (extramedullary) myelopoiesis and splenomegaly. Our data suggest an important role for G-CSF since increased plasma levels were measured in patients and our sJIA mouse model (**Chapter 5**). Finally, we characterised the different neutrophil subsets formed during extramedullary myelopoiesis as increasing reports were made describing the existence of distinct neutrophils subsets (264,434–436) (**Chapter 5**).

Objective 3: Elucidate lung complications in our sJIA mouse model

Recently, two studies reported lung complications (including lymphoplasmacytic infiltrates and mixed features of pulmonary alveolar proteinosis and endogenous lipoid pneumonia) in patients with sJIA (108,109). Lung involvement was equally demonstrated in the IFN-γ KO sJIA murine model. To gain understanding of the pulmonary complications in the sJIA mouse model, we studied the different (innate) cell population and cytokines in the lung. Furthermore, we wanted to evaluate lung disease by performing histological and functional measurements in mice upon induction of disease (**Chapter 6**).

CHAPTER 4

IL-1β DRIVES THE PATHOGENESIS OF SYSTEMIC JUVENILE IDIOPATHIC ARTHRITIS-FEATURES BY STIMULATING PRO-INFLAMMATORY IL-17 AND IL-22 EXPRESSION IN MICE

Manuscript in preparation

Bert Malengier-Devlies[1], Eline Bernaerts[1], Kourosh Ahmadzadeh[1], Jessica Vandenhaute[1], Maya Imbrechts[1], Amber De Visscher[1], Tania Mitera[1], Nele Berghmans[2], Louis Boon[3], Paul Proost[2], Laure Dumoutier[4], Carine Wouters[1,5,6], Patrick Matthys[1]

[1]KU Leuven Department of Microbiology, Immunology and Transplantation, Rega Institute for Medical Research, Laboratory of Immunobiology, Leuven, Belgium
[2]KU Leuven Department of Microbiology, Immunology and Transplantation, Rega Institute for Medical Research, Laboratory of Molecular Immunology, Leuven, Belgium
[3]Bioceros, Utrecht, The Netherlands
[4]UCLouvain Faculté de pharmacie et des sciences biomédicales, Institut de Duve, Woluwe-Saint-Lambert, Belgium
[5]University Hospitals Leuven, Division of Pediatric Rheumatology, Leuven, Belgium
[6]European Reference Network for Rare Immunodeficiency, Autoinflammatory and Autoimmune Diseases (RITA) at University Hospital Leuven, Leuven, Belgium

CHAPTER 4: IL-1β DRIVES THE PATHOGENESIS OF SYSTEMIC JUVENILE IDIOPATHIC ARTHRITIS-FEATURES BY STIMULATING PRO-INFLAMMATORY IL-17 AND IL-22 EXPRESSION IN MICE

Abstract

Systemic juvenile idiopathic arthritis (sJIA) is a childhood autoinflammatory disease of unknown aetiology. A pathogenic role of IL-1β has been proposed in the disease since antagonists are successfully being used in the treatment of sJIA. In this study, we took advantage of a mouse model to elucidate the role of IL-1β in the disease pathogenesis. The model is based on injection of complete Freund's adjuvant (CFA) in interferon-gamma (IFN-γ) knock-out (KO) mice thereby developing clinical and haematological features reminiscent of sJIA. We here report on increased levels of active caspase-1 in lymphoid organs of IFN-γ KO mice upon CFA challenge which was associated with increased plasma levels of active IL-1β. Treatment with neutralising anti-IL-1β antibodies inhibited several of the sJIA-like features and significantly reduced the number of $CD27^-$γδ T cells which are major sources of IL-17 and IL-22. While we previously demonstrated a pro-inflammatory role of IL-17 in the sJIA model, we here were also able to show this for IL-22. Translating the findings to the clinic, we found increased plasma levels of active IL-22 in sJIA patients with active disease. On cocultures of human $CD4^+$ T cells or γδ T cells and monocytes, it was found that IL-1β in combination with IL-22 strongly stimulated the production of IL-17. In conclusion, our results provide insights into the mechanism of action of IL-1 in the pathogenesis of sJIA and also explain why IFN-γ KO mice after immunisation with CFA are more prone than wildtype mice to develop autoinflammatory manifestations.

Introduction

Systemic juvenile idiopathic arthritis (sJIA) is a childhood auto-inflammatory immune disorder of unknown aetiology characterised by spiking fever, weight loss, rash, arthritis, splenomegaly, polyserositis, and systemic inflammation. The disease is associated with neutrophilia, leukocytosis, anaemia, and thrombocytosis. Among the different JIA subtypes, it has the highest morbidity since it can lead to a potentially lethal macrophage activation syndrome (MAS) (26,31,34,748). The plasma cytokine profile in sJIA patients shows high levels of interleukin-6 (IL-6), IL-18 as well as elevated levels of the C-reactive protein (CRP) and S100 acute phase proteins S100A8/A9 and S100A12 (749,750). Patients can successfully be treated with IL-1 blocking agents such as the recombinant IL-1 receptor antagonist (IL-1Ra) anakinra and the monoclonal antibody canakinumab, as well as IL-6 blocking agents such as the IL-6 receptor monoclonal antibody tocilizumab. IL-1 antagonism is beneficial especially as first-line therapy, underlining the importance of IL-1β at the disease onset (73,74,751,752). It has been recognised that sJIA follows a biphasic clinical course, in which the innate immune system is mainly involved at disease initiation, followed by the adaptive immune system which ultimately contributes to the arthritic phenotype (753).

Our laboratory has developed a mouse model for sJIA, that rely on the subcutaneous administration of complete Freund's adjuvant (CFA) in the tail of BALB/C mice (121). When CFA is injected in wild-type (WT) mice, the animals develop splenomegaly, lymphadenopathy, neutrophilia, thrombocytosis, and increased cytokine expression. When IFN-γ knock-out (KO) mice are challenged with CFA, they develop these symptoms more pronounced than WT mice and in addition develop weight loss, arthritis, anaemia, hemophagocytosis and show increased levels of interleukin-6 (IL-6). In the tail-draining lymph nodes (LNs), the mutant mice showed increased mRNA expression of IL-17 in both γδ T cells and Th17 cells, which are defined as IL-17 producing CD4+ T cells. Interestingly, the development of sJIA-like haematological and inflammatory changes could be prevented by using IL-17-neutralising antibodies (121,158). In line with our work in mice, Kessel *et al.* reported in sJIA patients an increase in blood γδ T cells with enhanced IL-17 production upon priming with IL-1β (147). Taken together, injection of CFA into IFN-γ KO mice results in a chronic immune condition that closely resembles sJIA in its clinical, haematological, and immune-cellular aspects.

IL-22, previously known as IL-10-related T cell-derived inducible factor, is often co-expressed with IL-17 in activated T cells or γδ T cells (209–212). The cytokine is upregulated in some chronic inflammatory diseases including psoriasis, rheumatoid arthritis (RA), and inflammatory bowel disease (IBD) (225,231,754). Although sJIA, psoriasis IBD and RA partially share pro-inflammatory cytokines involved in their pathogenesis (IL-1β, IL-23, and IL-6) (209,225,231,755–757), the role of IL-22 in the pathophysiology of sJIA remained unexplored. IL-22 signals through a heterodimeric receptor (758) resulting in the activation of proliferative and anti-apoptotic pathways or the induction of tissue-specific genes (234,759). For example, IL-22 may induce the release of antimicrobial peptides and acute phase proteins such as β-defensins or S100 proteins respectively (211,215,225,760). IL-22 can also upregulate the expression of pro-inflammatory molecules and synergise with IL-17 in the production of both IL-6 and G-CSF (209). The activity of IL-22 is tightly regulated by an IL-22 binding protein (IL-22BP), which is a soluble IL-22 receptor, blocking the IL-22 activity (220).

In contrast to the sJIA mouse model, in sJIA patients, no mutations in the genes for IFN-γ or its receptor have been described. At present, it is not clear how the absence of IFN-γ contributes to the sJIA-like phenotype predominantly found in IFN-γ KO mice. In the present study, we explored the hypothesis that enhanced production of IL-1β in IFN-γ KO mice, as compared to WT mice, might be involved. We indeed found enhanced IL-1β processing in the CFA-challenged IFN-γ KO mice and discovered an important upregulation of both IL-17 and IL-22, both playing an important role in the disease pathogenesis. Our findings endorse the relevance of the IFN-γ KO murine model to further unravel pathomechanisms of inflammation in sJIA patients.

Material and Methods

Mice and experimental design

IFN-γ KO and WT BALB/c mice were used for the experiments. Mice were bred under specific pathogen-free (SPF) conditions in the animal house of the REGA Institute for Medical Research, KU Leuven. Six- to 8-week-old mice were subcutaneously injected with CFA (Difco) added with heat-killed Mycobacterium (1.5 mg/ml) as previously described (12). Age- and sex-matched non-injected (NI) WT and IFN-γ KO mice were included as controls. Mice were weighed and examined visually. Inflammation at the injection site was scored (score 0: normal; score 1: redness and/or swelling at tail base; score 2: redness and/or swelling over entire tail; score 3: small wounds; score 4: wounds over entire tail; score 5: necrosis). Mice were euthanised between 16- and 21-days post-CFA-infection on the moment overt signs of inflammation were discernible. By intraperitoneal injection, mice received 200 µg of monoclonal antibodies against IL-1β (Ultra-LEAF Purified anti-mouse/rat IL-1β, clone B122, Biolegend) or against IL-22 (clone AM22.1, kindly provided by L. Dumoutier), twice a week starting on day-1. Mice injected with PBS were included as controls. All experiments were designed randomly and were approved by the Ethics Committee of KU Leuven (P182/2014).

Patients

During the study, 29 sJIA patients and 21 gender- and age-matched healthy controls were recruited. The study was performed at the University Hospital of Leuven, conducted according to the Declaration of Helsinki, and approved by the Ethics Committee of KU Leuven (S58814). The patient classification was based on the criteria of the International League of Associations for Rheumatology (16). Patients were divided according to their disease state into active (18) and inactive (11) patients. A detailed list of patient characteristics can be found in Supplementary Table 4.1. Samples were collected before any therapeutic intervention or at disease flares. Inactive patients were defined by the absence of fever, rash, arthritis, and inflammatory parameters.

Blood analysis and isolation of samples

Murine blood samples were collected by cardiac puncture with heparin (LEO Pharma, 500 IU/ml), complete blood cell analysis was performed with a Cell-Dyn 3700 Hematology Analyser (Abbott Diagnostic). Plasma was obtained and stored (-80°C) within two hours. Spleen and two inguinal LNs were weighed and passed through a cell-strainer (pore size 70 µm, BD Biosciences) to obtain single-cell suspensions. Red blood cells were lysed using Ammonium-Chloride-Potassium lysis buffer (Gibco). The patient's plasma was separated by centrifugation and stored (-80°C) within two hours after withdrawal of EDTA-anticoagulated blood. Human PBMCs were obtained by Pancoll density centrifugation and frozen in liquid nitrogen in cryopreservation medium (90% FCS, 10% DMSO).

Antibodies, flow cytometry, and FACS sorting

Cells were incubated with FcR-block (Miltenyi Biotec) and stained extracellularly in FACS buffer (PBS +2% FCS +2mM EDTA). The following antibodies were used in this study: γδ-TCR (GL3), CD11b (M1/70), CD122 (TM-β1), CD19 (6D5), CD3 (145-2C11), CD4 (RM4-5), CD49 (DX5), CD8 (53-6.7), Ly6C (HK1.4), Ly6G (1A8). For intracellular cytokine staining, cells were stimulated for 4-hours in RPMI + 10% FCS supplemented with 0.50 µg/ml phorbol 12-myristate 13-acetate (Sigma) and 0.75 µg/ml ionomycin (Sigma) in the presence of Brefeldin A (GolgiStop, 2 µg/ml, Biotechne). Unstimulated cells were used as negative controls for the cytokine staining. After the surface staining, cells were fixed and permeabilised using the Cytofix/Cytoperm kit (BD Bioscience) and stained intracellularly with the following antibodies: IL-17 (eBio17B7), IL-22 (1H8PWSR), FOXP3 (150D). All antibodies were obtained from Biolegend, eBioscience, or BD Biosciences. Before lineage gating, all populations were first gated on live cells by using Zombie Aqua 516 (Biolegend) or DAPI (Sigma). Forward and side scatter was used to limit debris and doublets. Cells were run on a BD LSRFortessa X20, a BD FACSymphony or on a BD FACS Aria III sorter equipped with the DIVA software. FACS data were analysed using FlowJo software (LLC, V10).

Cell enrichment

γδ T cells, CD4+ T cells, and monocytes were enriched from healthy donor PBMCs using the EasySep Human Gamma/Delta T cell Isolation Kit, the EasySep Human CD4 Positive Selection Kit II, and the

EasySep Human CD14 Positive Selection Kit II (all from Stemcell Technologies), according to the manufacturer's protocols.

***In vitro* T cell stimulation**

γδ T cells and CD4+ T cells (2x104 cells) were cultured alone or cocultured with heterologous monocytes (4x104 cells) in RPMI-1640 medium containing 10% FCS, penicillin (100 U/ml) and streptomycin (100 U/ml) at 37°C and 5% CO2. The medium was supplemented with IL-2 (100 units/ml, PeproTech). Cells were left unstimulated or were stimulated with combinations of lipopolysaccharide (LPS) (100 pg/ml, Sigma), recombinant IL-18 (10 ng/ml, MBL), IL-1β (10 ng/ml, PeproTech) or IL-22 (25 ng/ml, PeproTech) and/or anti-CD3/CD28 beads (10 µl/ml, Invitrogen). On day 3 and day 6 cultures were supplemented with 100 units/ml of recombinant IL-2. After 7 days, the supernatant was harvested, cleared from remnant cells, and analysed for cytokine expression using an ELISA assay as described below.

qRT-PCR

According to the manufacturer's protocol, total RNA was extracted using the PureLink RNA Mini kit (Invitrogen) or the RNeasy Micro kit (Qiagen), followed by the preparation of complementary DNA (cDNA) using Superscript II reverse transcriptase and random primers (Invitrogen). Real-time (RT) quantitative (q)PCR was performed using a TaqMan gene expression assay (Applied Biosystems) on a 7500 Real-Time PCR System Apparatus. The primer against IL-22 (Mm00444241_m1) was obtained from Thermo Fisher and RNA expression was normalized to the expression of GAPDH RNA (Mm99999915_g1) (primer from Integrated DNA Technologies) according to the delta-delta CT method.

Histologic cytospin analysis

For cytospin preparations, single-cell suspensions were spun on a glass slide and stained with haematoxylin and eosin (H&E).

ELISA, multiplex, and western blot

Mouse plasma cytokines were measured with a ProcartaPlex multiplex immunoassay (eBioscience) according to the manufacture's protocol. Meso Scale Discovery (MSD, Meso Scale Diagnostics, LLC) was used to measure human plasma cytokines according to the manufacturer's protocol. The ELISA MAX Deluxe Set Human IL-17A (Biolegend) was used to measure IL-17 levels in the supernatant of stimulated cells.

Splenocytes were lysed in RIPA buffer. Samples were centrifuged (15 min, 12000 g, 4°C) and the supernatant was used for further analysis. Protein concentration was quantified using a Bradford assay (Biorad). Protein samples (100 µg/lane) were resolved by a 16% Tris-Glys gel (Invitrogen) and then transferred to a polyvinylidene fluoride membrane. Monoclonal detection anti-IL-1β (DuoSet ELISA, R&D) and rat anti-Caspase 1 (Clone 5B10, Thermofisher) antibodies were incubated overnight after blocking with 5% NFDM. Streptavidin-HRP or horseradish peroxidase-conjugated anti-rat (Jackson) were incubated for 1 hour at RT. Signals were visualised by chemiluminescence detection using SuperSignal (Thermofisher) using the Fusion Solo S (Vilber).

Luciferase assay

The IL-22 activity was assessed by measuring the luciferase activity in cells transfected with the pGRR5 construct as previously described by Dumoutier *et al.* (220).

Statistical analyses

The two-tailed non-parametric Mann-Whitney U test was used for all single comparisons of two unpaired groups. For data with three or more groups, the non-parametric Kruskal-Wallis test (unpaired data) or Friedman test (paired data) was used and was followed by a Mann-Whitney U test. All data analysis was performed using the GraphPad Prism 7 software.

Results

Increased levels of active IL-1β are found in CFA-challenged IFN-γ KO mice, which are rescued from clinical and haematological abnormalities upon IL-1β neutralisation

Although IL-1β levels are hardly detected in patient sera, IL-1β is considered as one of the driving factors in the pathogenesis of sJIA, which is clearly demonstrated by the beneficial effects of anti-IL-1β treatment in patients. IL-1β is produced as an inactive precursor, termed pro-IL-1β, and needs to cleaved by theIL-1β-processing enzyme caspase-1. Caspase-1 in turn first needs to be cleaved - in an inflammasome-dependent way - from its pro-caspase 1 into its 20 kDa active form. By western blot (WB), splenocytes lysate was tested for the presence of inactive pro-IL-1β and active IL-1β, as well as of the activation state of caspase-1. Splenocytes derived from non-immunised mice (NI) contained only pro-caspase-1 and pro-IL-1β. Upon CFA-immunisation, splenocytes from WT mice showed a few processed intermediate forms of caspase-1. In contrast, splenocytes of immunised IFN-γ KO mice contained multiple processed intermediate form of caspase-1 as well as the 20 kDa chain of its active forms. Concordantly, higher active caspase-1 levels were accompanied by a conversion of pro-IL-1β into active IL-1β (Figure 4.1A). Next, plasma IL-1β-levels were measured by ELISA. In line with the increased activation of IL-1β found in CFA-immunised IFN-γ KO mice, a significantly increased plasma level of IL-1β was measured in the immunised IFN-γ KO mice as compared to WT counterparts (Figure 4.1A). These observations demonstrate that the development of sJIA-like features in IFN-γ KO mice is associated with the activation of caspase-1 and the proteolytic maturation of IL-1β.

To investigate the role of IL-1β in the pathogenesis of sJIA, CFA-challenged IFN-γ KO mice were treated with neutralising anti-IL-1β antibodies, starting one-day prior immunisation. Compared to PBS control-treated mice, anti-IL-1β antibodies prevented weight loss. Rash was assessed by the amount of overt tail inflammation (scoring is described in M&M). The highest score was measured in the CFA-immunised IFN-γ KO control-treated mice. Tail inflammation was significantly diminished by treatment with anti-IL-1β (Figure 4.1B). On day 16 post-CFA challenge mice were sacrificed. No significant decrease in splenomegaly nor in lymphadenopathy was measured in the anti-IL-1β-treated mice (Figure 4.1B). Haematological examination revealed a significantly reduced neutrophilia and thrombocytosis in the anti-IL-1β treated group when compared to the PBS-treated immunised IFN-γ KO mice (Figure 4.1C). In contrast, the lymphocyte count was not altered (Figure 4.1C). Anaemia was assessed by the number of red blood cells (RBCs), but no anaemic mice were found (data not shown). The plasma levels of IL-6 showed a non-significant reduction upon treatment with anti-IL-1β towards the level found in the CFA-immunised WT mice (Figure 4.1C). In conclusion, IL-1β neutralisation reduced some of the clinical symptoms and laboratory abnormalities of sJIA mice to the level of those found in WT mice.

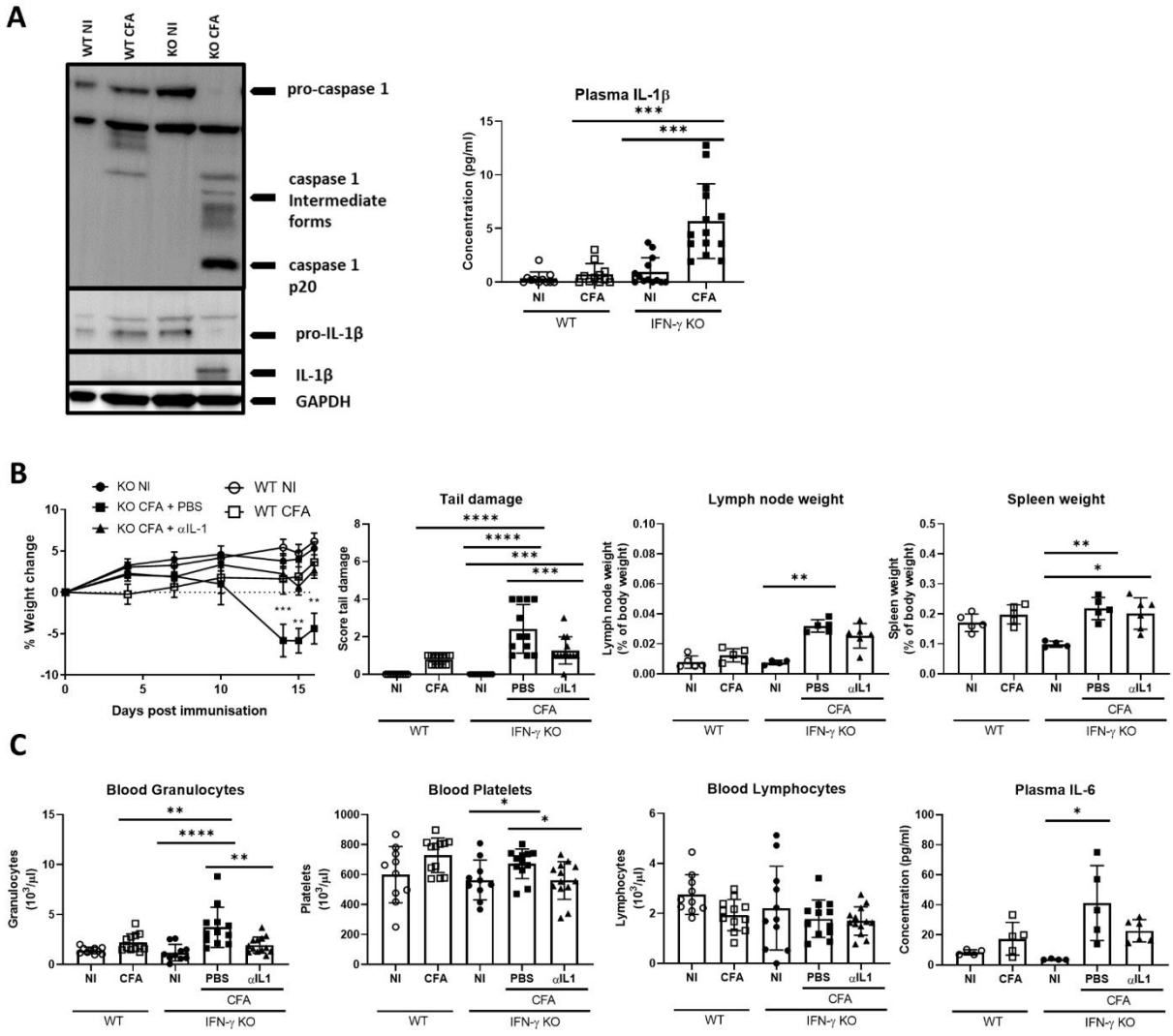

Figure 4.1. Increased levels of active IL-1β in CFA-challenged IFN-γ KO mice, which are rescued from clinical and haematological abnormalities upon IL-1β neutralisation

(A) The differential expression of the caspase-1 and IL-1β-isoforms in CFA-challenged wild-type (WT) and interferon-gamma (IFN-γ) knock-out (KO) mice at day 21 post-immunisation were compared to non-immunised (NI) littermates Within each group, splenocyte suspensions of three mice were pooled and lysed. Total protein (100 µg) was loaded for electrophoresis and blotted. The blotting membrane was incubated with an anti-caspase-1 antibody and anti-IL-1β antibody (as described in M&M). Caspase-1 isoforms: inactive pro-caspase-1, intermediate caspase-1 form and the active 20 kDa form (p20). IL-1β-isoformes: inactive IL-1β and active IL-1β. Expression of GAPDH was used as a loading control. Plasma IL-1β levels were measured by ELISA. (B) IFN-γ KO mice were injected with CFA alone or in combination with IL-1β-neutralising antibodies. 200 µg of anti-IL-1β (αIL-1β) was injected twice a week, one-day prior immunisation. Naïve (NI) IFN-γ KO and CFA-challenged or NI WT mice were included as controls. Percentage change in body weight and inflammation at the tail was scored as described in M&M. Lymph node (LN) weight and spleen weight was expressed as a percentage of total body weight. (C) Granulocyte count, platelet count and lymphocyte count in blood samples were measured with the blood cell analyser. ELISA measured plasma IL-6 levels. Graphs show results from two experiments, in which mice were analysed at day 17 p.i.. Dots represent individual mice, horizontal bars represent mean group values with standard error (SE). * p<0.05; ** p<0.01; *** p<0.001; **** p<0.0001 between indicated groups, by Kruskal-Wallis followed by a Mann-Whitney U test.

Reduced extramedullary myelopoiesis and reduced numbers of γδ T cells in anti-IL-1β-treated mice
Since CFA-immunisation is associated with important myelopoiesis in the spleen (761), flow-cytometric analysis of the splenocytes was performed. The analysis revealed non-significantly decreased percentages and absolute number of CD11b+Ly6G+ neutrophils and CD11b+Ly6C+ monocytes in the mice treated with anti-IL-1β when compared to PBS-injected mice (Figure 4.2A). Cytospin preparations of the spleen confirmed the reduced number of neutrophils and showed a shift toward more mature neutrophils at the expense of immature neutrophils having a banded circular and non-segmented nuclear morphology (Figure 4.2A). Next, flow-cytometry on LNs revealed no differences in the number of T lymphocytes nor the number of B cells between the anti-IL-1-treated and the PBS-treated immunised IFN-γ KO mice (Figure 4.2B). Interestingly, the absolute number of γδ T cells was significantly decreased in mice treated with anti-IL-1β as compared to the PBS-treated control group. Remark that the main reduction was seen in the CD27 negative γδ T cells (Figure 4.2B), which are known to be the IL-17 cytokine-producing subset. In conclusion anti-IL-1β affected in spleen tissue the myelopoiesis (although not significantly) and in LNs the γδ T.

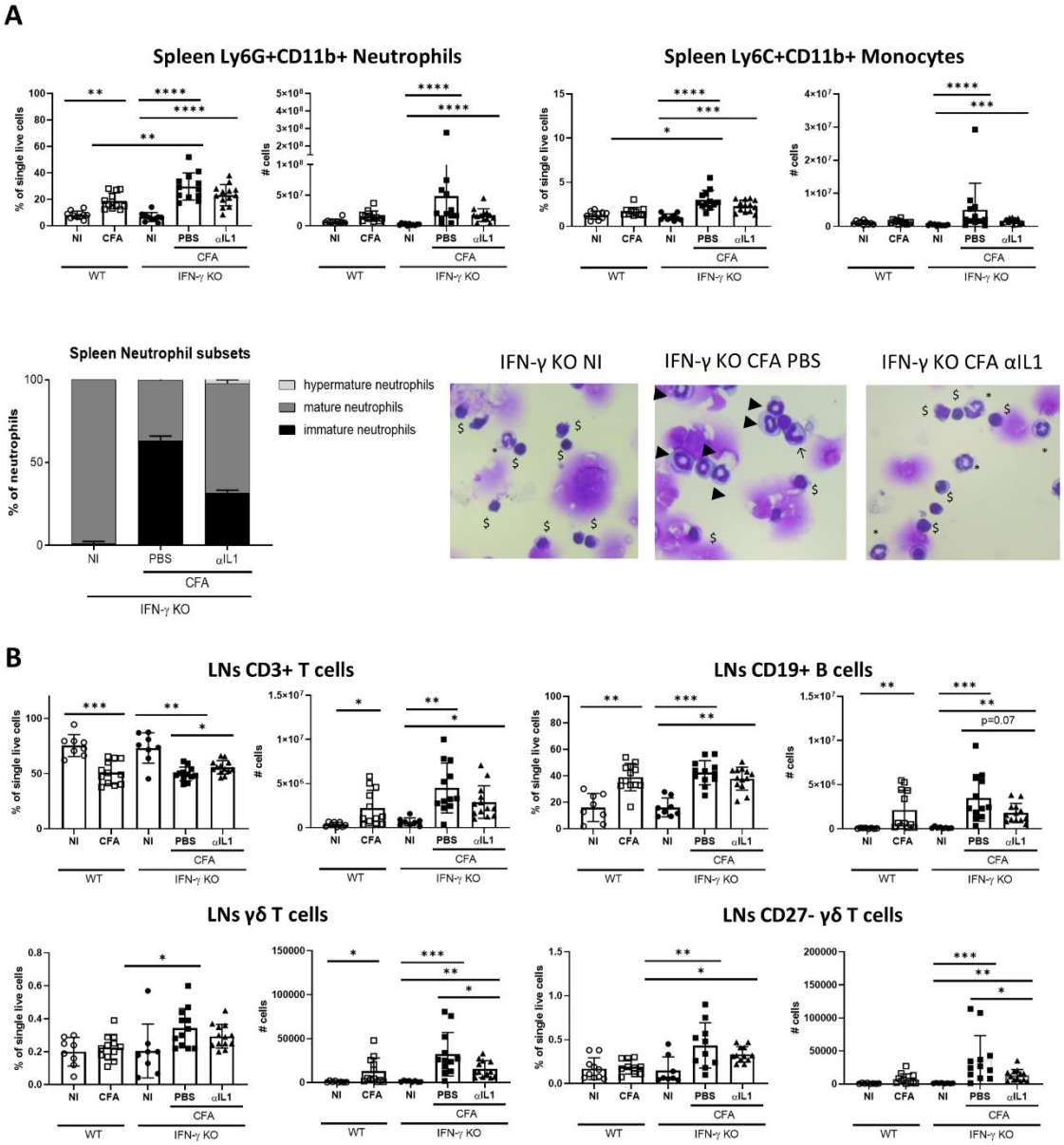

Figure 4.2. Splenocyte and lymph node cell number upon anti-IL-1β-treatment in CFA-challenged IFN-γ KO mice show reduced extramedullary myelopoiesis and reduced numbers of CD27 negative γδ T cells.

IFN-γ KO mice were injected with CFA alone or in combination with IL-1β-neutralising antibodies as described in legend of Figure 4.1. (A) Splenocytes were analysed by flow cytometry and cytospin. Absolute number and percentage of CD11b+Ly6G+ neutrophils and CD11b+Ly6C+ monocytes. Neutrophil subtypes were counted on cytospin. Representative cytospin photographs are shown (mature neutrophils (asterisk), immature neutrophils (arrow point), monocytes (arrow), lymphocytes (dollar sign)). (B) Lymph node cells were analysed by flow cytometry. Absolute number and percentage of CD3+ T cells, CD19+ B cells, CD3+γδTCR+ γδ T cells and CD27- γδ T cells. Graphs show results from two experiments, in which mice were analysed at day 17 p.i.. Dots represent individual mice, horizontal bars represent mean group values with standard error (SE). * p<0.05; ** p<0.01; *** p<0.001; **** p<0.0001 between indicated groups, by Kruskal-Wallis followed by Mann-Whitney U test.

IL-22 levels are increased in CFA-challenged IFN-γ KO mice and IL-22 neutralisation is associated with a partial reduction of sJIA disease symptoms

By qPCR on sorted LNs cells, we previously demonstrated that CD4+ T cells and γδ T cells are important sources of IL-17 in the CFA-immunised IFN-γ KO mice (121). In the present study, we analysed cytokines at the protein level by performing intracellular flow cytometry stainings. As can be seen in Figure 4.3A (left), we confirmed that the highest IL-17-expressing cells relative to all live lymph node cells were CD4+ T cells and γδ T cells in IFN-γ KO mice and to a much lesser extend in WT mice. When positive cells were calculated within each population, around 80% of the γδ T cells were positively stained for IL-17 in IFN-γ KO mice versus 40% in WT animals (Figure 4.3A right). In addition to IL-17, CD4+ T cells and γδ T cells also expressed IL-22 (Figure 4.3B). The percentages of IL-17- and IL-22-positive cells within all other investigated cell populations stayed below 4%. The enhanced cytokine expression of IL-22 was confirmed by real-time quantitative PCR specially the LNs and to a smaller extent in the lungs (Figure 4.3C). In the blood of CFA-challenged IFN-γ KO mice, increased plasma levels of IL-22 were determined compared to naïve control mice and CFA-challenged WT mice (Figure 4.3D). To understand the role of IL-22 in our mouse model, we analysed the effect of IL-22 neutralisation on the observed disease symptoms. Antibodies against IL-22 were administered on day -1, 3, 10, and 13 in CFA-challenged IFN-γ KO mice. This prophylactic treatment with anti-IL-22 antibodies could partially prevent disease symptoms. Initially, treated mice did not lose weight and showed reduced signs of skin inflammation around the tail (Figure 4.3E). Mice were sacrificed on day 17. No differences were found in either lymphadenopathy or splenomegaly (Figure 4.3F). Blood analysis showed that anti-IL-22 antibodies counteracted neutrophilia and thrombocytosis. No improvement of the lymphocytopenia was seen in CFA-injected mice (Figure 4.3G), nor differences in RBC count were found upon IL-22-neutralisation when compared to PBS-treated control mice (data not shown). Anti-IL-22 antibody treatment did not affect IL-6 levels in plasma (Figure 4.3H). Two follow-up experiments were performed, starting treatment at either day 5 or day 12. This confirmed the reduced weight loss, number of granulocytes, platelets. Nevertheless, a more pronounced effect was seen during early treatment, suggesting that IL-22 mainly plays a role during disease onset (data not shown). Taken together, increased IL-22 levels are measured in CFA-immunised IFN-γ KO mice and were mainly produced by CD4+ T cells and γδ T cells. Neutralisation of IL-22 in CFA-challenged IFN-γ KO mice – especially during early stages- results in partial inhibition of development of sJIA.

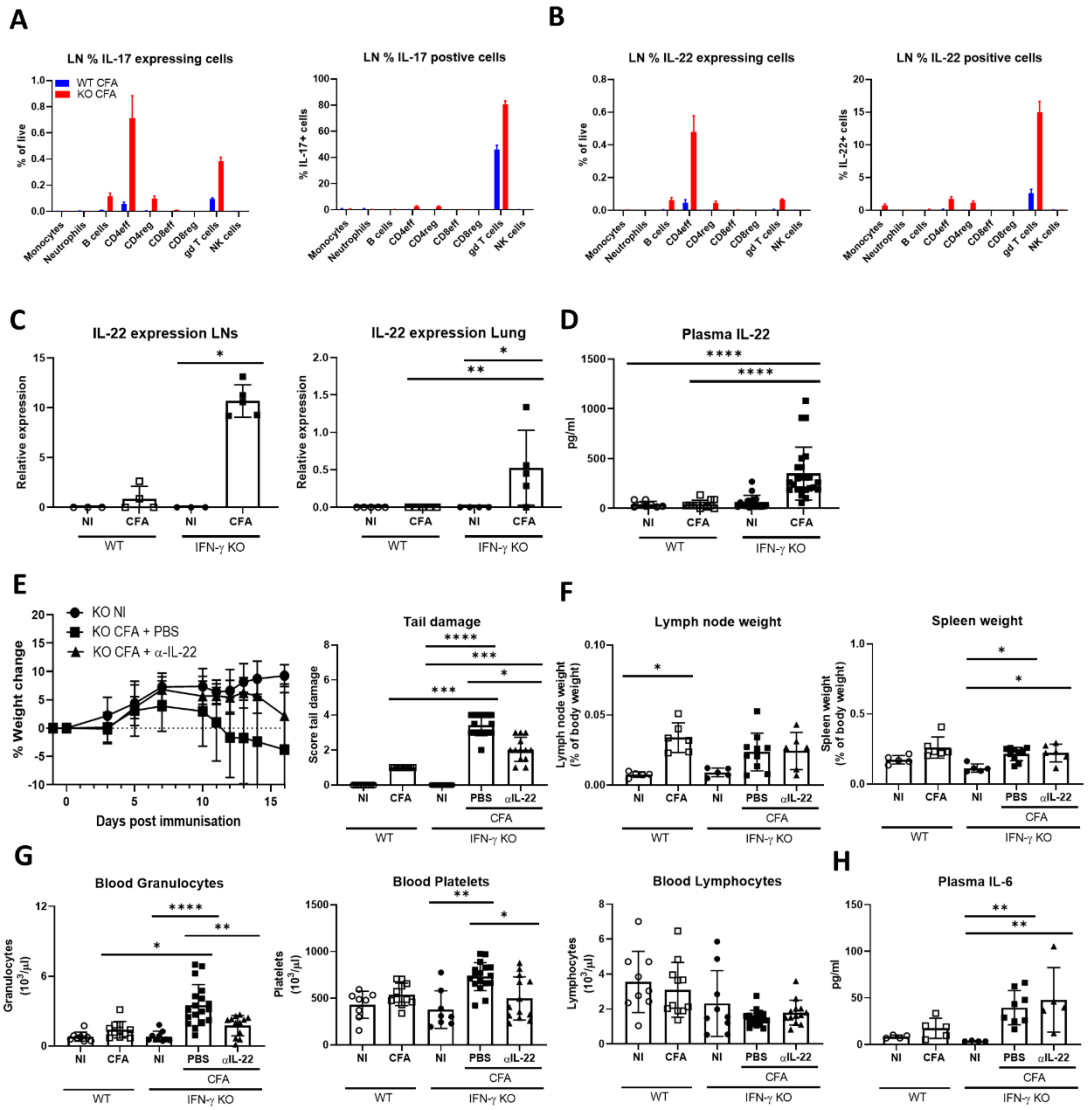

Figure 4.3. Increased IL-22 in CFA-challenged IFN-γ KO mice plays a partial role in the sJIA-like disease symptoms

IFN-γ knock-out (KO) mice and wild-type (WT) mice were either or not immunised with CFA. (A-B) IL-17 and IL-22 cytokine production was measured by intracellular flow cytometry in CD11b+Ly6C+ monocytes, CD11b+Ly6G+ neutrophils, CD19+ B cells, CD3+CD4+ T effector (CD4eff) cells, CD3+CD4+FoxP3+ regulatory T (CD4reg) cells, CD3+CD8+ T effector (CD8eff) cells, CD3+CD8+FoxP3+ regulatory T (CD8reg) cells, CD3+γδTCR+ γδ T cells and CD3-DX5+CD122+ NK cells. Data shows the percentage of IL-17 or IL-22 positive cells relative to all live cells (left) or within each cell population (right). (C) Expression levels of IL-22 were measured by RT-qPCR in the lymph nodes (LNs), and lungs. (D) Plasma levels of IL-22 were measured by ELISA. (E-H) IFN-γ KO mice were injected with CFA alone or in combination with IL-22-depleting antibodies. 200 µg of anti-IL-22 (αIL-22) was injected twice a week starting one day before immunisation. Non-injected (NI) IFN-γ KO and CFA-challenged or NI WT mice were included as controls. (E) Percentage change in body weight and inflammation at the tail was scored. (F) Lymph node weight and spleen weight were expressed as a percentage of total body weight. (G) Neutrophil count, platelet count and lymphocyte count in blood samples were measured with the blood cell analyser. (H) ELISA measured plasma IL-6 levels. Graphs show results from two experiments, in which mice were analysed at day 17 p.i.. Dots represent individual mice, horizontal bars represent mean group values with standard error (SE). * p<0.05; ** p<0.01; **** p<0.0001 between indicated groups, by Kruskal-Wallis followed by a Mann-Whitney U test.

Active-sJIA patients have increased plasma levels of active IL-22, potentiating the release of IL-17 from CD4+ T cells and γδ T cells

Finally, we wanted to test whether the observations made in mice could be translated to the clinical situation. Our study included three groups: a sJIA patient-group with active disease, a sJIA patient-group with inactive disease (after treatment), and a control group consisting of age- and gender-matched healthy controls (HC). The disease activity parameters of the recruited patients and HCs at the time of the study are shown in Supplementary Table 4.1. Clinical features and laboratory parameters were determined and the levels of twenty-two inflammatory cytokines were analysed in the plasma. Increased plasma levels of IL-6, IL-18, and CRP (published data) were found in the active sJIA patients (158). In contrast to another study (45), we were not able to confirm an increased plasma level of IL-17 in the active sJIA patient group (data not shown). A non-significant increased IL-22 level was seen in the plasma of the active sJIA patient group compared to the control groups (Figure 4.4A). Next, using a bioassay, we measured the amount of active IL-22 and showed a significantly increased IL-22 activity in the active sJIA patient group compared to either the inactive patient-group or the HCs (Figure 4.4B).

Kessel *et al.* showed that γδ T cells from patients with sJIA are primed to produce IL-17. In their study, they demonstrated that co-cultures of monocytes and γδ T cells in a sJIA-cytokine environment could cause this priming effect. Especially IL-1β was found as a driving factor and the use of canakinumab, a monoclonal antibody blocking IL-1β in patients, could abolish this effect (147). To test whether IL-22 could potentiate the release of IL-17, co-cultures were made from healthy donor γδ T cells or CD4+ T cells and monocytes. IL-22 alone could not promote the secretion of IL-17. Interestingly, the addition of IL-22 with IL-1β or IL-18 did increase IL-17 secretion in CD4+ T cells. Furthermore, this increased IL-17 secretion was even more pronounced in the γδ T cells. In our co-culture experiments, LPS was used as a positive control to produce IL-17 (Figure4C-D). This data shows increased levels of active IL-22 in patients with sJIA. In the sJIA inflammatory environment, IL-22 may synergise to induce the production of IL-17 by CD4+ T cells and γδ T cells.

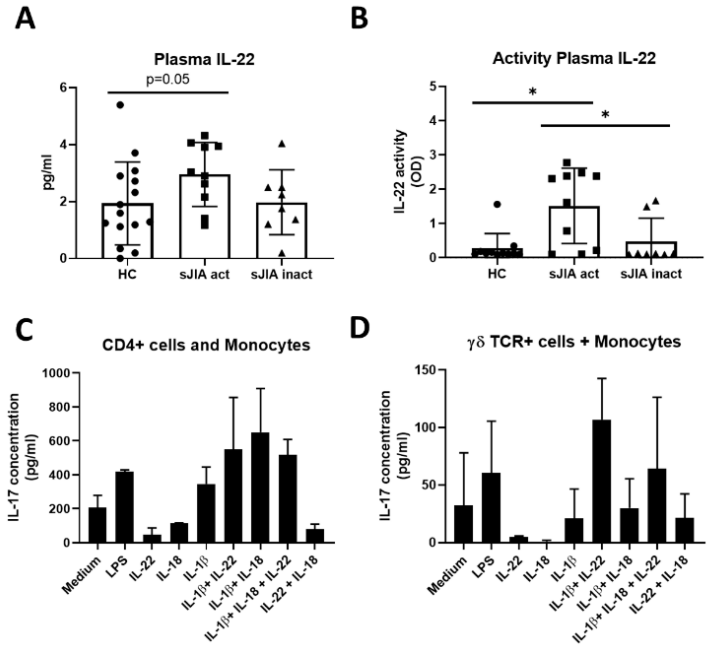

Figure 4.4. Plasma levels of active IL-22 levels are increased in patients with sJIA and active IL-22 can potentiate the release of IL-17 from healthy CD4+ T cells and γδ T cells

(A) Levels of IL-22 in plasma of healthy controls (HC) and patients with active and inactive sJIA. (B) IL-22 activity in HC, active and inactive sJIA patients. Dots represent individual patients, horizontal bars represent mean group values with standard error (SE). Results are from one experiment only. (C-D) Healthy donor (C) CD4+ T cells or (D) γδ T cells together with heterologous monocytes and IL-2 were left unstimulated or were stimulated with recombinant IL-18 (10 ng/ml), IL-1β (10 ng/ml), IL-22 (25 ng/ml) or LPS (100 pg/ml) as described in M&M. On day 6, levels of IL-17A in culture supernatants were quantified by ELISA. Horizontal bars represent mean group values with standard error (SE). * p<0.05 between indicated groups, by Kruskal-Wallis followed by Mann-Whitney U test or Wilcoxon matched-pairs signed-rank test.

Discussion

Systemic juvenile idiopathic arthritis (sJIA) is an autoinflammatory childhood immune disorder, thought to be caused by an excessive inflammatory immune reaction to a generally harmless trigger in predisposed children. We previously demonstrated that injection of IFN-γ KO mice with CFA, an adjuvant containing heat-killed mycobacteria, leads to a chronic immune syndrome with clinical and pathological features reminiscent of sJIA, including a storm of pro-inflammatory cytokines. In the model, IL-17 and IL-23 have been demonstrated as important driving factors as the use of neutralising antibodies against IL-17 or IL-12/IL-23p40 can cause amelioration of the disease symptoms (121,158).

Although the model is a clinically relevant animal model of sJIA, its applicability may be disputed given the absence of documented IFN-γ mutations in sJIA patients. The exact role of IFN-γ in patients with sJIA requires further research but its role is expected to be limited since the transcriptome analysis of peripheral blood mononuclear cells (PBMCs) in patients with sJIA showed an absence of IFN-γ upregulated genes, which is a remarkable observation considering the inflammatory nature of the disease (126,152,174). In our previous manuscripts, we demonstrated that susceptibility of IFN-γ KO mice to develop sJIA could at least partially, be explained by acquired defects in IL-10 production as IL-10 defects were found in B cells, regulatory T (Treg) cells, and natural killer (NK) cells (158). This defect in NK cell IL-10-production may be in line with the general NK cell defects seen in the absence of IFN-γ. Also, patients with sJIA show a decreased number of NK cells (126,138–140,144), aberrant NK cell phenotypes (137,142), or a defective NK cell function (137,139,140,143,144) The important regulatory role of NK cells in the prevention of sJIA has recently been described in our mouse model (257).

In the current manuscript, we point toward another important feature of the IFN-γ KO mice that could explain why these mice are more prone to develop sJIA-like features. We showed that IFN-γ KO mice, in contrast to WT mice, have increased conversion of pro-IL-1β into active IL-1β. This was associated with increased plasma levels of IL-1β in CFA-immunised IFN-γ KO mice. Multiprotein complexes called inflammasomes mediate this processing in a caspase 1-dependent way (762). Increased caspase-1 activation was seen upon CFA immunisation in IFN-γ KO mice when compared to WT mice. These results are in line with *in vitro* studies in mice, showing that IFN-γ could inhibit the production of IL-1β by blocking the transcription or the NLRP3 inflammasome-dependent activation of IL-1β in a STAT-1- or NO-dependent way (763–766). Also in the collagen-induced arthritis (CIA) model, a mouse model to study rheumatoid arthritis (RA), IFN-γR KO mice had increased levels of active caspase-1 and IL-1β, which were associated with a higher susceptibility to develop arthritis (767). In general, increased caspase-1 activation may explain why IFN-γ-ablated mice are more prone to develop various autoimmune and autoinflammatory diseases. This contrasts with *in vitro* studies performed in human cells, showing that IFN-γ rather potentiates the release of IL-β. The different regulation of IFN-γ-induced IL-1β release and its impact on IL-17 production between different species has been demonstrated and could explain the discrepancy seen between men and mice (764).

In the next step, we studied what role the increased IL-1β levels have in our CFA-challenged IFN-γ KO mice. Multiple sJIA symptoms can be explained by the overexpression of IL-1β including neutrophilia, thrombocytosis, cutaneous rash, and recurring fever due to the induction of PGE2 (prostaglandin E2). Besides this, IL-1β can induce the production of acute-phase proteins by hepatocytes, including IL-6. Furthermore, IL-1β can mediate bone erosion and cause arthritis (20,767–770). In patients with sJIA, associations with polymorphisms in genes of the IL-1 family have been found (174). The striking indication that IL-1β drives the pathogenesis of the disease came from the effective treatment nowadays using IL-1 targeting agents such as anakinra and canakinumab (74,171,751,771–774). In this manuscript, we showed that neutralisation of IL-1β by means of anti-IL-1β-neutralising antibodies in CFA-immunised IFN-γ KO mice, resulted in an alleviation of disease symptoms. Anti-IL-1β-injected mice presented with a reduced wasting and local inflammation. Furthermore, anti-IL-1β-treatment reduced neutrophilia, and thrombocytosis towards the level of CFA-challenged WT mice. Interestingly, IL-1β neutralisation reduced the amount of immature, band-shaped neutrophils, and instead, more mature

neutrophils were found on cytospin preparations of the spleen. Also in humans, increased numbers of banded $CD16^{dim}$ immature neutrophils were described in active patients with sJIA, which could be reduced upon anakinra treatment (129,775).

IL-1β-neutralised mice showed an important decrease in the number of γδ T cells - mainly cytokine-producing CD27 negative γδ T cells – that were measured in the lymphoid organs upon anti-IL1β-treatment. In several inflammatory conditions, including mycobacterial infections, RA, and psoriasis, it has been described that γδ T cells dominate an initial IL-17 response (776–778). This IL-17 production may promote an amplification loop further inducing Th17 cells (170). As IFN-γ induces STAT1 signalling and subsequently impair Th17 development, it may also explain why IFN-γ KO mice are more prone to develop sJIA (121,779). Although we previously showed that the CFA-induced disease symptoms are mediated by IL-17 in the sJIA mouse model, the role of the cytokine in patients is less clear. Increased plasma levels of IL-17 have been described in active patients with sJIA, but was not always confirmed (45,147,152). In patients, the number of CD4+ cells were found to be normal or slightly increased whereas γδ T cell numbers were decreased compared to healthy controls. Nevertheless, both Th1 and Th17 subpopulations were enriched in the peripheral blood of sJIA patients. Interestingly, Kessel *et al.* showed that γδ T cells isolated from patients with sJIA have an increased IL-17 secretion upon stimulation with S100 or TLR4 ligands. Furthermore, they showed that the serum of patients was sufficient to induce this increased secretion in γδ T cells of healthy controls. They also showed that this increased cytokine expression appeared to be partially sensitive to anti-IL-1 treatment, as neutralising free IL-1β with canakinumab could reduce the increased IL-17 secretion (147,162). Additionally, the synovial fluid of JIA patients contained elevated levels of CCL20, a chemokine able to attract CCR6-expressing IL-17 producing γδ T cells from the blood into the synovium of the inflamed joints whey they may drive local inflammation and cause active disease (780).

In addition to the important role of IL-1β, we point in this manuscript towards another potential pro-inflammatory mediator, IL-22, driving the pathogenesis of sJIA. Increased plasma levels of IL-22 were measured in the CFA-challenged IFN-γ KO mice, which were mainly produced by CD4+ T cells from the LNs. In patients with active sJIA, we showed non-significant increased levels of IL-22. However, since the activity of IL-22 is regulated by the balance of IL-22 and IL-22BP, it was more relevant to measure IL-22 activity (220,781). We found increased concentrations of active IL-22 in active sJIA patients compared to inactive patients or healthy controls. Remark that this should be validated in a bigger cohort of patients. It is interesting to point out that increased levels of active IL-22 in sJIA may be a consequence of their high IL-18 blood levels, as IL-18 downregulates IL-22BP (221,224). Vice versa, active IL-22 can upregulate the levels of IL-18 by enhancing the expression of pro-IL-18 in human keratinocytes and murine intestinal epithelial cells (222–224).

To study the *in vivo* role of IL-22 in sJIA, we neutralised IL-22 using anti-IL-22-neutralising antibodies. This allowed us to study the effect of the IL-22 pathway without influencing the IL-17A pathway. The neutralising experiments revealed a reduced wasting, local inflammation, granulocytosis, and thrombocytosis when compared to PBS-treated control mice. The reduced neutrophilia could be linked to the synergistic effect that has been described between IL-22 and IL-17 in stimulating epithelial cells to produce CXCL1 and CXCL2 in mice (or IL-8 in humans), which are the most important neutrophilic chemotactic factors (209,215). Neutralisation of IL-22 also may lead to a reduced IL-1β gene expression, which in turn may prevent further Th17 or γδ T cell activation. IL-22 neutralisation could only partially reduce the sJIA-like disease symptoms and was mainly effective at the early stages of the disease. Therefore, we concluded that IL-22 is rather enhancing sJIA than causing it. *In vitro* stimulation of human CD4+ T cells or γδ T cells with IL-22 showed that IL-22 could enhance the secretion of IL-17 when combined with the main pro-inflammatory sJIA mediators IL-1β or IL-18. It is however currently unknown whether this is a direct or indirect effect. Indirectly, IL-22 may enhance the secretion of S100A8 (calgranulin A) or S100A9 (calgranulin B) proteins, which were recently shown as important

inducers of γδ T cell IL-17-production and which are highly elevated in patients with sJIA (147). IL-22 may also enhance the lifespan of the cells which may explain the enhanced IL-17 secretion levels.

A biphasic sJIA disease model has been proposed by Nigrovic *et al.* The inflammatory phase is believed to be driven by the innate immune system whereas the seconded arthritic phase by the adaptive immune system. In this biphasic model, a "window of opportunity" has been proposed (753). Early treatment with biologicals agents, especially IL-1-targeting agents, may be effective in the early febrile innate-immunity driven phase, avoiding the chronic arthritic state. A recent paper indeed confirmed this hypothesis since first-line treatment with anakinra could prevent damage and functional limitations and could avoid an excessive glucocorticoid treatment. In more than half of the patients, inactive disease could be achieved within the first year of therapy (74). Our manuscript further broadens our knowledge in the pathophysiology of sJIA. In summary, our mouse model strengthens an early important role of IL-1β in the IL-17 and IL-22 expression of γδ T cells and CD4+ T cells, driving the pathogenesis of sJIA. Figure 4.5 summarises the main findings of this manuscript, supplemented with data from literature. Note that targeting IL-22 or its binding partner could potentially be used as a new therapeutic option. Currently, a phase II clinical trial on fezakinumab (an IL-22 neutralising antibody) in atopic dermatitis patients is tested (782). Whether targeting IL-22 could be used in the therapy of sJIA is an interesting area for further investigation.

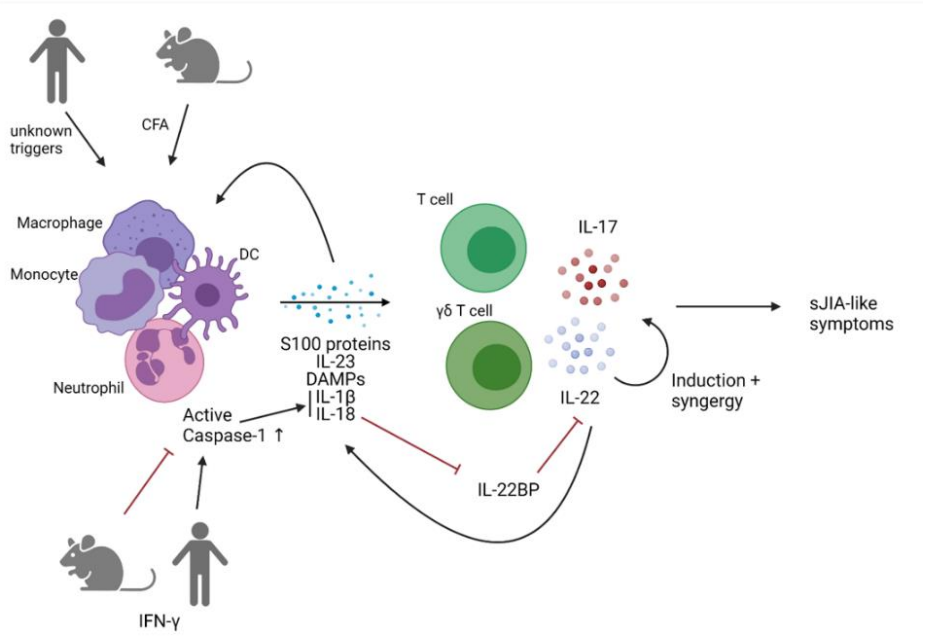

Figure 4.5: sJIA is associated with an aberrant innate immune activation of neutrophils, monocytes, macrophages, and DCs resulting in the release of pro-inflammatory cytokines (*e.g.* IL-1β or IL-18, IL-23), DAMPs (*e.g.* S100 proteins). In mice, activation is CFA-induced, whereas in patients no driving trigger could be demonstrated. Upon activation, T cells and γδ T cells are stimulated to produce IL-17. A direct link between IL-17 and sJIA-like symptoms was demonstrated in mice. IL-22 is often co-expressed with IL-17. IL-22 may directly or indirectly enhance further innate immune activation and IL-17 release, causing a positive amplification loop to induce sJIA pathology. High levels of IL-18 are measured in patients with sJIA. Since IL-18 may abort the expression of the natural IL-22-antagonist IL-22BP, increased IL-18 levels may explain the enhanced IL-22-activity that was measured in patients. In CFA-immunised IFN-γ KO mice, increased inflammasome activation and active caspase-1 activity were shown which were associated with increased pro-IL-1β cleavage. This increased inflammasome activation in the absence of IFN-γ may in part explain the increased susceptibility of IFN-γ KO mice to develop sJIA. In contrast, in patients, IFN-γ may rather stimulate inflammasome activation. Black lines represent active signalling, red lines represent inhibitory signalling. Figure based on literature data and own findings, in patients and in an IFN-γ KO mice model of sJIA.

Supplementary Tables

Supplementary Table 4.1: Patient characteristics

	HC	Active sJIA	Inactive sJIA
Male/Female	6/9	4/6	3/5
Age (years)	12 (0-27)	5 (1-16)	6 (2-16)
Clinical features			
Active arthritis	0/15	10/10	0/8
Fever	0/15	8/10	0/8
Rash	0/15	7/10	0/8
Laboratory features			
WBC count (x10^9/l)	ND	21.355 (4.8-30.3) *	6.6 (3.7-22.9)
Neutrophil count (x10^9/l)	ND	17.4 (3.1-27.0) *	2.6 (1.3-12.5)
Lymphocyte count (x10^9/l)	ND	2.3 (0.7-7.2)	2.95 (0.5-7.1)
Monocyte count (x10^9/l)	ND	1.05 (0.5-1.6) *	0.65 (0.2-1.1)
RBC count (x10^12/l)	ND	3.82 (3.2-4.5) *	4.455 (4.1-4.8)
Haemoglobin (g/dl)	ND	10.5 (7.9-11.9) **	12.15 (9.9-13.1)
Platelet count (x10^9/l)	ND	462 (210-757)	314.5 (172-759)
Aspartate transaminase (U/ml)	ND	31 (14-45)	29.5 (19-43)
Alanine transaminase (U/ml)	ND	14 (7-36)	20 (9-27)
Ferritin (µg/l)	ND	865 (49-3959)	ND
CRP (mg/l)	ND	115.55 (32.2-341.6) **	0.3 (0.3-4.5)
Treatment			
NSAID	0/15	5/10	0/8
Corticosteroids	0/15	2/10	2/8
Methotrexate	0/15	2/10	0/8
Biologicals (IL-6 or IL-1β)	0/15	2/10	5/8
Cytokine levels			
G-CSF (pg/ml)	12.3 (8.1-27.6)	58.2 (9.0-228.0) ## / *	19.0 (8.4-41.5)
GM-CSF (pg/ml)	0.4 (0.1-1.5)	0.4 (0.1-1.4)	0.3 (0.2-0.6)
IFN-γ (pg/ml)	2 (0-27.5)	5.3 (0.8-107.2)	2.7 (0-24.2)
IL-10 (pg/ml)	0.4 (0-2.1)	1.0 (0.2-7.9) *	0.2 (0-2.4)
IL-17 (pg/ml)	1.9 (0.7-5.1)	1.7 (0.8-3.2)	1.8 (1.1-2.7)
IL-18 (pg/ml)	688.5 (329-1247.1)	44540.6 (6972.1-290044.2) ####	2914.5 (792.3-163262.9) #
IL-1β (pg/ml)	0 (0-0.3)	0 (0-4.2)	0 (0-0.3)
IL-23 (pg/ml)	2.6 (0-12.6)	3.8 (1.3-12.5)	2.3 (0-50.1)
IL-6 (pg/ml)	0.4 (0.2-1.1)	15.5 (7.1-23.3) #### / *	5.5 (0.5-17.4) #
TNFα (pg/ml)	3.1 (0.9-6.1)	3.7 (1.9-13.3)	2.4 (1.1-6.1)

For age, laboratory features and cytokine levels, median with range are given. Inactive sJIA patients were defined by the absence of fever, rash, arthritis, and inflammatory parameters. HC = healthy. CRP = C-reactive protein. NSAID = non-steroidal anti-inflammatory drugs. ND = not determined. P values less than 0.05 were considered significant (* $p < 0.05$; ** $p < 0.01$ between active and inactive sJIA patients, by Wilcoxon matched-pairs signed rank test, or # $p < 0.05$; ## $p < 0.01$; ### $p < 0.001$; #### $p < 0.0001$ compared to HCs, by Kruskal–Wallis test, Dunn's post hoc test

CHAPTER 5

ROLE FOR G-CSF IN NEUTROPHILIC EXTRAMEDULLARY MYELOPOIESIS IN SYSTEMIC JUVENILE IDIOPATHIC ARTHRITIS

This chapter has been submitted to Arthritis and Rheumatology (In Revision)

Bert Malengier-Devlies[1], Eline Bernaerts[1], Kourosh Ahmadzadeh[1], Jessica Filtjens[1], Jessica Vandenhaute[1], Bram Broeckx[2,3], Oliver Burton[4,5,6], Amber De Visscher[1], Tania Mitera[1], Nele Berghmans[7], Adrian Liston[4,5,6], Diether Lambrechts[2,3], Paul Proost[7], Carine Wouters[1,8,9], Patrick Matthys[1]

[1]KU Leuven Department of Microbiology, Immunology and Transplantation, Rega Institute for Medical Research, Laboratory of Immunobiology, Leuven, Belgium
[2]VIB, Center for Cancer Biology, Leuven, Belgium
[3]KU Leuven Department of Human Genetics, Laboratory for Translational Genetics, Leuven, Belgium
[4]VIB, Center for Brain & Disease Research, Leuven, Belgium
[5]The Babraham Institute, Laboratory of Lymphocyte Signalling and Development, Cambridge, United Kingdom.
[6]KU Leuven Department of Microbiology, Immunology and Transplantation, Laboratory of adaptive immunology, Leuven, Belgium
[7]KU Leuven Department of Microbiology, Immunology and Transplantation, Rega Institute for Medical Research, Laboratory of Molecular Immunology, Leuven, Belgium
[8]University Hospitals Leuven, Division of Pediatric Rheumatology, Leuven, Belgium
[9]European Reference Network for Rare Immunodeficiency, Autoinflammatory and Autoimmune Diseases (RITA) at University Hospital Leuven, Leuven, Belgium

CHAPTER 5: ROLE FOR G-CSF IN NEUTROPHILIC EXTRAMEDULLARY MYELOPOIESIS IN SYSTEMIC JUVENILE IDIOPATHIC ARTHRITIS

Abstract

Objectives

Systemic juvenile idiopathic arthritis (sJIA) is an auto-inflammatory disease of childhood-onset. sJIA is associated with neutrophilia, including immature granulocytes, which might be driven by the growth factor granulocyte-colony stimulating factor (G-CSF). This study aimed to unravel the role of G-CSF in the pathology of sJIA.

Methods

Injection of complete Freund's adjuvant (CFA) in BALB/c mice induces mild inflammation and neutrophilia in wild-type (WT) mice and a more pronounced disease, reminiscent to sJIA patients, in interferon-γ (IFN-γ) knock-out (KO) mice. Extramedullary myelopoiesis was studied in CFA-immunised mice by single cell RNA-sequencing and the effect of G-CSFR-blockade on neutrophil development and sJIA pathology was evaluated. Additionally, in sJIA patients, plasma G-CSF levels were measured.

Results

Both in sJIA patients and in the corresponding mouse model plasma levels of G-CSF are increased. Our findings demonstrate that G-CSF is responsible for the observed neutrophilia and extramedullary myelopoiesis and the induction of immature neutrophils and myeloid-derived suppressor cells in the CFA-immunised IFN-γ KO mouse model of sJIA. Administration of a G-CSF-receptor antagonising antibody blocked the maturation and differentiation of neutrophils in CFA-immunised mice. In IFN-γ KO mice, anti-G-CSF-receptor antibody treatment was associated with almost complete inhibition of arthritis development.

Conclusion

We describe for the first time the role of G-CSF in a mouse model of sJIA and point towards an important G-CSF-induced myelopoiesis and neutrophilia, influencing the development of arthritis.

Introduction

Systemic juvenile idiopathic arthritis (sJIA) is a childhood inflammatory disorder characterised by arthritis and systemic inflammation such as quotidian fever, skin rash, weight loss, polyserositis, hepatosplenomegaly and lymphadenopathy. Haematological features include neutrophilia, lymphocytopenia, anaemia, thrombocytosis and increased levels of interleukin (IL)-6, IL-18 and S100 proteins (25,26,31,168,173,749). sJIA is considered as an autoinflammatory disease with a pathogenic role for IL-1β and IL-6 as evident by successful treatment with IL-1- or IL-6-antagonists (783).

Neutrophils are the most abundant innate immune effectors in the human circulation. Neutrophils kill pathogens through overlapping oxidative and non-oxidative mechanisms including phagocytosis and degranulation (259). Inappropriate activation of neutrophils in a sterile inflammatory setting can result in host tissue damage as described in several autoimmune and autoinflammatory disorders (784). Increasing evidence arises for neutrophils subsets with immunomodulatory properties (known as myeloid-derived suppressor cells (MDSCs)(265,785). In sJIA, the role of neutrophils remains largely unknown. Recently, an increased number of immature and hypermature neutrophils was described in patients with sJIA, which correlated with inflammatory disease parameters and which was reduced upon IL-1β blockage. Neutrophils are a key source of S100 proteins, amplifying the innate immune response. Furthermore, patients' neutrophils had an inflammatory gene expression and primed phenotype (126,129,130). The presence of immature granulocytes in blood of patients is indicative for extensive myelopoiesis.

Our laboratory developed a mouse model for sJIA mimicking the disease in its clinical, haematological and histological features (786). The model relies on administration of complete Freund's adjuvant (CFA) containing heat-killed Mycobacterium butyricum in BALB/C mice, and requires the use of IFN-γ deficient mice (IFN-γ knockout (KO) mice) since WT mice only develop a transient inflammatory disease reaction (786). While sJIA patients do not have mutations in the IFN-γ gene or its receptor, the clinical relevance of the model is related to the fact that NK-cells of these patients display profound defects in IL-18-induced IFN-γ production (137,139). Within two weeks post CFA-challenge, IFN-γ KO mice develop arthritis, lymphadenopathy, anaemia, thrombocytosis, and increased levels of IL-6. Moreover, the mice develop splenomegaly, extensive and poorly understood myelopoiesis and neutrophilia, characterised by the presence of immature neutrophils (786).

Granulocyte colony-stimulating factor (G-CSF) is the major regulator of granulocyte production. G-CSF signals through the G-CSF receptor (G-CSFR) expressed on myeloid progenitors, neutrophils, monocytes, macrophages, as well as endothelial cells (548). Administration of G-CSF increases peripheral blood neutrophil numbers and enhances their migration into tissues by promoting adhesion molecules expressed on neutrophils and endothelial cells (524,568). In the clinic, G-CSF is used to treat neutropenia or to mobilise hematopoietic stem cells for transplantation purposes (582).

Neutrophils may be a major contributor to the inflammatory cascade of sJIA, but studies in animal models are lacking. In an attempt to study the role of neutrophils in our sJIA model we previously used anti-Ly6G-depleting antibodies, but unfortunately, this approach only partially depleted immature neutrophils and the treatment was followed by a rebound of new neutrophils (787). In the current study, we hypothesised that G-CSF might be involved in driving myelopoiesis and the pathogenesis of sJIA. To this end, we treated sJIA mice with a G-CSFR-blocking monoclonal antibody and studied the extramedullary development of neutrophils and its effect on the development of disease. In a cohort of sJIA patients we measured colony stimulating factors.

Material and Methods

Patients

During the study, 7 sJIA-MAS patients, 28 sJIA patients and 15 gender- and age-matched healthy controls were recruited. The study was performed at the University Hospital of Leuven, conducted according to the Declaration of Helsinki, and approved by the Leuven's Ethics Committee (S58814). Patient classification was based on the criteria of the International League of Associations for Rheumatology (25). A detailed list of patient characteristics can be found in Supplementary Table 5.1. Samples were collected before any therapeutic intervention or at disease flares.

sJIA mouse model

The sJIA mouse model was induced in 6-9 week old WT and IFN-γ KO BALB/C mice as described (786). Induction of the sJIA model is detailly described in our supplementary M&M.

Anti-G-CSF antibody treatment

Mice were injected intraperitoneally (i.p.) with 200 µg anti-G-CSF-R (αG-CSF-R) (Ch5E2-VR81-mIgG1k) (586), twice a week starting one day prior to immunisation. CFA-immunised WT and IFN-γ KO mice injected i.p. with PBS were included as controls. To reduce any cage effect, all conditions were mixed among different cages. Mice were euthanised between day 16 and day 25. No mice were excluded in this study.

Blood analysis

Murine blood samples were obtained by heart puncture with heparin (Leo Pharma). Blood cell analysis was performed on a Cell-Dyn 3700 Hematology Analyser (Abott Diagnostics). Plasma was stored at -80°C. Human PBMCs were obtained by Lymphoprep density centrifugation. Cells were stored in liquid nitrogen in cryopreservation medium (90% FCS, 10% DMSO). Human plasma was isolated, centrifuged for 10min at 1000g and stored at -80°C.

Histologic and cytospin analysis

For cytospin analysis, single cell suspensions were spun on a slide, fixed with methanol, H&E stained and microscopically counted. For histological examination, forelimbs and hind limbs were fixed in 10% formalin and decalcified with formic acid. Paraffin sections were stained with H&E and scored blindly for: infiltration of mono- and polymorphonuclear cells, hyperplasia of the synovium and pannus formation. Severity was scored as: 0, absent; 1, mild; 2, average; 3, severe; 4, extensive.

In vitro osteoclast formation

Splenocytes were cultured in alpha-MEM REGA-3 and stimulated with RANKL (100 ng/mL, R&D Systems) and M-CSF (20 ng/mL, R&D Systems). After 3 days, cells were re-stimulated for 3 to 4 days, and stained for tartrate-resistant acid phosphatase (TRAP), as described (767). TRAP+ multinucleated cells (≥ three nuclei) were defined as osteoclasts.

Protein quantification

G-CSF, IL-1β, IL-6, IL-17, IL-22, and TNF-α were measured by the Procartaplex mouse multiplex ELISA (Thermofisher). Meso Scale Discovery's multiplex assay was used to measure human plasma C-reactive protein (CRP) and inflammatory cytokines. All according to the manufacturer's protocols.

Flow cytometry

Spleens were passed through a cell-strainer (70 µm) to obtain single-cell suspensions. Bone marrow was flushed from the femur. Red blood cells were lysed using ACK lysing-buffer (Gibco). Cells were incubated with FcR-blocking reagent (Miltenyi Biotec) and extracellularly stained. Dead cells were excluded using Zombie Aqua 516 (Biolegend). Intracellular staining of cytokines, perforin and granzymes was performed with the Fixation and Permeabilization kit (BD-Biosciences) according to the manufacturer's protocols. Prior to intracellular cytokine staining, samples were stimulated for 4 hours with phorbol myristate acetate (100 ng/mL) and ionomycin (500 ng/mL). Transcription factors were stained with the FoxP3/Transcription factor staining set (ThermoFisher Scientific). A list of the used antibodies is presented in Supplementary Table 5.3. Flow cytometry was performed on the BD LSR Fortessa X20, and data were analysed with FlowJo (LLC, V10).

Single-cell RNA sequencing

Single cell RNA sequencing was applied to sorted GR-1+ splenocytes of WT and IFN-γ KO mice immunised with CFA. The standard 10x Genomics Single Cell Protocols (10X Genomics) were followed. A library was generated and was sequenced on an Illumina HiSeq4000 platform using paired-end sequencing workflow. Sequencing coverage target was set at 50,000 reads per cell (Genomics core, KU Leuven).

Pre-processing and clustering of single-cell RNA sequencing data

The raw sequencing data were demultiplexed, aligned and counted with Cell Ranger V.2.0 pipelines (10X Genomics). Using the R package Seurat, gene and cell filtration, normalization, principle component analysis, variable gene finding, clustering analysis and t-distributed stochastic nearest neighbour embedding was performed on the obtained count matrixes. Analysis was performed according to standard pipelines with default parameters, unless stated otherwise. R package Slingshot was used to plot Pseudotime-trajectories in neutrophils (788).

Statistics

Data were analysed with GraphPad Prism software version 8.0. For comparison of two different groups, the two-tailed non-parametric Mann-Whitney U test was used. A non-parametric Kruskal-Wallis test followed by a Dunn’s post-hoc test was performed when three or more groups were compared. The Wilcoxon matched-pairs signed rank test was used for paired data. In our correlation studies, the non-parametric Spearman's rank correlation analysis was used.

Results

Active sJIA patients have increased levels of G-CSF that correlates with pro-inflammatory cytokines and number of neutrophils

Plasma G-CSF levels were measured in three groups of patients: MAS patients (n=7), active (n=10) and inactive sJIA patients (n=8), which were compared to age- and gender-matched healthy controls (HC) (n=15). The disease activity parameters are shown in Supplementary Table 5.1. Clinical features and laboratory parameters were determined and the levels of 10 inflammatory cytokines were analysed in the plasma. Increased plasma levels of IL-6, IL-18, CRP were measured (Supplementary Table 5.1). G-CSF levels were significantly increased in active sJIA patients (average [range] of 58.2 [9-228.0] pg/ml) compared to HCs (12.3 [8.1-27.6] pg/ml). In patients with inactive disease state, G-CSF levels were within normal range (19.0 [8.4-41.5] pg/ml) (Supplementary Figure 5.1A). Also, in MAS (43.2 [17.7-123.4] pg/ml) increased G-CSF levels were detected (Supplementary Figure 5.1A). Levels of GM-CSF were normal in all patients' groups (Supplementary Figure 5.1B). Correlation studies revealed a positive correlation between G-CSF and the number of WBCs, monocytes, neutrophils, and plasma levels of both IL-6 and IL-1β. Furthermore, a negative correlation between G-CSF and the number of lymphocytes was seen (Supplementary Figure 5.1C).

In mice, CFA-immunisation induces in IFN-γ KO mice a sJIA-like disease (786). In analogy with sJIA patients with active disease, increased levels of G-CSF were measured in the plasma upon immunisation. A significantly increased level was observed in immunised IFN-γ KO mice, when compared to WT mice (Supplementary Figure 5.1D). In conclusion, both in human sJIA and in the mouse model, plasma G-CSF levels are increased.

Effects of αG-CSFR antibody on CFA-induced inflammation in IFN-γ KO and WT mice

Next, we examined whether endogenous G-CSF causes CFA-induced inflammation by using a monoclonal antibody that blocks the G-CSF receptor (αG-CSFR). In sham-treated animals, we confirmed our previously reported findings that a single injection of CFA in the tail elicits local and systemic inflammation with symptoms including tail damage, weight loss, splenomegaly, lymphadenopathy, neutrophilia, lymphopenia, thrombocytosis, and anaemia. All these symptoms were either more pronounced or exclusively present in IFN-γ KO mice as compared to WT counterparts (Figure 5.1) (786). When CFA-challenged IFN-γ KO mice were treated with αG-CSFR antibody, tail damage was found to be increased and mild weight loss occurred (Figure 5.1A-B). In WT mice, αG-CSFR antibody injection had no effect on body weight changes (Figure 5.1A) and did not increase tail damage (not depicted). To investigate effects of αG-CSFR-injection on other sJIA-like symptoms, mice were euthanised between day 16 and day 25. αG-CSFR administration inhibited splenomegaly in both IFN-γ KO and WT mice, which was statistically significant in IFN-γ KO mice. While enlargement of lymph nodes was not affected by αG-CSFR antibody treatment in IFN-γ KO mice, those of WT animals had a trend towards reduction (p=0.1) (Figure 5.1C). Haematological analysis revealed G-CSFR administration completely inhibited neutrophilia in CFA-challenged IFN-γ KO, while lymphopenia, thrombocytosis and numbers of monocytes were not affected. In WT mice, lymphopenia was partially restored upon treatment (Figure 5.1D-E). Anaemia, evaluated by the drop in numbers of RBCs, was not affected by anti-G-CSFR antibody-treatment (Figure 5.1E). CFA-immunised IFN-γ KO mice showed a non-significant increased percentage of immature TER119+CD71+ RBCs, which was further increased upon antibody injection. In contrast, in WT mice, the immature RBCs were significantly reduced by α-GCSFR treatment (Figure 5.1F).

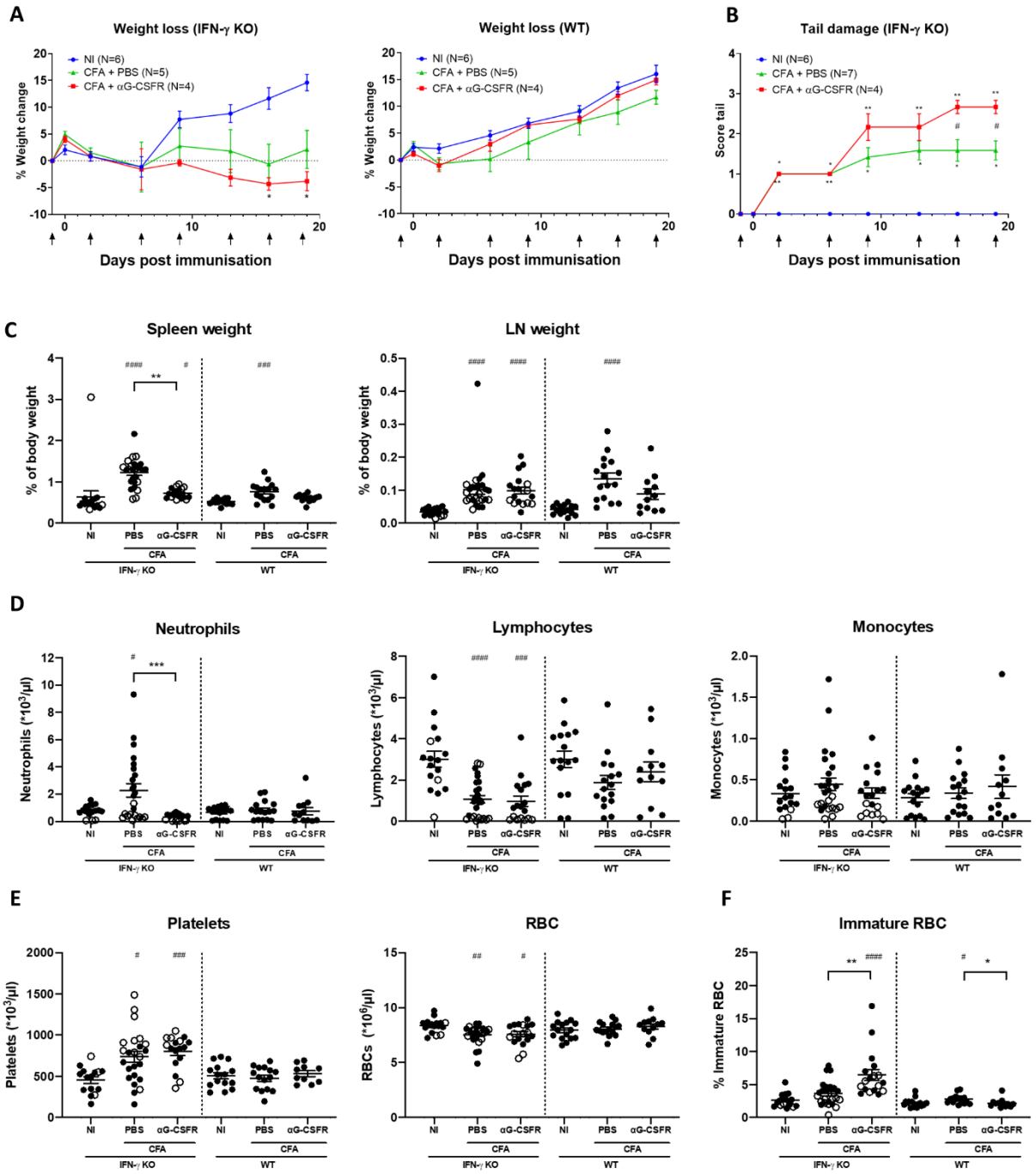

Figure 5.1: Effects of αG-CSFR antibody on CFA-induced inflammation. CFA-immunised IFN-γ KO and WT mice were injected with αG-CSFR (200 µg - i.p.) twice a week (black arrows). Mice were sacrificed between day 16 and 25 post-immunisation. PBS-injected CFA-immunised IFN-γ KO and WT mice were included as controls and compared to naive (NI) mice. (A) Percentage change in body weight. (B) Tail damage scored as Supplementary Table 5.2B. (C) Spleen weight and inguinal lymph node weight expressed as percentage of total body weight. (D) Neutrophil, lymphocyte, monocyte (E) blood platelet and RBC cell counts in blood samples were measured with a blood cell analyser. (F) Percentage immature RBCs were measured by flow cytometry (TER119+CD71+). Graphs show results from 3 pooled experiments. Each dot represents a single mouse, bars represent median group values with IQR. Closed circles: SPF-conditions; open circles: non-SPF-conditions. * $p < 0.05$; ** $p < 0.01$; *** $p < 0.001$ between indicated groups or # $p < 0.05$; ## $p < 0.01$; ### $p < 0.001$; #### $p < 0.0001$ compared to IFN-γ KO NI or WT NI mice, by Kruskal-Wallis test, Dunn's post hoc test.

When cytokines were analysed in plasma of mice, significantly increased levels of G-CSF, IL-1β, IL-6, TNF-α and IL-22 were measured in IFN-γ KO mice upon CFA-administration. In WT mice, CFA induced increased levels of G-CSF and TNF-α (Figure 5.2). An increase in G-CSF was seen after αG-CSFR administration in both IFN-γ KO and WT mice, which is most likely a direct consequence of blocking cytokine internalisation. In CFA-challenged IFN-γ KO mice, αG-CSFR antibody-injection slightly reduced plasma levels of IL-1β and IL-22. In contrast, IL-6, IL-17 and TNF-α were slightly elevated in αG-CSFR-injected CFA-immunised IFN-γ KO mice which was associated with increased weight loss, tail damage and haematological alterations when compared to PBS-treated mice. No elevated cytokine levels were seen in WT counterparts when treated with αG-CSFR antibody.

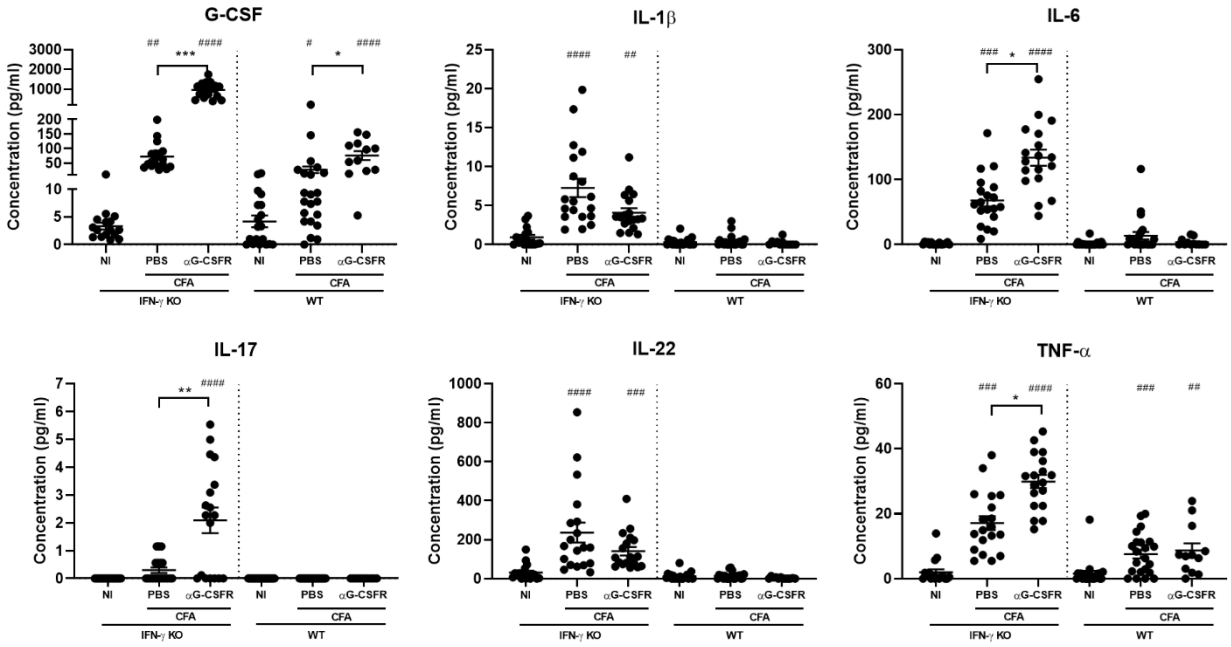

Figure 5.2: Altered plasma cytokine-levels in αG-CSFR-treated CFA-immunised IFN-γ KO mice. CFA-immunised IFN-γ KO and WT mice were injected twice a week with αG-CSFR (200 µg - i.p.). Mice were sacrificed between day 16 and 25 post-immunisation. PBS-injected CFA-immunised IFN-γ KO and WT mice were included as controls and compared to naïve (NI) mice. Plasma levels of G-CSF, IL-1β, IL-6, IL-17, IL-22 and TNF-α levels were measured by the Procarta-Multiplex system. Graphs show results from 3 pooled experiments. Each dot represents a single mouse, bars represent median group values with IQR. * p < 0.05; ** p < 0.01; *** p < 0.001 between indicated groups or # p < 0.05; ## p < 0.01; ### p < 0.001; #### p < 0.0001 compared to IFN-γ KO NI or WT NI, by Kruskal-Wallis test, Dunn's post hoc test.

In conclusion, the results demonstrate that G-CSF is responsible for the neutrophilia in CFA-immunised mice. αG-CSFR treatment caused an improvement of clinical and haematological features in IFN-γ KO mice, even though a modest increase of some systemic inflammatory features was observed.

Counteracting effects of G-CSFR-blockage on the development of arthritis

As we previously reported, around 40% of IFN-γ KO mice develop arthritis three weeks post CFA-challenge (786). Conventional animal housing is known to accelerate the onset and incidence of arthritis (789,790). In one our experimental set-ups, mice were housed in a conventional animal facility. As depicted in Figure 5.3A, joint inflammation was seen in CFA-immunised IFN-γ KO mice from day 13 onwards and reached an incidence over 80% during the time course of the experiment. At day 24, 9 out of 11 mice developed redness and swelling of the joints with an average arthritic score of 4.9 $\pm$ 1.7. In contrast, αG-CSFR antibody-treated mice developed less arthritis indicated by a lower incidence and a lower arthritic score (1.0 $\pm$ 0.4 in 4 out of 7 mice). Figure 5.3B shows representative images of the joint inflammation in the front and hind paws of IFN-γ KO mice. Representative histologic sections of joints of IFN-γ KO mice are displayed in figure 5.3C, and show hyperplasia of synovial tissue, infiltration of the synovium with mononuclear and polymorphonuclear cells and pannus formation with osteoclasts and bone destruction. Reduced severity of arthritis in the αG-CSFR antibody-treated mice was associated with an inhibition of cell infiltration, hyperplasia, and pannus formation.

To predict the possible development of arthritis, numbers of osteoclast precursor cells (CD3-B220-CD11b+CD115+ cells) in the spleen were determined as described (158,791). In IFN-γ KO mice, CFA-immunisation was associated with an increased number of osteoclast precursor cells, which was significantly reduced by αG-CSFR antibody. Likewise, in WT mice, CFA-immunisation induced the generation of osteoclast precursor cells, but not when mice were treated with anti-G-CSFR antibody (Figure 5.3D). In addition, when osteoclasts were generated in vitro, high numbers of multinucleated osteoclasts were generated from CFA-immunised IFN-γ KO mice, while those from mice treated with αG-CSFR antibody were found to be significantly lower (Figure 5.3E-F). In conclusion, αG-CSFR antibody treatment inhibited development of arthritis in CFA-immunised mice and reduced osteoclast formation.

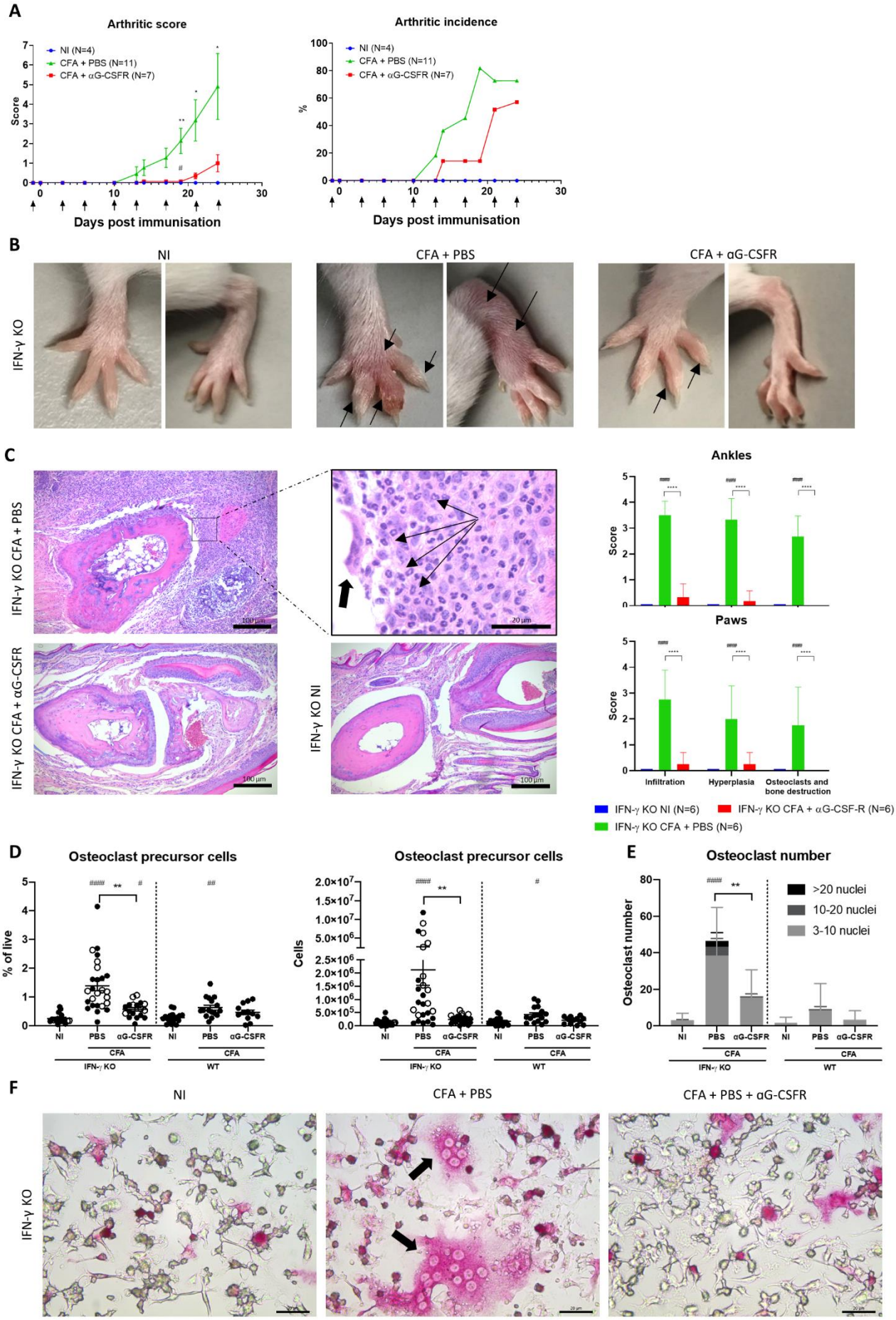
A
Arthritic score
NI (N=4)
CFA + PBS (N=11)
CFA + αG-CSFR (N=7)
Score
Days post immunisation
Arthritic incidence
%
B
NI
CFA + PBS
CFA + αG-CSFR
IFN-γ KO
C
IFN-γ KO CFA + PBS
IFN-γ KO CFA + αG-CSFR
IFN-γ KO NI
Ankles
Paws
Infiltration
Hyperplasia
Osteoclasts and bone destruction
IFN-γ KO NI (N=6)
IFN-γ KO CFA + αG-CSF-R (N=6)
IFN-γ KO CFA + PBS (N=6)
D
Osteoclast precursor cells
% of live
Cells
NI
PBS
αG-CSFR
CFA
IFN-γ KO
WT
E
Osteoclast number
>20 nuclei
10-20 nuclei
3-10 nuclei
F
NI
CFA + PBS
CFA + PBS + αG-CSFR
IFN-γ KO

Figure 5.3: Reduced arthritis and osteoclast formation upon αG-CSFR-treatment. CFA-immunised IFN-γ KO and WT mice were injected twice a week with αG-CSFR (200 µg - i.p.). Mice were sacrificed between day 16 and 25 post immunisation. PBS-injected CFA-immunised IFN-γ KO and WT mice were included as controls and compared to naive (NI) mice. (A) Arthritis score and incidence. (B) Representative photographs of front (left) and hind paw (right). Arrows show redness and/or swelling. (C) Representative photographs of H&E-stained ankle sections. Magnification shows synovial tissue infiltrated with neutrophils (arrows) and multinucleated osteoclast (large arrow). Histology scores were graded as described. (D) Number of osteoclast precursor cells (CD11b+CD115+) in the spleen. Graphs show results from 3 pooled experiments. Each dot represents a single mouse, bars represent median group values with IQR. Closed circles: SPF-conditions; open circles: non-SPF-conditions. (E) The number of in vitro generated TRAP+ multinucleated osteoclasts, with representative photographs (n=8-14). (F). Two osteoclasts are marked. * p < 0.05; ** p < 0.01; **** p < 0.0001 between indicated groups or # p < 0.05; ## p < 0.01; #### p < 0.0001 compared to IFN-γ KO NI or WT NI mice, by Kruskal-Wallis test, Dunn's post hoc test.

Major role for G-CSF-induced extramedullary myelopoiesis

To determine the effect of αG-CSFR-treatment on CFA-induced haematopoiesis and myelopoiesis, flow cytometric analysis was performed on LNs and spleen. In LNs, no aberrant differences were found in T-, B-, γδ- T- or NK-cells (data not shown). In spleen of CFA-immunised mice, both neutrophils (Ly6G+CD11b+) and monocytes (Ly6C+CD11b+) were significantly increased compared to non-immunised (NI) controls. A marked reduction of this myeloid compartment was seen upon treatment with αG-CSFR, reaching significance in the IFN-γ KO mice only. The increased number of DCs was reverted upon αG-CSFR-treatment (Figure 5.4A). Associated with the decreased myeloid compartment, mice showed a relative increased number of lymphocytes (data not shown). However, no differences were found in the absolute numbers of CD4+ T-cells (CD3+CD4+), CD8+ T-cells (CD3+CD8+) or B-cells (CD19+) (Figure 5.4B-C). In CFA-challenged IFN-γ KO mice, regulatory T-cells (Tregs) (CD3+FoxP3+) were significantly decreased compared with observations in non-immunised control mice. Unexpectedly, an increased number of Treg cells was found in the αG-CSFR group. In WT animals, the number of Tregs remained unaltered (Figure 5.4D). Both in IFN-γ KO and WT animals, the absolute number of NK-cells (CD122+DX5+) were decreased after immunisation although not altered in the antibody-injected mice (Figure 5.4E). Interestingly, both in CFA-immunised WT and IFN-γ KO mice, αG-CSFR-treatment induced a reduced number of γδ T-cells (Figure 5.4F). In conclusion, G-CSF is driving extramedullary myelopoiesis in the spleen of CFA-immunised mice and myeloid cells were suppressed by G-CSFR-blockade.

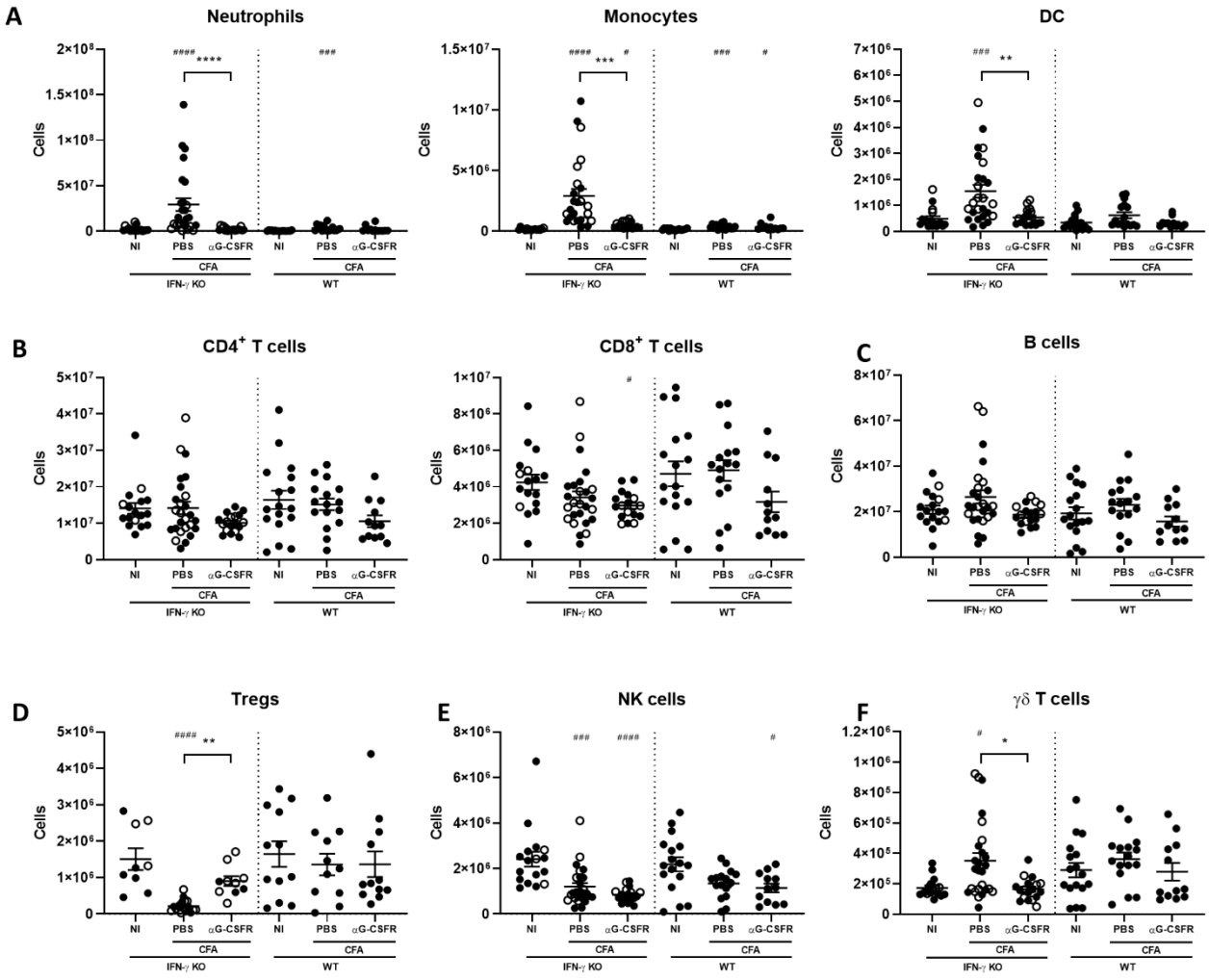

Figure 5.4: αG-CSFR-treatment induces a reduced splenic myelopoiesis in CFA-immunised mice. CFA-immunised IFN-γ KO and WT mice were injected twice a week with αG-CSFR (200 µg - i.p.). Mice were sacrificed between day 16 and 25 post-immunisation. PBS-injected CFA-immunised IFN-γ KO and WT mice were included as controls and compared to naive (NI) mice. Absolute number of different immune cells in the spleen (A) myeloid neutrophils, (CD11b+Ly6G+), monocytes (CD11b+Ly6C+), dendritic cells (CD11b+CD11c+), (B) lymphoid CD4+ T-cells (CD3+CD4+), CD8+ T-cells (CD3+CD8+), (C) B-cells, (D) Regulatory T-cells (CD3+CD25+), (E) NK-cells (CD3-CD122+DX5+) and (F) γδ T-cells (CD3+CD4+gdTCR+) were assessed by flow-cytometry. Graphs show results from 3 pooled experiments. Each dot represents a single mouse, bars represent median group values with IQR. Closed circles: SPF-conditions; open circles: non-SPF-conditions. * p < 0.05; ** p < 0.01; *** p < 0.001; **** p < 0.0001 between indicated groups or # p < 0.05; ### p < 0.001; #### p < 0.0001 compared to IFN-γ KO NI or WT NI, by Kruskal-Wallis test, Dunn's post hoc test.

Single cell sequencing identifies five neutrophil subsets formed during extramedullary myelopoiesis
CFA-immunisation is associated with an important de novo generation of neutrophils outside the bone marrow (BM). To characterise the cellular landscape of the different neutrophil subsets, single-cell RNA sequencing was applied to GR1-sorted splenocytes (depicting both Ly6G+ and Ly6C+ cells) from CFA-challenged WT and IFN-γ KO mice (Figure 5.5A). Unbiased clustering identified eight clusters (Figure 5.5B), and Supplementary Figure 5.2A shows a heat map of the top marker-genes. Based on the key neutrophil markers Ly6G and CXCR2, clusters 0, 1, 2, 3 and 5 were annotated as neutrophils. Cluster 4 represented monocytes, expressing high levels of CCR2 and Ly6C. Since Irf8 was found to be a main transcription factor in conventional and plasmacytoid dendritic cells (DCs), cluster 6 was annotated as DCs. Finally, a neglectable cluster 7 (<1% of sorted cells) was found representing NK-cells (Supplementary Figure 5.2A). Within neutrophils, five subsets could be found. Based on the expression transcription factors (Figure 5.5C), granule proteins (Figure 5.5D) and cell cycle genes (data not shown), neutrophils were divided into pre-neutrophils (cluster 5), immature neutrophils (cluster 1 and 3) and mature neutrophils (cluster 0 and 2). Within the immature neutrophils, two subsets were found showing no relevant biological difference. Mature neutrophils might also be divided into two (cluster 0 and 2) subsets, in which cluster 0 represents the inflammatory neutrophils, having an increased expression of *i.e.* IL-1β, G-CSFR (Csf3r) and CD101 (Figure 5.5E). Assessment of the different neutrophilic functions exposed that pre-neutrophils were highly proliferative cells whereas mature neutrophils had the highest antimicrobial and pro-inflammatory capacity (as seen in chemotaxis, phagocytosis, ROS, and activation scores) (Figure 5.1F/Supplementary Figure 5.2B). Using Slingshot, we reconstructed a one-branch neutrophil differentiation pathway (Figure 5.5G). Gene expression of proliferation, primary granules and early TFs decreased along the trajectory (*e.g.* Cdk1), pro-inflammatory marker gene expression increased (*e.g.* Il1b), while specific and gelatinase granule marker genes were expressed in between the differentiation path (*e.g.* Ltf) (Figure 5.1C-D/Supplementary Figure 5.3). Interestingly, we noticed a reduction in the number of UMIs along the differentiation path, corresponding to the gene silencing reported (data not shown). When we compared WT and IFN-γ KO mice, we confirmed a reduced number of mature neutrophils in the spleen of CFA-immunised IFN-γ KO mice (Figure 5.5B). Interestingly, both cluster 0 and cluster 4 showed a remarkable polarised distribution of WT and IFN-γ KO cells (Figure 5.5H). More in depth comparison between IFN-γ KO and WT mice in cluster 0 identified 115 significantly differentially expressed genes (DEG) (42 up, 73 down) (Figure 5.5I). 26 of these genes were associated with myeloid-derived suppressor cells (MDSC) *i.e.* Wfdc17, Ifitm1 and Igfbp6 and were increasingly expressed in the IFN-γ KO mice only. Furthermore, Cebpb, a transcription factor induced by G-CSF was highly upregulated in the IFN-γ KO mice (462).
In conclusion, in analogy to the BM (316), a similar G-CSF-driven differentiation pathway is found in the spleen. Compared to WT mice, CFA-immunised IFN-γ KO mice showed an increased number of immature neutrophils and MDSC-polarised mature neutrophils.

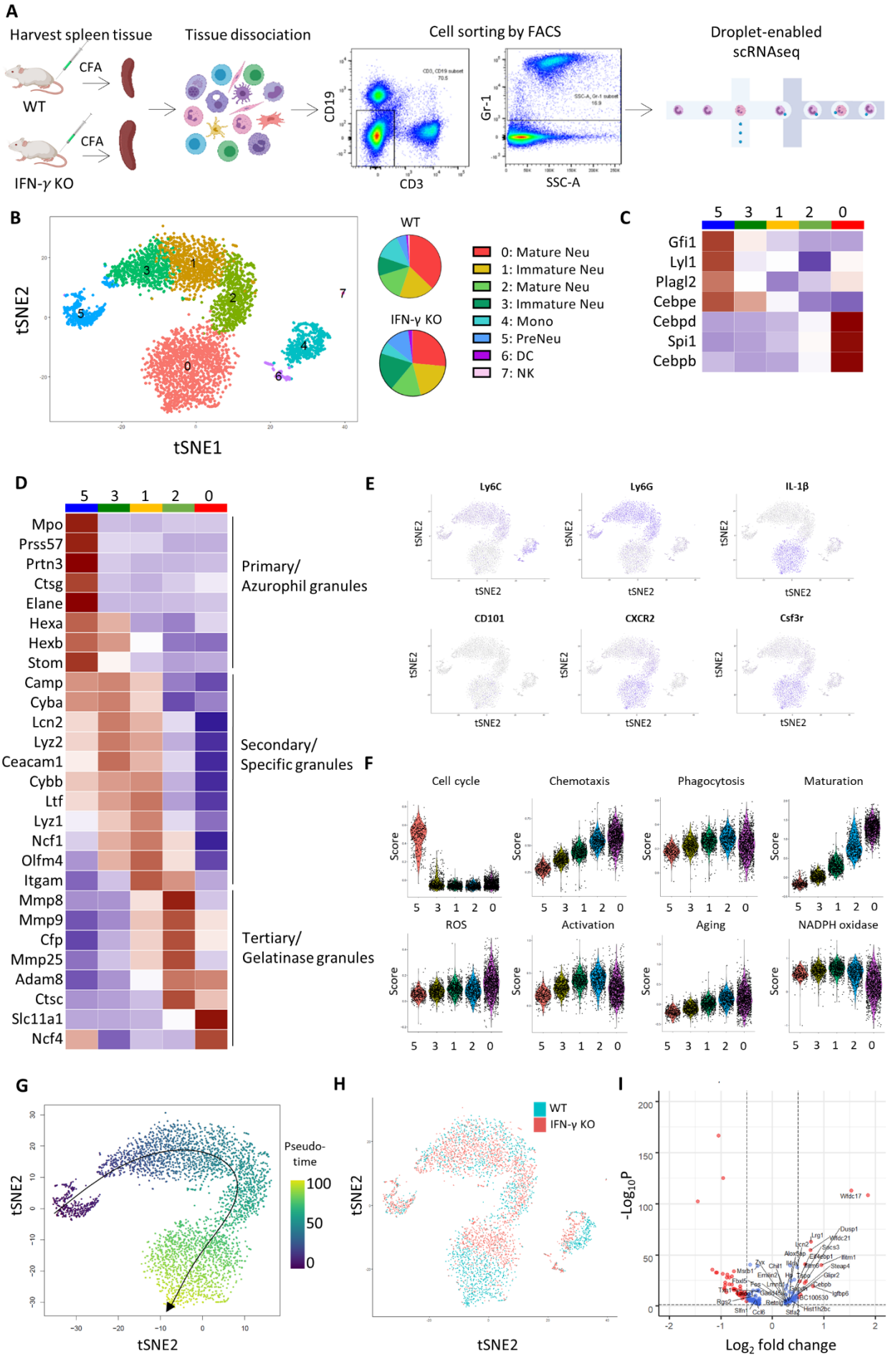
A
Harvest spleen tissue
Tissue dissociation
Cell sorting by FACS
Droplet-enabled scRNAseq
CFA
WT
IFN-γ KO
CD19
CD3
Gr-1
SSC-A
B
tSNE2
tSNE1
WT
IFN-γ KO
0: Mature Neu
1: Immature Neu
2: Mature Neu
3: Immature Neu
4: Mono
5: PreNeu
6: DC
7: NK
C
5 3 1 2 0
Gfi1
Lyl1
Plagl2
Cebpe
Cebpd
Spi1
Cebpb
D
5 3 1 2 0
Mpo
Prss57
Prtn3
Ctsg
Elane
Hexa
Hexb
Stom
Camp
Cyba
Lcn2
Lyz2
Ceacam1
Cybb
Ltf
Lyz1
Ncf1
Olfm4
Itgam
Mmp8
Mmp9
Cfp
Mmp25
Adam8
Ctsc
Slc11a1
Ncf4
Primary/ Azurophil granules
Secondary/ Specific granules
Tertiary/ Gelatinase granules
E
Ly6C
Ly6G
IL-1β
CD101
CXCR2
Csf3r
tSNE2
F
Cell cycle
Chemotaxis
Phagocytosis
Maturation
ROS
Activation
Aging
NADPH oxidase
Score
G
Pseudo-time
100
50
0
tSNE2
H
WT
IFN-γ KO
tSNE2
I
-Log10P
Log2 fold change

Figure 5.5: Single-cell RNA sequencing reveals five distinct neutrophil subsets in CFA-immunised IFN-γ KO and WT mice. (A) Approach overview for single-cell RNA sequencing (scRNA-seq) where CD3-CD19-GR1+ splenocytes were sorted from CFA-immunised IFN-γ and WT mice by FACS, followed by droplet-enabled scRNA-seq. (B) Seurat analysis of in total 4702 cells from CFA-immunised WT (2138 cells) and IFN-γ KO mice (2564 cells), in which 18177 genes were analysed are shown in a tSNE-projection. Colours indicate the distinct clusters of GR1+ splenocytes. Pie charts show the relative contribution of each cell type (in %) in CFA-immunised WT and IFN-γ KO mice. (C-D) Heatmap showing the expression of genes encoding myeloid development-related TF (C) and granule production (D) assessed in each neutrophil subcluster. (E) Main cell type markers were outlined in a dot plot. (F) Violin plots showing scores of cell cycle, chemotaxis, phagocytosis, maturation, ROS, activation, aging and NADPH oxidase by each neutrophil cell subcluster. (G) Pseudotime trajectory for neutrophils based on Slingshot. (H) tSNE-projection stratifying CFA-immunised WT and IFN-γ KO mice. (I) Volcano plot of all genes that were significantly differentially expressed in neutrophil cluster 0 between CFA-immunised WT and IFN-γ KO mice.

G-CSFR-blockade alters the relative distribution of neutrophil subsets

Spleen cytospin preparations confirmed the increased neutrophil-to-lymphocyte ratio measured by flow-cytometry in CFA-immunised mice (Figure 5.6A). Morphologically, neutrophils were divided in mature, immature and metamyelocytes (representing the pre-neutrophils). Mature neutrophils have a lobbed nucleus, whereas immature and metamyelocytes have a thin and thick banded nucleus, respectively (Supplementary Figure 5.4) (449). Quantification in the spleen revealed a relative increase in immature neutrophils. Interestingly, these emerge at day 10 post-immunisation, at the day mice start to develop overt signs of inflammation (data not shown). αG-CSFR-treatment restored the neutrophil-to-lymphocyte ratio but also induced a relatively increased percentage of metamyelocytes in CFA-immunised IFN-γ KO mice. In WT mice no major differences were observed (Figure 5.6B).

In addition, we performed a more in-depth analysis by flow cytometry. Based on two maturation markers, CD101 and CXCR2, mature (CD101+CXCR2+) and immature (CD101-CXCR2+) and metamyelocytes (CD101-CXCR2-) may be distinguished (316), which we confirmed (Figure 5.6C). As shown in Figure 5.6D-E, CFA-immunisation had no effect on the percentage of CD101-CXCR2- neutrophils, whereas it induces a relative increase in immature neutrophils, in IFN-γ KO mice only. Consequently, this results in a reduced percentage of mature neutrophils. Upon antibody treatment, the percentage of CD101-CXCR2- was increased in both IFN-γ KO and WT mice (not significant). Percentage immature and mature neutrophils were significantly decreased in CFA-immunised IFN-γ KO mice (Figure 5.6E). Interestingly, the reduced percentage of mature neutrophils was associated with a decreased percentage of IL-1β+ neutrophils (Figure 5.6F). Note that the absolute number of each neutrophil subtype was significantly decreased upon treatment. (Figure 5.6E-F). Supplementary Figure 5.5 shows the MFI of Ly6G, CD11b, CD101, CXCR2 and CXCR4 on neutrophils in the spleen. Together, these results indicate a αG-CSFR-mediated neutrophil maturation and differentiation deficiency in the spleen of CFA-immunised IFN-γ KO mice but not in CFA-immunised WT mice.

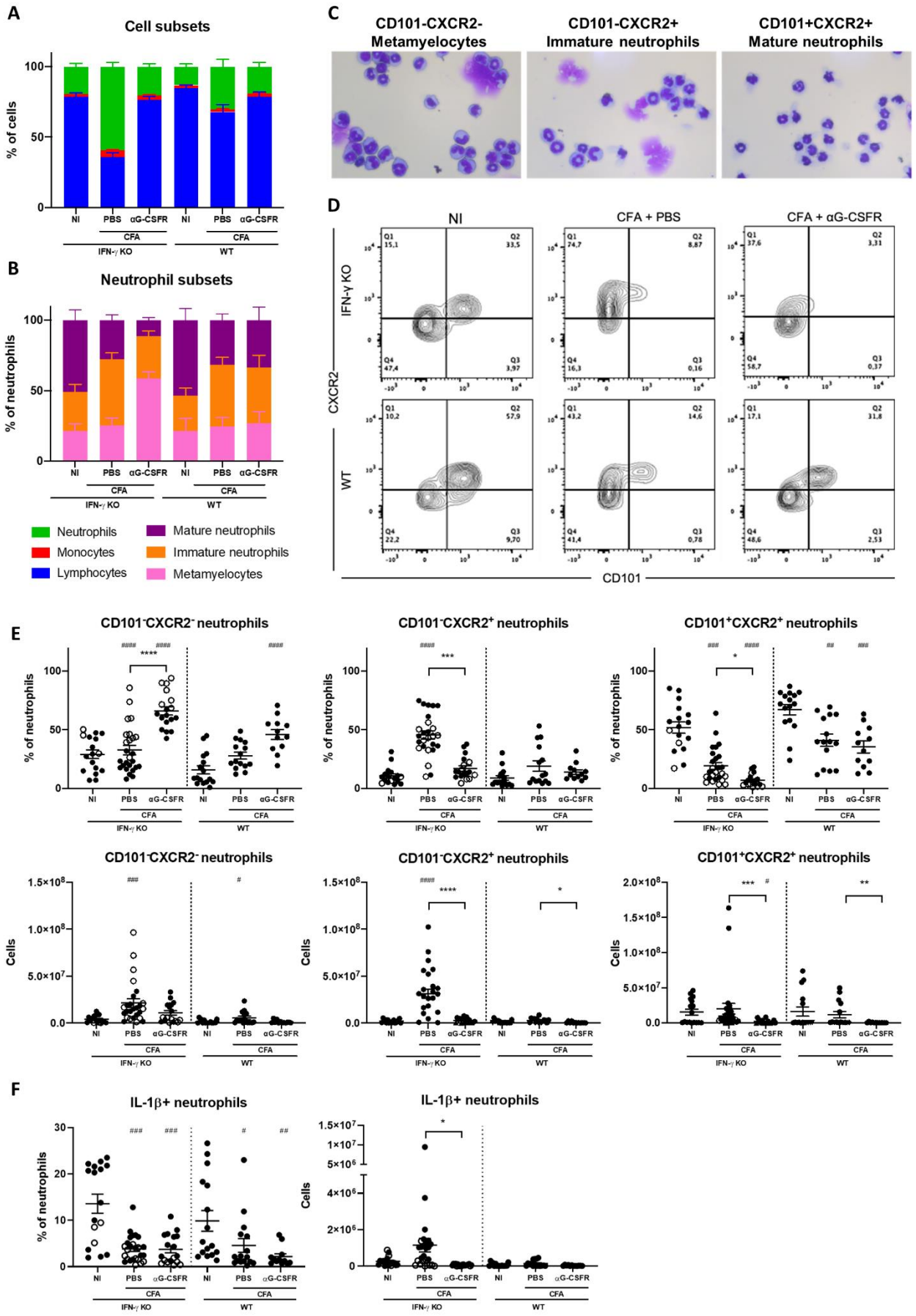
A
Cell subsets
% of cells
100
50
0
NI
PBS
αG-CSFR
NI
PBS
αG-CSFR
CFA
CFA
IFN-γ KO
WT
B
Neutrophil subsets
% of neutrophils
100
50
0
NI
PBS
αG-CSFR
NI
PBS
αG-CSFR
CFA
CFA
IFN-γ KO
WT
Neutrophils
Monocytes
Lymphocytes
Mature neutrophils
Immature neutrophils
Metamyelocytes
C
CD101-CXCR2-
Metamyelocytes
CD101-CXCR2+
Immature neutrophils
CD101+CXCR2+
Mature neutrophils
D
NI
CFA + PBS
CFA + αG-CSFR
IFN-γ KO
WT
CXCR2
CD101
Q1
15,1
Q2
33,5
Q4
47,4
Q3
3,97
Q1
74,7
Q2
8,87
Q4
16,3
Q3
0,16
Q1
37,6
Q2
3,31
Q4
58,7
Q3
0,37
Q1
10,2
Q2
57,9
Q4
22,2
Q3
9,70
Q1
43,2
Q2
14,6
Q4
41,4
Q3
0,78
Q1
17,1
Q2
31,8
Q4
48,6
Q3
2,53
E
CD101-CXCR2- neutrophils
CD101-CXCR2+ neutrophils
CD101+CXCR2+ neutrophils
% of neutrophils
100
50
0
Cells
1.5×10^8
1.0×10^8
5.0×10^7
0.0
2.0×10^8
1.5×10^8
1.0×10^8
5.0×10^7
0.0
NI
PBS
αG-CSFR
CFA
IFN-γ KO
WT
F
IL-1β+ neutrophils
IL-1β+ neutrophils
% of neutrophils
30
20
10
0
Cells
1.5×10^7
1×10^7
5×10^6
4×10^6
2×10^6
0

Figure 5.6: Left shift in neutrophil subsets upon αG-CSFR-treatment. CFA-immunised IFN-γ KO and WT mice were injected twice a week with αG-CSFR (200 µg - i.p.). Mice were sacrificed between day 16 and 25 post immunisation. PBS-injected CFA-immunised IFN-γ KO and WT CFA-immunised mice were included as controls and compared to naive (NI) mice. (A-B) Spleen cytospin preparations were counted (n=18-26). (C) Splenocytes were FACS-sorted based on CXCR2 and CD101. Cytospin preparations represent sorted metamyelocytes (CD101-CXCR2-), immature neutrophils (CD101-CXCR2+) and mature neutrophils (CD101+CXCR2+). (D) Representative flow cytometric plots showing different neutrophils subsets based on the markers CD101 and CXCR2 in all experimental groups. (E) The number of the different neutrophil subsets were assessed by flow cytometry. (F) Number of IL-1β-expressing neutrophils in the spleen. Graphs show results from 3 pooled experiments. Each dot represents a single mouse, bars represent median group values with IQR. Closed circles: SPF-conditions; open circles: non-SPF-conditions. * p < 0.05; ** p < 0.01; *** p <0.001; **** p < 0.0001 between indicated groups or # p < 0.05; ## p < 0.01; ### p < 0.001; #### p < 0.0001 compared to IFN-γ KO NI or WT NI, by Kruskal-Wallis test, Dunn's post hoc test.

Discussion

sJIA patients are characterised by increased neutrophilia and develop splenomegaly due to extramedullary myelopoiesis. Recently, two papers described the phenotypical and functional characteristics of circulating neutrophils in sJIA (129,130). Despite, the neutrophil developmental path during extramedullary myelopoiesis remains largely unknown. Here, we used a mouse model for sJIA , relying on injection of CFA in IFN-γ KO mice (786), to study the aetiology of CFA-induced myelopoiesis and neutrophilia as well as its functional importance in the development of sJIA-like features.

Our study highlights an important role for G-CSF in the pathophysiology of sJIA. Main findings are summarised in Supplementary Figure 5.6. Both in patients and our mouse model, increased plasma levels of G-CSF were detected correlating with the number of neutrophils. In mice, αG-CSFR-administration blocked splenomegaly, neutrophilia, and plasma IL-1β levels and reduced incidence, clinical severity, and histological abnormalities of arthritis in IFN-γ KO mice. These observations are in line with previous work that used these G-CSFR-blocking antibodies in the treatment of arthritis (586,587). In contrast, αGM-CSF-treatment in CFA-immunised IFN-γ KO mice had no effect on the sJIA-like symptoms (including weight loss, neutrophilia, thrombocytosis, or anaemia) (data not shown). Our results fit the 'remnant epitopes generate autoimmunity' model, stating that cells and molecules of the innate immune system, can start autoimmune reactions by cytokine-regulated proteolysis yielding remnant epitopes (3). In this regard it is worth mentioning that sJIA follows a biphasic clinical course, in which the innate immune system is mainly involved in the onset of the disease, whereas the adaptive immune system contributes to the later chronic arthritic phenotype (85).

scRNAseq identified 5 neutrophilic subsets associated with extramedullary myelopoiesis, to be identical with those found in BM (316). Interestingly, we confirmed that these subsets could be separated in spleen based on the expression of CD101 and CXCR2 (316). scRNA-seq additionally showed that mature neutrophils from IFN-γ KO mice had an increased expression of MDSCs related genes and C/EBPβ, a transcription factor associated with emergency granulopoiesis, induced by G-CSF (462). MDSCs are best described in cancer but also expand during chronic and acute inflammatory conditions including sepsis (425,792). Neutrophil transcriptome analysis in sJIA patients showed an inflammatory gene expression profile, overlapping with the transcriptome of sepsis (129,130,589). Studying the effect of G-CSF on neutrophil subsets, we showed that αG-CSFR-treatment caused a maturation deficiency and "left shift" in the spleen from mature towards more immature and pre-neutrophil in CFA-treated IFN-γ KO mice.

Generally, G-CSF is considered as one of the main regulators involved in the expansion and maturation of neutrophils (582,608,650). In inflammatory conditions, G-CSF is regulated by the IL-23-IL-17-G-CSF axis (427,793,794). In this pathway, IL-1β and IL-6 are released by early activation of neutrophils and

monocytes and along with IL-23 (mainly produced by activated DCs, macrophages, or monocytes), stimulate IL-17 expression in lymphocytes, subsequently regulating the systemic induction of G-CSF, eventually driving massive neutrophil release (170,795,796). In accordance with this auto-amplification mechanism, sJIA patients are successfully treated with IL-1β and IL-6-targeting agents. Innate immune cells including γδ T-cells are an additional important source of IL-17 (147,545,797). Moreover, a positive feedback loop between neutrophil-derived IL-1β or S100 proteins and γδ T-cells was demonstrated in active patients with sJIA (147). In our model, we identified that both IL-17 and IL-23 play a pivotal role in the pathogenesis of the disease and blockade almost completely abolished splenomegaly and granulocytosis (786). Since IFN-γ links the IL-23-17-G-CSF axis, its absence may partially explain the enhanced phenotype in IFN-γ KO mice, reflected by *i.e.* enhanced levels of G-CSF.

Unexpectedly, slight increases in IL-6, TNF-α and IL-17 were detected upon G-CSFR inhibition. This appears to be specific for IFN-γ KO mice only and associated with a mild increase in weight loss, tail damage and number of immature RBCs. Since neutrophils have both pro- and anti-inflammatory properties, the reduced number of neutrophils and more specifically MDSCs in CFA-immunised IFN-γ KO mice may explain this aggravated phenotype observed after αG-CSFR-blocking. Recently Rybakin *et al.* showed *in vitro* that neutrophil-derived MMP-9 reduces the abundance of signalling-competent IL-2. Therefore It may be that the reduced levels of neutrophils (and MMP-9) upon αG-CSFR-treatment increase the levels of active IL-2, leading to enhanced T-cell activation or numbers of Tregs (as demonstrated) (798). We postulate that the aggravated local inflammation around the tail-injection site is directly linked to the inherent function of neutrophils, since they are major phagocytic cells that rapidly infiltrate sites of inflammation, and clear foreign particles, in this case the killed mycobacteria that are present in CFA. Therefore, due to insufficient numbers of neutrophils, the killed mycobacteria might not be properly resolved and continuously stimulate the innate immune cells.

In conclusion G-CSFR-blockade is able to inhibit excessive extramedullary myelopoiesis and arthritis development in a sJIA murine model. Future research is needed to clarify the exact role of G-CSF in sJIA patients.

Supplementary material

Supplementary figures

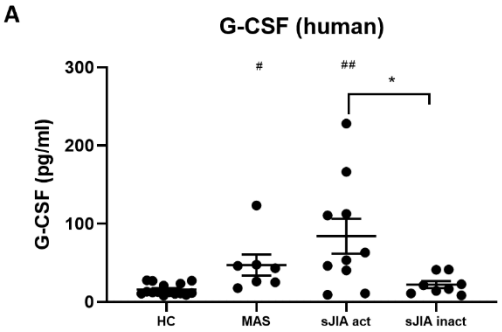

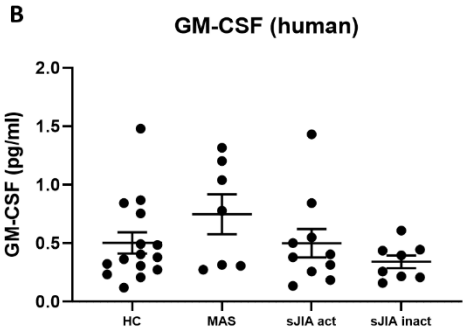

C

G-CSF	P-value	R^2
WBC	0.0003	0.9524
Monocytes	0.0003	0.9519
Neutrophils	0.0149	0.8095
IL-6	0.0298	0.7167
IL-1β	0.0377	0.6950
Lymphocytes	0.0501	-0.7066

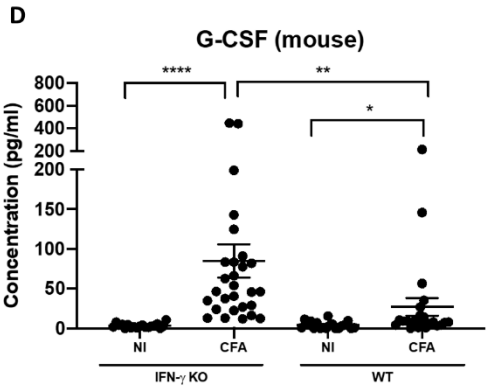

Supplementary Figure 5.1: sJIA patients display increased plasma levels of G-CSF. Plasma cytokine concentrations were measured with MSD multi-array technology. Levels of (A) G-CSF and (B) GM-CSF were measured in healthy controls (HC), macrophage activation syndrome (MAS) patients and systemic juvenile idiopathic arthritis (sJIA) patients with active or inactive disease status. Each dot represents a single measurement, horizontal bars represent median group values with IQR. * $p < 0.05$ between indicated group, by Wilcoxon matched-pairs signed rank test, or # $p < 0.05$; ## $p < 0.01$ compared to HCs, by Kruskal–Wallis test, Dunn's post hoc test. (C) Spearman correlations were found between levels of G-CSF and number of WBCs, monocytes, neutrophils and lymphocytes or plasma levels of IL-6 and IL-1β. (D) Mouse G-CSF levels measured in plasma by the Procarta-Multiplex system. Graphs show results from 3 pooled experiments. Each dot represents a single mouse, bars represent median group values with IQR. * $p < 0.05$; ** $p < 0.01$; ***0 $p < 0.0001$ between indicated groups, by Kruskal-Wallis test, Dunn's post hoc test.

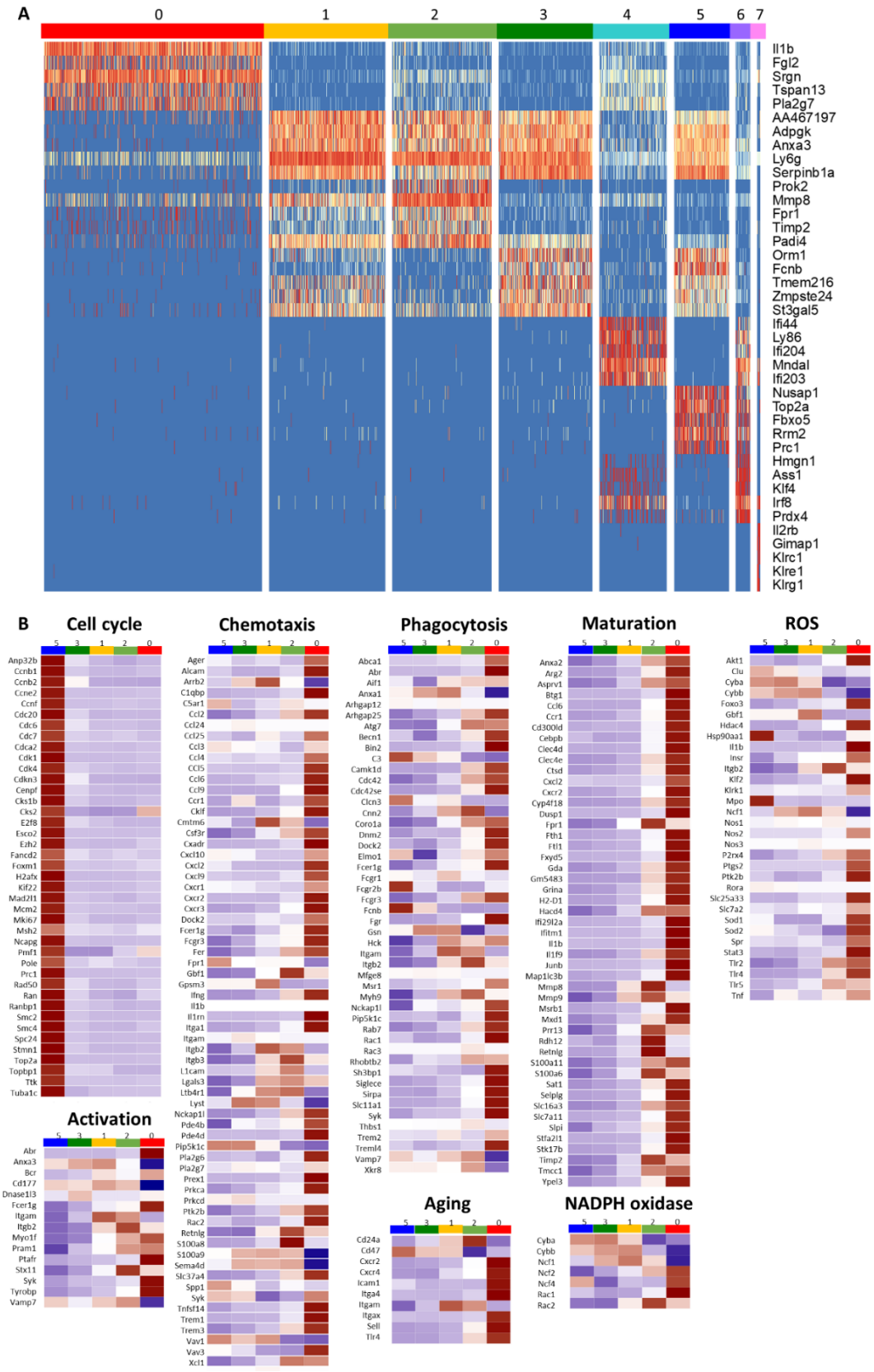

Supplementary Figure 5.2: Single-cell RNA sequencing reveals five distinct neutrophil subsets in CFA-immunised IFN-γ and WT mice. (A) Heatmap displaying the top marker genes within each cell cluster (by log fold change). (B) Heatmaps showing the expression of genes involved in ROS, phagocytosis, chemotaxis, cell cycle, maturation, aging and neutrophil activation in each neutrophil sub-cluster.

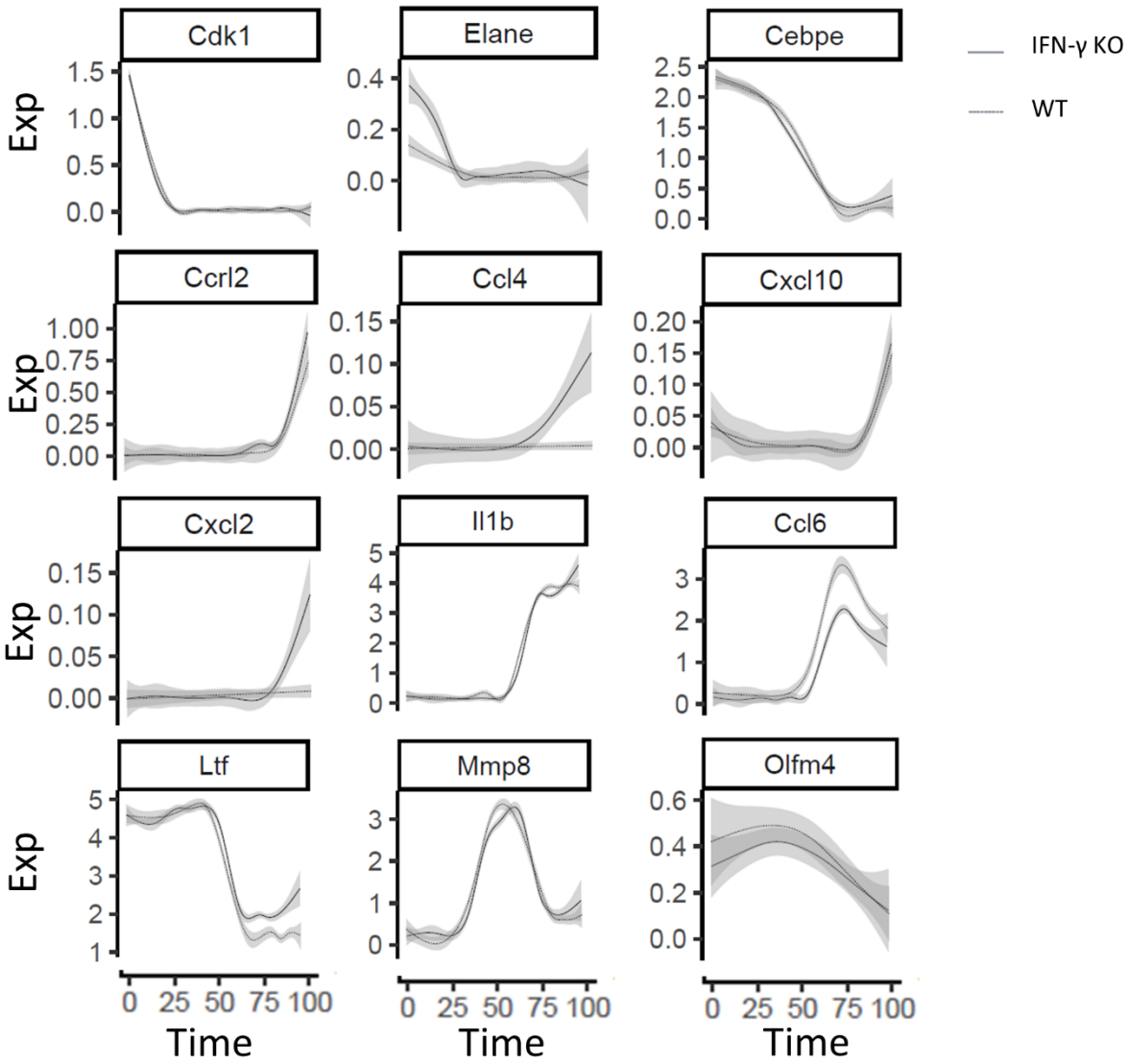

Supplementary Figure 5.3: Single-cell RNA sequencing reveals five distinct neutrophil subsets in CFA-immunised IFN-γ and WT mice. (A) Profiling of marker genes along the trajectories to confirm their functional annotation.

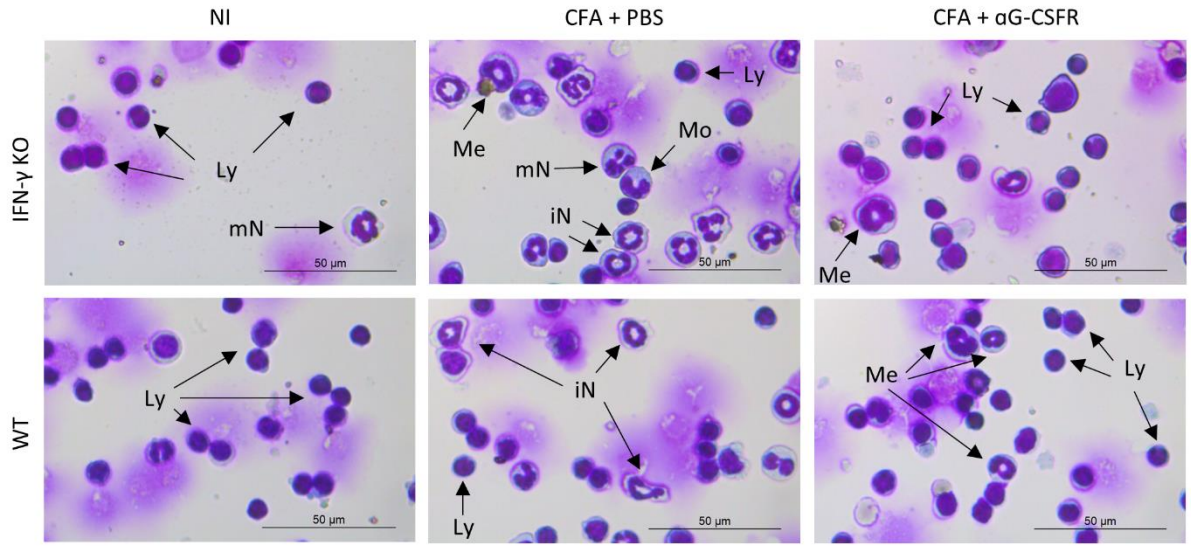

Supplementary Figure 5.4: Left shift in neutrophil subsets upon αG-CSFR-treatment. Representative photographs of H&E-stained cytospin preparations of splenocytes of NI IFN-γ KO and WT mice, CFA-immunised IFN-γ KO and WT mice with or without αG-CSFR-treatment. Arrows indicate different immune cells. Monocytes: Mo, lymphocytes: Ly, metamyelocytes: Me, immature neutrophils: iN, mature neutrophils: mM.

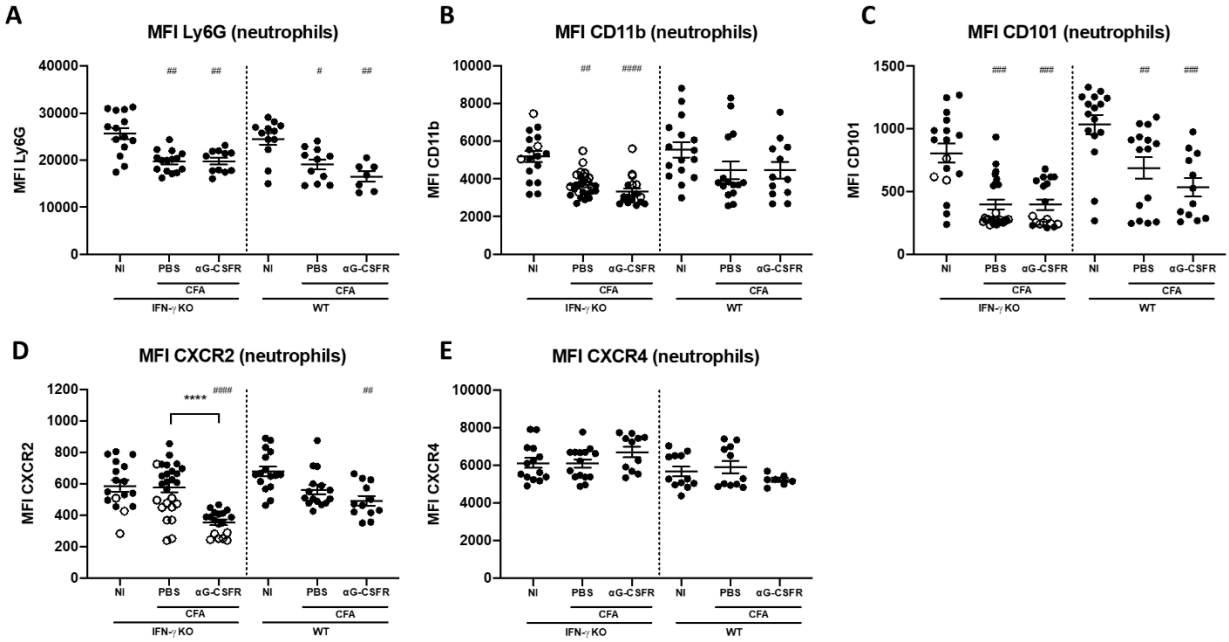

Supplementary Figure 5.5: Spleen neutrophil phenotype. CFA-immunised IFN-γ KO and WT mice were injected twice a week with αG-CSFR (200 µg - i.p.). Mice were sacrificed between day 16 and 25 post-immunisation. PBS-injected CFA-immunised IFN-γ KO and WT mice were included as controls and compared to naïve (NI) mice. Neutrophil expression levels of (A) Ly6G, (B) CD11b, (C) CD101, (D) CXCR2 and (E) CXCR4 were assessed in the spleen by flow cytometry. Graphs show results from 3 pooled experiments. Each dot represents a single mouse, bars represent median group values with IQR. Closed circles: SPF-conditions; open circles: non-SPF-conditions. **** $p < 0.0001$ between indicated groups or # $p < 0.05$; ## $p < 0.01$; ### $p < 0.001$; #### $p < 0.0001$ compared to IFN-γ KO NI or WT NI, by Kruskal-Wallis test, Dunn's post hoc test.

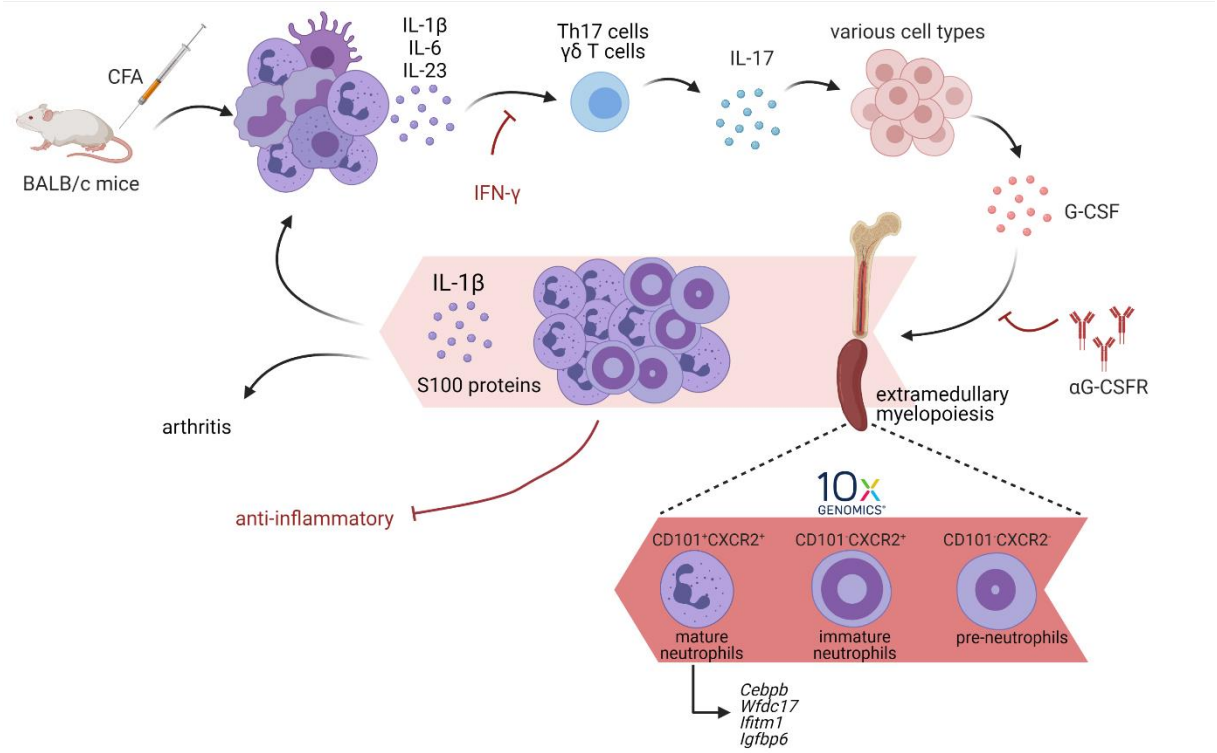

Supplementary Figure 5.6: The IL-23-IL-17-G-CSF-axis promotes extramedullary myelopoiesis in sJIA. CFA-immunisation evokes a local and systemic inflammatory reaction that is initiated by *i.e.* early infiltrating neutrophils and monocytes producing IL-1β, IL-6. Together with IL-23, these cytokines activate γδ T cells and Th17 cells to produce IL-17. Increased IL-17 subsequently lead to upregulation of G-CSF by diverse cell types including bone marrow (BM) stromal cells, endothelial cells, macrophages, or fibroblasts. G-CSFR-signalling promotes neutrophil expansion and extramedullary myelopoiesis in the spleen of CFA-immunised mice. Single cell sequencing was applied on spleen and revealed a neutrophil differentiation path reminiscent to the BM (316)**. IFN-γ tempers the induction of IL-17, and IFN-γ deficient (KO) mice have an exaggerated immune response characterised by increased levels of G-CSF. Excessive neutrophilia forms a positive feedback-system by the production of *i.e.* S100 proteins and IL-1β and furthermore results in the induction of arthritis in the joints. Boosted production of G-CSF in IFN-γ KO mice, phenotypically alters neutrophils and induces genes involved in emergency granulopoiesis and myeloid-derived suppressor cells. αG-CSFR-blockage could completely prevent neutrophilia, extramedullary myelopoiesis and arthritis development. In IFN-γ KO mice, depletion slightly increases pro-inflammatory cytokines due to absence of neutrophils that might have some anti-inflammatory effects.**

Supplementary Material and Methods

sJIA mouse model

Experiments with WT and IFN-γ KO BALB/c mice were performed at KU Leuven Experimental Animal Centre and were approved by our Ethical Committee (P182/2014-P005/2020). Mice were housed under specific pathogen-free (SPF) conditions, except where noted otherwise. The sJIA mouse model was induced in 6-9 week old mice by a subcutaneously injection of CFA (Difco) supplemented with heat-killed Mycobacterium butyricum (1.5 mg/mL) (786). Twice a week, mice were weighed and examined visually. Arthritis was assessed four times a week following a scoring system (Supplementary Table 5.2A). Tail damage was scored as described in Supplementary Table 5.2B. Non-immunised (NI) WT and IFN-γ KO littermates were included as controls.

Supplementary Tables

Supplementary Table 5.1: Patient characteristics

	HC	Active sJIA	Inactive sJIA	MAS
Male/Female	6/9	4/6	3/5	4/3
Age (years)	12 (0-27)	5 (1-16)	6 (2-16)	15 (0-34)
Clinical features				
Active arthritis	0/15	10/10	0/8	0/7
Fever	0/15	8/10	0/8	7/7
Rash	0/15	7/10	0/8	2/7
Laboratory features				
WBC count (x10^9/l)	ND	21.355 (4.8-30.3) *	6.6 (3.7-22.9)	7.3 (0.8-14.2)
Neutrophil count (x10^9/l)	ND	17.4 (3.1-27.0) *	2.6 (1.3-12.5)	1.7 (0.4-11.5)
Lymphocyte count (x10^9/l)	ND	2.3 (0.7-7.2)	2.95 (0.5-7.1)	1.5 (0.2-6.8)
Monocyte count (x10^9/l)	ND	1.05 (0.5-1.6) *	0.65 (0.2-1.1)	0.6 (0.1-0.8)
RBC count (x10^12/l)	ND	3.82 (3.2-4.5) *	4.455 (4.1-4.8)	4.655 (3.2-5.1)
Haemoglobin (g/dl)	ND	10.5 (7.9-11.9) **	12.15 (9.9-13.1)	11.1 (9.7-14.2)
Platelet count (x10^9/l)	ND	462 (210-757)	314.5 (172-759)	101 (31-366)
Aspartate transaminase (U/ml)	ND	31 (14-45)	29.5 (19-43)	189 (24-605)
Alanine transaminase (U/ml)	ND	14 (7-36)	20 (9-27)	124 (12-1164)
Ferritin (µg/l)	ND	865 (49-3959)	ND	5210.5 (1942-21151)
CRP (mg/l)	ND	115.55 (32.2-341.6) **	0.3 (0.3-4.5)	2.5 (0.4-339)
Treatment				
NSAID	0/15	5/10	0/8	1/7
Corticosteroids	0/15	2/10	2/8	1/7
Methotrexate	0/15	2/10	0/8	0/7
Biologicals (IL-6 or IL-1β)	0/15	2/10	5/8	2/7
Cytokine levels				
G-CSF (pg/ml)	12.3 (8.1-27.6)	58.2 (9.0-228.0) ## / *	19.0 (8.4-41.5)	43.2 (17.7-123.4)
GM-CSF (pg/ml)	0.4 (0.1-1.5)	0.4 (0.1-1.4)	0.3 (0.2-0.6)	0.8 (0.3-1.3)
IFN-γ (pg/ml)	2 (0-27.5)	5.3 (0.8-107.2)	2.7 (0-24.2)	45.5 (0-7285.2) #
IL-10 (pg/ml)	0.4 (0-2.1)	1.0 (0.2-7.9) *	0.2 (0-2.4)	7.4 (1.5-10.0) ###
IL-17 (pg/ml)	1.9 (0.7-5.1)	1.7 (0.8-3.2)	1.8 (1.1-2.7)	3.8 (0.8-5.3)
IL-18 (pg/ml)	688.5 (329-1247.1)	44540.6 (6972.1-290044.2) ####	2914.5 (792.3-163262.9) #	273378.9 (1949.8-1035449.8) ####
IL-1β (pg/ml)	0 (0-0.3)	0 (0-4.2)	0 (0-0.3)	0 (0-0.5)
IL-23 (pg/ml)	2.6 (0-12.6)	3.8 (1.3-12.5)	2.3 (0-50.1)	2.8 (0-4.7)
IL-6 (pg/ml)	0.4 (0.2-1.1)	15.5 (7.1-23.3) #### / *	5.5 (0.5-17.4) #	2.9 (0.6-52.5) #
TNFα (pg/ml)	3.1 (0.9-6.1)	3.7 (1.9-13.3)	2.4 (1.1-6.1)	7.0 (1.6-12.3)

For age, laboratory features and cytokine levels, median with range are given. Inactive sJIA patients were defined by the absence of fever, rash, arthritis, and inflammatory parameters. HC = healthy control. MAS = macrophage activation syndrome. AOSD = Adult onset Still's disease. CRP = C-reactive protein. NSAID = non-steroidal anti-inflammatory drugs. ND = not determined. P values less than 0.05 were considered significant (* $p < 0.05$; ** $p < 0.01$ between active and inactive sJIA patients, by Wilcoxon matched-pairs signed rank test, or # $p < 0.05$; ## $p < 0.01$; ### $p < 0.001$; #### $p < 0.0001$ compared to HCs, by Kruskal–Wallis test, Dunn's post hoc test.

Supplementary Table 5.2: Clinical scoring system arthritis and tail damage

A. Clinical score arthritis	
Score	**Meaning**
0	Normal
1	Redness and/or swelling in one joint
2	Redness and/or swelling in more than one joint
3	Redness and/or swelling in the entire paw
4	Deformity and/or ankylose.
For each mouse, a maximum score of 16 can be reached	
B. Clinical score tail	
Score	**Meaning**
0	No damage
1	Redness
2	Small open wound
3	Large open wound
4	Excessive damage

Supplementary Table 5.3: Antibody list

Antigen	Clone	Fluorochrome	Producent
γδ -TCR	eBioGL3 GL3	APC PE Cy7	Invitrogen Biolegend
B220	RA3-6B2	BV786	BD Biosciences
CD3	145-2C11 145-2C11 17A2 145-2C11	BUV395 BUV737 BV510 PercP Cy5.5	BD Biosciences BD Biosciences BioLegend Invitrogen
CD4	RM4-5 RM4-5 RM4-5	APC eF780 BV421 PercP Cy5.5	Invitrogen Biolegend Biolegend
CD8	53-6.7 53-6.7	BV711 PercP Cy5.5	Invitrogen/BD Biolegend
CD11b	M1/70	BUV395	BD BioScience
CD11c	N418	BV711	BD Bioscience
CD16/32	93	APC Cy7	BioLegend
CD19	6D5 eBIO1D3	BV510 PE	BioLegend eBioscience
CD25	PC61.5	PE Cy7	eBioscience
CD27	LG.7F9	FITC	eBioscience
CD34	RAM34	FITC	BD Bioscience
CD44	IM7	PE	BioLegend
CD49	DX5 DX5	BV421 PE Cy5	BD Bioscience Invitrogen
CD62L	MEL-14	APC	Invitrogen
CD69	H1.2F3 H1.2F3	BV786 PE Cy7	BioLegend Invitrogen
CD80	16-10A1	BV421	BD
CD86	GL1	PE	Invitrogen
CD101	307707 307707	Af647 APC	BD Bioscience invitrogen
CD115	AFS98	PE	eBioscience
CD117 (ckit)	2B8	PE Cy5	BioLegend
CD122	TM-β1 TM-β1	BV421 PE Cy7	BD Bioscience Biolegend
CD127	A7R34	BV605	BioLegend
CCR2	SA203G11	PE Cy7	BioLegend
CXCR2	SA045E1	PercP Cy5.5	BioLegend
CXCR4	L276F12	BV605	BioLegend
FOXP3	150D	Af488	BioLegend
F4/80	BM8	APC	Invitrogen
IL-1β	Pro-form-PE	PE	Miltenyi Biotec
IL-6	MP5-20F3	FITC	Invitrogen
IL-17	eBio17B7	eF450	Invitrogen
Ly6C	HK1.4 HK1.4	FITC PercP Cy5.5	BioLegend Invitrogen
Ly6G	1A8	BV786	BioLegend/BD Biosciences
KLRG1	2F1/KLRG1	PE-DAZZLE-594	BioLegend
MHCI	28-14-8	eF450	Invitrogen
MHCII	M5/114.15.2	PE	Invitrogen
TNF-α	MP6-XT22	APC FITC	Invitrogen BD Biosciences

Supplementary Table 5.4: sJIA characteristics in CFA-immunised mice

	WT CFA	WT CFA αG-CSFR	IFN-γ KO CFA	IFN-γ KO CFA αG-CSFR
General characteristics				
Weight loss	+	=	++	↑
Arthritis	-	=	+[a]	↓
Rash	-	=	+[a]	↑
Lymphadenopathy	+	↓	+	=
Splenomegaly	+	↓	++	↓
Hematologic				
Anaemia	-	=	+[a]	=
Granulocytosis	+	↓	++	↓
Lymphocytopenia	+	↓	+	=
Thrombocytosis	+	=	++	=↑
More specific characteristics				
IL-17, IL-6 and TNF-α levels	-	=↓ (IL-6)	+	↑
Immature RBCs	+	↓	+	↑

Features were graded as follows: +, present; ++, more pronounced present; and -, absent.
[a] In subsets of mice.
For WT and IFN-γ KO mice, a summary of 10 experiments was used to compose this table, and the list of features is founded on data published in Avau *et al.* (15). Arrows represent changes in αG-CSFR treated mice compared non-treated counterparts.

CHAPTER 6

LUNG FUNCTIONING AND INFLAMMATION IN A MOUSE MODEL OF SYSTEMIC JUVENILE IDIOPATHIC ARTHRITIS

Published manuscript:

Bert Malengier-Devlies[1], Tatjana Decaesteker[2], Kaat Decoster[3], Arno Vanstapel[2], Kourosh Ahmadzadeh[1], Fariba Poosti[4], Tania Mitera[1], Laura Seldeslachts[3], Erik Verbeken[5], Carine Wouters[1,6,7], Greetje Vande Velde[3], Jeroen Vanoirbeek[2], Patrick Matthys[1] (2021). Lung Functioning and inflammation in a mouse model of systemic juvenile idiopathic arthritis. Frontiers in Immunology, 12, Art.No. 642778.

[1] KU Leuven Department of Microbiology, Immunology and Transplantation, Rega Institute for Medical Research, Laboratory of Immunobiology, Leuven, Belgium
[2] KU Leuven Department of Chronic Diseases and Metabolism, Laboratory of Respiratory Diseases and Thoracic Surgery (BREATHE), Leuven, Belgium
[3] KU Leuven Department of Imaging & Pathology, Biomedical MRI, Leuven, Belgium
[4] KU Leuven Department of Microbiology, Immunology and Transplantation, Rega Institute for Medical Research, Laboratory of Molecular Immunology, Leuven, Belgium
[5] University Hospitals Leuven, Morphology and Molecular Pathology Section, Leuven, Belgium
[6] University Hospitals Leuven, Division of Pediatric Rheumatology, Leuven, Belgium
[7] European Reference Network for Rare Immunodeficiency, Autoinflammatory and Autoimmune Diseases (RITA) at University Hospital Leuven, Leuven, Belgium

CHAPTER 6: LUNG FUNCTIONING AND INFLAMMATION IN A MOUSE MODEL OF SYSTEMIC JUVENILE IDIOPATHIC ARTHRITIS

Abstract

Systemic juvenile idiopathic arthritis (sJIA) is an immune disorder characterised by fever, skin rash, arthritis and splenomegaly. Recently, increasing number of sJIA patients were reported having lung disease. Here, we explored lung abnormalities in a mouse model for sJIA relying on injection of IFN-γ deficient (IFN-γ KO) mice with complete Freund's adjuvant (CFA). Monitoring of lung changes during development of sJIA using microcomputer tomography revealed a moderate enlargement of lungs, a decrease in aerated and increase in non-aerated lung density. When lung function and airway reactivity to methacholine was assessed, gender differences were seen. While male mice showed an increased tissue hysteresivity, female animals were characterised by an increased airway hyperactivity, mirroring ongoing inflammation. Histologically, lungs of sJIA-like mice showed subpleural and parenchymal cellular infiltrates and formation of small granulomas. Flow cytometric analysis identified immature and mature neutrophils, and activated macrophages as major cell infiltrates. Lung inflammation in sJIA-like mice was accompanied by augmented expression of IL-1β and IL-6, two target cytokines in the treatment of sJIA. The increased expression of granulocyte colony stimulating factor, a potent inducer of granulopoiesis, in lungs of mice was striking considering the observed neutrophilia in patients. We conclude that development of sJIA in a mouse model is associated with lung inflammation which is distinct to the lung manifestations seen in sJIA patients. Our observations however underscore the importance of monitoring lung disease during systemic inflammation and the model provides a tool to explore the underlying mechanism of lung pathology in an autoinflammatory disease context.

Introduction

Systemic juvenile idiopathic arthritis (sJIA) is a childhood auto-inflammatory immune disorder, characterised by growth retardation, spiking fever, skin rash, arthritis, splenomegaly and polyserositis. Haematological changes, such as leucocytosis, neutrophilia, anaemia and thrombocytosis are typically seen. High levels of interleukin-6 (IL-6), IL-18, C-reactive protein (CRP) and S100 acute phase proteins are present in plasma of sJIA patients (25,26,31,168,173,749). Around 10-15% of patients develop a live-threatening complication, called macrophage activation syndrome (MAS) which is associated with pancytopenia, increased liver enzymes, high ferritin levels, and coagulopathy (31,59,60,132). MAS is associated with high production of IL-18 and interferon gamma (IFN-γ) (21). Part of sJIA patients can successfully be treated with biologics targeting IL-1β or IL-6, which replaced chronic high dose treatment with corticosteroids (73,78,81,771).

Chronic parenchymal lung disease (PLD) has only rarely been reported in sJIA (110,111). Kimura Y *et al* described for the first time 25 sJIA patients with chronic pulmonary disease, characterised by pulmonary arterial hypertension (PAH), interstitial lung disease (ILD) and pulmonary alveolar proteinosis (PAP) (799). Recently, two studies reported lung disease in patients with sJIA (108,109). Radiographic analysis demonstrated ground-glass opacities, subpleural reticulation, interlobular septal thickening and lymphadenopathy. Histopathological analysis revealed lymphoplasmacytic infiltration, mixed features of PAP or endogenous lipoid pneumonia (ELP), vasculopathy, alveolar epithelial cell hyperplasia and collagenous fibrosis. Although sJIA equally occurs in both sexes, a non-significant higher incidence of female patients with lung disease (66%) was reported (109). The incidence of lung disease cases has increased since 2010 and coincides with the increasing use of biologics, Nigrovic *et al.*, highlighted that 'lung disease in sJIA might be a dark cloud on the horizon in the management of sJIA' (112,800). Indeed, treatment with IL-1 or IL-6 inhibitors was demonstrated as a risk factor in the development of sJIA lung disease (109).

In this study, we investigated lung pathology in a mouse model for sJIA. The model relies on a single injection of BALB/C mice with complete Freund's adjuvant (CFA). While wild-type (WT) mice develop a transient and mild form of inflammation, IFN-γ-deficient (IFN-γ KO) mice develop a chronic inflammatory condition with clinical, haematological and biological characteristics reminiscent to sJIA (786). Although sJIA patients do not have mutations in the IFN-γ gene, defects in the production of IFN-γ by NK cells have been reported (139,157). Furthermore, the clinical relevance of the model lies in the many similarities with sJIA, including weight loss, arthritis, skin rash, splenomegaly, lymphadenopathy, anaemia, granulocytosis, thrombocytosis, NK cell defects and increased serum levels of IL-6 (Supplementary Table 6.1). To study lung inflammation, we evaluated the functional, histopathological and cellular aspects of lungs from CFA-injected IFN-γ KO mice (also designated as sJIA-like mice) and included CFA-injected WT mice for comparison.

Material and Methods

Mice immunisation

IFN-γ KO and WT BALB/c mice were bred under specific pathogen-free conditions. Six-to 8-week-old mice were either or not subcutaneously injected at the tail base with complete freund's adjuvant (CFA) (Difco) containing heat-killed *Mycobacterium butyricum* (1.5 mg/ml) as described (Supplementary Table 6.1) (786). All animals experiments were approved by the Ethics Committee of KU Leuven (P182/2014).

Micro-computed tomography

Micro-computed tomography was performed on day 0, day 12 and day 21 post CFA-immunisation. During the procedure, the mice were anesthetised by inhalation of 1.5-2% isoflurane in 100% oxygen and scanned in supine position using a dedicated small animal in vivo µCT scanner (Skyscan 1278, Bruker µCT, Kontich, Belgium) as previously described (801). The following parameters were used: 50 kVp X-ray source voltage and 346 µA current combined with a composite X-ray filter of 1 mm aluminium, 150 ms exposure time per projection, acquiring 3 projections per step with 0.9° increments over a total angle of 220°, and 10 cm field of view covering the whole body producing expiratory-weighted 3D data with 50 µm isotropic reconstructed voxel size. Each scan takes approximately 3 minutes and is associated with a measured radiation dose of 60-80 mGy (802). Software provided by the manufacturer (NRecon, DataViewer, and CTan) was used to reconstruct, visualise, and process µCT data as described previously (801–803). For Hounsfield unit (HU) calibration, a phantom was scanned consisting of an air-filled 1.5 mL tube inside a water-filled 50 mL tube. Based on full stack histograms of a volume-of-interest (VOI) containing only water or air, the main grayscale index of water (127) was set at 0 HU and grayscale index of air (6) at -1000 HU. The non-aerated lung volume, aerated lung volume, total lung volume and respective densities within these volumes were quantified for a manually delineated VOI covering the lung, avoiding the heart and main blood vessels. The aerated and non-aerated lung densities represents the density of air in the alveoli and the surrounding epithelial, capillary and extracellular matrix and small airways respectively. Oedema and accumulation of inflammatory cells are associated with an increased density whereas destruction of the alveoli would result in a decreased lung density. The threshold used to distinguish aerated from non-aerated lung volume was manually set at -180 HU and kept constant for all data sets.

Lung function measurements

At day 21 post CFA-infection, on the moment all overt signs of inflammation were discernible, lung function measurements were performed and mice were subsequently euthanised. During function measurements, mice were anaesthetised by an intraperitoneal (i.p.) injection of pentobarbital (70 mg/kg body weight). Lung function measurements were performed using a forced oscillation technique (FlexiVent 7.6, SCIREQ, Montreal, Canada), as described previously (804). Mice were quasi-sinusoidally ventilated with a tidal volume of 10 mL/kg at a frequency of 150 breaths/min and a positive end-expiratory pressure of 3 cm H_2O, to mimic the characteristics of spontaneous breathing. Airway resistance (Rn) was measured using the 'quick-prime 3' protocol, which induces oscillations of 1 to 20.5 Hz during 3 seconds. Lung volumes, such as forced expiratory volume in 0.1s ($FEV_{0.1}$), forced vital capacity (FVC) and peak expiratory flow (PEF) were measured by using the 'Negative Pressure Forced Oscillation' technique. After baseline measurements, each mouse was exposed to a methacholine aerosol, generated with an in-line nebulizer (Aeroneb Lab nebuliser, 2.5-4 µm, Aerogen, Galway, Ireland) and administered at increasing concentrations (0, 2.5, 5, 10, 20 and 40 mg/mL), each during 5 seconds, and Rn measured.

Histopathology and immunofluorescence staining

Lungs were fixed for 24 hours with 10% formalin and were kept inflated at constant pressure throughout the fixation process. Lung sections were stained with hematoxylin and eosin, and were evaluated blindly by two experienced lung pathologists. Images were taken with a Leica DFC295 microscope. Immunofluorescence staining was performed on 4 µm acetone-fixed frozen lung and kidney sections. Tissue sections were incubated with the primary anti-α-SMA (Cat. Nr: 61001, ProGen, Heidelberg, Germany) antibody for 1 h at RT. Binding of α-SMA primary antibody was detected by incubation with goat anti-mouse IgG2a FITC (Southern Biotech, Birmingham, AL, USA) for 30 min. Nuclei were stained with Hoechst, and sections were coverslipped with Prolong Gold antifade reagent (Invitrogen). All immunofluorescence images were taken with a Zeiss Axiovert 200M inverted microscope and AxioVision acquisition software (Carl Zeiss, Oberkochen, Germany).

Antibodies, flow cytometry and FACS sorting

To prepare single cell suspensions, lungs were digested for 45 min at 37°C in RPMI 1640 supplemented with 5 % FCS, 2 mM L-glutamine, 0.05 mM 2-mercaptoethanol, 100 U/ml penicillin, 100 mg/ml streptomycin (Invitrogen), 1 mg/ml collagenase type 2 (Worthington Biochemical), and 0.02 mg/ml DNase I (grade II from bovine pancreas, Ingelheim). Red blood cells were lysed using ACK Lysing Buffer (Gibco). Cells were incubated with FcR-block (Miltenyi Biotec) and stained extracellularly in FACS buffer (PBS +2% FCS +2mM EDTA). Antibodies used in this study are listed in Supplementary Table 6.2. Before lineage gating, all populations were first gated on live cells by using Zombie Aqua 516 (Biolegend). Forward and side scatter was used to limit debris and doublets. Cells were run on a BD LSRFortessa X20 or a BD FACSymphony equipped with the DIVA software and data were analysed using FlowJo software (LLC, V10).

qRT-PCR

Total RNA was extracted by PureLink RNA Mini kit (Invitrogen) or the RNeasy Micro kit (Qiagen), followed by the preparation of complementary DNA (cDNA) using Superscript II reverse transcriptase and random primers (Invitrogen). Real-time (RT) quantitative (q)PCR was performed using a TaqMan gene expression assay (Applied Biosystems) on a 7500 Real-Time PCR System Apparatus. Primers used are listed in Supplementary Table 6.3. All primers were obtained from Integrated DNA Technologies and RNA expression was normalized to the expression of GAPDH RNA (Mm99999915_g1) according to the delta-delta CT method.

Statistical analyses

The two-tailed non-parametric Mann-Whitney U test was used for all single comparisons of two unpaired groups. For data with three or more groups, the non-parametric Kruskal-Wallis test (unpaired data) or Friedman test (paired data) was used and was followed by a Mann-Whitney U test. Data of longitudinal µCT-derived biomarkers (mean lung density, total lung volume, non-aerated lung volume and aerated lung volume) were analysed using a mixed-effects model with Geisser-Greenhouse correction. For multiple comparison, Sidak's *post hoc* test was used. For correlation analysis, the Spearman correlation coefficient was determined. For all tests, statistical significance was assumed with * p-value < 0.05; ** p-value < 0.01; *** p-value < 0.001; **** p-value < 0.0001. All data analysis was performed using the GraphPad Prism 7 software.

Results

Changes in lung volume and lung density upon immunisation with CFA.

When BALB/C mice are injected s.c. at the base of the tail with CFA, they develop systemic inflammation within 21 days. While the inflammation is mild in WT animals, IFN-γ KO mice develop a more severe disease with symptoms and blood abnormalities that are similar to those reported in sJIA patients (Supplementary Table 6.1) (786). To identify potential lung disease during development of systemic inflammation, mice were monitored by high-resolution low-dose *in vivo* µCT before and after immunisation with CFA, *i.e.* at day 12 when sJIA symptoms started to appear and at day 21 when blood abnormalities are maximal in both groups of mice (786). Representation of µCT images and quantification of lung volume and lung densities are shown in Figure 6.1 and Supplementary Figure 6. 1. Visual inspection of the µCT images showed a moderate enlargement and a reduced density of the lungs over time in CFA-immunised mice (Figure 6.1a). Surprisingly, IFN-γ KO mice have a larger lung volume than WT mice, even before the start of immunisation despite the fact that the mean body weight in both groups was similar at day 0 (Figure 6.1b, body weights are not shown). Following CFA-immunisation, total lung volume increased in both WT and IFN-γ KO mice which was attributed to an increase in aerated lung volume. CFA-challenge also resulted in a decrease of mean lung density in both WT and IFN-γ KO mice (Figure 6.1b). While total and aerated lung densities decreased upon immunisation in both strains, the non-aerated density significantly increased in IFN-γ KO mice only (Figure 6.1c). When aerated and non-aerated lung densities were plotted, the changes reached statistical significance when data were separately quantified in females and males (Figure 6.1d). In conclusion, development of systemic inflammation elicited by CFA, is associate with a moderate increase in aerated lung volume and a decrease in aerated lung density, the latter being indicative for loss of alveolar integrity. The more severe inflammation in IFN-γ KO mice is associated with an increased non-aerated lung density, which may be indicative for inflammatory infiltrates (801).

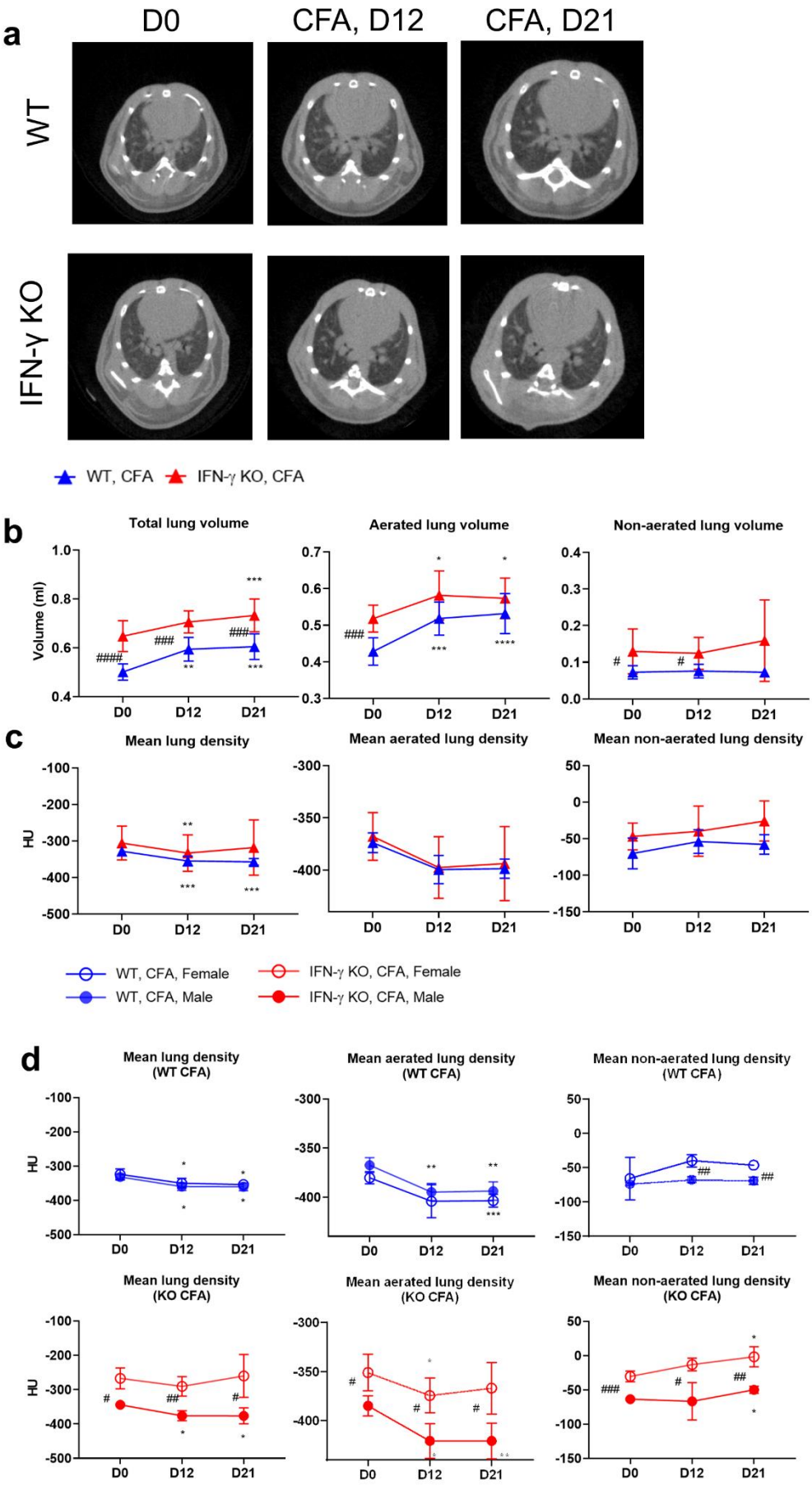
a
D0
CFA, D12
CFA, D21
WT
IFN-γ KO
WT, CFA
IFN-γ KO, CFA
b
Total lung volume
Aerated lung volume
Non-aerated lung volume
Volume (ml)
D0
D12
D21
c
Mean lung density
Mean aerated lung density
Mean non-aerated lung density
HU
WT, CFA, Female
WT, CFA, Male
IFN-γ KO, CFA, Female
IFN-γ KO, CFA, Male
d
Mean lung density (WT CFA)
Mean aerated lung density (WT CFA)
Mean non-aerated lung density (WT CFA)
Mean lung density (KO CFA)
Mean aerated lung density (KO CFA)
Mean non-aerated lung density (KO CFA)

Figure 6.1: WT mice and IFN-γ KO mice were immunised with CFA. Mice were scanned with µCT before (day D0) and at regular time points after the CFA-immunisation (day D12, day D21). (a) Representative transverse µCT images of a WT and KO CFA-immunised mice at the selected time points. The position of the shown images was choses at 100 z-positions after the first bifurcation of the airways. (b) Three lung volumes were established: total lung volume (ml), aerated long volume (ml) and non-aerated long volume (ml). (c-d) The mean lung density, aerated lung density and non-aerated lung density were measured and expressed in HU units. Data are represented as mean group values with standard error (SE). Blue graphs represent CFA-immunised WT mice, red graphs represent CFA-immunised IFN-γ KO mice. */# p<0.05; **/## p<0.01; */### p<0.001; ****/#### p<0.0001 by repeated measures two-way ANOVA. Asterisk represents time-based differences and hashtag represents differences between WT and IFN-γ KO mice.**

Functional lung alterations in CFA-challenged IFN-γ KO mice

On day 21, a time-point on which most systemic features were apparent (786), lung function and non-specific airway reactivity to methacholine was assessed. Distinct functional alterations were measured between male and female mice, therefore both sexes are shown separately. Lung forced vital capacity (FVC), forced expiratory volume 0.1 ($FEV_{0.1}$) and the FVC/$FEV_{0.1}$ ratio (also known as Tiffeneau-index 0.1) did not show any difference between the experimental groups (data not shown). In contrast, lung structural parameters, such as tissue damping (G) and tissue hysteresivity (eta=G/H) were significantly higher in male CFA-challenged IFN-γ KO mice compared to naïve IFN-γ KO mice. A significant lower airway resistance (Rn) in male IFN-γ KO mice compared with male WT mice, regardless of the CFA injection was also observed. These changes in G, eta and Rn were not seen in female mice (Figure 6.2a). After the baseline measurements, a dose-response challenge with methacholine was performed to evaluate the airway hyperreactivity. Airway resistance of female CFA-challenged IFN-γ KO mice was significantly higher at 20 and 40 mg/ml compared with other treatment groups (Figure 6.2b). This was also reflected in a significantly lower $FEV_{0.1}$ upon methacholine challenge with 20 and 40 mg/ml in female CFA-challenged IFN-γ KO mice (Figure 6.2c), confirming airway hyperreactivity in female CFA-challenged IFN-γ KO mice. In male mice, all dose-responses to methacholine were the same and no airway hyperreactivity could be measured (Figure 6.2b-c). In conclusion, CFA-immunisation leads to functional lung alterations in IFN-γ KO mice. Whereas male mice show increased tissue hysteresivity, female mice were characterised by an increased airway hyperreactivity.

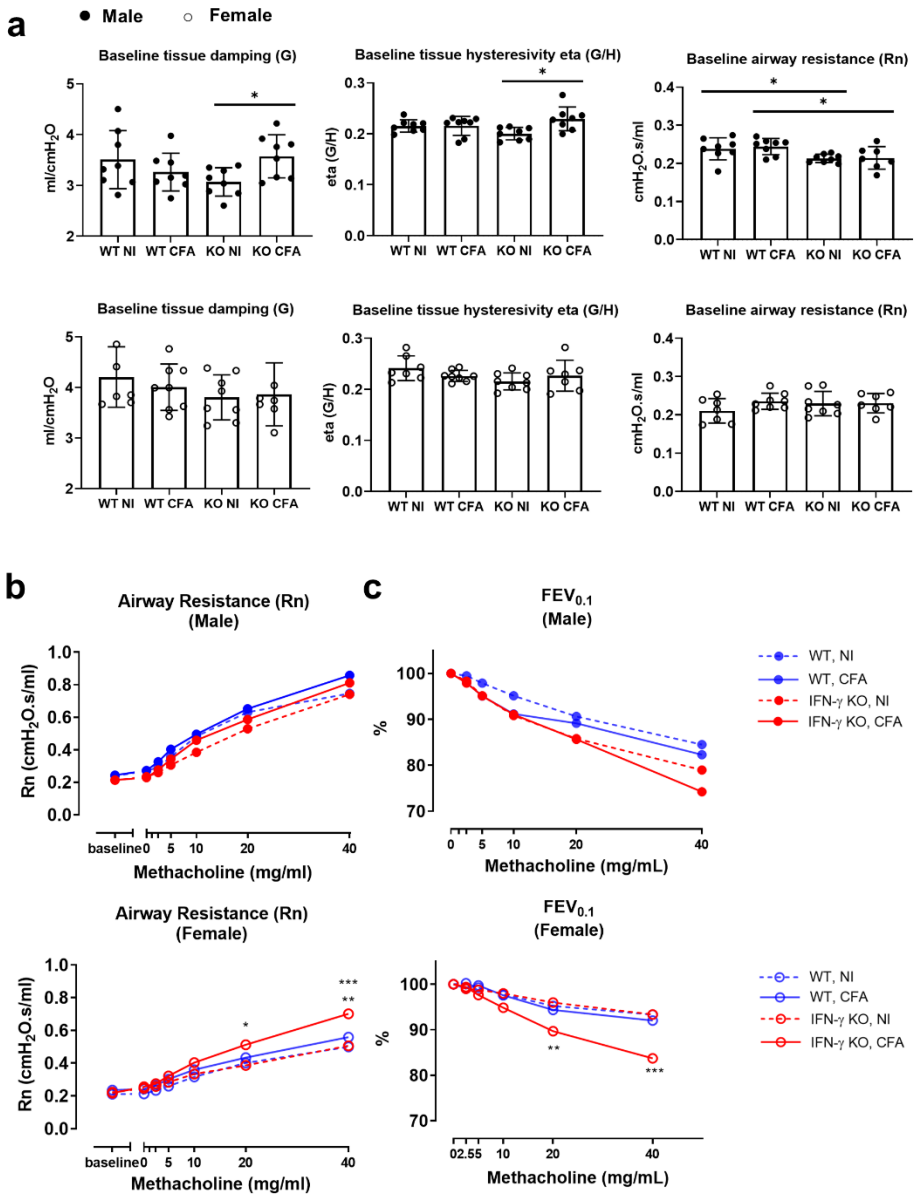

Figure 6.2: WT mice and IFN-γ KO mice were immunised with CFA. NI WT and IFN-γ KO mice were included as controls. Baseline lung function parameters and airway hyperreactivity were assessed at day 21 post CFA-injection. (a) Baseline tissue damping (G), tissue hysteresivity (eta = G/H) and airway resistance (Rn) were measured using a forced oscillation technique (QP3) in both male (closed) and female (open) mice. Data are represented as mean group values and individual data points. *p < 0.05 by by Kruskal-Wallis followed by Mann-Whitney U test. (b) The dose-response of the airway resistance to methacholine (0 – 40 mg/ml), in both male (closed) and female (open) mice, was measured using the forced oscillations technique (QP3). *p < 0.05 for IFN-γ KO CFA compared to IFN-γ KO NI at 20 mg/ml. **p < 0.01 and *** p < 0.001 for IFN-γ KO CFA compared to WT CFA and IFN-γ KO NI respectively at 40 mg/ml (Two-Way ANOVA). (c) The dose-response of the forced expiration volume in 0.1 sec (FEV0.1) to methacholine (0 – 40 mg/ml) was measured using a negative pressure forced expiration manoeuvre (NPFE), in male (closed) and female (open) mice. **p < 0.01 for IFN-γ KO CFA compared to IFN-γ KO NI at 20 mg/ml. ***p<0.001 for all groups compared to IFN-γ KO CFA at 40 mg/ml. (Two-Way ANOVA). Blue graphs represent CFA-immunised WT mice, red graphs represent CFA-immunised IFN-γ KO mice. Figure 6.2b and 2c show the mean values of Rn and FEV0.1, respectively, against the methacholine concentrations between 0 and 40 mg/ml. (n=7-8).

Histopathology reveals cell infiltration and granulomas in lungs of CFA-challenged mice

On day 21 post-immunisation, lungs of mice were histopathologically evaluated (Figure 6.3). Lungs of naïve WT and IFN-γ KO mice had a normal preserved parenchymal appearance without cellular infiltrates. In contrast, histological alterations were observed in both CFA-immunised WT and IFN-γ KO mice. Subpleural and parenchymal cellular infiltrates were present, ranging from small nodular lesions comprised of macrophages and lymphocytes to overt granulomatous inflammation, comprised of prominent multinucleated giant cells and mainly lymphocytic inflammation. No granulomas were reported in other organs including liver, kidney, brain or colon (786). Granulomas in IFN-γ KO mice were more extensively present and also contained scattered neutrophils. No necrosis nor neutrophilic inflammation was found in immunised WT mice. Furthermore, CFA-challenged IFN-γ KO mice showed a mild diffuse interstitial lymphocytic inflammation. In some of the immunised mice, widening of the alveolar spaces was observed, consistent with the observed decrease in aerated lung density. However, no intra-alveolar pathology was present and there was no evidence of PAP or oedema. No overt signs of fibrosis were observed and the absence of collagen deposition was confirmed by an immunohistochemical staining of Alpha-smooth muscle actin (α-SMA) (Supplementary Figure 6.2). In conclusion, a single injection of CFA at the base of the tail leads to a predominantly monocyte, macrophage and neutrophilic pulmonary infiltration in both WT and IFN-γ KO mice which was more pronounced in the sJIA-like animals.

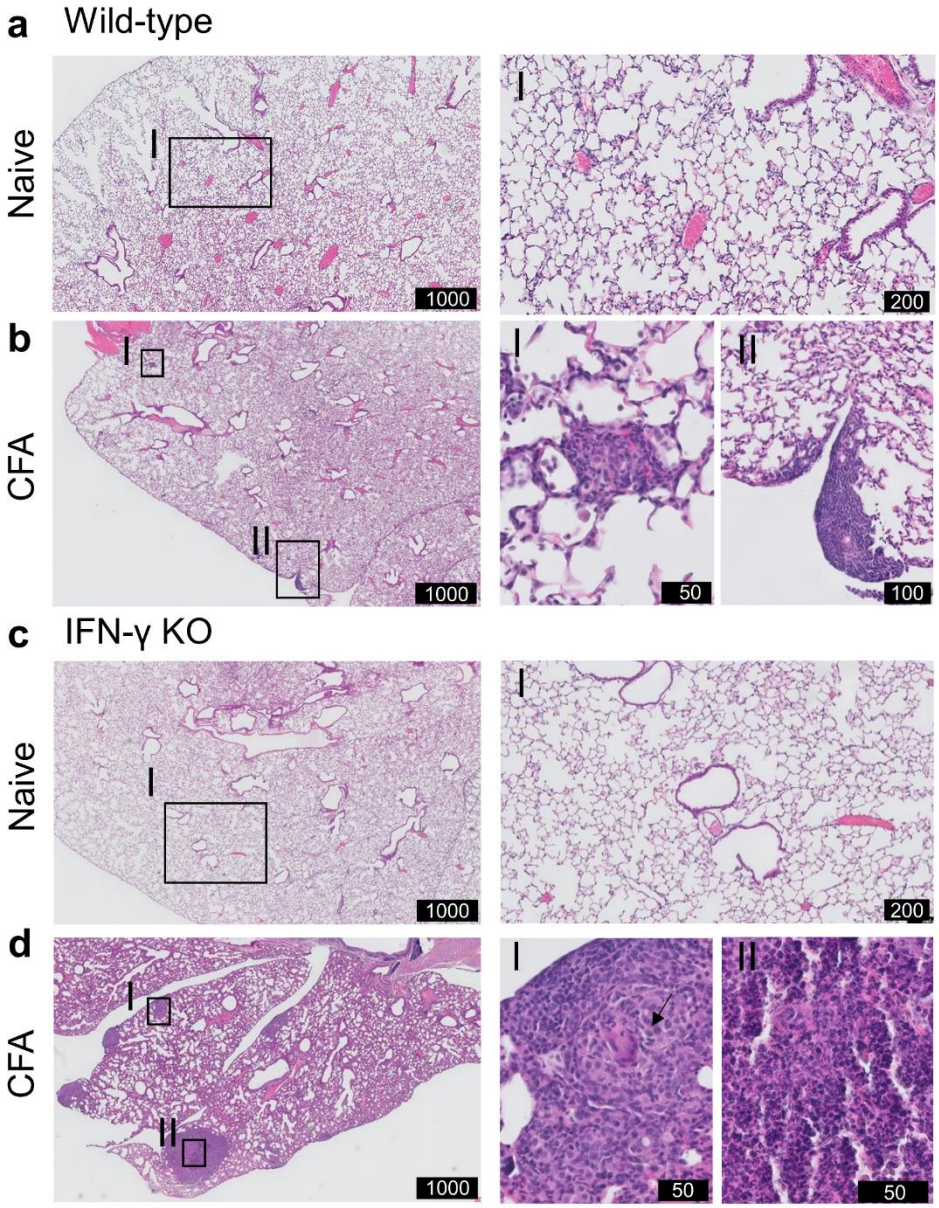

Figure 6.3: Histopathology of pulmonary involvement in CFA-immunised mice. WT and IFN-γ KO mice were immunised with CFA. NI WT and IFN-γ KO mice were include as controls. (a) Representative H&E-stained lung section of WT mice illustrating the normally preserved parenchyma. I is enlargement of the delineated area. (b) Representative H&E-stained lung section of CFA-challenged WT mice at day 21. I and II highlights the presence of subpleural nodules. The parenchyma is further normally preserved. (c) Representative H&E-stained lung section of KO mice illustrating the normally preserved parenchyma. I is enlargement of the delineated area.(d) Representative H&E-stained lung sections of CFA-challenged IFN-γ KO mice at day 21. I, II are enlargements of the delineated areas. Scale is indicated in the black boxes (in µm). Arrow indicate multinucleated giant cells in granuloma-like cells lesions.

Lungs of CFA-immunised IFN-γ KO mice present with elevated numbers of neutrophils and activated monocytes/macrophages

To further characterise the observed pulmonary inflammation, flow cytometric analysis was applied on single cell suspensions of lung tissues. As can be seen in Figure 6.4a, numbers of neutrophils were significantly increased in CFA-IFN-γ KO mice. Also, in BAL, neutrophils were significantly increased (data not shown). In sJIA patients with lung disease, it was hypothesised that the inflammatory milieu could polarise macrophage away from the phenotype necessary for recycling the surfactant (108). We therefore characterised four different subsets of monocytes/macrophages (MO/MA) in lung of our mice, more specifically classical inflammatory Ly6C^{+} MO/MA, non-classical patrolling Ly6C^{-} MO/MA, interstitial macrophages (IM) and alveolar macrophages (AM) (805). As shown in Figure 6.4a, the Ly6C+ MO/MA subset was found to be significantly increased in CFA-challenged KO mice, while other subsets remained unchanged. Interestingly, when CD80 positive macrophages were determined, which is considered as an activating marker and M1-like marker (806), CFA-immunised IFN-γ KO mice showed a significantly higher percentage of CD80^{+} Ly6C^{+} MO/MA, Ly6C^{-} MO/MA and IM (Figure 6.4b). Numbers of SiglecF+CD64- eosinophils, CD11b+ dendritic cells (DC) and CD103+ DCs were increased upon CFA-immunisation in WT mice, whereas they were only slightly elevated in immunised IFN-γ KO mice (Supplementary Figure 6.3a-c).

Number of lymphocytes were either unchanged (CD4+ T cells or B220+ B cells) or were significantly decreased in the diseased IFN-γ KO mice (CD8+ T cells and NK cells). In analogy with our previous data obtained in spleen and LNs (786), CFA-immunisation was associated with an increased number of γδ T cells in lungs of both WT and IFN-γ KO mice (Figure 6.4c). In all studied leukocyte populations, no differences were found between male and female mice. Nevertheless, the highest monocyte/macrophage activation was seen in the female mice. In conclusion, myeloid cell number and activation of macrophages are elevated in the lung tissues of CFA-immunised IFN-γ KO mice.

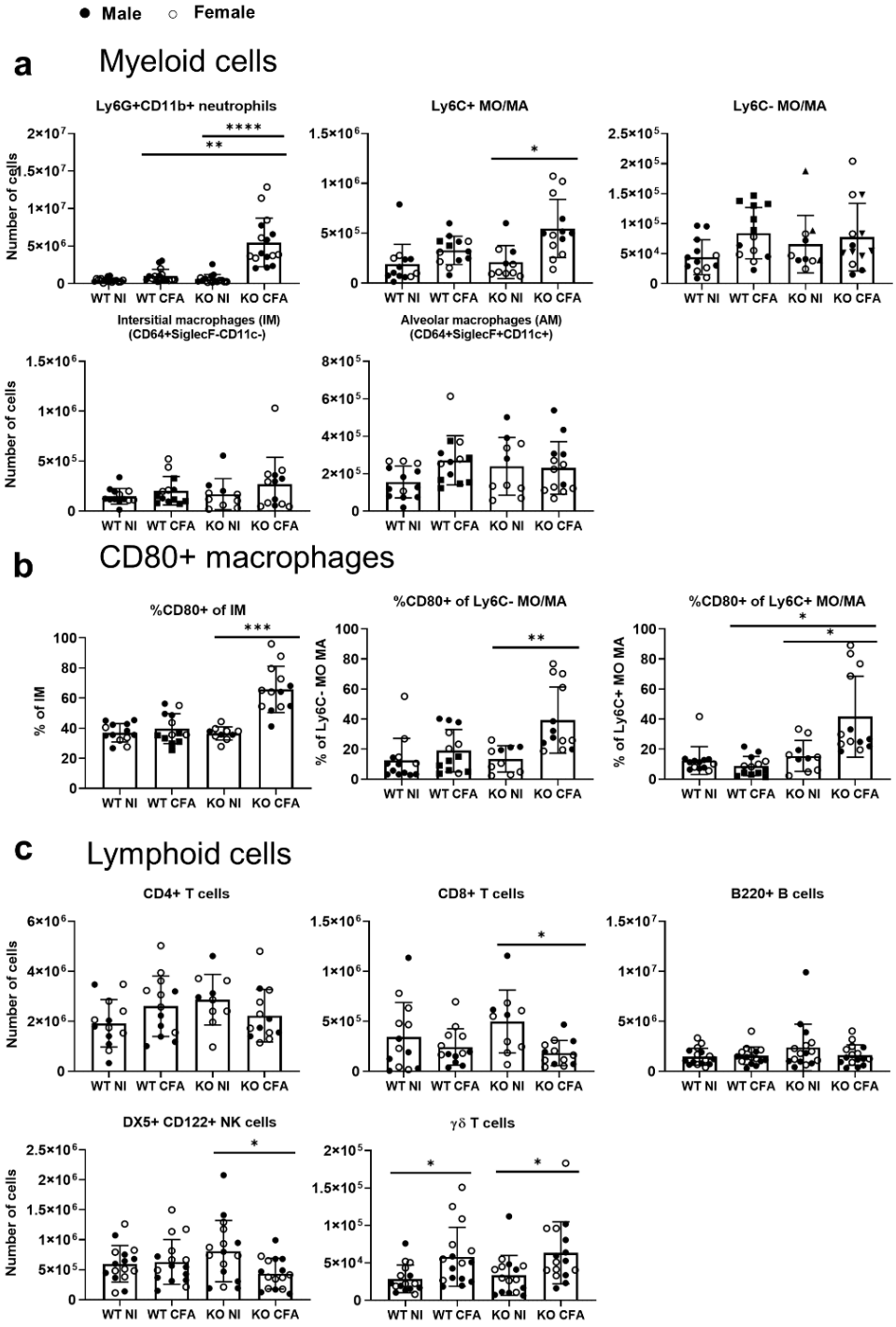

Figure 6.4: WT mice and IFN-γ KO mice were immunised with CFA. NI WT and IFN-γ KO mice were included as controls. Lung cells were analysed by flow cytometry. (a) Absolute number of Ly6G+CD11b+ neutrophils, CD11b+MHCII-Ly6C$_{pos}$ monocytes/macrophages (MO/MA), CD11b+MHCII-Ly6C$_{neg}$ MO/MA, CD64+SiglecF-CD11c- interstitial macrophages (IM) and CD64+SiglecF+CD11c+ alveolar macrophages (AM) were measured. (b) Percentage of CD80+, were determined within the interstitial macrophages (IM), Ly6C- MO/MA and the Ly6C+ MO/MA. (c) Absolute number of CD4+ T cells, CD8+ T cells, B220+ B cells, DX5+CD122+ NK cells and CD3+γδTCR+ γδ T cells were measured. Dots represent individual mice (male closed, female open), horizontal bars represent mean group values with standard error (SE). * p<0.05; ** p<0.01; **** p<0.0001 by Kruskal-Wallis followed by Mann-Whitney U test.

CFA-immunised IFN-γ KO mice show increased expression of inflammatory mediators in lung tissue

To assess the inflammatory mediators involved in the observed lung inflammation, mRNA levels of inflammatory cytokines and chemokines were measured by qPCR in lung tissue of the four groups of mice (Figure 6.5). Upon CFA-immunisation, expression of the pro-inflammatory cytokines IL-1β, IL-6, TNFα, IL-17 and IL-22 increased significantly in predominantly in IFN-γ KO mice. IL-10, an anti-inflammatory cytokine was significantly lower in CFA-challenged IFN-γ KO versus WT mice (Figure 6.5a). In a replicate experiment, cytokines were measured in the lungs, lymph nodes and spleens of CFA-immunised IFN-γ KO mice. Intriguingly, levels of IL-1β and IL-6 in lung tissue were similar or higher than levels found in lymph nodes and spleen respectively, pointing to the importance of a non-lympoid organ as source for these two cytokines (Figure 6. 5b). Analysis of the type I and the type II IFN genes, exposed an increased expression of CXCL9 and CXCL10 in CFA-immunised WT mice only (Supplementary Figure 6.4a). Since neutrophils and monocyte/macrophages were the most abundant infiltrating cells in lung tissue of CFA-challenged mice, we examined expression of the main neutrophil and monocyte/macrophage chemoattractants: keratinocyte chemoattractant (KC) (CXCL1), macrophage inflammatory protein 2 (MIP2 / CXCL2), granulocyte chemotactic protein 2 (GCP2 / CXLC6) and monocyte chemoattractant protein 1 (MCP1). All of the chemokines were significantly increased in immunised IFN-γ KO mice and two in WT counterparts. We further analysed granulocyte colony stimulating factor (G-CSF), a potent inducer of granulopoiesis, and found significant increased expression levels in lung tissue of CFA-induced IFN-γ KO mice, as compared to its naïve and WT counterparts, and these data may explain the observed neutrophilia in these mice (Figure 6.5c). Furthermore, a positive correlation was found between the number of neutrophils or the number of conventional inflammatory $Ly6C_{pos}$ monocytes and the relative expression of either IL-1β, IL-17, G-CSF or MCP-1. In addition, a positive correlation could be made between the absolute number of neutrophils and the expression levels of IL-22 (Supplementary Figure 6.4b-c). Cytokine concentrations in BAL fluid were too low to be detected (data not shown). From these results, we conclude that lungs of sJIA-like mice are represent a relevant basis of neutrophil and MO/MA-associated inflammatory mediators.

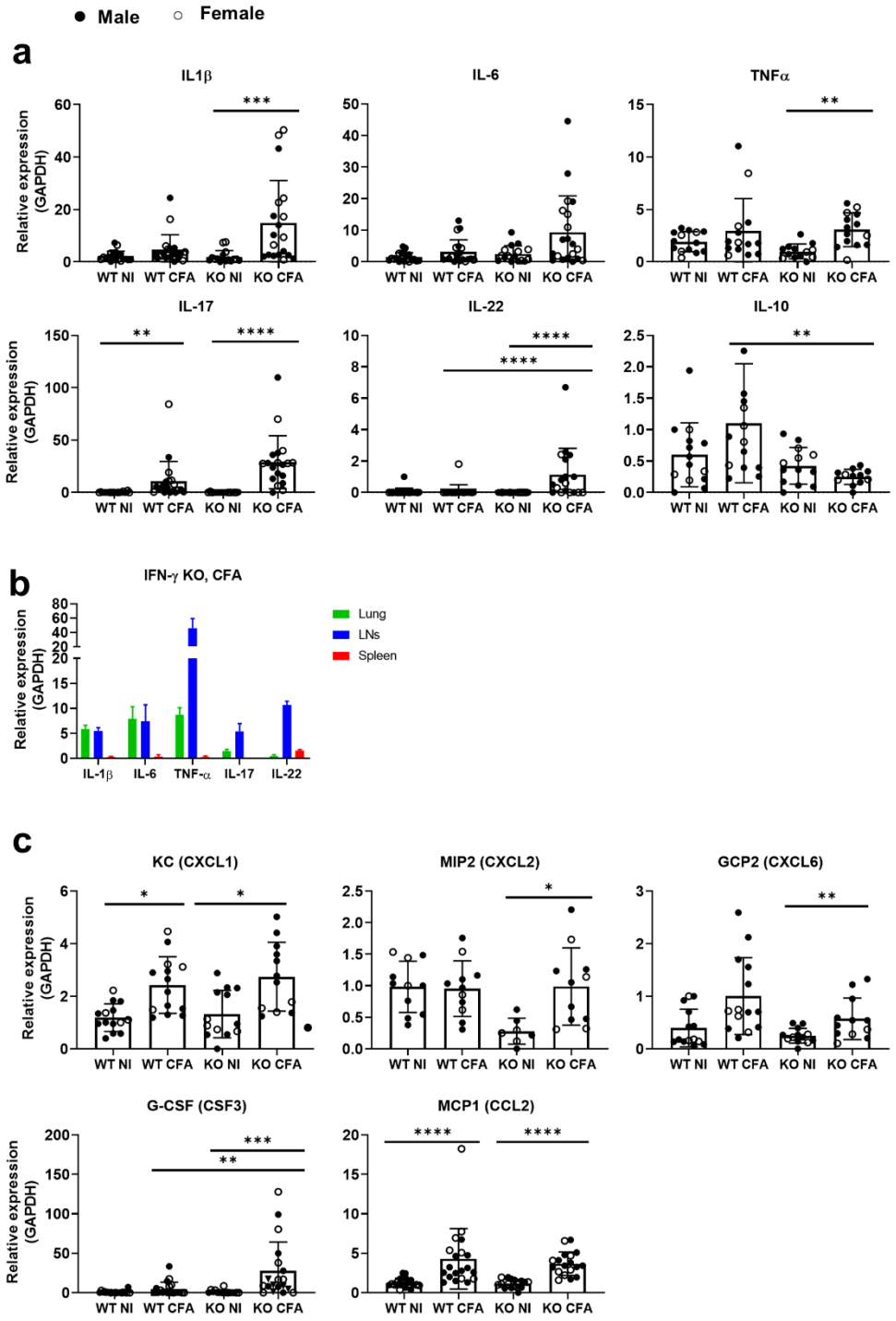

Figure 6.5: WT mice and IFN-γ KO mice were immunised with CFA. NI WT and IFN-γ KO mice were included as controls. (a) The relative RNA expression of IL-1β ,IL-6, TNFα, IL-17, IL-22 and IL-10 was measured in the lungs. (b) Expression levels of IL-1β, IL-6, TNF-α, IL-17 and IL-22 were compaed between lungs, lymph nodes and spleens. (c) Relative RNA expression of the main chemokines or growth factors: KC (CXCL1), MIP2 (CXCL2), GCP2 (CXCL6), G-CSF (CSF3) and MCP1 (CCL2) were determined in the lungs by qPCR. Dots represent individual mice (female open, male closed), horizontal bars represent mean group values with standard error (SE). * p<0.05; ** p<0.01; *** p<0.001; **** p<0.0001 by Kruskal-Wallis followed by Mann-Whitney U test.

Discussion

Pleuritis and pleural effusions are commonly seen in sJIA patients whereas PLD was rarely described until 2015 (110,111,799). Considering the increased reports on pulmonary manifestations in patients with sJIA (108,109), we investigated the physiological and potential inflammatory aspects of lungs in a CFA-based mouse model of sJIA. We found that following immunisation, mice display altered lung physiological responses and develop pulmonary inflammation with cellular infiltration and expression of pro-inflammatory cytokines. In comparison with CFA-challenged WT mice, IFN-γ KO mice showed a distinct and more severe pathology, which is in line with their increased expression of clinical, haematological and biological sJIA-like features.

Non-invasive μCT analysis was able to detect mild changes during the progression of the disease, including increases in lung volume and changes in lung density. The increased lung volume was mainly due to an increase in the aerated lung volume which is a phenomenon that has previously been described in mice having lung infections, inflammation or fibrosis, and which is absent in humans (801). This compensatory increase in the aerated lung volume may underestimate the presence of a restrictive lung disease during lung function volumetric readouts. In our study, lung function measurements showed indeed no difference in forced vital capacity. The overall or aerated lung density was decreased upon immunisation with CFA, without clear-cut differences between IFN-γ KO and WT mice. The gradual changes in aerated lung volume or density could reflect longitudinal changes measured in healthy adult mice but are probably neglectable since the short duration of the experiment (801). When lungs were subjected to functional measurements, subtle differences were found in IFN-γ KO mice, provided that females and males were analysed separately. The induction of sJIA-like disease in IFN-γ KO mice was associated with significantly increased long tissue damping and hysteresivity, in male mice and with an increased airway hyperreactivity in females. Although the observed functional changes in the lungs may be related to the increased infiltration of immune cells in the lungs of IFN-γ KO mice compared to WT counterparts, it needs to be said that no gender differences were observed in the flow cytometric and histological analysis. Note that also in sJIA patients, no gender differences were described. Histologically, the lungs of CFA-immunised mice (both WT and IFN-γ KO animals) showed subpleural and parenchyma cellular infiltrates with formation of granulomas. More extensive granulomas were found in IFN-γ KO mice, in line with the increased non-aerated lung consolidation on μCT. Flow cytometric analysis of lung tissue homogenates revealed significantly elevated numbers of neutrophils and $Ly6C_{pos}$ monocyte/macrophages in lungs of CFA-immunised IFN-γ KO mice, while numbers of cytotoxic T cells and NK cells were lower. γδ T cells were also increased in CFA-immunised mice. Little is known about the role of γδ T cells in lung disease, but the inflammatory environment of sJIA patients primes blood γδ T cells for IL-17 overproduction (147).

Although all data are in line with the hypothesis of an altered innate immune response in sJIA, the pulmonary manifestations in mice are clearly distinct to those in sJIA patients. At first, the immune cell infiltrates in the lung of CFA-immunised mice were predominantly monocytes, macrophages, and neutrophils, whereas in sJIA patients, mainly lymphoplasmacytic infiltrates were reported. Secondly, different inflammatory pathways are involved in humans and in mice. In humans, IFN-γ and IL-18 play a pivotal role in the activation of resident immune cells in the lungs, including macrophages. This is associated with elevated levels of CXCL9 and CXCL10 in the BAL fluid, which are important in the accumulation of immune cells establishing a self-sustained inflammatory response. Subsequently, this inflammatory response may polarise macrophages away from its surfactant recycling properties, and eventually results in the PAP-like features (108,109,799). The upregulated IFN-γ signature may also directly promote alveolar macrophage dysfunction since IFN-γ overexpression in T lymphocytes was shown to drive alveolar macrophage dysfunction and PAP-like lung pathology in mice (807). While, both CXCL9 and CXCL10 were upregulated in CFA-immunised WT mice, an IFN-signature was obviously not seen in our CFA-injected IFN-γ KO mice. In our mouse model, the infiltration of neutrophils and monocytes most likely lead to an enhanced production of IL-1β and IL-6 in the lung. Although we did not show direct involvement of these innate immune cells, a positive correlation was reported

between the number of neutrophils or Ly6C$_{pos}$ monocytes and the expression levels of *i.e.* IL-1β. An increased number of myeloid cells was seen in CFA-immunsed IFN-γ KO mice and can be linked to the increased extramedullary myelopoiesis that we previously described in IFN-γ KO mice, challenged with CFA (761,786), and is also reflected by the increased expression of G-CSF in the lung tissue. Furthermore, in CFA-challenged IFN-γ KO mice, both the IM, the Ly6C$_{pos}$ and the Ly6C$_{neg}$ monocytes/macrophages showed an increased pro-inflammatory activation state, which may possibly sharpen the lung pathology of the sJIA mouse model. Of note, IFN-γ can inhibit the production and/or activity of some pro-inflammatory cytokines or chemokines, including IL-17, TNF-α or GCP-2 however only IL-17 was higher in IFN-γ KO mice compared to WT mice (705,808,809).

Pathologically, sJIA patients showed ILD with mixed features of PAP and ELP. In our mouse model, we have no evidence of PAP-like features. The absence of PAP-like features may be attributed to differences between mice and humans. Alternatively, the systemic inflammation elicited by CFA as measured in our mouse model, might be insufficient to induce PAP-like lung pathology. In contrast, granulomas were formed in the lungs of CFA-immunised mice. These granulomas were an isolated phenomenon, restricted to the pulmonary environment and were absent in other organs including the liver, heart, kidneys, colon, and brain (data not shown). It indicates that lung expose to pathogen-associated molecular patterns or damage-associated molecular patterns in a systemic inflammatory setting may induce the formation of these granulomas. Note that larger granulomas in CFA-immunised IFN-γ KO mice may be related to the protective role that endogenous IFN-γ has on granuloma formation elicited with killed or live mycobacteria (810–814). No fibrosis was observed in the lung of CFA-immunised IFN-γ mice. This might also be attributed to the absence of IFN-γ, a cytokine that is required in development of bleomycin-induced pneumopathy and fibrosis (815,816). Of note, fibrosis was also not seen in CFA-challenged WT mice despite the fact that there is evidence of pulmonary inflammation (granuloma formation, infiltration of γδ T cells and a tendency for increased macrophage infiltration). It could also be that the development of fibrosis takes more time than 21 days, the time when our mice were euthanised. For ethical reasons, assessment of lung disease at later time points was not possible.

A fourth important point of difference between mice and humans, is the use of biologics. In patients, the clinical phenotype and severity of lung disease, coincidend with the introduction of IL-1 and IL-6-targetting biologics (and decreasing used of corticosteroids), suggesting potential contribution of drug exposure (108,817). In this study, no biologics were used. The exact role of cytokine depletion on lung pathophysiology requires further research.

Pulmonary manifestations are described in several other autoimmune and auto-inflammatory diseases including *i.e.* Adult-onset Still's disease (AOSD) – which is the adult spectrum of sJIA, rheumatoid arthritis (RA), systemic sclerosis and systemic lupus erythematosus, and are in part associated to the systemic nature of these diseases and the nature of the lungs that are especially vulnerable to a fast innate immune activation (818–820). In AOSD, PLD is reported in 2-12% of the patients. Two main kinds of PLD may be distinguished during AOSD and are either associated with acute respiratory distress syndrome (ARDS) or with another form. The latter is characterised by a predominant airway involvement (bronchiolitis and bronchitis) or ILD. Interestingly about half of the cases of non-ARDS PLD was neutrophilic. However, in contrast to our mouse model, no monocyte or macrophage infiltration was reported neither the formation of granulomas. In contrast to sJIA, the pathogenesis of ILD in AOSD has not been clarified yet. Hypercytokinemia with activation of inflammatory cytokines such as IL-6 are suggested to play a crucial role in the pathogenesis (111,821–823). Note that pulmonary granulomas can be formed in a wide spectrum of pathologies including non-infectious inflammatory sarcoidosis and RA. In RA, these are called rheumatoid nodules (824).

In conclusion, we provided a detailed histologic, immunologic and functional characterisation of the pulmonary manifestations in a mouse model of sJIA. We demonstrated early µCT alterations and

pulmonary inflammation in both WT and IFN-γ KO BALB/C mice upon CFA-immunisation. More extended granuloma formation, cellular infiltrates, cell activation and functional abnormalities were reported in the absence of IFN-γ. Although the pathology of lung inflammation in our model is distinct from human sJIA, it may be representative for a more IL-17-oriented systemic inflammation. Our observations provide evidence that lungs need to be considered as an important target organ in systemic autoinflammation and are a neglected source of pro-inflammatory cytokines that contribute to the cytokine storm. Our study underscore the importance of monitoring lung disease during systemic inflammation and the model provides a tool to explore the underlying mechanism of lung pathology in an autoinflammatory disease context.

Supplementary Material

Supplementary Figures

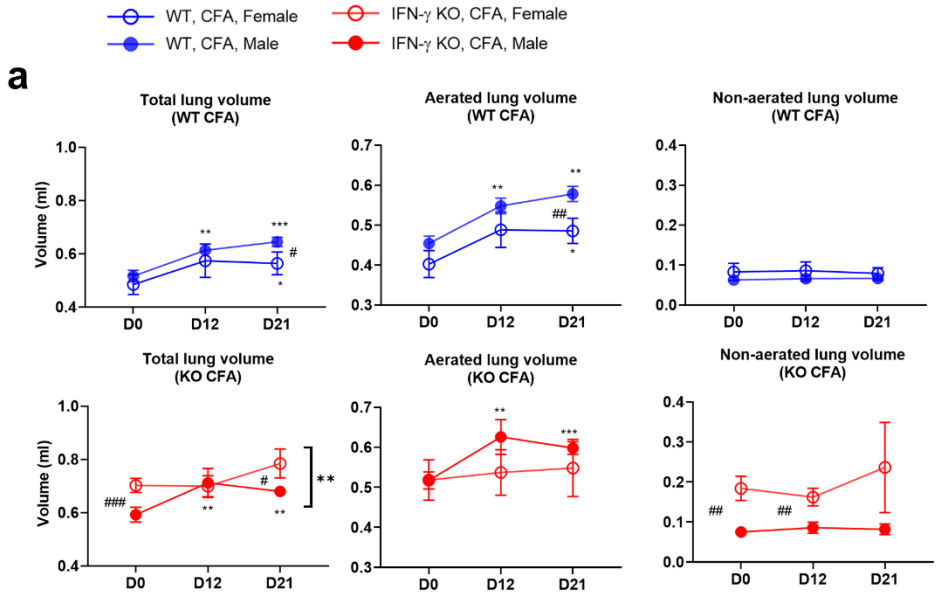

Supplementary Figure 6.1: WT mice and IFN-γ KO mice were immunised with CFA. Mice were scanned with µCT before (day D0) and at regular time points after the CFA-immunisation (day D12, day D21). (a) Three lung volumes were established: total lung volume (ml), aerated long volume (ml) and non-aerated long volume (ml). Data are represented as mean group values with standard error (SE). Blue graphs represent CFA-immunised WT mice, red graphs represent CFA-immunised IFN-γ KO mice. Closed symbols represent male mice, opens symbols represent female mice. */# p<0.05; **/## p<0.01; */### p<0.001; ****/#### p<0.0001 by repeated measures two-way ANOVA. Asterisk represents time-based differences and hashtag represents inter-group differences.**

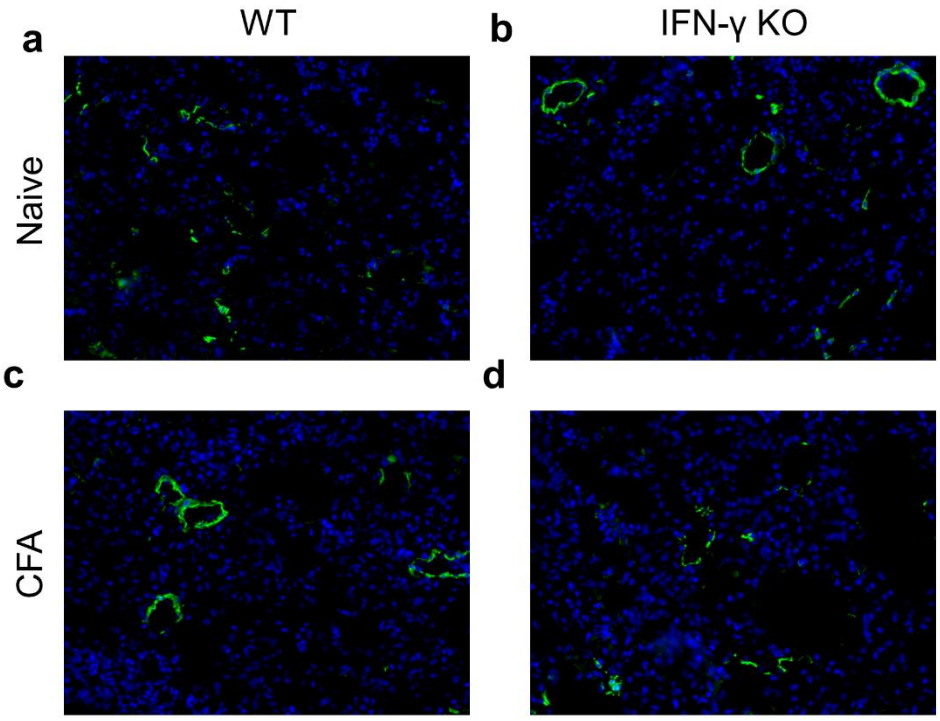

Supplementary Figure 6.2: Alpha-smooth muscle actin (α-SMA) (green) and DAPI (blue) expression were visualised by immunohistochemistry on lung sections of (a) WT NI mice, (b) IFN-γ KO NI mice, (c) CFA-immunised WT mice and (d) CFA-immunised IFN-γ KO mice.

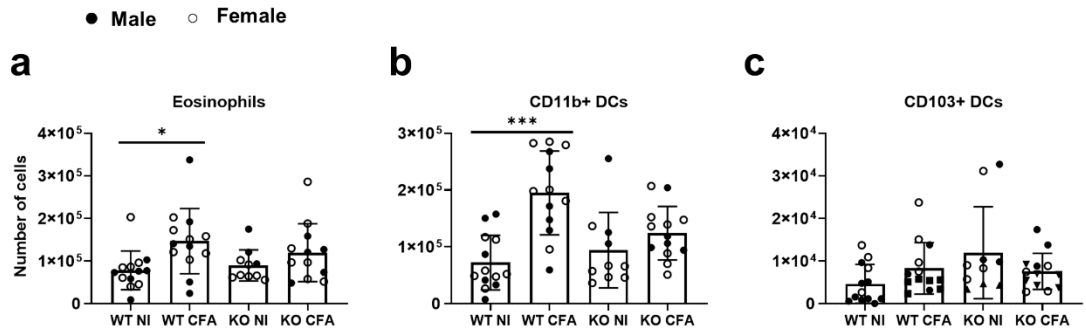

Supplementary Figure 6.3: WT mice and IFN-γ KO mice were immunised with CFA. NI WT and IFN-γ KO mice were included as controls. Lung cells were analysed by flow cytometry. Absolute number of (a) SiglecF+CD64- eosinophils, (b) CD11b+CD11C+MHCII+ dendritic cells (DCs) and (c) CD11C+CD103+ DCs were measured. Dots represent individual mice (male closed, female open), horizontal bars represent mean group values with standard error (SE). * p<0.05; ** p<0.01; *** p<0.001; **** p<0.0001 by Kruskal-Wallis followed by Mann-Whitney U test.

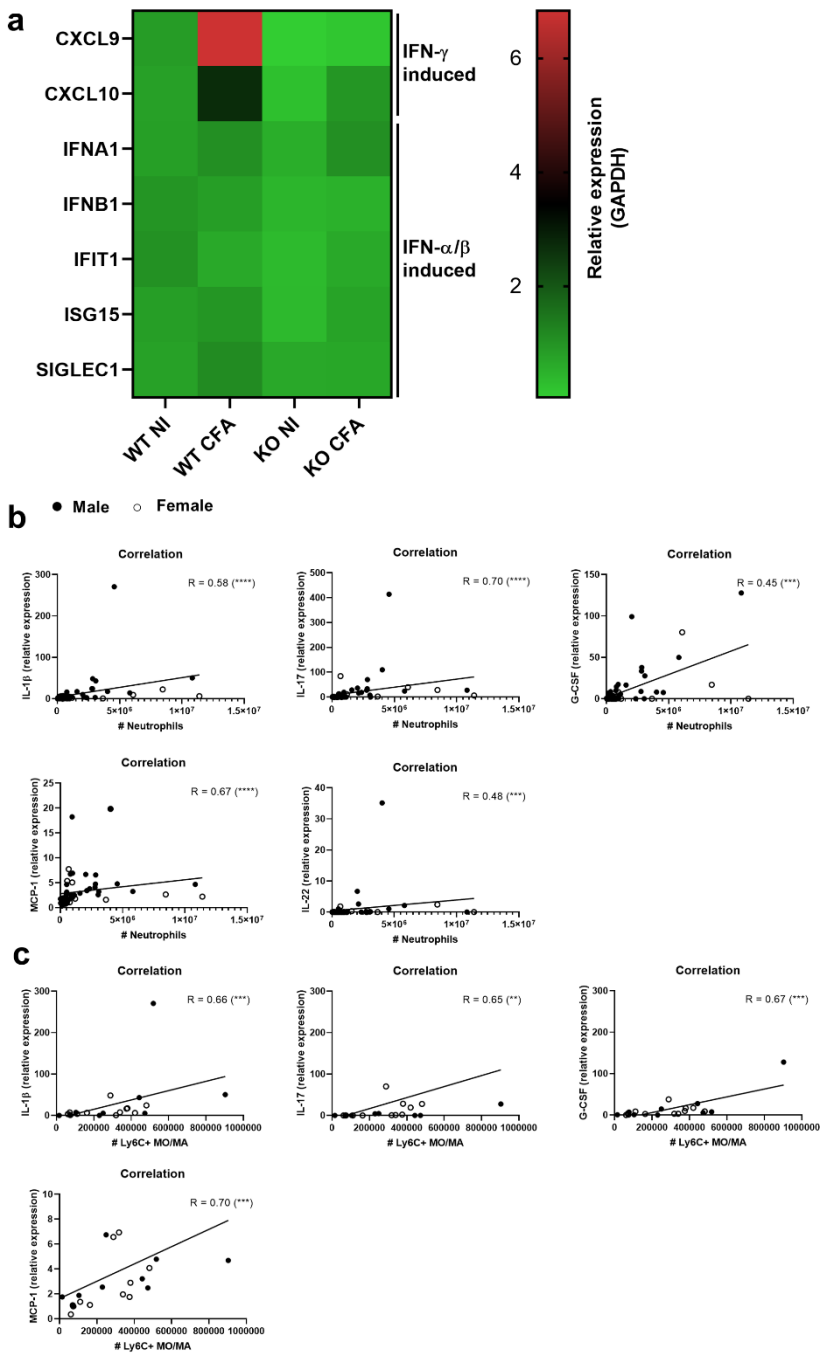

Supplementary Figure 6.4: WT mice and IFN-γ KO mice were immunised with CFA. NI WT and IFN-γ KO mice were included as controls. (a) The relative RNA expression of CXCL9, CXCL10, IFNA1, IFNB1, IFIT1, ISG15 and SIGLEC1 was measured in the lungs. Colour scheme represent relative expression compared to WT NI mice. (b) Correlations between the absolute number of neutrophils and the relative expression of IL-1β, IL-17, G-CSF, MCP-1 and IL-22. (c) Correlations between the absolute number of $Ly6C_{pos}$ monocytes and the relative expression of IL-1β, IL-17, G-CSF, and MCP-1. For every correlation the Spearman correlation coefficient is given.

Supplementary Tables

Supplementary Table 6.1

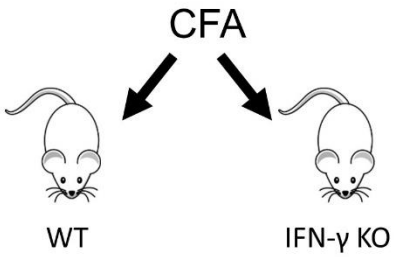

sJIA characteristics		
Clinical features		
- Fever	-	-
- Weight loss	+	++
- Arthritis	-	+[a]
- Skin rash	-	+[a]
- Splenomegaly	+	++
- Lymphadenopathy	+	+
Hematologic features		
- Neutrophilia	+	++
- Thrombocytosis	+	++
- Lymphocytopenia	-	+
- Anaemia	-	+[a]
Immune/inflammatory features		
- Increased IL-6	-	+
- Decreased NK cell functionality	-	+

Features were graded as follows: +, present; ++, more pronounced present; and -, absent.

[a] In subsets of mice.

For WT and IFN-γ KO mice, a summary of more than 10 experiments was used to compose this table, and the list of features is founded on data published in Avau *et al.*, Imbrechts *et al.* and Vandenhaute *et al.* (158,257,786)

Supplementary Table 6.2

Antigen	Fluorophore	Clone	Company
B220	BV786	RA3-6B2	BD
CD101	Af647	307707	BD
CD103	PerCpEF710	2E7	eBioscience
CD115	PE	AFS98	eBioscience
CD117	PE-Cy5	2B8	Biolegened
CD11b	BUV395	M1/70	BD
CD11b	BUV395	M1/70	BD
CD11c	BV711	N418	Biolegend
CD11c	BV711	N418	Biolegend
CD122	BV421	TM-b1	BD
CD16/32	APC-Cy7	93	Biolegend
CD163	APC	S150491	Biolegend
CD19	BV510	6D5	Biolegend
CD19	FITC	eBio1D3	eBioscience
CD206	BV605	C068C2	Biolegend
CD27	FITC	LG.7G9	eBioscience
CD3	BV510	17A2	Biolegend
CD3	FITC	145-2C11	eBioscience
CD3	BUV737	145-2C11	BD
CD34	FITC	RAM34	BD
CD4	PerCp-Cy5.5	RM4-5	eBioscience
CD4	APC-ef780	RM4.5	eBioscience
CD45	PE	30-F11	eBioscience
CD64	BV786	X54-5/7.1	BD
CD8	BV711	53-6.7	BD
CD80	BV421	16-1OA1	BD
CXCR2	PerCp-Cy5.5	SA045E1	Biolegend
CXCR4	BV605	L276F12	Biolegend
DX5	FITC	DX5	eBioscience
DX5	PE-Cy5	DX5	eBioscience
IL-17	eF450	eBio1787	eBioscience
IL-1β	PE	REA577	Milteny Biotec
IL-6	FITC	MP5-20F3	eBioscience
Ly6C	APC-Cy7	AL-21	BD
Ly6C	PerCp-Cy5.5	HK1.4	eBioscience
Ly6G	BV786	1A8	BD
Ly6G	FITC	1A8-LY6G	eBioscience
Ly6G	BV786	1A8	BD
MHCII	AlexaFluor700	M5/114.14.2	eBioscience
SiglecF	PE-CF594	E50-2440	BD
TNF-α	APC	MP6-XT22	eBioscience
ΓδTCR	APC	GL3	Biolegend
ΓδTCR	PE-Cy7	GL3	Biolegend

Supplementary Table 6.3

Gene	Primer name	Company
IL1β	Mm.PT.58.42940223	IDT
IL-6	Mm. PT.58.10005566	IDT
TNF-α	Mm.PT.58.1257581	IDT
IL-17	Mm.PT.58.6531092	IDT
IL-22	Mm00444241_m1	Thermo Fisher
IL-10	Mm.PT.58.13531087	IDT
KC	Mm.PT.58.42076891	IDT
MIP2	Mm.PT.58.10456839	IDT
GCP2	Mm00436451_g1	Thermo Fisher
G-CSF	Mm.PT58.7976206.gs	IDT
MCP1	Mm.PT.58.42151692	IDT
GAPDH	Mm.PT.39a.1	IDT
IFNA1	Mm.PT.58.43426930.g	IDT
IFNB1	Mm.PT.58.30132453.g	IDT
CXCL9	Mm.PT.58.5726745	IDT
CXCL10	Mm.PT.58.43575827	IDT
IFIT1	Mm.PT.58.32674307	IDT
ISG15	Mm.PT.58.41476392.g	IDT
SIGLEC1	Mm.PT.58.8446763	IDT

CHAPTER 7

GENERAL DISCUSSION AND FUTURE PERSPECTIVES

CHAPTER 7: GENERAL DISCUSSION AND FUTURE PERSPECTIVES

Introduction

Current knowledge and gap in the pathogenesis of sJIA

sJIA is a rare childhood immune disorder, thought to be caused by a relatively innocent trigger in predisposed children. According to the ILAR, sJIA is defined by arthritis of unknown aetiology starting at a juvenile age, accompanied by systemic features including quotidian fever, skin rash, lymphadenopathy, hepatosplenomegaly, or serositis (25,26). The pathogenesis of sJIA remains incompletely understood. It is hypothesised that sJIA follows a biphasic clinical course, in which initial disease can be considered as a polygenic autoinflammatory disease, followed by an autoimmune afebrile arthritis phase. Initially, the disease is driven by the innate immune system, whereas later, also the adaptive immune system has a potential driving role (6,85). In **Chapter 1**, the different clinical and laboratory features of sJIA have been summarised.

The disease course in sJIA patients can be self-limiting monophasic, polycyclic, or persistent requiring appropriate treatment. Nowadays, sJIA can successfully be controlled in subsets of patients using biologicals (targeting IL-1 or IL-6). Unfortunately, some patients become refractory to treatment or develop MAS, a potentially life-threatening complication, characterised by a systemic immune-inflammatory response (6,34,748). More recently, also lung disease has been associated with sJIA and is alarmingly being induced upon treatment (112). Therefore, the quest for novel and more effective treatments and insights is still warranted.

In this doctoral dissertation, we aimed to gain new insights into the pathogenesis of sJIA by focusing on the innate immune system and more specifically on the neutrophils and γδ T cells. Special attention was attributed to the different molecular mediators that regulate the kinetics of neutrophil ontogenesis (*i.e.* G-CSF and IL-1β). Neutrophil homeostasis in health and disease was comprehensively overviewed in **Chapter 2**. The results of this doctoral work were presented in three main chapters (**Chapter 4-6**). This thesis was supplemented by **Addendum 1**, in which the *in vivo* limitations of neutrophil-depleting antibodies in systemic inflammatory disorders were highlighted. In **Addendum 2**, we described the phenotypical and functional characteristics of neutrophils in FMF and PAAND.

Decreasing the knowledge gap by using a sJIA-like mouse model

Animal models are valuable tools to study the pathogenesis of human diseases and to uncover potential new therapeutic targets. Due to ethical reasons, this is not always possible in humans. In this doctoral thesis, we made use of a mouse model described by Avau *et al.* (121). In this model, injection of WT BALB/C with CFA results in mild disease symptoms. In contrast, CFA-immunisation in IFN-γ KO mice is associated with an ongoing and more pronounced immune response, resembling most of the sJIA-like features (121). In the model, the inflammatory and haematological abnormalities could be prevented by treating the mice with anti-IL-12/IL-23p40 or anti-IL-17 antibodies (121). No beneficial effects were noticed upon treatment with anakinra, anti-IL-6, anti-IL6R, anti-IL-18, IL-18BP or anti-GM-CSF (unpublished results Dr. Avau).

The pathogenesis of sJIA: a summarising model

Based on the results obtained in this doctoral thesis and considering the current literature, we schematically overviewed the onset and progression of sJIA (Figure 7.1). According to Figure 1, we divided this discussion into six different parts (Parts I-VI). In each part, we draw an important aspect of the sJIA pathogenesis. We describe the current knowledge and question if our newly obtained results confirm or rather challenge this knowledge or could provide us with some new insights. At the end of each part, we raise some unanswered questions and future perspectives.

In the sJIA mouse model, an enhanced inflammasome activation was associated with increased levels of IL-1β. Using neutralising anti-IL-1β antibodies we could partially reduce the sJIA-like features. In Part I of this discussion, we describe the role of inflammasome activation in sJIA. Part II focuses on γδ T cells as kick-starters of the initial innate immune response. In our mouse model, reduced numbers of IL-17- and IL-22-producing CD27-negative γδ T cells were associated with the beneficial effects that were noticed upon anti-IL-1β-treatment. The pathogenic role of IL-17 in the model was previously demonstrated (121). In this doctoral thesis, we additionally investigated the role of IL-22 and showed a partial role in the induction of disease symptoms by synergistically increasing the production of IL-17. In Part III of this discussion, we describe how neutrophils are recruited via the IL-17 - G-CSF axis. In Part IV, we delineate the transition from the initial febrile phase towards the chronic arthritic phase. Here, both the Th17 cells and the neutrophils might be important players. In Part V of this discussion, we highlight the dual role of neutrophils. While neutrophils can amplify the initial innate immune response and drive the development of arthritis, also some anti-inflammatory properties were attributed to the neutrophils. Finally, in Part VI, we describe the lung pathology in the sJIA mouse model. There, we exposed the lungs as an important source of innate cells and pro-inflammatory cytokines.

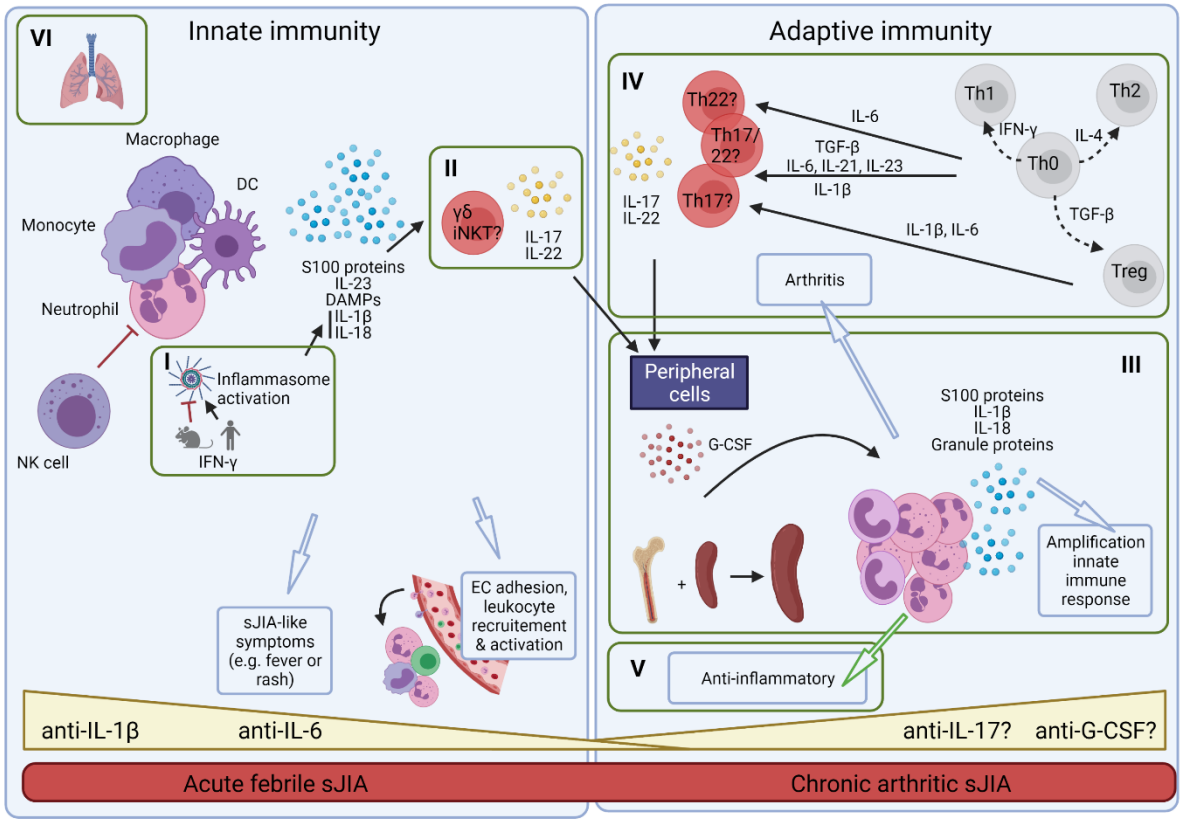

Figure 7.1: CFA immunisation results in a local inflammatory reaction with activation of innate immune cells including neutrophils, monocytes, macrophages, or DCs. NK cells have a disease tempering role. In patients, an infectious trigger is suspected to induce an aberrant innate inflammatory response in predisposed children. Inflammasome activation triggers increased processing and activation of IL-1β, or IL-18 (Part I), and could induce IL-17, or IL-22 in e.g. γδ T cells (Part II). The first innate immune response is strengthened by an adaptive immune response consisting of Th17 and Th22 cells. Neutrophil ontogenesis and recruitment are stimulated via the IL-17 - G-CSF axis. The recruited neutrophils may further amplify the immune response by releasing pro-inflammatory mediators including IL-1β, granule proteins, or S100 proteins (Part III). Neutrophils are eventually also involved in the induction of arthritis (Part IV). The high need for new neutrophils results in extensive extramedullary myelopoiesis, triggering the development of myeloid-derived suppressor cells (MDSCs). This subset of neutrophils may partially temper the excessive immune response (Part V). Considering the biphasic model of sJIA, the innate immune system is mainly involved in the initial acute febrile phase, whereas the differentiation of adaptive Th17 cells leads to the chronic arthritic phase. The neutrophils can be considered important cells that may glue together the two clinical phases. Considering the important role of IL-1β (and IL-6) at disease initiation, the use of drugs targeting IL-1β or IL-6 should mainly be considered at the early disease stages. Tempering signalling through G-CSF or IL-17 could be considered as an alternative treatment during the arthritic phase. The use of G-CSF-targeting drugs should be used with care in systemic inflammatory diseases like sJIA. Finally, we demonstrated an important innate immune activation in the lungs, together with the recent findings in patients (108,109,112), this organ should not be neglected while studying sJIA pathogenesis (Part VI).

Part I: sJIA is an autoinflammatory disease, initiated by an aberrant inflammasome activation

Current insights and new findings

Autoinflammatory diseases are hereditary fever syndromes, induced by genetic mutations in genes that cause an aberrant immune action without the presence of autoantibodies, autoreactive T cells, or HLA class II associations (1–3). The group of autoinflammatory disorders can be divided into at least 8 categories including IL-1β activation disorders (inflammasomopathies), NF-κB activation syndromes, protein misfolding disorders, complement regulatory diseases, cytokine signalling disturbances, MAS, ubiquitination disorders, and type I interferonopathies (6,19).

The initial stage of sJIA clinically mimics the monogenic inflammasomopathies and can be linked to high levels of IL-1β or IL-18. Both in sJIA and MAS, it is hypothesised that unusual TLR signalling or inflammasome overactivation by a relatively harmless infectious agent, may cause an excessive innate immune response in genetically susceptible children (31,34,35,825). In our sJIA mouse model, systemic inflammation is induced by the subcutaneous injection of CFA at the base of the tail. During immunisation, the mycobacterial substances present in CFA may serve as PAMPs, locally activating and recruiting diverse innate immune cells including neutrophils, γδ T cells, monocytes, macrophages, and DCs (255). IFN-γ is a crucial factor in the eradication of intracellular pathogens (826). Consequently, reduced clearance of *M. butyricum* in the IFN-γ KO mice as compared to WT mice may promote a sustained innate immune activation, explaining in part their aggravated phenotype. Remark that in patients, no pathogens have been demonstrated to induce sJIA, and diagnosis implies the absence of any infection.

In contrast to the monogenic inflammasomopathies, no single gene mutations are reported in sJIA patients. Aberrant inflammasome activation might however be related to the sJIA and MAS pathology (827,828). In sJIA patients, associations were made with NLRP3 inflammasome polymorphisms (829). Next, the TLR or IL-1R pathways, required to induce the inflammasome components, were found to be upregulated in sJIA patients (124), and the inflammasome components AIM2 and NLRC4 were highly expressed in neutrophils from sJIA patients (129). Elevated serum levels of N-terminal GASDMD in patients with active AOSD and sJIA additionally suggest inflammasome activation and GASDMD-dependent pyroptosis in patients (830). Recently, a heterozygous missense variant in the gene encoding pro-caspase-1 was described to be associated with sJIA and recurrent MAS. The reported patient showed an increased NLRP3 inflammasome and NF-κB activation (49). Also the *LACC1* mutation, reported in a patient with sJIA, may prime NLRP3 inflammasome activation by increased ROS production (831). Finally, it is important to note that S100 proteins, highly expressed in sJIA patients, also stimulate NLRP3 activation (64,832,833).

In **Chapter 4**, we demonstrate an enhanced inflammasome activation in CFA-immunised IFN-γ KO mice. The enhanced inflammasome activation was associated with increased cleavage of IL-1β and increased plasma levels of active IL-1β. Like in patients, we showed that treatment with neutralising anti-IL-1β antibodies could partially inhibit the sJIA-like symptoms.

The role of innate immune activation in the development of MAS is equally important, as indicated by MAS models that are based on LPS and CpG injections, or viral infection (115,116,834–838). In sJIA patients, MAS mainly develops during the systemic inflammatory phase (6), which could be related to the proposed threshold model. In this model, combinations of genetic predisposition, an underlying inflammatory state like sJIA, or additional infection triggers may reach the threshold linked to a clinically relevant cytokine storm syndrome (105,839). Whereas predisposition to MAS is not associated with the NLRP3 inflammasome (840), gain-of-function mutations in NLRC4 were associated with increased IL-18 production and recurrent MAS in patients (841). The relevance of NLRC4 in MAS was recently confirmed in mice (827,835,842).

Future perspectives

Considering the involvement of aberrant inflammasome activation in sJIA and MAS, it will be highly informative to explore the following questions:

- *What are the main cellular sources of IL-1β and IL-18 in sJIA?*

Gene expression analysis of murine immune cells and tissue suggests that neutrophils may be better producers of IL-1β compared to monocytes or macrophages, whereas IL-18 may be largely produced by the epithelial cells (843). Note that neutrophils have a relatively high expression of pro-IL-1β and do not necessarily need a priming signal. In sJIA, both neutrophils and monocytes are an important sources of IL-1β, especially taking into account the high numbers of neutrophils (6,129,130,842). In our murine model, we have evidence that IL-1β is mainly derived from the neutrophils. The cellular source of IL-18 in sJIA remains poorly understood (6).

- *Can we target inflammasome components in the treatment of sJIA or MAS?*

Thus far, medications used to target excessive inflammasome activation primarily focused on the inhibition of the pro-inflammatory cytokine IL-1 (72–79,844). Interestingly, some of the beneficial effects of using NSAIDs might be attributed to the inhibitory role that COX-2 blockade has on the NLRP3 inflammasome complex (845). Currently, clinical trials evaluating the safety and efficacy of anti-IL-18 antibodies in sJIA-MAS are ongoing (846,847). In NLRC4-mediated MAS, a single case report described successful treatment with recombinant IL-18BP (841,848). In AOSD IL18BP treatment was found to be safe and showed early sign of efficacy (849).

- *What is the role of inflammasome activation in the progression towards MAS?*

Whereas inflammasome activation finally results in the cleavage and activation of IL-1β, IL-18, or GASDMD, the clinical phenotype of sJIA and MAS is highly variable and suggests a cell, tissue, or inflammasome-specific clinical phenotype. The expression of each inflammasome is cell- or tissue-dependent and each inflammasome has a preference to process either IL-1β, IL-18, or GASDMD. NLRP3 preferentially activates IL-1β, whereas NLRC4 predominantly stimulates IL-18 (850). Since the development of sJIA or MAS is more dependent on IL-1β or IL-18, respectively, it will be interesting to understand if an altered inflammasome activation may trigger the conversion from sJIA to MAS. Also, the exploration of different triggers that may induce excessive immune activation in sJIA and MAS requires further research.

- *May enhanced inflammasome activation in IFN-γ KO mice explain their enhanced susceptibility to autoimmune or autoinflammatory?*

Compared to WT mice, IFN-γ KO mice showed an increased inflammasome activation upon CFA immunisation. Also, in the CIA model, increased levels of active caspase-1 were described in the absence of IFN-γ signalling (767). Enhanced inflammasome activation in IFN-γ KO should be investigated in other models but can in part be explained by the inhibitory role of IFN-γ on the NLRP3 oligomerisation (765,766,851,852). In contrast, in humans, IFN-γ potentiates the release of IL-1β (764). This could partially clarify the different roles of IFN-γ in mice and humans.

PART II: γδ T cells are an important source of IL-17 and IL-22, driving the sJIA-like symptoms

Current insights and new findings

γδ T cells represent a small subset of invariant T lymphocytes with features of both the innate and the adaptive immune systems (853,854). Activation depends on the presentation of phosphorylated antigens by non-classical MHC I molecules in the presence of IL-23, IL-1β, IL-6, and TGF-β. In mice, γδ T cells can be pre-programmed in the thymus (853,854). In contrast to regular T cells, these cells acquired their effector function during development and do not require antigen presentation to become activated. These cells can directly be activated by IL-1β and IL-23 (170,855–858). IL-17-producing γδ cells are characterised by upregulation of CCR6 and the loss of CD27. The expression of IL-17 depends on RORγt (855,859,860). In mice, IL-17 production is mainly restricted to the Vγ4+ or the Vγ6+ γδ T cells, largely present in the non-lymphoid tissues (853,854). Interestingly, in sJIA patients, increased peripheral blood IL-17-producing γδ T cells were reported (861). Also, invariant NKT (iNKT) cells were proposed to link innate and adaptive immune responses via IL-17 expression (147,862,863). Limited research has been performed on these cells in sJIA but iNKT cells were shown to be significantly increased in patients (864). Considering the high levels of IL-18 in patients with sJIA it is worth stressing that the IL-18R is highly expressed on γδ T cells or iNKT cells, and that IL-18 signalling may drive the IL-17 expression in these cells (147,862,865).

In **Chapter 4**, we showed that the number of γδ T cells was significantly increased in the CFA-immunised IFN-γ KO mice. These γδ T cells may provide a fast IL-17 response, fuelling the early stages of inflammation and creating a cytokine environment that can spill over to trigger an adaptive immune response, including the *in vivo* activation of Th17 or Th22 cells (147,170). We indeed demonstrated that the γδ T cells together with the CD4+ T cells, are an important source of both IL-17 and IL-22. Interestingly, we could show a reduced number of IL-17-producing CD27 negative γδ T cells upon IL-1β neutralisation. Indirectly, the reduced cytokine expression was linked to the ameliorated disease symptoms. These results in mice are in line with the work of Kessel *et al.* in patients showing that γδ T cells overexpressed the IL-17 cytokine, which could be normalised upon therapeutic IL-1-blockade (147). The role of IL-17 in the sJIA mouse model was previously reported (121). Next, we studied the role of IL-22 in sJIA. IL-22 can be induced in T cells and innate immune cells like γδ T cells, NKT cells, and ILCs upon IL-6 or IL-23 stimulation. Additionally in γδ T cells, TLR signalling can drive IL-22 expression, whereas in Th17 cells or ILC3 cells IL-1β may synergistically induce IL-22 (170,213,857,866–868). **Chapter 4** describes increased expression and plasma levels of IL-22 in CFA-immunised IFN-γ KO mice. Using IL-22 neutralising antibodies we could demonstrate a partial role of IL-22 on the observed sJIA-like symptoms. In sJIA patients with active disease, we also could measure increased levels of active IL-22. The increased activity of IL-22 could be explained by a reduction of the IL-22BP, the natural antagonist of IL-22. IL-18 can downregulate IL-22BP, and active IL-22 upregulates pro-IL-18 expression, creating a positive feedback loop (221–224). The exact mechanism of IL-22 remains unclear, but we could demonstrate that IL-22 together with IL-1β synergistically induced IL-17 production in both the γδ T cells and the CD4+ T cells.

Considering the results on single IL-17 and IL-22 depletion, we questioned whether depletion of either γδ T cells or CD4+ T cells could also ameliorate some of the disease symptoms. Although additional repeat experiments are needed, depletion of either CD4+ T cells or γδ T cells in the sJIA mouse model demonstrated that indeed both cells are required for at least part of the CFA-induced inflammation, but in contrast to IL-1β or IL-17 depletion, symptoms could only be partially inhibited (Malengier-Devlies *et al.*, unpublished results). The difference between *in vivo* depletion of CD4+ cells or γδ T cells and IL-17 neutralisation, indicates that cell type single depletions are insufficient to abolish IL-17 completely in the model.

Future perspectives

Taken together we describe an important role for IL-17 and IL-22 in the induction of sJIA-like symptoms. Whether IL-22 can be used as a possible therapeutic candidate in sJIA requires further research. Additionally, two fundamental questions remain to be answered:

- *What is the mode of action of IL-22 in sJIA?*

The mechanism of action of IL-22 remains ununderstood. The cytokine may induce the release of antimicrobial peptides, increase the lifespan of cells, induce acute-phase proteins including S100 proteins and synergistically upregulate pro-inflammatory molecules including G-CSF and IL-6 (209,211,215,225,760). During the arthritic phase, IL-22 may induce the proliferation of synovial fibroblasts (231), may stimulate synovial production of the CCL2 monocyte-attracting chemokine (231), and may induce RANKL expression that promotes osteoclastogenesis (232). Interestingly, in sJIA patients, γδ T cells might be attracted to the inflamed joints in a CCR6-dependent way since elevated CCL20 levels were measured in the synovial fluid of sJIA patients (861). In view of the close association of IL-22 with psoriatic lesions, IL-22 should also be investigated in the light of skin inflammation (869).

- *Which are the cellular sources of IL-22 in sJIA?*

The cellular sources of IL-22 in patients with sJIA remain unknown. The main candidates are the γδ T cells, Th22 cells, subsets of NK cells, NKT cells, and group 3 innate lymphoid cells (ILC3) (209–212). Th22 cells are a distinct CD4+ T-helper subset that produces high levels of IL-22 without the co-production of IL-17. Th22 are found at sites of infections and play a role in a range of inflammatory diseases (870). Initially, IL-22 was linked with Th17 cells but clear functional differences between Th17 and Th22 are evident as transferred Th22 cells, but not Th17 cells, can rescue susceptible mice from enteropathogenic bacterial infection (870). Comparative transcriptome analysis of Th22 and Th17 cells revealed differential expression of several hundred genes. Additionally, it showed that Th22 cells develop independently of the Th17 lineage (213,871). In its development, Th22 cells depend on IL-6 and the transcription factors Tbet and AhR whereas RORγt acts as a negative regulator (214,215). Interestingly, strong plasticity exists between Th17 cells, Th22 cells, and iTreg cells depending on the balance of IL-6 and TGF-β. For example, after the maturation of Th17 cells, reduced TGF-β levels skew the development of intermediary Th17/Th22 cells that produce both IL-17 and IL-22. Whereas IL-23 augments IL-22 expression, it is not necessary to develop Th22 cells.

In the sJIA mouse model, we demonstrated increased expression of IL-22 in γδ T cells and T cells. If T cells solely express IL-22 or in combination with IL-17 requires more in-depth analysis. Additionally, next to T cells and γδ T cells, the other cellular sources of IL-22 should be investigated.

PART III: Neutrophils are recruited via the IL-17 - G-CSF axis and amplify the innate immune response by releasing pro-inflammatory mediators

Current insights and new findings

Neutrophils are the first cells to enter the site of inflammation and are an important source of pro-inflammatory mediators that initiate a proper immune response (259). When studying neutrophils in mice, it is important to note that there are some important intrinsic differences with human cells. First, the number of blood neutrophils at homeostasis is significantly lower in mice compared to humans, representing 10-25% and 50-70% of the total white blood cells, respectively. Mice lack the expression of defensin. Next, some antimicrobial enzymes, including myeloperoxidase and lysozyme, show lower activity in mice (872,873). Finally, mice lack CXCL8 (IL-8), and neutrophil attraction in mice rather depends on CXCL1 (KC), CXCL2 (MIP-2), and CXCL6 (GCP-2) (874).

During systemic inflammation, as described in sJIA, granulopoiesis is switched from steady-state to emergency granulopoiesis with high plasma levels of G-CSF, meeting the high demand for new neutrophils (520–525). IL-17 is a potent inducer of G-CSF, and in inflammatory conditions, G-CSF is controlled by the IL-23 - IL-17 - G-CSF axis (427,793,794). In **Chapter 5**, we demonstrated increased levels of G-CSF in our sJIA mouse model. Levels were especially high in immunised IFN-γ KO mice

compared to WT mice and could be linked to the enhanced IL-17 release in these mice. In analogy, increased plasma G-CSF levels were measured in sJIA patients with active disease. Furthermore, the levels were positively correlating with some inflammatory mediators including the number of neutrophils, and plasma levels of IL-6 and IL-1β. Using our model, we could clearly demonstrate that upon CFA-immunisation, G-CSF is responsible for the observed neutrophilia and splenomegaly, which both were aborted upon anti-G-CSFR treatment. The increase of neutrophils in IFN-γ KO mice was mainly noticed between days 10-14 post-immunisation. Interestingly, this is the time-point associated with the induction of disease symptoms, including rash and weight loss.

The newly recruited neutrophils may further enhance inflammation in an inflammasome-mediated way (Part I). Considering the important role of neutrophils in strengthening the innate response, it is worth noting that high numbers of neutrophils or neutrophil-associated genes were indeed correlating with a beneficial response to anakinra or canakinumab (45,130,875) Neutrophils may also provide an important source of alarmins or DAMPs, further amplifying the activation of the innate immune system. In sJIA, there is a growing interest in these molecules, with special attention to the S100 proteins. S100 proteins may activate innate immune cells, predominantly monocytes, and macrophages, upon binding the RAGE receptor or TLRs by enhancing the secretion of pro-inflammatory molecules (749). High concentrations of S100 proteins (both S100A8/A9 and S100A12) are measured in patients with sJIA and therefore these molecules were proposed as biomarkers (67,166,241,244,250,252,253,876). In WBCs or monocytes from sJIA patients, the release of IL-1 and other inflammatory cytokines was reduced by depleting S100A8/A9 from the serum of sJIA patients or by preventing the S100A12 complex formation (6,166,877). Additionally, together with IL-1β, the S100 proteins may promote Th17, γδ T cell development, or induce IL-17 expression in autoreactive CD8+ T cells, sustaining an important amplification loop (6,147,245,246).

Future perspectives

Given our results, the following additional questions may be presented:

- *Are the neutrophils formed during extramedullary myelopoiesis distinct from the neutrophils formed in the BM?*

By single-cell sequencing, we could demonstrate that during extramedullary myelopoiesis, similar neutrophils are formed (including pre-neutrophils, immature neutrophils, and mature neutrophils), via a G-CSF-driven developmental trajectory (**Chapter 5**). However, it remains to be established whether extramedullary-derived neutrophils have another functionality or plasticity than neutrophils generated in the BM. Next, it will be important to understand the functional differences between mature and immature neutrophils. In SLE for example, immature neutrophils have an increased capacity to form NETs (878), whereas in sepsis they were described to have a reduced phagocytic capacity compared to mature neutrophils (879).

- *Can we link defective NK cells or B cells in CFA-immunised IFN-γ KO mice to enhanced plasma levels of G-CSF, explaining their aggravated phenotype?*

It is hypothesised that NK cells can terminate the inflammatory response by eliminating activated cells. Inappropriate elimination may result in persistent immune stimulation with a self-amplifying inflammatory response (106,141,168). The role of NK cells in the sJIA model was demonstrated upon NK cell depletion or NKG2D blockade (257). IFN-γ KO mice have inborn deficiencies in NK cells making them more susceptible to induce sJIA. However, like in patients, the defects in NK cells might also be attributed to the cytokine environment. Especially high levels of IL-18 and IL-6 may abort NK cell functionality (880). Interestingly, also high levels of G-CSF may inhibit the functionality of NK cells (539). Additionally, it has been described that mature neutrophils are required to properly mature NK cells (881). We might also speculate that the "left shift" from mature to immature neutrophils during systemic inflammation described in sJIA, might block NK cells at the CD11b+CD27+ stage which may explain their hyperresponsiveness. In the mouse model, this was indeed shown in the blood of anti-Ly6G-depleted CFA-immunised IFN-γ KO mice (Bert Malengier-Devlies, unpublished). Similarly, the shift away from lymphopoiesis in the BM might explain the reduced number of B cells which serve as an important source of IL-10 in sJIA (158).

- *What is the role of other DAMPs in the context of sJIA?*

Next to S100 proteins, other alarmins are released upon intracellular stress or tissue injury in processes like necrosis or pyroptosis and should be studied in the setting of sJIA. One proposed candidate includes the high-mobility group box 1 (HMGB1). The HMGB1 has chemotactic or cytokine-inducing effects and is increased in patients with sJIA (882–888). The formation of NETs by neutrophils may also act as an alarm signal activating other immune cells. Various components of NETs including DNA are sensed by macrophages or dendritic cells and may induce a pro-inflammatory immune response (889,890). Additionally, the release of NETs can cause tissue injury and augment tissue inflammation (891–893).

Part IV: Th17 cells and neutrophils are linking the acute autoinflammatory febrile phase to the chronic autoimmune arthritic phase

Current insights and new findings

Untreated sJIA can progress towards an arthritic phase, molecularly distinct from the febrile phase (894), with clinical features typical of autoimmune conditions and similar as described in the other JIA subtypes (6,895–898). Autoimmune diseases root in the breakdown of immunologic self-tolerance, induction of autoantibodies or autoreactive T cells, and MHC class II allele associations. Although specific autoantibodies are less common in patients with sJIA (899), associations are made with the HLA-DRB1*11 allele (53), and increasing antinuclear antibodies (ANA) or rheumatoid factor (RF) titers are reported during the sJIA disease progression (900).

Next, another hallmark of autoimmune diseases is the disbalance between Th17 cells, driving autoimmunity, and periphery-derived Tregs (pTregs) as inhibiting elements (901,902). Whereas both Th17 cells and pTregs require TGF-β for their initial differentiation, Th17 cell differentiation additionally requires interaction with the innate immune system. The Th17 transcription factor RORγt is induced upon combined TCR/CD28 and IL-6 signalling and bolstered by other pro-inflammatory cytokines like IL-1β, IL-21, IL-23, and TNF-α (902–904). Interestingly, IL-1β can substitute TGF-β in the IL-6-driven generation of Th17 cells (905). Full differentiation of Th17 cells additionally requires IL-23 signalling, which receptor is induced in a RORγt-dependent way.

In sJIA, no autoantigens have been described questioning the *in vivo* activation of Th17 cells. Interestingly, it has been described that Th17 activation may be independent of TCR signalling. In JIA for example, CD31 ligation of synovial $CD28^{null}CD31^{+}CD4^{-}CD8^{-}$ αβ T cells is sufficient to induce RORγt expression and subsequent IL-17 production. In the synovium, fibrocyte-like cells (FLC) were proposed as key ligating cells via its expression of CD38, a known ligand for CD31. CD38 can be upregulated on FLCs by IL-17 (derived from γδ T cells or iNKT cells) (906). *In vitro* studies additionally showed that IL-23 and IL-1β could also promote non-anergic Th17 cell development in the absence of CD28 (907).

In **Chapter 4**, we reported increased numbers of IL-17-producing T cells in CFA-immunised IFN-γ KO mice and reduction of these cells upon anti-IL-1β-treatment. IFN-γ can abort the development of Th17 cells, elucidating their increased susceptibility to develop sJIA (908). Since C57BL/6 preferentially mount an IFN-γ-mediated Th1 response, it might explain their reduced susceptivity to develop sJIA, compared to BALB/C mice (909). In patients with JIA, including sJIA, an abnormal ratio of Th17 to Treg cells was described, correlating to the arthritic severity (780,895,910). Remark that enhanced Th17 cell differentiation and IL-17 expression is not restricted to autoimmune disease but has also been reported in autoinflammatory diseases including CAPS (911) or FMF (6,912). It is important to note that IL-1β appears to be less important during the arthritic phase since sJIA patients with an increased number of active joints are less likely to respond to treatment with anakinra (45,72).

The remnant epitopes generate autoimmune (REGA) model states that cells and molecules of the innate immune system (including neutrophils) can start the autoimmune reaction by cytokine-regulated proteolysis yielding remnant epitopes (3). Next, neutrophils are considered important cells in the development of arthritis since they can destroy the cartilage by *e.g.* releasing granule proteins (913,914). Recently an additional pathogenic role was linked to the neutrophil-DC hybrid subset that may serve as antigen-presenting cells (421,423). In the joints of JIA patients, neutrophils were abundantly present (915,916) and the presence of S100A12 in synovial fluids from JIA patients (252) confirms their involvement in arthritis development. Interestingly, we recently also demonstrated increased numbers of neutrophil-DC hybrid cells in the synovial fluid from patients with JIA (746). Corresponding with the involvement of neutrophils in the arthritis pathology, we demonstrated in **Chapter 5** that blockage of the G-CSFR could clearly inhibit the development of arthritis, which was indirectly associated with a reduced neutrophilia. These results were in line with other arthritic studies blocking the G-CSFR (586,587).

Future perspectives

In conclusion, in sJIA, neutrophils may play an important role in the induction of arthritis. In light of the presented results, it will be important to answer the following question:

- *Are the neutrophils that drive arthritis in the synovial tissue, phenotypically or functionally distinct to the neutrophils characterised in the blood?*

In blood, patient neutrophils have a primed phenotype with enhanced degranulation, ROS production, or S100A8/A9 release (130). At the transcriptional level, the gene expression profile is overlapping with sepsis having an upregulation of *e.g.* components of inflammasomes, IL-8, and genes involved in the NF-κB pathway (129,130,589). Although the neutrophils were extensively studied in the blood of patients with sJIA, it remains particularly interesting to understand the functional and phenotypical features of neutrophils in the joints. This may help us to understand their role in the pathophysiology and the discrimination between the arthritic and febrile phases of the disease.

Part V: Neutrophil homeostasis: too much, too little? Dual role of neutrophils in sJIA

Current insights and new findings

Considering the important role of neutrophils in the release of IL-1β, their role in the amplification phase, and their involvement in the development of arthritis, it is tempting to speculate that depletion of neutrophils would result in an amelioration of the sJIA-like disease symptoms. Neutrophil-depleting antibodies are an easy tool to study the *in vivo* role of neutrophils in murine models. In **Addendum 1** however, we demonstrated that upon CFA-immunisation, neutrophils were incompletely depleted irrespective of the antibody dosage that was used. Importantly, we showed that especially the CXCR2 negative immature neutrophils were depleted less efficiently and speculated that a high expression of Ly6G is needed for proper depletion. Interestingly, neutrophil depletion in the sJIA mouse model was associated with a significantly increased proliferation in the spleen, causing a fast rebound of new immature neutrophils. Unexpectedly, when we evaluated the early clinical features upon depletion, we noticed an enhanced weight loss and aggravated tail damage from which we concluded that the neutrophils are required for removing the heat-killed *Mycobacterium* in the tail (Malengier-Devlies *et al.*, unpublished results).

In **Chapter 5**, we used an alternative method to study indirectly the effect of neutrophil depletion in our sJIA mouse model. Using G-CSFR-blocking antibodies, we could inhibit G-CSF signalling, and treated mice were characterised by a reduced neutrophilia, myelopoiesis, and associated IL-1β release. Although arthritis could completely be prevented, clinical evaluation demonstrated a mild aggravation of the disease symptoms in CFA-immunised IFN-γ KO mice. Interestingly, blocking the G-CSFR signalling caused no aggravation of clinical symptoms in other arthritic models (586,587), whereas in a cancer study, increased activation of CD4+ T cells was noticed (540).

In cancer, the neutrophil-mediated ongoing immune response was presented as “the wound that cannot be healed”(917,918). In normal wounds or injuries, neutrophils are the first responders and play a crucial role in antimicrobial host defence by generating ROS, granule proteins, or NETs. The elimination of the acute insult is followed by a resolution phase in which neutrophils are cleared through efferocytosis, monocytes are recruited, and thrombosis, angiogenesis, or stromal remodelling is initiated. However, in the context of cancer, there is an ongoing inflammatory response resulting in a persistent demand for new neutrophils and neutrophilic activation. Next to GM-CSF and IL-6, the IL-23 - IL-17 - G-CSF pathway has been proposed to drive this excessive myelopoiesis. The massive recruitment of neutrophils was also associated with the induction of MDSCs. Since these MDSCs have a tempering role, they might be a compensatory mechanism of the body to avoid excessive inflammation (427,465,633,919–923). In **Chapter 5**, we also demonstrated that high levels of G-CSF were associated with the development of MDSCs in immunised IFN-γ KO mice. In the sJIA model, these cells showed a mature phenotype associated with high levels of CEBP/β, a transcription factor previously linked to emergency granulopoiesis. The MDSCs were significantly reduced upon anti-G-CSFR-blockage in the CFA-immunised mice. Eventually, this may partially explain their aggravated phenotype.

Future perspectives

Concluding, G-CSF-targeted therapy can be used to block the development of arthritis but should be used with care in sJIA patients. Below, we propose some unanswered questions:

- *Are neutrophil-associated proteins potential new targets in the treatment of sJIA?*

It remains extremely interesting to translate the studied effects concerning G-CSFR depletion in mice to the human situation. We might speculate whether, similar to what has been reported for IL-1β, there would exist a window of opportunity in which G-CSF-targeting drugs could be considered (*e.g.* in patients that do not respond to IL-1 or IL-6 therapies or during the arthritic stage of the disease). Next, we could envisage to study the clinical effects of drugs targeting neutrophil migration. This could be drugs that block its main chemokine receptors (*e.g.* CXCR1 and CXCR2), ligands (*e.g.* CD11b), or attracting molecules [*e.g.* IL-8 (CXCL8) in humans or GCP-2 (CXCL6), KC (CXCL1), and MIP-2 (CXCL2) in mice]. These strategies may reduce the influx of new neutrophils without influencing the balance between mature and immature neutrophils. CXCL8-neutralising treatment is currently tested in settings of cancer and COVID19 (924,925).

- *Which mechanisms are used by neutrophils to temper the inflammatory response?*

Mature neutrophils are fully equipped with all kinds of pro-inflammatory properties and are responsible for the quick elimination of pathogens. Their decreased number upon G-CSFR-blockage may result in a delayed CFA clearance and consequently ensure a lasting immune activation. A maturational block at an immature (and potentially less functional) neutrophil stage may also explain their reduced functionality. In contrast, in patients, the "left shift" towards a more immature phenotype may be a protective mechanism to abort an ongoing immune response during excessive inflammation. Next, several mechanisms have been proposed by which MDSCs could suppress the activation and proliferation of T cells including the induction of NO via iNOS (427), the release of hydrogen peroxide (428), the depletion of L-arginine by arginase (429,926,927) or the direct cell contact between PD-L1 or Mac-1 (430,431). Finally, our lab recently demonstrated that the tertiary granule protein MMP-9, which is highly expressed by neutrophils, could proteolytically process IL-2 yielding IL-2 with lower receptor affinity (798). Therefore, the reduced number of neutrophils upon anti-G-CSFR usage could be linked to an enhanced T cell activation. Additionally, it may also explain the increased numbers of Tregs observed upon antibody administration in the CFA-immunised IFN-γ KO mice (**Chapter 5**).

- *What are the consequences of G-CSF administration in MAS?*

Granulocytopenia and agranulocytosis are common in MAS patients, therefore, the administration of G-CSF is an effective strategy. However, Zhao *et al.* suggested that G-CSF could promote the production of cytokines and hemophagocytosis in MAS (928). Considering neutrophils as an important source of pro-inflammatory cytokines, this hypothesis should not be neglected. Confirming this idea, therapy with granulocyte colony-stimulating factor in SLE was associated with severe flares (929). In contrast, administration of G-CSF in MAS patients may also have some disease tempering effects through the accumulation of myeloid-derived suppressor cells (MDSCs). The emergence of these cells has mainly been studied in (breast) cancer patients receiving G-CSF after chemotherapy (930). Whereas in cancer patients, the emergency of MDSCs might be detrimental through immune evasion and metastasis promotion, in MAS patients, tempering T cell activation is warranted. The exact (beneficial) role of G-CSF in MAS remains largely unexplored and might be the subject of future fruitful research.

Part VI: The lungs are an underestimated target organ in the pathogenesis of sJIA

Current insights and new findings

Considering the increasing number of sJIA patients having lung disease (108,109,112), in **Chapter 6**, we extensively described lung abnormalities in our sJIA mouse model. We demonstrated more extensively present functional, histological, and radiological abnormalities in CFA-immunised IFN-γ KO mice. Next, the flow-cytometric analysis showed increased infiltration of (immature and mature) neutrophils and monocytes in CFA-immunised IFN-γ KO mice and an increased activation state of the macrophages. Interestingly, when comparing the expression of pro-inflammatory cytokines in the lungs, we noticed that the lungs were a main source of IL-1β, IL-6, TNF-α, IL-17, and G-CSF.

In our sJIA mouse model, the pulmonary manifestations were distinct from those seen in sJIA patients. In the discussion part of **Chapter 6**, we summarised the four main differences between lung pathology in CFA-immunised IFN-γ KO mice and sJIA patients. First, different cell infiltrates were involved. Whereas in our model, infiltrates were mainly myeloid-derived, a more lymphocyte-orientated inflammation was described in humans. Next, inflammation in mice was mainly IL-17-driven whereas in patients a dominating role for IFN-γ and IL-18 was reported. Also, the clinical presentation was highly variable between mice and humans, revealing PLD with the formation of granulomas in mice, and ILD with mixed features of PAP and ELP in patients. Finally, we studied lung disease in the absence of any treatment with biologics whereas, in patients, treatment with inhibitors of IL-1 or IL-6 was demonstrated as a potential risk factor in the development of sJIA lung disease (109). Recently, in a patient with a missense variant in the pro-caspase-1 gene, presenting with sJIA and recurrent MAS, dual IL-1 and IL-6 blockade was beneficial to abort systemic disease symptoms, but interstitial lung inflammation progressed with a reduced lung diffusing capacity (49). Future experiments using anti-IL-1β in our sJIA mouse model may help to understand a potential role of biologics in the development of lung complications.

Future perspectives

Although our mouse model failed to reflect the full pathophysiological alterations seen in patients, it underlines the importance of the lungs in the pathological phenotype of sJIA. Considering our results, we also raise some important questions:

- *How does local inflammation in the tail induce pulmonary complications?*

The formation of granulomas and pulmonary manifestations are described in several other autoimmune and autoinflammatory diseases including AOSD, RA, systemic sclerosis, and systemic lupus erythematosus. They are in part associated with the systemic nature of these diseases and the nature of the lungs being especially vulnerable to a fast-innate immune activation (818–820). In our mouse model, the formation of granuloma-like structures with giant cells is typical for infection with mycobacteria (810,811). Although it seems acceptable that *M. butyricum*, as part of the injected CFA, induced the formation of granulomas, it remains remarkable that immunisation in the tail induces excessive inflammation in the lungs. The route by which the *M. butyricum* travel towards the lungs remains unknown. Transport might be explained by passive bacterial leakage into the venous system and pulmonary capillary trapping or active transport by macrophages or neutrophils. Using fluorescently labelled *M. butyricum* we however could not demonstrate the presence of *M. butyricum* in the lungs of our immunised mice [Bert Malengier-Devlies *et al.*, unpublished results and Schurgers *et al.*(812)].

- *Are the observed lung manifestations described in patients related to a susceptibility to develop MAS?*

In sJIA patients with lung disease, the pulmonary activation of resident immune cells in the lungs, including macrophages, are linked to increased levels of IFN-γ and IL-18 (108). Additionally, CXCL9 and CXCL10, both IFN-induced chemokines, were elevated in the BAL fluids of patients (108). Together with IFN-γ, these chemokines are strongly associated with the development of MAS (100,931,932). Interestingly, the inflammatory environment that drives MAS, including the upregulated IFN-γ, may promote alveolar macrophage dysfunction eventually resulting in a reduced surfactant clearance and eventually result in PAP-like features (807). Indeed, PAP has been linked to alterations in alveolar macrophages with impaired maturation and polarisation (933–936).

sJIA is a heterogeneous condition, and it is conceivable that patients with severe refractory systemic inflammatory disease and/or susceptibility to develop MAS are at a higher risk to develop lung disease. The initial reports on the pulmonary disease in sJIA were especially seen during acute MAS (107,110,111). Furthermore, Schulert *et al.* describe that the majority of sJIA patients with lung disease had associations with a history of MAS, and MAS was proposed as an important risk factor in the induction of pulmonary complications (108). In contrast, Saper *et al.* showed that MAS at sJIA onset was increased in children exposed to IL-1/IL-6 inhibitors but this was not associated with LD features. Pre-exposure to cytokine-inhibition, possibly associated with concomitant reduction of steroids, was the predominant phenotype in this series. Almost one-third of patients with lung disease had their first MAS episode at or after diagnosis of lung involvement, suggesting that lung disease may trigger systemic inflammation (109). Considering the reported associations with MAS, it's important to evaluate the development of lung complications in well-accepted MAS models. Just recently, Gao *et al.* extensively described pulmonary inflammation in the CpG MAS model (937). In this paper, researchers showed that CpG-immunisation is associated with a CD4-predominant perivascular interstitial inflammation with elevated levels of IFN-γ and IFN-γ-related chemokines. Single-cell sequencing showed the emergence of monocytes and macrophage populations including an IFN-γ-induced pro-inflammatory MAS-specific macrophage population. During the resolution phase, mice continued to have pulmonary interstitial inflammation, but alveolar macrophages switched to an anti-inflammatory phenotype. In recurrent MAS, a more extensive inflammation was noticed. Alveolar macrophages were increased, and cells were re-switched to their pro-inflammatory phenotype. Like in our sJIA mouse model, CpG-immunised MAS mice did not develop PAP, suggesting that MAS alone is not sufficient to completely mimic the sJIA lung disease described in patients. Considering the role of Bach1 in some forms of PAP, the downregulation of the gene during the resolution phase was interesting (935). Concluding, the work of Gao *et al.* demonstrates that IFN-γ is essential for alveolar macrophage-driven pulmonary inflammation.

It is known that IL-1 blockade can potentiate an IFN response in children with sJIA (72,135). This may explain the increased susceptibility to develop lung complications in patients treated with biologicals. The effect of biologics on pulmonary inflammation in both the sJIA and MAS mouse models remains unknown and requires further research. Additionally, it will be of interest to study immune cell activation in the lungs of sJIA patients with and without overt pulmonary involvement to determine lung disease prevalence and uncover molecular mechanisms of this potentially fatal complication.

ADDENDUM 1

LIMITATIONS OF NEUTROPHIL DEPLETION BY ANTI-LY6G ANTIBODIES IN TWO HETEROGENIC IMMUNOLOGICAL MODELS

Published manuscript:

Pollenus, E. [1*], Malengier-Devlies, B. [2*], Vandermosten, L. [1], Thao-Thy, P. [1], Mitera, T. [2], Possemiers, H. [1], Boon, L. [3], Opdenakker, G. [2], Matthys, P. [2*], Van den Steen, P.E[1*]. (2019). Limitations of neutrophil depletion by anti-Ly6G antibodies in two heterogenic immunological models. Immunology Letters, *212*, 30-36

* equal contribution

[1]KU Leuven Department of Microbiology, Immunology and Transplantation, Rega Institute for Medical Research, Laboratory of Immunoparasitology, Leuven, Belgium
[2]KU Leuven Department of Microbiology, Immunology and Transplantation, Rega Institute for Medical Research, Laboratory of Immunobiology, Leuven, Belgium
[3]Bioceros, Utrecht, The Netherlands

ADDENDUM 1: LIMITATIONS OF NEUTROPHIL DEPLETION BY ANTI-LY6G ANTIBODIES IN TWO HETEROGENIC IMMUNOLOGICAL MODELS

Abstract

Neutrophil-depleting antibodies, such as anti-GR1 (RB6-8C5) and anti-Ly6G (1A8), are commonly used to study the in vivo function of neutrophils in murine disease models. Anti-Ly6G antibodies became the standard, because in contrast to anti-GR1, these do not bind Ly6C. The efficiency of the depletion needs to be carefully analysed as flow cytometry plots may be misinterpreted. For example, the staining intensity of GR1 on neutrophils (CD11b+ GR1hi) drops upon anti-Ly6G administration. We show that this drop is due to competition between anti-GR1 and anti-Ly6G antibodies. Neutrophil depletion with anti-Ly6G in naive mice was organ- and strain-specific. Furthermore, an incomplete anti-Ly6G-dependent neutrophil depletion was obtained in two immune-mediated mouse models, *i.e.* in malaria-infected C57BL/6 mice and in complete Freund's adjuvant (CFA)-challenged BALB/c mice. BrdU-incorporation studies show a slight increase in proliferating bone marrow neutrophils upon depletion in naive mice. Strikingly, depletion with anti-Ly6G in CFA-challenged BALB/c mice resulted in a significant increase in proliferating splenic neutrophils, causing a fast rebound of new immature neutrophils. In conclusion, our results emphasise the importance of careful panel design, gating strategies and duration of neutrophil depletion and highlight the context-dependent Ly6G depletion efficiency. It furthermore underlines the need for new tools to understand the in vivo role of neutrophils in immunological models.

Introduction

Neutrophils are the most abundant white blood cells in the circulation. These short-lived cells have the capacity to infiltrate into sites of inflammation and are rapidly replenished in adult bone marrow pools by myelopoiesis (650). In mice, neutrophils are defined as CD11b+ Ly6G+ Ly6Cint cells and have a variety of functions (259,360,938). Many disease models are characterised by an expansion of neutrophil numbers in the circulation and/or in different organs, where they are considered as important drivers of immune responses and critical players in the resolution process. Nevertheless, their exact role is often poorly understood. One way to study the in vivo function of neutrophils is by using neutrophil-depleting antibodies, which can be administered at different time points during the disease process. Two different antibodies are commonly used for this approach in mice: anti-Ly6G (clone 1A8) and anti-GR1 (clone RB6-8C5). Ly6G expression is restricted to neutrophils and is involved in recruitment and transmigration. Ly6C, another member of the Ly6 family, is expressed on neutrophils and other leukocyte populations, and plays a role in the adhesion to the endothelium (938,939). The anti-GR1 antibodies bind both to Ly6G and Ly6C and may thereby also deplete subpopulations of dendritic cells, monocytes, macrophages and lymphocytes (939,940). Since the anti-Ly6G antibodies are more specific for neutrophils compared to the anti-GR1 antibodies, they became the standard approach for neutrophil depletion experiments.

In tumour biology, different concerns have been raised in using neutrophil-depleting antibodies. In an editorial by Ma and Greten, the authors stressed the importance of properly checking the depletion efficacy (941). These authors underlined the fact that neutrophil depletion efficacy may be misinterpreted by the method, timing and location of neutrophil depletion analysis. However, despite the release of this editorial, Ly6G-depleting antibodies are still widely used, which may be related to the lack of appropiate alternatives. Here, we describe some experimental pitfalls of Ly6G-depleting antibodies in two immunological models to warn for misinterpretations.

The first model is a mouse model to study malaria-associated acute respiratory distress syndrome (MA-ARDS). Thereby, C57BL/6 mice are infected with the Plasmodium berghei NK65-Edinburgh line (PbNK65) (942), resulting in the development of experimental MA-ARDS at day 9 post infection (p.i.). The pathology in these mice resembles the histopathological findings in MA-ARDS patients (943). MA-ARDS pathology in both patients and mice is characterised by severe interstitial and alveolar edema and a vast infiltration of mononuclear leukocytes and neutrophils (944). In this mouse model, CD8+ T cells were shown to be essential for the pathogenesis (945), but the role of neutrophils remains unclear. In another model for malaria-associated acute lung injury (*i.e.* the infection of DBA/2 mice with P. berghei ANKA), neutrophils were suggested to play an essential role in the pathogenesis based on depletion experiments with the less specific anti-GR1 antibody (946).

The second model is based on the injection of complete Freund's adjuvants (CFA) in BALB/c mice (121). CFA consists of an oil emulsion containing heat-killed mycobacteria (255). It is the most commonly used immunoadjuvant in animal models for the production of (auto)antibodies and for the induction of experimental autoimmune diseases (255,761). A single subcutaneous (s.c.) injection of CFA is sufficient to induce a local and systemic inflammation in the mice. The mycobacterial component of CFA elicits myelopoiesis in both bone marrow and in spleen (designated as extramedullary myelopoiesis) and is associated with neutrophilia (255,761). This model is used to study activated hematopoiesis or myelopoiesis (121).

In this research letter, we show incomplete neutrophil depletion in two heterogenic immunological models. We also report organ-specific and genetic background-related differences in the efficacy of neutrophil depletion with anti-Ly6G, and demonstrate the importance of adequately verifying the neutrophil depletion efficacy.

Materials and methods

Mice and cell isolation

Seven to eight weeks old C57BL/6 mice were purchased from Janvier Labs (Le Genest-Saint-Isle, France) and housed in a conventional or specific pathogen-free (SPF) facility. Six to eight weeks old SPF BALB/c mice were bred in the animal house of the Rega Institute for Medical Research, KU Leuven. All mice were housed in individually ventilated cages. All experiments were performed at the KU Leuven according to the regulations of the European Union (directive 2010/63/EU) and the Belgian Royal Decree of 29 May 2013, and were approved by the Animal Ethics Committee of the KU Leuven (License LA1210186, Belgium). Murine blood samples were obtained by cardiac punction in heparinised (LEO, Pharma, Lier, Belgium) syringes followed by transcardial perfusion. Ciculating leukocytes were obtained from blood after lysis of red blood cells (RBC) with 0.83% ammoniumchloride (NH4Cl) in 10 mM Tris (pH 7.2). Bone marrow was extracted from the tibia of one of the hind legs. Single cell leukocytes of the lungs were obtained using the gentle MACS dissociator (Miltenyi Biotec, Leiden, The Netherlands) followed by a collagenase D (2 mg/ml, Roche, Mannheim, Germany) and DNase (40 U/ml, Roche) digest for 30 min at 37 °C in HEPES buffer. Next, pulmonary leukocytes were purified using density gradient centrifugation with 40% and 72% Percoll solutions (GE healthcare, Upsala, Sweden). Spleens were passed through a cell strainer (70 µm) and RBCs were lysed with 0.83% NH4Cl. Cell numbers were manually counted with a Bürker chamber upon staining with trypan-blue (VWR, Heverlee, Belgium) to exclude dead cells.

Antibody competition test

To test competition between anti-Ly6G and anti-GR1, splenocytes from C57BL/6 mice were incubated with or without non-labeled anti-Ly6G (200 µg/ml, corresponding to depletion concentration, clone 1A8, Bio X cell, Huisen, The Netherlands) prior to staining with fluorescently labeled anti-GR1 (clone RB6-8C5, Biolegend, London, UK). In parallel, competition between fluorescently labeled anti-Ly6C (2.4 µg/ml, concentration as used for Ly6C staining, clone AL-21, BD Biosciences, Erembodegem, Belgium) and anti-GR1 was tested in the same manner.

Ly6G depletion in naive mice

Naive C57BL/6 and BALB/c mice were intraperitoneally (i.p.) injected with 200 or 500 µg of anti-Ly6G (clone 1A8, Bio X cell) or with IgG2a isotype control (anti-β-Gal, clone GL117). Mice were euthanised two days later.

Ly6G depletion in the PbNK65 infection-model

Mice were infected with PbNK65 by i.p. injection of 104 infected RBCs as described previously (947). Infected C57BL/6 mice received ad libitum high-energy food (Ssniff Spezialdiäte GMBH, Soest, Germany) and water, which was supplemented with 0.422 mg/ml 4-amino-benzoic acid sodium (PABA) (Sigma-Aldrich, Bornem, Belgium) for optimal parasite growth. On day 9 p.i., mice were euthanised. Age- and sex-matched non-infected littermates were included as controls. Mice were i.p. treated with 200 µg or 500 µg of anti-Ly6G (clone 1A8, Bio X cell) or with an IgG2a isotype control (anti-β-Gal, clone GL117) on days -1, 3 and 7 after infection.

Ly6G depletion in the CFA-based immunisation model

BALB/c mice were s.c. injected with CFA (Difco, Franklin Lakes, NJ, USA) together with heat-killed mycobacteria (1.5 mg/ml) as previously described [13]. Mice were euthanised and analysed on day 21 post CFA-challenge. Age- and sex-matched non-injected littermates were included as controls. Mice were treated i.p. with 250 µg or 600 µg of anti-Ly6G (clone 1A8, Bio X cell) or with an IgG2a isotype control (anti-β-Gal, clone GL117) on day 14 and 17 post CFA-challenge (unless specified otherwise).

Flow cytometry

Cells were incubated with FcR-block (Miltenyi Biotec) and stained extracellularly in Brilliant stain buffer (BD Biosciences). The following mouse antibodies were used in this study: anti-CD45 (clone 30-F11, Biolegend), anti-Ly6C (clone AL-21, BD Biosciences), anti-CD11b (clone M1/70, eBioscience, San Diego, CA, USA), anti-GR1 (clone RB6-8C5, Biolegend), anti-CD3 (clone 17A2, Biolegend), anti-CD19 (clone 6D5, Biolegend), anti-NK1.1 (clone PK136, Biolegend) and anti-CXCR2 (clone SA045E1, Biolegend). Forward and side scatter analysis was used to limit debris and doublets. All leukocyte populations were gated on CD45+ live cells. Cells positive for lineage-specific markers were excluded (with CD3, CD19 and NK1.1 as exclusion markers). Neutrophils were gated as specified. Cells were run on a LSRFortessa X20 (BD Biosciences) equipped with the DIVA software and analysed with FlowJo software (LLC, V10, Ashland, OR, USA).

Fluorescence-activated cell sorting of gated neutrophils and inflammatory monocytes

PbNK65-infected C57BL/6 mice were i.p. injected with 500 µg anti-Ly6G (clone 1A8) or isotype control (anti-β-Gal, clone GL117) on days -1, 3 and 7 after infection. On day 9 p.i., mice were sacrificed and lung cells were isolated. The pulmonary leukocytes were stained as described above with anti-CD45 (clone 30-F11, Biolegend), anti-Ly6C (clone HK1.4, eBioscience), anti-GR1 (clone RB6-8C5, eBioscience), anti-CD3 (clone 17A2, Biolegend), anti-CD19 (clobe 6D5, Biolegend) and anti-NK1.1 (clone PK136, eBioscience). Neutrophils and inflammatory monocytes were sorted on a BD Melody (BD Biosciences) equipped with the BD FACS Chorus software 1.0 according to the gating as shown in Fig. A1.1. Cytospins were prepared from the sorted cells using the Shandon cytospin 2 (Thermo Fischer Scientific, Aalst, Belgium). After the slides were air-dried, they were stained with Hemacolour (Merck, Darmstadt, Germany). Pictures were made under a 40x magnification using a Leica DM2000 LED microscope (Leica microsystems, Diegem, Belgium).

BrdU incorporation assay

One day before analysis, mice received a single i.p. injection of 1.5 mg 5-bromo-2'-deoxyuridine (BrdU, Sigma-Aldrich). BrdU positive cells were visualised with the BrdU flow kit from BD as described by the manufacturer's protocol. In brief, cells were extracellularly stained, fixed and permeabilised. To detect incorporated BrdU, cells were treated with DNase (300 µg/ml) and stained with a PE-labeled anti-BrdU antibody (BD Biosciences).

Statistical analysis

GraphPad Prism Software (GraphPad Software, San Diego, CA, USA) was used for all statistical analyses. The non-parametric Kruskal-Wallis test followed by Dunn's nonparametric comparison was used to calculate significance levels for the differences between groups. Significance levels were indicated as follows: *$p < 0.05$, **$p < 0.01$, ***$p < 0.001$, **** $p < 0.0001$. Non-siginificant differences were not indicated.

Results

Optimising a gating strategy to evaluate the efficiency of neutrophil depletion after injection with anti-Ly6G (clone 1A8)

In this study, flow cytometry was used to determine the efficiency of depletion in naive mice and two murine immunological models. For instance, in the lungs of PbNK65-infected C57BL/6 mice, anti-Ly6G depletion resulted in the apparent disappearance of neutrophils, when defined as CD11b+ GR1hi double positive (Fig. A1.1, upper dot plots, red gate). However, GR1/Ly6C plots of the CD11b+ subset clearly showed that neutrophils (GR1int/hi Ly6Cint) were not fully depleted but that instead, the GR1 intensity decreased (Fig. A1.1, lower dot plots, green gate). Therefore, determination of depletion efficiency in GR1/CD11b plots results in wrong conclusions, since the neutrophil population is masked by the Ly6Chi inflammatory monocytes (CD11b+ Ly6Chi) upon anti-Ly6G depletion. The drop in GR1 intensity was independent of the dosage used (200 µg or 500 µg, data not shown) and is most likely explained by competition between staining anti-GR1 and depleting anti-Ly6G antibodies. In an in vitro competition experiment, anti-Ly6G at 200 µg/ml, which approximates the concentration that might be reached in an in vivo depletion experiment, clearly competed for the binding of the detection anti-GR1 antibody (Suppl. Fig. A1.1). Furthermore, a parallel competition experiment showed that the anti-Ly6C antibody, at 2.4 µg/ml used for detection of Ly6C in our gating strategy, does not compete with the detection anti-GR1 antibody. Therefore, to enumerate the neutrophils in a correct way, these were gated as GR1int/hi Ly6Cint CD11b+ cells. Microscopy analysis of sorted GR1int/hi Ly6Cint CD11b+ and Ly6Chi CD11b+ cells, confirmed that these cells are, respectively, neutrophils and inflammatory monocytes (Fig. A1.1). In contrast to other studies, forward scatter (FSC) and side scatter (SSC) could not be used upon PbNK65 infection to assess the depletion efficacy, as the inflammatory monocytes and neutrophils overlap in the FSC/SSC plot (Fig. A1.1) (948).

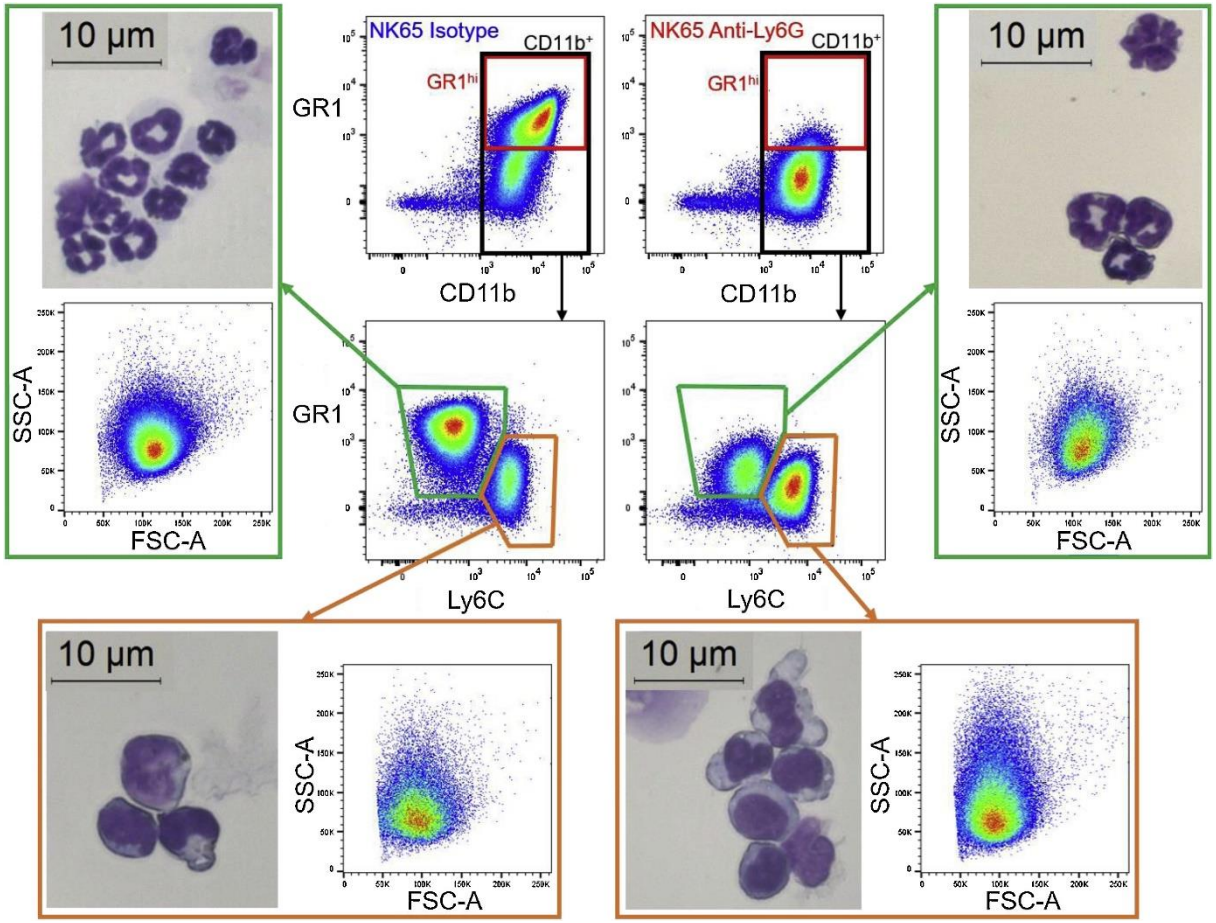

Fig. A1.1. Gating strategy used to evaluate the efficiency of neutrophil depletion.
Representative flow cytometry plots show the gating strategy of neutrophils from pulmonary leukocytes of PbNK65-infected C57BL/6 mice that were either i.p. injected on day -1, 3 and 7 p.i. with 500 µg isotype control (IgG2a) or 500 µg anti-Ly6G (1A8). First, live CD45+ CD11b+ cells were gated (black gate). Neutrophils were gated as GR1int/hi Ly6Cint (green gate). Monocytes were gated as Ly6Chi (orange gate). Both were gated after exclusion of CD3+, CD19+ or NK1.1+ cells. Red gate represents live CD45+ CD11b+ GR1hi cells. Gated GR1int/hi Ly6Cint and Ly6Chi cells were sorted and representative microscopic pictures and FSC/SSC plots were shown. The graphs show data from one representative sample out of 2 independent experiments.

Depletion efficacy in naive BALB/c and C57BL/6 mice

In naive C57BL/6 and BALB/c mice, the efficacy of neutrophil depletion after anti-Ly6G injection was evaluated in different organs, including lungs, spleen, blood and bone marrow. Depletion with 200 µg of anti-Ly6G resulted in a reduction of pulmonary neutrophils of ±43% in C57BL/6 mice and ± 96% in BALB/c mice (Fig. A1.2A). Comparable results were found in the spleen: a reduction of ± 67% and ± 96% in C57BL/6 and BALB/c mice, respectively, upon depletion with 200 µg of anti-Ly6G (Fig. A1.2B). Depletion of neutrophils with 200 µg anti-Ly6G was efficient in blood, with a reduction of ± 87% and ±95% in C57BL/6 and BALB/c mice, respectively, after depletion with 200 µg anti-Ly6G (Fig. A1.2C). Similar depletion efficacies were found after injection of 500 µg anti-Ly6G in all three organs (Fig. A1.2A–C). The decrease in neutrophils after depletion with 200 µg or 500 µg anti-Ly6G was significant in all three organs in both C57BL/6 and BALB/c mice, with only a trend in lungs ($p = 0.0540$) and blood ($p = 0.0669$) after depletion with 500 µg anti-Ly6G in C57BL/6 mice. In contrast, neutrophil depletion in the bone marrow was incomplete, since the number of neutrophils was at best decreased with ±33% in C57BL/6 mice and ±66% in BALB/c mice (Fig. A1.2D). Interestingly, in spleen, blood and lungs, the depletion appeared to be less efficient for CXCR2− neutrophils (Suppl. Fig. A1.2). In all four organs, we observed a higher GR1 expression on neutrophils of BALB/c mice compared to C57BL/6 mice (Fig. A1.2E–H), despite a similar Ly6C expression (data not shown). This suggests that the lower percentual depletion efficiency in C57BL/6 mice versus BALB/c mice might be related to a lower Ly6G expression on the neutrophils or due to lower number of neutrophils in the different organs of naive C57BL/6 mice.

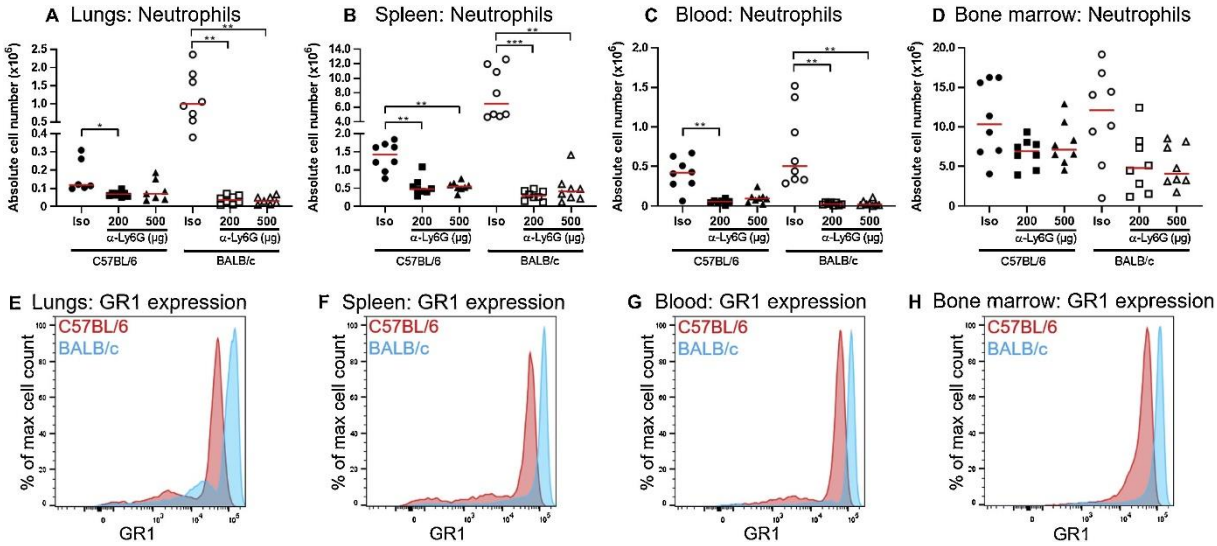

Fig. A1.2. Efficiency of neutrophil depletion with anti-Ly6G in naive C57BL/6 and BALB/c mice. C57BL/6 and BALB/c mice were injected i.p. with 200 or 500 µg of anti-Ly6G (1A8) or isotype control (IgG2a). Two days after administration, lung, spleen, blood and bone marrow leukocytes were collected and analysed with flow cytometry. A–D) Absolute cell number of neutrophils (GR1int/hi Ly6Cint CD11b+) present in lungs (A), spleen (B), blood (C) and bone marrow (D) (n = 8). Results pooled from 2 independent experiments. E–H) Representative plots of the intensity of GR1 expression of CD11b+ ly6Cint/− cells in lungs (E), spleen (F), blood (G) and bone marrow (H) of isotype injected C57BL/6 (red) and BALB/c mice (blue). The graphs show data from one representative experiment out of 2 independent experiments.

Incomplete depletion of neutrophils in both PbNK65-infected C57BL/6 mice and CFA-challenged BALB/c mice

Using the above described gating procedure, we quantified the absolute number of neutrophils in the target organs of two immunological models and calculated the neutrophil depletion efficiency of the anti-Ly6G antibody. Infection of C57BL/6 mice with PbNK65 resulted in an increased number of neutrophils in the lungs (Fig. A1.3A). Challenging BALB/c mice with CFA caused increased neutrophil numbers in the spleen, a consequence of myelopoiesis as described before (Fig. A1.3B) [14,15]. Depletion of neutrophils was incomplete and independent of anti-Ly6G dosage. Upon administration of 200 or 500 µg anti-Ly6G on days -1, 3 and 7 p.i. in PbNK65-infected C57BL/6 mice, the number of pulmonary neutrophils was only reduced by ±48% or ±59%, respectively (Fig. A1.3A). Also, in CFA-challenged BALB/c mice, depletion was incomplete. When 250 or 600 µg of anti-Ly6G was administrated on day 14 and 17 post CFA-challenge, a splenic neutrophil reduction of less than ±65% was seen at day 21 (Fig. A1.3B). In contrast, when neutrophils would have been gated as CD11b+ GR1hi (Fig. A1.1, red gating), more than 90% depletion would have been apparently observed in lungs of PbNK65-infected C57BL/6 mice and in the spleen of CFA-challenged BALB/c mice, demonstrating the risk of wrong interpretations.

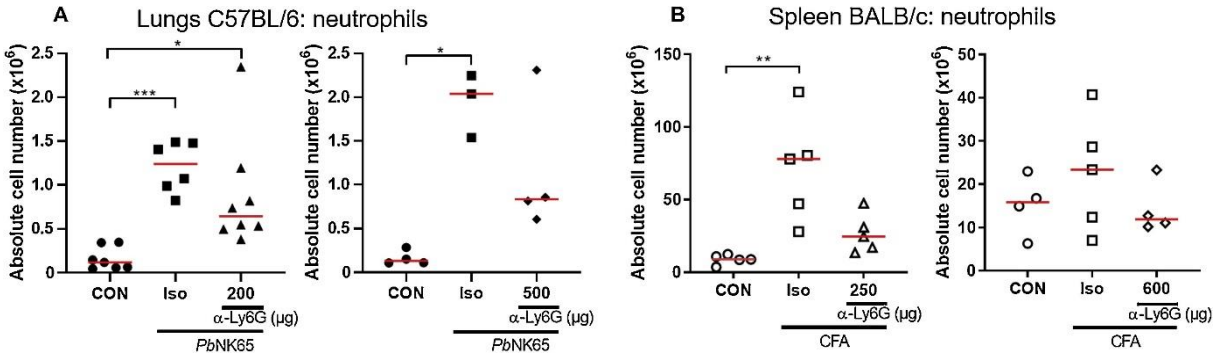

Fig. A1.3. Incomplete depletion of neutrophils with anti-Ly6G in PbNK65-infected C57BL/6 mice and CFA-challenged BALB/c mice.

A) PbNK65-infected C57BL/6 mice were injected i.p. on day -1, 3 and 7 p.i. with 200 or 500 µg of anti-Ly6G (1A8) or with the corresponding amount of isotype control (IgG2a). On day 9 p.i., mice suffered from MA-ARDS and were sacrificed. Absolute numbers of pulmonary neutrophils were determined (n = 3–7). B) CFA-challenged BALB/c mice were injected i.p. with 250 or 600 µg of anti-Ly6G (1A8) or with isotype control (IgG2a) on day 14 and 17 post challenge. On day 21, mice were sacrificed and the number of neutrophils in the spleen were determined (n = 4–5). A–B) Graphs represent the absolute number of neutrophils after gating as described in Fig. A1.1. Panel A left graph, pooled data from 2 independent experiments; panel A right graph and panel B, graphs show data from one representative experiment out of 2 independent experiments.

Depletion of neutrophils is associated with increased proliferation

To understand the importance of a proper timing of the administration of depleting antibodies, we performed a BrdU incorporation test in naive mice. 24 h after BrdU injection, approximately 10% of the bone marrow neutrophils (GR1int/hi Ly6Cint CD11b+) incorporated BrdU in isotype control-treated mice (Fig. A1.4A). Upon single-dose neutrophil depletion 24 h before BrdU injection, bone marrow neutrophils showed a significantly increased BrdU incorporation in both C57BL/6 and BALB/c mice (non-significant trend in case of 500 µg anti-Ly6G in C57BL/6, p = 0.0709) (Fig. A1.4A). In the spleen of naive C57BL/6 and BALB/c mice, no significant differences were found upon depletion with anti-Ly6G (Fig. A1.4B). However, CFA-challenged BALB/c mice that received 600 µg anti-Ly6G on days 14 and 17 post CFA-challenge showed a significant increase in the percentage of proliferating splenic neutrophils (Fig. A1.4C). This increased proliferation seen in the spleen, may explain the limited and temporary depletion capacity of the antibody in this model. When mice were treated with 250 µg of anti-Ly6G antibodies twice a week, starting immediately after CFA administration (on day -1, 3, 6, 10, 14, 17 and 20), the number of splenic neutrophils increased profoundly on day 21 post CFA-injection (Suppl. Fig. A1.3A). These neutrophils had an immature phenotype which is characterised by a banded nuclear morphology, suggesting a rapid infiltration of new neutrophils (Suppl. Fig. A1.3B and C) (449).

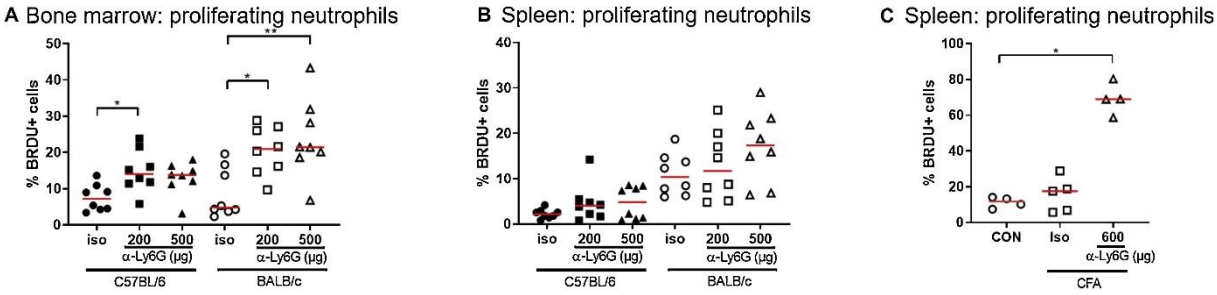

Fig. A1.4. Proliferation of neutrophils upon depletion with anti-Ly6G.

A–B) Percentage of BrdU+ bone marrow (A) and splenic (B) neutrophils (GR1int/hi Ly6Cint CD11b+) in naive C57BL/6 and BALB/c mice two days after depletion with 200 or 500 µg of anti-Ly6G (1A8) or upon injection with isotype control (IgG2a). BrdU was injected 24 h prior to dissection (*i.e.* one day after depletion) (n = 8). Results pooled from 2 independent experiments. C) Percentage of BrdU+ splenic neutrophils (GR1int/hi Ly6Cint CD11b+) in CFA-challenged BALB/c mice that were depleted with 600 µg of anti-Ly6G (1A8) or injected with isotype control (IgG2a) on day 14 and 17 and dissected on day 21. BrdU was injected 24 h prior to dissection (day 20) (n = 4–5). Data from one representative experiment out of 2 independent experiments.

Discussion

Neutrophil-depleting antibodies are frequently used in vivo to assess the role of neutrophils in disease models. Often, the neutrophil depletion efficacy is inadequately verified, for example by only determining the depletion in the circulation [6]. Moreover, a common mistake is the use of anti-Ly6G (clone 1A8) for both detection and depletion of the neutrophils (940,949). One can better opt for a different antibody, for example anti-GR1 (clone RB6-8C5), for the detection of neutrophils after depletion with anti-Ly6G. The use of a different antibody clone is also a good solution. However, we demonstrated that competition exists between the anti-Ly6G and anti-GR1 antibodies, which resulted in a lower GR1 staining and an apparent disappearance of the GR1hi population. Such staining procedure may lead to the misinterpretation that depletion was successful, while neutrophils were still present but masked by other GR1int/lo populations, *e.g.* the inflammatory Ly6Chi monocytes. These results emphasise the importance of careful panel design and gating strategies during neutrophil depletion studies. Using naive mice, we demonstrated that an efficient depletion (>80%) of neutrophils was obtained in the blood, lungs and spleen but not in the bone marrow of BALB/c mice. In contrast, efficient depletion of neutrophils was only reached in the blood of naive C57BL/6 mice and not in the organs, such as lungs, spleen and bone marrow. These findings stress the importance of confirming the depletion efficacy in the organ of interest, rather than only in the blood. Interestingly, the depletion appeared less efficient for the CXCR2− neutrophils, which may have either an immature or aged character, in blood, spleen and lungs. CXCR2 is upregulated during maturation and regulates neutrophil egress from the bone marrow (950). Aged neutrophils decrease their CXCR2 expression, facilitating them to reverse-migrate back to the bone marrow, where they can be eliminated by the macrophages (951).

Interestingly, increased numbers of neutrophils and higher GR1-staining were found in BALB/c compared to C57BL/6 mice. This suggested that the higher percentual depletion efficiency seen in BALB/c mice might be related to a higher Ly6G expression or elevated neutrophil numbers before depletion. However, other factors might also play a role, such as potential differences in complement activation or phagocytosis, as it was shown that Ly6G depletion depends on the presence of macrophages (952). In our study, we were unable to obtain efficient depletion of neutrophils in both PbNK65-infected C57BL/6 mice and CFA-challenged BALB/c mice, and showed that this limited depletion was dosage independent. In normal situations, the turnover of neutrophils is tightly regulated (650,730). Depletion of neutrophils causes a G-CSF-dependent positive feedback loop that triggers the expansion of new neutrophils in the bone marrow at the expense of thrombopoietic and red cell precursors (532). The BrdU incorporation studies indeed document that, upon depletion, an increased proliferation of neutrophils occured in the bone marrow of naive mice, two days after anti-Ly6G depletion. In the CFA-induced inflammation model, the duration of the depletion is an important limiting factor. In this model, long persistent depletion, twice a week starting one day prior to CFA challenge, resulted in a profound increased number of immature neutrophils in the spleen, associated with an increased number of BrdU+ splenic neutrophils. The increased number of proliferating splenic neutrophils was also found in the CFA-challenged BALB/c mice that were depleted with 600 µg of anti-Ly6G on day 14 and 17 and dissected on day 21. This nicely illustrated the temporary depletion capacity of the antibodies in this CFA-based model.

In conclusion, neutrophil depletion is organ-, strain- and timing-specific and should thus be analysed carefully. This study describes the incomplete depletion in two immunological models and underlines the need for new tools to understand the role of neutrophils in vivo.

Supplementary Material

Supplementary Figures

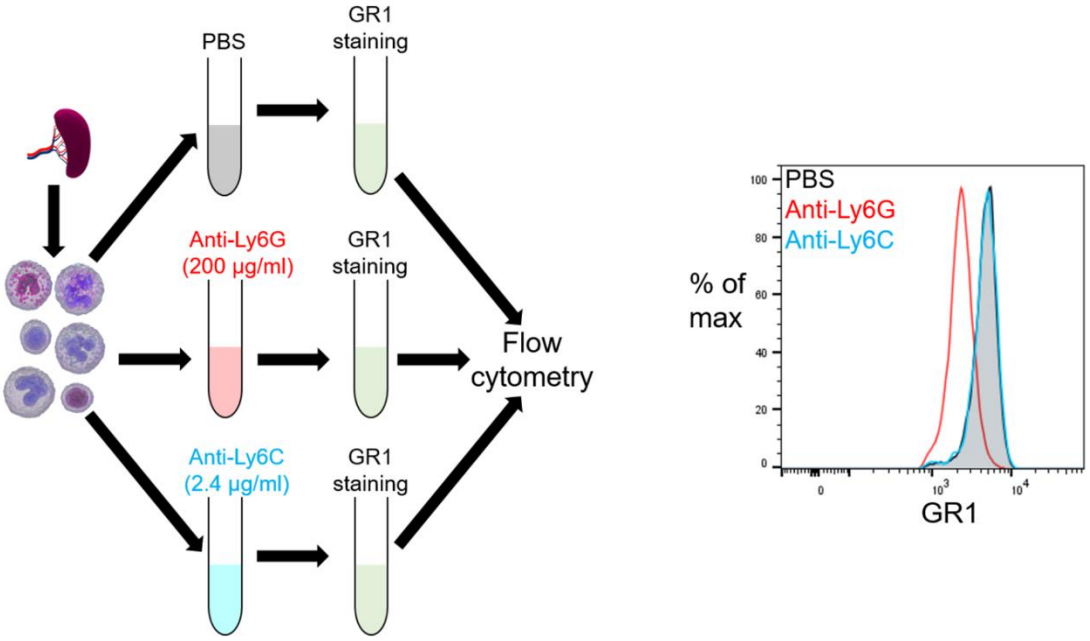

Suppl. Fig. A1.1. Competition between the anti-Ly6G or anti-Ly6C and anti-GR1 antibodies.
Spleen leukocytes were isolated from naive C57BL/6 mice and stained with anti-CD45, anti-CD11b and anti-GR1 after prior incubation with PBS (grey), unlabeled depleting anti-Ly6G antibodies (200 µg/ml, red) or fluorescently labeled anti-Ly6C antibodies (2.4 µg/ml, blue). Subsequently, flow cytometry analysis was performed to assess the mean fluorescence intensity (MFI) of the GR1 staining. Neutrophils were gated as CD11b+ GR1int/hi. The graphs show data from one representative experiment out of 2 independent experiments.

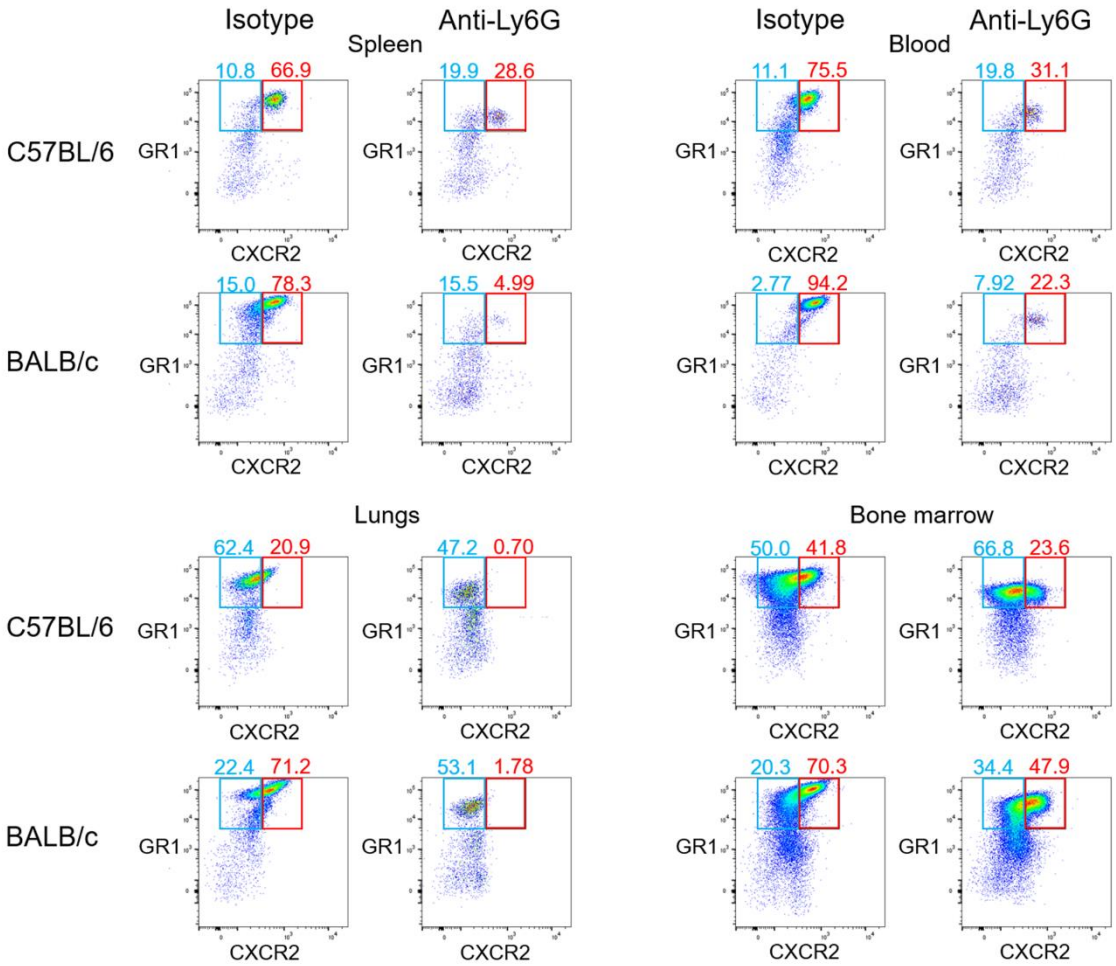

Suppl. Fig. A1.2. CXCR2- neutrophils are less efficiently depleted by anti-Ly6G than CXCR2+ neutrophils.

Naive C57BL/6 and BALB/c mice were injected i.p. with 200 µg of anti-Ly6G (1A8) or isotype control (IgG2a). Two days after injection, lung, spleen, blood and bone marrow leukocytes were collected and analysed with flow cytometry. Representative flow cytometry plots of the expression of GR1 and CXCR2 on CD11b+ Ly6Cint/lo cells are shown. Neutrophils were defined as GR1int/hi CXCR2+ (red gate) and GR1int/hi CXCR2- (blue gate). The graphs show data from one representative sample out of 2 independent experiments.

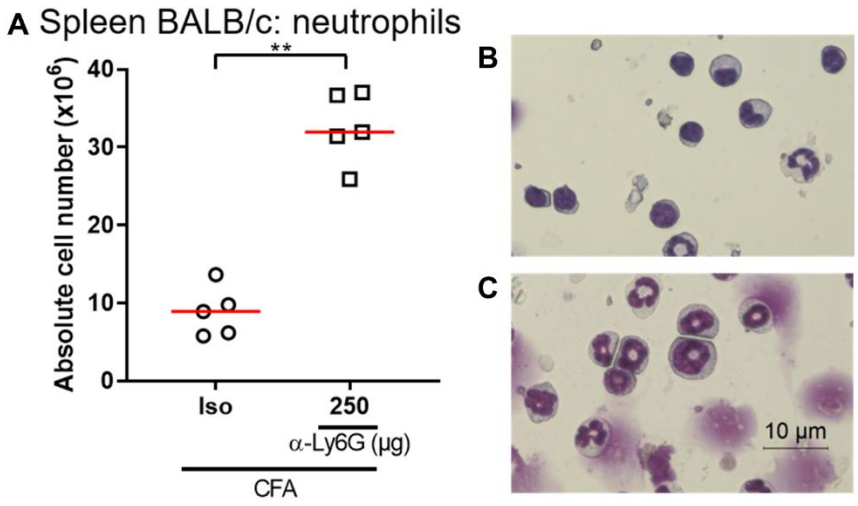

Suppl. Fig. A1.3. Early depletion of neutrophils with anti-Ly6G in CFA-challenged BALB/c mice induces a reactive repopulation.
A) CFA-challenged BALB/c mice were i.p. injected, twice a week starting one day prior to challenge (on day -1, 3, 6, 10, 14, 17 and 20), with 250 µg of anti-Ly6G (1A8) or with isotype control (IgG2a). Mice were sacrificed on day 21 post CFA-injection and number of neutrophils in the spleen were measured. Graphs represent the absolute number of neutrophils (n=5). B-C) Representative cytospin preparations of the splenocytes upon treatment with isotype control (B) or anti-Ly6G (C). The graphs show data from one representative experiment out of 3 independent experiments.

ADDENDUM 2

PHENOTYPICAL AND FUNCTIONAL CHARACTERISATION OF NEUTROPHILS IN TWO PYRIN-ASSOCIATED AUTO-INFLAMMATORY DISEASES

Published manuscript:

Bert Malengier-Devlies[1,*], Mieke Metzemaekers[2,*], Mieke Gouwy[2], Erika Van Nieuwenhove[3], Albrecht Betrains[4], Maaike Cockx[2], Lotte Vanbrabant[2], Noëmie Pörtner[2], Jurgen Vercauteren[5], Lien De Somer[1,3,6], Sofie Struyf[2], Steven Vanderschueren[4,7], Ellen De Langhe[8,9], Paul Proost[2,*], Patrick Matthys[1,*] and Carine Wouters[1,3,6,*](2021). Journal of Clinical Immunology

* equal contribution

[1]KU Leuven Department of Microbiology, Immunology and Transplantation, Rega Institute for Medical Research, Laboratory of Immunobiology, Leuven, Belgium
[2]KU Leuven Department of Microbiology, Immunology and Transplantation, Rega Institute for Medical Research, Laboratory of Molecular Immunology, Leuven, Belgium
[3]University Hospitals Leuven, Division of Pediatric Rheumatology, Leuven, Belgium
[4]KU Leuven Department of Microbiology, Immunology and Transplantation, Laboratory of Clinical Infectious and Inflammatory Disorders, Leuven, Belgium
[5]KU Leuven Department of Microbiology, Immunology and Transplantation, Rega Institute for Medical Research, Laboratory of Clinical and Epidemiological Virology, KU Leuven, Leuven, Belgium
[6]European Reference Network for Rare Immunodeficiency, Autoinflammatory and Autoimmune Diseases (RITA) at University Hospital Leuven, Leuven, Belgium
[7]University Hospitals Leuven, Division of General Internal Medicine, Leuven, Belgium
[8]University Hospitals Leuven, Division of Rheumatology, Leuven, Belgium
[9]KU Leuven, Laboratory of Tissue Homeostasis and Disease, Leuven, Belgium

Reproduced with permission from Springer Nature

ADDENDUM 2: PHENOTYPICAL AND FUNCTIONAL CHARACTERISATION OF NEUTROPHILS IN TWO PYRIN-ASSOCIATED AUTO-INFLAMMATORY DISEASES

Abstract

Purpose Familial Mediterranean Fever (FMF) and Pyrin-Associated Autoinflammation with Neutrophilic Dermatosis (PAAND) are clinically distinct autoinflammatory disorders caused by mutations in the pyrin-encoding gene *MEFV*. We investigated the transcriptional, phenotypical, and functional characteristics of patient neutrophils to explore their potential role in FMF and PAAND pathophysiology.

Methods RNA sequencing was performed to discover transcriptional aberrancies. The phenotypical features, degranulation properties, and phagocytic capacity of neutrophils were assessed by flow cytometry. Production of reactive oxygen species (ROS), myeloperoxidase (MPO) release, and chemotactic responses were investigated via chemiluminescence, ELISA, and Boyden chamber assays, respectively.

Results Neutrophils from PAAND and FMF patients showed a partially overlapping, activated gene expression profile with increased expression of S100A8, S100A9, S100A12, IL-4R, CD48, F5, MMP9, and NFKB. Increased MMP9 and S100A8/A9 expression levels were accompanied by high plasma concentrations of the encoded proteins. Phenotypical analysis revealed that neutrophils from FMF patients exhibited an immature character with downregulation of chemoattractant receptors CXCR2, C5aR, and BLTR1 and increased expression of Toll-like receptor 4 (TLR4) and TLR9. PAAND neutrophils displayed an increased random, but reduced CXCL8-induced migration. A tendency for enhanced random migration was observed for FMF neutrophils. PAAND neutrophils showed a moderately but significantly enhanced phagocytic activity as opposed to neutrophils from FMF patients. Neutrophils from both patient groups showed increased MPO release and ROS production.

Conclusions Neutrophils from patients with FMF and PAAND, carrying different mutations in the *MEFV* gene, share a proinflammatory phenotype yet demonstrate diverse features, underscoring the distinction between both diseases

Introduction

Autoinflammatory syndromes typically present with recurrent episodes of non-infectious fever accompanied by systemic and/or local inflammation predominantly driven by dysregulation of innate immune mechanisms, in the absence of autoimmunity hallmarks such as high-titer autoantibodies or autoreactive T cells (953,954). Multiple autoinflammatory syndromes are caused by mutations in inflammasome-related genes (955). Inflammasomes are composed of a cytoplasmic sensor that recognises pathogen- or danger-associated conserved structural motifs or perturbations in intracellular homeostasis, an adaptor protein, and a caspase (11,13,956). Activation of the sensor causes inflammasome assembly and results in consecutive activation of caspase 1, interleukin (IL-)1β, and IL-18. A major cytoplasmic sensor is pyrin, which is found primarily in neutrophils, eosinophils, and monocytes/ macrophages (957–959). Human pyrin is encoded by the *MEFV* (Mediterranean fever) gene. During homeostasis, Rho A effector protein kinases N1 and N2 (PKN1 and PKN2) mediate phosphorylation of pyrin at residues S208 and S242, thereby facilitating binding to 14-3-3 proteins, keeping pyrin inactive (960). Pyrin inhibition is halted upon stimulation with bacterial Type III Secretion System (T3SS) effector molecules or Rho-inactivating toxins, that inactivate Rho A and PKN1/2 resulting in loss of phosphorylation and 14-3-3 protein dissociation (961–964). Mutations in pyrin cause Familial Mediterranean Fever (FMF), the prototype monogenic autoinflammatory disorder (24,953,954). The precise underlying mechanisms of FMF are not fully understood but increased activation of the pyrin inflammasome has been demonstrated. Clinical characteristics are recurrent febrile episodes lasting for 1 to 3 days accompanied by arthritis and/or serositis, with or without erysipelas-like rash (965). Recently, two novel mutations in exon 2 of pyrin were linked to an autoinflammatory disorder with a distinct clinical phenotype termed Pyrin-Associated Autoinflammation with Neutrophilic Dermatosis (PAAND) (22,23). These mutations, namely S242R and E244K, disrupt a phosphorylation site or its +2 position, and binding of pyrin to 14-3-3. PAAND is a chronic recurrent neutrophilic dermatosis with long-lasting inflammatory episodes (23). Most FMF patients carry homozygous or compound heterozygous mutations, especially in exon 10 in the *MEFV* gene, whereas PAAND is caused by a single *MEFV* mutation. FMF patients can be treated with colchicine (966). In PAAND patients, successful treatment with anakinra (recombinant IL-1RA) was achieved in one patient (23). Tumor necrosis factor (TNF) blockage proved more effective in another patient with limited responsiveness to IL-1β-targeted therapy (22). Neutrophils are the predominant cells in skin lesions from PAAND patients, and are the most abundant circulating leukocytes during inflammatory attacks in FMF. These innate leukocytes have important pro-inflammatory, anti-microbial effector functions including phagocytosis, production of reactive oxygen species (ROS), and release of neutrophil extracellular traps (NETs) (338,784). The functional role as well as transcriptional and phenotypical characteristics of neutrophils in the pathology of pyrin-associated autoinflammatory syndromes are currently unknown (for PAAND) or have been unraveled only partially (for FMF) (967–970). In the present study, we isolated peripheral blood neutrophils during disease remission (no flare) from PAAND and FMF patients and healthy controls (HCs). The freshly isolated cells were used for comprehensive gene expression analysis by RNA sequencing (RNAseq) and for extensive phenotypical and functional characterisation.

Patients and Methods

Patients

Seven PAAND patients, thirteen FMF patients, and thirty healthy controls (HCs) were recruited at the University Hospital Leuven (Suppl. Table S1) after informed consent according to the declaration of Helsinki. Patients were under treatment and displayed low disease activity at the moment of sampling (Suppl. Table S1). The Ethics Committee of University Hospitals Leuven approved this study (S59874).

Cytokine, S100A8/A9, and Matrix Metalloproteinase (MMP)-9 Measurements

Plasma concentrations of IL-1β, IL-6, IL-10, IL-18, IL-1RA, TNF-α, interferon (IFN)-γ, and CXCL8 were determined using Meso Scale Discovery multiplex technology. S100A8/ A9 levels were measured by DuoSet ELISA (R&D Systems, Minneapolis, MN) and MMP-9 activity by zymography as described (971).

Neutrophil Isolation

Neutrophils were isolated from fresh peripheral blood (within 30 min after blood donation) by density gradient centrifugation (10 min, 20 °C, 218g) in Pancoll (PAN Biotech GmbH, Aidenbach, Germany). Erythrocytes were eliminated by hypotonic shock (30 s) prior to induction experiments, analysis of production of ROS, and chemotaxis assays. Alternatively, neutrophils were directly isolated from whole blood using the EasySep™ Direct Human Neutrophil Isolation Kit (Stemcell Technologies, Vancouver, Canada) and used for extensive phenotyping, analysis of phagocytosis, degranulation, and RNAseq. To evaluate the effects of colchicine on the phenotypical and functional properties of neutrophils, cells were stimulated for 30 min at 37 °C with 150 pg/ml or 250 pg/ml of colchicine (Sigma, Saint Louis, MO).

RNA Sequencing

RNA was extracted from neutrophils using the RNeasy Mini Kit (Qiagen, Hilden, Germany). RNAseq, preparative techniques, and gene counting were performed by the KU Leuven Genomics core as described in the supplementary Patients & Methods. Count-based differential expression analysis between neutrophils from HCs and patients with FMF and PAAND was done with R-based Bioconductor package DESeq2 (972). Reported p-values were adjusted for multiple testing with the Benjamini-Hochberg procedure, which controls the false discovery rate (FDR). To select significantly differentially expressed genes (DEGs), a cut-off on fold change with an absolute log2-ratio below 0.5 was combined with a FDR value less than 0.05. Graphical visualisation of DEGs was done using the R-based packages Pheatmap and Enhancedvolcano. Gene expression levels were validated using a TaqMan gene expression assay (Applied Biosystems, Waltham, MA). Primers used are listed in Suppl. Table 2.

Flow Cytometry

Cells were incubated with FcR-block (Miltenyi Biotec, Bergisch Gladbach, Germany) and stained extracellularly in FACS buffer [phosphate buffered saline (PBS) + 2% (v/v) fetal calf serum (FCS) + 2 mM ethylenediaminetetraacetic acid (EDTA)]. Antibodies are listed in Suppl. Table S3. For intracellular staining (TLR9), cells were fixed and permeabilised using the Cytofix/ Cytoperm kit (BD Biosciences, Franklin Lakes, NJ) and stained with anti-human CD289. Before lineage gating, all populations were first gated on live cells visualised using Zombie Aqua 516 (Biolegend, San Diego, CA) or FVS620 (BD Biosciences). Forward and side scatter were used to exclude debris and doublets. After acquisition on a BD LSRFortessa X20, samples were analysed using FlowJo (LLC, V10).

Degranulation and Phagocytosis Assay

Cells were stimulated with 50 ng/ml TNF-α (PeproTech, Rocky Hill, NJ) or 10 µg/ml ultrapure lipopolysaccharide (LPS) from E. coli (Invivogen, San Diego, CA) in [PBS + 2 mM EDTA] at 37 °C. After 30 min, pHrodo red S. aureus bioparticles (Invitrogen, Waltham, MA) were added and incubated for 30 min at 37 °C. Negative controls were placed on ice without stimulation. Results were analysed by flow cytometry (vide supra). Degranulation was assessed based on the expression of granule-associated markers CD63, CD66b, CD11b, and CD35 (Suppl. Table S3) as described (973).

Respiratory Burst Assay

ROS production by neutrophils was determined with a chemiluminescence-based assay as described in the supplementary Patients & Methods. Cells were stimulated with 150 ng/ml phorbol 12-myristate 13-acetate (PMA; Sigma) or 50 ng/ml TNF-α in the presence of 5 mM luminol (Sigma).

Production of Myeloperoxidase (MPO)

Neutrophils [2 × 106 cells/ml in RPMI1640 complemented with 10% (v/v) FCS + 50 µg/ml gentamycin (Gibco, Waltham, MA)] were stimulated with 200 ng/ml ultrapure LPS from E. coli (Invivogen, San Diego, CA). Supernatants were collected after 4 h at 37 °C and analysed for MPO using commercially available DuoSet ELISA kits (R&D Systems).

48-Well Boyden Chamber Chemotaxis Assay

The migratory responses of neutrophils towards 10 ng/ml C5a (R&D Systems), 10 ng/ml CXCL8 (72AA; PeproTech) and 10−8 M N-formylmethionyl-leucyl-phenylalanine (fMLF; Sigma) were compared using the 48-well Boyden chamber chemotaxis assay as described (974).

Statistics

A linear mixed model was used to detect statistical differences between the study groups. Correction for multiple samples per patient was done using a random intercept model. Statistical analysis was performed using R.

Results

Neutrophils from Patients with PAAND and FMF Show a Primed Gene Expression Profile

An in-depth analysis of the neutrophil transcriptome was performed by RNAseq on purified neutrophils from PAAND patients (n = 5), FMF patients (n = 5), and HCs (n = 4). Patients were under treatment with low disease activity at the moment of sampling, except for one FMF patient (Suppl. Table S1). The purity of the neutrophil transcriptome was confirmed using the cell type enrichment tool CTen. The top 50 most expressed genes are shown in a heatmap (Suppl. Fig. A2.1A). Principal components analysis (PCA) revealed a partial overlap between neutrophils from FMF and PAAND patients, suggesting a similar transcriptome (Fig. A2.1A). In contrast, transcriptomes from patient and HC neutrophils were distinct, showing a minor overlap only in the PCA plot (Fig. A2.1A). Based on the count-based DEGs, we determined the genes that were significantly up- or downregulated after adjusting for multiple testing (adjusted p-values <0.05 were considered significant). Complete lists of DEGs are shown in Suppl. Tables S4-6. Fig. A2.1B shows a heatmap of the top 70 DEGs between the different groups. Comparing the neutrophil transcriptome of FMF patients and HCs revealed 481 DEGs, with 165 and 316 genes, respectively, being up- and downregulated in FMF. Between PAAND and HCs, 233 genes were differentially expressed, 162 genes were significantly upregulated and 71 genes were significantly downregulated in neutrophils from PAAND patients. Interestingly, 83 overlapping genes were significantly different in both PAAND and FMF when compared to HCs (Suppl. Table S7). Gene ontology showed that DEGs were involved in positive regulation of the respiratory burst, phagocytosis, and neutrophil regulation (Suppl. Fig. A2.1B). In contrast, only 58 genes were significantly altered in FMF compared to PAAND patients of which 19 were upregulated in FMF and 39 were downregulated in FMF. Fig. A2.1C shows the volcano plots of DEGs in neutrophils from PAAND or FMF patients compared to HCs (cut off adjusted p value: 0.05, cut off fold-change: 0.5). Genes upregulated in patient neutrophils included nuclear factor kappa-light-chain-enhancer of activated B cells (NFKB), factor V (F5), and IL-4R, all genes indicative of a primed phenotype. Alarmins S100A8/9 and S100A12 were significantly upregulated only in PAAND patients, while a non-significantly increased expression was measured in FMF neutrophils. In contrast, both MMP9 and CD48 were significantly upregulated in FMF whereas PAAND patients only showed a non-significantly increased expression. Importantly, increased MMP9 and S100A8/A9 expression levels were accompanied by high levels of the encoded proteins in plasma (Table 1). Analysis of S100A8, S100A9, S100A12, IL-4R, CD48, F5, MMP9, and NFKB expression levels in a second batch of RNA samples from PAAND patients (n = 7), FMF patients (n = 6), and HCs (n = 10) by single-target qPCRs revealed upregulation of all genes in both patient groups (Suppl. Fig. A2.2). Results from single-target qPCR analysis, but not RNAseq data, suggested upregulation of MMP8 and IL-1β expression by neutrophils from PAAND and FMF patients as compared to HCs (Suppl. Fig. A2.2). Collectively, these data suggest that peripheral blood neutrophils from patients with PAAND and FMF are activated cells. We could not identify a group of functionally relevant genes that was specifically related to FMF or PAAND.

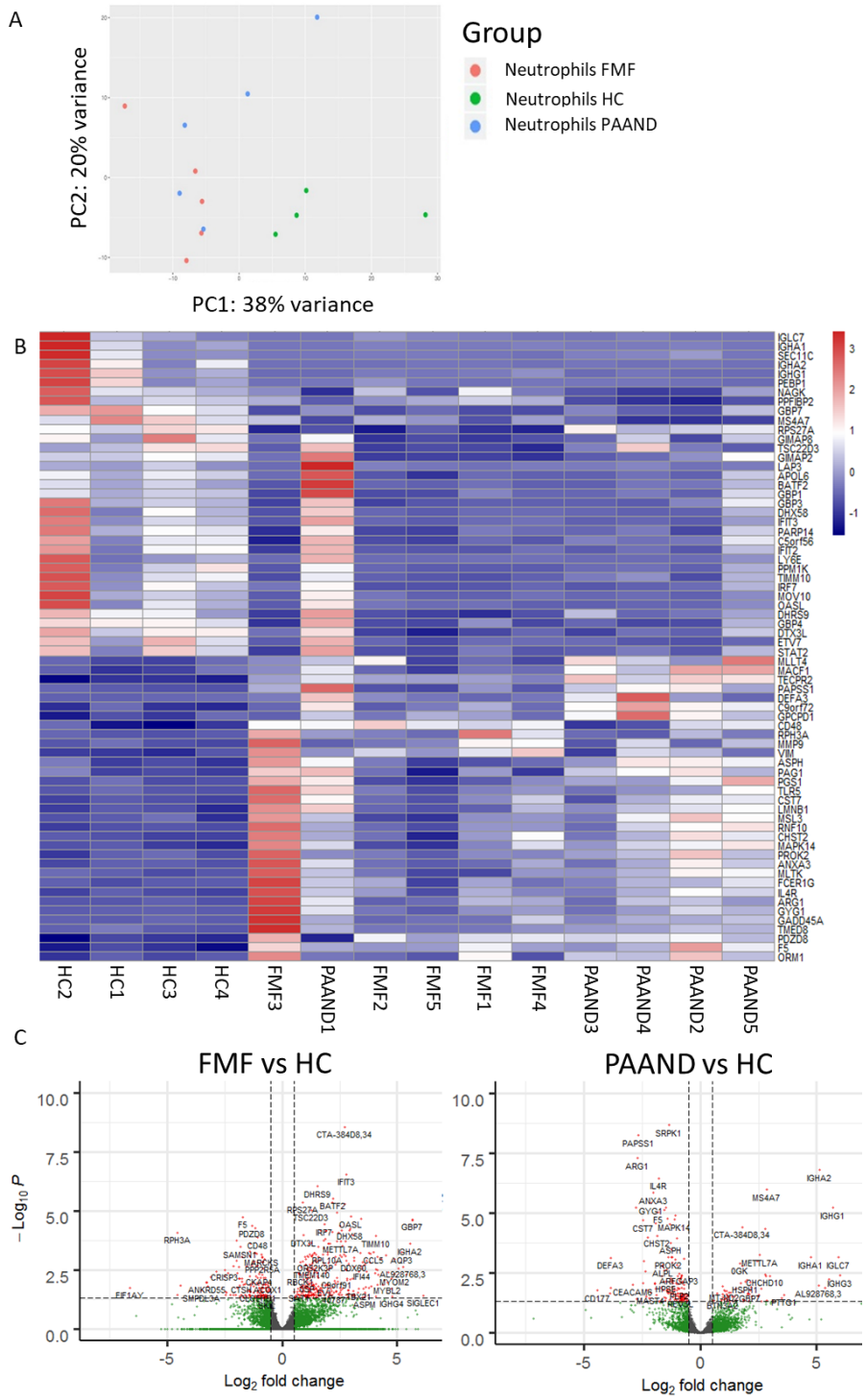

Fig. A2.1. Distinct gene expression profile in neutrophils from PAAND or FMF patients
RNA-sequencing was performed on neutrophils from 5 PAAND patients, 5 FMF patients and 4 HCs. Neutrophils were isolated by immunomagnetic negative selection. (A) Principle component analysis (PCA) using the most variable genes (B) Heatmap of DEGs. Colours indicate expression profiles (as Z-scores:red high, blue low expression). (C) Vulcano plot of DEGs with adjusted p-values. Plot shows statistical significance versus magnitude of gene expression change (fold-change). A cut-off of 0.05 and 0.5 was (dotted lines) chosen for the adjusted p-values and fold-change, respectively.

Neutrophils from Patients with PAAND and FMF Display Phenotypical Differences and Have Altered Maturation States

Results from gene expression studies (vide supra) sparked our interest to perfom an extensive phenotypical and functional analysis of patient neutrophils. First, the inflammatory environment was assessed in the blood by determining the concentration of 7 cytokines, CXCL8, S100A9/A9, and MMP-9 (Table 1). Quantification of inflammasome-related cytokines IL-1β and IL-18 revealed enhanced IL-18 concentrations in plasma from FMF patients as compared to individuals with PAAND or HCs (Table 1). Compared to HCs and FMF patients, PAAND patients displayed elevated plasma concentrations of IFN-ɣ and a tendency towards increased IL-6 and TNF-α levels. Plasma concentrations of the neutrophil-attracting chemokine CXCL8 and anti-inflammatory cytokines IL-10 and IL-1RA did not vary significantly between the study groups. Taken together, these results support the idea that FMF and PAAND are featured by distinct plasma cytokine profiles (17). Next, neutrophils were isolated from the blood. Neutrophil numbers were significantly higher in PAAND patients compared to HCs, whereas they were not altered in FMF (Table 1).

Table 1. Plasma cytokine levels

	HCs	PAAND	FMF
Age in years	28 (18-64)	49 (19-76)	34.5 (20-62)
Gender (M/F)	11/19	4/3	6/7
IL-1β (pg/ml)	0,01 (0.01-0.01) (n = 12)	0,01 (0.01-4.10) (n = 6)	0,01 (0.01 -0.42) (n = 8)
IL-6 (pg/ml)	0,47 (0.08-0.96) (n = 12)	2,64 (0.43-15.11) (n = 6)	0,43 (0.04-46.4) (n = 8)
IL-10 (pg/ml)	0,18 (0.11-0.57) (n = 12)	0,27 (0.07-5.01) (n = 6)	0,29 (0.03-1.92) (n = 8)
IL-18 (pg/ml)	440,9 (310.1-1684.0) (n = 12)	939,1 (567.9-1571.0) $ (n = 6)	4330,0 (1262.0-20076.0) *,$ (n = 8)
IL-1RA (pg/ml)	150,4 (72.64-316.0) (n = 12)	209,1 (143.5-13910.0) (n = 6)	187,0 (93.1-597.7) (n = 8)
IFN-γ (pg/ml)	7,13 (4.20-15.96) (n = 12)	21,80 (4.13-336.30) *,$ (n = 6)	6,3 (1.0-16.2) $ (n = 8)
TNF-α (pg/ml)	1,63 (0.22-7.31) (n = 12)	2,68 (1.17-22.70) (n = 6)	1,7 (0.5-5.1) (n = 8)
CXCL8 (pg/ml)	2,34 (1.05-2.71) (n = 12)	2,24 (1.14-12.32) (n = 6)	2,1 (1.1-10.5) (n = 8)
S100A8/A9 (ng/ml)	249,4 (69.4-597.0) (n = 12)	3287 (741.8-5710) (n = 6)	2495 (1102-97687) (n = 8)
MMP-9 (pmol/ml)	1,95 (0.48-5.07) (n = 12)	3,34 (0.44-30.20) (n = 6)	2,83 (1.29-19.68) (n = 8)
Neutrophils (cells/ml)	$1{,}65*10^6$ (0.77-2.24)	$2{,}375*10^6$ (1.06-3.34) ***,$	$1{,}475*10^6$ (0.85-3.64) $

Overview of patients and controls (HCs). Age, neutrophil numbers (determined after immuno-magnetic purification as cells per ml of blood), plasma cytokine and S100A8/A9 concentrations and MMP-9 activities are represented as median (range). Results were statistically analysed using a linear mixed model. A random intercept model was used to correct for multiple samples per patient. * $p<0.05$, *** $p<0.001$; for statistical differences between patients and HCs, $ $p<0.05$; for statistical differences between patient groups

No significant differences were found in the mean fluorescent intensity (MFI) of the neutrophil lineage-markers CD66b and CD15 (Suppl. Fig. A2.3A-B). The expression of the Fcγ receptor III (CD16) was moderately but significantly decreased on neutrophils from FMF patients (Suppl. Fig. A2.3C). The chemoattractant receptor CXCR1 was slightly but significantly upregulated on neutrophils from PAAND patients as compared to HC cells (Suppl. Fig. A2.4A). Neutrophils from FMF patients were featured by significantly lower levels of CXCR2, C5aR (C5a complement receptor), and BLTR1 (leukotriene B4 receptor) as compared to HCs or PAAND patients (Suppl. Fig. A2.4B-D). No differences in protein expression of IL-1R2 or CD11b were found on neutrophils from patients with PAAND or FMF (Suppl. Fig. A2.5A-B). Evaluation of the expression of TLR2, TLR4, TLR6, and TLR9 revealed significantly increased levels of TLR4 and TLR9 on neutrophils from FMF patients as compared to PAAND patients (TLR4) or HCs (TLR4 and TLR9) (Suppl. Fig. A2.6). CD10 expression, which is restricted to mature cells

(975), was moderately but significantly decreased only on neutrophils from FMF patients (Fig. A2.2A). To assess neutrophil maturation characteristics in more detail, the expression of CD16 and CD62L (L-selectin) was assessed (Fig. A2.2B–C, Suppl. Fig. A2.5C). In non-inflammatory conditions, nearly all circulating neutrophils are mature, CD16highCD62Lhigh cells with 3–4 nuclear lobes. Immature neutrophils have a banded nucleus and are CD16dimCD62Lhigh. Hypersegmented neutrophils are phenotypically defined as CD16highCD62Llow cells and have more than 4 nuclear lobes. A non-significant (p = 0.07) increased percentage of immature neutrophils was found in FMF patients compared to HCs (Fig. A2.2B, D, F). One PAAND patient showed an increased percentage of hypersegmented neutrophils (Fig. A2.2C, E). Since FMF patients and two PAAND patients were treated with colchicine, we evaluated the effects of colchicine on the phenotypical characteristics of HC neutrophils (Suppl. Fig. A2.7). In line with the observations made in FMF patients, a decreased expression of CXCR2, C5aR, and BLTR1 was measured on colchicine-treated neutrophils. No differences were observed in maturation state (as evidenced by the MFI of CD10) or TLR expression, but a shedding of CD62L was measured upon colchicine treatment. Taken together, neutrophils from FMF patients, but not PAAND neutrophils, showed a reduced maturation and have increased expression of TLR4 and TLR9. Alterations in expression of CXCR2, C5aR and BLTR1 on neutrophils potentially result from colchicine therapy.

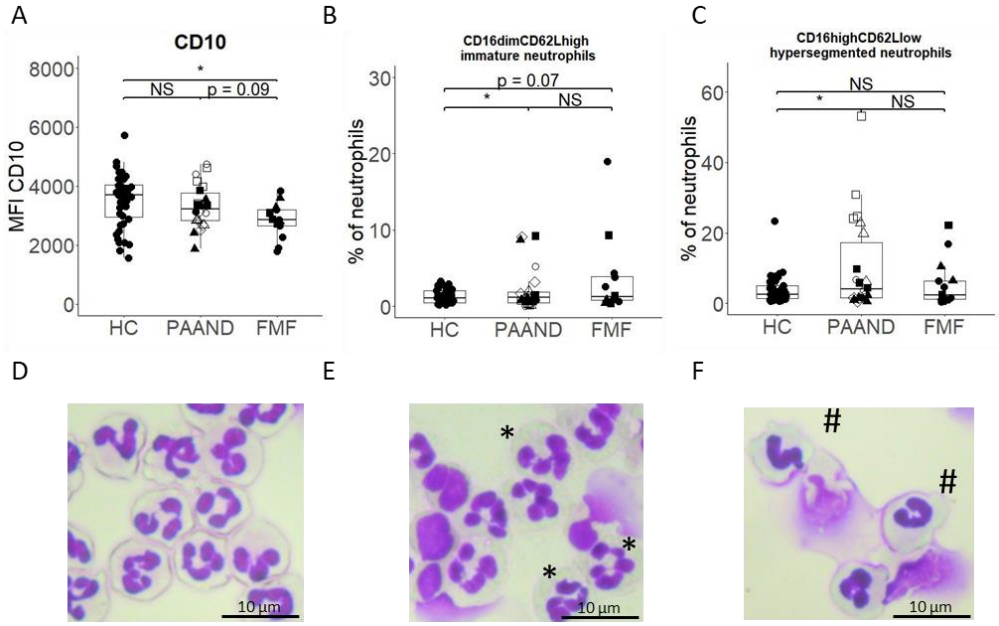

Fig. A2.2. Phenotypical analysis of neutrophils from patients with pyrin-associated autoinflammation

Neutrophils from PAAND patients, FMF patients and HCs were isolated by immunomagnetic negative selection and analysed by flow cytometry and cytospin. (A) Box whisker plot indicate expression levels on neutrophils [mean fluorescence intensity (MFI)] of CD10. (B-C) Based on CD16 and CD62L expression, neutrophils were divided into immature ($CD16^{dim}CD62L^{high}$) (B) and hypersegmented neutrophils ($CD16^{high}CD62L^{low}$) (C) and their relative number was shown. (D-F) Representative neutrophil cytospin images from a HC (D), a PAAND patient (E) and an FMF patient (F). Hypersegmented neutrophils and immature neutrophils were indicated by an asterisk (*) or a hashtag (#), respectively. Each dot represents an individual donor (n ≥ 6). Symbols with the same shape in the PAAND patient group represent replicate measurements of the same patient assessed at different time points. Symbols in the FMF group represent patients with a homozygous (●), a heterozygous (■) or a compound heterozygous (▲) mutation, respectively (Suppl. Table S1). Results were statistically analysed using a linear mixed model. A random intercept model was used to correct for multiple samples per patient. *p<0.05

Neutrophils from Patients with PAAND and FMF Display Altered Pro-inflammatory Activities

Upon activation, neutrophils may execute multiple proinflammatory activities including the release of ROS and phagocytosis. FMF neutrophils, in particular those from patients with homozygous mutations, displayed significantly enhanced ROS production under basal conditions as well as after stimulation with TNF-α compared to neutrophils from HCs (Fig. A2.3A–B). Neutrophils from PAAND patients also displayed enhanced basal and TNF-α-induced ROS production as compared to HCs (Fig. A2.3A–B). Colchicine treatment had no major impact on the basal ROS production of HC neutrophils (Suppl. Fig. A2.8A). Numbers of phagocytosing neutrophils were not significantly different between the study groups, although a tendency towards an increased percentage of cells having beads engulfed was observed for PAAND patients (Fig. A2.3C). The number of engulfed beads (represented by the MFI)was significantly lower for FMF neutrophils compared to HCs whereas PAAND neutrophils showed a moderately but significantly enhanced phagocytic activity (Fig. A2.3D). Colchicine did not affect the phagocytic capacity of HC neutrophils (Suppl. Fig. A2.8B-C). Examination of cell culture supernatants 4 h after sub-cultivation under basal conditions or in the presence of LPS revealed a tendency towards an increased release of MPO—an enzyme stored in azurophilic granules that coverts H_2O_2 to hypochlorous acid—by neutrophils from some PAAND and FMF patients (Fig. A2.3E–F). Our results indicate that neutrophils from PAAND and FMF patients show a tendency of elevated pro-inflammatory activity.

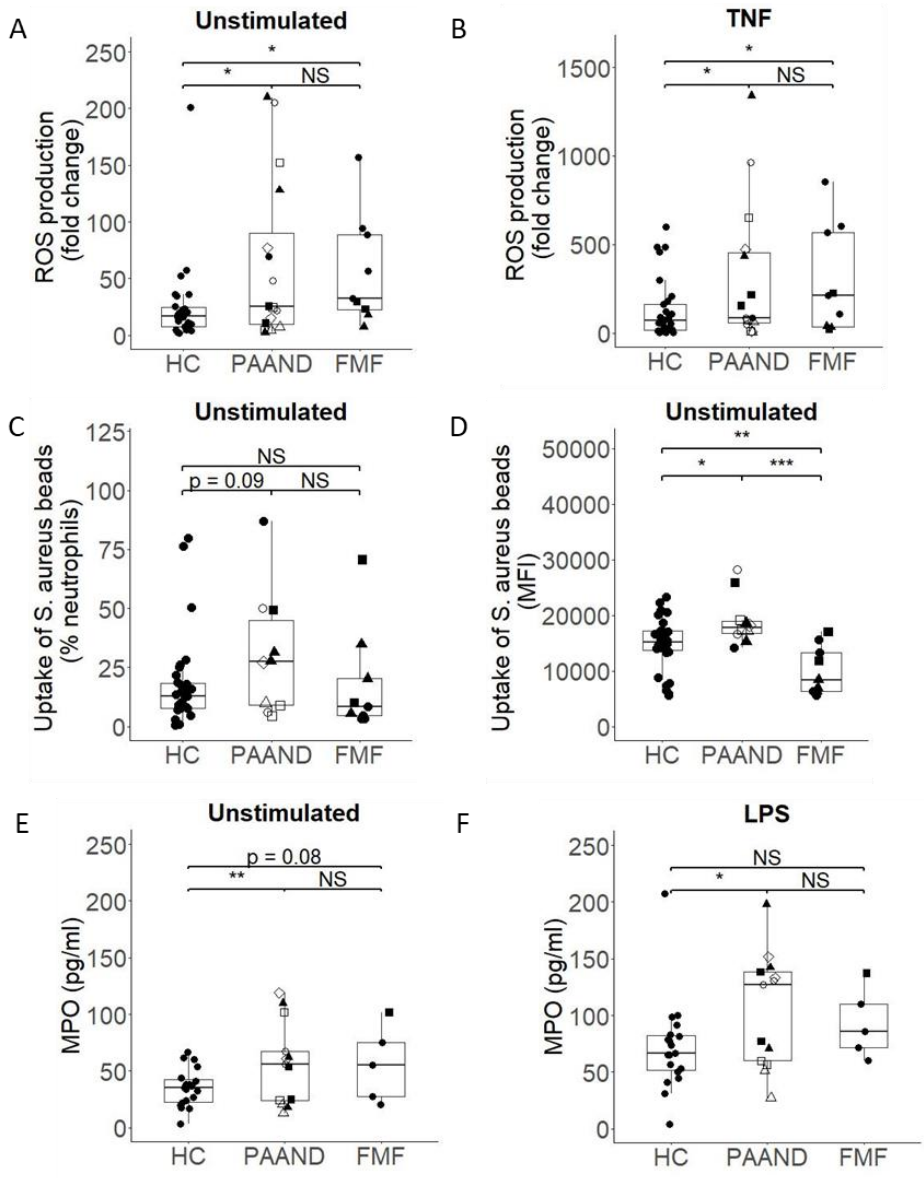

Fig. A2.3. Altered ROS production and phagocytic activity of neutrophils from patients with pyrin-associated autoinflammation

(A-B) Neutrophils from PAAND patients, FMF patients and HCs were exposed to (A) RPMI1640 medium alone or (B) 50 ng/ml TNF-α in the presence of 5 mM luminol and kinetic measurements of luminol oxidation where performed during 3 h at 37°C. ROS production was assessed by calculating fold changes of luminol oxidation, *i.e.* the differences between the lowest value and the maximal value during the incubation period. (C-D) Neutrophils were incubated with pHrodo red *S. aureus* bioparticles™ during 30 min at 37°C and bead uptake was evaluated by flow cytometry. Results are presented as (C) percentage of cells that engulfed beads and (D) the amount of engulfed beads/cell (represented by the MFI). (E-F) Neutrophils were cultured in the absence (E) or presence of 200 ng/ml ultrapure LPS (F). Supernatants were collected after 4h of incubation at 37°C and MPO concentrations were determined by ELISA. Each dot in box whisker plots represents an individual donor (n ≥ 6). Symbols with the same shape in the PAAND patient group represent replicate measurements of the same patient assessed at different time points. Symbols in the FMF group represent patients with a homozygous (●), a heterozygous (■) or a compound heterozygous (▲) mutation, respectively (Suppl. Table S1). Results were statistically analysed using a linear mixed model. A random intercept model was used to correct for multiple samples per patient. *p<0.05, ** p<0.01, *** p<0.001.

Neutrophils from Patients with PAAND and FMF Show a Primed Phenotype

Neutrophil priming occurs when quiescent neutrophils are (continuously) exposed to inflammatory agents or mechanical stress, and results in increased responsiveness to subsequent stimulation. The activated gene expression profile, increased ROS production, and the observed tendency towards increased concentrations of the granule-associated protease MMP-9 and cytosolic alarmin S100A8/A9 in plasma from FMF and PAAND patients already suggested enhanced neutrophil activation (Table 1). Interestingly, an increased percentage of small and large granular neutrophils was found in most PAAND patients as compared to FMF patients or HCs (Fig. A2.4A–B). Degranulation of neutrophils upon in vitro stimulation with LPS or TNF-α was studied (Fig. A2.4 and Suppl. Fig. A2.9) based on surface expression of CD35 (secretory vesicles), CD66b (specific granules), CD11b (specific granules, gelatinase granules, secretory vesicles), and CD63 (azurophilic granules) (976). No significant differences in expression of CD35 were detected (Fig. A2.4C and Suppl. Fig. A2.9). PAAND neutrophils displayed significantly higher levels of CD66b and CD63 upon stimulation with TNF-α, but not after LPS stimulation or in medium conditions, as compared to HCs (Fig. A2.4D/F). Additionally, neutrophils from PAAND patients showed enhanced CD11b expression in medium conditions but no significant differences were found upon LPS or TNF-α stimulation (Fig. A2.4E & Suppl. Fig. A2.9). In conclusion, neutrophils from PAAND patients show a tendency of increased degranulation that is reflected by the increased plasma levels of S100A8/9 and MMP-9.

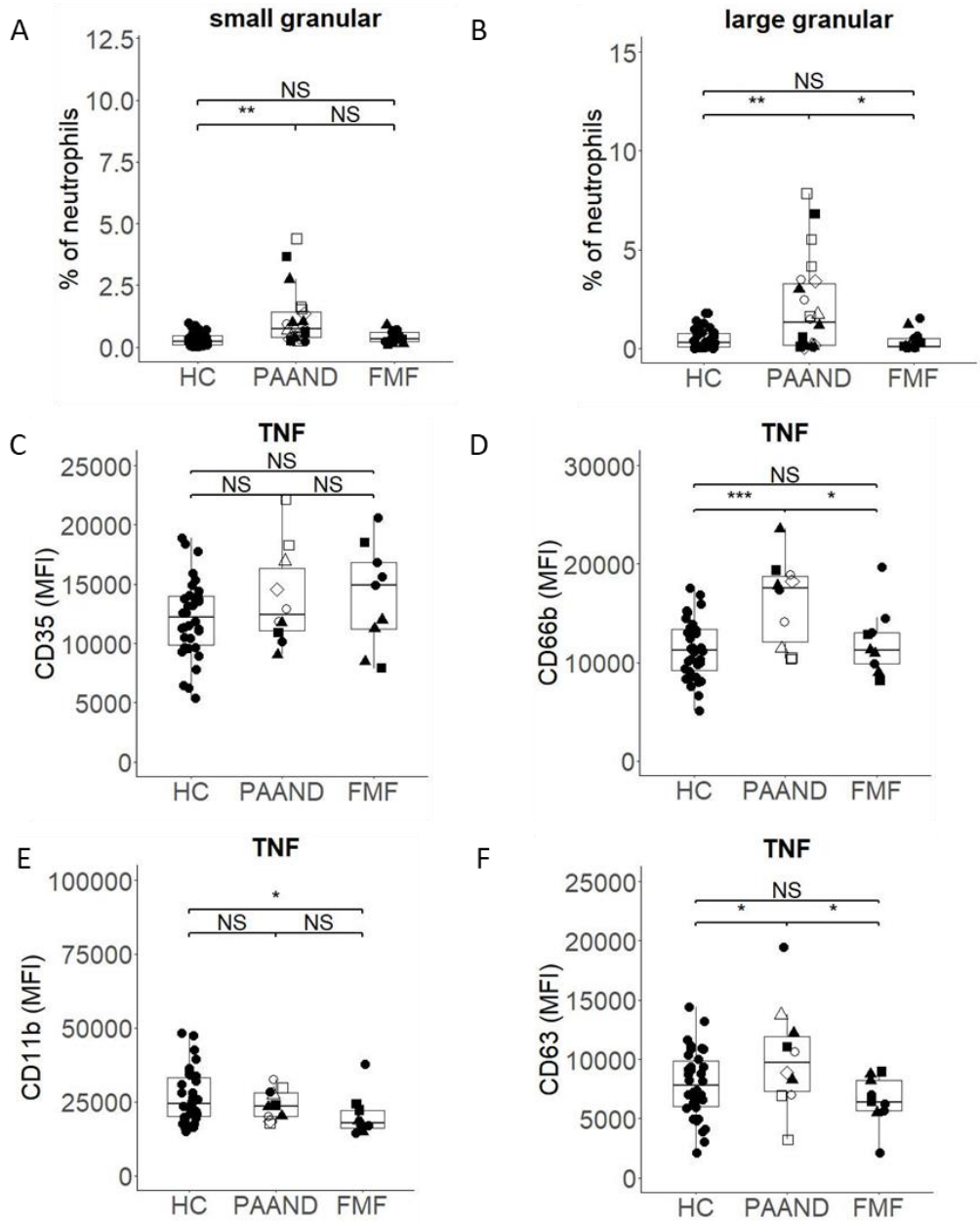

Fig. A2.4. Altered granularity and degranulation capacity of neutrophils from patients with pyrin-associated autoinflammation

(A-B) Forward scatter (FSC) and side scatter (SSC) were used to evaluate the neutrophil size and granularity. (A-B) Percentage of small and large granular neutrophils in HCs, patients with PAAND or FMF. (C-F) Neutrophils were cultured for 1 h with 50 ng/ml TNF-α at 37°C. Relative expression levels (MFI) of CD35 (secretory vesicles), CD66b (specific vesicles), CD11b (gelatinase vesicles) and CD63 (azurophilic vesicles) were plotted to assess degranulation of neutrophils. Each dot represents an individual donor (n ≥ 5). Symbols with the same shape in the PAAND patient group represent replicate measurements of the same patient assessed at different time points. Symbols in the FMF group represent patients with a homozygous (●), a heterozygous (■) or a compound heterozygous (▲) mutation, respectively (Suppl. Table S1). Results were statistically analysed using a linear mixed model. A random intercept model was used to correct for multiple samples per patient. *p<0.05, ** p<0.01, *** p<0.001.

Random Migration and Chemotactic Responses of Neutrophils from PAAND and FMF Patients

The migratory behaviour of PAAND, FMF, and HC neutrophils was evaluated in vitro. As compared to HCs, neutrophils from PAAND patients displayed enhanced spontaneous migration, and a tendency towards increased random migration was observed for FMF (Fig. A2.5A). Migration induced by the classical neutrophil-chemoattractants CXCL8, C5a, and fMLF was examined by calculating the chemotactic indices migration (Fig. A2.5D). However, in terms of absolute cell numbers, neutrophils from FMF patients showed a tendency towards enhanced fMLF-induced chemotaxis (Suppl. Fig. A2.10). Colchicine treatment did not affect migration of HC neutrophils (Suppl. Fig. A2.11). Taken together, neutrophils from PAAND and FMF patients showed a (tendency towards) increased spontaneous migration versus reduced chemoattractant-directed migration.

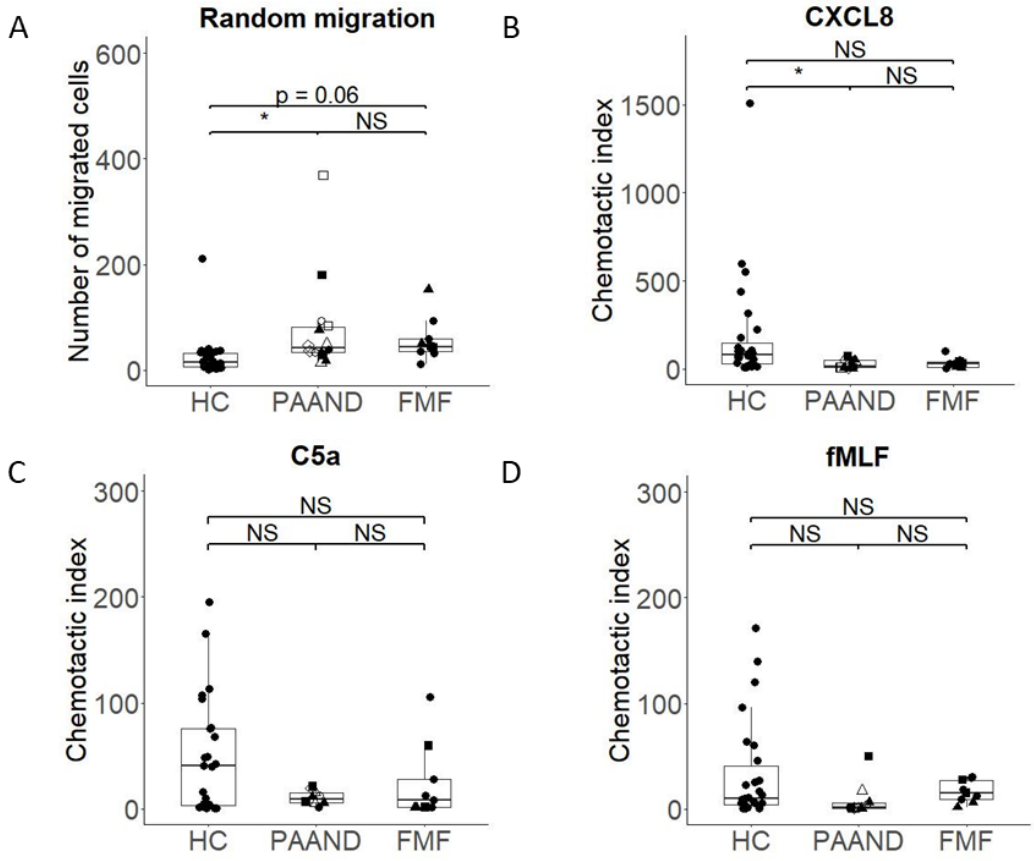

Fig. A2.5. Migratory behaviour of neutrophils from patients with pyrin-associated autoinflammation
Random and chemoattractant-induced migratory responses of freshly isolated neutrophils from PAAND patients, FMF patients and HCs were investigated *in vitro* using the 48-well Boyden chamber chemotaxis assay. Cells were seeded in the top well of the chamber and exposed in the lower well to (A) buffer alone, (B) 10 ng/ml CXCL8, (C) 10 ng/ml C5a or (D) 10 nM fMLF and migration was allowed during 45 min at 37°C. Results are represented as number of migrated cells in 10 high power microscopic fields or as chemotactic indices (*i.e.* total number of neutrophils that migrated in response to chemoattractant divided by the number of cells that migrated in response to buffer alone) for random and chemoattractant-induced migration, respectively. Each dot represents an individual donor (n ≥ 6). Symbols with the same shape in the PAAND patient group represent replicate measurements of the same patient assessed at different time points. Symbols in the FMF group represent patients with a homozygous (●), a heterozygous (■) or a compound heterozygous (▲) mutation, respectively (Suppl. Table S1). Results were statistically analysed using a linear mixed model. A random intercept model was used to correct for multiple samples per patient. *p<0.05.

Discussion

PAAND and FMF are caused by disease-specific mutations in the *MEFV* gene, resulting in an excessive pyrin-dependent maturation of IL-1β and IL-18. In contrast to FMF, patients with PAAND have severe recurrent neutrophilic dermatosis and prolonged fever attacks (17, 18). Distinct mechanisms of pyrin activation may contribute to the disparate clinical features in FMF and PAAND patients. Indeed, whereas mutations causative for PAAND presumably result in loss of phosphorylation and spontaneous activation of pyrin, no scientific consensus exists regarding the precise underlying mechanism of pyrin activation in FMF.

FMF and PAAND patients typically present with neutrophilia and a massive influx of neutrophils into affected tissues (2, 18). Neutrophils express high pyrin levels, and were identified as important IL-1β source in several models of inflammation and infection (977–983). However, only limited transcriptional, functional, and phenotypical data are available on neutrophils from PAAND and FMF patients. Published results revealed that neutrophils from FMF patients display an activated phenotype at the mRNA level, even during disease remission (967). Consistently, FMF neutrophils displayed enhanced spontaneous CD62L shedding during the first 2 h of ex vivo subcultivation (970). In addition, the formation of NETs is proposed to play a major role during inflammatory attacks in FMF (969).

These clinical and experimental findings support the notion that neutrophils may play an important pathological role in pyrin-associated autoinflammation, sparking our interest to study neutrophils from FMF and PAAND patients. The present study is the first to provide a detailed overview of transcriptional, phenotypical, and functional characteristics of neutrophils derived from the patients' peripheral blood. The study population included seven related PAAND patients with a S242R mutation, thirteen FMF patients with M680I or M694V mutations, and thirty age- and sex-matched HCs. All included individuals were adults and patients had low disease activity when samples were collected.

In-depth analysis of the neutrophil transcriptome by RNAseq and single-target qPCRs revealed that neutrophils from FMF and PAAND patients have an activated gene expression profile, as indicated by enhanced expression of S100A8, S100A9, S100A12, IL-1β, IL-4R, CD48, F5, MMP8, MMP9, and NFKB, among others. As expected, profound differences were observed between neutrophils from HCs and the two patient groups, while a partial overlap was found between the transcriptomes of FMF and PAAND neutrophils. We did not identify a group of functionally relevant genes that is specifically related to FMF or PAAND.

Analysis of the neutrophil maturation state uncovered an increased number of immature neutrophils—a hallmark of systemic inflammation—in FMF. In contrast, one PAAND patient showed an increased percentage of hypersegmented neutrophils, which are prone to activation and associated with inflammation. Compared to HCs, neutrophils from FMF patients showed a reduced phagocytic activity, increased ROS release, and a tendency towards increased MPO production. Enhanced spontaneous MPO production by FMF neutrophils was recently described in another patient cohort 5 h after subcultivation (970). PAAND neutrophils showed a significantly increased phagocytic response, displayed an enhanced granularity, and elevated ROS production. These data suggest that neutrophils from patients with pyrin-associated autoinflammation display a primed phenotype, even during the remission phase.

Plasma cytokine levels were determined to provide more insights into the original environment of isolated neutrophils. We confirmed the differential cytokine profiles in both patient groups (22). In line with the more profound features of systemic inflammation in FMF, increased concentrations of IL-18 were detected in plasma from FMF patients. Interestingly, recent experimental evidence suggests that neutrophils from FMF patients are a potentially important source of IL-18 (970). PAAND patients showed increased plasma concentrations of IFN-ɣ and a tendency towards enhanced IL-6. A tendency

towards increased MMP-9 activity was observed in plasma from FMF and PAAND patients. Moreover, levels of S100A8/A9 were at least ten times higher in plasma from FMF and PAAND patients as compared to HCs. These observations are in line with the increased expression of the corresponding genes.

In addition to neutrophil activation, also neutrophil migration requires tight regulation. We found that neutrophils from PAAND patients show increased spontaneous migration. FMF neutrophils also displayed a tendency towards enhanced random migration. The spontaneous migration was recently reported to be significantly increased in another cohort of FMF patients (984). When we analysed the chemoattractant-directed migration, a significantly reduced migration in response to CXCL8 for neutrophils from PAAND patients was found if chemotactic indices were assessed. Neutrophils from FMF patients also displayed a tendency towards impaired chemoattractant-induced migration. The reduced chemoattractant-directed migratory responses can be explained partially by the observed increased random migration of patient neutrophils. Moreover, the moderately but significantly reduced protein levels of the major chemoattractant receptors CXCR2, BLTR1, and C5aR on neutrophils from FMF patients may also contribute to the reduced chemotactic response, although the expression levels of chemoattractant receptors on cells do not necessarily recapitulate the functional response induced upon ligand stimulation (344,985–987). Worth mentioning, the differences in chemoattractant receptor levels were only found at the protein level and suggest an altered receptor turn-over rate rather than transcriptional differences.

We acknowledge that our sample size is small due to the rarity of PAAND and the practical limitations that come with neutrophil experiments (including the need for freshly isolated cells). Individual PAAND patients were included multiple times at different time points. We corrected for the presence of replicates of individual patients by using a random intercept statistical model. Additionally, FMF patients had distinct mutation states and patients were at different treatment strategies (Suppl. Table S1). The use of colchicine, in particular, may interfere with downstream analyses. This inhibitor of microtubule polymerisation accumulates in neutrophils and may interfere with cellular processes including migration and adhesion, phagocytosis, and production of cytokines and superoxide (988–992). In our hands, colchicine-treatment induced a reduction of CXCR2 and C5aR expression levels on HC neutrophils and promoted TNF-α-induced ROS production, but did not affect basal ROS production, phagocytosis, and chemotaxis.

To conclude, our results indicate that neutrophils from patients with PAAND and FMF have an activated gene expression profile and are characterised by unique primed phenotypes with enhanced pro-inflammatory properties (Suppl. Table S8 summarises our main conclusion). Comparison between neutrophils from the two pyrin-associated autoinflammatory syndromes favors the idea that PAAND and FMF are distinct diseases.

Supplementary Material

Supplementary Material & Methods

Respiratory burst assay

Cells were suspended in Roswell Park Memorial Institute medium 1640 (RPMI1640, Gibco, Paisley, Scotland) (without phenol red) at a final concentration of 1.5 x 10^6 cells per ml, seeded in a white 96-well plate (PerkinElmer, Waltham, MA) and stimulated in duplicate. Kinetic measurements of luminol oxidation were performed during 3 h at 37°C using a Clariostar Monochromator Microplate Reader (BMG Labtech, Orthenberg, Germany). The results were subtracted by values obtained with PMA stimulation in the absence of luminol and converted to fold changes of luminol oxidation *i.e.* (maximum – minimum)/minimum. The maximum and minimum values refer to the maximum and minimum luminescence values during the 3 h incubation period.

RNA sequencing, library preparation and quality check

Sequence libraries were prepared with the Lexogen QuantSeq 3' mRNA-Seq Library prep kit according to the manufacturer's protocol. Samples were indexed to allow for multiplexing. Library quality and size range was assessed using a Bioanalyzer (Agilent Technologies) with the DNA 1000 kit (Agilent Technologies) according to the manufacturer's recommendations. Libraries were diluted to a final cDNA concentration of 2 nM and subsequently sequenced on an Illumina HiSeq4000 platform according to the manufacturer's recommendations. Single-end reads of 50 bp length were produced with a minimum of 1M reads per sample. Quality control of raw reads was performed with FastQC v0.11.7. (993). Adapters were filtered with ea-utils fastq-mcf v1.05. (https://github.com/ExpressionAnalysis/ea-utils). Splice-aware alignment was performed with Hisat2 (http://daehwankimlab.github.io/hisat2/) against the human reference genome hg19 using the default parameters. Reads mapping to multiple loci in the reference genome were discarded. Resulting BAM alignment files were handled with Samtools v1.5. (994). Quantification of reads per gene was performed with HT-seq Count v2.7.14.

Supplementary Figures

A

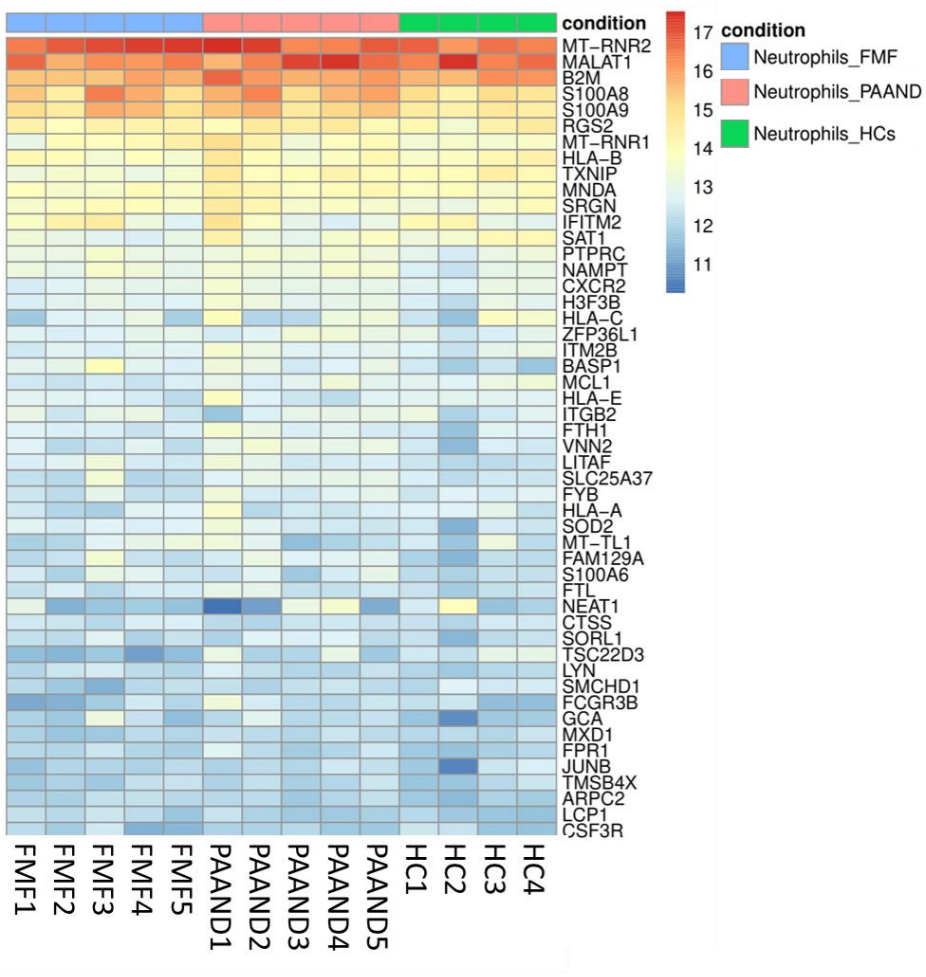

B

GO biological process complete	Number of genes	Adjusted p value
B cell receptor signaling pathway	132	8,25E-04
regulation of immune system process	1734	1,12E-03
humoral immune response	386	1,41E-03
phagocytosis, recognition	106	2,09E-03
defense response to protozoan	25	2,10E-03
positive regulation of respiratory burst	9	4,58E-03
phagocytosis, engulfment	131	5,51E-03
regulation of immune effector process	476	5,64E-03
neutrophil degranulation	482	6,00E-03
glomerular filtration	13	7,69E-03
complement activation, classical pathway	161	9,74E-03
defense response to Gram-positive bacterium	99	1,06E-02
humoral immune response mediated by circulating immunoglobulin	167	1,11E-02
positive regulation of B cell activation	170	1,19E-02
negative regulation of immune response	345	1,21E-02
innate immune response in mucosa	22	2,08E-02
hormone-mediated signaling pathway	134	3,28E-02
opsonization	73	3,62E-02
cellular response to steroid hormone stimulus	144	4,09E-02
regulation of signal transduction	3164	4,12E-02
translational initiation	144	4,13E-02
negative regulation of macromolecule metabolic process	2928	4,14E-02
retina homeostasis	79	4,33E-02
negative regulation of response to external stimulus	565	4,84E-02

Suppl. Fig. A2.1. Top 50 expressed genes identified from the transcriptome of neutrophils
RNA-sequencing was performed on neutrophils from 5 PAAND patients, 5 FMF patients and 4 HCs. Neutrophils were isolated by immunomagnetic negative selection. Heatmap showing the top 50 highly expressed genes. Colours indicate normalized gene expression (scale represents number of counts x10 000)

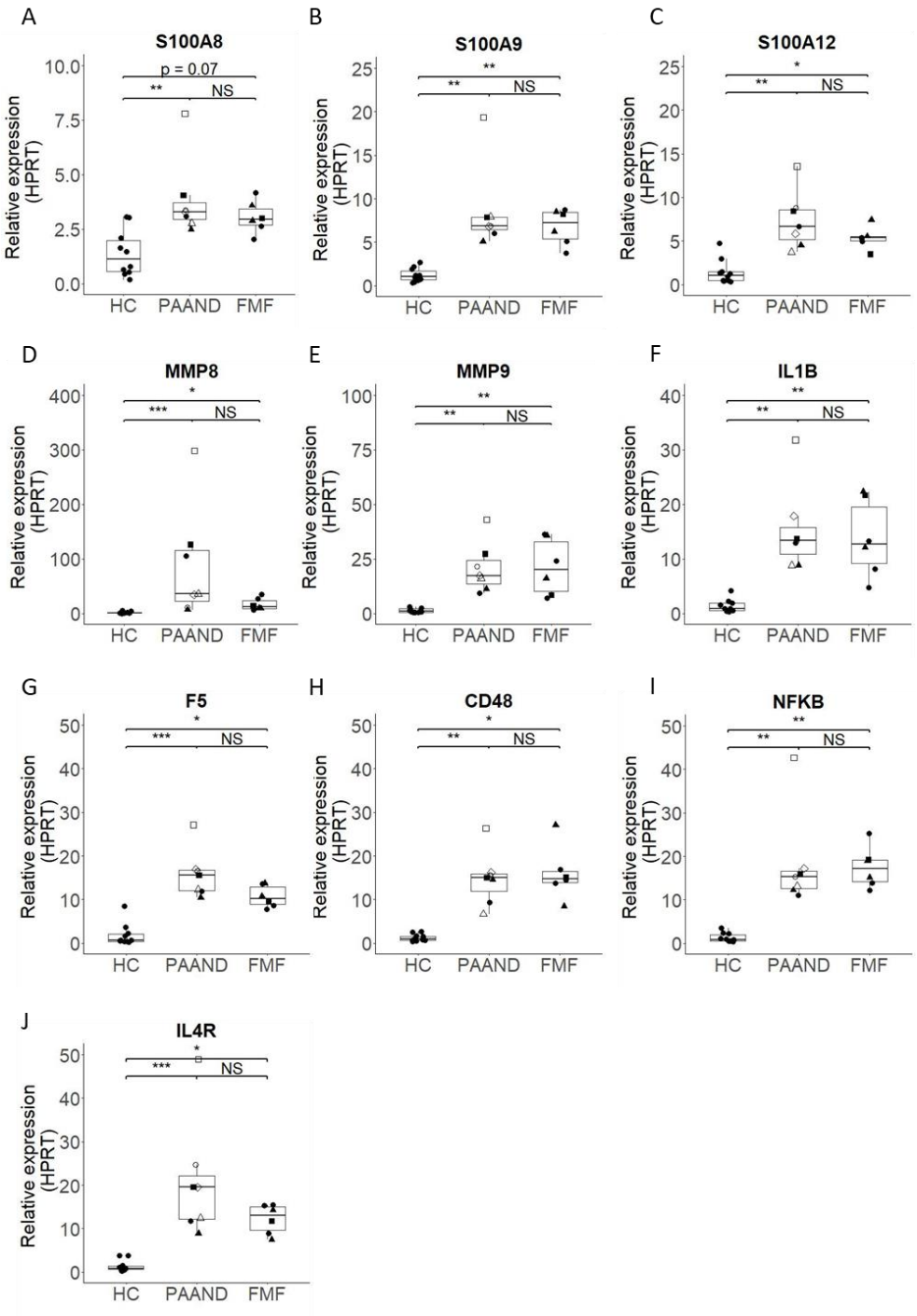

Suppl. Fig. A2.2. Analysis of gene expression by qPCR

Neutrophils from PAAND patients, FMF patients and HCs were isolated by immunomagnetic negative selection and analysed by flow cytometry. RNA was extracted and relative expression levels were analyzed by qPCR. (A-J) Box whisker plot show the expression levels of *S100A8* (A), *S100A9* (B), *S100A12* (C), *MMP8* (D), *MMP9* (E), *IL1B* (F), *F5* (G), *CD48* (H), *NFKB* (I) and *IL4R* (J), normalized to expression of hypoxanthine guanine phosphoribosyltransferase (*HPRT)* for each individual patient. Each dot represents an individual donor (n ≥ 6). Symbols with the same shape in the PAAND patient group represent replicate measurements of the same patient assessed at different time points. Symbols in the FMF group represent patients with a homozygous (●), a heterozygous (■) or a compound heterozygous (▲) mutation, respectively (Suppl. Table S1). Results were statistically analysed using a linear mixed model. A random intercept model was used to correct for multiple samples per patient. *p<0.05, ** p<0.01, *** p<0.001.

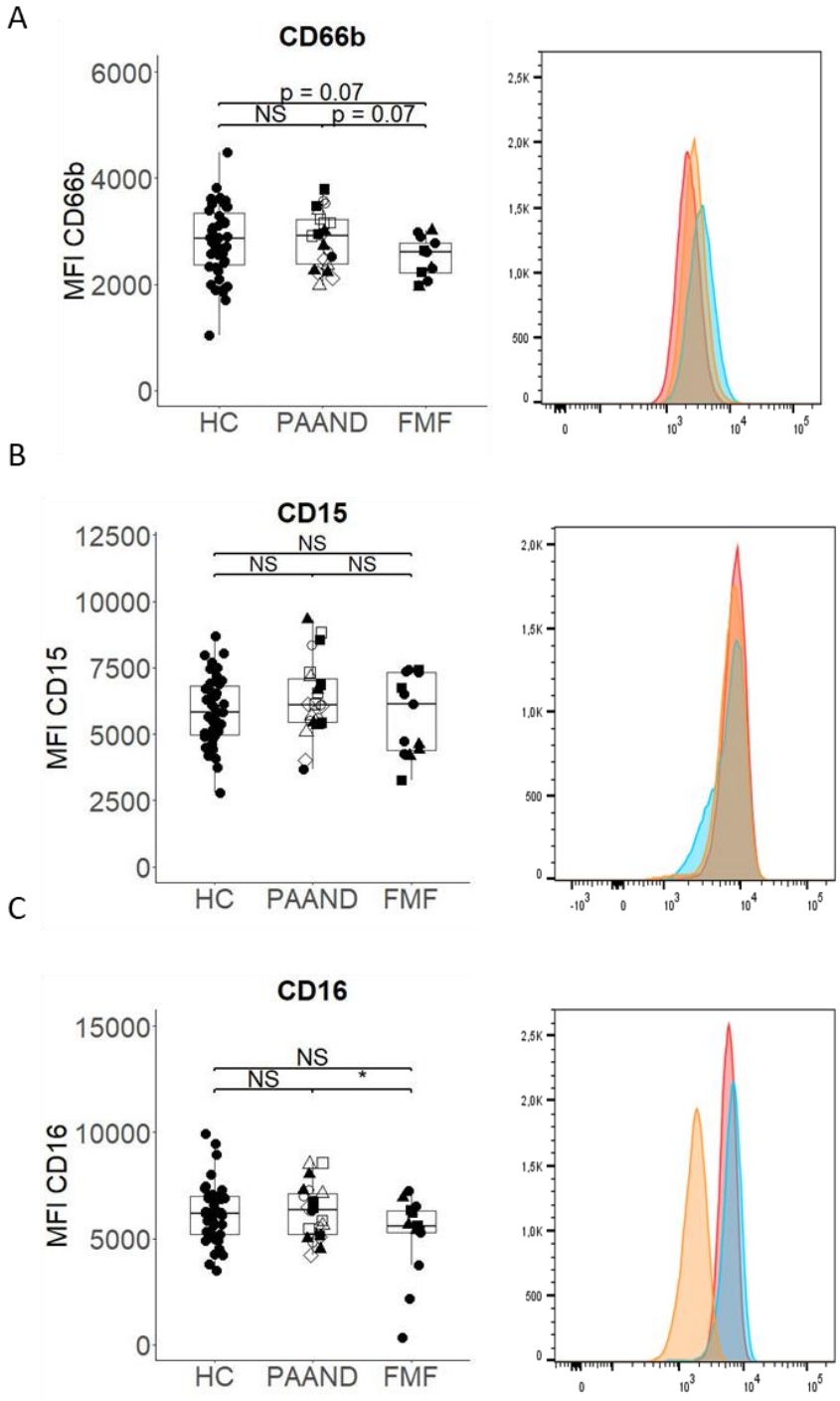

Supp. Fig. A2.3. Phenotypical analysis of neutrophils from patients with PAAND and FMF.
Neutrophils from PAAND patients, FMF patients and HCs were isolated by immunomagnetic negative selection and analysed by flow cytometry. (A-C) Box whisker plots indicate expression levels on neutrophils [mean fluorescence intensity (MFI)] of CD66b (A), CD15 (B) and CD16 (C), for individual patients. Representative histograms were plotted showing the expression levels (MFI) on purified neutrophils of HC (red), PAAND patients (blue) and FMF patients (yellow). Each dot represents an individual donor (n ≥ 6). Symbols with the same shape in the PAAND patient group represent replicate measurements of the same patient assessed at different time points. Symbols in the FMF group represent patients with a homozygous (●), a heterozygous (■) or a compound heterozygous (▲) mutation, respectively (Suppl. Table S1). Results were statistically analysed using a linear mixed model. A random intercept model was used to correct for multiple samples per patient. *p<0.05.

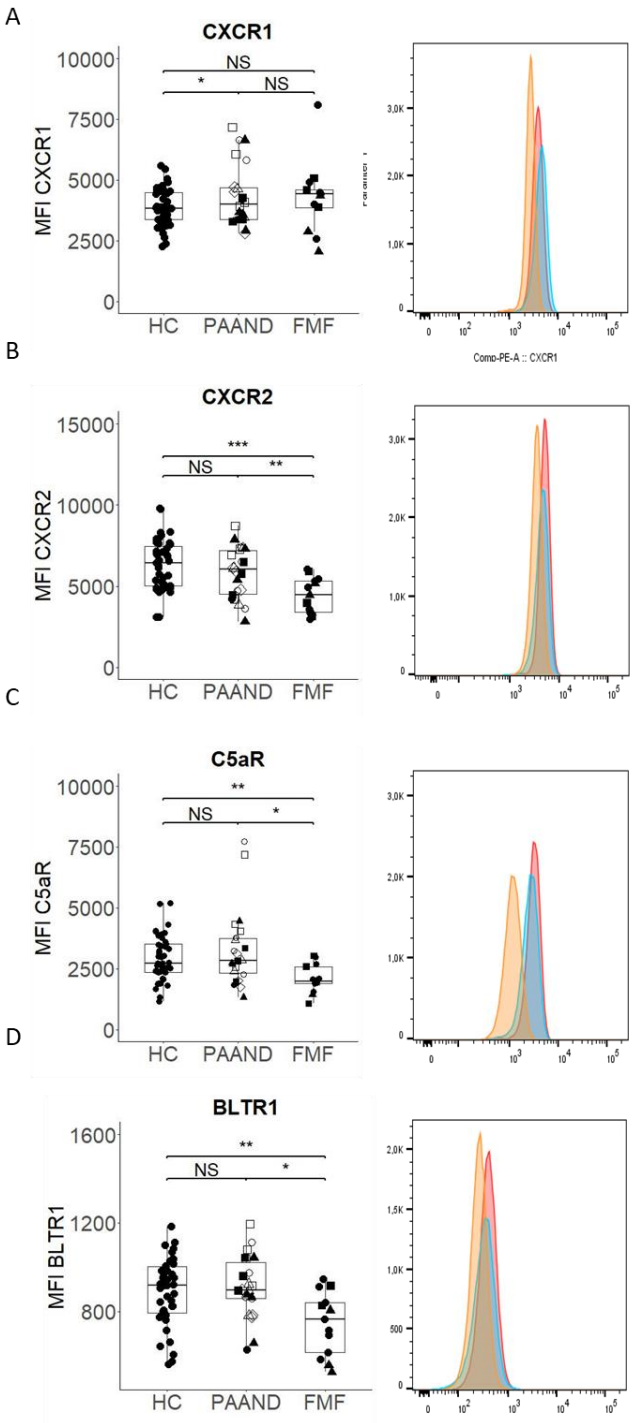

Supp. Fig. A2.4. Phenotypical analysis of neutrophils from patients with PAAND and FMF.
Neutrophils from PAAND patients, FMF patients and HCs were isolated by immunomagnetic negative selection and analysed by flow cytometry. (A-D) Box whisker plots indicate expression levels on neutrophils [mean fluorescence intensity (MFI)] of CXCR1 (A), CXCR2 (B), C5aR (C) and BLTR1 (D), for individual patients. Representative histograms were plotted showing the expression levels (MFI) on purified neutrophils of HC (red), PAAND patients (blue) and FMF patients (yellow). Each dot represents an individual donor (n ≥ 6). Symbols with the same shape in the PAAND patient group represent replicate measurements of the same patient assessed at different time points. Symbols in the FMF group represent patients with a homozygous (●), a heterozygous (■) or a compound heterozygous (▲) mutation, respectively (Suppl. Table S1). Results were statistically analysed using a linear mixed model. A random intercept model was used to correct for multiple samples per patient. *p<0.05, ** p<0.01, *** p<0.001.

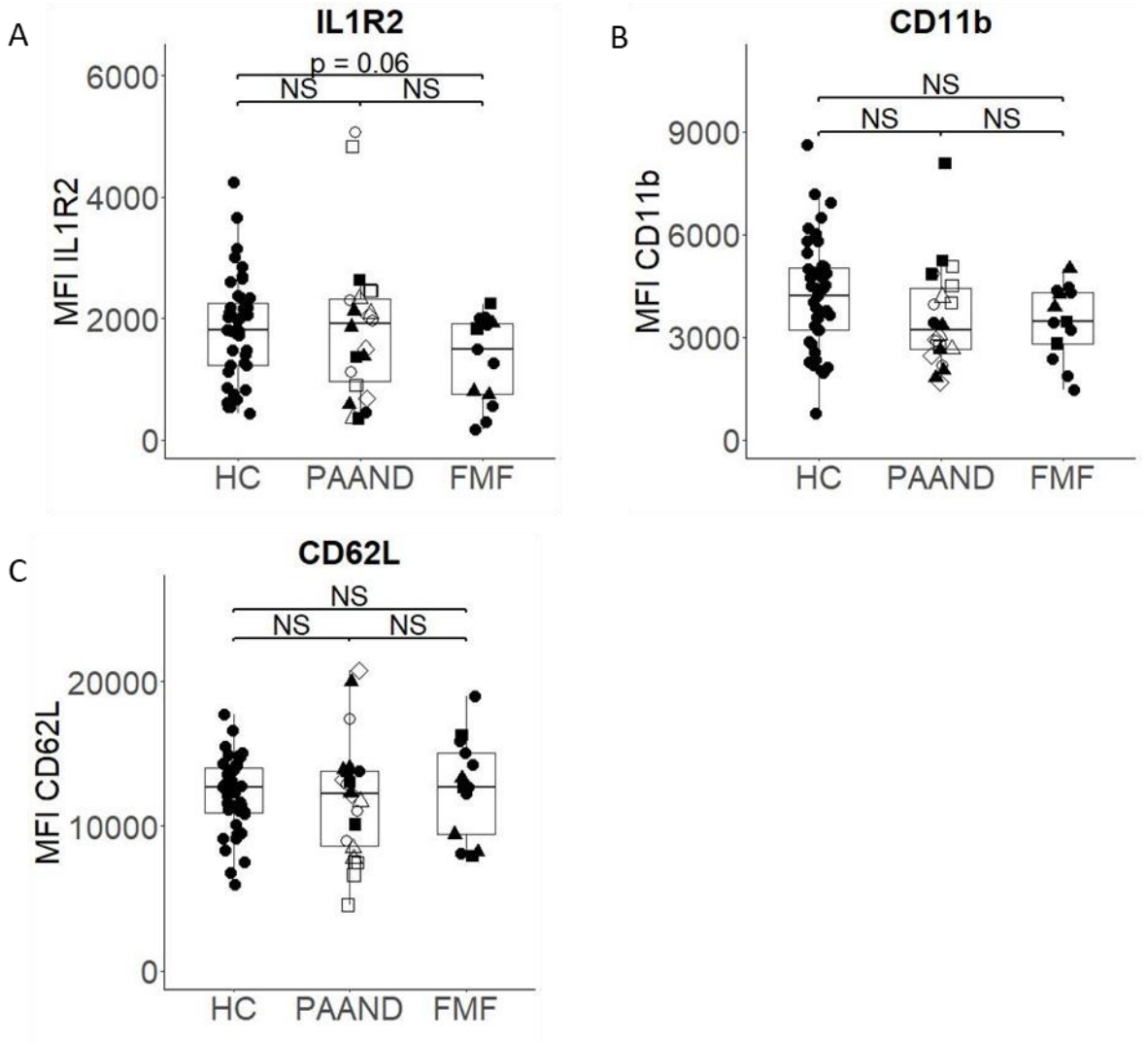

Suppl. Fig. A2.5. Phenotypical analysis of neutrophils from patients with PAAND and FMF.
Neutrophils from PAAND patients, FMF patients and HCs were isolated by immunomagnetic negative selection and analysed by flow cytometry. Expression levels (MFI) of IL-1R2 (A), CD11b (B) and CD62L (C) were measured on neutrophils and are shown for the individual patients. Each dot represents an individual donor (n ≥ 6). Symbols with the same shape in the PAAND patient group represent replicate measurements of the same patient assessed at different time points. Symbols in the FMF group represent patients with a homozygous (●), a heterozygous (■) or a compound heterozygous (▲) mutation, respectively (Suppl. Table S1). Results were statistically analysed using a linear mixed model. A random intercept model was used to correct for multiple samples per patient. *p<0.05.

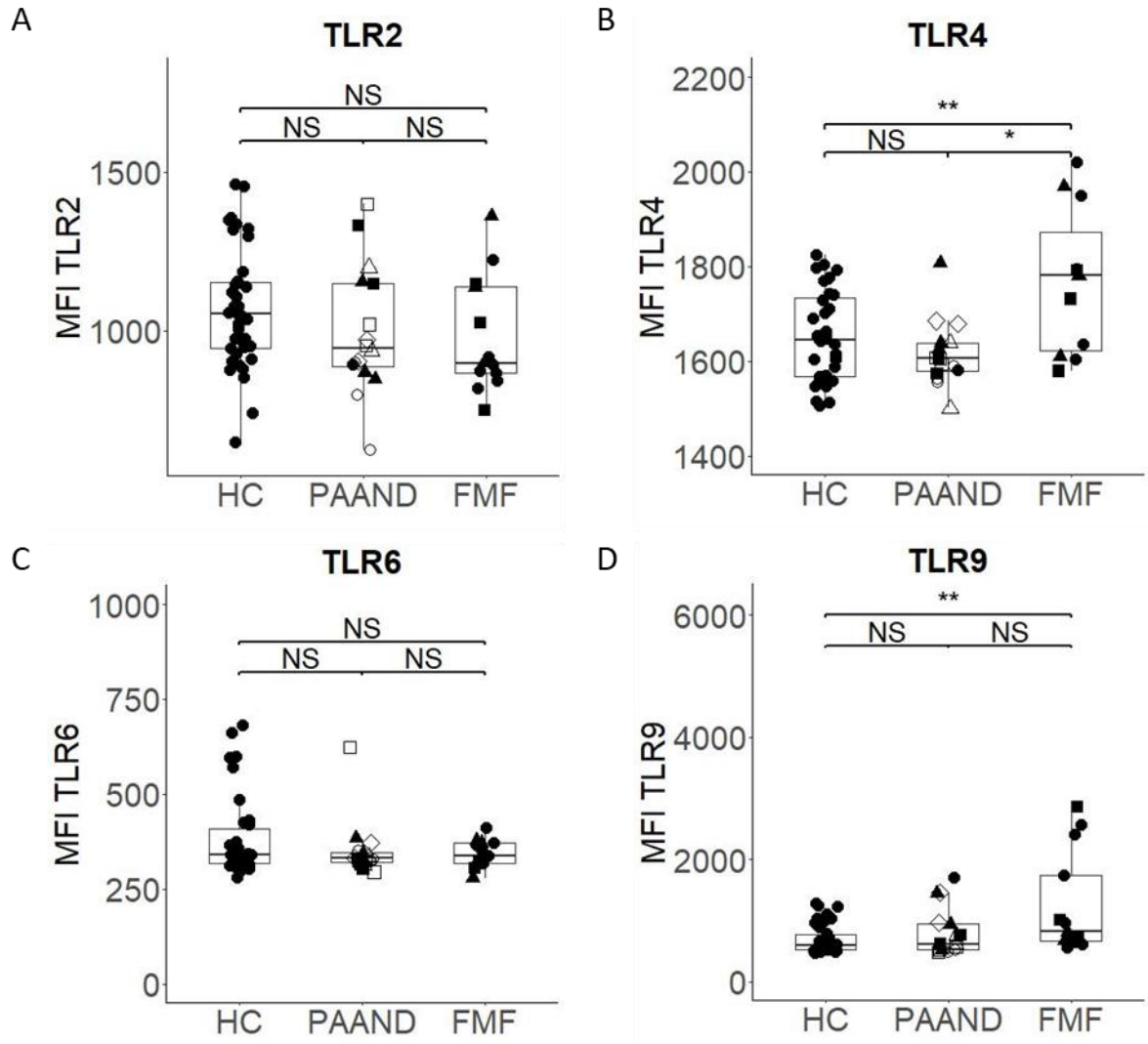

Suppl. Fig. A2.6. Phenotypical analysis of neutrophils from patients with PAAND and FMF.
Neutrophils from PAAND patients, FMF patients and HCs were isolated by immunomagnetic negative selection and analysed by flow cytometry. (A-D) Box whisker plots indicate expression levels on neutrophils [mean fluorescence intensity (MFI)] of TLR2 (A), TLR4 (B), TLR6 (C) and TLR9 (D), for individual patients. Each dot represents an individual donor (n ≥ 6). Symbols with the same shape in the PAAND patient group represent replicate measurements of the same patient assessed at different time points. Symbols in the FMF group represent patients with a homozygous (●), a heterozygous (■) or a compound heterozygous (▲) mutation, respectively (Suppl. Table S1). Results were statistically analysed using a linear mixed model. A random intercept model was used to correct for multiple samples per patient. *p<0.05, ** p<0.01.

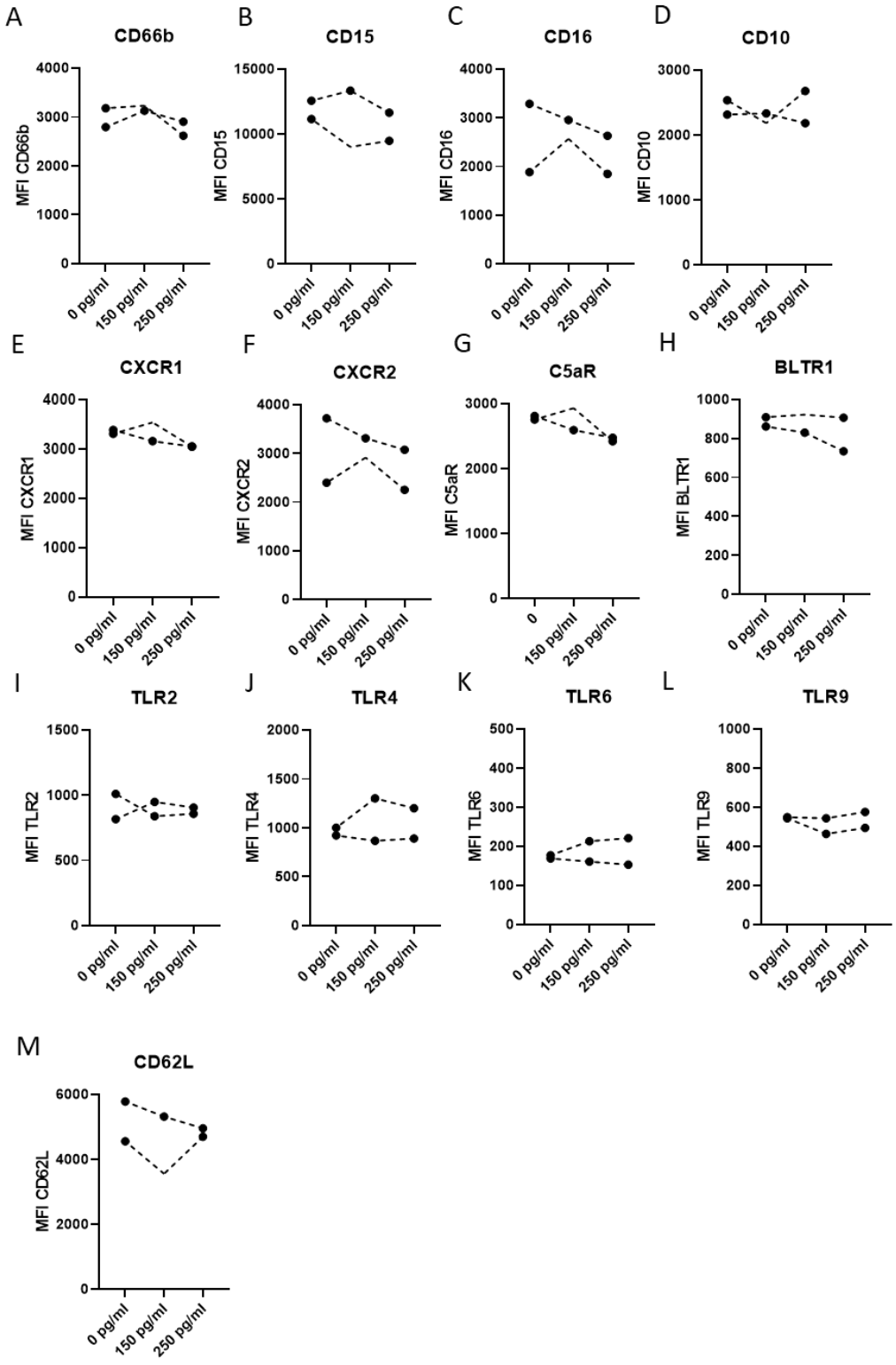

Suppl. Fig. A2.7. Effects of colchicine treatment on the phenotypical characteristics of neutrophils. **HC neutrophils were isolated by immunomagnetic negative selection, stimulated with vehicle or colchicine (150 pg/ml or 250 pg/ml) and analysed by flow cytometry. Expression levels [mean fluorescence intensity (MFI)] of CD66b (A), CD15 (B), CD16 (C), CD10 (D), CXCR1 (E), CXCR2 (F), C5aR (G), BLTR1 (H), TLR2 (I), TLR4 (J), TLR6 (K), TLR9 (L) and CD62L (M) were measured on neutrophils and are shown for neutrophils from two healthy controls.**

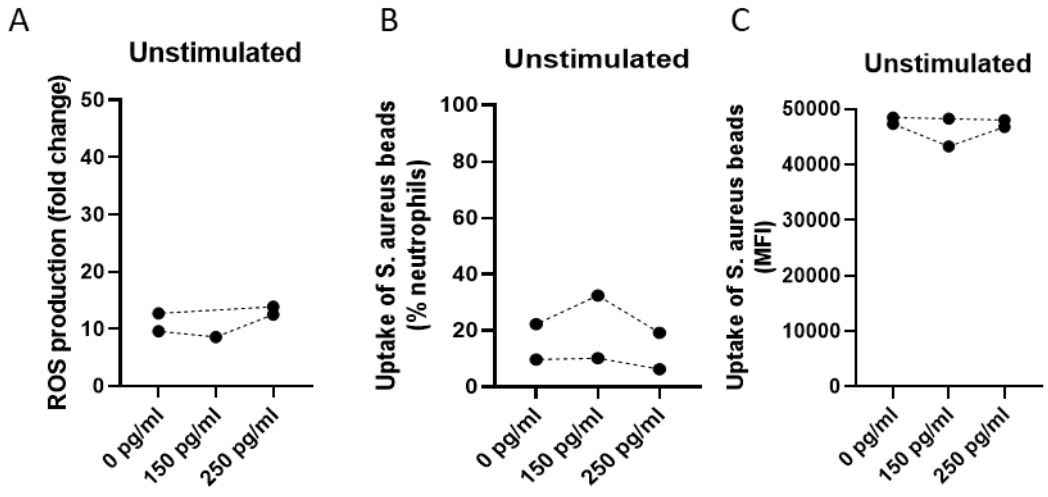

Suppl. Fig. A2.8. Effects of colchicine treatment on ROS production and phagocytosis
HC neutrophils were isolated by centrifugation in a density gradient (for ROS production assays) or immunomagnetic negative selection (for phagocytosis experiments) and incubated for 30 min in the presence of vehicle or colchicine (150 pg/ml or 250 pg/ml).(A) Cells were exposed to RPMI1640 medium supplemented with 5 mM luminol and kinetic measurements of luminol oxidation were performed during 3 h at 37°C. ROS production was assessed by calculating fold changes of luminol oxidation, *i.e.* the differences between the value at the start of the incubation and the maximal value. (B-C) Neutrophils were incubated with pHrodo red *S. aureus* bioparticles™ during 30 min at 37°C and bead uptake was evaluated by flow cytometry. Results are presented as (B) percentage of neutrophils that engulfed beads and (C) the amount of engulfed beads/cell (represented by the MFI).

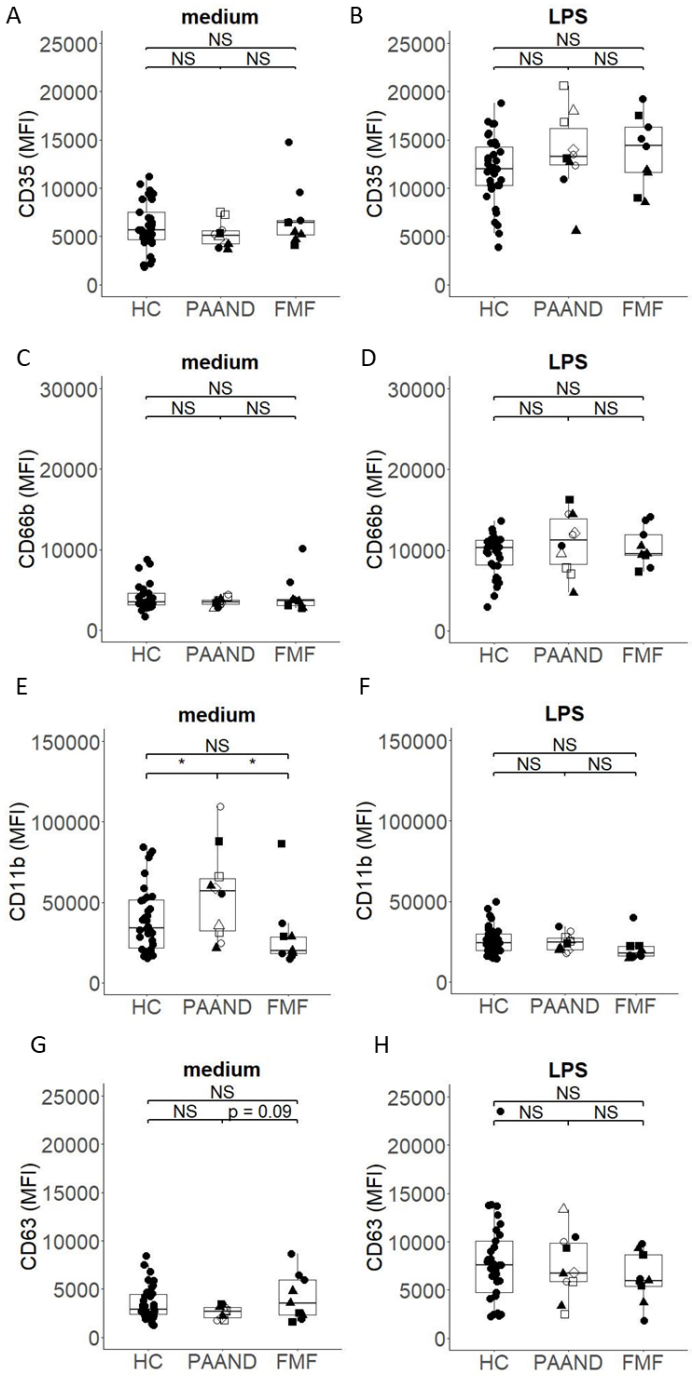

Suppl. Fig. A2.9. Activation state of neutrophils from PAAND and FMF patients upon *in vitro* stimulation

(A-H) Neutrophils from PAAND patients, FMF patients and HCs were cultured for 1 h without (A, C, E, G) or with 10 µg/ml ultrapure LPS (B, D, F, H) at 37°C. Relative expression levels (MFI) of CD35 (secretory vesicles) (A-B), CD66b (specific vesicles) (C-D), CD11b (gelatinase vesicles) (E-F) and CD63 (azurophilic vesicles) (G-H) were plotted to assess degranulation of neutrophils. Each dot represents an individual donor (n ≥ 5). Symbols with the same shape in the PAAND patient group represent replicate measurements of the same patient assessed at different time points. Symbols in the FMF group represent patients with a homozygous (●), a heterozygous (■) or a compound heterozygous (▲) mutation, respectively (Suppl. Table S1). Results were statistically analysed using a linear mixed model. A random intercept model was used to correct for multiple samples per patient. *p<0.05.

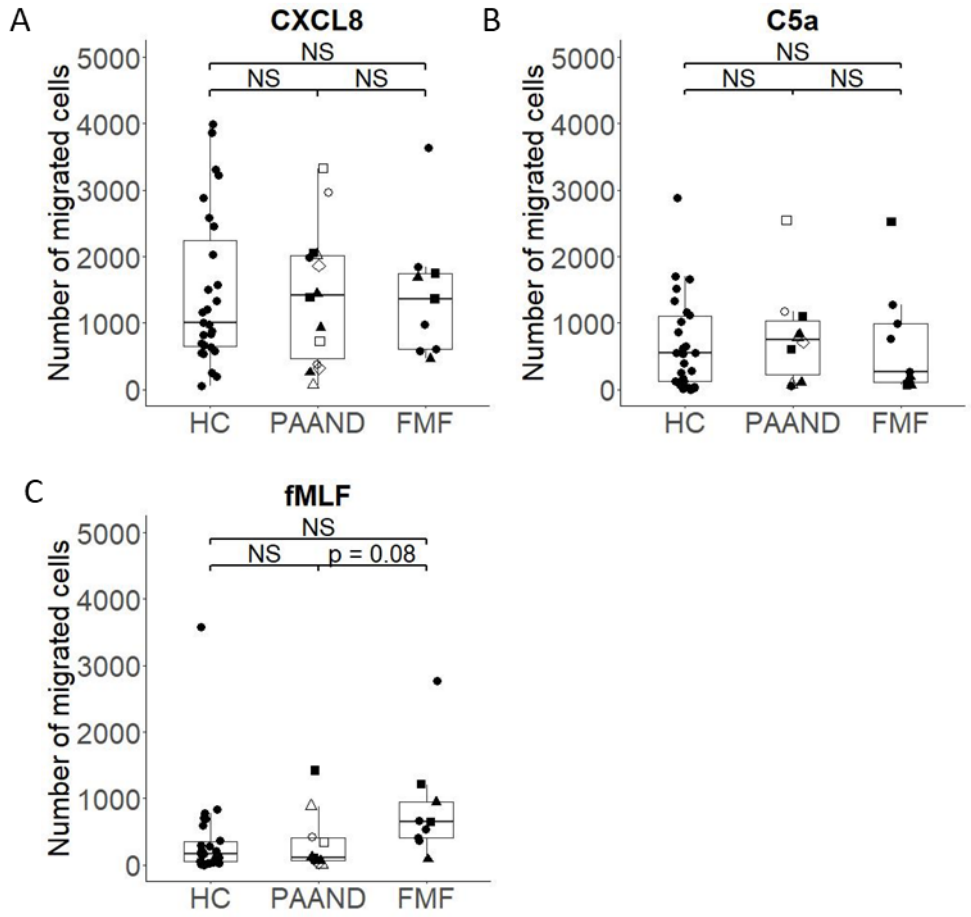

Suppl. Fig. A2.10. Altered migration behaviour of neutrophils from patients with pyrin-associated autoinflammation.

Chemotactic responses of neutrophils from PAAND patients, FMF patients and HCs were investigated *in vitro* using the 48-well Boyden chamber chemotaxis assay. Cells were added to the upper well of the chamber and exposed in the bottom well to (A) 10 ng/ml CXCL8, (B) 10 ng/ml C5a or (C) 10 nM fMLF and migration was allowed during 45 min at 37°C. Results are represented as absolute number of migrated cells microscopically counted in 10 high power fields. Each dot represents an individual donor (n ≥ 6). Symbols with the same shape in the PAAND patient group represent replicate measurements of the same patient assessed at different time points. Symbols in the FMF group represent patients with a homozygous (●), a heterozygous (■) or a compound heterozygous (▲) mutation, respectively (Suppl. Table S1). Results were statistically analysed using a linear mixed model. A random intercept model was used to correct for multiple samples per patient.

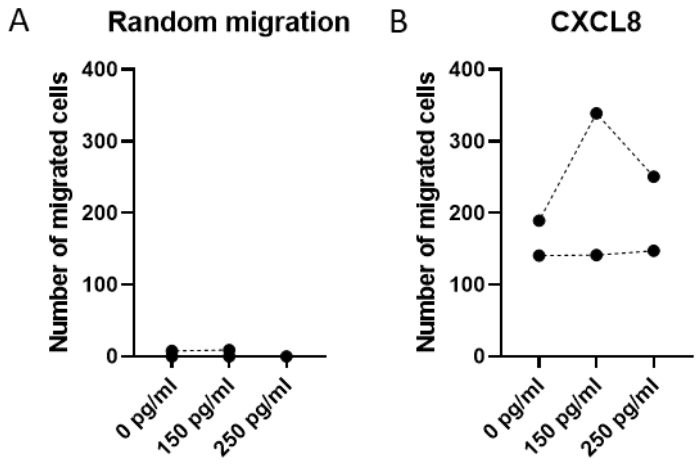

Suppl. Fig. A2.11. Effects of colchicine treatment on migration
HC neutrophils were isolated by centrifugation in a density gradient and incubated for 30 min in the presence of vehicle or colchicine (150 pg/ml or 250 pg/ml).(A-B) Random and chemoattractant-induced migratory responses of neutrophils were investigated *in vitro* using the 48-well Boyden chamber chemotaxis assay. Cells were loaded in the upper part of the chamber and (A) buffer alone or (B) 10 ng/ml CXCL8 (72 amino acid form) were added below the chemotaxis membrane. Migration was allowed during 45 min at 37°C and migrated cells were counted by microscopy. Results are represented as number of migrated cells in ten high power fields.

Supplementary Tables

Supplementary Table S1. Patient characteristics

Patient	Disease	Age in years [a]	Gender (M/F)	Ethnicity	Mutation statue	Gene	Mutation	Treatment	Number of times sampled	Disease state at the moment of blood collection	Symbol used in figures
FMF1	FMF	29	M	Armenian	Homozygous	*MEFV*	M680I	Colchicine	2	remission	●
FMF2	FMF	20	F	Turkish	Homozygous	*MEFV*	M694V	Colchicine	1	remission	●
FMF3	FMF	48	M	Turkish	Heterozygous	*MEFV*	M680I	Colchicine, NSAIDs	2	remission (once), flare (once)	■
FMF4	FMF	31	F	N.D.	Homozygous	*MEFV*	M694V	Colchicine, NSAIDs	1	remission	●
FMF5	FMF	35	F	N.D.	Homozygous	*MEFV*	M694V	Colchicine	1	remission	●
FMF6	FMF	33	F	Turkish	Compound heterozygous	*MEFV*	V726A/E167D - F479L	Colchicine	1	remission	▲
FMF7	FMF	20	F	Turkish	Homozygous	*MEFV*	M694V	Colchicine, canakinumab	1	remission	●
FMF8	FMF	46-48	M	Turkish	Heterozygous	*MEFV*	M694V	Colchicine, canakinumab	2	remission	■
FMF9	FMF	62	M	Turkey	Homozygous	*MEFV*	M694V	Colchicine, canakinumab	1	remission	●
FMF10	FMF	40	M	Turkey	Homozygous	*MEFV*	M694V	Colchicine, canakinumab	1	remission	●
FMF11	FMF	49	F	Turkey	Homozygous	*MEFV*	M694V	Colchicine	1	remission	●
FMF12	FMF	34	M	Armenia	Compound heterozygous	*MEFV*	V726A/M680I	Colchicine	1	remission	▲
FMF13	FMF	23	F	Armenia	Compound heterozygous	*MEFV*	A761H/M694V	Colchicine, canakinumab	1	remission	▲
PAAND1	PAAND	53-54	M	Caucasian	Heterozygous	*MEFV*	S242R	Colchicine, anakinra, methylprednisolone , metoprolol	3	remission	Δ
PAAND2	PAAND	19-20	F	Caucasian	Heterozygous	*MEFV*	S242R	Etanercept, methotrexate	4	remission	▲
PAAND3	PAAND	46-48	F	Caucasian	Heterozygous	*MEFV*	S242R	No treatment	3	remission	◊
PAAND4	PAAND	52-53	M	Caucasian	Heterozygous	*MEFV*	S242R	Adalimumab, methylprednisolone, tramadol, acetaminophen, fentanyl, NSAIDs, metoprolol	4	remission	□
PAAND5	PAAND	24-25	M	Caucasian	Heterozygous	*MEFV*	S242R	Mycofenolate mofetil, tacrolimus, amlodipine, acetaminophen	4	remission	○
PAAND6	PAAND	75-76	M	Caucasian	Heterozygous	*MEFV*	S242R	Colchicine, methylprednisolone	3	remission	■
PAAND7	PAAND	50	F	Caucasian	Heterozygous	*MEFV*	S242R	NSAIDs, sulfalazine	1	remission	●

[a]Some patients were sampled more than once. In that case an age range is indicated for the sampling period.
NSAID, non-steroidal anti-inflammatory drug

Supplementary Table S2. Overview of primers used for qPCR

Gene	Primer	Company
S100A8	Hs.PT.58.19654111.gs	Integrated DNA Technologies
S100A9	Hs.PT.58.20989743	Integrated DNA Technologies
S100A12	Hs.PT.58.39942209	Integrated DNA Technologies
IL1B	Hs.PT.58.1518186	Integrated DNA Technologies
NFKB	Hs.PT.58.20344216	Integrated DNA Technologies
F5	Hs.PT.58.2237261	Integrated DNA Technologies
IL4R	Hs.PT.58.14553110	Integrated DNA Technologies
CD48	Hs.PT.58.3602385	Integrated DNA Technologies
MMP8	Hs.PT.58.38449046	Integrated DNA Technologies
MMP9	Hs.PT.58.22814824.g	Integrated DNA Technologies
GAPDH	Hs.PT.39a.22214836	Integrated DNA Technologies
HPRT	Hs.PT.39a.22214821(1)	Integrated DNA Technologies

Supplementary Table S3. Overview of antibodies used for flow cytometry

Antigen	Clone	Company	Dilution	Host species	Colour	Cat. number
BLTR-1	203/14F11	BD	1/200	Mouse	BV510	744913
CD10	HI10a	BD	1/100	Mouse	BV786	564960
CD11b	ICRF44	BD	1/66	Mouse	BV510	563088
CD11b	ICRF44	Biolegend	1/100	Mouse	PE-Cy5	301308
CD121a	Polyclonal	R&D	1/500	Goat	PE	FAB269P
CD121b	REA744	Miltenyi Biotec	1/66	Recombinant human	FITC	130-111-274
CD14	61D3	Invitrogen	1/160	Mouse	PE-Cy5	15-0149-42
CD15	HI98	BD	1/100	Mouse	BUV395	563872
CD15	W6D3	BD	1/200	Mouse	BV786	741013
CD16	3G8	BD	1/200	Mouse	AlexaFluor700	557920
CD16	3G8	BD	1/200	Mouse	BUV395	563784
CD181	5A12	BD	1/20	Mouse	PE	555940
CD182	6C6	BD	1/10	Mouse	FITC	551126
CD282	11G7	BD	1/100	Mouse	BV421	565350
CD284	HTA125	Invitrogen	1/20	Mouse	AlexaFlur488	53-9917-42
CD286	TLR6.127	Biolegend	1/20	Mouse	PE	334708
CD289	eB72-1665	Invitrogen	1/20	Rat	APC	17-9099-82
CD35	E11	Biolegend	1/100	Mouse	FITC	333404
CD62L	DREG-56	Invitrogen	1/100	Mouse	APC	17-0627-42
CD63	H5C6	Biolegend	1/100	Mouse	PERCPCy5.5	353020
CD66b	G10F5	BD	1/100	Mouse	BV421	562940
CD66b	G10F5	Biolegend	1/14	Mouse	PerCP5.5	305108
CD88	S5/1	Biolegend	1/40	Mouse	PerCPCy5.5	344312

Supplementary Table S4: Differentially expressed genes in PAAND neutrophils versus HC neutrophils
Significantly differentially expressed genes as determined by RNA-sequencing in purified neutrophils from 5 PAAND patients and 4 age-matched HCs. The logFC represents the logarithm of the fold change (FC) comparing the HC neutrophil gene expression to the PAAND neutrophil gene expression. Genes with an expression logFC > |0.5| and false discovery rate (FDR) <0.05 were considered significant. FC.

Supplementary Table S5: Differentially expressed genes in FMF neutrophils versus HC neutrophils
Significantly differentially expressed genes as determined by RNA-sequencing in purified neutrophils from 5 FMF patients and 4 age-matched HCs. The logFC represents the logarithm of the FC comparing the HC neutrophil gene expression to the FMF neutrophil gene expression. Genes with an expression logFC > |0.5| and FDR <0.05 were considered significant. FC. Fold change; FDR. False discovery rate.

Supplementary Table S6: Differentially expressed genes in FMF neutrophils versus PAAND neutrophils
Significantly differentially expressed genes as determined by RNA-sequencing in purified neutrophils from 5 FMF patients and 5 PAAND patients. The logFC represents the logarithm of the FC comparing the PAAND neutrophil gene expression to the FMF neutrophil gene expression. Genes with an expression logFC > |0.5| and FDR <0.05 were considered significant. FC. Fold change; FDR. False discovery rate.

Supplementary Table S7: Overlapping differentially expressed genes in FMF and PAAND neutrophils versus HC neutrophils
Overlapping significantly differentially expressed genes as determined by RNA-sequencing in purified neutrophils from 5 FMF patients and 5 PAAND patients compared to 4 age-matched HCs.

Supplementary Table S4

Gene Symbol	logFC	FDR
SRPK1	-1.3	2.0e-09
PAPSS1	-2.7	5.5e-09
ARG1	-2.7	5.1e-08
IGHA2	5.1	1.6 e-07
IL4R	-1.8	3.4e-07
MS4A7	2.8	1.0e-06
ANXA3	-2.0	1.4 e-06
GYG1	-2.1	3.9 e-06
IGHG1	5.7	5.9 e-06
LMNB1	-1.5	5.9 e-06
MLLT4	-2.8	5.9 e-06
GADD45A	-1.5	7.3e-06
F5	-1.8	9.0e-06
C9orf72	-1.1	1.3 e-05
MACF1	-1.4	1.6e-05
MAPK14	-1.1	1.8e-05
CST7	-2.5	2.0e-05
MLTK	-1.9	2.7e-05
PAG1	-1.3	2.8e-05
CTA-384D8.34	1.8	3.8 e-05
PEBP1	2.8	4.5e-05
CHST2	-1.8	8.7e-05
TLR5	-2.2	0.000108
FCER1G	-1.0	0.0001186
ASPH	-1.3	0.000177
PGS1	-1.3	0.00032
METTL7A	2.5	0.0005761
IGHA1	4.7	0.00074
IGLC7	6.0	0.000714
PROK2	-1.4	0.000714
RNF10	-1.2	0.000714
TMED8	-1.2	0.000714
DEFA3	-3.9	0.000725
TECPR2	-0.7	0.00080287
GPCPD1	-1.1	0.000887
PPFIBP2	2.4	0.0010
ORM1	-2.4	0.0010
MSL3	-1.2	0.0012
NAGK	1.7	0.0012
ALPL	-1.6	0.00154
EIF1AY	-8.1	0.0015
KCNJ15	-1.0	0.0015
MPEG1	1.8	0.0016
TSPO	-1.6	0.00183
CD44	-1.5	0.00238
EMILIN2	-1.5	0.0025
KCNQ1OT1	-2.4	0.0027
ARFGAP3	-0.9	0.00333
CHCHD10	2.8	0.00386
IGHG3	6.0	0.0040
SH3GLB1	-0.8	0.0041
FGD2	2.8	0.0042
SERPINB1	-1.0	0.0042
ATF6	-0.8	0.0043
ATP5G1	3.0	0.0043
CASP5	-1.6	0.0043
ZNF438	-0.8	0.005076
ACSL1	-0.8	0.0055
SNX3	-1.3	0.0055
MZB1	5.5	0.006069
GALM	2.0	0.0061
HRH2	-0.9	0.0061
ST3GAL4	-1.2	0.0061
SYNE1	-1.2	0.0061
IGHG4	8.1	0.00637
HPSE	-1.5	0.0071
ATP11B	-0.8	0.00734
DHRS13	-1.2	0.00753
UPP1	-1.6	0.00753
HSPH1	1.9	0.00765
SAMSN1	-1.3	0.00765
FMNL2	2.2	0.008053
WDFY3	-0.8	0.00818
TMEM260	-1.0	0.00836
CDKN1C	1.7	0.0087
C19orf59	-2.5	0.0087
OSBPL1A	-2.0	0.0087
POR	-1.2	0.0087
STAT5B	-0.8	0.0087
GPR97	-1.0	0.009005
RP11-290F20.1	-2.0	0.00941
USB1	-0.9	0.00941
CEACAM6	-2.9	0.0097
TBC1D15	-0.7	0.0098
AL928768.3	5.1	0.011
AC074289.1	1.0	0.011
BMX	-1.2	0.013
CECR1	2.2	0.013
ZDHHC2	-1.7	0.013
IGLC2	5.4	0.013
HP	-3.9	0.013
ATP2B4	-1.0	0.014
FAM129A	-0.8	0.014
PABPC4	1.5	0.014
PLP2	-0.9	0.014
ZNF254	-1.9	0.014
FAM118A	2.6	0.014
FLOT2	-0.9	0.014
CDK5RAP2	-1.4	0.015
CR1	-1.1	0.015

Supplementary Table S5

Gene Symbol	logFC	FDR
CTA-384D8.34	2.7	2.7e-09
IFIT3	2.8	2.8e-07
DHRS9	1.5	9.1e-07
BATF2	2.2	2.9e-06
GIMAP2	2.2	4.3e-06
RPS27A	0.9	4.3e-06
GBP3	2.7	5.0e-06
TSC22D3	1.3	9.2e-06
IFIT2	2.4	1.2e-05
OASL	3.0	1.7e-05
F5	-1.7	1.8e-05
SEC11C	3.4	2.2e-05
GBP7	5.7	2.3e-05
LY6E	5.7	2.5e-05
IRF7	1.8	3.7e-05
LAP3	2.5	4.4e-05
PDZD8	-1.3	4.4e-05
VIM	-1.2	5.4e-05
DHX58	2.9	5.7e-05
APOL6	1.7	6.4e-05
ETV7	2.9	6.4e-05
STAT2	1.9	6.4e-05
MOV10	2.6	6.6e-05
PARP14	1.9	7.0e-05
GIMAP8	2.2	7.7e-05
RPH3A	-4.6	8.1e-05
GBP4	2.4	8.5e-05
PPM1K	3.1	0.00010
DTX3L	0.9	0.00010
TIMM10	4.1	0.00012
CD48	-1.1	0.00013
GBP1	1.9	0.00015
C5orf56	1.8	0.00017
MMP9	-2.0	0.00017
METTL7A	2.6	0.00019
PARP12	2.4	0.00019
TREX1	2.7	0.00020
APOL1	1.3	0.00023
GBP1P1	2.0	0.00024
IFIH1	2.0	0.00024
IFIT5	2.1	0.00024
IGHA2	5.6	0.00024
NQO2	-1.4	0.00024
RPL37A	1.2	0.00026
FRMD3	2.6	0.00030
RPL5	1.6	0.00034
SAMSN1	-1.8	0.00034
TRIM22	1.8	0.00038
CTB-61M7.2	-1.4	0.00050
CCL5	4.0	0.00057
RPL10A	2.0	0.00057
AQP3	5.2	0.00057
FGD2	3.8	0.00058
DDX58	1.4	0.00058
GPR97	-1.2	0.00058
IGHG1	3.4	0.00058
CDA	-1.2	0.00060
UBE2L6	1.4	0.00062
TRIB2	3.8	0.00062
FBXW2	-1.1	0.00065
MARCKS	-0.9	0.00070
ODF3B	1.5	0.00070
RNF213	1.3	0.00070
RPS12	1.2	0.00070
RPS4X	1.8	0.00070
HLA-DRB1	2.7	0.00071
SERPING1	2.0	0.00072
RTP4	4.5	0.00073
PEBP1	2.5	0.00078
STAT1	1.3	0.00078
DSE	-1.4	0.00079
SAMHD1	1.3	0.00079
RPS19	1.1	0.00081
IFI6	2.7	0.00082
CHMP5	1.1	0.00087
GBE1	-1.8	0.00087
RARRES3	1.6	0.00087
TAP1	1.0	0.00087
OAS1	4.2	0.00087
S100A10	2.3	0.00087
LDHB	2.6	0.00089
MT2A	3.1	0.00091
OXSR1	-0.9	0.00096
IFI44L	4.3	0.0011
OAS2	4.9	0.0011
TAP2	1.0	0.0011
MEGF9	-0.8	0.0011
OR52K3P	1.4	0.0012
SAMD9L	1.6	0.0012
DDX60	3.1	0.0013
PDIA4	2.8	0.0013
ZDHHC2	-2.0	0.0013
ISG15	3.7	0.0013
ACPP	-1.2	0.0013
SP140	1.5	0.0014
NUB1	0.9	0.0014
PPP2R5A	-0.8	0.0014
FBL	2.3	0.0015
GNG2	-0.9	0.0015

Supplementary Table S6

Gene Symbol	logFC	FDR
G0S2	-1.3	3.0e-06
PSMB8	1.1	4.0e-06
LL22NC03-2H8.5	3.2	2.6e-05
GZMA	4.2	0.00018
EMR2	1.0	0.00021
HSPA6	0.8	0.00031
MACF1	1.2	0.00040
CLEC2B	1.3	0.00043
LACTB	1.1	0.00051
GZMB	3.1	0.00065
SNHG6	1.2	0.0011
MT-ND1	-1.1	0.0012
DOCK4	1.6	0.0035
MT-ND2	-1.4	0.0035
GNLY	3.1	0.0046
IRF1	0.7	0.0053
HCAR3	1.0	0.0058
ARL4C	2.3	0.0077
KLRB1	4.8	0.0086
C9orf72	0.7	0.0092
SLK	0.6	0.015
DHRS9	1.2	0.016
HIP1	-1.4	0.016
MAML2	1.0	0.016
TXNIP	0.8	0.016
MT-CYB	-1.3	0.018
MT-ND5	-1.3	0.018
MT-ND4L	-1.5	0.021
RPS27A	0.7	0.021
GIMAP2	2.0	0.023
CD247	2.7	0.024
GIMAP4	1.3	0.024
NASP	1.0	0.024
CCL5	3.8	0.024
SAMD3	3.6	0.024
PAPSS1	1.9	0.025
RPS20	0.9	0.027
VCL	-1.0	0.028
MTND2P28	-2.2	0.030
ZFAS1	0.6	0.032
TSC22D3	1.0	0.032
GBP3	2.1	0.032
DIAPH2	-1.1	0.033
ERO1L	-0.9	0.034
ZYG11B	-0.8	0.034
C5orf56	1.4	0.034
MT-ND4	-1.2	0.035
PPFIBP2	-1.7	0.036
NXPE3	-1.2	0.040
TBX21	3.0	0.040
TRAF3IP3	-1.0	0.042
ZEB2	0.7	0.042
CNPY3	-0.6	0.045
SETD8	-1.1	0.046
FCGR2C	1.2	0.048
PGLYRP1	-1.2	0.048
HNRNPU-AS1	1.5	0.048
VNN2	0.7	0.051

Supplementary Table S7: Overlapping differentially expressed genes in FMF and PAAND neutrophils versus HC neutrophils

Gene Symbol
CTA-384D8.34
F5
SEC11C
GBP7
PDZD8
METTL7A
IGHA2
NQO2
SAMSN1
FGD2
GPR97
IGHG1
MARCKS
RPS4X
PEBP1
NAMPTL
OR52K3P
PDIA4
ZDHHC2
PPP2R5A
ITM2C
RGL4
RPL4
CAMP
OSBPL1A
HMGB2
AL928768.3
IFRD1
IGJ
SRGAP2
ARHGAP24
RNASE3
RPS8
MZB1
SOS2
IGHG3
BMX
ARG1
SRPK1
ZNF281
LAMTOR5
IRAK3
SYNE1
IGHA1
SSR4
RABGAP1L
CHURC1
PTTG1
LPIN2
EIF1AY

Gene Symbol
GADD45A
IGLC7
TEP1
BASP1
SNX3
POR
ZBTB16
BTN3A2
GALM
CST7
KIF1B
PADI2
CLSTN1
CALR
CD44
ALPL
CD177
IRF4
ORM1
PLP2
PABPC4
ACSL1
ANKRD36BP2
DEFA3
NFIL3
IGHG4
IL4R
RPS28
EMBP1
CHCHD10
MS4A7
PYGL
CLSTN1

Overlapping significantly differentially expressed genes as determined by RNA-sequencing in purified neutrophils from 5 FMF patients and 5 PAAND patients compared to 4 age-matched HCs.

Supplementary Table S8. Summary

Feature	PAAND	FMF
Number of neutrophils	↑	=
Maturation	=	Immature
MFI chemoattractant receptors (CXCR2, C5aR,BLTR1)	=	↓
MFI TLR4/TLR9	=	↑
ROS production	↑	↑
Phagocytosis	↑	↓
MPO release	↑	↑ (n.s.)
Granularity neutrophils	↑	=
Degranulation	↑	=?
Random migration	↑	↑ (n.s.)
Gene expression	Activated gene expression profile	Activated gene expression profile

Abbreviations: n.s.; not significant; ↑, ↓ and = indicate enhanced, decreased or unaltered parameters compared to healthy controls

SUMMARY

SUMMARY

Systemic juvenile idiopathic arthritis (sJIA) is a severe autoinflammatory childhood-onset immune disorder, classified as one of the JIA subtypes. Patients clinically present with fever, skin rash, enlarged lymph nodes (LNs), spleen and/or liver, and develop arthritis. Haematologically, neutrophilia (including immature neutrophils), leukocytosis, anaemia, and thrombocytosis is noticed. Patients have high plasma cytokine levels of interleukin-6 (IL-6), IL-18, C-reactive proteins, and S100 proteins (S100A8/A9 and S100A12). Among all JIA subtypes, sJIA has the highest mortality rate since the disease is associated with a severe life-threatening complication macrophage activation syndrome (MAS). MAS is a hyperinflammatory syndrome with excessive activation of macrophages and T cells resulting in a cytokine storm and is associated with hemophagocytosis. More recently sJIA was also associated with pulmonary complications that include interstitial lung disease (ILD), and pulmonary alveolar proteinosis (PAP).

In this doctoral thesis, we aimed to understand the role of the innate immune system in the pathogenesis of the sJIA. More specifically we aimed to gain insights into the successful use of IL-1 antagonists in patients considering that IL-1β blood levels are barely detectable. Next, we aimed to understand the effects of IL-1 on both the neutrophils and the γδ T cells. Considering the high numbers of neutrophils in blood of patients and the splenomegaly as a characteristic of sJIA, we studied extramedullary granulopoiesis and the role of neutrophils in the disease pathogenesis. Finally, we aimed to answer why sJIA patients show lung disorders, and more specifically investigated whether this is rather an epiphenomenon, or whether lung inflammation participates in the disease initiation.

To address these aims, we took advantage of a described mouse model of sJIA that is based on the injection of complete Freund's adjuvant (CFA) in interferon-gamma (IFN-γ) knock-out (KO) mice. These mice develop all clinical and haematological features reminiscent of sJIA, whereas CFA-immunisation in wild-type (WT) animals only results in a partial, self-resolving immune response. We demonstrated increased inflammasome activation in immunised IFN-γ KO mice, as evident by increased levels of active caspase-1 and IL-1β in the lymphoid organs and the blood. This could in part explain their increased susceptibility to develop sJIA. Using neutralising anti-IL-1β antibodies, the sJIA-like features could partially be prohibited and treated mice showed reduced weight loss, rash, granulocytosis, and thrombocytosis, and had reduced plasma IL-6 levels. Interestingly, the number of IL-17- and IL-22-producing CD27 negative γδ T cells and CD4+ T cells were decreased upon treatment. Beneficial effects of IL-17-depletion were reported in the initial description of the mouse model. In this doctoral thesis, we explored the role of IL-22 in the pathogenesis of sJIA. Increased IL-22 plasma levels were measured in the CFA-immunised IFN-γ KO mice. Using IL-22 neutralising antibodies we showed a partial role of IL-22 in the mouse model since neutralisation was associated with reduced weight loss, tail damage, neutrophilia, and thrombocytosis. In sJIA patients with active disease increased plasma levels of active IL-22 were measured. Using healthy donor γδ T cells or CD4+ cells, we could show a synergistic effect of IL-22 and IL-1β in the production of IL-17.

To understand the role of neutrophils in the sJIA pathophysiology, we made use of anti-Ly6G (1A8) depleting antibodies. Anti-Ly6G can be used to study the *in vivo* role of neutrophils in murine models and became the gold standard considering its neutrophil-specific depletion. In the CFA-challenged BALB/C model, we demonstrated an incomplete anti-Ly6G-mediated neutrophil depletion. Furthermore, using BrdU incorporation, we demonstrated an increased proliferation in the bone marrow (BM) upon depletion, and a massive neutrophilic proliferation in the spleen, showing that a temporary depletion is followed by a fast rebound of new immature neutrophils that cannot be depleted. Therefore, we used an alternative approach in which we targeted granulocyte-colony stimulating factor (G-CSF) signalling. G-CSF is the main growth factor involved in the proliferation, maturation, release, and functionality of neutrophils. G-CSF release can be stimulated by IL-17. During

excessive myelopoiesis, it can drive the formation of myeloid-derived suppressor cells (MDSCs), having an immune-tempering capacity. Increased plasma levels of G-CSF were measure in the CFA-immunised IFN-γ KO mice. Also, in patients with active disease increased plasma G-CSF levels were reported. Interestingly, these levels were correlating with some inflammatory mediators including the number of neutrophils and plasma levels of IL-6 or IL-1β. The role of G-CSF was studied in our mouse model using G-CSF receptor (G-CSFR)-blocking antibodies. We could demonstrate that G-CSF is responsible for the observed neutrophilia and extramedullary myelopoiesis. Next, by blocking the G-CSFR, we could inhibit the development of arthritis. However, treated mice showed a mild aggravation of some of the disease symptoms including weight loss, tail damage, number of immature RBCs, and had slightly increased plasma levels of IL-6, IL-17, and TNF-α. Single-cell sequencing revealed that neutrophil development in the spleen follows a similar developmental path as described in the BM and also includes stages of pre-neutrophils, immature neutrophils, and mature neutrophils. When we compared CFA-immunised WT and IFN-γ KO mice, the latter were characterised by the development of MDSCs, having a mature phenotype with high levels of CEBP/β. Administration of the G-CSFR-antagonising antibody could block the maturation and differentiation of neutrophils in CFA-immunised mice. The reduced numbers of MDSCs could in part explain their aggravated phenotype.

In the final part of this doctoral thesis, lung abnormalities in our sJIA mouse model were the subject of research considering the recent lung complications that were described in patients. Using microcomputer tomography, a moderate enlargement of the lungs was measured upon CFA-immunisation as well as a decrease in aerated lung density. In the IFN-γ KO mice only, an increased non-aerated lung density was found. Next, functional alterations were noticed in the CFA-immunised IFN-γ KO mice, with male mice showing an increased tissue hysteresivity and tissue damping, female mice presented with increased airway hyperactivity. Histopathology revealed subpleural and parenchymal cellular infiltrates associated with the formation of granulomas. Using flow cytometry and quantitative PCR, we demonstrated an excessive innate immune activation with infiltration of mainly immature and mature neutrophils or monocytes, increased γδ T cells, activated macrophages, and increased expression of both IL-1β, IL-6, TNF-α, IL-17, and IL-22. Associated with increased neutrophilic infiltrates, high levels of G-CSF and neutrophil-attracting chemokines were measured in the CFA-injected IFN-γ KO mice. Although the pulmonary manifestations in mice were distinct to those described in sJIA patients, the work demonstrates an important innate immune activation in our model. It underlines that lung inflammation should not be neglected when the pathophysiology of sJIA is studied.

Expanding our knowledge on neutrophils in autoinflammatory diseases, we studied neutrophils in both pyrin-associated inflammation with neutrophilic dermatosis (PAAND) and familial Mediterranean fever (FMF). PAAND and FMF are two IL-1β-driven autoinflammatory syndromes caused by distinct mutations in the same *MEFV* gene. Considering their high numbers of neutrophils in the blood and affected tissues, the transcriptional, functional, and phenotypical characteristics of neutrophils were extensively analysed. At the transcriptional level patients showed a partially overlapping activated phenotype with increased expression of S100 proteins, IL-4R, CD48, F5, MMP9, and NF-κB. Increased levels of MMP9 and S100A8/A9 were validated in plasma. Flow cytometric analysis demonstrated an immature character, an increased expression of TLR4 and TLR9, whereas a decreased expression of CXCR2, C5aR, and BLTR1 was observed on neutrophils from FMF patients only. PAAND patients showed an enhanced granularity and a functional increased random, but reduced CXCL8-induced migration. Similarly, in FMF patients a tendency for enhanced random migration and reduced chemoattractant-induced migration was noticed. Neutrophils from both FMF and PAAND patients showed an increased basal and TNF-α-induced ROS production and had an elevated release of the azurophilic granule protein myeloperoxidase (MPO). Analysing the phagocytic capacity, we showed enhanced activity in PAAND patients but reduced activity in FMF patients. Together our data describe the neutrophil abnormalities in two pyrin-associated diseases and underlines that FMF and PAAND are two distinct diseases.

SAMENVATTING

SAMENVATTING

Systemische juveniele idiopathische artritis (sJIA) is een ernstige auto-inflammatoire immuunziekte bij kinderen. Klinisch vertonen de patiënten koorts, huiduitslag, vergrote lymfeklieren, vergrote milt en/of lever en ontwikkelen ze uiteindelijk ook artritis. Hematologisch worden patiënten gekenmerkt door neutrofilie (inclusief een stijging van het aantal immature neutrofielen), leukocytose, anemie en trombocytose. Bij patiënten worden verhoogde cytokinespiegels in plasma gemeten voor interleukine-6 (IL-6), IL-18, CRP en S100-eiwitten (S100A8/A9 en S100A12). Van alle JIA-subtypes heeft sJIA de hoogste mortaliteit aangezien de ziekte geassocieerd wordt met een ernstige en levensbedreigende complicatie: macrofaagactivatiesyndroom (MAS). MAS is een inflammatoir syndroom met overmatige activatie van macrofagen en T-cellen en resulteert uiteindelijk in een cytokinestorm. Verder wordt MAS ook geassocieerd met hemofagocytose. Recent werden bij patiënten met sJIA ook pulmonale complicaties vastgesteld waaronder interstitiële longziekte (ILD) en pulmonale alveolaire proteïnose (PAP).

In dit doctoraat wilden we de rol van het aangeboren immuunsysteem in de pathogenese van de sJIA beter begrijpen. Concreet wilden we inzicht krijgen in het succesvolle gebruik van IL-1-antagonisten bij patiënten, rekening houdend met het feit dat de IL-1β-bloedspiegels nauwelijks detecteerbaar zijn. Vervolgens wilden we de effecten van IL-1 op zowel de neutrofielen als de γδ T-cellen beter begrijpen. De aanmaak van neutrofielen (buiten het beenmerg) en hun rol in sJIA werden bestudeerd omwille van hun hoge aantal in de afwezigheid van enige infectie. Tot slot wilden we een antwoord vinden op de vraag waarom sJIA-patiënten ook longaandoeningen ontwikkelen. We vroegen ons af of dit eerder een bijverschijnsel is, of dat deze longontsteking daadwerkelijk ook een rol speelt bij het ontstaan van de ziekte.

Om deze vragen te beantwoorden, hebben we gebruik gemaakt van een beschreven muismodel voor sJIA dat gebaseerd is op de injectie van Compleet Freund's Adjuvant (CFA) in interferon-gamma (IFN-γ) knock-out (KO) muizen. Deze muizen ontwikkelen nagenoeg alle klinische en hematologische kenmerken die doen denken aan sJIA. Bij wildtype (WT) dieren resulteert CFA-immunisatie slechts in een gedeeltelijke immuunrespons. In dit onderzoek toonden we aan dat de verhoogde inflammatie in de geïmmuniseerde IFN-γ KO muizen toe te schrijven is aan verhoogde niveaus van actief caspase-1 en IL-1β in de lymfoïde organen en het bloed. Dit zou ook de verhoogde vatbaarheid voor het ontwikkelen van sJIA kunnen verklaren in deze IFN-γ KO muizen. Met behulp van neutraliserende anti-IL-1β-antilichamen konden de kenmerkende ziektesymptomen van sJIA gedeeltelijk voorkomen worden. Behandelde muizen vertoonden namelijk minder gewichtsverlies, huiduitslag, granulocytose en trombocytose. Verder werden deze behandelde muizen ook gekenmerkt door verlaagde IL-6-spiegels in plasma. Overigens zagen we dat het aantal IL-17- en IL-22-producerende CD27-negatieve γδ T-cellen en CD4+ T-cellen was afgenomen na behandeling. Het gunstige effect van IL-17-depletie werd eerder al gerapporteerd in de eerste beschrijving van het muismodel. In dit doctoraat hebben we de rol van IL-22 in de pathogenese van sJIA verder onderzocht. Verhoogde plasmaspiegels van IL-22 werden gemeten in de CFA-geïmmuniseerde IFN-γ KO-muizen. Met behulp van een antilichaam dat IL-22 neutraliseert, toonden we een gedeeltelijke rol aan van IL-22 in het ziekteproces. Zo was neutralisatie geassocieerd met verminderd gewichtsverlies, staartschade, neutrofilie en trombocytose. Ook in actieve sJIA-patiënten werden verhoogde plasmaspiegels van actief IL-22 gemeten. Tenslotte, konden we met behulp van γδ T-cellen of CD4+ cellen van gezonde humane donoren aantonen dat IL-22 en IL-1β synergetisch de productie van IL-17 induceren.

Om de rol van neutrofielen in de pathofysiologie van sJIA te begrijpen hebben we gebruik gemaakt van anti-Ly6G (1A8) depleterende antilichamen. Deze antilichamen kunnen gebruikt worden om de *in vivo* rol van neutrofielen te bestuderen in muizenmodellen en worden aanzien als de gouden standaard omwille van hun specifieke depletiecapaciteit. Wij toonden echter aan dat toedienen van anti-Ly6G antilichamen de neutrofielen onvolledig depleteert in CFA-geïmmuniseerde muizen. Verder toonden we met BrdU-opname-experimenten aan dat depletie geassocieerd is met een verhoogde proliferatie in het beenmerg en een massale proliferatie van neutrofielen in de milt. Dit duidt aan dat de tijdelijke depletie gevolgd wordt door een snelle rebound van nieuwe immature neutrofielen die niet kunnen worden gedepleteerd. Daarom maakten we in ons onderzoek gebruik van een alternatieve aanpak waarbij we ons richtten op de granulocyt-kolonie-stimulerende factor (G-CSF). G-CSF is de belangrijkste groeifactor die betrokken is bij de proliferatie, rijping, vrijzetting en functionaliteit van neutrofielen. De aanmaak van G-CSF kan worden gestimuleerd door IL-17. Verhoogde plasmaspiegels van G-CSF werden gemeten in de CFA-geïmmuniseerde IFN-γ KO-muizen. Ook bij sJIA-patiënten worden verhoogde G-CSF-spiegels in plasma gemeten. Deze verhoogde concentraties werden gecorreleerd met ontstekingsmediatoren, waaronder het aantal neutrofielen en plasmaniveaus van IL-6 of IL-1β. De rol van G-CSF werd bestudeerd in ons muismodel met behulp van een antilichaam dat de G-CSF-receptor (G-CSFR) blokkeert. We tonen aan dat G-CSF verantwoordelijk is voor de waargenomen neutrofilie en extramedullaire myelopoëse. Verder kon de ontwikkeling van artritis worden afgeremd wanneer we de G-CSFR blokkeerden. De behandelde muizen vertoonden echter ook een lichte verergering van enkele van de ziektesymptomen, waaronder gewichtsverlies, staartbeschadiging en het aantal immature rode bloedcellen. Ook werden licht verhoogde plasmaspiegels van IL-6, IL-17 en TNF-α gemeten. Single-cell sequencing toonde aan de ontwikkeling van neutrofielen in de milt gelijkaardig is als deze in het beenmerg en eveneens bestaat uit pre-neutrofielen, immature en mature neutrofielen. Wanneer WT en IFN-γ KO muizen werden vergeleken, werden deze laatste gekenmerkt door de ontwikkeling van immuun-onderdrukkende myeloïde suppressorcellen (MDSC's). Aangezien G-CSFR blokkade resulteert in een verminderde maturatie en differentiatie van neutrofielen kan het verergerde fenotype in de IFN-γ KO muizen deels verklaard worden door het verlaagde aantal MDSC's.

Rekening houdend met de recente longcomplicaties beschreven in sJIA-patiënten, werden de longafwijkingen bestudeerd in het sJIA muismodel. Met behulp van microcomputertomografie werd een milde vergroting gemeten van de longen na CFA-immunisatie, evenals een afname van de dichtheid van het luchtgedeelte. In de IFN-γ KO-muizen werd ook een verhoogde dichtheid gemeten van het niet-luchtgedeelte. Een afwijkende longfunctionaliteit werd gemeten in de CFA-geïmmuniseerde IFN-γ KO muizen. Deze waren verschillend bij mannelijke en vrouwelijke muizen. Mannetjesmuizen vertoonden een verhoogde weefselhysteresiviteit en weefseldemping, vrouwtjes daarentegen vertoonden een verhoogde hyperactiviteit van de luchtwegen. Vervolgens onthulde histopathologie subpleurale en parenchymale cellulaire infiltraten alsook de vorming van granulomen. Met behulp van flowcytometrie en kwantitatieve PCR toonden we een overmatige immuunactivatie aan met infiltratie van voornamelijk immature en mature neutrofielen of monocyten, verhoogde γδ-T-cellen, geactiveerde macrofagen en verhoogde expressie van zowel IL-1β, IL-6, TNF-α, IL-17 als IL-22. Geassocieerd met deze verhoogde infiltratie van neutrofielen, werd ook een verhoogde expressie van G-CSF en neutrofiel-geassocieerde chemokinen gemeten in de CFA-geïnjecteerde IFN-γ KO-muizen. Alhoewel de pulmonale manifestaties bij muizen anders waren dan bij sJIA-patiënten, beklemtoont dit onderzoek het belang van longontsteking in de pathofysiologie van sJIA.

Neutrofielen werden verder onderzocht in twee auto-inflammatoire ziektes geassocieerd met IL-1β: pyrine-geassocieerde auto-inflammatie met neutrofiele dermatose (PAAND) en Familiale Middellandse zeekoorts (FMF). De twee aandoeningen worden veroorzaakt door verschillende mutaties in hetzelfde *MEVV*-gen. Gezien hun hoge aantal neutrofielen in het bloed en aangetaste weefsels, werden de neutrofielen transcriptioneel, functioneel en fenotypisch onderzocht. Op transcriptioneel niveau vertoonden patiënten een gedeeltelijk overlappend geactiveerd fenotype met verhoogde expressie van zowel S100-eiwitten, IL-4R, CD48, F5, MMP9 als NF-KB. Verhoogde concentraties van MMP9 en S100A8/A9 werden gevalideerd in het plasma. Flowcytometrische analyse toonde aan dat neutrofielen van FMF-patiënten een immatuur karakter hebben, een verhoogde expressie van TLR4 en TLR9 en een verlaagde expressie van CXCR2, C5aR en BLTR1. PAAND-patiënten vertoonden een verhoogde granulariteit en een verhoogde willekeurige migratie. De CXCL8-geïnduceerde migratie was echter gedaald. Ook de neutrofielen van FMF-patiënten vertoonden een verhoogde willekeurige migratie en verlaagde chemoattractant-geïnduceerde migratie. De neutrofielen van zowel FMF- als PAAND-patiënten vertoonden een verhoogde basale en TNF-α-geïnduceerde ROS-productie en hadden een verhoogde afgifte van het azurofiele granule-eiwit myeloperoxidase (MPO). Ten slotte toonden we aan de neutrofielen van PAAND-patiënten een verhoogde fagocyterende capaciteit hebben terwijl deze gedaald is bij FMF-patiënten. Concluderend kunnen we stellen dat PAAND en FMF-patiënten neutrofilaire afwijkingen vertonen die verschillend zijn ten opzichte van elkaar. Dit duidt op discrepantie tussen deze twee pyrine-geassocieerde ziektes.

REFERENCES

REFERENCES

1. Krainer, J., Siebenhandl, S. & Weinhäusel, A. Systemic autoinflammatory diseases. *J. Autoimmun.* **109**, 102421 (2020).
2. Doria, A. *et al.* Autoinflammation and autoimmunity: Bridging the divide. *Autoimmun Rev* **12**, 22–30 (2012).
3. Opdenakker, G., El-asrar, A. A. & Van Damme, J. Remnant Epitopes Generating Autoimmunity : From Model to Useful Paradigm. *Trends Immunol.* **41**, 367–378 (2020).
4. Mcdermott, M. F. *et al.* Germline Mutations in the Extracellular Domains of the 55 kDa TNF Receptor , TNFR1 , Define a Family of Dominantly Inherited Autoinflammatory Syndromes. *Cell* **97**, 133–144 (1999).
5. Hashkes, P. J. & Laxer, R. M. Current practices for the genetic diagnosis of autoinflammatory diseases: results of a European Molecular Genetics Quality Network Survey. in *Textbook of Autoinflammation* 225–237 (2019).
6. Kessel, C., Hedrich, C. M. & Foell, D. Innately Adaptive or Truly Autoimmune : Is There Something Unique About Systemic Juvenile Idiopathic Arthritis ? *Arthritis Rheumatol.* **72**, 210–219 (2020).
7. Peckham, D., Scambler, T., Savic, S. & Mcdermott, M. F. The burgeoning field of innate immune-mediated disease and autoinflammation. *J. Pathol.* **241**, 123–139 (2017).
8. Kawasaki, T. & Kawai, T. Toll-like receptor signaling pathways. *Front. Immunol.* **5**, 461 (2014).
9. Newton, K. & Dixit, V. M. Signaling in Innate Immunity and Inflammation. *Cold Spring Harb Perspect Biol* **4**, a006049 (2012).
10. Kubelkova, K. & Macela, A. Innate Immune Recognition : An Issue More Complex Than Expected. *Front. Cell. Infect. Microbiol.* **9**, 241 (2019).
11. Mathur, A., Hayward, J. A. & Man, S. M. Molecular mechanisms of inflammasome signaling. *J. Leukoc. Biol.* **103**, 233–257 (2018).
12. Hayward, J. A., Mathur, A. & Ngo, C. Cytosolic Recognition of Microbes and Pathogens : Inflammasomes in Action. *Am. Soc. Microbiol.* **82**, e00015-18 (2018).
13. Liston, A. & Masters, S. L. Homeostasis-altering molecular processes as mechanisms of inflammasome activation. *Nat Rev Immunol* **17**, 208–214 (2017).
14. Schroder, K. & Tschopp, J. The Inflammasomes. *Cell* **140**, 821–832 (2010).
15. Martinon, F., Mayor, A. & Tschopp, J. The Inflammasomes: Guardians of the Body. *Annu. Rev. Immunol.* **27**, 229–265 (2009).
16. Schnappauf, O., Chae, J. J., Kastner, D. L. & Aksentijevich, I. The Pyrin Inflammasome in Health and Disease. *Front. Immunol.* **10**, 1–15 (2019).
17. Fink, S. L. & Cookson, B. T. Apoptosis , Pyroptosis , and Necrosis : Mechanistic Description of Dead and Dying Eukaryotic Cells. *Infect. Immun.* **73**, 1907–1916 (2005).
18. Liu, X. & Lieberman, J. *A Mechanistic Understanding of Pyroptosis : The Fiery Death Triggered by Invasive Infection*. *Advances in Immunology* **135**, (2017).
19. Manthiram, K., Zhou, Q., Aksentijevich, I. & Kastner, D. L. The monogenic autoinflammatory diseases define new pathways in human innate immunity and inflammation. *Nat. Immunol.* **18**, 832–842 (2017).
20. Gabay, C., Lamacchia, C. & Palmer, G. IL-1 pathways in inflammation and human diseases. *Nat. Rev. Rheumatol.* **6**, 232–241 (2010).
21. Prencipe, G., Bracaglia, C. & De Benedetti, F. Interleukin-18 in pediatric rheumatic diseases. *Curr. Opin. Rheumatol.* **31**, 421–427 (2019).
22. Moghaddas, F. *et al.* A novel Pyrin-Associated Autoinflammation with Neutrophilic Dermatosis mutation further defines 14-3-3 binding of pyrin and distinction to Familial Mediterranean Fever. *Ann. Rheum. Dis.* **76**, 2085–2094 (2017).
23. Masters, S. L. *et al.* Familial autoinflammation with neutrophilic dermatosis reveals a regulatory mechanism of pyrin activation. *Sci. Transl. Med.* **8**, 332ra45 (2016).
24. Manukyan, G. & Aminov, R. Update on Pyrin Functions and Mechanisms of Familial Mediterranean Fever. *Front. Microbiol.* **7**, 456 (2016).
25. Petty, R. E. *et al.* International League of Associations for Rheumatology Classification of Juvenile Idiopathic Arthritis : Second Revision, Edmonton, 2001. *J. Rheumatol.* **31**, 390–392 (2004).
26. Prakken, B., Albani, S. & Martini, A. Juvenile idiopathic arthritis. *Lancet* **377**, 2138–2149 (2011).
27. Ravelli, A. & Martini, A. Juvenile idiopathic arthritis. *Lancet* **369**, 767–778 (2007).
28. Gowdie, P. J. & Tse, S. M. L. Juvenile Idiopathic Arthritis. *Pediatr. Clin. NA* **59**, 301–327 (2012).
29. Still, G. F. On a Form of Chronic Joint Disease in Children. *Med Chir Trans* **80**, 47–60 (1896).
30. Gerfaud-Valentin, M., Jamilloux, Y., Iwaz, J. & Sève, P. Adult-onset Still's disease. *Autoimmun. Rev.* **13**, 708–722 (2014).
31. Woo, P. Systemic juvenile idiopathic arthritis: diagnosis, management, and outcome. *Nat. Clin. Pract. Rheumatol.* **2**, 28–34 (2006).
32. Gurion, R., Lehman, T. J. A. & Moorthy, L. N. Systemic Arthritis in Children : A Review of Clinical Presentation and Treatment. *J Inflam* **2012**, 271569 (2012).
33. Behrens, E. M. *et al.* Evaluation of the presentation of systemic onset juvenile rheumatoid arthritis : data from the Pennsylvania Systemic Onset Juvenile Arthritis Registry Evaluation of the Presentation of Systemic Onset Juvenile Rheumatoid Arthritis : Data from the Pennsylva. *J Rh* **35**, 343–348 (2008).
34. Mellins, E. D., Macaubas, C. & Grom, A. A. Pathogenesis of systemic juvenile idiopathic arthritis : some answers ,

more questions. *Nat. Rev. Rheumatol.* **7**, 416–426 (2011).
35. Sikora, K. A. & Grom, A. A. Update on the pathogenesis and treatment of systemic idiopathic arthritis. *Curr Opin Pediatr.* **23**, 640–646 (2012).
36. Date, Y. *et al.* Identification of a genetic risk factor for systemic juvenile rheumatoid arthritis in the 5'-flanking region onf the TNFa gene and HLA genes. *Arthritis Rheum.* **42**, 2577–2582 (1999).
37. Stock, C. J. W. *et al.* Comprehensive association study of genetic variants in the IL-1 gene family in systemic juvenile idiopathic arthritis. *Genes Immun.* **9**, 349–357 (2008).
38. Fishman, D., Humphries, S. & Woo, P. The effect of novel polymorphisms in the interleukin-6 (IL-6) gene on IL-6 transcription and plasma IL-6 levels , and an association with systemic-onset juvenile chronic arthritis. *J. Clin. Invest.* **102**, 1369–1376 (1998).
39. Ogilvie, E. M. *et al.* The -174G Allele of the Interleukin-6 Gene Confers Susceptibility to Systemic Arthritis in Children. *Arthritis Rheum.* **48**, 3202–3206 (2003).
40. Möller, J. C. *et al.* IL10 promoter polymorphisms are associated with systemic onset juvenile idiopathic arthritis (SoJIA). *Clin. Exp. Rheumatol.* **28**, 912–918 (2010).
41. Omoyinmi, E. *et al.* Association of the IL-10 Gene Family Locus on Chromosome 1 with Juvenile Idiopathic Arthritis (JIA). *PLoS One* **7**, e47673 (2012).
42. De Benedetti, F. *et al.* Functional and Prognostic Relevance of the - 173 Polymorphism of the Macrophage Migration Inhibitory Factor Gene in Systemic-Onset Juvenile Idiopathic Arthritis. *Arthritis Rheum.* **48**, 1398–1407 (2003).
43. Lamb, R., Thomson, W., Ogilvie, E. M. & Donn, R. Positive Association of SLC26A2 Gene Polymorphisms With Susceptibility to Systemic-Onset Juvenile Idiopathic Arthritis. *Arthritis Rheum.* **56**, 1286–1291 (2007).
44. Gattorno, M. *et al.* The pattern of response to anti-interleukin-1 treatment distinguishes two subsets of patients with systemic-onset juvenile idiopathic arthritis. *Arthritis Rheum.* **58**, 1505–1515 (2008).
45. Gattorno, M. *et al.* Pattern of Interleukin-1beta Secretion in Response to Lipopolysaccharide and ATP Before and After Interleukin-1 Blockade in Patients With CIAS1 Mutations. *Arthritis Rheum.* **56**, 3138–3148 (2007).
46. Fife, M. S. *et al.* Novel IL10 gene family associations with systemic juvenile idiopathic arthritis. *Arthritis Res. Ther.* **8**, 8–12 (2006).
47. Pardeo, M. *et al.* Early Treatment and IL1RN Single-Nucleotide Polymorphisms Affect Response to Anakinra in Systemic Juvenile Idiopathic Arthritis. *Arthritis Rheumatol.* **73**, 1053–1061 (2021).
48. Wakil, S. M. *et al.* Association of a Mutation in LACC1 With a Monogenic Form of Systemic Juvenile Idiopathic Arthritis. *Arthritis Rheumatol.* **67**, 288–295 (2015).
49. Jørgensen, S. E. *et al.* Systemic juvenile idiopathic arthritis and recurrent macrophage activation syndrome due to a CASP1 variant causing inflammasome hyperactivation. *Rheumatology* **59**, 3099–3105 (2020).
50. Schlenner, S. *et al.* NFIL3 mutations alter immune homeostasis and sensitise for arthritis pathology. *Ann. Rheum. Dis.* annrheumdis-2018-213764 (2018). doi:10.1136/annrheumdis-2018-213764
51. Schulert, G. S. *et al.* Brief Report: Novel UNC13D Intronic Variant Disrupting an NF-κB Enhancer in a Patient With Recurrent Macrophage Activation Syndrome and Systemic Juvenile Idiopathic Arthritis. *Arthritis Rheumatol.* **70**, 963–970 (2018).
52. Hazen, M. M. *et al.* Mutations of the hemophagocytic lymphohistiocytosis-associated gene UNC13D in a patient with systemic juvenile idiopathic arthritis. *Arthritis Rheumatol.* **58**, 567–70 (2008).
53. Ombrello, M. J. *et al.* HLA-DRB1 * 11 and variants of the MHC class II locus are strong risk factors for systemic juvenile idiopathic arthritis. *Proc. Natl. Acad. Sci.* **112**, 15970–15975 (2015).
54. Prahalad, S. *et al.* Quantification of the familial contribution to juvenile idiopathic arthritis. *Arthritis Rheum.* **62**, 2525–2529 (2010).
55. Prahalad, S. *et al.* Familial aggregation of juvenile idiopathic arthritis. *Arthritis Rheum.* **50**, 4022–7 (2004).
56. Singh-Grewal, D., Schneider, R., Bayer, N. & Feldman, B. M. Predictors of Disease Course and Remission in Systemic Juvenile Idiopathic Arthritis Significance of Early Clinical and Laboratory Features. *Arthritis Rheum.* **54**, 1595–1601 (2006).
57. Martini, A. Systemic juvenile idiopathic arthritis. *Autoimmun. Rev.* **12**, 56–59 (2012).
58. Nirmala, N., Grom, A. & Gram, H. Biomarkers in systemic juvenile idiopathic arthritis : a comparison with biomarkers in cryopyrin- associated periodic syndromes. *Curr. Opin. Rheumatol.* **26**, 543–552 (2014).
59. Grom, A. A. & Mellins, E. D. Macrophage activation syndrome : advances towards understanding pathogenesis. *Curr. Opin. Rheumatol.* **22**, 561–566 (2010).
60. Ravelli, A., Davì, S. & Cron, R. Macrophage Activation Syndrome. *Hematol Oncol Clin N Am* **29**, 927–941 (2015).
61. Macaubas, C. *et al.* Alternative activation in systemic juvenile idiopathic arthritis monocytes. *Clin. Immunol.* **142**, 362–372 (2012).
62. Sen, E. S., Clarke, S. L. N. & Ramanan, A. V. Macrophage Activation Syndrome. *Indian J Pediatr* **83**, 248–253 (2016).
63. Lehmberg, K. *et al.* Differentiating Macrophage Activation Syndrome in Systemic Juvenile Idiopathic Arthritis from Other Forms of Hemophagocytic Lymphohistiocytosis. *J. Pediatr.* **162**, 1245–1251 (2013).
64. Gohar, F., Kessel, C., Lavric, M., Holzinger, D. & Foell, D. Review of biomarkers in systemic juvenile idiopathic arthritis : helpful tools or just playing tricks ? *Arthritis Res. Ther.* **18**, 163 (2016).
65. Wilson, D. C. *et al.* Follistatin-like-protein-1 is a mesenchyme-derived inflammatory protein and may represent a biomarker for systemic-onset juvenile rheumatoid arthritis. *Arthritis Rheum* **62**, 2510–2516 (2011).
66. Holzinger, D. *et al.* The Toll-like receptor 4 agonist MRP8 / 14 protein complex is a sensitive indicator for disease

activity and predicts relapses in systemic-onset juvenile idiopathic arthritis. *Ann Rheum Dis* **11**, 974–980 (2012).
67. Wittkowski, H. *et al.* S100A12 is a Novel Molecular Marker Differentiating Systemic Onset Juvenile Idiopathic Arthritis from other Causes of Fever of Unknown Origin. *Arthritis Rheum.* **58**, 3924–3931 (2008).
68. Lotito, A. P. N., Campa, A., Silva, C. A. A., Kiss, M. H. B. & Mello, S. B. V. Interleukin 18 as a Marker of Disease Activity and Severity in Patients with Juvenile Idiopathic Arthritis. *J Rheumatol* **34**, 823–830 (2007).
69. Shimizu, M., Inoue, N., Mizuta, M., Nakagishi, Y. & Yachie, A. Serum Leucine-Rich α2-Glycoprotein as a Biomarker for Monitoring Disease Activity in Patients with Systemic Juvenile Idiopathic Arthritis. *J. Immunol. Res.* **2019**, 3140204 (2019).
70. Jelušić, M. *et al.* Interleukin-18 as a mediator of systemic juvenile idiopathic arthritis. *Clin Rheumatol* **26**, 1332–1334 (2007).
71. Ferrara, G. *et al.* Methotrexate in juvenile idiopathic arthritis : advice and recommendations from the MARAJIA expert consensus meeting. *Pediatr. Rheumatol.* **16**, 46 (2018).
72. Quartier, P. *et al.* A multicentre, randomised, double-blind, placebo-controlled trial with the interleukin-1 receptor antagonist anakinra in patients with systemic-onset juvenile idiopathic arthritis (ANAJIS trial). *Ann Rheum Dis* **70**, 747–754 (2011).
73. Pascual, V., Allantaz, F., Arce, E., Punaro, M. & Banchereau, J. Role of interleukin-1 (IL-1) in the pathogenesis of systemic onset juvenile idiopathic arthritis and clinical response to IL-1 blockade. *J. Exp. Med.* **201**, 1479–86 (2005).
74. ter Haar, N. M. *et al.* Treatment to Target Using Recombinant Interleukin-1 Receptor Antagonist as First-Line Monotherapy in Onset Systemic Juvenile Idiopathic Arthritis : Results From a Five-Year Follow-Up Study. *Arthritis Rheumatol.* **71**, 1163–1173 (2019).
75. Horneff, G. *et al.* Experience with etanercept , tocilizumab and interleukin-1 inhibitors in systemic onset juvenile idiopathic arthritis patients from the BIKER registry. *Arthritis Res. Ther.* **19**, 256 (2017).
76. Tarp, S. *et al.* Efficacy and safety of biological agents for systemic juvenile idiopathic arthritis : a systematic review and meta-analysis of randomized trials. *Rheumatology* **55**, 669–679 (2016).
77. Woerner, A., Uettwiller, F., Melki, I., Mouy, R. & Wouters, C. Biological treatment in systemic juvenile idiopathic arthritis : achievement of inactive disease or clinical remission on a first , second or third biological agent. *RMD open* **1**, e000036 (2015).
78. Ruperto, N. *et al.* Two Randomized Trials of Canakinumab in Systemic Juvenile Idiopathic Arthritis. *N. Engl. J. Med.* **367**, 2396–2406 (2012).
79. Ilowite, N. T. *et al.* Randomized , Double-Blind , Placebo-Controlled Trial of the Efficacy and Safety of Rilonacept in the Treatment of Systemic Juvenile Idiopathic Arthritis. *Arthritis Rheumatol.* **66**, 2570–2579 (2014).
80. De Benedetti, F. *et al.* Randomized Trial of Tocilizumab in Systemic Juvenile Idiopathic Arthritis. *N. Engl. J. Med.* **367**, 2385–2395 (2012).
81. Yokota, S. *et al.* Efficacy and safety of tocilizumab in patients with systemic-onset juvenile idiopathic arthritis : a randomised , double-blind , placebo-controlled , withdrawal phase III trial. *Lancet* **371**, 998–1006 (2008).
82. Yokota, S. *et al.* Tocilizumab in systemic juvenile idiopathic arthritis in a real-world clinical setting : results from 1 year of postmarketing surveillance follow-up of 417 patients in Japan. *Ann Rheum Dis* **75**, 1654–1660 (2016).
83. Woo, P. *et al.* Research article Open label phase II trial of single , ascending doses of MRA in Caucasian children with severe systemic juvenile idiopathic arthritis : proof of principle of the efficacy of IL-6 receptor blockade in this type of arthritis and demonstrati. *Arthritis Res.* **7**, 1281–1288 (2005).
84. Vastert, S. J. *et al.* Anakinra in children and adults with Still's disease. *Rheumatology* **58**, vi9–vi22 (2019).
85. Nigrovic, P. A. Is There a Window of Opportunity for Treatment of Systemic Juvenile Idiopathic Arthritis ? *Arthritis Rheumatol.* **66**, 1405–1413 (2014).
86. Quartier, P. *et al.* Efficacy of Etanercept for the Treatment of Juvenile Idiopathic Arthritis According to the Onset Type. *Arthritis Rheum.* **48**, 1093–1101 (2003).
87. Brinkman, D. M. C. *et al.* Autologous Stem Cell Transplantation in Children With Severe Progressive Systemic or Polyarticular Juvenile Idiopathic Arthritis Long-Term Followup of a Prospective Clinical Trial. *Arthritis Rheum.* **56**, 2410–2421 (2007).
88. Wulffraat, M. *et al.* Autologous Stem Cell Transplantation for Refractory Juvenile Idiopathic Artrhitis : Current Results and Perspectives. *Transplanation Proc.* **34**, 2925–2926 (2002).
89. Wulffraat, N. M. *et al.* Long-term follow-up of autologous stem cell transplantation for refractory juvenile idiopathic arthritis. *Bone Marrow Transplant.* **32**, S61–S64 (2003).
90. Behrens, E. M. *et al.* Occult Macrophage Activation Syndrome in Patients with Systemic Juvenile Idiopathic Arthritis. *J. Rheumatol.* **34**, 1133–1138 (2007).
91. Ravelli, A., Grom, A. A., Behrens, E. M. & Cron, R. Q. Macrophage activation syndrome as part of systemic juvenile idiopathic arthritis : diagnosis , genetics , pathophysiology and treatment. *Genes Immun.* **13**, 289–298 (2012).
92. Gupta, A. *et al.* Successful use of tocilizumab in amyloidosis secondary to systemic juvenile idiopathic arthritis. *Rheumatol. Int.* **40**, 153–159 (2020).
93. Bechtold, S. & Simon, D. Growth abnormalities in children and adolescents with juvenile idiopathic arthritis. *Rheumatol Int* **34**, 1483–1488 (2014).
94. Roth, J. *et al.* Osteoporosis in juvenile idiopathic arthritis- a practical approach to diagnosis and therapy. *Eur J Pediatr* **166**, 775–784 (2007).
95. Lattanzi, B. *et al.* Macrophage activation syndrome. *Indian J. Rheumatol.* **7**, 27–35 (2012).

96. Minoia, F. *et al.* Clinical Features , Treatment , and Outcome of Macrophage Activation Syndrome Complicating Systemic Juvenile Idiopathic Arthritis. *Arthritis Rheumatol.* **66**, 3160–3169 (2014).
97. Ravelli, A. *et al.* 2016 Classification Criteria for Macrophage Activation Syndrome Complicating Systemic Juvenile Idiopathic Arthritis. *Arthritis Rheumatol.* **68**, 566–76 (2016).
98. Henter, J.-I. *et al.* HLH-2004 : Diagnostic and Therapeutic Guidelines for Hemophagocytic Lymphohistiocytosis. *Pediatr Blood Cancer* **48**, 124–131 (2007).
99. Bleesing, J. *et al.* The Diagnostic Significance of Soluble CD163 and Soluble Interleukin-2 Receptor alpha-Chain in Macrophage Activation Syndrome and Untreated New-Onset Systemic Juvenile Idiopathic Arthritis. *Arthritis Rheum.* **56**, 965–971 (2007).
100. Bracaglia, C. *et al.* Elevated circulating levels of interferon- γ and interferon- γ -induced chemokines characterise patients with macrophage activation syndrome complicating systemic juvenile idiopathic arthritis. *Ann Rheum Dis* **76**, 166–172 (2017).
101. Shimizu, M. *et al.* Interleukin-18 for predicting the development of macrophage activation syndrome in systemic juvenile idiopathic arthritis. *Clin. Immunol.* **160**, 277–281 (2015).
102. Lee, P. Y. *et al.* Adenosine deaminase 2 as a biomarker of macrophage activation syndrome in systemic juvenile idiopathic arthritis. *Ann Rheum Dis* **79**, 225–231 (2020).
103. Mizuta, M., Shimizu, M., Irabu, H. & Usami, M. Comparison of serum cytokine profiles in macrophage activation syndrome complicating different background rheumatic diseases in children. *Rheumatology* **60**, 231–238 (2021).
104. Rigante, D., Emmi, G., Fastiggi, M., Silvestri, E. & Cantarini, L. Macrophage activation syndrome in the course of monogenic autoinflammatory disorders. *Clin Rheumatol* **34**, 1333–1339 (2015).
105. Brisse, E., Wouters, C. H. & Matthys, P. Advances in the pathogenesis of primary and secondary haemophagocytic lymphohistiocytosis : differences and similarities. *Br. J. Haematol.* **147**, 203–217 (2016).
106. Brisse, E., Wouters, C. H. & Matthys, P. Hemophagocytic lymphohistiocytosis (HLH): A heterogeneous spectrum of cytokine-driven immune disorders. *Cytokine Growth Factor Rev.* **26**, 263–280 (2015).
107. Kimura, Y. *et al.* Pulmonary Hypertension and Other Potentially Fatal Pulmonary Complications in Systemic Juvenile Idiopathic Arthritis. *Arthrtis Care Res.* **65**, 745–752 (2013).
108. Schulert, G. S. *et al.* Systemic Juvenile Idiopathic Arthritis-Lung Disease: Characterization and Risk Factors. *Arthritis Rheumatol.* **71**, 1943–1954 (2019).
109. Saper, V. E. *et al.* Emergent high fatality lung disease in systemic juvenile arthritis. *Ann Rheum Dis.* **78**, 1722–1731 (2019).
110. Schultz, È., Mattila, J., Gappa, M. & Verronen, P. Development of Progressive Pulmonary Interstitial and Intra-Alveolar Cholesterol Granulomas (PICG) Associated With Therapy-Resistant Chronic Systemic Juvenile Arthritis (CJA). *Pediatr. Pulmonol.* **402**, 397–402 (2001).
111. Athreya BH, Doughty RA, Bookspan M, Schumacher HR, Sewell EM, C. J. Pulmonary manifestations of juvenile rheumatoid arthritis. A report of eight cases and review. *Clin Chest Med* **1**, 361–74 (1980).
112. Nigrovic, P. A. Storm warning: lung disease in systemic juvenile idiopathic arthritis. *Arthritis Rheumatol.* **71**, 1773–1775 (2019).
113. De Benedetti, F. *et al.* Interleukin 6 Causes Growth Impairment in Transgenic Mice through a Decrease in Insulin-like Growth Factor-I A Model for Stunted Growth in Children with Chronic Inflammation. *J. Clin. Invest.* **99**, 643–650 (1997).
114. De Benedetti, F., Meazza, C. & Martini, A. Role of Interleukin-6 in Growth Failure : An Animal Model Role of Interleukin-6 in Growth Failure : An Animal Model. *Horm. Res.* **58**, 24–27 (2002).
115. Strippoli, R. *et al.* Amplification of the Response to Toll-like Receptor Ligands by Prolonged Exposure to Interleukin-6 in Mice Implication for the Pathogenesis of Macrophage Activation Syndrome. *Arthritis Rheum.* **64**, 1680–1688 (2012).
116. Prencipe, G., Caiello, I., Pascarella, A., Grom, A. A. & Bracaglia, C. Neutralization of IFN-gamma reverts clinical and laboratory features in a mouse model of macrophage activation syndrome. *J. Allergy Clin. Immunol.* **141**, 1439–1449 (2017).
117. Minoia, F. *et al.* Clinical Features , Treatment , and Outcome of Macrophage Activation Syndrome Complicating Systemic Juvenile Idiopathic Arthritis. *Arthritis Rheumatol.* **66**, 3160–3169 (2014).
118. Kawane, K., Tanaka, H., Kitahara, Y., Shimaoka, S. & Nagata, S. Cytokine-dependent but acquired immunity-independent arthritis caused by DNA escaped from degradation. *Proc. Natl. Acad. Sci.* **107**, 9–14 (2010).
119. Kawane, K. *et al.* Chronic polyarthritis caused by mammalian DNA that escapes from degradation in macrophage. *Nature* **443**, 998–1002 (2006).
120. Yoshida, H., Okabe, Y., Kawane, K., Fukuyama, H. & Nagata, S. Lethal anemia caused by interferon-beta produced in mouse embryos carrying undigested DNA. *Nat. Immunol.* **6**, 49–56 (2005).
121. Avau, A. *et al.* Systemic Juvenile Idiopathic Arthritis-like Syndrome in Mice Following Stimulation of the Immune System With Freund ' s Complete Adjuvant. *Arthritis Rheumatol.* **66**, 1340–1351 (2014).
122. Jung, J., Kim, J., Suh, C. & Kim, H. Roles of Interactions Between Toll-Like Receptors and Their Endogenous Ligands in the Pathogenesis of Systemic Juvenile Idiopathic Arthritis and Adult-Onset Still ' s Disease. *Front. Immunol.* **11**, 583513 (2020).
123. Allantaz, F. *et al.* Blood leukocyte microarrays to diagnose systemic onset juvenile idiopathic arthritis and follow the response to IL-1 blockade. *J. Exp. Med.* **204**, 2131–2144 (2007).

124. Barnes, M. G. *et al.* Subtype-Specific Peripheral Blood Gene Expression Profiles in Recent-Onset Juvenile Idiopathic Arthritis. *Arthritis Rheum.* **60**, 2102–2112 (2009).
125. Ogilvie, E. M., Khan, A., Hubank, M., Kellam, P. & Woo, P. Specific Gene Expression Profiles in Systemic Juvenile Idiopathic Arthritis. *Arthritis Rheum.* **56**, 1954–1965 (2007).
126. Fall, N. *et al.* Gene Expression Profiling of Peripheral Blood From Patients With Untreated New-Onset Systemic Juvenile Idiopathic Arthritis Reveals Molecular Heterogeneity That May Predict Macrophage Activation Syndrome. *Arthritis Rheum.* **56**, 3793–3804 (2007).
127. Cepika, A.-M. *et al.* A multidimensional blood stimulation assay reveals immune alterations underlying systemic juvenile idiopathic arthritis. *J. Exp. Med.* **214**, 3449–3466 (2017).
128. Guiducci, C. *et al.* RNA recognition by human TLR8 can lead to autoimmune inflammation. *J. Exp. Med.* **210**, 2903–2919 (2013).
129. Brown, R. A. *et al.* Neutrophils From Children With Systemic Juvenile Idiopathic Arthritis Exhibit Persistent Proinflammatory Activation Despite Long-Standing Clinically Inactive Disease. *Front. Immunol.* **9**, 2995 (2018).
130. ter Haar, N. M. *et al.* Reversal of Sepsis-Like Features of Neutrophils by Interleukin-1 Blockade in Patients With Systemic-Onset Juvenile Idiopathic Arthritis. *Arthritis Rheumatol.* **70**, 943–956 (2018).
131. Hinze, C. H. *et al.* Immature cell populations and an erythropoiesis gene-expression signature in systemic juvenile idiopathic arthritis: implications for pathogenesis. *Arthritis Res. Ther.* **12**, R123 (2010).
132. Macaubas, C. *et al.* Distribution of circulating cells in systemic juvenile idiopathic arthritis across disease activity states. *Clin. Immunol.* **134**, 206–216 (2010).
133. Shimizu, M. & Yachie, A. Compensated inflammation in systemic juvenile idiopathic arthritis : Role of alternatively activated macrophages. *Cytokine* **60**, 226–232 (2012).
134. Macaubas, C. *et al.* Altered signaling in systemic juvenile idiopathic arthritis monocytes. *Clin. Immunol.* **163**, 66–74 (2016).
135. Sikora, K. A., Fall, N., Thornton, S. & Grom, A. A. The Limited Role of Interferon-γ in Systemic Juvenile Idiopathic Arthritis Cannot Be Explained by Cellular Hyporesponsiveness. *Arthritis Rheum* **64**, 3799–3808 (2012).
136. Muller, K., Herner, E., Stagg, A., Bendtzen, K. & Woo, P. Inflammatory cytokines and cytokine antagonists in whole blood cultures of patients with systemic juvenile chronic arthritis. *Br. J. Rheumatol.* **37**, 562–569 (1998).
137. Put, K. *et al.* Inflammatory Gene Expression Profile and Defective Interferon-γ and Granzyme K in Natural Killer Cells From Systemic Juvenile Idiopathic Arthritis Patients. *Arthritis Rheumatol.* **69**, 213–224 (2017).
138. Wouters, C. H. P., Ceuppens, J. L. & Stevens, E. A. M. Different circulating lymphocyte profiles in patients with different subtypes of juvenile idiopathic arthritis. *Clin. Exp. Rheumatol.* **20**, 239–248 (2002).
139. de Jager, W. *et al.* Defective phosphorylation of interleukin-18 receptor beta causes impaired natural killer cell function in systemic-onset juvenile idiopathic arthritis. *Arthritis Rheumatol.* **60**, 2782–2793 (2009).
140. Villanueva, J. *et al.* Natural killer cell dysfunction is a distinguishing feature of systemic onset juvenile rheumatoid arthritis and macrophage activation syndrome. *Arthritis Res. Ther.* **7**, 30–37 (2005).
141. Grom, A. A. *et al.* Natural killer cell dysfunction in patients with systemic-onset juvenilie rheumatoid arthritis and macropahge activation syndrome. *J. Pediatr.* **142**, 292–296 (2003).
142. Wulffraat, N. M., Rijkers, G. T., Elst, E., Brooimans, R. & Kuis, W. Reduced perforin expression in systemic juvenile idiopathic arthritis is restored by autologous stem-cell transplantation. *Rheumatology* **42**, 375–379 (2003).
143. Vastert, S. J. *et al.* Mutations in the perforin gene can be linked to macrophage activation syndrome in patients with systemic onset juvenile idiopathic arthritis. *Rheumatology* **49**, 441–449 (2010).
144. Zhou, J., Tang, X., Ding, Y., An, Y. & Zhao, X. Natural killer cell activity and frequency of killer cell immunoglobulin-like receptors in children with different forms of juvenile idiopathic arthritis. *Pediatr. Allergy Immunol.* **24**, 691–696 (2013).
145. Behrens, E. M. Caught in the Act : Dissecting Natural Killer Cell Function in Systemic Juvenile Idiopathic Arthritis. *Arthritis Rheumatol.* **69**, 6–8 (2017).
146. Vandenhaute, J., Wouters, C. H. & Matthys, P. Natural Killer Cells in Systemic Autoinflammatory Diseases : A Focus on Systemic Juvenile Idiopathic Arthritis and Macrophage Activation Syndrome. *Front. Immunol.* **10**, 3089 (2020).
147. Kessel, C. *et al.* Proinflammatory Cytokine Environments Can Drive Interleukin-17 Overexpression by γ/δ T Cells in Systemic Juvenile Idiopathic Arthritis. *Arthritis Rheumatol.* **69**, 1480–1494 (2017).
148. Pascual, V., Allantaz, F., Arce, E., Punaro, M. & Banchereau, J. Role of interleukin-1 (IL-1) in the pathogenesis of systemic onset juvenile idiopathic arthritis and clinical response to IL-1 blockade. *J. Exp. Med.* **201**, 1479–1486 (2005).
149. Prahalad, S. *et al.* Elevated serum levels of soluble CD154 in children with juvenile idiopathic arthritis. *Pediatr. Rheumatol.* **6**, 8 (2008).
150. Yilmaz, M., Kendirli, S. G., Altintas, D., Bingöl, G. & Antmen, B. Cytokine Levels in Serum of Patients with Juvenile Rheumatoid Arthritis. *Clin. Rheumatol.* **20**, 30–35 (2001).
151. De Benedetti, F. *et al.* Circulating levels of interleukin 1 beta and of interleukin 1 receptor antagonist in systemic juvenile chronic arthritis. *Clin Exp Rheumatol* **13**, 779–84 (1995).
152. de Jager, W. *et al.* Blood and synovial fluid cytokine signatures in patients with juvenile idiopathic arthritis: a cross-sectional study. *Ann. Rheum. Dis.* **66**, 589–598 (2008).
153. Rooney, M. *et al.* Inflammatory cytokine responses in juvenile chronic arthritis. *Br J Rheumatol.* **34**, 454–60 (1995).
154. Pignatti, P. *et al.* Abnormal Regulation of Interleukin 6 in Systemic Juvenile Idiopathic Arthritis. *J Rheumatol* **28**, 1670–1676 (2001).

155. De Benedetti, F. *et al.* Correlation of serum interleukin-6 levels with joint involement and thrombocytosis in systemic juvenile rheumatoid arthritis. *Arthritis Rheum.* **34**, 1158–1163 (1991).
156. Lepore, L. *et al.* Study of IL-2, IL-6, TNF alpha, IFN gamma and beta in the serum and synovial fluid of patients with juvenile chronic arthritis. *Clin Exp Rheumatol* **12**, 561–32 (1994).
157. Shimizu, M. *et al.* Tocilizumab masks the clinical symptoms of systemic juvenile idiopathic arthritis-associated macrophage activation syndrome : The diagnostic significance of interleukin-18 and interleukin-6. *Cytokine* **58**, 287–294 (2012).
158. Shimizu, M. *et al.* Distinct cytokine profiles of systemic-onset juvenile idiopathic arthritis-associated macrophage activation syndrome with particular emphasis on the role of interleukin-18 in its pathogenesis. *Rheumatology* **49**, 1645–1653 (2010).
159. Put, K. *et al.* Inflammatory Gene Expression Profile and Defective Interferon-γ and Granzyme K in Natural Killer Cells From Systemic Juvenile Idiopathic Arthritis Patients. *Arthritis Rheumatol.* **69**, 213–224 (2017).
160. Imbrechts, M. *et al.* Insufficient IL-10 Production as a Mechanism Underlying the Pathogenesis of Systemic Juvenile Idiopathic Arthritis. *J. Immunol.* **201**, 2654–2663 (2018).
161. Raziuddin, S., Bahabri, S., Al-dalaan, A., Siraj, A. K. & Al-sedairy, S. A Mixed Th1 / Th2 Cell Cytokine Response Predominates in Systemic Onset Juvenile Rheumatoid Arthritis : Immunoregulatory IL-10 Function. *Clin. Immunol. Immunopathol.* **86**, 192–198 (1998).
162. Omoyinmi, E. *et al.* Th1 and Th17 cell subpopulations are enriched in the peripheral blood of patients with systemic juvenile idiopathic arthritis. *Rheumatology* **51**, 1881–1886 (2012).
163. Muhsin, H. Y., Ad'hiah, A. H. & AL-Mossawei, M. T. *Role of Cytokine in Pathogenesis of Juvenile Idiopathic Arthritis*. (2018).
164. Chen, O. *et al.* The imbalance of IL-18 / IL-18BP in patients with systemic juvenile idiopathic arthritis. *Acta Biochim Biophys Sin* **45**, 339–341 (2013).
165. Frosch, M. *et al.* Expression of Myeloid-Related Proteins 8 and 14 in Systemic-Onset Juvenile Rheumatoid Arthritis. *Arthritis Rheum.* **48**, 2622–2626 (2003).
166. Frosch, M. *et al.* The Myeloid-Related Proteins 8 and 14 Complex , a Novel Ligand of Toll-Like Receptor 4, and Interleukin-1beta Form a Positive Feedback Mechanism in Systemic-Onset Juvenile Idiopathic Arthritis. *Arthritis Rheum.* **60**, 883–891 (2009).
167. Meazza, C. *et al.* Macrophage Migration Inhibitory Factor in Patients With Juvenile Idiopathic Arthritis. *Arthritis Rheum.* **46**, 232–237 (2002).
168. Avau, A., Put, K., Wouters, C. H. & Matthys, P. Cytokine balance and cytokine-driven natural killer cell dysfunction in systemic juvenile idiopathic arthritis. *Cytokine Growth Factor Rev.* **26**, 35–45 (2015).
169. Eder, C. Mechanisms of interleukin-1β release. *Immunobiology* **214**, 543–553 (2009).
170. Sutton, C. E. *et al.* Interleukin-1 and IL-23 Induce Innate IL-17 Production from gamma delta T Cells , Amplifying Th17 Responses and Autoimmunity. *Immunity* **31**, 331–341 (2009).
171. Giancane, G. *et al.* IL-1 inhibition in systemic juvenile idiopathic arthritis. *Front. Pharmacol.* **7**, 467 (2016).
172. Miettunen, P. M., Narendran, A., Jayanthan, A., Behrens, E. M. & Cron, R. Q. Successful treatment of severe paediatric rheumatic disease-associated macrophage activation syndrome with interleukin-1 inhibition following conventional immunosuppressive therapy: case series with 12 patients. *Rheumatol.* **50**, 417–419 (2011).
173. Mellins, E. D., Macaubas, C. & Grom, A. A. Pathogenesis of systemic juvenile idiopathic arthritis : some answers , more questions. *Nat. Rev. Rheumatol.* **7**, 416–426 (2011).
174. Stock, C. J. W. *et al.* Comprehensive association study of genetic variants in the IL-1 gene family in systemic juvenile idiopathic arthritis. *Genes Immun.* **9**, 349–357 (2008).
175. Palomo, J., Dietrich, D., Martin, P., Palmer, G. & Gabay, C. The interleukin (IL)-1 cytokine family - Balance between agonists and antagonists in inflammatory diseases. *Cytokine* **76**, 25–37 (2015).
176. Arend, W. P., Malyak, M. & Guthridge, C. J. Interleukin-1 receptor antagonist: Role in Biology. *Annu. Rev. Immunol.* **16**, 27–55 (1998).
177. Colotta, F., Dower, S. K., Sims, J. E. & Mantovani, A. The type II ' decoy ' receptor : a novel regulatory pathway for interleukin 1. *Immunol Today* **15**, 562–6 (1994).
178. Burger, D., Chicheportiche, R., Giri, J. G. & Dayer, J. The inhibitory activity of human interleukin-1 receptor antagonist is enhanced by type II interleukin-1 soluble receptor and hindered by type I interleukin-1 soluble receptor. *J. Clin. Invest.* **96**, 38–41 (1995).
179. Martin, P. *et al.* Mouse neutrophils express the decoy type 2 interleukin-1 receptor (IL-1R2) constitutively and in acute inflammatory conditions. *J. Leukoc. Biol.* **94**, 791–802 (2013).
180. Sambo, P. *et al.* Reactive oxygen intermediates cause rapid release of the interleukin-1 decoy receptor from human myelomonocytic cells. *Blood* **87**, 1682–1686 (1996).
181. Colotta, B. F. *et al.* Chemoattractants induce rapid release of the interleukin 1 type II decoy receptor in human polymorphonuclear cells. *J. Exp. Med.* **181**, 2181–2188 (1995).
182. Dinarello, C. A., Novick, D., Kim, S. & Kaplanski, G. Interleukin-18 and IL-18 binding protein. *Front. Immunol.* **4**, 289 (2013).
183. Novick, D., Kim, S., Kaplanski, G. & Dinarello, C. A. Interleukin-18 , more than a Th1 cytokine. *Semin. Immunol.* **25**, 439–448 (2013).
184. Put, K. *et al.* Cytokines in systemic juvenile idiopathic arthritis and haemophagocytic lymphohistiocytosis: Tipping

the balance between interleukin-18 and interferon-γ. *Rheumatology* **54**, 1507–1517 (2015).
185. Billiau, A. & Matthys, P. Interferon-gamma : A historical perspective. *Cytokine Growth Factor Rev.* **20**, 97–113 (2009).
186. Lin, F. & Young, H. A. The talented interferon-gamma. *Adv. Biosci. Biotechnol.* **4**, 6–13 (2013).
187. Kelchtermans, H., Billiau, A. & Matthys, P. How interferon-γ keeps autoimmune diseases in check. *Trends Immunol.* **29**, 479–486 (2008).
188. Schroder, K., Hertzog, P. J., Ravasi, T. & Hume, D. A. Interferon- γ : an overview of signals , mechanisms and functions. *J. Leukoc. Biol.* **75**, 163–189 (2004).
189. Green, D. S., Young, H. A. & Valencia, J. C. Current prospects of type II interferon-g signaling and autoimmunity. *J. Biol. Chem.* **292**, 13925–13933 (2017).
190. Hu, X. & Ivashiv, L. B. Cross-regulation of Signaling and Immune Responses by IFN-γ and STAT1. *Immunity* **31**, 539–550 (2010).
191. Tanaka, T. & Kishimoto, T. Targeting Interleukin-6 : All the Way to Treat Autoimmune and Inflamma- tory Diseases. *Int. J. Biol. Sci.* **8**, 1227–1236 (2012).
192. Hunter, C. A. & Jones, S. A. IL-6 as a keystone cytokine in health and disease. *Nat. Immunol.* **16**, 448–458 (2015).
193. De Benedetti, F. & Martini, A. Targeting the Interleukin-6 Receptor : A New Treatment for Systemic Juvenile Idiopathic Arthritis? *Arthritis Rheum.* **52**, 687–693 (2005).
194. Zhang, S. The role of transforming growth factor b in T helper 17 differentiation. *Immunology* **155**, 24–35 (2018).
195. Geginat, J. *et al.* The light and the dark sides of Interleukin-10 in immune-mediated diseases and cancer . *Cytokine Growth Factor Rev.* **30**, 87–93 (2016).
196. Hedrich, C. M. & Bream, J. H. Cell type-specific regulation of IL-10 expression in inflammation and disease. *Immunol Res* **47**, 185–206 (2010).
197. Iyer, S. S. & Cheng, G. Role of Interleukin 10 Transcriptional Regulation in Inflammation and Autoimmune Disease. *Crit Rev Immunol* **32**, 23–63 (2012).
198. Moore, K. W., Malefyt, R. D. W., Robert, L. & Garra, A. O. Interleukin-10 and the Interleukin-10 receptor. *Annu Rev Immunol* **19**, 683–765 (2001).
199. Mosser, D. M. & Zhang, X. Interleukin-10 : new perspectives on an old cytokine. *Immunol. Rev.* **226**, 205–218 (2008).
200. Ouyang, W., Rutz, S., Crellin, N. K., Valdez, P. A. & Hymowitz, S. G. Regulation and Functions of the IL-10 Family of Cytokines in Inflammation and Disease. *Annu Rev Immunol* **29**, 71–109 (2011).
201. Sabat, R. *et al.* Biology of interleukin-10. *Cytokine Growth Factor Rev.* **21**, 331–344 (2010).
202. Fillatreau, S. & Garra, A. O. *Current Topics in Microbiology and Immunology Interleukin-10 in Health and Disease*. (2014).
203. Kuwabara, T., Ishikawa, F., Kondo, M. & Kakiuchi, T. The Role of IL-17 and Related Cytokines in Inflammatory Autoimmune Diseases. *Mediators Inflamm.* **2017**, 3908061 (2017).
204. Moseley, T. A., Haudenschild, D. R., Rose, L. & Reddi, A. H. Interleukin-17 family and IL-17 receptors. *Cytokine Growth Factor Rev.* **14**, 155–174 (2003).
205. Roark, C. L., Simonian, P. L., Fontenot, A. P., Born, W. K. & Brien, R. L. O. gd T cells : an important source of IL-17. *Curr. Opin. Immunol.* **20**, 353–357 (2008).
206. Omoyinmi, E. *et al.* Th1 and Th17 cell subpopulations are enriched in the peripheral blood of patients with systemic Juvenile idiopathic arthritis. *Rheumatology* **51**, 1881–1886 (2012).
207. Sabat, R., Ouyang, W. & Wolk, K. Therapeutic opportunities of the IL-22–IL-22R1 system. *Nat. Rev. Drug Discov.* **13**, 23–38 (2014).
208. Zenewicz, L. A. & Zenewicz, L. A. IL-22 : There Is a Gap in Our Knowledge IL-22 : There Is a Gap in Our Knowledge. *ImmunoHorizons* **2**, 198–207 (2020).
209. Dudakov, J. A. *et al.* Interleukin-22: immunobiology and pathology. *Annu Rev Immunol.* **33**, 747–785 (2015).
210. Rao, R. *et al.* Interleukin 17-Producing γδ T Cells Promote Hepatic Regeneration in Mice. *Gastroenterology* **147**, 473–484 (2014).
211. Wolk, K. & Sabat, R. Interleukin-22 : A novel T- and NK-cell derived cytokine that regulates the biology of tissue cells. *Cytokine Growth Factor Rev.* **17**, 367–380 (2006).
212. Victor, A. R. *et al.* Interleukin-18 drives ILC3 proliferation and promotes interleukin-22 production via NF-κB. *J Immunol.* **199**, 2333–2342 (2018).
213. Liang, S. C. *et al.* Interleukin (IL)-22 and IL-17 are coexpressed by Th17 cells and cooperatively enhance expression of antimicrobial peptides. *J. Exp. Med.* **203**, 2271–2279 (2006).
214. Honda, K. IL-22 from T Cells : Better Late than Never. *Immunity* **37**, 952–954 (2012).
215. Rutz, S., Eidenschenk, C. & Ouyang, W. IL-22, not simply a Th17 cytokine. *Immunol. Rev.* **252**, 116–132 (2013).
216. Veldhoen, M. *et al.* The aryl hydrocarbon receptor links Th17-cell-mediated autoimmunity to environmental toxins. *Nature* **453**, 2–6 (2008).
217. Veldhoen, M., Hirota, K., Christensen, J., Garra, A. O. & Stockinger, B. Natural agonists for aryl hydrocarbon receptor in culture medium are essential for optimal diff erentiation of Th17 T cells. *J. Exp. Med.* **206**, 43–49 (2009).
218. Yeste, A. *et al.* IL-21 induces IL-22 production in CD4+ T-cells. *Nat. Commun.* **5**, 3753 (2014).
219. Kotenko, S. V *et al.* Identification, Cloning, and Characterization of a Novel Soluble Receptor That Binds IL-22 and Neutralizes Its Activity. *J Immunol.* **166**, 7096–7103 (2001).
220. Dumoutier, L., Lejeune, D., Colau, D. & Renauld, J. Cloning and Characterization of IL-22 Binding Protein, a Natural Antagonist of IL-10-Related T Cell-Derived Inducible Factor/IL-22. *J Immunol* **166**, 7090–7095 (2001).

221. Huber, S. *et al.* IL-22BP is regulated by the inflammasome and modulates tumorigenesis in the intestine. *Nature* **491**, 259–264 (2012).
222. Eidenschenk, C. *et al.* Interleukin-22 Induces Interleukin-18 Expression from Epithelial Cells during Intestinal Infection. *Immunity* **42**, 321–331 (2015).
223. Kim, Y. *et al.* The pathogenic role of interleukin-22 and its receptor during UVB-induced skin inflammation. *PLoS One* **12**, e0178567 (2017).
224. Mühl, H. & Bachmann, M. IL-18 / IL-18BP and IL-22 / IL-22BP : Two interrelated couples with therapeutic potential. *Cell. Signal.* **63**, 109388 (2019).
225. Wolk, K. *et al.* IL-22 Increases the Innate Immunity of Tissues. *Immunity* **21**, 241–254 (2004).
226. Zheng, Y. *et al.* Interleukin-22 mediates early host defense against attaching and effacing bacterial pathogens. *Nat. Med.* **14**, 282–289 (2008).
227. Raffatellu, M. *et al.* Lipocalin-2 resistance of Salmonella enterica serotype Typhimurium confers an advantage during life in the inflamed intestine. *Cell Host Microbe* **5**, 476–486 (2010).
228. Sugimoto, K. *et al.* IL-22 ameliorates intestinal inflammation in a mouse model of ulcerative colitis. *J. Clin. Invest.* **118**, 534–544 (2008).
229. Pinto, L. G. *et al.* Joint production of IL-22 participates in the initial phase of antigen-induced arthritis through IL-1beta production. *Arthritis Res. Ther.* **17**, 235 (2015).
230. Geboes, L. *et al.* Proinflammatory Role of the Th17 Cytokine Interleukin-22 in Collagen-Induced Arthritis in C57BL / 6 Mice. *Arthritis Rheum.* **60**, 390–395 (2009).
231. Ikeuchi, H. *et al.* Expression of Interleukin-22 in Rheumatoid Arthritis Potential Role as a Proinflammatory Cytokine. *Arthritis Rheum.* **52**, 1037–1046 (2005).
232. Kim, K. *et al.* Interleukin-22 Promotes Osteoclastogenesis in Rheumatoid Arthritis Through Induction of RANKL in Human Synovial Fibroblasts. *Arthritis Rheum.* **64**, 1015–1023 (2012).
233. Wolk, K. *et al.* IL-22 regulates the expression of genes responsible for antimicrobial defense , cellular differentiation , and mobility in keratinocytes : a potential role in psoriasis. *Eur. J. Immunol.* **36**, 1309–1323 (2006).
234. Radaeva, S., Sun, R., Pan, H., Hong, F. & Gao, B. Interleukin 22 (IL-22) Plays a Protective Role in T Cell-mediated Murine Hepatitis: IL-22 Is a Survival Factor for Hepatocytes via STAT3 Activation. *Hepatology* **39**, 1332–1342 (2004).
235. Zenewicz, L. A. *et al.* Innate and Adaptive Interleukin-22 Protects Mice from Inflammatory Bowel Disease. *Immunity* **29**, 947–957 (2008).
236. Zenewicz, L. A. *et al.* Interleukin-22 but Not Interleukin-17 Provides Protection to Hepatocytes during Acute Liver Inflammation. *Immunity* **27**, 647–659 (2007).
237. Bradley, J. R. TNF-mediated inflammatory disease. *J. Pathol.* **214**, 149–160 (2008).
238. Sedger, L. M. & McDermott, M. F. TNF and TNF-receptors : From mediators of cell death and inflammation to therapeutic giants – past , present and future. *Cytokine Growth Factor Rev.* **25**, 453–472 (2014).
239. Calandra, T. & Roger, T. Macrophage migration inhibitory factor: a regulator of innate immunity. *Nat. Rev. Immunol.* **3**, 791–800 (2003).
240. Kim, K. & Kim, H. Macrophage migration inhibitory factor : a potential therapeutic target for rheumatoid arthritis. *Korean J. Intern. Med.* **31**, 634–642 (2016).
241. Foell, D., Wittkowski, H. & Roth, J. Mechanisms of Disease : a ' DAMP ' view of inflammatory arthritis. *Nat. Clin. Pract. Rheumatol.* **3**, 382–390 (2007).
242. Hofmann, M. A. *et al.* RAGE Mediates a Novel Proinflammatory Axis : A Central Cell Surface Receptor for S100 / Calgranulin Polypeptides. *Cell* **97**, 889–901 (1999).
243. Hofmann, M. *et al.* RAGE and arthritis: the G82S polymorphism amplifies the inflammatory response. *Genes Immun.* **3**, 123–135 (2002).
244. Foell, D. *et al.* Proinflammatory S100A12 can activate human monocytes via toll-like receptor 4. *Am. J. Respir. Crit. Care Med.* **187**, 1324–1334 (2013).
245. Loser, K. *et al.* The Toll-like receptor 4 ligands Mrp8 and Mrp14 are crucial in the development of autoreactive CD8 + T cells. *Nat. Med.* **16**, 713–718 (2010).
246. Reinhardt, K. *et al.* Monocyte-Induced Development of Th17 Cells and the Release of S100 Proteins Are Involved in the Pathogenesis of Graft-versus-Host Disease. *J. Immunol.* **193**, 3355–3365 (2020).
247. Schmidt, A. M., Yan, S. F. & Stern, D. M. The multiligand receptor RAGE as a progression factor amplifying immune and inflammatory responses. *J. Clin. Invest.* **108**, 949–955 (2001).
248. Lander, H. M. *et al.* Activation of the Receptor for Advanced Glycation End Products Triggers a p21 ras -dependent Mitogen-activated Protein Kinase Pathway Regulated by Oxidant Stress. *J. Biol. Chem.* **272**, 17810–17814 (1997).
249. Yeh, C. *et al.* Protein Kinases in RAGE-Mediated Nuclear Factor-kB Transcriptional Activation and Cytokine Secretion. *Diabetes* **50**, 1495–1504 (2001).
250. Holzinger, D., Foell, D. & Kessel, C. The role of S100 proteins in the pathogenesis and monitoring of autoinflammatory diseases. *Mol. Cell. Pediatr.* **5**, 7 (2018).
251. Foell, D. & Roth, J. Proinflammatory S100 Proteins in Arthritis and Autoimmune Disease. *Arthritis Rheum.* **50**, 3762–3771 (2004).
252. Foell, D. *et al.* Monitoring Neutrophil Activation in Juvenile Rheumatoid Arthritis By S100A12 Serum Concentrations. *Arthritis Rheum.* **50**, 1286–1295 (2004).
253. Frosch, M., Foell, D., Ganser, G. & Roth, J. Arthrosonography of hip and knee joints in the follow up of juvenile

rheumatoid arthritis. *Ann Rheum Dis* 242–244 (2003).
254. Canna, S. W. Interferon-gamma : Friend or Foe in Systemic Juvenile Idiopathic Arthritis and Adult-Onset Still ' s Disease? *Arthritis Rheum.* **66**, 1072–1076 (2014).
255. Billiau, A. & Matthys, P. Modes of action of Freund ' s adjuvants in experimental models of autoimmune diseases. *J. Leukoc. Biol.* **70**, 849–860 (2001).
256. Dalton, D. *et al.* Multiple defects of immune cell function in mice with disrupted interferon-gamma genes. *Science (80-.).* **259**, 1739–1742 (1993).
257. Vandenhaute, J. *et al.* Regulatory Role for NK Cells in a Mouse Model of Systemic Juvenile Idiopathic Arthritis. *J. Immunol.* **203**, 3339–3348 (2019).
258. Bettelli, E., Korn, T. & Kuchroo, V. K. Th17: the third member of the effector T cell trilogy. *Curr. Opin. Immunol.* **19**, 652–657 (2007).
259. Nauseef, W. M. & Borregaard, N. Neutrophils at work. *Nat. Immunol.* **15**, 602–11 (2014).
260. Lima, S. S. S. *et al.* Neutropenic patients and their infectious complications at a University Hospital. *Rev Bras Hematol Hemoter.* **35**, 18–22 (2013).
261. Kumar, V. & Sharma, A. Neutrophils: Cinderella of innate immune system. *Int. Immunopharmacol.* **10**, 1325–1334 (2010).
262. Borregaard, N. Neutrophils , from Marrow to Microbes. *Immunity* **33**, 657–670 (2010).
263. Tecchio, C., Micheletti, A. & Cassatella, M. A. Neutrophil-derived cytokines: Facts beyond expression. *Front. Immunol.* **5**, 508 (2014).
264. Scapini, P. & Cassatella, M. A. Social networking of human neutrophils within the immune system. *Blood* **124**, 710–720 (2017).
265. Silvestre-Roig, C., Hidalgo, A. & Soehnlein, O. Neutrophil heterogeneity: Implications for homeostasis and pathogenesis. *Blood* **127**, 2173–2181 (2016).
266. Ballesteros, I. *et al.* Co-option of Neutrophil Fates by Tissue Environments. *Cell* **183**, 1282–1297 (2020).
267. Jaillon, S. *et al.* Neutrophil diversity and plasticity in tumour progression and therapy. *Nat. Rev. Cancer* **20**, 485–503 (2020).
268. Summers, C. *et al.* Neutrophil kinetics in health and disease. *Trends Immunol.* **31**, 318–324 (2010).
269. Ley, K. *et al.* Neutrophils : New insights and open questions. *Sci. Immunol.* **3**, eaat4579 (2018).
270. Wirths, S., Bugl, S. & Kopp, H. G. Neutrophil homeostasis and its regulation by danger signaling. *Blood* **123**, 3563–3566 (2014).
271. Manz, M. G. & Boettcher, S. Emergency granulopoiesis. *Nat Rev Immunol* **14**, 302–314 (2014).
272. Baggiolini, M. Chemokines in pathology and medicine. *J. Intern. Med.* **250**, 91–104 (2001).
273. Castanheira, F. V. S. & Kubes, P. Neutrophils and NETs in modulating acute and chronic inflammation. *Blood* **133**, 2178–2185 (2019).
274. Gao, H., Ying, S. & Dai, Y. Pathological Roles of Neutrophil-Mediated Inflammation in Asthma and Its Potential for Therapy as a Target. *J. Immunol. Res.* **2017**, 3743048 (2017).
275. Kruger, P. *et al.* Neutrophils : Between Host Defence , Immune Modulation , and Tissue Injury. *PLoS Pathog.* **11**, e1004651 (2015).
276. Phillipson, M. & Kubes, P. The neutrophil in vascular inflammation. *Nat. Med.* **17**, 1381–1390 (2011).
277. Wipke, B. T. & Allen, P. M. Essential Role of Neutrophils in the Initiation and Progression of a Murine Model of Rheumatoid Arthritis. *J Immunol* **167**, 1601–1608 (2001).
278. Witko-Sarsat, V., Rieu, P., Descamps-Latscha, B., Lesavre, P. & Halbwachs-Mecarelli, L. Neutrophils : Molecules , Functions and Pathophysiolgical Aspects. *Lab. Investig.* **80**, 617–653 (2000).
279. Fodil, N., Langlais, D. & Gros, P. Primary Immunodeficiencies and Inflammatory Disease: A Growing Genetic Intersection. *Trends Immunol.* **37**, 126–140 (2017).
280. Dinauer, M. C. Inflammatory consequences of inherited disorders affecting neutrophil function. *Blood* **133**, 2130–2139 (2019).
281. Burg, N. D. & Pillinger, M. H. The Neutrophil : Function and Regulation in Innate and Humoral Immunity. *Clin. Immunol.* **99**, 7–17 (2001).
282. Bunting, M., Harris, E. S., McIntyre, T., Prescott, S. & Zimmerman, G. A. Leukocyte adhesion deficiency syndromes: adhesion and tethering defects involving β 2 integrins and selectin ligands. *Curr. Opin. Hematol.* **9**, 30–35 (2002).
283. Friedman, A. D. Transcriptional regulation of granulocyte and monocyte development. *Oncogene* **1**, 3377–3390 (2002).
284. Rosmarin, A. G., Yang, Z. & Resendes, K. K. Transcriptional regulation in myelopoiesis : Hematopoietic fate choice , myeloid differentiation , and leukemogenesis. *Exp. Hematol.* **33**, 131–143 (2005).
285. Ding, L., Saunders, T. L., Enikolopov, G. & Morrison, S. J. Endothelial and perivascular cells maintain haematopoietic stem cells. *Nature* **481**, 457–462 (2012).
286. Ding, L. & Morrison, S. J. Haematopoietic stem cells and early lymphoid progenitors occupy distinct bone marrow niches. *Nature* **495**, 231–235 (2013).
287. Cvejic, A. Mechanisms of fate decision and lineage commitment during haematopoiesis. *Immunol. Cell Biol.* **94**, 230–235 (2016).
288. Akashi, K. *et al.* Transcriptional accessibility for genes of multiple tissues and hematopoietic lineages is hierarchically controlled during early hematopoiesis. *Blood* **101**, 383–390 (2003).

289. Miyamoto, T. *et al.* Myeloid or Lymphoid Promiscuity as a Critical Step in Hematopoietic Lineage Commitment. *Dev. Cell* **3**, 137–147 (2002).
290. Nandakumar, S. K., Ulirsch, J. C. & Sankaran, V. G. Advances in understanding erythropoiesis : evolving perspectives. *Br. J. Haematol.* **173**, 206–218 (2016).
291. Notta, F. *et al.* Distinct routes of lineage development reshape the human blood hierarchy across ontogeny. *Science (80-.).* **351**, 139 (2016).
292. Paul, F. *et al.* Transcriptional Heterogeneity and Lineage Commitment in Myeloid Progenitors Article Transcriptional Heterogeneity and Lineage Commitment in Myeloid Progenitors. *Cell* **163**, 1663–1677 (2015).
293. Akashi, K., Traver, D. & Miyamoto, T. A clonogenic common myeloid progenitor that gives rise to all myeloid lineages. *Nature* **404**, 193–197 (2000).
294. Warren, L., Bryder, D., Weissman, I. L. & Quake, S. R. Transcription factor profiling in individual hematopoietic progenitors by digital RT-PCR. *Proc. Natl. Acad. Sci.* **103**, 17807–17812 (2006).
295. David, L. A. *et al.* Diet rapidly and reproducibly alters the human gut microbiome. *Nature* **505**, 559–63 (2014).
296. Ward, A. C., Loeb, D. M., Soede-bobok, A. A., Touw, I. P. & Friedman, A. D. Regulation of granulopoiesis by transcription factors and cytokine signals. *Leukemia* **14**, 973–990 (2000).
297. Mora-Jensen, H. *et al.* Technical Advance : Immunophenotypical characterization of human neutrophil differentiation. *J. Leukoc. Biol.* **90**, 629–634 (2011).
298. Klausen, P., Bjerregaard, M. D., Borregaard, N. & Cowland, J. B. End-stage differentiation of neutrophil granulocytes in vivo is accompanied by up-regulation of p27kip1 and down-regulation of CDK2, CDK4, and CDK6. *J. Leukoc. Biol.* **75**, 569–578 (2004).
299. Cowland, J. B. & Borregaard, N. Granulopoiesis and granules of human neutrophils. *Immunol. Rev.* **273**, 11–28 (2016).
300. Lawrence, S. M., Corriden, R. & Nizet, V. The Ontogeny of a Neutrophil : Mechanisms of Granulopoiesis and Homeostasis. *Microbiol. Mol. Biol. Rev.* **82**, e00057-17 (2018).
301. Xie, X. *et al.* Single-cell transcriptome profiling reveals neutrophil heterogeneity and orchestrated maturation during homeostasis and bacterial infection. *Nat Immunol.* **21**, 1119–1133 (2020).
302. Skokowa, J. *et al.* LEF-1 is crucial for neutrophil granulocytopoiesis and its expression is severely reduced in congenital neutropenia. *Nat. Med.* **12**, 1191–1198 (2006).
303. Guo, H., Ma, O., Speck, N. A. & Friedman, A. D. Runx1 deletion or dominant inhibition reduces Cebpa transcription via conserved promoter and distal enhancer sites to favor monopoiesis over granulopoiesis. *Blood* **119**, 4408–4418 (2012).
304. Johansen, L. M. *et al.* c-Myc Is a Critical Target for C/EBPa in Granulopoiesis. *Mol. Cell. Biol.* **21**, 3789–3806 (2001).
305. Wang, Q. & Friedman, A. D. CCAAT / enhancer-binding proteins are required for granulopoiesis independent of their induction of the granulocyte colony-stimulating factor receptor. *Blood* **99**, 2776–2785 (2002).
306. Obaya, A. J., Mateyak, M. K. & Sedivy, J. M. Mysterious liaisons : the relationship between c-Myc and the cell cycle. *Oncogene* **18**, 2934–2941 (1999).
307. Shahrin, N. H., Diakiw, S., Dent, L. A., Brown, A. L. & Andrea, R. J. D. Conditional knockout mice demonstrate function of Klf5 as a myeloid transcription factor. *Blood* **128**, 55–59 (2016).
308. Giladi, A. *et al.* Single-cell characterization of haematopoietic progenitors and their trajectories in homeostasis and perturbed haematopoiesis. *Nat. Cell Biol.* **20**, 836–846 (2018).
309. Olsson, A. *et al.* Single-cell analysis of mixed-lineage states leading to a binary cell fate choice. *Nature* **537**, 698–702 (2016).
310. Kurotaki, D. *et al.* IRF8 inhibits C/EBPa activity to restrain mononuclear phagocyte progenitors from differentiating into neutrophils. *Nat. Commun.* **5**, 1–15 (2014).
311. Yanez, A., Ng, M. Y., Hassanzadeh-kiabi, N. & Goodridge, H. S. Regular Article IRF8 acts in lineage-committed rather than oligopotent progenitors to control neutrophil vs monocyte production. *Blood* **125**, 1452–1459 (2015).
312. Bartels, M. *et al.* Acetylation of C/EBPe is a prerequisite for terminal neutrophil differentiation. *Blood* **125**, 1782–1792 (2015).
313. Liu, Q. & Dong, F. Gfi-1 Inhibits the Expression of Eosinophil Major Basic Protein (MBP) during G-CSF-Induced Neutrophilic Differentiation. *Int J Hematol.* **95**, 640–647 (2013).
314. Sheshachalam, A., Srivastava, N., Mitchell, T., Lacy, P. & Eitzen, G. Granule protein processing and regulated secretion in neutrophils. *Front. Immunol.* **5**, 448 (2014).
315. Bjerregaard, M. D., Jurlander, J., Klausen, P., Borregaard, N. & Cowland, J. B. The in vivo profile of transcription factors during neutrophil differentiation in human bone marrow. *Blood* **101**, 4322–4332 (2003).
316. Evrard, M. *et al.* Developmental Analysis of Bone Marrow Neutrophils Reveals Populations Specialized in Expansion , Trafficking , and Effector Functions. *Immunity* **48**, 364–379 (2018).
317. Yamanaka, R. *et al.* Impaired granulopoiesis , myelodysplasia , and early lethality in CCAAT¯enhancer binding protein e -deficient mice. *Proc. Natl. Acad. Sci.* **94**, 13187–13192 (1997).
318. Clements, W. K. *et al.* A somitic Wnt16/Notch pathway specifies haematopoietic stem cells. *Nature* **474**, 220–224 (2011).
319. Pellmé, S. *et al.* Localization of human neutrophil interleukin-8 (CXCL-8) to organelle(s) distinct from the classical granules and secretory vesicles. *J. Leukoc. Biol.* **79**, 564–573 (2006).
320. Ng, L. G., Ostuni, R. & Hidalgo, A. Heterogeneity of neutrophils. *Nat. Rev. Immunol.* **19**, 255–265 (2019).
321. Marini, O. *et al.* Mature CD10 + and immature CD10 - neutrophils present in G-CSF-treated donors display opposite

effects on T cells. *Blood* **129**, 1343–1356 (2017).
322. Kim, M., Yang, D., Kim, M., Kim, S. & Kim, D. A late-lineage murine neutrophil precursor population exhibits dynamic changes during demand- adapted granulopoiesis. *Sci. Rep.* **7**, 39804 (2017).
323. Zhu, Y. P. *et al.* Identification of an Early Unipotent Neutrophil Progenitor with Pro-tumoral Activity in Mouse and Human Bone Marrow. *Cell Rep.* **24**, 2329-2341.e8 (2018).
324. Xie, X. *et al.* Single-cell transcriptome profiling reveals neutrophil heterogeneity in homeostasis and infection. *Nat. Immunol.* **21**, 119–1133 (2020).
325. Zilionis, R. *et al.* Single-Cell Transcriptomics of Human and Mouse Lung Cancers Reveals Conserved Myeloid Populations across Individuals and Species. *Immunity* **50**, 1–18 (2019).
326. Devi, S. *et al.* Neutrophil mobilization via plerixafor- mediated CXCR4 inhibition arises from lung demargination and blockade of neutrophil homing to the bone marrow. *J. Exp. Med.* **210**, 2321–2336 (2013).
327. Kawaia, T. & Malechb, H. L. WHIM Syndrome: Congenital Immune Deficiency Disease. *Curr Opin Hematol.* **16**, 20–26 (2009).
328. Semerad, C. L. *et al.* G-CSF Is an Essential Regulator of Neutrophil Trafficking from the Bone Marrow to the Blood. *Immunity* **17**, 413–423 (2002).
329. Kim, H. K. *et al.* G-CSF down-regulation of CXCR4 expression identified as a mechanism for mobilization of myeloid cells. *Blood* **108**, 812–820 (2006).
330. Kohler, A. *et al.* G-CSF – mediated thrombopoietin release triggers neutrophil motility and mobilization from bone marrow via induction of Cxcr2 ligands. *Blood* **117**, 4349–4357 (2011).
331. Bonig, H. & Papayannopoulou, T. Hematopoietic stem cell mobilization: updated conceptual renditions. *Leukemia* **27**, 24–31 (2013).
332. Starckx, S., Van den Steen, P. E., Wuyts, A., Van Damme, J. & Opdenakker, G. Neutrophil Gelatinase B and Chemokines in Leukocytosis and Stem Cell Mobilization. *Leuk. Lymphoma* **43**, 233–241 (2002).
333. Haese, A. D. *et al.* In Vivo Neutrophil Recruitment by Granulocyte Chemotactic Protein-2 Is Assisted by Gelatinase B / MMP-9 in the Mouse. *J. Interf. cytokine Res.* **20**, 667–674 (2000).
334. Grassi, L. *et al.* Dynamics of Transcription Regulation in Human Bone Marrow Myeloid Differentiation to Mature Blood Neutrophils. *Cell Rep.* **24**, 2784–2794 (2018).
335. Doerschuk, C. M., Beyers, N., Coxson, H. O., Wiggs, B. & Hogg, J. C. Comparison of neutrophil and capillary diameters and their relation to neutrophil sequestration in the lung. *J Appl Physiol* **74**, 3040–5 (1985).
336. Price, T. H. & Dale, D. C. Neutrophil preservation : the effect of short-term storage on in vivo kinetics. *J Clin Invest* **59**, 475–480 (1977).
337. Athens, J. W. *et al.* Leukokinetic studies. IV. The total blood, circulating and marginal granulocyte pools and the granulocyte turnover rate in normal subjets. *J Clin Invest* **40**, 989–995 (1961).
338. Nauseef, W. M. & Borregaard, N. Neutrophils at work. *Nat. Immunol.* **15**, 602–11 (2014).
339. Bierman, H. R. *et al.* The Release of Leukocytes and Platelets from the Pulmonary Circulation by Epinephrine. *Blood* **7**, 683–692 (1952).
340. Bierman, H. R., Kelly, K. H., King, F. w. & Petrakis, N. L. The Pulmonary Circulation as a Source of Leucocytes and Platelets in Man. *Science (80-.).* **114**, 276–277 (1951).
341. Yipp, B. G. *et al.* The Lung is a Host Defense Niche for Immediate Neutrophil-Mediated Vascular Protection. *Sci. Immunol.* **2**, eaam8929 (2017).
342. Sadik, C. D. & Luster, A. D. Lipid-cytokine-chemokine cascades orchestrate leukocyte recruitment in inflammation. *J. Leukoc. Biol.* **91**, 207–215 (2012).
343. Petri, B. & Sanz, M. Neutrophil chemotaxis. *Cell Tissue Res.* **371**, 425–436 (2018).
344. Metzemaekers, M., Gouwy, M. & Proost, P. Neutrophil chemoattractant receptors in health and disease : double-edged swords. *Cell. Mol. Immunol.* **17**, 433–450 (2020).
345. Schramm, R. & Thorlacius, H. Neutrophil recruitment in mast cell-dependent inflammation : inhibitory mechanisms of glucocorticoids. *Inflamm. Res.* **53**, 644–652 (2004).
346. Kolaczkowska, E. & Kubes, P. Neutrophil recruitment and function in health and inflammation. *Nat. Rev. Immunol.* **13**, 159–175 (2013).
347. Ley, K., Laudanna, C., Cybulsky, M. I. & Nourshargh, S. Getting to the site of inflammation : the leukocyte adhesion cascade updated. *Nat. Rev. Immunol.* **7**, 678–689 (2007).
348. Filippi, M. Neutrophil transendothelial migration : updates and new perspectives. *Blood* **133**, 2149–2158 (2019).
349. Nourshargh, S., Hordijk, P. L. & Sixt, M. Breaching multiple barriers : leukocyte motility through venular walls and the interstitium. *Nat. Rev. Mol. Cell Biol.* **11**, 366–378 (2010).
350. Morikis, V. A. *et al.* Neutrophil Mechanosignaling Promotes Integrin Engagement With Endothelial Cells and Motility Within Inflamed Vessels. *Front. Immunol.* **9**, 1–14 (2018).
351. Maas, S. L., Soehnlein, O. & Viola, J. R. Organ-Specific Mechanisms of Transendothelial Neutrophil Migration in the Lung, Liver, Kidney, and Aorta. *Front. Immunol.* **9**, 2739 (2018).
352. Mantovani, A., Cassatella, M. a, Costantini, C. & Jaillon, S. Neutrophils in the activation and regulation of innate and adaptive immunity. *Nat. Rev. Immunol.* **11**, 519–531 (2011).
353. Miralda, I., Uriarte, S. M. & Mcleish, K. R. Multiple Phenotypic Changes Define Neutrophil Priming. *Front. Cell. Infect. Microbiol.* **7**, 217 (2017).
354. Adrover, M. *et al.* A Neutrophil Timer Coordinates Immune Defense and Vascular Protection. *Immunity* **50**, 390–402

(2019).
355. Adrover, J. M., Nicolás-ávila, J. A. & Hidalgo, A. Aging : A Temporal Dimension for Neutrophils. *Trends Immunol.* **37**, 334–345 (2016).
356. Adrover, J. M. *et al.* Programmed 'disarming' of the neutrophil proteome reduces the magnitude of inflammation. *Nat. Immunol.* **21**, 135–144 (2020).
357. Casanova-Acebes, M. *et al.* Rhythmic Modulation of the Hematopoietic Niche through Neutrophil Clearance. *Cell* **153**, 1025–1035 (2013).
358. A-Gonzalez, N. *et al.* Apoptotic Cells Promote Their Own Clearance and Immune Tolerance through Activation of the Nuclear Receptor LXR. *Immunity* **31**, 245–258 (2009).
359. Stark, M. A. *et al.* Phagocytosis of Apoptotic Neutrophils Regulates Granulopoiesis via IL-23 and IL-17. *Immunity* **22**, 285–294 (2005).
360. Amulic, B., Cazalet, C., Hayes, G. L., Metzler, K. D. & Zychlinsky, A. Neutrophil function: from mechanisms to disease. *Annu. Rev. Immunol.* **30**, 459–489 (2012).
361. Mócsai, A. Diverse novel functions of neutrophils in immunity, inflammation, and beyond. *J. Exp. Med.* **210**, 1283–99 (2013).
362. Lee, W. L., Harrison, R. E. & Grinstein, S. Phagocytosis by neutrophils. *Microbes Infect.* **5**, 1299–1306 (2003).
363. Nordenfelt, P. & Tapper, H. Phagosome dynamics during phagocytosis by neutrophils. *J. Leukoc. Biol.* **90**, 271–284 (2011).
364. Futosi, K., Fodor, S. & Mócsai, A. Neutrophil cell surface receptors and their intracellular signal transduction pathways. *Int. Immunopharmacol.* **17**, 638–650 (2013).
365. Dupuy, A. G. & Caron, E. Integrin-dependent phagocytosis – spreading from microadhesion to new concepts. *J. Cell Sci.* **121**, 1773–1783 (2008).
366. Dale, D. C., Boxer, L. & Liles, W. C. The phagocytes : neutrophils and monocytes. *Blood* **112**, 935–945 (2008).
367. Soehnlein, O. Direct and alternative antimicrobial mechanisms of neutrophil-derived granule proteins. *J Membr Biol* **87**, 1157–1164 (2009).
368. Faurschou, M. & Borregaard, N. Neutrophil granules and secretory vesicles in inflammation. *Microbes Infect.* **5**, 1317–1327 (2003).
369. Påhlman, L. I. *et al.* Streptococcal M Protein : A Multipotent and Powerful Inducer of Inflammation 1. *J. Immunol.* **177**, 1221–1228 (2006).
370. Soehnlein, O. & Lindbom, L. Phagocyte partnership during the onset and resolution of inflammation. *Nat. Rev. Immunol.* **10**, 427–439 (2010).
371. Taekema-Roelvink, M. E. J., Van Kooten, C., Van der Kooij, S., Heemskerk, E. & Daha, M. R. Proteinase 3 Enhances Endothelial Monocyte Chemoattractant Protein-1 Production and Induces Increased Adhesion of Neutrophils to Endothelial Cells by Upregulating Intercellular Cell Adhesion Molecule-1. *J. Am. Soc. Nephrol.* **8**, 932–940 (2001).
372. Soehnlein, O. *et al.* Neutrophil secretion products pave the way for inflammatory monocytes. *Blood* **112**, 1461–1471 (2008).
373. Parker, H. & Winterbourn, C. C. Reactive oxidants and myeloperoxidase and their involvement in neutrophil extracellular traps. *Front. Immunol.* **3**, 1–6 (2013).
374. Winterbourn, C. C. & Kettle, A. J. Redox Reactions and Microbial Killing in the Neutrophil Phagosome. *Antioxid. Redox Signal.* **18**, 642–660 (2013).
375. Nauseef, W. M. Biological Roles for the NOX Family NADPH Oxidases. *J. Biol. Chem.* **283**, 16961–16965 (2008).
376. Reeves, E. P. *et al.* Killing activity of neutrophils is mediated through activation of proteases by K+ flux. *Nature* **416**, 291–297 (2002).
377. Leto, T. L. & Geiszt, M. Role of Nox Family NADPH Oxidases in Host Defense. *Antioxid. Redox Signal.* **8**, 1549–1561 (2006).
378. Curnutte, J., Kpnes, R. & Babior, B. Defect in pyridine nucleotide dependent superoxide production by a particulate fraction from the cranulocytes of patients with chronic granulomatous disease. *N. Engl. J. Med.* **293**, 628–632 (1975).
379. Timar, C. I. *et al.* Antibacterial effect of microvesicles released from human neutrophilic granulocytes. *Blood* **121**, 510–518 (2013).
380. Gasser, O. & Schifferli, J. A. Activated polymorphonuclear neutrophils disseminate anti-inflammatory microparticles by ectocytosis. *Blood* **104**, 2543–2548 (2004).
381. Gasser, O., Hess, C., Miot, S., Deon, C. & Sanchez, J. Characterisation and properties of ectosomes released by human polymorphonuclear neutrophils. *Exp. Cell Res.* **285**, 243–257 (2003).
382. Angelillo-Scherrer, A. Leukocyte-Derived Microparticles in Vascular Homeostasis. *Circ. Res.* **110**, 356–369 (2012).
383. Brinkmann, V. *et al.* Neutrophil Extracellular Traps Kill Bacteria. *Science (80-.).* **303**, 1532–6 (2004).
384. Delgado-Rizo, V., Martínez-Guzmán, M. A., Iñiguez-Gutierrez, L. & Fafutis-Morris, M. Neutrophil extracellular Traps and its implications in inflammation : An Overview. *Front. Cell. Infect. Microbiol.* **8**, 1–20 (2017).
385. Schauer, C. *et al.* Aggregated neutrophil extracellular traps limit inflammation by degrading cytokines and chemokines. *Nat. Med.* **20**, 511–517 (2014).
386. Wright, H. L., Moots, R. J. & Edwards, S. W. The multifactorial role of neutrophils in rheumatoid arthritis. *Nat. Rev. Rheumatol.* **10**, 593–601 (2014).
387. Frangou, E., Vassilopoulos, D., Boletis, J. & Boumpas, D. T. Autoimmunity Reviews An emerging role of neutrophils and NETosis in chronic inflammation and fibrosis in systemic lupus erythematosus (SLE) and ANCA-associated

vasculitides (AAV): Implications for the pathogenesis and treatment. *Autoimmun. Rev.* **18**, 751–760 (2019).
388. He, Y., Yang, F. Y. & Sun, E. W. Neutrophil Extracellular Traps in Autoimmune Diseases. *Chinese Midical J.* **131**, 1513–1519 (2018).
389. Salemme, R., Peralta, L. N., Meka, S. H. & Pushpanathan, N. The Role of NETosis in Systemic Lupus Erythematosus. *J Cell Immunol* **1**, 33–42 (2019).
390. De Candia, E. NETosis in arterial and venous thrombosis : a one size fits all mechanism? *Intern. Emerg. Med.* **12**, 9–11 (2017).
391. Moschonas, I. C. & Tselepis, A. D. The pathway of neutrophil extracellular traps towards atherosclerosis and thrombosis. *Atherosclerosis* **288**, 9–16 (2019).
392. Martinod, K. & Wagner, D. D. Thrombosis : tangled up in NETs. *Blood* **123**, 2768–2776 (2014).
393. Collison, J. Preventing NETosis to reduce thrombosis. *Nat. Rev. Rheumatol.* **15**, 317 (2019).
394. Berthelot, J., Le, B., Neel, A. & Maugars, Y. NETosis : At the crossroads of rheumatoid arthritis , lupus , and vasculitis. *Jt. Bone Spine* **84**, 255–262 (2017).
395. Grayson, P. C. & Kaplan, M. J. At the Bench : Neutrophil extracellular traps (NETs) highlight novel aspects of innate immune system involvement in autoimmune diseases. *J. Leukoc. Biol.* **99**, 253–264 (2016).
396. Branzk, N. & Papayannopoulos, V. Molecular mechanisms regulating NETosis in infection and disease. *Semin. Immunopathol.* **35**, 513–530 (2013).
397. Cassatella, M. A. Neutrophil-Derived Proteins : Selling Cytokines by the Pound. *Adv. Immunol.* **73**, 369–509 (1999).
398. Tecchio, C. & Cassatella, M. A. Neutrophil-derived chemokines on the road to immunity. *Semin. Immunol.* **28**, 119–128 (2016).
399. Scapini, P., Lapinet-vera, J. A. & Cassatella, M. A. The neutrophil as a cellular source of chemokines. *Immunol. Rev.* **177**, 195–203 (2000).
400. Sica, A. *et al.* IL-1 transcriptionally activates the neutrophil chemotactic factor / IL-8 gene in endothelial cells. *Immunology* **199**, 548–553 (1990).
401. Kasama, T. *et al.* Neutrophil-Derived Cytokines: Potential Therapeutic Targets in Inflammation. *Curr. Drug Targets - Inflamm. Allergy* **4**, 273–279 (2005).
402. Benigni, G. *et al.* CXCR3/CXCL10 Axis Regulates Neutrophil − NK Cell Cross-Talk Determining the Severity of Experimental Osteoarthritis. *J. Immunol.* **198**, 2115–2124 (2017).
403. Nathan, C. Neutrophils and immunity: challenges and opportunities. *Nat. Rev. Immunol.* **6**, 173–182 (2006).
404. Subrahmanyam, Y. V. B. K. *et al.* RNA expression patterns change dramatically in human neutrophils exposed to bacteria. *Blood* **97**, 2457–2468 (2001).
405. Kobayashi, S. D., Voyich, J. M., Buhl, C. L., Stahl, R. M. & Deleo, F. R. Global changes in gene expression by human polymorphonuclear leukocytes during receptor-mediated phagocytosis : Cell fate is regulated at the level of gene expression. *Proc. Natl. Acad. Sci.* **99**, 6901–6906 (2002).
406. Meyer-Hoffert, U. & Wiedow, O. Neutrophil serine proteases : mediators of innate immune responses. *Curr. Opin. Hematol.* **18**, 19–24 (2011).
407. Pekarek, B. L. A., Starr, B. A., Toledano, A. Y. & Schreiber, H. Inhibition o f Tumor Growth by Elimination o f Granulocytes. *J. Exp. Med.* **181**, 435–440 (1995).
408. Tecchio, C., Scapini, P., Pizzolo, G. & Cassatella, M. A. On the cytokines produced by human neutrophils in tumors. *Semin. Cancer Biol.* **23**, 159–170 (2013).
409. Puga, I. *et al.* B cell – helper neutrophils stimulate the diversification and production of immunoglobulin in the marginal zone of the spleen. *Nat. Immunol.* **13**, 170–180 (2013).
410. Schwaller, J. *et al.* Neutrophil-derived APRIL concentrated in tumor lesions by proteoglycans correlates with human B-cell lymphoma aggressiveness. *Blood* **109**, 331–338 (2007).
411. Huard, B. *et al.* APRIL secreted by neutrophils binds to heparan sulfate proteoglycans to create plasma cell niches in human mucosa Find the latest version : APRIL secreted by neutrophils binds to heparan sulfate proteoglycans to create plasma cell niches in human mucosa. *J. Clin. Invest.* **8**, 2887–2895 (2010).
412. Scapini, P., Bazzoni, F. & Cassatella, M. A. Regulation of B-cell-activating factor (BAFF)/ B lymphocyte stimulator (BLyS) expression in human neutrophils. *Immunol. Lett.* **116**, 1–6 (2008).
413. Bennouna, S. & Denkers, E. Y. Microbial Antigen Triggers Rapid Mobilization of TNFα to the Surface of Mouse Neutrophils Transforming Them into Inducers of High-Level Dendritic Cell TNFα Production. *J. Immunol.* **174**, 4845–4851 (2005).
414. Van Gisbergen, K. P. J. M., Sanchez-hernandez, M., Geijtenbeek, T. B. H. & Van Kooyk, Y. Neutrophils mediate immune modulation of dendritic cells through glycosylation- dependent interactions between Mac-1 and DC-SIGN. *J. Exp. Med.* **201**, 1281–1292 (2005).
415. Megiovanni, A. M. *et al.* Polymorphonuclear neutrophils deliver activation signals and antigenic molecules to dendritic cells : a new link between leukocytes upstream of T lymphocytes and mutually influence the two leukocyte popula- cesses occurring upstream of the interactions be. *J. Leukoc. Biol.* **79**, 977–988 (2006).
416. Charmoy, M., Auderset, F., Allenbach, C. & Tacchini-Cottier, F. The Prominent Role of Neutrophils during the Initial Phase of Infection by Leishmania Parasites. *J. ofBiomedicine Biotechnol.* **2010**, 719361 (2010).
417. Beauvillain, C. *et al.* CCR7 is involved in the migration of neutrophils to lymph nodes. *Blood* **117**, 1196–204 (2011).
418. Abadie, V. *et al.* Neutrophils rapidly migrate via lymphatics after Mycobacterium bovis BCG intradermal vaccination and shuttle live bacilli to the draining lymph nodes. *Blood* **106**, 1843–1850 (2005).

419. Balazs, M., Martin, F., Zhou, T. & Kearney, J. F. Blood Dendritic Cells Interact with Splenic Marginal Zone B Cells to Initiate T-Independent Immune Responses. *Immunity* **17**, 341–352 (2002).
420. Duffy, D. *et al.* Neutrophils Transport Antigen from the Dermis to the Bone Marrow , Initiating a Source of Memory CD8+ T cells. *Immunity* **37**, 917–929 (2012).
421. Matsushima, H. *et al.* Neutrophil differentiation into a unique hybrid population exhibiting dual phenotype and functionality of neutrophils and dendritic cells. *Blood* **121**, 1677–1689 (2013).
422. Müller, I., Munder, M., Kropf, P. & Hänsch, G. M. Polymorphonuclear neutrophils and T lymphocytes : strange bedfellows or brothers in arms ? *Trends Immunol.* **30**, 522–530 (2009).
423. Geng, S. *et al.* Emergence , origin , and function of neutrophil-dendritic cell hybrids in experimentally induced inflammatory lesions in mice. *Blood* **121**, 1690–1700 (2013).
424. Peters, J. H. *et al.* Signals required for differentiating dendritic cells from human monocytes in vitro. *Adv. Exp. Med. Biol.* **329**, 275–276 (1993).
425. Gabrilovich, D. I. & Nagaraj, S. Myeloid-derived suppressor cells as regulators of the immune system. *Nat. Rev. Cancer* **9**, 162–174 (2009).
426. Pillay, J. *et al.* A subset of neutrophils in human systemic inflammation inhibits T cell responses through Mac-1 A subset of neutrophils in human systemic inflammation inhibits T cell responses through Mac-1. *J. Clin. Invest.* **122**, 327–336 (2012).
427. Coffelt, S. B. *et al.* IL-17-producing gamma delta T cells and neutrophils conspire to promote breast cancer metastasis. *Nature* **522**, 345–348 (2015).
428. Schmielau, J. & Finn, O. J. Activated Granulocytes and Granulocyte-derived Hydrogen Peroxide Are the Underlying Mechanism of Suppression of T-Cell Function in Advanced. *Cancer Res.* **61**, 4756–4760 (2001).
429. Munder, M. *et al.* Suppression of T-cell functions by human granulocyte arginase. *Blood* **108**, 1627–1634 (2006).
430. de Kleijn, S. *et al.* IFN-γ-Stimulated Neutrophils Suppress Lymphocyte Proliferation through Expression of PD-L1. *PLoS One* **8**, e72249 (2013).
431. Pillay, J. *et al.* A subset of neutrophils in human systemic inflammation inhibits T cell responses through Mac-1. **122**, 327–336 (2012).
432. Jaeger, B. N. *et al.* Neutrophil depletion impairs natural killer cell maturation , function , and homeostasis. *J. Exp. Med.* **209**, 565–580 (2012).
433. Chakravarti, A., Raquil, M., Tessier, P. & Poubelle, P. E. Surface RANKL of Toll-like receptor 4 – stimulated human neutrophils activates osteoclastic bone resorption. *Blood* **114**, 1633–1644 (2009).
434. Silvestre-Roig, C., Hidalgo, A. & Soehnlein, O. Neutrophil heterogeneity: implications for homeostasis and pathogenesis. *Blood* **127**, 2173–2182 (2017).
435. Garley, M. & Jabłońska, E. Heterogeneity Among Neutrophils. *Arch. Immunol. Ther. Exp. (Warsz).* **66**, 21–30 (2018).
436. Bonavita, O. *et al.* Flow Cytometry Detection of Chemokine Receptors for the Identification of Murine Monocyte and Neutrophil Subsets. *Methods Enzymol.* **570**, 441–456 (2016).
437. Becher, B. *et al.* High-dimensional analysis of the murine myeloid cell system. *Nat. Immunol.* **15**, 1181–1189 (2014).
438. Deniset, J. F. & Kubes, P. Neutrophil heterogeneity : Bona fide subsets or polarization states? *J Leukoc Biol.* **103**, 829–838 (2018).
439. Fridlender, Z. G. *et al.* Polarization of Tumor-Associated Neutrophil Phenotype by TGF-beta : ‘“ N1 ”’ versus ‘“ N2 ”’ TAN. *Cancer Cell* **16**, 183–194 (2009).
440. Piccard, H., Muschel, R. J. & Opdenakker, G. On the dual roles and polarized phenotypes of neutrophils in tumor development and progression. *Crit. Rev. Oncol. Hematol.* **82**, 296–309 (2012).
441. Mishalian, I., Granot, Z. & Fridlender, Z. G. Immunobiology The diversity of circulating neutrophils in cancer. *Immunobiology* **222**, 82–88 (2017).
442. Shaul, M. E. & Fridlender, Z. G. Cancer related circulating and tumor-associated neutrophils - subtypes, sources and function. *FEBS J.* **285**, 4316–4342 (2018).
443. Granot, Z. & Jablonska, J. Distinct Functions of Neutrophil in Cancer and Its Regulation. *Mediators Inflamm.* **2015**, 1–11 (2015).
444. Giese, M. A., Hind, L. E. & Huttenlocher, A. Neutrophil plasticity in the tumor microenvironment. *Blood* **133**, 2159–2167 (2019).
445. Sionov, R. V., Fridlender, Z. G. & Granot, Z. The Multifaceted Roles Neutrophils Play in the Tumor Microenvironment. *Cancer Microenviron.* **8**, 125–158 (2015).
446. Rosales, C. Neutrophil : A Cell with Many Roles in Inflammation or Several Cell Types ? *Front. Physiol.* **9**, 113 (2018).
447. Fridlender, Z. G. & Albelda, S. M. Tumor-associated neutrophils : friend or foe? *Carcinogenesis* **33**, 949–955 (2012).
448. Youn, J. I., Nagaraj, S., Collazo, M. & Gabrilovich, D. I. Subsets of myeloid-derived suppressor cells in tumor-bearing mice . *J. Immunol. (Baltimore, Md. 1950)* **181**, 5791–5802 (2008).
449. Pillay, J., Tak, T., Kamp, V. M. & Koenderman, L. Immune suppression by neutrophils and granulocytic myeloid-derived suppressor cells: Similarities and differences. *Cell. Mol. Life Sci.* **70**, 3813–3827 (2013).
450. Oliveira, S. De, Rosowski, E. E. & Huttenlocher, A. Neutrophil migration in infection and wound repair : going forward in reverse. *Nat. Publ. Gr.* **16**, 378–391 (2016).
451. Buckley, C. D. *et al.* Identification of a phenotypically and functionally distinct population of long-lived neutrophils in a model of reverse endothelial migration. *J. Leukoc. Biol.* **79**, 303–311 (2006).
452. Christoffersson, G. *et al.* VEGF-A recruits a proangiogenic MMP-9 – delivering neutrophil subset that induces

angiogenesis in transplanted hypoxic tissue. *Blood* **120**, 4653–4662 (2012).
453. Massena, S. *et al.* Identification and characterization of VEGF-A- responsive neutrophils expressing CD49d , VEGFR1 , and CXCR4 in mice and humans. *Blood* **126**, 2016–2026 (2016).
454. Kaplan, M. J. Neutrophils in the pathogenesis and manifestations of SLE. *Nat. Rev. Rheumatol.* **7**, 691–699 (2011).
455. Hacbarth, E. & Kajdacsy-Balla, a. Low density neutrophils in patients with systemic lupus erythematosus, rheumatoid arthritis, and acute rheumatic fever. *Arthritis Rheum.* **29**, 1334–42 (1986).
456. Carmona-Rivera, C. & Kaplan, M. J. Low-density granulocytes: A distinct class of neutrophils in systemic autoimmunity. *Semin. Immunopathol.* **35**, 455–463 (2013).
457. Chakravarti, A., Rusu, D., Flamand, N., Borgeat, P. & Poubelle, P. E. Reprogramming of a subpopulation of human blood neutrophils by prolonged exposure to cytokines. *Lab. Investig.* **89**, 1084–1099 (2009).
458. Silvestre-Roig, C., Fridlender, Z. G., Glogauer, M. & Scapini, P. Neutrophil Diversity in Health and Disease. *Trends Immunol.* **40**, 565–583 (2019).
459. Chatfield, S. M. & Thieblemont, N. Expanding Neutrophil Horizons : New Concepts in Inflammation. *J. Innatre Immun.* **10**, 422–431 (2018).
460. Christoffersson, G. & Phillipson, M. The neutrophil : one cell on many missions or many cells with different agendas ? *Cell Tissue Res.* **371**, 415–423 (2018).
461. Hellebrekers, P., Vrisekoop, N. & Koenderman, L. Neutrophil phenotypes in health and disease. *Eur J Clin Invest.* **48**, e12943 (2018).
462. Manz, M. G. & Boettcher, S. Emergency granulopoiesis. *Nat Rev Immunol* **14**, 302–314 (2014).
463. Cain, D. W., Snowden, P. B., Sempowski, G. D. & Kelsoe, G. Inflammation triggers emergency granulopoiesis through a density-dependent feedback mechanism. *PLoS One* **6**, e19957 (2011).
464. Solinas, G., Germano, G., Mantovani, A. & Allavena, P. Tumor-associated macrophages (TAM) as major players of the cancer-related inflammation. *J. Leukoc. Biol.* **86**, 1065–1073 (2009).
465. Gabrilovich, D. I., Ostrand-rosenberg, S. & Bronte, V. Coordinated regulation of myeloid cells by tumours. *Nat. Rev. Immunol.* **12**, 253–268 (2012).
466. Cortez-Retamozo, V. *et al.* Origins of tumor-associated macrophages and neutrophils. *Proc. Natl. Acad. Sci.* **109**, 2491–2496 (2012).
467. Fujii, W. *et al.* Myeloid-Derived Suppressor Cells Play Crucial Roles in the Regulation of Mouse Collagen-Induced Arthritis. *J. Immunol.* **191**, 1073–1081 (2013).
468. Croker, B. A., Silke, J. & Gerlic, M. Fight or Flight - Regulation of Emergency Hematopoiesis by Pyroptosis and Necroptosis. *Curr. Opin. Hematol.* **22**, 293–301 (2016).
469. Boettcher, S. & Manz, M. G. Regulation of Inflammation- and Infection-Driven Hematopoiesis. *Trends Immunol.* **38**, 345–357 (2017).
470. Boettcher, S. *et al.* Cutting Edge: LPS-Induced Emergency Myelopoiesis Depends on TLR4-Expressing Nonhematopoietic Cells. *J. Immunol.* **188**, 5824–5828 (2012).
471. Nagai, Y. *et al.* Toll-like Receptors on Hematopoietic Progenitor Cells Stimulate Innate Immune System Replenishment. *Immunity* **24**, 801–812 (2006).
472. Chicha, L., Jarrossay, D. & Manz, M. G. Clonal Type I Interferon – producing and Dendritic Cell Precursors Are Contained in Both Human Lymphoid and Myeloid Progenitor Populations. *J. Exp. Med.* **200**, 1519–1524 (2004).
473. Luca, K. De *et al.* The TLR1 / 2 agonist PAM 3 CSK 4 instructs commitment of human hematopoietic stem cells to a myeloid cell fate. *Leukemia* **23**, 2063–2074 (2009).
474. Sioud, M. & Fløisand, Y. TLR agonists induce the differentiation of human bone capable of inducing a Th1-type response. *Eur. J. Clin. Invest.* **37**, 2834–2846 (2007).
475. Sioud, M., Fløisand, Y., Forfang, L. & Lund-Johansen, F. Signaling through Toll-like Receptor 7 / 8 Induces the Differentiation of Human Bone Marrow CD34 + Progenitor Cells along the Myeloid Lineage. *J. Mol. Biol.* **364**, 945–954 (2006).
476. Schmid, M. A. *et al.* Bone marrow dendritic cell progenitors sense pathogens via Toll-like receptors and subsequently migrate to inflamed lymph nodes. *Blood* **118**, 4829–4840 (2011).
477. Bugl, S. *et al.* Steady-state neutrophil homeostasis is dependent on TLR4/TRIF signaling. *Blood* **121**, 723–733 (2013).
478. Burberry, A. *et al.* Infection Mobilizes Hematopoietic Stem Cells through Cooperative NOD-like Receptor and Toll-like Receptor Signaling. *Cell Host Microbe* **15**, 779–791 (2014).
479. Schürch, C. M., Riether, C. & Ochsenbein, A. F. Cytotoxic CD8 + T Cells Stimulate Hematopoietic Progenitors by Promoting Cytokine Release from Bone Marrow Mesenchymal Stromal Cells. *Cell Stem Cell* **14**, 460–472 (2014).
480. Watari, K. *et al.* Serum granulocyte colony-stimulating factor levels in healthy volunteers and patients with various disorders as estimated by enzyme immunoassay. *Blood* **73**, 117–22 (1989).
481. Kawakami, M. *et al.* Levels of serum granulocyte colony-stimulating factor in patients with infections. *Blood* **76**, 1962–4 (1990).
482. Cebon, J., Layton, J. E., Maher, D. & Morstyn, G. Endogenous haemopoietic growth factors in neutropenia and infection. *Br. J. Haematol.* **86**, 265–274 (1994).
483. Cheers, C. *et al.* Production of Colony-Stimulating Factors (CSFs) during Infection : Separate Determinations of Macrophage-, Granulocyte-,Granulocyte-Macrophage-, and Multi-CSFs. *Infect. Immun.* **56**, 247–251 (1988).
484. Selig, C. & Nothdurft, W. Cytokines and Progenitor Cells of Granulocytopoiesis in Peripheral Blood of Patients with Bacterial Infections. *Infect. Immun.* **63**, 104–109 (1995).

485. Presneill, J. *et al.* Plasma granulocyte colony-stimulating factor and granulocyte-macrophage colony-stimulating factor levels in critical illness including sepsis and septic shock: Relation to disease severity, multiple organ dysfunction, and mortality. *Crit. Care Med.* **28**, 2344–2354 (2000).
486. Waring, P. M. *et al.* Differential alterations in plasma colony-stimulating factor concentrations in meningococcaemia. *Clin Exp Immunol* **102**, 501–506 (1995).
487. Tanaka, H., Ishikawa, K., Nishino, M., Shimazu, T. & Yoshioka, T. Changes in Granulocyte Colony-Stimulating Factor Concentration in Patients with Trauma and Sepsis. *J. Trauma Inj. Infect. Crit. Care* **40**, 718–726 (1996).
488. Honda, T., Uehara, T., Matsumoto, G., Arai, S. & Sugano, M. Neutrophil left shift and white blood cell count as markers of bacterial infection. *Clin. Chim. Acta* **457**, 46–53 (2016).
489. Cavallazzi, R., Bennin, C., Hirani, A., Gilbert, C. & Marik, P. E. Is the Band Count Useful in the Diagnosis of Infection ? An Accuracy Study in Critically Ill Patients. *J. Intensive Care Med.* **25**, 353–357 (2010).
490. Mare, T. A. *et al.* The diagnostic and prognostic significance of monitoring blood levels of immature neutrophils in patients with systemic inflammation. *Crit. Care* **19**, 57 (2015).
491. Leliefeld, P. H. C. *et al.* Differential antibacterial control by neutrophil subsets. *Blood Adv.* **2**, 1344–1355 (2018).
492. Tak, T. *et al.* Human CD62L dim neutrophils identified as a separate subset by proteome pro fi ling and in vivo pulse-chase labeling. *Blood* **129**, 3476–3485 (2017).
493. Hirai, H. *et al.* C/EBPbeta is required for 'emergency' granulopoiesis. *Nat. Immunol.* **7**, 732–739 (2006).
494. Satake, S. *et al.* C/EBP β Is Involved in the Amplification of Early Granulocyte Precursors during Candidemia-Induced '"Emergency"' Granulopoiesis. *J. Immunol.* **189**, 4546–4555 (2012).
495. Hayashi, Y. *et al.* C/EBPbeta promotes BCR-ABL-mediated myeloid expansion and leukemic stem cell exhaustion. *Leukemia* **27**, 619–628 (2013).
496. Hirai, H., Yokota, A., Tamura, A., Sato, A. & Maekawa, T. Non-steady-state hematopoiesis regulated by the C/EBPβ transcription factor. *Cancer Sci.* **106**, 797–802 (2015).
497. Bugl, S. *et al.* Steady-state neutrophil homeostasis is dependent on TLR4 / TRIF signaling. **121**, 723–734 (2017).
498. Hirai, H. *et al.* Cyclic AMP Responsive Element Binding Proteins Are Involved in ' Emergency ' Granulopoiesis through the Upregulation of CCAAT / Enhancer Binding Protein beta. *PLoS One* **8**, e54862 (2013).
499. Kim, M. *et al.* Neutrophil survival and c-kit ƨ -progenitor proliferation in Staphylococcus aureus – infected skin wounds promote resolution. *Blood* **117**, 3343–3352 (2011).
500. Jones, L. C. *et al.* Expression of C / EBPbeta from the C/ebpapha gene locus is sufficient for normal hematopoiesis in vivo. *Blood* **99**, 2032–2036 (2002).
501. Porse, B. T., Pedersen, T. A., Xu, X., Lindberg, B. & Wewer, U. M. E2F Repression by C/EBPalpha Is Required for Adipogenesis and Granulopoiesis In Vivo. *Cell* **107**, 247–258 (2001).
502. Wang, H. *et al.* C / EBPalpha Arrests Cell Proliferation through Direct Inhibition of Cdk2 and Cdk4. *Mol. Cell* **8**, 817–828 (2001).
503. Sebastian, T. & Johnson, P. F. Stop and Go: Anti-proliferative and Mitogenic Functions of the Transcription Factor C/EBPbeta. *Cell Cycle* **5**, 953–957 (2006).
504. Akagi, T. *et al.* Impaired response to GM-CSF and G-CSF , and enhanced apoptosis in C/EBPbeta-deficient hematopoietic cells. *Blood* **111**, 2999–3004 (2008).
505. Zhang, H. *et al.* STAT3 controls myeloid progenitor growth during emergency granulopoiesis. *Blood* **116**, 2462–2471 (2010).
506. Hall, C. J. *et al.* Infection-Responsive Expansion of the Hematopoietic Stem and Progenitor Cell Compartment in Zebrafish Is Dependent upon Inducible Nitric Oxide. *Cell Stem Cell* **10**, 198–209 (2012).
507. Kim, C. H. Homeostatic and pathogenic extramedullary hematopoiesis. *J. Blood Med.* **1**, 13–9 (2010).
508. Hosseinzadeh, M., Omidifar, N. & Kumar, P. V. Pulmonary Extramedullary Hematopoiesis in a Patient with Chronic Asthma Resembling Lung Cancer: A Case Report. *Case Rep. Med.* 3–6 (2012). doi:10.1155/2012/231787
509. Koch, C. A., Li, C.-Y., Mesa, R. A. & Tefferi, A. Nonhepatosplenic Extramedullary Hematopoiesis: Associated Diseases, Pathology, Clinical Course, and Treatment. *Mayo Clin. Proc.* **78**, 1223–1233 (2003).
510. Johns, J. L. & Christopher, M. M. Extramedullary Hematopoiesis: A New Look at the Underlying Stem Cell Niche , Theories of Development , and Occurrence in Animals. *Vet. Pathol.* **49**, 508–523 (2012).
511. Lefrançais, E. *et al.* The lung is a site of platelet biogenesis and a reservoir for haematopoietic progenitors. *Nature* **544**, 105–109 (2017).
512. Tubo, N. *et al.* Immunosurveillance by Hematopoietic Progenitor Cells Trafficking through Blood, Lymph, and Peripheral Tissues. *Cell* **131**, 994–1008 (2007).
513. Inra, C. N. *et al.* A perisinusoidal niche for extramedullary haematopoiesis in the spleen. *Nature* **527**, 466–471 (2015).
514. Yvan-Charvet, L. & Ng, L. G. Granulopoiesis and Neutrophil Homeostasis : A Metabolic , Daily Balancing Act. *Trends Immunol.* **40**, 598–612 (2019).
515. Robbins, C. S. & Swirski, F. K. The multiple roles of monocyte subsets in steady state and inflammation. *Cell. Mol. Life Sci.* **67**, 2685–2693 (2010).
516. Wu, C. *et al.* Spleen mediates a distinct hematopoietic progenitor response supporting tumor- promoting myelopoiesis Find the latest version : Spleen mediates a distinct hematopoietic progenitor response supporting tumor-promoting myelopoiesis. *J. Clin. Invest.* **128**, 3425–3438 (2018).
517. Alshetaiwi, H. *et al.* Defining the emergence of myeloid-derived suppressor cells in breast cancer using single-cell transcriptomics. *Sci Immunol.* **5**, eaay6017 (2020).

518. Marigo, I. *et al.* Tumor-Induced Tolerance and Immune Suppression Depend on the C/EBPbeta Transcription Factor. *Immunity* **32**, 790–802 (2010).
519. Lechner, M. G. *et al.* Functional characterization of human Cd33 + And Cd11b + myeloid-derived suppressor cell subsets induced from peripheral blood mononuclear cells co-cultured with a diverse set of human tumor cell lines. *J. Transl. Med.* **9**, 90 (2011).
520. Sivakumar, R. G-CSF: A Friend or Foe? *Immunome Res.* **01**, 1–8 (2014).
521. Roberts, A. W. G-CSF: A key regulator of neutrophil production, but that's not all! *Growth Factors* **23**, 33–41 (2005).
522. Metcalf, D. Hematopoietic cytokines. *Blood* **111**, 485–491 (2008).
523. Nicola, N. A., Metcalf, D., Johnson, G. R. & Burgess, A. W. Separation of functionally distinct human granulocyte-macrophage colony-stimulating factors. *Blood* **54**, 614–27 (1979).
524. Liu, F., Wu, H. Y., Wesselschmidt, R., Kornaga, T. & Link, D. C. Impaired Production and Increased Apoptosis of Neutrophils in Granulocyte Colony-Stimulating Factor Receptor – Deficient Mice. *Immunity* **5**, 491–501 (1996).
525. Lieschke, G. J. *et al.* Mice lacking granulocyte colony-stimulating factor have chronic neutropenia, granulocyte and macrophage progenitor cell deficiency, and impaired neutrophil mobilization. *Blood* **84**, 1737–46 (1994).
526. Richards, M. K., Liu, F., Iwasaki, H., Akashi, K. & Link, D. C. Pivotal role of granulocyte colony-stimulating factor in the development of progenitors in the common myeloid pathway. *Blood* **102**, 3562–3568 (2003).
527. Lord, B. I. *et al.* The kinetics of human granulopoiesis following treatment with granulocyte colony-stimulating factor in vivo. *Proc. Natl. Acad. Sci.* **86**, 9499–9503 (1989).
528. Basu, S., Hodgson, G., Katz, M. & Dunn, A. R. Evaluation of role of G-CSF in the production , survival , and release of neutrophils from bone marrow into circulation. *Blood* **100**, 854–861 (2008).
529. Brühl, H., Cohen, C. D., Linder, S., Kretzler, M. & Mack, M. Post-translational and cell type-specific regulation of CXCR4 expression by cytokines. *Eur. J. Immunol.* **33**, 3028–3037 (2003).
530. Nagase, H. *et al.* Cytokine-mediated regulation of CXCR4 expression in human neutrophils. *J. Leukoc. Biol.* **71**, 711–717 (2002).
531. Petit, I. *et al.* G-CSF induces stem cell mobilization by decreasing bone marrow SDF-1 and up-regulating CXCR4. *Nat. Immunol.* **3**, 687–694 (2002).
532. Bajrami, B. *et al.* G-CSF maintains controlled neutrophil mobilization during acute inflammation by negatively regulating CXCR2 signaling. *J. Exp. Med.* **213**, 1999–2018 (2016).
533. Spiekermann, K., Roesler, J., Emmendoerffer, A., Elsner, J. & Welte, K. Functional features of neutrophils induced by G-CSF and GM-CSF treatment: Differential effects and clinical implications. *Leukemia* **11**, 466–78 (1997).
534. Altznauer, F. *et al.* Inflammation-associated Cell Cycle – independent Block of Apoptosis by Survivin in Terminally Differentiated Neutrophils. *J. Exp. Med.* **199**, 1343–1354 (2004).
535. Colotta, F., Re, F., Polentarutti, N., Sozzani, S. & Mantovani, A. Modulation of granulocyte survival and programmed cell death by cytokines and bacterial products. *Blood* **80**, 2012–20 (1992).
536. Kawano, Y. *et al.* G-CSF-induced sympathetic tone provokes fever and primes antimobilizing functions of neutrophils via PGE 2. *Blood* **129**, 587–597 (2017).
537. Chow, A. *et al.* Bone marrow CD169+ macrophages promote the retention of hematopoietic stem and progenitor cells in the mesenchymal stem cell niche. *J. Exp. Med.* **208**, 261–271 (2010).
538. Semerad, C. L. *et al.* G-CSF potently inhibits osteoblast activity and CXCL12 mRNA expression in the bone marrow. *Blood* **106**, 3020–3027 (2005).
539. Schlahsa, L., Jaimes, Y., Blasczyk, R. & Figueiredo, C. Granulocyte-colony-stimulatory factor: A strong inhibitor of natural killer cell function. *Transfusion* **51**, 293–305 (2011).
540. Morris, K. T. *et al.* Anti-G-CSF treatment induces protective tumor immunity in mouse colon cancer by promoting protective NK cell, macrophage and T cell responses. *Oncotarget* **6**, 22338–22347 (2015).
541. Sano, E. *et al.* A Possible Role of Autogenous IFN-b for Cytokine Productions in Human Fibroblasts. *J. Cell. Biochem.* **100**, 1459–1476 (2007).
542. Fossiez, F. *et al.* T Cell Interleukin-17 Induces Stromal Cells to Produce Proinflammatory and Hematopoietic Cytokines. *J. Exp. Med.* **183**, 2593–260 (1996).
543. Panopoulos, A. D. & Watowich, S. S. Granulocyte colony-stimulating factor : Molecular mechanisms of action during steady state and 'emergency' hematopoiesis. *Cytokine* **42**, 277–288 (2008).
544. Watari, K. *et al.* Production of Human Granulocyte Colony Stimulating Factor by Various Kinds of Stromal Cells In Vitro Detected by Enzyme Immunoassay and In Situ Hybridization. *Stem Cells* **12**, 416–423 (1994).
545. Eyles, J. L. *et al.* A key role for G-CSF – induced neutrophil production and trafficking during inflammatory arthritis. *Blood* **112**, 5193–5202 (2008).
546. Lord, B. I. *et al.* Myeloid cell kinetics in mice treated with recombinant interleukin-3, granulocyte colony-stimulating factor (CSF), or granulocyte-macrophage CSF in vivo. *Blood* **77**, 2154–9 (1991).
547. Boettcher, S. *et al.* Endothelial cells translate pathogen signals into G-CSF-driven emergency granulopoiesis. *Blood* **124**, 1393–403 (2014).
548. Demetri, G. D. & Griffin, J. D. Granulocyte colony-stimulating factor and its receptor. *Blood* **78**, 2791–808 (1991).
549. Nicholson, S. E., Starr, R., Novak, U., Hilton, D. J. & Layton, J. E. Tyrosine Residues in the Granulocyte Colony-stimulating Factor (G-CSF) Receptor Mediate G-CSF-induced Differentiation of Murine Myeloid Leukemic (M1) Cells. *J. Biol. Chem.* **271**, 26947–26953 (1996).
550. Novak, U., Ward, A. C., Hertzog, P. J., Hamilton, J. A. & Paradiso, L. Aberrant Activation of JAK/STAT Pathway

Components in Response to G-CSF, Interferon-a/p and Interferon-y in NFS-60 Cells. *Growth Factors* **13**, 251–260 (1996).
551. Ward, B. A. C. *et al.* Tyrosine-Dependent and -Independent Mechanisms of STAT3 Activation by the Human Granulocyte Colony-Stimulating Factor (G-CSF) Receptor Are Differentially Utilized Depending on G-CSF Concentration. *Blood* **93**, 113–124 (1999).
552. Ward, A. C., van Aesch, Y. M., Schelen, A. M. & Touw, I. P. Defective internalization and sustained activation of truncated granulocyte colony-stimulating factor receptor found in severe congenital neutropenia/acute myeloid leukemia. *Blood* **93**, 447–58 (1999).
553. O'Shea, J. J., Gadina, M. & Schreiber, R. D. Cytokine Signaling in 2002 : New Surprises in the Jak / Stat Pathway. *Cell* **109**, 121–131 (2002).
554. Snow, J. W. *et al.* STAT5 promotes multilineage hematolymphoid development in vivo through effects on early hematopoietic progenitor cells. *Blood* **99**, 95–101 (2002).
555. Moriggl, R. *et al.* Stat5 tetramer formation is associated with leukemogenesis. *Cancer Cell* **7**, 87–99 (2005).
556. Bunting, K. D. *et al.* Reduced lymphomyeloid repopulating activity from adult bone marrow and fetal liver of mice lacking expression of STAT5. *Blood* **99**, 479–487 (2002).
557. Teglund, S. *et al.* Stat5a and Stat5b Proteins Have Essential and Nonessential, or Redundant, Roles in Cytokine Responses. *Cell* **93**, 841–850 (1998).
558. Durbin, J. E., Simon, M. C. & Levy, D. E. Targeted Disruption of the Mouse Stat1 Gene Results in Compromised Innate Immunity to Viral Disease. *Cell* **84**, 443–450 (1996).
559. Meraz, M. A. *et al.* Targeted Disruption of the Stat1 Gene in Mice Reveals Unexpected Physiologic Specificity in the JAK – STAT Signaling Pathway. *Cell* **84**, 431–442 (1996).
560. Chakraborty, A. & Tweardy, D. J. Stat3 and G-CSF-induced myeloid differentiation. *Leuk. Lymphoma* **30**, 433–442 (1998).
561. Panopoulos, A. D. *et al.* STAT3 governs distinct pathways in emergency granulopoiesis and mature neutrophils. *Blood* **108**, 3682–3691 (2017).
562. Lee, C. *et al.* STAT3 Is a Negative Regulator of Granulopoiesis but Is Not Required for G-CSF-Dependent Differentiation. *Immunity* **17**, 63–72 (2002).
563. Welte, T. *et al.* STAT3 deletion during hematopoiesis causes Crohn ' s disease-like pathogenesis and lethality : A critical role of STAT3 in innate immunity. *Proc. Natl. Acad. Sci.* **100**, 1879–1884 (2003).
564. Kamezaki, K. *et al.* Roles of Stat3 and ERK in G-CSF Signaling. *Stem Cells* **23**, 252–263 (2005).
565. Croker, B. A. *et al.* SOCS3 Is a Critical Physiological Negative Regulator of G-CSF Signaling and Emergency Granulopoiesis. *Immunity* **20**, 153–165 (2004).
566. Zhang, D. *et al.* Absence of granulocyte colony-stimulating factor signaling and neutrophil development in CCAAT enhancer binding protein alpha-deficient mice. *Proc. Natl. Acad. Sci.* **94**, 569–574 (1997).
567. Betsuyaku, T. *et al.* A functional granulocyte colony-stimulating factor receptor is required for normal chemoattractant-induced neutrophil activation. *J. Clin. Invest.* **103**, 825–832 (1999).
568. Lieschke, G. J. *et al.* Mice lacking granulocyte colony-stimulating factor have chronic neutropenia , granulocyte and macrophage progenitor cell deficiency , and impaired neutrophil mobilization. *Blood* **847**, 1737–1746 (1994).
569. Sinha, S., Zhu, Q. S., Romero, G. & Corey, S. J. Deletional Mutation of the External Domain of the Human Granulocyte Colony-Stimulating Factor Receptor in a Patient With Severe Chronic Neutropenia Refractory to Granulocyte Colony-Stimulating Factor. *J Pediatr Hematol Oncol* **25**, 791–796 (2003).
570. Druhan, L. J. *et al.* Novel mechanism of G-CSF refractoriness in patients with severe congenital neutropenia. *Blood* **105**, 584–591 (2005).
571. Skokowa, J. *et al.* Interactions among HCLS1 , HAX1 and LEF1 proteins are essential for G-CSFtriggered granulopoiesis. *Nat. Med.* **18**, 1550–9 (2012).
572. Zeidler, C., Germeshausen, M., Klein, C. & Welte, K. Clinical implications of ELA2-, HAX1-, and G-CSF-receptor (CSF3R) mutations in severe congenital neutropenia. *Br. J. Haematol.* **144**, 459–67 (2009).
573. Basu, S. *et al.* 'Emergency' granulopoiesis in G-CSF-deficient mice in response to Candida albicans infection. *Blood* **95**, 3725–33 (2000).
574. Zhan, B. Y., Lieschke, G. J., Grail, D., Dunn, A. R. & Cheers, C. Essential Roles for Granulocyte-Macrophage Colony-Stimulating Factor (GM-CSF) and G-CSF in the Sustained Hematopoietic Response of Listeria monocytogenes – Infected Mice. *Blood* **91**, 863–869 (1998).
575. Seymour, J. F. *et al.* Mice lacking both granulocyte colony-stimulating factor (CSF) and granulocyte-macrophage CSF have impaired reproductive capacity, perturbed neonatal granulopoiesis, lung disease, amyloidosis, and reduced long-term survival. *Blood* **90**, 3037–49 (1997).
576. Hibbs, M. L. *et al.* Mice Lacking Three Myeloid Colony-Stimulating Factors (G-CSF, GM-CSF, and M-CSF) Still Produce Macrophages and Granulocytes and Mount an Inflammatory Response in a Sterile Model of Peritonitis. *J. Immunol.* **178**, 6435–6443 (2007).
577. Tamura, M. *et al.* Induction of neutrophilic granulocytosis in mice by administration of purified human native granulocyte colony-stimulating factor (G-CSF). *Biochem. Biophys. Res. Commun.* **142**, 454–60 (1987).
578. Dührsen, U. *et al.* Effects of recombinant human granulocyte colony-stimulating factor on hematopoietic progenitor cells in cancer patients. *Blood* **72**, 2074–81 (1988).
579. Bronchud, M. H. *et al.* Phase I / II study of recombinant human granulocyte colony-stimulating factor in patients

receiving intensive chemotherapy for small cell lung cancer. *Br J Cancer* **56**, 809–813 (1987).
580. Gabrilove, J. L. *et al.* Effect of Granulocyte Colony-Stimulating Factor on Neutropenia and Associated Morbidity Due to Chemotherapy for Transitional-Cell Carcinoma of the Urothelium. *N. Engl. J. Med.* **318**, 1414–1422 (1988).
581. Mehta, H. M., Malandra, M. & Corey, S. J. G-CSF and GM-CSF in Neutropenia. *J. Immunol.* **195**, 1341–1349 (2016).
582. Roberts, A. W. G-CSF: a key regulator of neutrophil production, but that's not all! *Growth factors* **23**, 33–41 (2005).
583. Anasetti, C. *et al.* Peripheral-Blood Stem Cells versus Bone Marrow from Unrelated Donors. *N. Engl. J. Med.* **367**, 1487–1496 (2012).
584. Lawlor, K. E. *et al.* Critical role for granulocyte colony-stimulating factor in inflammatory arthritis. *Proc. Natl. Acad. Sci.* **101**, 11398–11403 (2004).
585. Campbell, I. K., Rich, M. J., Bischof, R. J. & Hamilton, J. A. The colony-stimulating factors and collagen-induced arthritis : exacerbation of disease by M-CSF and G-CSF and requirement for endogenous M-CSF Abstract : There is increasing evidence that the colony-stimulating factors (CSFs) may play a part studies sh. *J. Leukoc. Biol.* **68**, 144–150 (2000).
586. Campbell, I. K. *et al.* Therapeutic Targeting of the G-CSF Receptor Reduces Neutrophil Trafficking and Joint Inflammation in Antibody-Mediated Inflammatory Arthritis. *J. Immunol.* **197**, 4392–4402 (2016).
587. Scalzo-Inguanti, K. *et al.* A neutralizing anti–G-CSFR antibody blocks G-CSF–induced neutrophilia without inducing neutropenia in nonhuman primates. *J. Leukoc. Biol.* **102**, 537–549 (2017).
588. Lee, M. *et al.* G-CSF Receptor Blockade Ameliorates Arthritic Pain and Disease. *J. Immunol.* **198**, 3565–3575 (2017).
589. Ramanathan, K. *et al.* Neutrophil activation signature in juvenile idiopathic arthritis indicates the presence of low-density granulocytes. *Rheumatology* **57**, 488–498 (2018).
590. Ramanathan, K. *et al.* Neutrophil activation signature in juvenile idiopathic arthritis indicates the presence of low-density granulocytes. *Rheumatology* **57**, 488–498 (2018).
591. Hamilton, J. A. GM-CSF in inflammation and autoimmunity. *Trends Immunol.* **23**, 403–408 (2002).
592. Fleetwood, A. J., Cook, A. D. & Hamilton, J. A. Functions of granulocyte-macrophage colony-stimulating factor. *Crit Rev Immunol* **25**, 405–28 (2005).
593. Fukuzawa, H. *et al.* Identification of GM-CSF in Paneth cells using single-cell RT-PCR. *Biochem. Biophys. Res. Commun.* **312**, 897–902 (2003).
594. El-Behi, M. *et al.* The encephalitogenicity of Th17 cells is dependent on IL-1- and IL-23-induced production of the cytokine GM-CSF. *Nat. Immunol.* **12**, 568–575 (2011).
595. Lukens, J. R., Barr, M. J., Chaplin, D. D., Chi, H. & Kanneganti, T.-D. Inflammasome-Derived IL-1 β Regulates the Production of GM-CSF by CD4 + T Cells and γ δ T Cells. *J. Immunol.* **188**, 3107–3115 (2012).
596. Duhen, T. & Campbell, D. J. IL-1 β Promotes the Differentiation of Polyfunctional Human CCR6 + CXCR3 + Th1/17 Cells That Are Specific for Pathogenic and Commensal Microbes. *J. Immunol.* **193**, 120–129 (2014).
597. Codarri, L. *et al.* RORgt drives production of the cytokine GM-CSF in helper T cells , which is essential for the effector phase of autoimmune neuroinflammation. *Nat. Immunol.* **12**, 560–657 (2011).
598. Ozawa, H., Aiba, S., Nakagawa, S. & Tagami, H. Interferon-γ and interleukin-10 inhibit antigen presentation by Langerhans cells for T helper type 1 cells by suppressing their CD80 (B7-1) expression. *Eur. J. Immunol.* **26**, 648–652 (1996).
599. Jansen, J. H., Wientjens, G. J., Fibbe, W. E., Willemze, R. & Kluin-Nelemans, H. C. Inhibition of human macrophage coloy formation by interleukin 4. *J. Exp. Med.* **170**, 577–82 (1989).
600. Sagawa, K. *et al.* Suppression by IL-10 and IL-4 of cytokine production induced by two-way autologous mixed lymphocyte reaction. *Cytokine* **8**, 501–506 (1996).
601. Adcock, I. M. & Caramori, G. Cross-talk between pro-inflammatory transcription factors and glucocorticoids. *Immunol. Cell Biol.* **79**, 376–384 (2001).
602. Gasson, J. C. Molecular physiology of granulocyte-macrophage colony-stimulating factor. *Blood* **77**, 1131–45 (1991).
603. Lang, R. A. *et al.* Transgenic Mice Expressing a Hemopoietic Growth Factor Gene (GM-CSF) Develop Accumulations of Macrophages, Blindness, and a Fatal Syndrome of Tissue Damage. *Cell* **51**, 675–686 (1987).
604. Metcalf, D. *et al.* Hemopoietic Responses in Mice Injected With Purified Recombinant Murine GM-CSF. *Exp. Hematol.* **15**, 1–9 (1987).
605. Burgess, A. W., Camakaris, J. & Metcalf, D. Purification and Properties of Colony-stimulating from Mouse Lung-conditioned Medium. *J. Biol. Chem.* **252**, 1998–2003 (1977).
606. Hercus, T. R. *et al.* The granulocyte-macrophage colony-stimulating factor receptor : linking its structure to cell signaling and its role in disease. *Blood* **114**, 1289–1298 (2009).
607. Hansen, G. *et al.* The Structure of the GM-CSF Receptor Complex Reveals a Distinct Mode of Cytokine Receptor Activation. *Cell* **134**, 496–507 (2008).
608. Hamilton, J. A. & Achuthan, A. Colony stimulating factors and myeloid cell biology in health and disease. *Trends Immunol.* **34**, 81–89 (2013).
609. Uchida, K. *et al.* GM-CSF Autoantibodies and Neutrophil Dysfunction in Pulmonary Alveolar Proteinosis. *N. Engl. J. Med.* **356**, 567–579 (2007).
610. Sakagami, T. *et al.* Human GM-CSF Autoantibodies and Reproduction of Pulmonary Alveolar Proteinosis. *N. Engl. J. Med.* **361**, 2679–2681 (2014).
611. van Pelt, L. J., de Craen, A. J. M., Langeveld, N. E. & Weening, R. S. Granulocyte-Macrophage Colony-Stimulating Factor (GM-CSF) Ameliorates Chemotherapy- Induced Neutropenia in Children with Solid Tumors. *Pediatr. Hematol.*

Oncol. **14**, 539–545 (1997).
612. Shiomi, A. & Usui, T. Pivotal Roles of GM-CSF in Autoimmunity and Inflammation. *Mediators Inflamm.* **2015**, 568543 (2015).
613. van Nieuwenhuijze, A. *et al.* GM-CSF as a therapeutic target in inflammatory diseases. *Mol. Immunol.* **56**, 675–682 (2013).
614. Okuda, K., Foster, R. & Griffin, J. D. Signaling Domains of the beta c Chain of the GM-CSF/IL-3/IL-5 Receptor. *Ann. N. Y. Acad. Sci.* **872**, 305–313 (1999).
615. Blalock, W. L. *et al.* Signal transduction , cell cycle regulatory , and anti-apoptotic pathways regulated by IL-3 in hematopoietic cells : possible sites for intervention with anti-neoplastic drugs. *Leukemia* **13**, 1109–1166 (1999).
616. van de Laar, L., Coffer, P. J. & Woltman, A. M. Regulation of dendritic cell development by GM-CSF : molecular control and implications for immune homeostasis and therapy. *Blood* **119**, 3383–3393 (2012).
617. Matsumura, I. *et al.* Transcriptional regulation of the cyclin D1 promoter by STAT5 : its involvement in cytokine-dependent growth of hematopoietic cells. *EMBO J.* **18**, 1367–1377 (1999).
618. Lehtonen, A., Matikainen, S., Miettinen, M. & Julkunen, I. Granulocyte-macrophage colony-stimulating factor (GM-CSF)-induced STAT5 activation and target-gene expression during human monocyte / macrophage differentiation. *J. Leukoc. Biol.* **71**, 511–519 (2002).
619. Mui, A. L., Wakao, H., Farrell, A. O., Harada, N. & Miyajima, A. Interleukin-3, granulocyte-macrophage colony stimulating and interleukin-5 transduce signals through two STAT5 homologs. *EMBO J.* **14**, 1166–1175 (1995).
620. Choi, J. K., Kim, K. H., Park, H., Park, S. R. & Choi, B. H. Granulocyte macrophage-colony stimulating factor shows anti-apoptotic activity in neural progenitor cells via JAK / STAT5-Bcl-2 pathway. *Apoptosis* **16**, 127–134 (2011).
621. Katz, S., Zsiros, V., Dóczi, N. & Kiss, A. L. Inflammation-Induced Epithelial-to-Mesenchymal Transition and GM-CSF Treatment Stimulate Mesenteric Mesothelial Cells to Transdifferentiate into Macrophages. *Inflammation* **41**, 1825–1834 (2018).
622. Yang, T., Chang, P., Kuo, T. & Lu, S. Electronegative L5-LDL induces the production of G-CSF and GM-CSF in human macrophages through LOX-1 involving NFkB and ERK2 activation. *Atherosclerosis* **267**, 1–9 (2017).
623. Stanley, E. *et al.* Granulocyte/macrophage colony-stimulating factor-deficient mice show no major perturbation of hematopoiesis but develop a characteristic pulmonary pathology. *Proc. Natl. Acad. Sci.* **91**, 5592–5596 (1994).
624. Kingston, D. *et al.* The concerted action of GM-CSF and Flt3-ligand on in vivo dendritic cell homeostasis. *Blood* **114**, 835–843 (2009).
625. Zhan, Y. & Cheers, C. Haemopoiesis in mice genetically lacking granulocyte-macrophage colony stimulating factor during chronic infection with Mycobacterium avium. *Immunol. Cell Biol.* **78**, 118–123 (2000).
626. Zhang, P. *et al.* Upregulation of interleukin 6 and granulocyte colony-stimulating factor receptors by transcription factor CCAAT enhancer binding protein alpha (C/EBP alpha) is critical for granulopoiesis. *J. Exp. Med.* **188**, 1173–84 (1998).
627. Collins, S. J., Ulmer, J., Purton, L. E. & Darlington, G. Multipotent hematopoietic cell lines derived from C/EBPa (-/-) knockout mice display granulocyte macrophage – colony-stimulating factor , granulocyte – colony-stimulating factor , and retinoic acid – induced granulocytic differentiation. *Blood* **96**, 2382–2388 (2001).
628. Zhang, P. *et al.* Induction of granulocytic differentiation by 2 pathways. *Blood* **99**, 4406–4412 (2002).
629. Lotfi, N., Thome, R., Rezaei, N., Zhang, G. & Rezaei, A. Roles of GM-CSF in the Pathogenesis of Autoimmune Diseases : An Update. *Front. Immunol.* **10**, 1265 (2019).
630. Campbell, I. K. *et al.* Protection from collagen-induced arthritis in granulocyte-macrophage colony-stimulating factor-deficient mice. *J. Immunol.* **161**, 3639–44 (1998).
631. McQualter, J. L. *et al.* Granulocyte macrophage colony-stimulating factor: a new putative therapeutic target in multiple sclerosis. *J. Exp. Med.* **194**, 873–82 (2001).
632. Bozinovski, S., Jones, J. E., Vlahos, R., Hamilton, J. A. & Anderson, G. P. Granulocyte / Macrophage-Colony-stimulating Factor (GM-CSF) Regulates Lung Innate Immunity to Lipopolysaccharide through Akt / Erk Activation of NFkB and AP-1 in Vivo. *J. Biol. Chem.* **277**, 42808–42814 (2002).
633. Casbon, A. *et al.* Invasive breast cancer reprograms early myeloid differentiation in the bone marrow to generate immunosuppressive neutrophils. *Proc. Natl. Acad. Sci.* **112**, E566-75 (2015).
634. Piper, C. *et al.* T Cell Expression of Granulocyte-Macrophage Colony-Stimulating Factor in Juvenile Arthritis Is Contingent Upon Th17 Plasticity. *Arthritis Rheumatol.* **66**, 1955–1960 (2014).
635. Gattorno, M. *et al.* Synovial fluid T cell clones from oligoarticular juvenile arthritis patients display a prevalent Th1 / Th0-type pattern of cytokine secretion irrespective of immunophenotype. *Clin. Exp. Immunol.* **109**, 4–11 (1997).
636. Kolls, J. K. & Linde, A. Interleukin-17 Family Members. *Immunity* **21**, 467–476 (2004).
637. Yao, Z. *et al.* Herpesvirus Saimiri encodes a new cytokine, IL-17, which binds to a novel cytokine receptor. *Immunity* **3**, 811–21 (1995).
638. Laan, M., Prause, O., Miyamoto, M., Sjo, M. & Hyto, A. M. A role of GM-CSF in the accumulation of neutrophils in the airways caused by IL-17 and TNF-a. *Eur Respir J* **21**, 387–393 (2003).
639. Schwarzenberger, P. *et al.* Requirement of Endogenous Stem Cell Factor and Granulocyte-Colony-Stimulating Factor for IL-17-Mediated Granulopoiesis. *J Immunol* **164**, 4783–4789 (2000).
640. Onishi, R. M. & Gaffen, S. L. Interleukin-17 and its target genes: mechanisms of interleukin-17 function in disease. *Immunology* **129**, 311–321 (2010).
641. Ye, P. *et al.* Requirement of Interleukin 17 Receptor Signaling for Lung CXC Chemokine and Granulocyte Colony-

stimulating Factor Expression , Neutrophil Recruitment , and Host Defense. *J. Exp. Med.* **194**, 519–527 (2001).
642. Griffin, G. K. *et al.* IL-17 and TNFα Sustain Neutrophil Recruitment during Inflammation through Synergistic Effects on Endothelial Activation. *J. Immunol.* **188**, 6287–6299 (2012).
643. Bunte, K. & Beikler, T. Th17 Cells and the IL-23 / IL-17 Axis in the Pathogenesis of Periodontitis and Immune-Mediated Inflammatory Diseases. *Int J Mol Sci* **20**, 3394 (2019).
644. Cua, D. J. & Tato, C. M. Innate IL-17-producing cells : the sentinels of the immune system. *Nat. Rev. Immunol.* **10**, 479–89 (2010).
645. Iwakura, Y. & Ishigame, H. The IL-23/IL-17 axis in inflammation. *J Clin Invest* **116**, 1218–1222 (2006).
646. Smith, E. *et al.* IL-23 Is Required for Neutrophil Homeostasis in Normal and Neutrophilic Mice. *J Immunol* **179**, 8274–9 (2007).
647. Pietras, E. M. *et al.* Chronic interleukin-1 exposure drives haematopoietic stem cells towards precocious myeloid differentiation at the expense of self-renewal. *Nat. Cell Biol.* **18**, 607–618 (2016).
648. Ueda, Y., Cain, D. W., Kuraoka, M., Kondo, M. & Kelsoe, G. IL-1R Type I-Dependent Hemopoietic Stem Cell Proliferation Is Necessary for Inflammatory Granulopoiesis and Reactive Neutrophilia. *J. Immunol.* **182**, 6477–6484 (2009).
649. Gallicchio, V. S., Watts, T. D. & DellaPuca, R. Synergistic action of recombinant-derived murine interleukin-1 on the augmentation of colony stimulating activity on murine granulocyte-macrophage hematopoietic stem cells in vitro. *Exp Cell Biol* **55**, 83–92 (1987).
650. Opdenakker, G., Fibbe, W. E. & Van Damme, J. The molecular basis of leukocytosis. *Immunol. Today* **19**, 182–189 (1998).
651. Walker, F. *et al.* IL6 / sIL6R complex contributes to emergency granulopoietic responses in G-CSF- and GM-CSF-deficient mice. *Blood* **111**, 3978–3985 (2008).
652. Dinarello, C. A. Biologic basis for interleukin-1 in disease. *Blood* **15**, 2095–147 (1996).
653. Biondo, C. *et al.* The Interleukin-1b/CXCL1/2/Neutrophil Axis Mediates Host Protection against Group B Streptococcal Infection. *Infect. Immun.* **82**, 4508–4517 (2014).
654. Strieter, R. M. *et al.* Endothelial cell gene expression of a neutrophil chemotactic factor by TNF-alpha, LPS, and IL-1 beta. *Science (80-.).* **243**, 1467–9 (1989).
655. Mitroulis, I. *et al.* Neutrophil Extracellular Trap Formation Is Associated with IL-1b and Autophagy-Related Signaling in Gout. *PLoS One* **6**, e29318 (2011).
656. Prince, L. R. *et al.* The Role of Interleukin-1b in Direct and Toll-Like Receptor 4-Mediated Neutrophil Activation and Survival. *Am. J. Pathol.* **165**, 1819–1826 (2004).
657. Yagisawa, M. *et al.* Stimulation and priming of human neutrophils by IL-1 alpha and IL-1 beta: complete inhibition by IL-1 receptor antagonist and no interaction with other cytokines. *Exp Hematol* **23**, 603–8 (1995).
658. Kopf, M. *et al.* Impaired immune and acute-phase respones in interleukin-6-deficient mice. *Nature* **368**, 815–818 (1994).
659. Maeda, K. *et al.* IL-6 blocks a discrete early step in lymphopoiesis. *Blood* **106**, 879–885 (2005).
660. Biswas, B. P. *et al.* Interleukin-6 Induces Monocyte Chemotactic Protein-1 in Peripheral Blood Mononuclear Cells and in the U937 Cell Line. *Blood* **91**, 258–265 (1998).
661. Pojda, Z. & Tsuboi, A. In Vivo Effects of Human Recombinant Interleukin 6 on Hemopoietic Stem and Progenitor Cells and Circulating Blood Cells in Normal Mice. *Exp. Hematol.* **18**, 1034–7 (1990).
662. Suwa, T., Hogg, J. C., English, D. & Van Eeden, S. F. Interleukin-6 induces demargination of intravascular neutrophils and shortens their transit in marrow. *Am J Physiol Hear. Circ Physiol* **279**, 2954–2960 (2000).
663. Ulich, T. R., Castillo, J. del & Guo, K. In vivo hematologic effects of recombinant interleukin-6 on hematopoiesis and circulating numbers of RBCs and WBCs. *Blood* **73**, 108–110 (1989).
664. Hashizume, M., Higuchi, Y., Uchiyama, Y. & Mihara, M. IL-6 plays an essential role in neutrophilia under inflammation. *Cytokine* **54**, 92–99 (2011).
665. Walker, F. *et al.* IL6/sIL6R complex contributes to emergency granulopoietic responses in G-CSF- and GM-CSF-deficient mice. *Blood* **111**, 3978–3985 (2008).
666. Suwa, T., Hogg, J. C., Klut, M. E., Hards, J. & Van Eeden, S. F. Interleukin-6 Changes Deformability of Neutrophils and Induces Their Sequestration in the Lung. *Am J Respir Crit Care Med* **163**, 970–976 (2001).
667. Reynaud, D. *et al.* IL-6 controls leukemic multipotent progenitor cell fate and contributes to chronic myelogenous leukemia development. *Cancer Cell* **20**, 661–673 (2012).
668. Romani, L. *et al.* Impaired Neutrophil Response and CD4+ T Helper Cell 1 Development in Interleukin 6-deficient Mice Infected with Candida albicans. *J. Exp. Med.* **183**, 1345–1355 (1996).
669. Emery, P. *et al.* IL-6 receptor inhibition with tocilizumab improves treatment outcomes in patients with rheumatoid arthritis refractory to anti-tumour necrosis factor biologicals : results from a 24-week multicentre randomised placebo-controlled trial. *Ann Rheum Dis* **67**, 1516–1523 (2008).
670. Genovese, M. C. *et al.* Interleukin-6 Receptor Inhibition With Tocilizumab Reduces Disease Activity in Rheumatoid Arthritis With Inadequate Response to Disease-Modifying Antirheumatic Drugs The Tocilizumab in Combination With Traditional Disease-Modifying Antirheumatic Drug. *Arthritis Rheum.* **58**, 2968–2980 (2008).
671. Smolen, J. S. *et al.* Effect of interleukin-6 receptor inhibition with tocilizumab in patients with rheumatoid arthritis (OPTION study): a double-blind, placebo-controlled, randomised trial. *Lancet* **371**, 987–997 (2008).
672. Maini, R. N. *et al.* Double-Blind Randomized Controlled Clinical Trial of the Interleukin-6 Receptor Antagonist ,

Tocilizumab , in European Patients With Rheumatoid Arthritis Who Had an Incomplete Response to Methotrexate. *Arthritis Rheum.* **54**, 2817–2829 (2006).
673. Jones, G. *et al.* Comparison of tocilizumab monotherapy versus methotrexate monotherapy in patients with moderate to severe rheumatoid arthritis : the AMBITION study. *Ann Rheum Dis* **69**, 88–96 (2010).
674. Nakamura, I., Omata, Y., Naito, M. & Ito, K. Blockade of Interleukin 6 Signaling Induces Marked Neutropenia in Patients with Rheumatoid Arthritis. *J Rheumatol* **36**, 459 (2009).
675. Collins, S. J., Ulmer, J., Purton, L. E. & Darlington, G. Multipotent hematopoietic cell lines derived from C/EBPa (-/-) knockout mice display granulocyte macrophage – colony-stimulating factor , granulocyte – colony-stimulating factor , and retinoic acid – induced granulocytic differentiation. *Blood* **98**, 2382–2388 (2001).
676. Heinrich, P. C. *et al.* Principles of interleukin (IL)-6-type cytokine signalling and its regulation. *Biochemistry* **374**, 1–20 (2003).
677. Marin, V. *et al.* Chemotactic agents induce IL-6Ra shedding from polymorphonuclear cells : involvement of a metalloproteinase of the TNFa -converting enzyme (TACE) type. *Eur. J. Immunol.* **32**, 2965–2970 (2002).
678. Rabe, B. *et al.* Transgenic blockade of interleukin 6 transsignaling abrogates inflammation. *Blood* **111**, 1021–1028 (2008).
679. Hurst, S. M. *et al.* IL-6 and Its Soluble Receptor Orchestrate a Temporal Switch in the Pattern of Leukocyte Recruitment Seen during Acute Inflammation. *Immunity* **14**, 705–714 (2001).
680. Marin, V. *et al.* The IL-6-Soluble IL-6R α Autocrine Loop of Endothelial Activation as an Intermediate Between Acute and Chronic Inflammation: an Experimental Model Involving Thrombin. *J. Immunol.* **167**, 3435–3442 (2001).
681. Gabay, C. Interleukin-6 and chronic inflammation. *Arthritis Res. Ther.* **8**, S3 (2006).
682. Romano, M. *et al.* Role of IL-6 and Its Soluble Receptor in Induction of Chemokines and Leukocyte Recruitment. *Immunity* **6**, 315–325 (1997).
683. Xing, Z. *et al.* IL-6 Is an Antiinflammatory Cytokine Required for Controlling Local or Systemic Acute Inflammatory Responses. *J. Clin. Invest.* **101**, 311–320 (1998).
684. Atreya, R. *et al.* Blockade of interleukin 6 trans signaling suppresses T-cell resistance against apoptosis in chronic intestinal inflammation : Evidence in Crohn disease and experimental colitis in vivo. *Nat. Med.* **6**, 583–588 (2000).
685. Alonzi, B. T. *et al.* Interleukin 6 Is Required for the Development of Collagen-induced Arthritis. *J. Exp. Med.* **187**, 461–468 (1998).
686. Yamamoto, M., Yoshizaki, K., Ito, H. & Alerts, E. IL-6 Is Required for the Development of Th1 Cell-Mediated Murine Colitis. *J. Immunol.* **164**, 4878–4882 (2000).
687. Tanaka, T., Narazaki, M. & Kishimoto, T. IL-6 in Inflammation, Immunity, and Disease. *Cold Spring Harb Perspect Biol.* **6**, a016295 (2014).
688. Dienz, O. *et al.* Essential role of IL-6 in protection against H1N1 influenza virus by promoting neutrophil survival in the lung. *Nature* **5**, 258–266 (2012).
689. Wright, H. L., Cross, A. L., Edwards, S. W. & Moots, R. J. Effects of IL-6 and IL-6 blockade on neutrophil function in vitro and in vivo. *Rheumatology* **53**, 1321–1331 (2014).
690. Afford, S. C. *et al.* The Induction by Human Interleukin-6 of Apoptosis in the Promonocytic Cell Line U937 and Human Neutrophils. *J. Biol. Chem.* **267**, 21612–21616 (1992).
691. Biffl, W. L., Moore, E. E., Moore, F. A. & Banett Jr, C. C. Interleukin-6 suppression of neutrophil apoptosis is neutrophil concentration dependent. *J. Leukoc. Biol.* **58**, 582–584 (1995).
692. Mcnamee, J. P., Bellier, P. V, Kutzner, B. C. & Wilkins, R. C. Effect of pro-inflammatory cytokines on spontaneous apoptosis in leukocyte sub-sets within a whole blood culture. *Cytokine* **31**, 161–167 (2005).
693. Ottonello, L. *et al.* Differential regulation of spontaneous and immune complex- induced neutrophil apoptosis by proinflammatory cytokines . Role of oxidants , Bax and caspase-3. *J. Leukoc. Biol.* **72**, 125–132 (2002).
694. Wilkinson, A. N. *et al.* Granulocytes Are Unresponsive to IL-6 Due to an Absence of gp130. *J. Immunol.* **200**, 3547–3555 (2018).
695. Calzetti, F., Tamassia, N., Arruda-Silva, F., Gasperini, S. & Cassatella, M. A. The importance of being “pure” neutrophils. *J. Allergy Clin. Immunol.* **139**, 352-355.e6 (2017).
696. Leung, B. P. *et al.* A Role for IL-18 in Neutrophil Activation. *J. Immunol.* **167**, 2879–2886 (2001).
697. Elbim, C., Dang, P. M. C., Pedruzzi, E., Benna, J. El & Bichat, C. H. X. Interleukin-18 Primes the Oxidative Burst of Neutrophils in Response to Formyl-Peptides : Role of Cytochrome b558 Translocation and N-Formyl Peptide Receptor Endocytosis. *Clin. Diagn. Lab. Immunol.* **12**, 436–446 (2005).
698. Fortin, C. F., Ear, T. & Mcdonald, P. P. Autocrine role of endogenous interleukin-18 on inflammatory cytokine generation by human neutrophils. *FASEB J.* **23**, 194–203 (2009).
699. Müller, A. A., Dolowschiak, T., Sellin, M. E., Felmy, B. & Verbree, C. An NK Cell Perforin Response Elicited via IL-18 Controls Mucosal Inflammation Kinetics during Salmonella Gut Infection. *PLoS Pathog.* **12**, e1005723 (2016).
700. Baldridge, M. T., King, K. Y., Boles, N. C., Weksberg, D. C. & Goodell, M. A. Quiescent haematopoietic stem cells are activated by IFN-gamma in response to chronic infection. *Nature* **465**, 793–797 (2010).
701. De Bruin, A. M., Voermans, C. & Nolte, M. A. Impact of interferon-γ on hematopoiesis. *Blood* **124**, 2479–2486 (2014).
702. Ramakrishna, C. & Cantin, E. M. IFNγ inhibits G-CSF induced neutrophil expansion and invasion of the CNS to prevent viral encephalitis. *PLoS Pathog.* **14**, e1006822 (2018).
703. de Bruin, A. M. *et al.* IFN-gamma induces monopoiesis and inhibits neutrophil development during inflammation. *Blood* **119**, 1543–1554 (2012).

704. Snoeck, H. W. *et al.* Interferon-gamma and interleukin-4 reciprocally regulate the production of monocytes/macrophages and neutrophils through a direct effect on committed monopotential bone marrow progenitor cells. *Eur. J. Immunol.* **23**, 1072–7 (1993).
705. Cruz, A. *et al.* Cutting Edge: IFN- γ Regulates the Induction and Expansion of IL-17-Producing CD4 T Cells during Mycobacterial Infection. *J. Immunol.* **177**, 1416–1420 (2006).
706. Desvignes, L. & Ernst, J. D. Interferon-gamma-Responsive Nonhematopoietic Cells Regulate the Immune Response to Mycobacterium tuberculosis. *Immunity* **31**, 974–985 (2009).
707. Pearl, J. E., Saunders, B., Ehlers, S., Orme, I. M. & Cooper, A. M. Inflammation and Lymphocyte Activation during Mycobacterial Infection in the Interferon-gamma-Deficient Mouse. *Cell. Immunol.* **50**, 43–50 (2001).
708. Norose, K., Naoi, K., Fang, H. & Yano, A. In vivo study of toxoplasmic parasitemia using interferon- γ deficient mice : Absolute cell number of leukocytes , parasite load and cell susceptibility. *Parasitol. Int.* **57**, 447–453 (2008).
709. Ellison, M. A., Gearheart, C. M., Porter, C. C. & Ambruso, D. R. IFN-γ alters the expression of diverse immunity related genes in a cell culture model designed to represent maturing neutrophils. *PLoS One* **12**, e0185956 (2017).
710. Ellis, T. N. & Beaman, B. L. Interferon-γ activation of polymorphonuclear neutrophil function. *Immunology* **112**, 2–12 (2004).
711. Marchi, L. F., Ignacchiti, M. D. C. & Mantovani, B. In vitro activation of mouse neutrophils by recombinant human interferon-gamma : Increased phagocytosis and release of reactive oxygen species and pro-in fl ammatory cytokines. *Int. Immunopharmacol.* **18**, 228–235 (2014).
712. Pfister, O. *et al.* Chronic overexpression of membrane-bound flt3 ligand by T lymphocytes in severe aplastic anaemia. *Br. J. Rheumatol.* **109**, 211–220 (2000).
713. Drexler, H. G. & Quentmeier, H. FLT3: Receptor and Ligand. *Growth factors* **22**, 71–73 (2009).
714. Jörgen Adolfsson, 1 *et al.* Upregulation of Flt3 Expression within the Bone Marrow Lin- Sca1+ c-kit+ Stem Cell Compartment Is Accompanied by Loss of Self-Renewal Capacity. *Immunity* **15**, 659–669 (2001).
715. Stirewalt, D. L. & Radich, J. P. The role of FLT3 in haematopoietic maligancies. *Nat. Rev. Cancer* **3**, 650–666 (2003).
716. Kazi, J. U. & Rönnstrand, L. The role of SRC family kinases in FLT3 signaling. *Int. J. Biochem. Cell Biol.* **107**, 32–37 (2019).
717. Staudt, D. *et al.* Targeting Oncogenic Signaling in Mutant FLT3 Acute Myeloid Leukemia : The Path to Least Resistance. *Int. J. Mol. Sci* **19**, 3198 (2018).
718. Lyman, S. D. & Jacobsen, S. E. c-kit ligand and Flt3 ligand: stem/progenitor cell factors with overlapping yet distinct activities. *Blood* **91**, 1101–34 (1998).
719. Maraskovsky, E. *et al.* In vivo generation of human dendritic cell subsets by Flt3 ligand. *Blood* **96**, 878–884 (2000).
720. McKenna, H. J. *et al.* Mice lacking flt3 ligand have deficient hematopoiesis affecting hematopoietic progenitor cells, dendritic cells, and natural killer cells. *Blood* **95**, 3489–97 (2000).
721. Onai, N., Obata-Onai, A., Schmid, M. A. & Manz, M. G. Flt3 in Regulation of Type I Interferon-Producing Cell and Dendritic Cell Development. *Ann NY Acad Sci* **1106**, 253–61 (2007).
722. Hammum, C. *et al.* Ligand for FLT3/FLK2 receptor tyrosine kinase regulates growth of haematopoietic stem cells and is encodes by variant RNAs. *Nature* **368**, (1994).
723. Lyman, B. S. D. *et al.* Cloning of the human homologue of the murine flt3 ligand: a growth factor for early hematopoietic progenitor cells. *Blood* **83**, 2795–2801 (1994).
724. Sonoda, Y. *et al.* Human FLT3 ligand acts on myeloid as well as multipotential progenitors derived from purifiedkD34 ' bfoodv progenitors expressing different levels of c-kit protein. *Eur. J. Haematol.* **58**, 257–264 (1997).
725. Rosborough, B. R. *et al.* Flt3 ligand mediates STAT3-independent expansion, but STAT3- dependent activation of myeloid-derived suppressor cells. *J. Immunol.* **192**, 3470–3473 (2015).
726. Ramos, M. I. *et al.* FMS-related tyrosine kinase 3 ligand (Flt3L)/ CD135 axis in rheumatoid arthritis. *Arthritis Res. Ther.* **15**, R209 (2013).
727. Dehlin, M. *et al.* Intra-Articular Fms-Like Tyrosine Kinase 3 Ligand Expression Is a Driving Force in Induction and Progression of Arthritis. *PLoS One* **3**, e3633 (2008).
728. Lean, J. M., Fuller, K. & Chambers, T. J. FLT3 ligand can substitute for macrophage colony-stimulating factor in support of osteoclast differentiation and function. *Blood* **98**, 2707–2713 (2001).
729. Ramos, M. I. P. *et al.* Absence of Fms-like tyrosine kinase 3 ligand (Flt3L) signalling protects against collagen-induced arthritis. *Ann Rheum Dis* **74**, 211–219 (2015).
730. Bugl, S., Wirths, S., Müller, M. R., Radsak, M. P. & Kopp, H. G. Current insights into neutrophil homeostasis. *Ann. N. Y. Acad. Sci.* **1266**, 171–178 (2012).
731. Furze, R. C. & Rankin, S. M. The role of the bone marrow in neutrophil clearance under homeostatic conditions in the mouse. *FEBS J.* **22**, 3111–3119 (2008).
732. Gordy, C., Pua, H., Sempowski, G. D. & He, Y. Regulation of steady-state neutrophil homeostasis by macrophages. *Blood* **117**, 618–629 (2011).
733. Aroca-Crevillén, A., Adrover, J. M. & Hidalgo, A. Circadian Features of Neutrophil Biology. *Front. Immunol.* **11**, 576 (2020).
734. Ella, K. & Attila, M. Circadian regulation of neutrophils : Control by a cell-autonomous clock or systemic factors? *Eur J Clin Invest* **48**, e12965 (2018).
735. Haspel, J. A. *et al.* Perfect timing : circadian rhythms , sleep , and immunity — an NIH workshop. *JCI Insight* **5**, e131487 (2020).

736. Zhang, D. *et al.* Neutrophil ageing is regulated by the microbiome. *Nature* **525**, 528–32 (2015).
737. Jung, T. M. & Dailey, M. O. Rapid modulation of homing receptors (gp90MEL-14) induced by activators of protein kinase C . Receptor shedding due to accelerated proteolytic cleavage at the cell Information about subscribing to The Journal of Immunology is online at : Receptor Sheddi. *J. Immunol.* **144**, 3130–3136 (1990).
738. Demaret, J. *et al.* Marked alterations of neutrophil functions during sepsis-induced immunosuppression. *J. Leukoc. Biol.* **98**, 1081–1090 (2015).
739. Kahn, J., Ingraham, R. H., Shirley, F., Migaki, G. I. & Kishimoto, T. K. Membrane proximal cleavage of L-selectin: identification of the cleavage site and a 6-kD transmembrane peptide fragment of L-selectin. *J Cell Biol.* **125**, 461–70 (1994).
740. Komiya, A. *et al.* Neutrophil CD64 is upregulated in patients with active adult-onset Still ' s disease. *Scand. J. Rheumatol.* **41**, 156–158 (2012).
741. Liu, Y., Xia, C., Chen, J., Fan, C. & He, J. Elevated circulating pro-inflammatory low-density granulocytes in adult-onset Still ' s disease. *Rheumatology* **60**, 297–303 (2021).
742. Nirmala, N. *et al.* Gene-expression analysis of adult-onset Still ' s disease and systemic juvenile idiopathic arthritis is consistent with a continuum of a single disease entity. *Pediatr. Rheumatol.* **13**, 50 (2015).
743. Omoyinmi, E. *et al.* Mitochondrial and oxidative stress genes are differentially expressed in neutrophils of sJIA patients treated with tocilizumab : a pilot microarray study. *Pediatr. Rheumatol.* **14**, 7 (2016).
744. Arend, W. P. The Innate Immune System in Rheumatoid Arthritis. *Arthritis Rheum.* **44**, 2224–2234 (2001).
745. Cecchi, I., Arias, I., Rosa, D., Menegatti, E. & Roccatello, D. Neutrophils : Novel key players in Rheumatoid Arthritis . Current and future therapeutic targets. *Autoimmun. Rev.* **17**, 1138–1149 (2018).
746. Metzemaekers, M. *et al.* Synovial fluid neutrophils from patients with juvenile idiopathic arthritis display a hyperactivated phenotype. *Arthritis Rheumatol.* **73**, 875–884 (2021).
747. Gustafsson, K., Herrmann, T. & Dieli, F. Editorial: Understanding Gamma Delta T Cell Multifunctionality - Towards Immunotherapeutic Applications. *Front. Immunol.* **11**, (2020).
748. Bruck, N., Schnabel, A. & Hedrich, C. M. Current understanding of the pathophysiology of systemic juvenile idiopathic arthritis (sJIA) and target-directed therapeutic approaches. *Clin. Immunol.* **159**, 72–83 (2015).
749. Kessel, C., Holzinger, D. & Foell, D. Phagocyte-derived S100 proteins in autoinflammation : Putative role in pathogenesis and usefulness as biomarkers. *Clin. Immunol.* **147**, 229–241 (2013).
750. Avau, A., Put, K., Wouters, C. H. & Matthys, P. Cytokine balance and cytokine-driven natural killer cell dysfunction in systemic juvenile idiopathic arthritis. *Cytokine Growth Factor Rev.* **26**, 35–45 (2015).
751. Nigrovic, P. A. *et al.* Anakinra as First-Line Disease-Modifying Therapy in Systemic Juvenile Idiopathic Arthritis Report of Forty-Six Patients From an International Multicenter Series. *Arthritis Rheum.* **63**, 545–555 (2011).
752. Vastert, S. J. *et al.* Effectiveness of First-Line Treatment With Recombinant Interleukin-1 Receptor Antagonist in Steroid-Naive Patients With New-Onset Systemic Juvenile Idiopathic Arthritis Results of a Prospective Cohort Study. *Arthritis Rheumatol.* **66**, 1034–1043 (2014).
753. Nigrovic, P. A. Is There a Window of Opportunity for Treatment of Systemic Juvenile Idiopathic Arthritis? *Arthritis Rheumatol.* **66**, 1405–1413 (2014).
754. Andoh, A. *et al.* Interleukin-22, a Member of the IL-10 Subfamily, Induces Inflammatory Responses in Colonic Subepithelial Myofibroblasts. *Gastroenterology* **129**, 969–984 (2005).
755. Zhang, N., Pan, H. F. & Ye, D. Q. Th22 in inflammatory and autoimmune disease: Prospects for therapeutic intervention. *Mol. Cell. Biochem.* **353**, 41–46 (2011).
756. Ma, H. *et al.* IL-22 is required for Th17 cell – mediated pathology in a mouse model of psoriasis-like skin inflammation. **118**, 597–607 (2008).
757. Geboes, L. *et al.* Proinflammatory Role of the Th17 Cytokine Interleukin-22 in Collagen-Induced Arthritis in C57BL / 6 Mice. **60**, 390–395 (2009).
758. Xie, M. *et al.* Interleukin (IL) -22 , a Novel Human Cytokine That Signals through the Interferon Receptor-related Proteins CRF2 – 4 and IL-22R *. *J. Biol. Chem.* **275**, 31335–31339 (2000).
759. Ouyang, W., Rutz, S., Crellin, N. K., Valdez, P. A. & Hymowitz, S. G. Regulation and Functions of the IL-10 Family of Cytokines in Inflammation and Disease. *Annu. Rev. Immunol.* **29**, 71–109 (2011).
760. Kotenko, S. V *et al.* Identification of the Functional Interleukin-22 (IL-22). *J. Biol. Chem.* **276**, 2725–2732 (2001).
761. Matthys, P. *et al.* Enhanced autoimmune arthritis in IFN-γ receptor-deficient mice Is conditioned by Mycobacteria in Freund's adjuvant and by increased expansion of Mac-11 myeloid cells. *J Immunol* **163**, 3505–3510 (1999).
762. Lamkanfi, M. & Dixit, V. M. Mechanisms and functions of inflammasomes. *Cell* **157**, 1013–1022 (2014).
763. Eigenbrod, T., Bode, K. A. & Alexander, H. Early Inhibition of IL-1 β Expression by IFN- γ Is Mediated by Impaired Binding of NF-κB to the IL-1 β Promoter but Is Independent of Nitric Oxide. *J Immunol* **190**, 6533–6541 (2003).
764. Masters, S. L. *et al.* Regulation of interleukin-1beta by interferon-gamma is species specific, limited by suppressor ofcytokine signalling 1 and influences interleukin-17 production. *EMBO Rep.* **11**, 640–646 (2010).
765. Mishra, B. B. *et al.* Nitric oxide controls the immunopathology of tuberculosis by inhibiting NLRP3 inflammasome-dependent processing of IL-1β. *Nat. Immunol.* **14**, 52–60 (2013).
766. de Boer, M. L., Hu, J., Kalvakolanu, D. V, Hasday, J. D. & Cross, A. S. IFN-gamma Inhibits Lipopolysaccharide-Induced Interleukin-1beta in Primary Murine Macrophages via a Stat1-Dependent Pathway. *J. Interf. cytokine Res.* **21**, 485–494 (2001).
767. De Klerck, B. *et al.* Enhanced osteoclast development in collagen-induced arthritis in interferon- γ receptor knock-

out mice as related to increased splenic CD11b + myelopoiesis. *Arthritis Res. Ther.* **6**, R220–R231 (2004).
768. Frosch, M. *et al.* Myeloid-related proteins 8 and 14 are specifically secreted during interaction of phagocytes and activated endothelium and are useful markers for monitoring disease activity in pauciarticular-onset juvenile rheumatoid arthritis. *Arthritis Rheum.* **43**, 628–637 (2000).
769. Kramer, F. *et al.* Interleukin-1beta stimulates acute phase response and C-reactive protein synthesis by inducing an NFkB- and C/EBPbeta-dependent autocrine interleukin-6 loop. **45**, 2678–2689 (2008).
770. Dayer, J., Oliviero, F. & Punzi, L. A Brief History of IL-1 and IL-1 Ra in Rheumatology. *Front. Pharmacol.* **8**, 293 (2017).
771. Shenoi, S. Update on the management of systemic juvenile idiopathic arthritis and role of IL-1 and IL-6 inhibition. *Adolesc Heal. Med Ther* **8**, 125–135 (2017).
772. Burger, D., Dayer, J. M., Palmer, G. & Gabay, C. Is IL-1 a good therapeutic target in the treatment of arthritis? *Best Pract. Res. Clin. Rheumatol.* **20**, 879–896 (2006).
773. Toplak, N., Blazina, Š. & Avčin, T. The role of IL-1 inhibition in systemic juvenile idiopathic arthritis: current status and future perspectives. *Drug Des. Devel. Ther.* **12**, 1633–1643 (2018).
774. Rondeau, J. M., Ramage, P., Zurini, M. & Gram, H. The molecular mode of action and species specificity of canakinumab, a human monoclonal antibody neutralizing IL-1beta. *MAbs* **7**, 1151–1160 (2015).
775. ter Haar, N. *et al.* Monocytes and neutrophils in the inflammatory cascade of systemic onset Juvenile Idiopathic Arthritis. *Pediatr. Rheumatol.* **13**, O54 (2015).
776. Lockhart, E., Green, A. M. & Flynn, J. L. IL-17 Production Is Dominated by T Cells rather than CD4 T Cells during Mycobacterium tuberculosis Infection. *J. Immunol.* **177**, 4662–4669 (2006).
777. Roark, C. L. *et al.* γδ T cells clonally expand, produce IL-17, and are pathogenic in collagen-induced arthri. **179**, 5576–5583 (2009).
778. Cai, Y. *et al.* Pivotal Role of Dermal IL-17-producing γδ T Cells in Skin Inflammation. *Immunity* **35**, 596–610 (2011).
779. Villarino, A. V, Gallo, E., Abbas, A. K. & Alerts, E. STAT1-Activating Cytokines Limit Th17 Responses through Both T-bet − Dependent and − Independent Mechanisms. *J Immunol* **185**, 6461–71 (2010).
780. Nistala, K. *et al.* Interleukin-17 – Producing T Cells Are Enriched in the Joints of Children With Arthritis , but Have a Reciprocal Relationship to Regulatory T Cell Numbers. **58**, 875–887 (2008).
781. Heslan, M. *et al.* Interleukin-22 binding protein (IL-22BP) is constitutively expressed by a subset of conventional dendritic cells and is strongly induced by retinoic acid. *Mucosal Immunol.* **7**, 101–13 (2014).
782. Guttman-Yassky, E. *et al.* Efficacy and safety of fezakinumab (an IL-22 monoclonal antibody) in adults with moderate-to-severe atopic dermatitis inadequately controlled by conventional treatments : A randomized , double-blind , phase 2a trial. *J. Am. Dermatology* **78**, 872-881.e6 (2018).
783. Cannya, S. & Mellins, E. New frontiers in the treatment of systemic juvenile idiopathic arthritis. *F1000Res.* **6**, 971 (2017).
784. Liew, X. P. X. & Kubes, P. The neutrophil's role during health and disease. *Physiol Rev* **99**, 1223–1248 (2019).
785. Leliefeld, P. H. C., Wessels, C. M., Leenen, L. P. H., Koenderman, L. & Pillay, J. The role of neutrophils in immune dysfunction during severe inflammation. *Crit. Care* **20**, 73 (2016).
786. Avau, A. *et al.* Systemic Juvenile Idiopathic Arthritis – like Syndrome in Mice Following Stimulation of the Immune System With Freund ' s Complete Adjuvant. *Arthritis Rheumatol.* **66**, 1340–1351 (2014).
787. Pollenus, E. *et al.* Limitations of neutrophil depletion by anti-Ly6G antibodies in two heterogenic immunological models. *Immunol. Lett.* **212**, 30–36 (2019).
788. Street, K. *et al.* Slingshot: cell lineage and pseudotime inference for single-cell transcriptomics. *BMC Genomics* **19**, 477 (2018).
789. Thornton, S. & Strait, R. T. Head-to-head comparison of protocol modifications for the generation of collagen-induced arthritis in a specific-pathogen free facility using DBA/1 mice. *Biotechniques* **60**, 119–28 (2016).
790. Liu, X. *et al.* Role of the Gut Microbiome in Modulating Arthritis Progression in Mice. *Sci. Rep.* **6**, 30594 (2016).
791. Li, P. *et al.* Systemic tumor necrosis factor alpha mediates an increase in peripheral CD11bhigh osteoclast precursors in tumor necrosis factor alpha-transgenic mice. *Arthritis Rheum* **50**, 265–76 (2004).
792. Schrijver, I. T., Théroude, C. & Roger, T. Myeloid-Derived Suppressor Cells in Sepsis. *Front. Immunol.* **10**, 327 (2019).
793. D'Angelo, M. A., Gomez-Cavazos, J. S., Mei, A., Lackner, D. H. & Hetzer, M. W. A Change in Nuclear Pore Complex Composition Regulates Cell Differentiation. *Dev. Cell* **22**, 446–458 (2012).
794. Schwarzenberger, P. *et al.* Requirement of Endogenous Stem Cell Factor and Granulocyte-Colony-Stimulating Factor for IL-17-Mediated Granulopoiesis. *J. Immunol.* **164**, 4783–4789 (2000).
795. Chung, Y. *et al.* Critical Regulation of Early Th17 Cell Differentiation by Interleukin-1 Signaling. *Immunity* **30**, 576–587 (2009).
796. Mei, J. *et al.* Cxcr2 and Cxcl5 regulate the IL-17 / G-CSF axis and neutrophil homeostasis in mice. *J. Clin. Invest.* **122**, 974–986 (2012).
797. Papotto, P. H., Ribot, J. C. & Silva-santos, B. IL-17+ γδ T cells as kick-starters of inflammation. *Nat. Rev. Immunol.* **18**, 604–611 (2017).
798. Rybakin, V. *et al.* Gelatinase B / matrix metalloproteinase-9 and other neutrophil proteases switch off interleukin-2 activity. *Biochem. J.* **476**, 2191–2208 (2019).
799. Kimura, Y. *et al.* Pulmonary hypertension and other potentially fatal pulmonary complications in systemic juvenile idiopathic arthritis. *Arthritis Care Res.* **65**, 745–752 (2013).
800. Klotsche, J. *et al.* Outcome and Trends in Treatment of Systemic Juvenile Idiopathic Arthritis in the German National

Pediatric Rheumatologic Database , 2000 – 2013. *ARTHRITIS Rheumatol.* **68**, 3023–3034 (2016).
801. Vande Velde, G. *et al.* Longitudinal micro-CT provides biomarkers of lung disease that can be used to assess the effect of therapy in preclinical mouse models , and reveal compensatory changes in lung volume. *Dis. Model. Mech.* **9**, 91–98 (2016).
802. Berghen, N. *et al.* Radiosafe micro-computed tomography for longitudinal evaluation of murine disease models. *Sci. Rep.* **9**, 17598 (2019).
803. Vande Velde, G. *et al.* Magnetic Resonance Imaging for Noninvasive Assessment of Lung Fibrosis Onset and Progression Cross-Validation and Comparison of Different Magnetic Resonance Imaging Bleomycin-Induced Mouse Model. *Invest. Radiol.* **49**, 691–698 (2014).
804. Devos, F. C. *et al.* Forced expiration measurements in mouse models of obstructive and restrictive lung diseases. *Respir Res.* **18**, 123 (2017).
805. Misharin, A. V., Morales-Nebreda, L., Mutlu, G. M., Budinger, G. R. S. & Perlman, H. Major Technical Advances Flow Cytometric Analysis of Macrophages and Dendritic Cell Subsets in the Mouse Lung. *Am. J. Respir. Cell Mol. Biol.* **49**, 503–510 (2013).
806. Tarique, A. A. *et al.* Phenotypic , Functional , and Plasticity Features of Classical and Alternatively Activated Human Macrophages. *Am. J. Respir. Cell Mol. Biol.* **53**, 676–688 (2015).
807. Iriguchi, S. *et al.* Regular Article T-cell – restricted T-bet overexpression induces aberrant hematopoiesis of myeloid cells and impairs function of macrophages in the lung. *Blood* **125**, 370–382 (2015).
808. Chu, C. *et al.* Interferon-gamma Regulates Susceptibility to Collagen-Induced Arthritis Through Suppression of Interleukin-17. *Arthritis Rheum.* **56**, 1145–1151 (2007).
809. Kelchtermans, H. *et al.* Protective role of IFN-g in collagen-induced arthritis conferred by inhibition of mycobacteria-induced granulocyte chemotactic protein-2 production. *J. Leukoc. Biol.* **81**, 1044–1053 (2006).
810. Tomashefski, J. f. J. & Farver, C. F. Tuberculosis and Nontuberculous Mycobacterial Infection. in *Dail and Hammer's Pulmonary Pathology* **1**, 316–348 (2008).
811. Gilbert, S., Steinbreck, D. S., Landas, S. K. & Hunninghake, G. W. Amounts of angiotensin-converting enzyme mRNA reflect the burden of granulomas in granulomatous lung disease. *Am. Rev. Respir. Dis.* **148**, 483–486 (1993).
812. Schurgers, E. *et al.* Pulmonary inflammation in mice with collagen- induced arthritis is conditioned by complete Freund ' s adjuvant and regulated by endogenous IFN- γ. *Eur J Immunol.* **42**, 3223–3234 (2012).
813. Kamijo, R. *et al.* Mice That Lack the Interferon-g Receptor Have Profoundly Altered Responses to Infection with Bacillus Calmette-Guérin and Subsequent Challenge with Lipopolysaccharide. *J. Exp. Med.* **178**, 1435–1440 (1993).
814. Flynn, B. J. L. *et al.* An Essential Role for Interferon-gamma in Resistance to Mycobacterium tuberculosis Infection. *J. Exp. Med.* **178**, 2249–2254 (1993).
815. Chen, E. S., Greenlee, B. M., Wills-karp, M. & Moller, D. R. Attenuation of Lung Inflammation and Fibrosis in Interferon-gamma-Deficient Mice after Intratracheal Bleomycin. *Am. J. Respir. Cell Mol. Biol.* **24**, 545–555 (2001).
816. Ulloa, L., Doody, J. & Massagué, J. Inhibition of transforming growth factor-beta/SMAD signalling by the interferon-gamma/STATpathway. *Nature* **601**, 710–713 (1999).
817. Kimura, Y. *et al.* Pulmonary Hypertension and Other Potentially Fatal Pulmonary Complications in Systemic Juvenile Idiopathic Arthritis. *Arthritis Care Res. (Hoboken).* **65**, 745–752 (2013).
818. Alamoudi, O. S. B. & Attar, S. M. Pulmonary manifestations in systemic lupus erythematosus : Association with disease activity. *Respirology* **20**, 474–480 (2015).
819. Solomon, J. J. *et al.* Scleroderma lung disease. *Eur Respir J* **22**, 6–19 (2013).
820. Yunt, Z. X. & Solomon, J. J. Lung Disease in Rheumatoid Arthritis. *Rheum Dis Clin North Am.* **41**, 225–236 (2015).
821. Gerfaud-Valentin, M. *et al.* Parenchymal lung involvement in adult-onset Still disease. *Medicine (Baltimore).* **95**, e4258 (2016).
822. Guerrieri, A., Angeletti, G., Mazzolini, M., Bassi, I. & Nava, S. Respiratory Medicine Case Reports Pulmonary involvement in adult Still ' s disease : Case report and brief review of literature. *Respir. Med. Case Reports* **22**, 91–94 (2017).
823. Takakuwa, Y. *et al.* Adult-onset Still ' s disease-associated interstitial lung disease represents severe phenotype of the disease with higher rate of haemophagocytic syndrome and relapse. *Clin. Exp. Rheumatol.* **27**, S23–S27 (2019).
824. Ohshimo, S., Guzman, J., Costabel, U. & Bonella, F. Differential diagnosis of granulomatous lung disease : clues and pitfalls. *Eur Respir J* **26**, 170012 (2017).
825. Vastert, S. J., Kuis, W. & Grom, A. A. Systemic JIA: New Developments in the Understanding of the Pathophysiology and Therapy. *Best Pract. Res. Clin. Rheumatol.* **23**, 655–664 (2010).
826. Lalvani, A. & Millington, K. A. T Cells and Tuberculosis : Beyond Interferon-gamma. *J. Infect. Dis.* **197**, 941–943 (2008).
827. Weiss, E. S. *et al.* Interleukin-18 diagnostically distinguishes and pathogenically promotes human and murine macrophage activation syndrome. *Blood* **131**, 1442–1455 (2018).
828. Grom, A. A., Horne, A. & Benedetti, F. De. Macrophage activation syndrome. *Nat. Rev. Immunol.* **12**, 259–268 (2016).
829. Yang, C. *et al.* Association of NLRP3 and CARD8 genetic polymorphisms with juvenile idiopathic arthritis in a Taiwanese population. *Scand. J. Rheumatol.* **43**, 146–152 (2014).
830. Nagai, H. *et al.* Elevated serum gasdermin D N-terminal implicates monocyte and macrophage pyroptosis in adult-onset Still' s disease. *Rheumatology* Online ahead of print (2021). doi:10.1093/rheumatology/keaa814
831. Cader, M. Z. *et al.* C13orf31 (FAMIN) is a central regulator of immunometabolic function. *Nat. Rev. Immunol.* **17**, 1046–1056 (2016).

832. Foell, D. *et al.* Methotrexate Withdrawal at 6 vs 12 Months in Juvenile Idiopathic Arthritis in Remission. *Am. Med. Assoc.* **303**, 1266–1273 (2010).
833. Aljaberi, N. *et al.* The use of S100 proteins testing in juvenile idiopathic arthritis and autoinflammatory diseases in a pediatric clinical setting: a retrospective analysis. *Pediatr. Rheumatol.* **18**, 7 (2020).
834. Behrens, E. M. *et al.* Repeated TLR9 stimulation results in macrophage activation syndrome-like disease in mice. *J. Clin. Invest.* **9**, 2254–2277 (2011).
835. Girard-guyonvarc, C. *et al.* Unopposed IL-18 signaling leads to severe TLR9-induced macrophage activation syndrome in mice. *Blood* **131**, 1430–1441 (2018).
836. Canna, S. W. *et al.* Interferon-gamma Mediates Anemia but Is Dispensable for Fulminant Toll-like Receptor 9-Induced Macrophage Activation Syndrome and Hemophagocytosis in Mice. *Arthritis Rheum.* **65**, 1764–1775 (2013).
837. Brisse, E. *et al.* Mouse Cytomegalovirus Infection in BALB/c Mice Resembles Virus-Associated Secondary Hemophagocytic Lymphohistiocytosis and Shows a Pathogenesis Distinct from Primary Hemophagocytic Lymphohistiocytosis. *J. Immunol.* **196**, 3124–34 (2016).
838. Wang, A. *et al.* Specific sequences of infectious challenge lead to secondary hemophagocytic lymphohistiocytosis-like disease in mice. *PNAS* **116**, 2200–2209 (2019).
839. Strippoli, R., Caiello, I. & Benedetti, F. De. Reaching the Threshold : A Multilayer Pathogenesis of Macrophage Activation Syndrome. *J. Rheumatol.* **40**, 761–767 (2013).
840. Alehashemi, S. & Goldbach-Mansky, R. Human Autoinflammatory Diseases and NLRC4-Inflammasome Dysregulation Updates on Diagnosis, Treatment, and the Respective Roles of IL-1 and IL-18. *Front Immunol.* **11**, 1840 (2020).
841. Canna, S. W. *et al.* Life-threating NLRC4-associated hyperinflammation successfully treated with IL-18 inhibition. *J Allergy Clin Immunol* **139**, 1698–1701 (2017).
842. Nichols, R. D., Von Moltke, J. & Vance, R. E. NAIP/NLRC4 inflammasome activation in MRP8+ cells is sufficient to cause systemic inflammatory disease. *Nat. Commun.* **8**, 2209 (2017).
843. Weiss, E. S. *et al.* Interleukin-18 diagnostically distinguishes and pathogenically promotes human and murine macrophage activation syndrome. *Blood* **131**, 1442–1455 (2018).
844. McCoy, S. S., Stannard, J. & Kahlenberg, J. M. Targeting the Inflammasome in Rheumatic Diseases. *Transl Res* **167**, 125–137 (2017).
845. Hua, K. *et al.* Cyclooxygenase-2 Regulates NLRP3 In fl ammasome-Derived IL-1b Production. *J. Cell. Physiol.* **230**, 863–874 (2015).
846. Nariai, Y., Kamino, H., Obayashi, E., Kato, H. & Sakashita, G. Generation and characterization of antagonistic anti-human interleukin (IL)-18 monoclonal antibodies with high affinity : Two types of monoclonal antibodies against full-length IL-18 and the neoepitope of inflammatory caspase-cleaved active IL-18. *Arch. Biochem. Biophys.* **663**, 71–82 (2019).
847. Tsutsumi, N. *et al.* An innate interaction between IL-18 and the propeptide that inactivates its precursor form. *Sci. Rep.* **9**, 6160 (2019).
848. Canna, S. W. *et al.* An activating NLRC4 inflammasome mutation causes autoinflammation with recurrent macrophage activation syndrome. *Nat. Genet.* **46**, 1140–1146 (2015).
849. Gabay, C. *et al.* Open-label, multicentre, dose-escalating phase II clinical trial on the safety and efficacy of tadekinig alfa (IL-18BP) in adult-onset Still's disease. *Ann Rheum Dis.* **77**, 840–847 (2018).
850. Pereira, F. *et al.* Inflammasome genetics and complex diseases : a comprehensive review. *Eur. J. Hum. Genet.* **28**, 1307–1321 (2020).
851. Mao, K. *et al.* Nitric oxide suppresses NLRP3 inflammasome activation and protects against LPS-induced septic shock. *Cell Res.* **23**, 201–212 (2013).
852. Hernandez-cuellar, E. *et al.* Cutting Edge: Nitric Oxide Inhibits the NLRP3 Inflammasome. *J. Immunol.* **189**, 5113–5117 (2012).
853. Papotto, P. H., Ribot, J. C. & Silva-Santos, B. IL-17 + γδ T cells as kick-starters of inflammation. *Nat. Immunol.* **18**, 604–611 (2017).
854. Fiala, G. J., Gomes, A. Q. & Silva-santos, B. From thymus to periphery : Molecular basis of effector γδ -T cell differentiation. *Immunol. Rev.* **298**, 47–60 (2020).
855. Haas, J. D. *et al.* CCR6 and NK1 . 1 distinguish between IL-17A and IFN-gamma-producing gamma delta effector T cells. *Eur. J. Immunol.* **39**, 3488–3497 (2009).
856. Barros-Martins, J. *et al.* Effector γ δ T Cell Differentiation Relies on Master but Not Auxiliary Th Cell Transcription Factors. *J. Immunol.* **196**, 3642–3652 (2016).
857. Martin, B., Hirota, K., Cua, D. J., Stockinger, B. & Veldhoen, M. Interleukin-17-Producing gd T Cells Selectively Expand in Response to Pathogen Products and Environmental Signals. *Immunity* **31**, 321–330 (2009).
858. Papotto, P. H. *et al.* IL- 23 drives differentiation of peripheral gamma delata 17 T cells from adult bone marrow-derived precursors. *EMBO Rep.* **18**, 1957–1967 (2017).
859. Ribot, J. C. *et al.* CD27 is a thymic determinant of the balance between interferon-gamma- and interleukin 17-producing gamma delta T cell subsets. *Nat Immunol.* **10**, 427–436 (2009).
860. Jensen, K. D. C. *et al.* Thymic Selection Determines gamma delta T Cell Effector Fate: Antigen-Naive Cells Make Interleukin-17 and Antigen-Experienced Cells Make Interferon gamma. *Immunity* **29**, 90–100 (2008).
861. Papotto, P. H., Reinhardt, A., Prinz, I. & Silva-santos, B. Innately versatile : gamma delta 17 T cells in inflammatory and autoimmune diseases. **87**, 26–37 (2018).

862. Lalor, S. J. *et al.* Caspase-1 − Processed Cytokines IL-1β and IL-18 Promote IL-17 Production by γδ and CD4 T Cells That Mediate Autoimmunity. *J. Immunol.* **186**, 5738–5748 (2011).
863. Moreira-Teixeira, L. *et al.* Proinflammatory environment dictates the IL-17-producing capacity of human invariant NKT cells. *J. Immunol.* **186**, 5758–65 (2011).
864. Nieuwenhove, E. Van *et al.* Machine learning identifies an immunological pattern associated with multiple juvenile idiopathic arthritis subtypes. *Ann Rheum Dis* **78**, 617–628 (2019).
865. Lind, S. M. *et al.* IL-18 skews the invariant NKT-cell population via autoreactive activation in atopic eczema. *Eur. J. Immunol.* **39**, 2293–2301 (2009).
866. Zheng, Y. *et al.* Interleukin-22 , a Th17 cytokine , mediates IL-23-induced dermal inflammation and acanthosis. *Nature* **445**, 23–26 (2007).
867. Doisne, J. *et al.* Cutting Edge: Crucial Role of IL-1 and IL-23 in the Innate IL-17 Response of Peripheral L ymph Node NK1.1 − Invariant NKT Cells to Bacteria. *J. Immunol.* **186**, 662–666 (2011).
868. Wang, X. *et al.* GPR34-mediated sensing of lysophosphatidylserine released by apoptotic neutrophils activates type 3 innate lymphoid cells to mediate tissue repair. *Immunity* **8**, 1123-1136.e8. (2021).
869. Nograles, K. E. *et al.* Th 17 cytokines interleukin (IL) - 17 and IL- 22 modulate distinct inflammatory and keratinocyte-response pathways. *Br. J. Dermatology* **159**, 1092–1102 (2008).
870. Basu, R. *et al.* Th22 Cells Are an Important Source of IL-22 for Host Protection against Enteropathogenic Bacteria. *Immunity* **37**, 1061–1075 (2012).
871. Plank, M. W. *et al.* Th22 Cells Form a Distinct Th Lineage from Th17 Cells In Vitro with Unique Transcriptional Properties and Tbet-Dependent Th1 Plasticity. *J. Immunol.* **198**, 2182–2190 (2017).
872. Mestas, J. & Hughes, C. C. W. Of Mice and Not Men: Differences between Mouse and Human Immunology. *J. Immunol.* **172**, 2731–2738 (2004).
873. Zschaler, J., Schlorke, D. & Arnhold, J. Differences in Innate Immune Response between Man and Mouse Differences in Innate Immune Response between Man and Mouse. *Crit Rev Immunol* **34**, 433–454 (2014).
874. Wuyts, A. *et al.* NH 2 - and COOH-Terminal Truncations of Murine Granulocyte Chemotactic Protein-2 Augment the In Vitro and In Vivo Neutrophil Chemotactic Potency. *J. Immunol.* **163**, 6155–6163 (1999).
875. Verweyen, E. L., Pickering, A., Grom, A. A. & Schulert, G. S. Distinct Gene Expression Signatures Characterize Strong Clinical Responders Versus Nonresponders to Canakinumab in Children With Systemic Juvenile Idiopathic Arthritis. *Arthritis Rheumatol.* **73**, 1334–1340 (2021).
876. La, C. *et al.* Serum calprotectin (S100A8 / A9): a promising biomarker in diagnosis and up in different subgroups of juvenile idiopathic arthritis. *RMD open* **7**, e001646 (2021).
877. Kessel, C. *et al.* Calcium and zinc tune autoinflammatory Toll-like receptor 4 signaling by S100A12. *J Allergy Clin Immunol* **142**, 1370–1373 (2018).
878. Kaplan, M. J. Neutrophils in the pathogenesis and manifestations of SLE. *Nat. Rev. Rheumatol.* **7**, 691–699 (2011).
879. Taneja, R., Sharma, A. P., Hallett, M. B., Findlay, G. P. & Morris, M. R. Immature circulating neutrophils in sepsis have impaired phagoctosis and calcium signaling. *Shock* **30**, 618–622 (2008).
880. Crayne, C. B., Albeituni, S., Nichols, K. E. & Cron, R. Q. The Immunology of Macrophage Activation Syndrome. *Front. Immunol.* **10**, 119 (2019).
881. Donadieu, J. *et al.* Neutrophil depletion impairs natural killer cell maturation , function , and homeostasis. *J. Exp. Med.* **209**, 565–580 (2012).
882. Bobek, D., Grčević, D., Kovačić, N., Lukić, I. K. & Jelušić, M. The presence of high mobility group box-1 and soluble receptor for advanced glycation end-products in juvenile idiopathic arthritis and juvenile systemic lupus erythematosus. *Pediatr. Rheumatol.* **12**, 50 (2014).
883. Harris, H. E., Andersson, U. & Pisetsky, D. S. HMGB1: A multifunctional alarmin driving autoimmune and inflammatory disease. *Nat. Rev. Rheumatol.* **8**, 195–202 (2012).
884. Kang, R. *et al.* HMGB1 in Health and Disease. *Mol Asp. Med.* **0**, 1–116 (2014).
885. Yang, H. *et al.* Identification of CD163 as an antiinflammatory receptor for HMGB1-haptoglobin complexes. *JCI Insight* **1**, e85375 (2018).
886. Holzinger, D. *et al.* S100A12 as diagnostic tool in the differential diagnosis of sJIA associated MAS vs. hereditary or acquired HLH. *Pediatr. Rheumatol.* **13**, 12–13 (2015).
887. Chan, J. K. *et al.* Alarmins : awaiting a clinical response. *J. Clin. Invest.* **122**, 2711–2719 (2012).
888. Donato, R. *et al.* Functions of S100 Proteins. *Curr Mol Med.* **13**, 24–57 (2013).
889. Lande, R. *et al.* Neutrophils Activate Plasmacytoid Dendritic Cells by Releasing Self-DNA–Peptide Complexes in Systemic Lupus Erythematosus. *Sci. Transl. Med.* **3**, 73ra19 (2011).
890. Donis-Maturano, L. *et al.* Prolonged exposure to neutrophil extracellular traps can induce mitochondrial damage in macrophages and dendritic cells. *Springerplus* **4**, 161 (2015).
891. Caudrillier, A. *et al.* Platelets induce neutrophil extracellular traps in transfusion-related acute lung injury. *J. Clin. Invest.* **122**, 2661–2671 (2012).
892. Narasaraju, T. *et al.* Excessive Neutrophils and Neutrophil Extracellular Traps Contribute to Acute Lung Injury of Influenza Pneumonitis. *Am. J. Pathol.* **179**, 199–210 (2011).
893. Rossaint, J. *et al.* Synchronized integrin engagement and chemokine activation is crucial in neutrophil extracellular trap-mediated sterile inflammation. *Blood* **123**, 2573–2584 (2014).
894. Gohar, F. *et al.* Molecular signature characterisation of different inflammatory phenotypes of systemic juvenile

idiopathic arthritis. *Ann Rheum Dis* **78**, 1107–1113 (2019).
895. Mahmud, S. A. & Binstadt, B. A. Autoantibodies in the Pathogenesis , Diagnosis , and Prognosis of Juvenile Idiopathic Arthritis. *Front Immunol.* **9**, 3168 (2019).
896. Vehe, R. K., Begovich, A. B. & Nepom, B. S. HLA susceptibility genes in rheumatoid factor positive juvenile rheumatoid arthritis. *J Rheumatol Suppl.* 11–5 (1990).
897. Silvestri, A. De *et al.* HLA-DRB1 alleles and juvenile idiopathic arthritis : Diagnostic clues emerging from a meta-analysis. *Autoimmun. Rev.* **16**, 1230–1236 (2017).
898. Hersh, A. O. & Prahalad, S. Immunogenetics of juvenile idiopathic arthritis : A comprehensive review. *J. Autoimmun.* **64**, 113–124 (2015).
899. Glerup, M., Herlin, T. & Twilt, M. Remission rate is not dependent on the presence of antinuclear antibodies in juvenile idiopathic arthritis. *Clin Exp Rheumatol.* **36**, 671–676 (2017).
900. Hügle, B., Hinze, C., Lainka, E., Fischer, N. & Haas, J. Development of positive antinuclear antibodies and rheumatoid factor in systemic juvenile idiopathic arthritis points toward an autoimmune phenotype later in the disease course. *Pediatr. Rheumatol.* **12**, 28 (2014).
901. Zambrano-Zaragoza, J. F., Romo-Martínez, E. J., Durán-Avelar, M. D. J., García-Magallanes, N. & Vibanco-Pérez, N. Th17 cells in autoimmune and infectious diseases. *Int. J. Inflam.* **2014**, 651503 (2014).
902. Lee, G. R. The Balance of Th17 versus Treg Cells in Autoimmunity. *Int. J. Mol. Sci.* **19**, 730 (2018).
903. Omenetti, S. & Pizarro, T. T. The Treg / Th17 Axis : A Dynamic Balance Regulated by the Gut Microbiome. *Front. Immunol.* **6**, 639 (2015).
904. Geginat, J. *et al.* Plasticity of Human CD4 T Cell Subsets Plasticity of human CD4 T cell subsets. *Front Immunol.* **5**, 630 (2014).
905. Ghoreschi, K. *et al.* Generation of pathogenic TH17 cells in the absence of TGF-beta signalling. *Nature* **467**, 967–971 (2010).
906. Ferguson, I. D. *et al.* T Cell Receptor-Independent, CD31/IL-17A-Driven Inflammatory Axis Shapes Synovitis in Juvenile Idiopathic Arthritis. *Front. Immunol.* **9**, 1802 (2018).
907. Revu, S. *et al.* IL-23 and IL-1β Drive Human Th17 Cell Differentiation and Metabolic Reprogramming in Absence of CD28 Costimulation. *Cell Rep.* **22**, 2642–2653 (2018).
908. Schurgers, E., Billiau, A. & Matthys, P. Collagen-Induced Arthritis as an Animal Model for Rheumatoid Arthritis : Focus on Interferon-gamma. *J. Interf. cytokine Res.* **31**, 917–926 (2011).
909. Güler, M. L. *et al.* Genetic Susceptibility to Leishmania: IL-12 Responsiveness in TH1 Cell Development. *Science (80-.).* **27**, 984–7 (1996).
910. Maggi, L. *et al.* Th17 and Th1 Lymphocytes in Oligoarticular Juvenile Idiopathic Arthritis. *Front. Immunol.* **10**, 450 (2019).
911. Meng, G., Zhang, F., Fuss, I., Kitani, A. & Strober, W. A Mutation in the Nlrp3 Gene Causing Inflammasome Hyperactivation Potentiates Th17 Cell-Dominant Immune Responses. *Immunity* **30**, 860–874 (2009).
912. Ovadia, A. *et al.* T helper 17 polarization in familial Mediterranean fever. *Genes Immun.* **14**, 212–216 (2013).
913. Elemam, N. M., Hannawi, S. & Maghazachi, A. A. Role of Chemokines and Chemokine Receptors in Rheumatoid Arthritis. *ImmunoTargets Ther.* **9**, 43–56 (2020).
914. Pillinger, M. H. & Abramson, S. B. The neutrophil in rheumatoid arthritis. *Rheum Dis Clin North Am* **21**, 691–714 (1995).
915. Jarvis, J. N., Jiang, K., Petty, H. R. & Centola, M. Neutrophils : the forgotten cell in JIA disease pathogenesis. *Pediatr. Rheumatol.* **5**, 13 (2007).
916. Hu, Z., Jiang, K., Barton, M., Chen, Y. & Jarvis, J. N. Modeling Transcriptional Rewiring in Neutrophils Through the Course of Treated Juvenile Idiopathic Arthritis. *Sci. Rep.* **8**, 7805 (2018).
917. Dvorak, H. F. Tumors: wounds that do not heal. Similarities between tumor stroma generation and wound healing. *N. Engl. J. Med.* **315**, 1650–9 (1986).
918. Singel, K. L. & Segal, B. H. Neutrophils in the tumor microenvironment: trying to heal the wound that cannot heal. *Immunol. Rev.* **273**, 329–343 (2016).
919. Chung, A. S. *et al.* An interleukin-17 – mediated paracrine network promotes tumor resistance to anti-angiogenic therapy. *Nat. Med.* **19**, 1114–1123 (2013).
920. Langowski, J. L., Kastelein, R. A. & Oft, M. Swords into plowshares : IL-23 repurposes tumor immune surveillance. *Trends Immunol.* **28**, 207–212 (2007).
921. Grivennikov, S. I. *et al.* Adenoma-linked barrier defects and microbial products drive IL-23/IL-17-mediated tumour growth. *Nature* **491**, 254–258 (2012).
922. Tosolini, M. *et al.* Clinical Impact of Different Classes of Infiltrating T Cytotoxic and Helper Cells (Th1 , Th2 , Treg , Th17) in Patients with Colorectal Cancer. *Cancer Res.* **71**, 1263–71 (2011).
923. Marigo, I. *et al.* Tumor-Induced Tolerance and Immune Suppression Depend on the C / EBPb Transcription Factor. *Immunity* **32**, 790–802 (2010).
924. Pum, A., Ennemoser, M., Adage, T. & Kungl, A. J. Cytokines and Chemokines in SARS-CoV-2 Infections — Therapeutic Strategies Targeting Cytokine Storm. *Biomolecules* **11**, 91 (2021).
925. Ha, H., Debnath, B. & Neamati, N. Role of the CXCL8-CXCR1 / 2 Axis in Cancer and Inflammatory Diseases. *Theranostics* **7**, 1543–1588 (2017).
926. Rotondo, R. *et al.* IL-8 induces exocytosis of arginase 1 by neutrophil polymorphonuclears in nonsmall cell lung

cancer. *Int. J. Cancer* **893**, 887–893 (2009).
927. Rotondo, R. *et al.* Exocytosis of azurophil and arginase 1-containing granules by activated polymorphonuclear neutrophils is required to inhibit T lymphocyte proliferation. *J. Leukoc. Biol.* **89**, 721–727 (2011).
928. Zhao, Y. *et al.* Clinical features and outcomes of patients with hemophagocytic lymphohistiocytosis at onset of systemic autoinflammatory disorder and compare with Epstein-Barr virus (EBV)-related hemophagocytic lymphohistiocytosis. *Medicine (Baltimore).* **99**, e18503 (2020).
929. Vasiliu, I. M., Petri, M. A. & Baer, A. N. Therapy with granulocyte colony-stimulating factor in systemic lupus erythematosus may be associated with severe flares. *J Rheumatol* **33**, 1878–80 (2006).
930. Liu, L., Liu, Y., Yan, X., Zhou, C. & Xiong, X. The role of granulocyte colony-stimulating factor in breast cancer development: A review. *Mol Med Rep* **21**, 2019–2029 (2020).
931. Schulert, G. S. & Grom, A. A. Pathogenesis of Macrophage Activation Syndrome and Potential for Cytokine- Directed Therapies. *Annu. Rev. Med.* **66**, 145–159 (2015).
932. Hinze, T. *et al.* A dysregulated interleukin-18/interferon-γ/CXCL9 axis impacts treatment response to canakinumab in systemic juvenile idiopathic arthritis. *Rheumatology* Online ahead of print (2021).
933. Suzuki, T. *et al.* Familial pulmonary alveolar proteinosis caused by mutations in CSF2RA. *J Exp Med* **205**, 2703–10 (2008).
934. Martinez-Moczygemba, M. *et al.* Pulmonary alveolar proteinosis caused by deletion of the GM-CSFRalpha gene in the X chromosome pseudoautosomal region 1. *J Exp Med* **205**, 2711–6 (2008).
935. Ebina-Shibuya, R. *et al.* The double knockout of Bach1 and Bach2 in mice reveals shared compensatory mechanisms in regulating alveolar macrophage function and lung surfactant homeostasis. *J Biochem* **160**, 333–344 (2016).
936. Carey, B. & Trapnell, B. C. The molecular basis of pulmonary alveolar proteinosis. *Clin. Immunol.* **135**, 223–35 (2010).
937. Gao, D. *et al.* IFNγ Is Essential for Alveolar Macrophage Driven Lung Inflammation in Macrophage Activation Syndrome. in *ACR Convergence 2020* 72 (suppl 10) (2020).
938. Lee, P. Y., Wang, J.-X., Parisini, E., Dascher, C. C. & Nigrovic, P. A. Ly6 family proteins in neutrophil biology. *J. Leukoc. Biol.* **94**, 585–94 (2013).
939. Daley, J. M., Thomay, A. A., Connolly, M. D., Reichner, J. S. & Albina, J. E. Use of Ly6G-specific monoclonal antibody to deplete neutrophils in mice. *J. Leukoc. Biol.* **83**, 64–70 (2008).
940. Schumak, B. *et al.* Specific depletion of Ly6Chi inflammatory monocytes prevents immunopathology in experimental cerebral malaria. *PLoS One* **10**, e0124080 (2015).
941. Ma, C. & Greten, T. F. Editorial: "Invisible" MDSC in tumor-bearing individuals after antibody depletion: fact or fiction? *J. Leukoc. Biol.* **99**, 794–794 (2016).
942. Van den Steen, P. E. *et al.* Immunopathology and dexamethasone therapy in a new model for malaria-associated acute respiratory distress syndrome. *Am. J. Respir. Crit. Care Med.* **181**, 957–968 (2010).
943. Duarte, M. I., Corbett, C. E., Boulos, M. & Amato Neto, V. Ultrastructure of the lung in falciparum malaria. *Am. J. Trop. Med. Hyg.* **34**, 31–5 (1985).
944. Van den Steen, P. E. *et al.* Pathogenesis of malaria-associated acute respiratory distress syndrome. *Trends Parasitol.* **29**, 346–358 (2013).
945. Pham, T.-T. *et al.* Pathogenic CD8+ T Cells Cause Increased Levels of VEGF-A in Experimental Malaria-Associated Acute Respiratory Distress Syndrome, but Therapeutic VEGFR Inhibition Is Not Effective. *Front. Cell. Infect. Microbiol.* **7**, 416 (2017).
946. Sercundes, M. K. *et al.* Targeting Neutrophils to Prevent Malaria-Associated Acute Lung Injury/Acute Respiratory Distress Syndrome in Mice. *PLoS Pathog.* **12**, e1006054 (2016).
947. Vandermosten, L. *et al.* Experimental malaria-associated acute respiratory distress syndrome is dependent on the parasite-host combination and coincides with normocyte invasion. *Malar. J.* **17**, 102 (2018).
948. Rose, S., Misharin, A. & Perlman, H. A novel Ly6C/Ly6G-based strategy to analyze the mouse splenic myeloid compartment. *Cytom. Part A* **81 A**, 343–350 (2012).
949. Rocha, B. C. *et al.* Type I interferon transcriptional signature in neutrophils and high frequency of low-density granulocytes are associated with tissue damage in malaria. *Cell Rep.* **13**, 2829–2841 (2015).
950. Eash, K. J., Greenbaum, A. M., Gopalan, P. K. & Link, D. C. CXCR2 and CXCR4 antagonistically regulate neutrophil trafficking from murine bone marrow. *J. Clin. Invest.* **120**, 2423–2431 (2010).
951. Möhle, R. *et al.* Modulation of CXC chemokine receptor expression and function in human neutrophils during aging in vitro suggests a role in their clearance from circulation. *Mediators Inflamm.* **2009**, 790174 (2009).
952. Bruhn, K. W., Dekitani, K., Nielsen, T. B., Pantapalangkoor, P. & Spellberg, B. Ly6G-mediated depletion of neutrophils is dependent on macrophages. *Results Immunol.* **6**, 5–7 (2016).
953. Masters, S. L., Simon, A., Aksentijevich, I. & Kastner, D. L. Horror Autoinflammaticus : The Molecular Pathophysiology of Autoinflammatory Disease ∗. *Annu Rev Immunol* **27**, 621–68 (2009).
954. de Jesus, A. A., Canna, S. W., Liu, Y. & Goldbach-Mansky, R. Molecular Mechanisms in Genetically Defined Autoinflammatory Diseases : Disorders of Amplified Danger. *Annu. Rev. Immunol.* **33**, 823–74 (2015).
955. Harapas, C. R., Steiner, A., Davidson, S., Masters, S. L. & Davidson, S. An Update on Autoinflammatory Diseases : Inflammasomopathies. *Curr Rheumatol Rep.* **21**, 261–9 (2014).
956. Hayward, J. A., Mathur, A., Ngo, C. & Man, S. M. Cytosolic Recognition of Microbes and Pathogens: Inflammasomes in Action. *Microbiol Mol Biol Rev.* **82**, e00015-18 (2018).
957. Centola, M. *et al.* The gene for familial Mediterranean fever, MEFV, is expressed in early leukocyte development and

is regulated in response to inflammatory mediators. *Blood* **95**, 3223–31 (2000).
958. Heilig, R. & Broz, P. Function and mechanism of the pyrin inflammasome. *Eur J Immunol.* **48**, 230–238 (2018).
959. Torre-Minguela, C. de, Castillo, P. M. Del & Pelegrín, P. The NLRP3 and Pyrin Inflammasomes: Implications in the Pathophysiology of Autoinflammatory Diseases. *Front Immunol.* **8**, 43 (2017).
960. Park, Y. H., Wood, G., Kastner, D. L. & Chae, J. J. Pyrin inflammasome activation and RhoA signaling in the autoinflammatory diseases FMF and HIDS. *Nat Immunol.* **17**, 914–21 (2016).
961. Aubert, D. F. *et al.* A Burkholderia Type VI Effector Deamidates Rho GTPases to Activate the Pyrin Inflammasome and Trigger Inflammation. *Cell Host Microbe.* **19**, 664–74 (2016).
962. Xu, H. *et al.* Innate immune sensing of bacterial modifications of Rho GTPases by the Pyrin inflammasome. *Nature* **513**, 237–41 (2014).
963. Gavrilin, M. A. *et al.* Activation of the pyrin inflammasome by intracellular Burkholderia cenocepacia. *J Immunol.* **188**, 3469–77 (2012).
964. Dumas, A. *et al.* The inflammasome pyrin contributes to pertussis toxin-induced IL-1β synthesis, neutrophil intravascular crawling and autoimmune encephalomyelitis. *PLoS Pathog.* **10**, e1004150 (2014).
965. Federici, S. *et al.* Evidence-based provisional clinical classification criteria for autoinflammatory periodic fevers. *Ann Rheum Dis.* **74**, 799–80 (2015).
966. Ozen, S. *et al.* EULAR recommendations for the management of familial Mediterranean fever. *Ann Rheum Dis.* **75**, 644–51 (2016).
967. Manukyan, G. *et al.* Activated phenotype of circulating neutrophils in familial Mediterranean fever. *Immunobiology* **218**, 892–8 (2013).
968. Mitroulis, I., Kourtzelis, I., Kambas, K., Chrysanthopoulou, A. & Ritis, K. Evidence for the involvement of mTOR inhibition and basal autophagy in familial Mediterranean fever phenotype. *Hum Immunol* **72**, 135–8 (2011).
969. Apostolidou, E. *et al.* Neutrophil extracellular traps regulate IL-1β-mediated inflammation in familial Mediterranean fever. *Ann Rheum Dis* **75**, 269–77 (2016).
970. Stoler, I. *et al.* Gene-Dose Effect of MEFV Gain-of-Function Mutations Determines ex vivo Neutrophil Activation in Familial Mediterranean Fever. *Front Immunol.* **11**, 716 (2020).
971. Vandooren, J., Geurts, N., Martens, E., Van Den Steen, P. E. & Opdenakker, G. Zymography methods for visualizing hydrolytic enzymes. *Nat. Methods* **10**, 211–220 (2013).
972. Love, M. I., Huber, W. & Anders, S. Moderated estimation of fold change and dispersion for RNA-seq data with DESeq2. *Genome Biol.* **15**, 550 (2014).
973. Metzemaekers, M., Vandendriessche, S., Berghmans, N., Gouwy, M. & Proost, P. Truncation of CXCL8 to CXCL8(9-77) enhances actin polymerization and in vivo migration of neutrophils. *J Leukoc Biol* **107**, 1167–1173 (2020).
974. De Buck, M. *et al.* Serum amyloid A1α induces paracrine IL-8/CXCL8 via TLR2 and directly synergizes with this chemokine via CXCR2 and formyl peptide receptor 2 to recruit neutrophils. *J Leukoc Biol* **98**, 1049–60 (2015).
975. Marini, O. *et al.* Mature CD10 + and immature CD10 - neutrophils present in G-CSF-treated donors display opposite effects on T cells. *Blood* **129**, 1343–1356 (2017).
976. Sengeløv, H. *et al.* Mobilization of granules and secretory vesicles during in vivo exudation of human neutrophils. *J Immunol* **154**, 4157–65 (1995).
977. Guma, M. *et al.* Caspase 1-independent activation of interleukin-1beta in neutrophil-predominant inflammation. *Arthritis Rheumatol.* **60**, 3642–50 (2009).
978. Mankan, A. K., Dau, T., Jenne, D. & Hornung, V. The NLRP3/ASC/Caspase-1 axis regulates IL-1β processing in neutrophils. *Eur J Immunol.* **42**, 710–5 (2012).
979. Karmakar, M. *et al.* Neutrophil IL-1β processing induced by pneumolysin is mediated by the NLRP3/ASC inflammasome and caspase-1 activation and is dependent on K+ efflux. *J Immunol* **194**, 1763–75 (2015).
980. Chen, K. W. *et al.* The neutrophil NLRC4 inflammasome selectively promotes IL-1β maturation without pyroptosis during acute Salmonella challenge. *Cell Rep.* **8**, 570–82 (2014).
981. Pérez-Figueroa, E. *et al.* Activation of NLRP3 inflammasome in human neutrophils by Helicobacter pylori infection. *Innate Immun* **22**, 103–12 (2016).
982. Mohammadi, N. *et al.* Neutrophils Directly Recognize Group B Streptococci and Contribute to Interleukin-1β Production during Infection. *PLoS One* **11**, e0160249 (2016).
983. Karmakar, M., Sun, Y., Hise, A. G., Rietsch, A. & Pearlman, E. Cutting edge: IL-1β processing during Pseudomonas aeruginosa infection is mediated by neutrophil serine proteases and is independent of NLRC4 and caspase-1. *J Immunol* **189**, 4231–5 (2012).
984. Balci-Peynircioglu, B. *et al.* Potential role of pyrin, the protein mutated in familial Mediterranean fever, during inflammatory cell migration. *Clin. Exp. Rheumatol.* **36**, 116–124 (2018).
985. Ramos, M. V. *et al.* Association of haemolytic uraemic syndrome with dysregulation of chemokine receptor expression in circulating monocytes. *Clin Sci* **129**, 235–44 (2015).
986. Ravi, A. K. *et al.* COPD monocytes demonstrate impaired migratory ability. *Respir Res* **18**, 90 (2017).
987. D'Amico, G. *et al.* Uncoupling of inflammatory chemokine receptors by IL-10: generation of functional decoys. *Nat Immunol.* **1**, 387–91 (2000).
988. Lidar, M. *et al.* Colchicine nonresponsiveness in familial Mediterranean fever: clinical, genetic, pharmacokinetic, and socioeconomic characterization. *Semin Arthritis Rheum* **33**, 273–82 (2004).
989. Bonfoco, E., Ceccatelli, S., Manzo, L. & Nicotera, P. Colchicine induces apoptosis in cerebellar granule cells. *Exp Cell*

Res **218**, 189–200 (1995).
990. Dalbeth, N., Lauterio, T. J. & Wolfe, H. R. Mechanism of action of colchicine in the treatment of gout. *Clin Ther* **36**, 1465–79 (2014).
991. Coelho, F. M. *et al.* The chemokine receptors CXCR1/CXCR2 modulate antigen-induced arthritis by regulating adhesion of neutrophils to the synovial microvasculature. *Arthritis Rheumatol.* **58**, 2329–37 (2008).
992. Angelidis, C. *et al.* Colchicine Pharmacokinetics and Mechanism of Action. *Curr Pharm Des* **24**, 659–663 (2018).
993. Wingett, S. W. & Andrews, S. FastQ Screen: A tool for multi-genome mapping and quality control. *F1000Research* **7**, 1338 (2018).
994. Li, H. *et al.* The Sequence Alignment/Map format and SAMtools. *Bioinformatics* **25**, 2078–2079 (2009).

ACKNOWLEDGMENTS, PERSONAL CONTRIBUTION, AND CONFLICT OF INTEREST STATEMENT

ACKNOWLEDGMENTS, PERSONAL CONTRIBUTION, AND CONFLICT OF INTEREST STATEMENT

Acknowledgments

The Research Foundation-Flanders (FWO-Vlaanderen) (G0A3218N), KU Leuven ("C1" grant C16/17/010), the Rega Foundation, and the European Union's Horizon 2020 research and innovation program (No 779295) supported this research. We thank all donors who participated in this research and all internship students who assisted with the experiments. Anti-G-CSF-receptor antibodies (Ch5E2-VR81-mIgG1k) were kindly provided by CSL Limited Australia. We thank Jens Wouters, Sofie Knoops, and Erik Martens for their excellent technical help. We thank our lab members for their insightful discussions.

My sincere thanks go to Prof. Ghislain Opdenakker who critically reviewed Chapters 1-3 and Chapter 5. Thanks to Dr. Lisa Lindqvist, Dr. Helen Cao, and Dr. Judith Field from CSL Limited Australia for their help and critical review of Chapter 5.

Author contributions

Cover

BMD designed the cover with Biorender software.

Chapter 1

BMD wrote the first draft of the manuscript and designed figures with Biorender software. MM, PP, CW, and PM critically read and edited the manuscript.

Chapter 2

BMD wrote the first draft of the manuscript and designed figures with Biorender software. MM, PP and PM critically read and edited the manuscript.

Chapter 3

BMD wrote the chapter and PP, and PM critically read and edited the chapter.

Chapter 4

BMD, and PM designed the study. BMD, EB, KA, JV, MI, ADV, TM, NB, and LD performed experiments. *In vivo* experiments and flow cytometry were performed by BMD, EB, KA, JV, MI, ADV, TM, and NB. CW was responsible for diagnosis and recruitment of patients. BMD, JV, MI, and LD performed the cytokine measurements. *In vitro* assays, histology, and western blot were performed by BMD, TM, NB, and EB. LD and LB kindly provided the *in vivo* antibodies. LD performed the luciferase assay. LD, PP, CW, and PM supervised the project. BMD wrote the first draft of the manuscript and designed the figures. All authors critically read, edited, and approved the final manuscript.

Chapter 5

BMD, EB, and PM designed the study. BMD, EB, KA, JF, JV, BB, OB, ADV, TM and NB performed experiments. *In vivo* experiments and flow cytometry were performed by BMD, EB, KA, JF, JV, ADV, TM and NB. CW was responsible for diagnosis and recruitment of patients. BMD, EB, JV, and TM performed the cytokine measurements. *In vitro* assays and histology were performed by BMD, EB, TM, and NB. *In vitro* osteoclast formation was performed by TM. BMD, OB, and BB performed the single-cell RNA sequencing experiments and analyses. AL, DL, PP, CW, and PM supervised the project. BMD and EB wrote the first draft of the manuscript and designed the figures. All authors critically read, edited, and approved the final manuscript.

Chapter 6
BMD, TD, and PM designed the study. BMD, TD, KD, AV, KA, FP, TM, LS, and EV performed experiments and analysed data under the supervision of PM, JV, GV, CW, and EV. *In vivo* experiments and flow cytometry were performed by BMD, KA, and TM. TD was involved in the lung function measurements. KD and LS performed the micro-computed tomography experiments. BMD and FP performed the immunofluorescence stainings. Histopathological stainings were evaluated by AV and EV. BMD, TD, PM, JV, and GV were involved in study conceptualisation and design. BMD wrote the initial manuscript, which was critically revised by all other authors. All authors approved the final version of the manuscript.

Chapter 7
Chapter discussion was written by BMD and critically read and edited by PP, and PM. Figure was designed with Biorender software.

Addendum 1
EP, BMD, PM, and PVD designed the study. EP, BMD, LV, TM, TP, and HP performed the experiments. *In vivo* experiments and flow cytometry were performed by EP, BMD, LV, TM, TP, and HP. EP performed the antibody competition test. FACS experiments were performed by EP and TM. EP and BMD analysed the data. PM, GO, and PVDS conceived the study. LB provided the IgG2a isotype control antibodies. EP, BMD, PM, and PVDS wrote the first drafts of the manuscript. All authors critically read and edited the manuscript. All authors read and approved the final manuscript.

Addendum 2
All authors contributed to the study's conception and design. BMD performed flow cytometry, zymography experiments, and analysed RNAseq data. BMD and MM were responsible for RNA extraction and qPCR experiments. MM carried out induction and chemotaxis experiments with the assistance of MG, LV, and NP. BMD, MM, LV, and NP quantified cytokines and chemokines, MPO, and S100 proteins levels in plasma. MM and MC performed NETosis and apoptosis experiments (data not shown). MM and LV performed ROS production experiments. EVN, AB, LDS, SV, EDL, and CW were responsible for the diagnosis and recruitment of patients and/or collection of clinical data. BMD and MM wrote the first draft of the manuscript. All authors critically read and edited the manuscript and approved the final manuscript.

Conflict of interest statement
The authors declare no conflict of interest with the contents of this thesis. None of the sponsors of this work had a role in the study design, the collection, analysis, or interpretation of this data, and in the writing of the thesis manuscript.

CURRICULUM VITAE

CURRICULUM VITAE

Personal information

Name	Bert Malengier-Devlies
E-mail	bert.malengier@kuleuven.be
Tel	+32 493 700 844
Nationality	Belgian
Date of birth	January 3th, 1993
Place of birth	Roeselare
Address	Brouwersstraat 17, box 403, 3000 Leuven, Belgium
Driver's licence B	



Education

2016-2021	**Doctoral training in Biomedical Sciences** Laboratory of Immunobiology, Rega Institute, KU Leuven Promotor: Prof. Dr. Patrick Matthys Co-promotors: Prof. Dr. Carine Wouters / Prof. Dr Paul Proost
2014-2016	**Master of Science in the Biomedical Sciences** Graduated *magna cum laude* KU Leuven, Belgium Master's thesis: "Characterisation of *Nup210* knockout mice: implications for the adaptive immune system" Laboratory of Genetics of Autoimmunity, KU Leuven Promotor: Prof. Dr. Adrian Liston
2014	**Honours college project** Université Métropolitaine (Université Mons, Université Lille, KULAK)
2011-2014	**Bachelor of Science in the Biomedical Sciences** Graduated *magna cum laude* KULAK, KU Leuven, Belgium
2005-2011	**Sciences – Mathematics** Graduated *cum laude* Klein Seminarie, Roeselare

Official Certificates and training

Radio Safety, KU Leuven (2019); Single cell sequencing, VIB (2019); Scientific Integrity Part I and II, KU Leuven (2016/2018); Single cell sequencing, KU Leuven (2018); Writing Clinic for Biomedical Researchers, KU Leuven (2018); Effective poster sessions, KU Leuven (2016); FELASA B Laboratory Animal Sciences, Module I, KU Leuven (2014); First aid, KULAK (2011)

Internships

2015-2016	Lab Internship, KU Leuven • Translational Research Centre for Gastrointestinal Disorders (TARGED) (Prof. Dr. Gianluca Matteoli) • Laboratory for Disease Mechanisms in Cancer (Prof. Dr. Kim De Keersmaecker) • Laboratory of Molecular Bacteriology (Prof. Dr. Tassos Economou)
2014	Student-Researcher (LVSO) at the Laboratory for Thrombosis Research (Prof. Dr. Simon Demeyer), KULAK

Skills

Languages	Dutch: mother tongue, English: excellent, French: good
Software	Office, Outlook, GraphPad Prism, R studio, FlowJo, Loupe Cell Browser, IDEAS, IncuCyte
Expertise	Immunological assays: (multiplex) ELISA, Meso Scale Discovery, primer design, RNA/DNA extraction, (q)PCR, WB Cellular biology: mammalian cell culture, cell culture assays Flow cytometry: multicolour panel design, BD FACSCanto II, BD LSRFortessa, BD FACSymphony, cell sorting Single-cell sequencing: Seurat single-cell sequencing analysis Animal models: mouse handling and injection, gavage, mouse necropsy and preparation of single cell suspensions from diverse organs

Science communication

2021	27th European Paediatric Rheumatology Congress. *Lung functioning and inflammation in a mouse model of systemic juvenile idiopathic arthritis* Poster presentation
2021	Virtual European Congress of Immunology. *Role for G-CSF in neutrophilic extramedullary myelopoiesis in systemic juvenile idiopathic arthritis* Oral presentation
2020	Seminars in immunology, Leuven, Belgium. *Phenotypical and functional characterisation of neutrophils in two pyrin-associated autoinflammatory diseases* Oral presentation, together with Mieke Metzemaekers
2019	16th International Conference on Innate Immunity, Rhodes, Greece. *Innate γδ-T cells initiate disease pathogenesis in a mouse model of systemic juvenile idiopathic arthritis, an autoinflammatory immune disorder*. Oral presentation
2018	Doctoral research seminar, Leuven, Belgium. *Neutrophils and γδ-T cells are main players in the onset of systemic juvenile idiopathic arthritis via the pro-inflammatory cytokines IL-22 and IL-1β* Oral presentation
2018	European Congress of Immunology, Amsterdam, The Netherlands. *IL17- and IL22-producing γδ-T cells in the pathogenesis of systemic juvenile idiopathic arthritis* Poster presentation

Awards

2019	Aegean Travel Award for oral presentation - 16th International Conference on Innate Immunity
2018	Abstract selected for an EFIS-ACTERIA travel grant - European Congress of Immunology

Educational activities

2017-2021	Supervisor of Master's thesis "Biological role of neutrophils in systemic juvenile idiopathic arthritis and method optimisation for characterisation of neutrophil subsets" by Lise De Smedt, Pharmaceutical Sciences (KU Leuven) "Unravelling the biological role of gamma delta (γδ) T cells and neutrophils in Systemic Juvenile Idiopathic Arthritis" by Hanne Engels, Bioscience Engineering (KU Leuven) "Unravelling the effect of interferon-gamma on inflammasome activation and characterisation of the lung pathology in Systemic Juvenile Idiopathic Arthritis" by Jalina Op de Beeck, Bioscience Engineering (KU Leuven) "Neutrophil subsets during extramedullary myelopoiesis" by Eline Bernaerts, Biochemical Sciences (KU Leuven) "Synovial macrophages: targets for pathological programming in inflammatory disease?" Evelyne Hellinck, Biomedical Sciences (KU Leuven)
2019-2020	Supervisor Bachelor's thesis "The effect of anti-IL-1β on the lung pathology in the sJIA mouse model" Gilles Verbinnen, Biochemistry and Biotechnology (KU Leuven)
2017-2021	Supervision and guidance in practical courses and workshops of Immunology (2nd Bachelor students, Biomedical Sciences, KU Leuven, and KULAK)
2015-2019	Supervisor in multiple lab internships (1st master students, Biomedical Sciences, KU Leuven)

Articles

Accepted articles

First or equally first author

1. Pollenus E.*, **Malengier-Devlies B.***, Vandermosten L., Pham T-T., Mitera T., Possemiers H., Boon L., Opdenakker G., Matthys P.*, Van den Steen PE.* (2019). Limitations of neutrophil depletion by anti-Ly6G antibodies in two heterogenic immunological models. *Immunology Letters*, 212, 30-36. (IP 3.7)
   * equally contribution
2. Sanchez-Felipe L.*, Vercruysse T.*, Sharma S.*, Ma J., Lemmens V.*, Van Looveren D.*, Arkalagud Javarappa M. P.*, Boudewijns R.*, **Malengier-Devlies B**.*, Liesenborghs L.*, Kaptein S. J. F., De Keyzer C., Bervoets L., Debaveye S., Rasulova M., Seldeslachts L., Li L., Jansen S., Yakass M. B., Verstrepen B. E., Böszörményi K. P., Kiemenyi-Kayere G., van Driel N., Quaye O., Zhang X., ter Horst S., Mishra N., Deboutte W., Matthijnssens J., Coelmont L., Vandermeulen C., Heylen E., Vergote V., Schols D., Wang Z., Bogers W., Kuiken T., Verschoor E., Cawthorne C., Van Laere K., Opdenakker G., Vande Velde G., Weynand B., Teuwen D. E., Matthys P., Neyts J.*, Thibaut H. J.*, Dallmeier K.* (2020). A single-dose live-attenuated YF17D-vectored SARS-CoV2 vaccine candidate. *Nature*, 590 (7845) (IP 49.9)
   * equally contribution
3. **Malengier-Devlies, B.,** Decaesteker, T., Dekoster, K., Vanstapel, A., Ahmadzadeh, K., Poosti, F., Mitera, T., Seldeslachts, L., Verbeken, E., Wouters, C., Vande Velde, G., Vanoirbeek, J., Matthys, P. (2021). Lung Functioning and Inflammation in a Mouse Model of Systemic Juvenile Idiopathic Arthritis. *Frontiers in Immunology*, 12, Art.No. ARTN 642778 (IP 7.6)
4. **Malengier-Devlies, B.*,** Metzemaekers, M.*, Gouwy, M., Van Nieuwenhove, E., Betrains, A., Cockx, M., Vanbrabant, L., Portner, N., Vercauteren, J., De Somer, L., Struyf, S., Vanderschueren, S., De Langhe, E., Proost*, P., Matthys, P.*, Wouters, C*. (2021). Phenotypical and Functional Characterization of Neutrophils in Two Pyrin-Associated Auto-inflammatory Diseases. *Journal of Clinical Immunology* (IP 8.3)
   * equally contribution

Co-author

5. Van Nieuwenhove, E., Barber, J.S., Neumann, J., Smeets, E., Willemsen, M., Pasciuto, E., Prezzemolo, T., Lagou, V., Seldeslachts, L., **Malengier-Devlies, B.**, Metzemaekers, M., Haßdenteufel, S., Kerstens, A., van der Kant, R., Rousseau, F., Schymkowitz, J., Di Marino, D., Lang, S., Zimmermann, R., Schlenner, S., Munck, S., Proost, P., Matthys, P., Devalck, C., Boeckx, N., Claessens, F., Wouters, C., Humblet-Baron, S., Meyts, I., Liston, A. (2020). Defective Sec61α1 underlies a novel cause of autosomal dominant severe congenital neutropenia. *Journal of Allergy and Clinical Immunology*, 146 (5), 1180-1193 (IP 10.8)
6. Vandenhaute, J., Avau, A., Filtjens, J., **Malengier-Devlies, B**., Imbrechts, M., Van den Berghe, N., Ahmadzadeh, K., Mitera, T., Boon, L., Leclercq, G., Wouters, C., Matthys, P. with Wouters, C. (joint last author), Matthys, P. (2019). Regulatory Role for NK Cells in a Mouse Model of Systemic Juvenile Idiopathic Arthritis. *Journal of Immunology*, 203(12):3339-3348 (IP 5.4)
7. Imbrechts M., Avau A., Vandenhaute J., **Malengier-Devlies B.**, Put K., Mitera T., Berghmans N., Burton O., Junius S., Liston A., De Somer L., Wouters C., Matthys P. (2018). Insufficient IL-10 Production as a Mechanism Underlying the Pathogenesis of Systemic Juvenile Idiopathic Arthritis. *Journal of Immunology*, 201(9), 2654-2663 (IP 5.4)
8. Van Nieuwenhuijze A., Burton O., Lemaitre P., Denton AE., Cascalho A., Goodchild RE., **Malengier-Devlies B.**, Cauwe B., Linterman MA., Humblet-Baron S., Liston A. (2018). Mice Deficient in Nucleoporin Nup210 Develop Peripheral T Cell Alterations. *Frontiers of Immunology*, 9, Art.No. 2234 (IP 7.6)
9. Wauters, E., Van Mol, P., Garg, A., Jansen, S., Van Herck, Y., Vanderbeke, L., Bassez, A., Boeckx, B., **Malengier-Devlies, B.**, Timmerman, A., Van Brussel, T., Van Buyten, T., Schepers, R., Heylen, E., Dauwe, D., Dooms, C., Gunst, J., Hermans, G., Meersseman, P., Testelmans, D., Yserbyt, J., Tejpar, S., De Wever, W., Matthys, P., CONTAGIOUS collaborators, , Neyts, J., Wauters, J., Qian, J., Lambrechts, D., Bosisio, F.M., Casaer, M., De Smet, F., De Munter, P., Humblet-Baron, S., Liston, A., Lorent, N., Martinod, K., Proost, P., Raes, J., Thevissen, K., Vos, R., Weynand, B., Wouters, C., Neyts, J., Wauters, J., Qian, J., Lambrechts, D. (2021). Discriminating mild from critical COVID-19 by innate and adaptive immune single-cell profiling of bronchoalveolar lavages. *Cell Research*, 31(3):272-290 (IP 25.6)
10. Metzemaekers, M., **Malengier-Devlies, B.**, Yu, K., Vandendriessche, S., Yserbyt, J., Matthys, P., De Somer, L., Wouters, C., Proost, P. (2021). Synovial Fluid Neutrophils From Patients With Juvenile Idiopathic Arthritis Display a Hyperactivated Phenotype. *Arthritis & Rheumatology*, 73 (5), 896-897 (IP 11.0)

11. Penttilä PA, Van Gassen S, Panovska D, Vanderbeke L, Van Herck Y, Quintelier K, Emmaneel A, Filtjens J, **Malengier-Devlies B**, Ahmadzadeh K, Van Mol P, Borras DM, Antoranz A, Bosisio FM, the CONTAGIOUS consortium, Wauters E, Matthys P, Saeys Y, Garg AD, Wauters J, De Smet F (2021). High-dimensional profiling identifies longitudinal blood immunotypes in critically ill COVID19 patients. *Cellular and Molecular Life Sciences*, 78 (8), 3987-4002 (IP 9.3)
12. Metzemaekers, M., Cambier, S., Blanter, M., Vandooren, J., de Carvalho, A.C., **Malengier-Devlies, B.**, Vanderbeke, L., Jacobs, C., Coenen, S., Martens, E., Portner, N., Vanbrabant, L., Van Mol, P., Van Herck, Y., Van Aerde, N., Hermans, G., Gunst, J., Borin, A., Pereira, B.T N., Gomes, A.B D S P., Muraro, S.P., de Souza, G.F., Farias, A.S., Proenca-Modena, J.L., Vinolo, M.A R., Consortium, C., Marques, P.E., Wouters, C., Wauters, E., Struyf, S., Matthys, P., Opdenakker, G., Marques, R.E., Wauters, J., Gouwy, M., Proost, P. (2021). Kinetics of peripheral blood neutrophils in severe coronavirus disease 2019. *Clinical & Translational Immunology*, 10 (4), Art.No. e1271. (IP 6.1)
13. Vennekens A., Laporte E., Hermans F., Cox B., Modave E., Janiszewski A., Nys C., Kobayashi H., **Malengier-Devlies B.**, Chappell J., Matthys P., Garcia M., Pasque V., Lambrechts D., Vankelecom H. (2021). Single-cell transcriptomics uncovers interleukin-6 as pituitary stem cell-activating factor which quenches at aging, coinciding with an elevated inflammatory state of the gland. *Proceedings of the National Academy of Science* (IP 11.2)

<u>Submitted articles / articles in revision</u>

First or equally first author

14. **Malengier-Devlies B.**, Bernaerts E., Ahmadzadeh K., Filtjens J., Vandenhaute J., De Visscher A., Mitera T., Berghmans N., Burton O., Liston A., Proost P., Wouters C., Matthys P. Role for G-CSF in neutrophilic extramedullary myelopoiesis in mouse model of systemic juvenile idiopathic arthritis. *Arthritis & Rheumatology* (IP 11.0) --> In revision
15. **Malengier-Devlies B.**, Metzemaekers M., Wouters C., Proost P., Matthys P. Neutrophil homeostasis and emergency granulopoiesis in systemic inflammation: the example of systemic juvenile idiopathic arthritis. *Frontiers of Immunology* (IP 7.6) --> In revision
16. **Malengier-Devlies B.***, Filtjens J.*, Ahmadzadeh K., Boeckx B., Vandenhaute J., De Visscher A., Bernaerts E., Mitera T., Vanderbeke L., Van Mol P., Van Herck Y., Hermans G., Meersseman P., Wilmer A., the CONTAGIOUS consortium, Gouwy M., Garg A.D., Humblet-Baron S., De Smet F., Martinod K., Wauters E., Proost P., Wouters C., Leclercq G., Lambrechts D.*, Wauters J.* and Matthys P.* Phenotypical and functional assessment of natural killer cells in a cohort of COVID-19 patients. *Journal of Clinical Investigation* (IP 14.8) --> Submitted
    * equally contribution

Co-author

17. Vandenhaute J., Filtjens J.#, Ahmadzadeh K.#, De Visscher A.#, **Malengier-Devlies B.**, Imbrechts M., Berghmans N., Mitera T., Bernaerts E., Zhang J., Boon L., Vanderschueren S., De Langhe E., De Somer L., C. Gabay, Dierckx T., Walzer T., Leclercq G., Wouters C.*, Matthys P.* STAT1-dependent expansion of inflammatory group 1 Innate Lymphoid cells in Macrophage Activation Syndrome. *Proceedings of the National Academy of Science* (IP 11.2) --> In revision
    # equally contribution
    * equally contribution
18. Cambier S., Metzemaekers M., de Carvalho A.C., Nooyens A., Jacobs C., Vanderbeke L., **Malengier-Devlies B.**, Gouwy M., Heylen E., Meersseman P., Hermans G., Wauters E., Wilmer A., the CONTAGIOUS Consortium, Schols D., Matthys P., Opdenakker G., Elias Marques R., Wauters J.*, Vandooren J.*, Proost P.* Atypical response to co-infection and persistent neutrophilic 1 inflammation in the lungs distinguish critical COVID-19 from influenza. *Cellular & Molecular Immunology* (IP 9.3) –> Submitted
    * equally contribution
19. Metzemaekers M., **Malengier-Devlies B**., Gouwy M., De Somer L., de Queiroz Cunha F, Opdenakker G., Proost P. Fast and furious: the neutrophil and its armamentarium in health and disease. *Annual Review of Immunology* (IP 28.5) --> Submitted